University of Alberta

Synthesis and Characterization of Cross-Conjugated Macrocycles and Exploratory Study of their Organometallic Chemistry

by

Mojtaba Gholami

A thesis submitted to the Faculty of Graduate Studies and Research
in partial fulfillment of the requirements for the degree of

Doctor of Philosophy

Department of Chemistry

Fall 2009
Edmonton, Alberta

Examining Committee

Dr. Rik R. Tykwinski, Department of Chemistry

Dr. James Harynuk, Department of Chemistry

Dr. Josef Takats, Department of Chemistry

Dr. Jeffrey M. Stryker, Department of Chemistry

Dr. William C. McCaffrey, Department of Chemical and Materials Engineering

Dr. Robin G. Hicks, Department of Chemistry, University of Victoria

Abstract

This thesis covers the synthesis, characterization and physical studies of cross-conjugated macrocycles, expanded radialenes, as well as their related derivatives. The main synthetic protocol that is used throughout this thesis is based on the Pd-mediated Sonogashira cross coupling reaction of a desilylated *iso*-polydiacetylene with a dibromoolefin.

To initiate the synthesis, a series of [3]–, [4]–, and [5]expanded radialenes was synthesized, characterized, and studied by UV-vis spectroscopy, electrochemistry, and solid-state analysis. The results confirm the macrocycles are achievable in reasonable yields and suitable for further physical studies without any concerns for their stability in the solid or solution phase.

At the same time, the use of tetrabromoethene in analogous Sonogashira cross coupling reactions afforded bisexpanded radialenes and radiaannulenes that exhibited interesting physical properties according to UV-vis spectroscopy and cyclic voltammetric analysis.

This thesis also covers some interesting results, in particular, for [3]expanded radialenes that undergo cycloaddition reactions. As well, physical studies of the target radialenes show that as the macrocycles become more strained, they exhibit more unique and unexpected electronic and optical properties.

Having the first series of the radialenes in hand, the synthetic plan shifted towards the synthesis of functional expanded radialenes, which were produced in

good to very good yields. In particular, the existence of a [4]expanded radialene carrying triisopropylsilylethynyl groups as exocyclic substituents provided an opportunity for derivatization of the expanded radialene framework.

The general protocol for radialene synthesis was also applied using tetrabromides of anthracenylidene and pentacenylidene in Sonogashira reactions. These efforts afforded structurally unique bisexpanded radialene and radiaannulene products.

Because of their shape and structure, radialenes have potential for use in organometallic chemistry or as ligands in inorganic chemistry. Exploratory studies have been focused on [3]– and [4]expanded radialenes. By all accounts, [3]radialenes reacted more easily with selected precursors such $Pt(PPh_3)_4$ and $Co_2(CO)_8$.

Throughout this thesis, all the major radialene frameworks are established in terms of solid-state structures by X-ray crystallography. Finally, electrochemical analyses show that the new series radialenes reported in this work are generally reduced at higher potentials when compared to the previous generation of expanded radialenes based on butadiynyl building blocks.

Acknowledgement

First of all, my deep appreciation to professor Rik R. Tykwinski, my supervisor, for his support, help and coming along with me during my PhD. study. I thoroughly believe our research achievements opened a window for future students to further explore radialene chemistry.

Special thanks to professor Jeffrey M. Stryker, my co-supervisor, who let me to use his group facility, for his research advice and proof–reading of my thesis and also all the Stryker group members who have been cooperative and friendly.

My warm appreciation also goes to professor Josef Takats for his helps during my graduate study, his memorable teaching and his general care to the graduate students.

I have to thank and mention all my group colleagues from past to present in the Tykwinski group; Dr. Katie Campbell, Dr. Sara Eisler, Andreea Spantulescu, Jamie Kendall, Dr. Thanh Luu, Amber Sadowy, Wes Chalifoux, Dan Lehnherr, Erin Graham, Shar Ramsaywack, B.J. Medos, Adrain Murray, Myron Wilde, Dr. Yasuhiro Morisaki, Dr. Khalid Azyat, and Dr. Eike Jahnke, for their help and great memories that remain for ever.

Special thanks and appreciation to four departmental laboratories, mass spectrometry laboratory, Drs. Randy Whittal and Angie Morales-Izquierdo, and Ms. Jing Zheng and NMR laboratory, Dr. Albin Otter, Mr. Mark Miskolzie, Mr. Glen Bigam, Ms. Nupur Dabral and Ms. Lai Kong and also X-ray crystallography

laboratory Drs. Robert McDonald and Michael J. Ferguson as well as analytical and instrumentation laboratory, Mr. Wayne Moffat, not only for all their help, time and efforts with regard to my research but also for providing good expertise. Furthermore, I should thank Mr. Eric Pelletier from professor Dennis Hall's group for HPLC experiments.

I have to acknowledge the people of machine shop specially Mr. Paul Crothers, Mr. Randy Benson and Mr. Richard Tomski and glass shop Mr. Gerald Streefkerk, Mr. Todd Carter, Mr. Jason Dibbs and of course the man in charge of chemstore Mr. Bernie Hippel and his colleagues Mr. Ryan Lewis and Mr. Andrew Yeung for their great help.

I have to specially thank our group secretary Ms. Diane Dowhaniuk for her help and assistance.

My great appreciation and thanks to professor Luis Echgoyen, Dr. Manuel N. Chaur and Dr. Fredric Melin, Department of Chemistry, Clemson University, SC, USA, for the electrochemistry experiments.

Finally, I have to really thank my family, especially my mother and father for their priceless support, patience and love.

Table of Contents

List of Tables

List of Figures

List of Schemes

Structures of Synthesized Macrocyclic Compounds

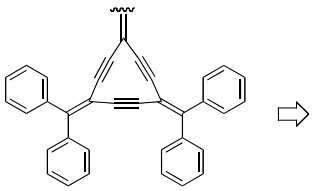

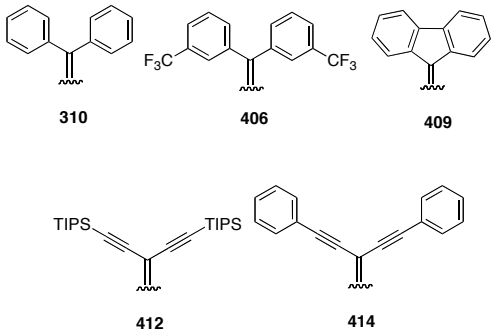

310 406 409

412 414

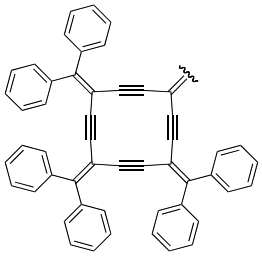

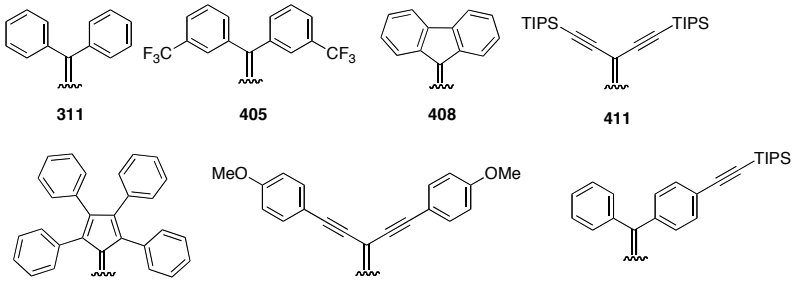

311 405 408 411

433 510 519

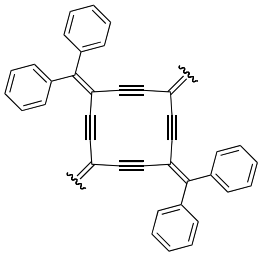

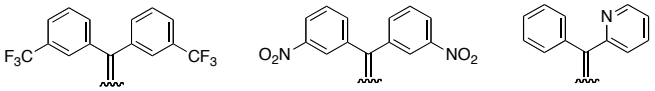

404 428 431

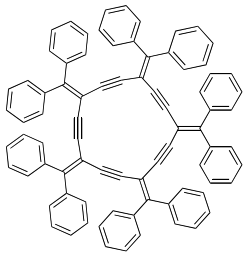

312

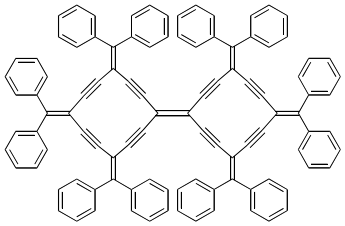

315a

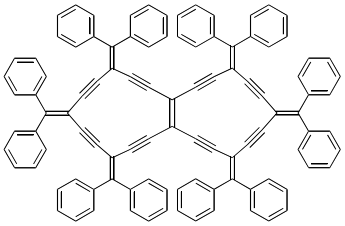

315b

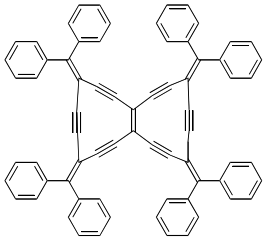

316a

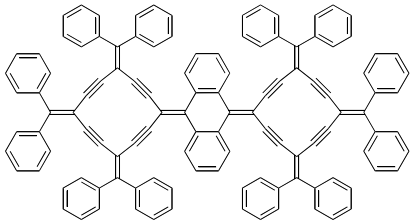

502 (and its isomer)

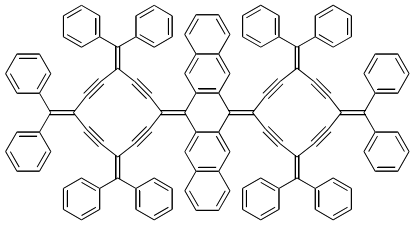

504 (and its isomer)

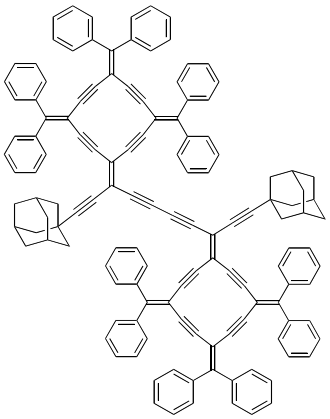

507

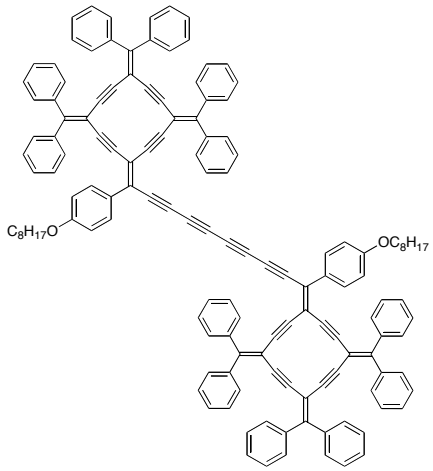

508

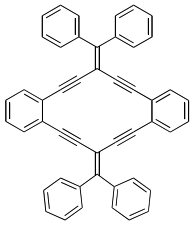

526

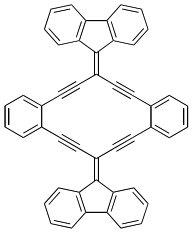

528

List of Abbreviations

Ac	acetyl
acac	acetylacetonate
OAc	acetate
app	apparent
Aq	aqueous
Bpy	bipyridine
BHT	butylated hydroxytoluene
Bu	*n*-butyl
CD	circular dichroism
CEE	cyanoethynylethylene
cm	centimeter
COD	cyclooctadiene
CV	cyclic voltammetry
d	doublet
decomp.	decomposition
DMF	*N, N*–dimethylformamide
dppee	1,2-bis(diphenylphosphino)ethane
DOKE	differential optical Kerr effect
DCTB	*trans*-2-[3-(4-*tert*-butylphenyl)-2-methyl-2-propenylidene]malononitrile
EI	electron ionization
Et	ethyl
ESI	electrospray ionization

Fc	ferrocenyl
g	gram(s)
G	grease or silicon grease
H	hexanes
h	hour(s)
HOMO (H)	highest occupied molecular orbital
HRMS	high resolution mass spectrometry
Hz	hertz
i	*iso*
IR	infrared
LR	low resolution
HR	high resolution
LUMO (L)	lowest unoccupied molecular orbital
m	multiplet
M	molar
MALDI	matrix–assisted laser desorption ionization
Me	methyl
MHz	megahertz
mL	milliliter
MLCT	metal–to–ligand–charge–transfer
mmol	millimole
MO	molecular orbital

Mp	melting point
MS	mass spectrometry
NLO	nonlinear optical
nm	nanometer
NMR	nuclear magnetic resonance
ORTEP	Oak Ridge Thermal Ellipsoid Plot
OTf	triflate ($–OSO_2CF_3$)
PDA	polydiacetylene
Ph	phenyl
ppm	part per million
PPV	poly(*p*-phenylenevinylene)
PTA	polytriacetylene
Py	pyridine
q	quartet
rt	room temperature
t	triplet
TBAF	tetrabutylammonium fluoride
TBDMS	tert-butyldimethylsilyl
TEE	tetraethylenethene
TES	triethylsilyl
THF	tetrahyrofuran
TIPS	triisopropylsilyl

tht	tetrahydrothiophene
TLC	thin layer chromatography
TMEDA	*N*, *N*, *N*′, *N*′,–tetramethylethylenediamine
TOF	time of flight
TTF	tetrathiafulvalene
UV–vis	ultraviolet visible

List of Symbols

Å	Angstrom
δ	chemical shift
ε	extinction coefficient or molar absorptivity
λ_{max}	wavelength of maximal absorption

Chapter 1:

Introduction to Cross-Conjugated Skeletons

1.1 Cross-conjugated skeletons †

The presence of π-electrons in the skeletons of organic or organometallic compounds motivated synthetic and theoretical chemists to explore their physical and chemical properties. This is not only from a theoretical point of view but also for their potential applications in materials science.[1]

Conjugated organic compounds play a primary role in the development of a new generation of optical and electronic materials. Monomers, oligomers, and polymers with carbon, heteroatomic, or organometallic frameworks have been widely explored as media for electroluminescence, data storage, and nonlinear optics.[1] The most intensely studied conjugated molecules with carbon-rich frameworks feature extended, linearly-conjugated π-systems. There are, however, alternative modes of π-electron communication, including cross conjugation[2] and omniconjugation[3] that can also produce electronically interesting materials. One of the most notable literature discussion concerning the "cross-conjugated" phenomenon is by Nelson F. Phelan and Milton Orchin.[2c] According to their definition a cross-conjugated compound may be defined as a compound possessing three unsaturated groups, two of which although conjugated to a third unsaturated center are not conjugated to each other as it is demonstrated by the molecules in Scheme **1.1**.

---

† This chapter adapted from "Gholami, M.; Tykwinski, R. R. *Chem. Rev*. **2006**, *106*, 4997–5027".

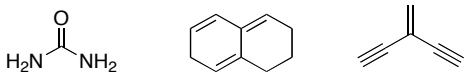

Scheme 1.1 Some examples of cross-conjugated compounds

Basically two approaches were considered to explain the cross-conjugation by Phelan and Orchin, based on Valance Bond (VB) and Molecular Orbital (MO) theories. These studies, according to a MO approach concerned the presence of conjugation (or bonding) between the unsaturated bonds centers for 3-methylene-1,4-pentadiene in three possible conformations as shown in Scheme **1.2**.[2c]

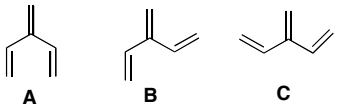

3-methylene-1,4-pentadiene

Scheme 1.2 Communication of vinyl groups in a cross-conjugated molecule

Regardless to the geometry for 3-methylene-1,4-pentadiene (**A**–**C**) that could be planner or close to planner the molecular orbital outcome is the same. All the six carbons have parallel 2pπ orbitals that are participated in the π system and all the six electrons delocalized over all carbon atoms and there are no "intact" vinyl groups. In terms of the molecular orbitals, there are three bonding at –20.16, –16.06 and –14.05 ev respectively and there are three antibonding orbitals at –8.27, –6.06, and –2.16 ev respectively.[2c] The MO approach not only gives a semi-quantitative understanding of the π-electron distribution in this cross-conjugated molecule, but also provides insight into the expected electronic absorptions. This is important because UV-vis spectroscopic studies are

essential and informative to account for differences between linear conjugated molecules in comparison to their cross-conjugated analogues. In the cross-conjugated compounds, the π-electron density cannot be as readily delocalized over the entire molecule such as that which is expected for linear conjugated compounds. Thus, for cross-conjugated molecules the electronic properties are often determined by the longest linear conjugated fragment that is present in the molecule. This premise has been explore experimentally by van Walree and co-workers.[2a,b] Their findings confirm that the extension of the conjugated system is not accompanied by a bathochromic shift of λ_{max} values in the UV spectra of a series of cross-conjugated model compounds. The most interesting outcome of this study is, perhaps, that cross-conjugated materials are good candidates for optoelectronic applications that rely on transparency in the visible region, such as nonlinear optical materials.[2a,b]

In comparison to linearly-conjugated materials, oligomeric and polymeric compounds with a fully cross-conjugated carbon backbone are relatively unexplored. This is not to say, however, that molecules with a cross-conjugated frameworks are rare.[4] The situation is, in fact, quite the opposite. Cross conjugation can be found in a wide range of molecules, including such examples as quinones, radialenes, fulvalenes, and fused aromatics. It has only been recently, however, that nonaromatic cross-conjugated frameworks have emerged as a versatile platform for the synthesis of expanded cyclic and acyclic systems. As a result, trends in the structural, physical, and electronic properties of

materials with a fully cross-conjugated π-backbone are only now starting to reveal themselves. The cross-conjugated isomers that arise as the constitutional isomers of their linearly-conjugated analogues; dendralenes, *iso*-polydiacetylenes (*iso*-PDAs), *iso*-polytriacetylenes (*iso*-PTAs), and *iso*–poly(phenylenevinylidene)s (*iso*-PPVS) are outlined by Scheme **1.3**. The obvious difference between the two classes of compounds is that π-electron density in the cross-conjugated isomers cannot be readily delocalized along the carbon framework in a manner analogous to that in their linearly-conjugated counterparts in accord with classical resonance theory.[2] Nonetheless, evidence of π-electron communication via cross conjugation in such systems is often observable and provides molecular systems of both fundamental and practical importance.

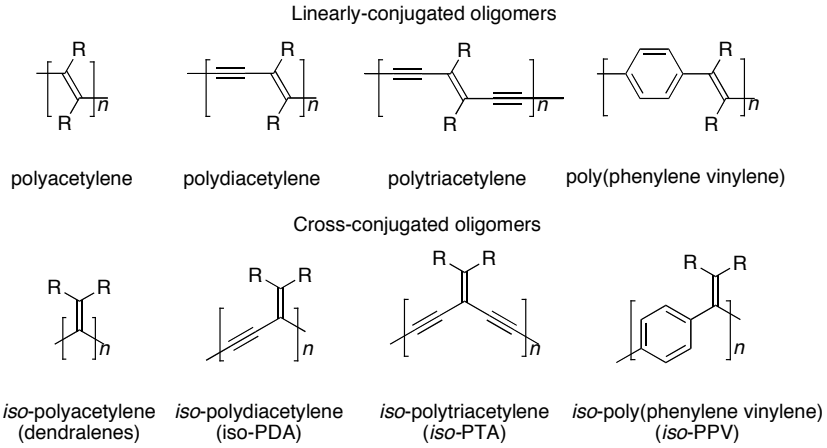

Scheme 1.3 Linear conjugated and cross-conjugated oligomers

While not yet classified as a dendralene, the inclusion of pendent and/or terminal functionalization onto the 1,3–butadienyl framework provides molecules with a range of cross-conjugated interactions, as outlined in Scheme **1.4**.[4-8]

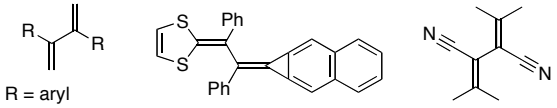

Scheme 1.4 Examples of cross-conjugated molecules

One of the examples for the formation of an acyclic cross-conjugated skeleton is the formation of 2,3-diethynyl-1,3-butadiene via the Pd catalyzed dimerization of a cumulene that was explored by Suzuki et al., giving a potentially interesting building block for cross-conjugated oligomers and polymers via desilylation and further elaboration as shown in Scheme **1.5**.[9]

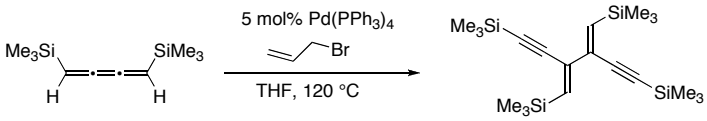

Scheme 1.5 Synthesis of an acyclic cross-conjugated enyne

1.2 Acyclic cross-conjugated skeletons

In terms of classification of linear cross-conjugated oligomers, and with regard to our focused discussion here it could tentatively be divided into three major categories including dendralenes, *iso*-polydiacetylenes, and polytriacetylenes. The first family of cross-conjugated oligomers are the [n]dendralenes, which feature a conjugated skeleton composed of sp^2-hybridized carbon atoms. Sherburn and co-workers reported one of the most important contributions in the synthesis of dendralenes that was based on the concept of masking the terminal butadiene moiety as a sulfolene.[10] The masked precursors were assembled using a sequence of Stille coupling reactions, and the dendralene products were obtained by heating at 450 °C. UV absorption analysis

confirmed that conjugation does not increase as a function of length, as it proceeds from **100** to **101** and **101** to **103** (Scheme **1.6**)

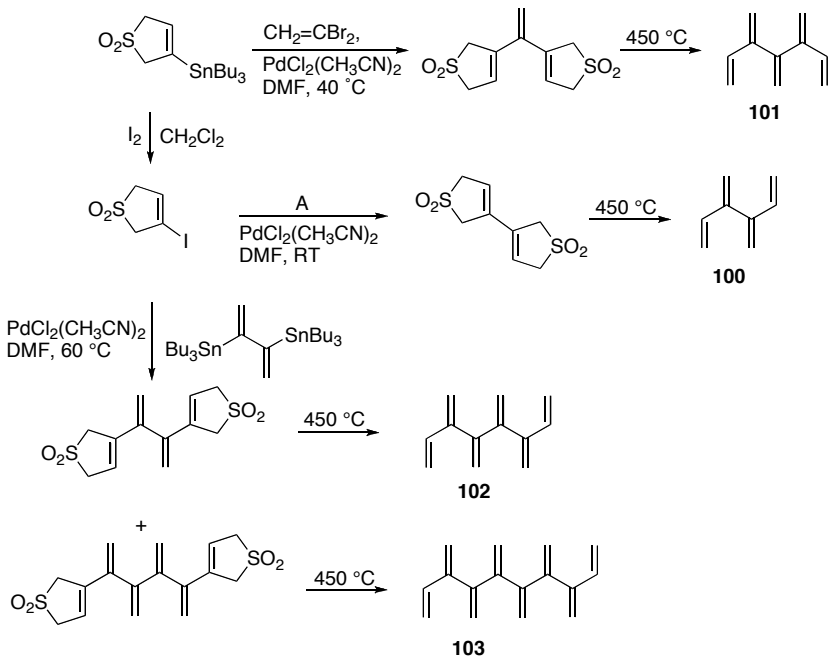

Scheme 1.6 Synthesis of dendralene series

Iso-polydiacetylenes prepared by an insertion of an acetylene group between the intervening olefins of a dendralene skeleton affords the *iso*-polydiacetylenes (*iso*-PDAs, also called expanded dendralenes). While dendralenes had been the object of study for some time, *iso*-PDAs were unknown until quite recently. The first series to be studied, **104-105**, were based on an isopropylidene framework as reported by Tykwinski and Zhao in 1999 (Scheme **1.7**).[11,12] The solid-state structure of a trimeric *iso*-PDA (**104** n = 3) showed a completely planar, cross-conjugated framework. The electronic characteristics of the monodisperse oligomers **104** and **105** were analyzed by UV–vis spectroscopy in solution and as thin films.[13] By comparing to the dimeric

species, **106** and **107**, which contain the longest linearly-conjugated segment of each oligomer (Scheme **1.7**), this study suggested that π-electron communication is present along the enyne framework of the *iso*-PDAs, but quickly reaches saturation by the stage of nonamer (**105** $n = 9$). The solubility and kinetic stability of both series, **104** and **105**, were, however, less than ideal.

The use of pendent cyclohexylidene groups was explored toward improving solubility (**109**), but resulted in *iso*-PDAs with even lower kinetic stability, while the use of alternating isopropylidene and cyclohexylidene (**110**) units faired a little better.[14] The adamantylidene series of *iso*-PDAs (**112**) was reported, and while kinetic stability was improved versus **104**, solubility remained a serious issue.[13] The most successfully studied *iso*–PDAs are the perphenylated derivatives **112**. Monodisperse oligomers, ranging from dimer **108** to pentadecamer **113**, were synthesized using a palladium-catalyzed cross-coupling protocol as shown in Scheme **1.8**. Following desilylation of each precursor, and coupling with a vinyl triflate as the partner gave the desired oligomers, as shown in Scheme **1.8**.[15]

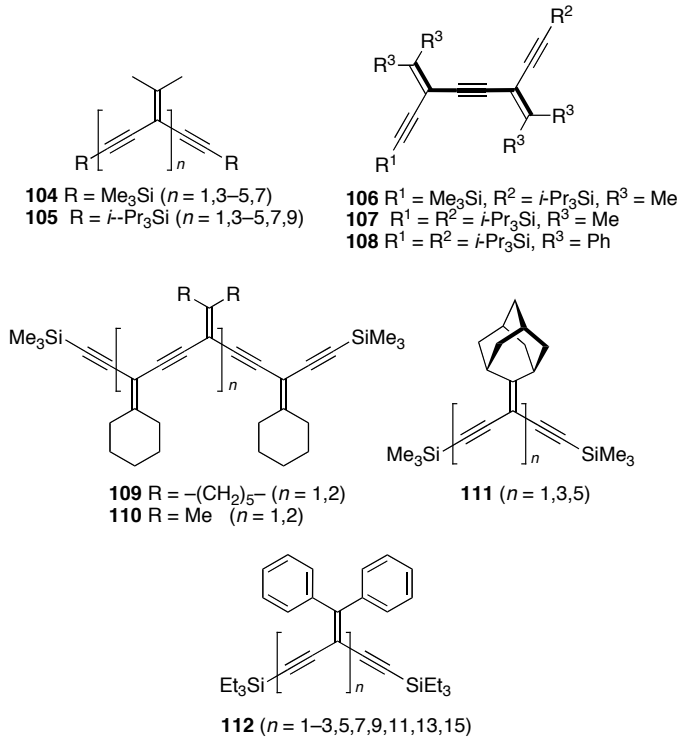

104 R = Me_3Si (*n* = 1,3–5,7)
105 R = *i*-Pr_3Si (*n* = 1,3–5,7,9)

106 R^1 = Me_3Si, R^2 = *i*-Pr_3Si, R^3 = Me
107 R^1 = R^2 = *i*-Pr_3Si, R^3 = Me
108 R^1 = R^2 = *i*-Pr_3Si, R^3 = Ph

109 R = $-(CH_2)_5-$ (*n* = 1,2)
110 R = Me (*n* = 1,2)

111 (*n* = 1,3,5)

112 (*n* = 1–3,5,7,9,11,13,15)

Scheme 1.7 Examples of expanded dendralenes

Pentadecamer **113a** is the longest monodisperse *iso*–PDA oligomer synthesized to date, and it consists of a cross-conjugated enyne backbone composed of 62 sp– and sp^2–hybridized carbons. Structural characteristics determined by X-ray crystallographic analysis for several derivatives demonstrated a non-planar backbone conformation for the oligomers as a result of steric interactions between neighboring alkylidene phenyl groups. The electronic absorption spectra of the oligomers show a slight red-shift of the maximum absorption wavelength as the chain length increases from dimer **108** to pentadecamer **113a**, a trend that has saturated by the stage of the nonamer **112** (n = 9) (Scheme **1.8**). Fluorescence spectroscopy confirmed that the pendent phenyl groups enhanced emission, and the relative emission intensity consistently increased as a function of chain length *n*. Molecular modeling and

spectroscopic studies suggest that *iso*–PDA oligomers ($n > 7$) adopt a coiled, helical conformation in solution.[15]

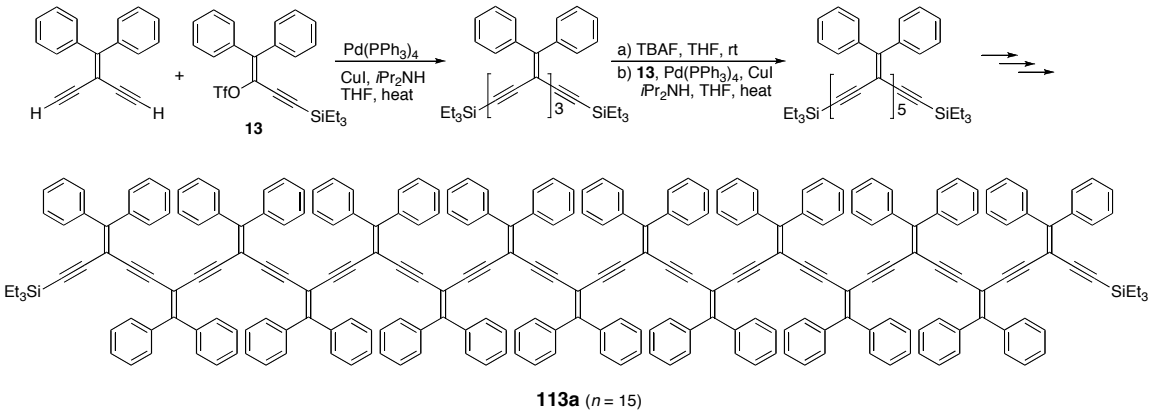

Scheme 1.8 Synthesis of *iso*-PDA series

The π-electron-rich framework of cross-conjugated *iso*-PDAs, in combination with their electronic transparency in the visible region of the spectrum, made them interesting candidates as NLO materials, and molecular third-order nonlinearities, γ, for the oligomers **112** were measured via the differential optical Kerr effect (DOKE).[16,17] While the nonresonant γ-values were modest, the molecular hyperpolarizabilities did show a superlinear increase as a function of the oligomer chain length *n*.

The first series of donor (**114**), acceptor (**115**), and donor-acceptor (**116**) *iso*-PDAs was reported by Tykwinski and Ciulei, and it included monomeric, dimeric, and trimeric species of each class (Scheme **1.9**).[18] Evidence for intramolecular charge-transfer via cross conjugation came from UV-vis spectroscopy, which showed that D-A monomer **116** has a low energy absorption tail that extends out beyond 450 nm, whereas **115** and **114** were transparent.

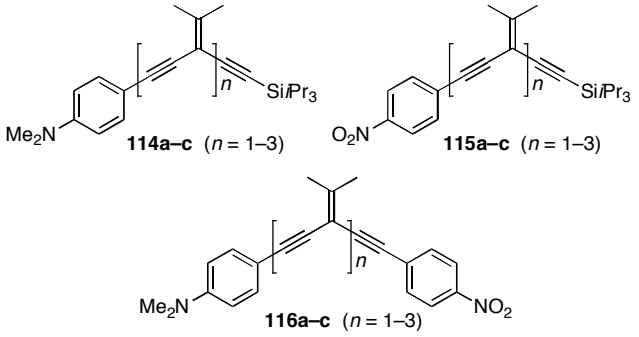

Scheme 1.9 *iso*-PDA donor-acceptor series

Insertion of a diacetylene group between the intervening olefins of the dendralene skeleton affords the next series of cross-conjugated oligomers, the *iso*-polytriacetylenes (*iso*-PTAs). The first members of this series **117**, were reported by Diederich and co-workers in 1995 and were based on the tetraethynylethene building block.[19] A one-pot homocoupling procedure was employed, and individual oligomers were then isolated by column chromatography. The *iso*-PTAs **117** were air- and light-stable solids, and even the longer derivatives (n = 3 and 4) showed melting points above 100 °C. Trimer **118** was reported by the same group , differing only in the terminal silyl groups. Tykwinski and co-workers reported the synthesis of two series of *iso*-PTAs, with pendent isopropylidene groups, **120** and **121**. The members of both series were assembled using an iterative approach similar to their synthesis of *iso*-PDAs described above (Scheme **1.8**).[20,21] For the purpose of comparison, dimeric species **122-124** were also synthesized because they contain the longest linearly-conjugated enyne segment of the *iso*-PTAs oligomers (shown in bold).

Unlike the peralkynylated derivatives **117-118**, the longer oligomers of both series **120** and **121** showed much reduced kinetic stability, decomposing

over a period of days, even when stored under nitrogen at low temperature. The same kinetic instability was found for *iso*-PTAs **119** based on the cyclohexylidene subunit, reported by Diederich and co-workers.[22]

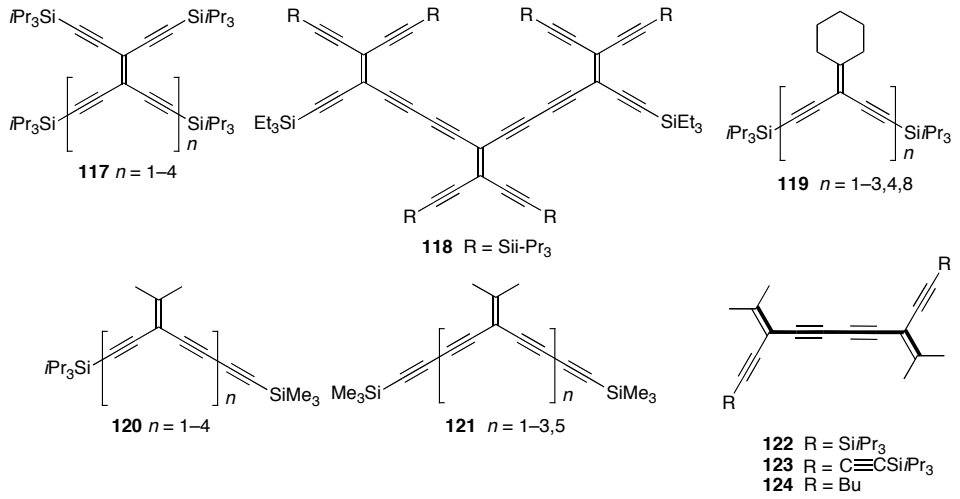

Scheme 1.10 *Iso*-PTA series

The octamer **119** (n = 8), composed of 40 sp- and sp^2-carbon atoms, represents the longest *iso*-PTA synthesized to date. The electronic characteristics of all the *iso*-PDA series have been examined by UV-vis spectroscopy. While little evidence for a lowering of the HOMO-LUMO gap was found for either the TEE (**117**)[19] or isopropylidene (**120** and **121**)[21] series, analysis of the cyclohexylidene (**119**) series by three different methods demonstrated a consistent drop in HOMO-LUMO energy as the length was increased,[22] suggesting a contribution from cross conjugation to the overall electronic makeup of the molecules. The electronic delocalization of *iso*-PTAs in comparison to linearly-conjugated PTAs has also been studied theoretically by Lüthi and coworkers and also Solomon and coworkers.[23, 24, 25] Similar in structure

to **122**–**124**, symmetrical dimeric *iso*-PTAs with a range of terminal and pendent functionality have been reported to date, and their structures are summarized in Scheme **1.11**.[29, 30] In nearly all cases, these molecules are readily available via an oxidative homocoupling reaction connecting the two halves via the central bond. Derivatives with pendent phenyl (**125**) and bromo (**126**)[25,26] substituents are known, while those with isopropylidene building blocks (**127**) have been used to look at the electronic effects of terminal donor or acceptor groups via cross conjugation.[27] Using a combination of spectroscopic and electrochemical analyses, Diederich has extensively explored the effects of substituents in the pendent alkylidene positions of TEE dimers **128**, including electronically neutral (aryl, arylethynyl, silyl)[19] as well as donor (*p*-$R_2NC_6H_4$) and acceptor (*p*-$O_2NC_6H_4$) groups.[28] A similar study by the same group looked at cyanoethynylethylenes (CEEs) **129**.[29] Extended TTF derivatives **130** have been studied, and the interesting azulene-terminated dimer **131** was synthesized by Ito and co-workers.[30] Unsymmetrical substituted *iso*-PTA dimers are more difficult to synthesize, since homo-coupling reactions are either inappropriate or lead to mixtures of products that are typically tedious to separate. Nonetheless, a number of highly functionalized examples are known, including TEE dimers **132** and **133**[28] and the extended donor-acceptor systems **134** and **135** (Scheme **1.12**).[29] A very thorough experimental and theoretical study of the ground-state properties of **134** and **135**, in comparison to smaller analogues, showed that more extensive π-conjugation could lead to molecules with higher HOMO-LUMO

gaps. This results suggested that, for molecules with strong electron donor/acceptors, evaluation of π-conjugation by UV-vis spectroscopy alone could provide misleading results (Scheme **1.12**).[29, 30]

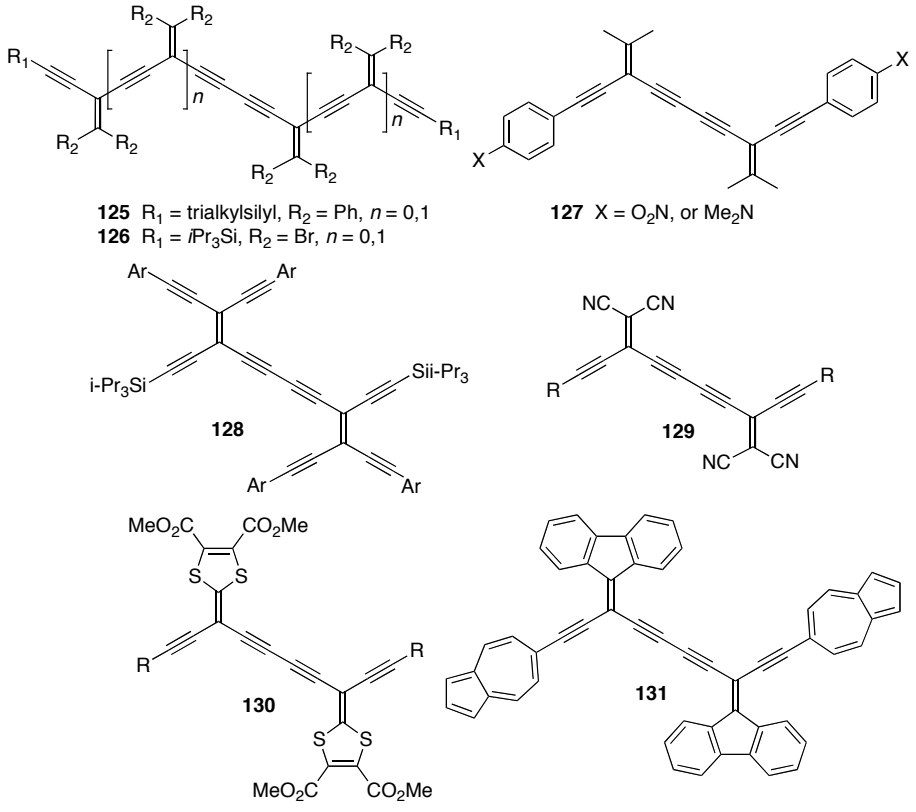

125 R_1 = trialkylsilyl, R_2 = Ph, n = 0,1
126 R_1 = iPr$_3$Si, R_2 = Br, n = 0,1

127 X = O_2N, or Me_2N

128

129

130

131

Scheme 1.11 Cross-conjugated oligomers with different functional groups

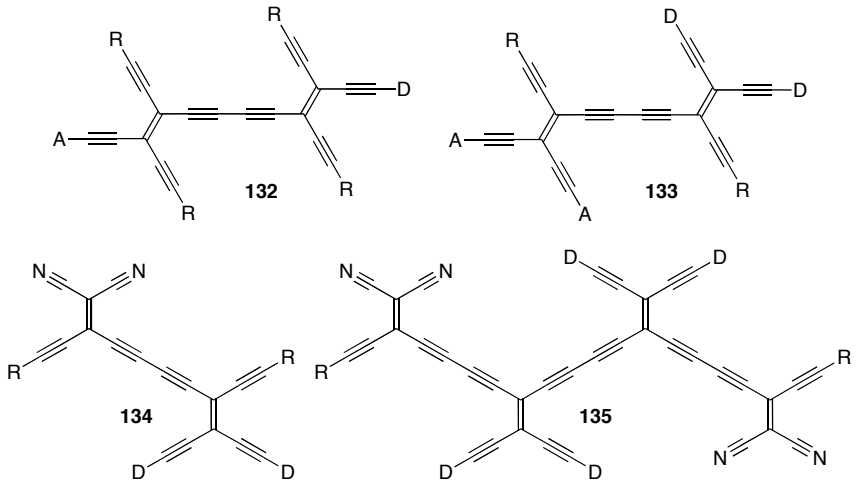

R = iPr$_3$Si, D = pMe$_2$NC$_6$H$_4$, A = pO$_2$NC$_6$H$_4$

Scheme 1.12 Cross-conjugated oligomers with donor-acceptor groups

1.3 Cyclic cross-conjugated systems, history and discoveries

Radialenes are the cyclic analogues of dendralenes, with general formula $C_{2n}H_{2n}$ and containing *n* ring atoms and *n*-exocyclic double bonds (Scheme **1.13**).[31] They are named in a manner similar to that of dendralenes, according to their ring size, i.e., [*n*]radialene.[32] Early syntheses of radialenes have been summarized by Hopf and Maas[32] and a recent review by Gholami and Tykwinski[33] covered synthesis and physical studies of cross-conjugated systems including radialenes that have been synthesized in the last 25 years.

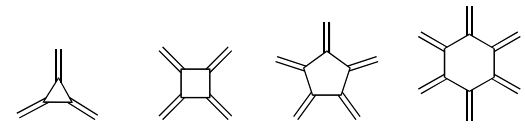

Scheme 1.13 Radialene series

Hopff and Wick reported the first member of the radialene family in 1961. As it is outlined in Scheme **1.13** [6]radialene **137** was synthesized as a mixture of diastereomers from the hexahalide **136** via reaction with Mg metal.[34]

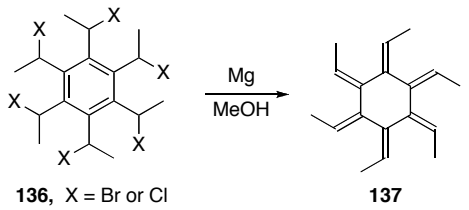

136, X = Br or Cl **137**

Scheme 1.14 The first synthesis of a radialene

The first [3]radialene, **138**, was synthesized shortly thereafter in 1965 by Köbrich and Heinemann in 2% yield as a colorless solid via the addition of the isopropylidene carbenoid **140** to cumulene **141** (Scheme **1.15**).[35]

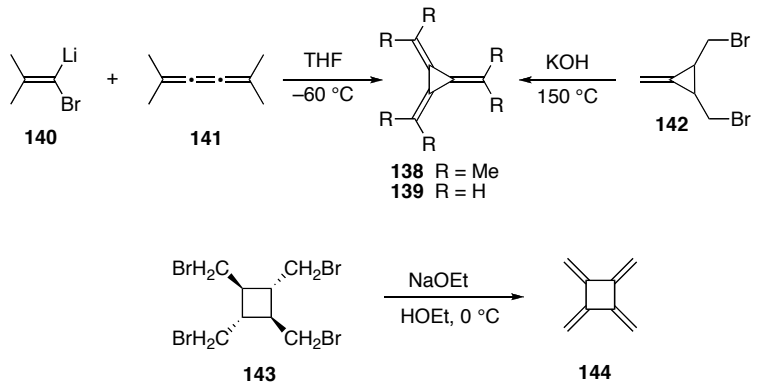

140 **141** **138** R = Me **139** R = H **142** **143** **144**

Scheme 1.15 The first synthesis of [3]– and [4]radialenes

The same year the parent [3]radialene (**139**) was reported by Dorko. It was obtained in 47% yield when the dibromocyclopropane derivative **142** was refluxed at 150 °C in the presence of KOH.[36,37] The lowest energy UV absorption for **138**, at λ_{max} = 309.5 nm (in hexanes), was an indication of electronic

communication between the three double bonds,[35] while λ_{max} for the parent radialene **139** was found at slightly higher energy, at 295 nm (in EtOH).[36] Griffin and Peterson in 1962 achieved the first synthesis of a [4]radialene **144** in 50% yield, as a result of reaction of **143** with NaOEt in ethanol. (Scheme **1.15**).[37, 38]

Completing the series of [*n*]radialenes, the first [5]radialene, **145** (Scheme **1.16**) was synthesized by Iyoda and co-workers in 1986 using the same carbenoid precursor used by Köbrich in Scheme **1.14** (compound **140**).[39] In this case, transmetalation to Cu(I) afforded relatively good yields of both **145** and **146** in 32% and 30%, yields respectively.

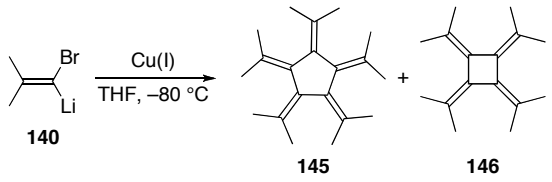

140 **145** **146**

Scheme 1.16 Synthesis of [4]– and [5]radialenes

1.3.1 [3]Radialenes

Because [3]radialenes are very strained macrocycles with interesting physical properties, synthetic chemists have been fascinated by these compounds for a long time. The most notable [3]radialene discoveries are contributions by four groups including Diederich, Oda, Stell, and Matsumoto.

Diederich and co-workers based on Fukunaga's[40] method used pentadiyne **147** and tetrachlorocyclopropene to synthesize [3]radialene **148** (Scheme **1.17**).[41] The perethynylated **148** was isolated as a dark red solid (λ_{max} = 567 nm). X-ray crystallographic analysis showed a planar cross-conjugated framework, and the

C–C bond lengths of the cyclic fragment showed values from 1.420(5) Å to 1.431(3) Å, which were fairly close to those of the parent [3]radialene **139** and its hexamethyl derivative **138**. (Scheme **1.17**)[42-44]

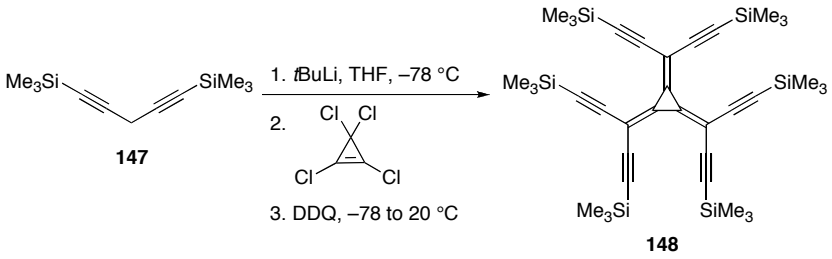

Scheme 1.17 Synthesis of [3]radialene with silylethynyl arms

Oda and co-workers synthesized [3]radialenes **149** and **150a-h** according to Fukunaga's method (Scheme **1.18**).[45,46] These compounds showed two reversible reductions, and cyclic voltammetry also showed that the reduction potentials increased in the order of **150f** < **150e** < **150d** < **150b**, reflecting the electronic nature of the aryl substituents. X-ray crystallography of **150e** showed the radialene core to be planar and the two phenyl rings on each corner to be twisted with regard to the central core. [3]Radialenes bearing either 2– or 3– or 4–pyridyl groups including **151**–**153** were synthesized and reported simultaneously by two groups Steel and Matsumoto (Scheme **1.18**).[47-49]

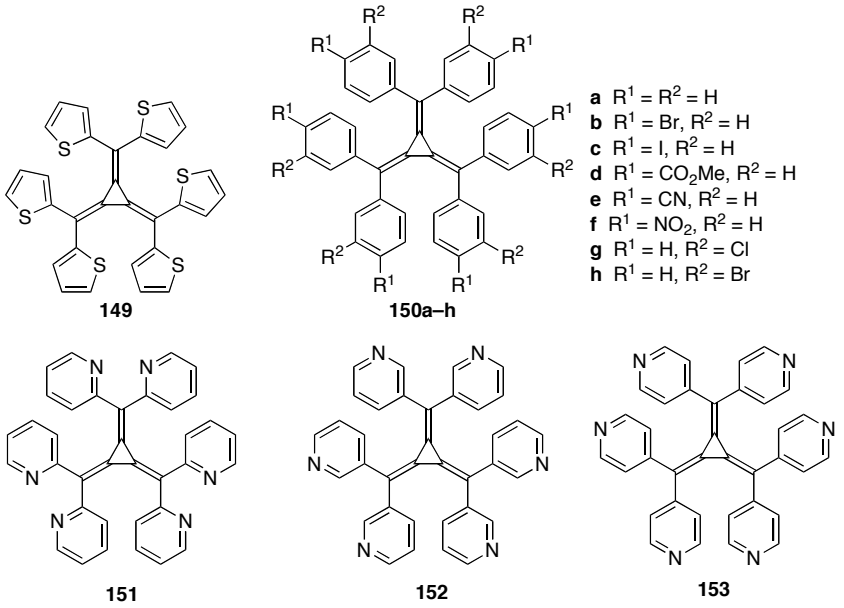

Scheme 1.18 [3]Radialenes with different functional groups

1.3.2 [4]Radialenes

There has been much attention devoted to the synthesis of [4]radialenes. In a series of reports, Uno and co-workers reported the synthesis of a diastereomeric series of [4]radialenes **154a**-**d** based on the coupling of a carbenoid intermediate (Scheme**1.19**).[50,51] Thermal isomerization experiments showed that when the all *Z*-radialenes **154b** were heated in tetralin at 170–200 °C, a mixture of [4]radialenes in a ratio of approximately **154a**:**154b**:**154c**:**154d** = 1 : 10 : 5 : 1 was produced. When the isomeric mixtures were heated in the solid state at the same temperature, however, selective isomerization took place to give **154b** isomers in >90%. Photochemical irradiation of the isomers **154b** caused isomerization to a mixture of ca. **154a:154b:154c:154d** = 1 : 1 : 24 : 24 (Scheme **1.19**).

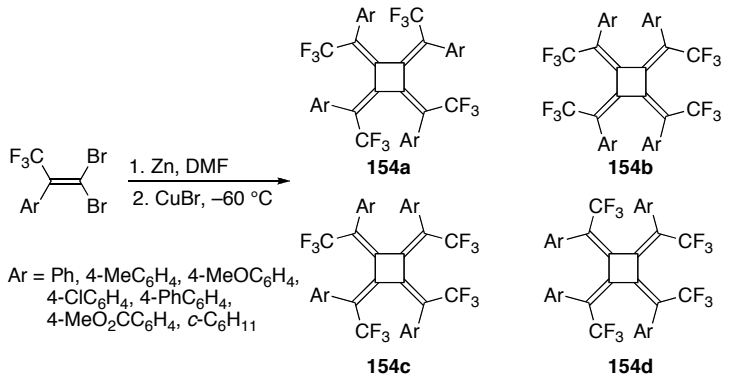

Scheme 1.19 Synthesis of [4]radialenes carrying CF_3 groups

Iyoda and co-workers developed a synthesis of radialenes **155** based on Ni-catalyzed cyclodimerization of [5]cumulenes (hexapentaenes).[52] The reaction yields ranged from 13 to 64% dependent on the catalyst and reaction conditions (Scheme **1.20**). This protocol has been expanded to include the incorporation of alkyl substituents, giving **156** and **157**.[53] The outcome of the dimerization reaction depended on the steric requirements of the cumulene. Head to tail dimerization was observed in the formation of **156** (and the benzo-analogue), while the C_4 symmetrical radialene **157** formed when the steric requirements of the substituents were increased even further. Thermal dimerization of [5]cumulenes was also explored and gave *C*4 symmetrical [4]radialenes **158**-**160** in 21–69% yield through regioselective reaction only at the central double bond (Scheme **1.20**). X-ray crystallographic study of **159** showed the radialene core to be perfectly planar, whereas that of **160** was slightly puckered.

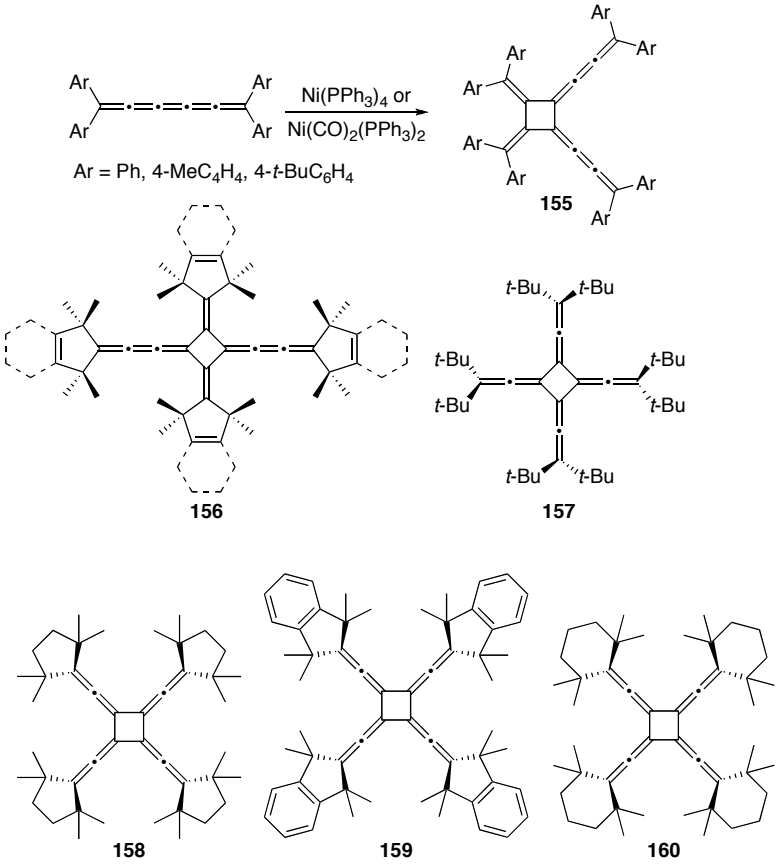

Scheme 1.20 A series of [4]radialene macrocycle

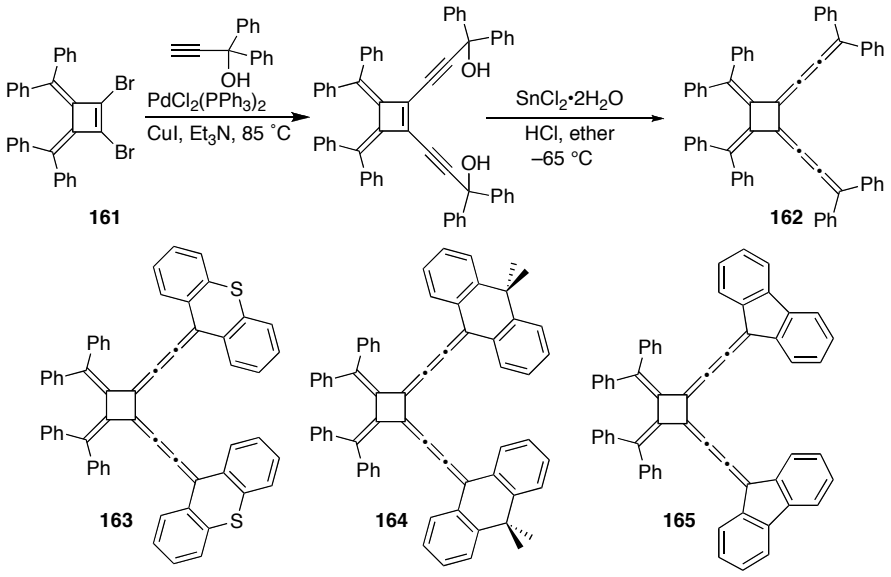

Scheme 1.21 Synthesis of [4]radialene macrocycles

A stepwise procedure was devised for [4]radialenes **162**-**165**.[54] Starting

with dibromide **161**, the Pd-catalyzed Sonogashira coupling with various alkynes was followed by reductive dehydroxylation to the radialene, as shown for the phenyl derivative **162**. The radialenes carrying thioxanthracene (**163**) and dihydroanthrancene (**164**) moieties showed a remarkably low rotational barrier about the butatriene bonds ($\Delta G^{\neq}$ = 13.7 and 14.9 kcal/mol, respectively), while this barrier for **165** was measured to be slightly higher ($\Delta G^{\neq}$ = 17.8 kcal/mol) due to reduced steric repulsion in the ground state of this derivative (Scheme **1.21**).

1.3.3 [5]Radialenes

Compared to [3]– and [4]radialenes, fewer [5]radialene syntheses have been reported. Sakurai and co-workers reported the synthesis of [4]radialene **166** that also provided the [5]radialene analogue **167** (Scheme **1.22**).[55-57] X-ray crystallography showed that neutral **167** adopted an envelope conformation. Upon reduction with Li, however, structural analysis of the corresponding tetraanion showed that the 10–carbon radialene core is nearly planar due to the involvement of these atoms in delocalization of the negative charge.

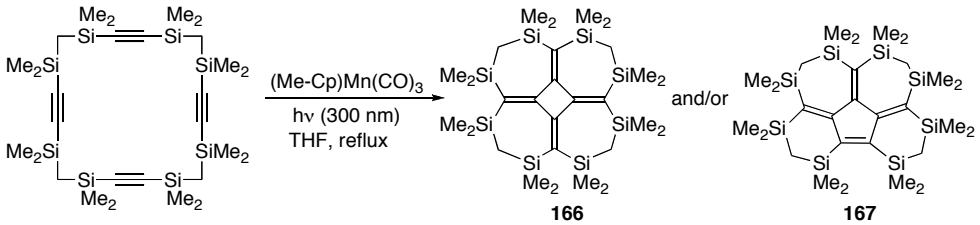

Scheme 1.22 Synthesis of a [5]radialene analogue

Yoshida and co-workers described usage of a common intermediate, radialenone **168**, as a starting material for synthesis of a series of [5]radialenes

169–171 (Scheme **1.23**)**.** Compounds **169**–**171** could be readily oxidized by $NOBF_4$ or $NOPF_6$ in CH_3CN to the corresponding tetracations.[58] Cyclic voltammetry of **169** showed a single-wave, four-electron transfer from the potent donor **169**, giving $\mathbf{169}^{4+}$. This process was explained by aromatic stabilization of the cyclopentadienide ring of the tetracation and rearrangement of the benzodithiol groups to a nonplanar conformation that reduced intramolecular Columbic repulsion and steric hindrance.

Iyoda and co-workers reported the synthesis of extended [5]radialenones **172** and **173** based on Ni-catalyzed dimerization of [5]cumulenes (Scheme **1.23**), reactions that also gave [4]radialenes, as described earlier. [53] X-ray analysis of **172** confirmed that it adopted a planar structure in the solid state, and electronic absorption studies revealed that both **172** and **173** showed strong solvatochromism, with λ_{max} shifting to lower energy as a function of increasing solvent polarity. Radialenone **172** was subsequently converted to [5]radialene **174** through reaction with MeLi.

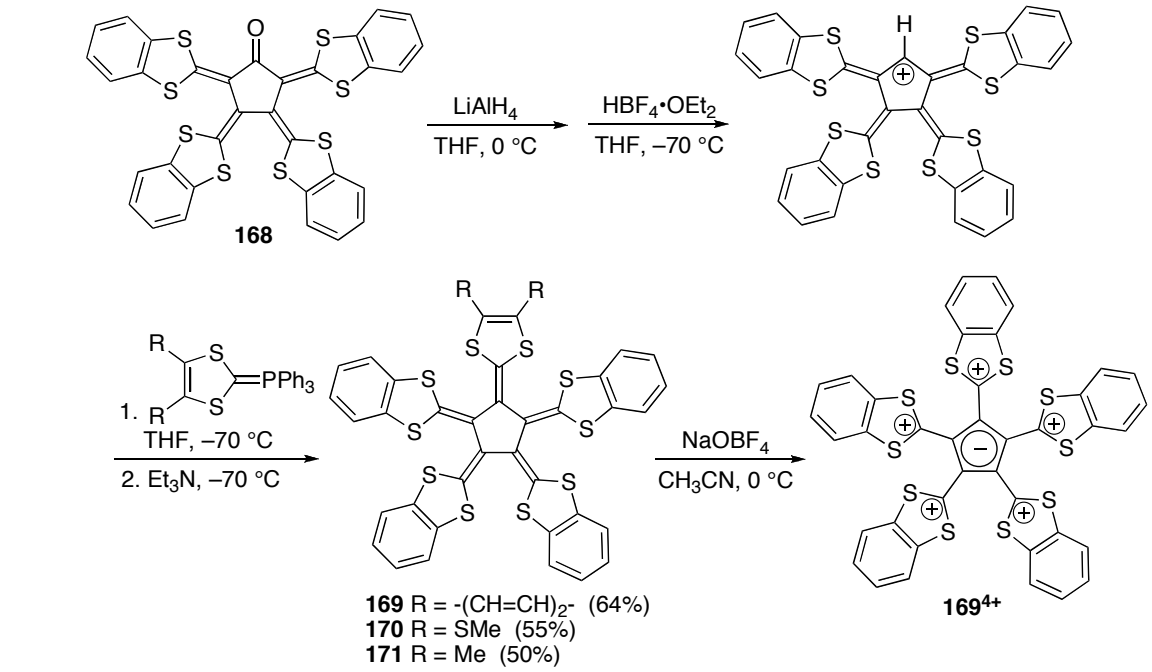

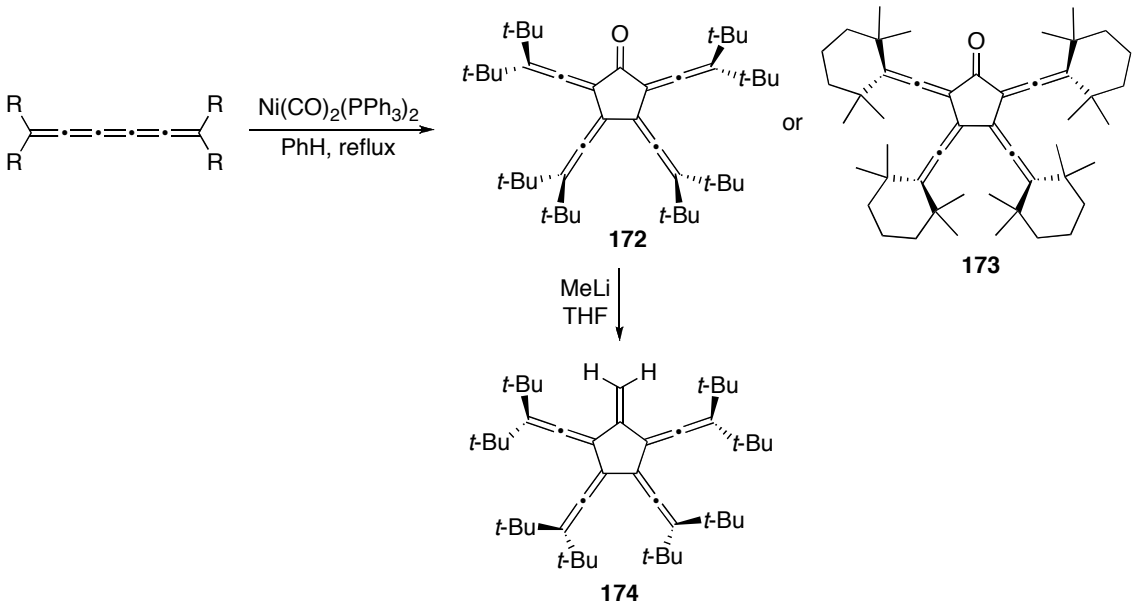

Scheme 1.23 Synthesis of [5]radialenes and their derivatives

1.3.4 [6]Radialenes

After over 40 years, the original synthesis of [6]radialene **137** (Scheme **1.14**) was revisited by Hopf and coworkers.[59] It became clear that the synthesis of **137** produced up to five other diastereomers according to GC/MS analysis, and one of these isomers could be separated using preparative thin layer chromatography (Scheme **1.24**).[59a] Analysis by NMR spectroscopy identified the byproduct as most likely ***cccaca*-137** over the other possibilities of ***ccccca*-137** and ***ccccaa*-137**. Hopf and co-workers have also recently reported the X-ray crystal structure of [6]radialene **175** which revealed that derivative adopted a chair conformation with a structure quite close to that reported for the hexamethyl analogue **137**.[59b]

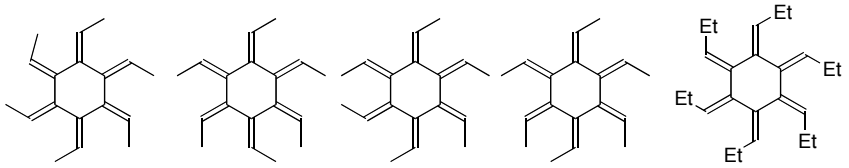

137 ***cccaca*-137** ***ccccca*-137** ***ccccaa*-137** **175**

Scheme 1.24 [6]radialene isomer series

Stanger and co-workers have synthesized the hexabromo[6]radialene **176** and its valence isomer **177** in a 2:3 ratio using a Ni-catalyst (Scheme **1.25**).[60] Heat or radical impurities cleanly transformed **176** into **177**. X-ray single-crystal analysis confirmed that this [6]radialene also adopted a chair conformation, while the core of **177** was planar.

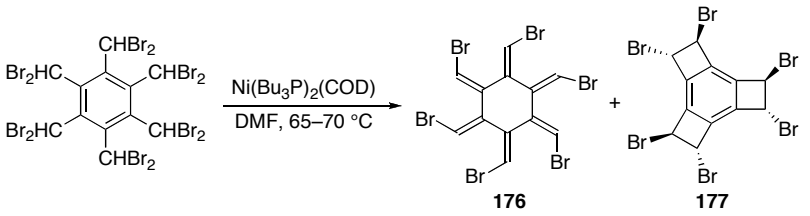

Scheme 1.25 Synthesis of a [6]radialene and its isomer

Very recently, the synthesis of planar [6]radialenes was reported by Bendikov and co-workers.[61] Compounds **180** and **181** were prepared according to Scheme **1.26**, when $Ni(COD)_2$ reacted with either **178** or **179** in the presence of 1,5-cyclooctadiene in DMF at 70 °C. **180** and **181** were characterized fully, including the solid-state structure. According to X-ray data, both compounds were shown to be planar with D_{3h} symmetry. Based on NICS (nucleus-independent chemical shifts, a calculation based on the functional density method, at B3LYP/6-31G(d)//B3LYP/6-31G(d) level)[61] calculations, compounds **180** and **181** are non-aromatic while all the carbons are sp^2 hybridized and the radialenes are planar (**182** and **183** were known prior to this synthesis).

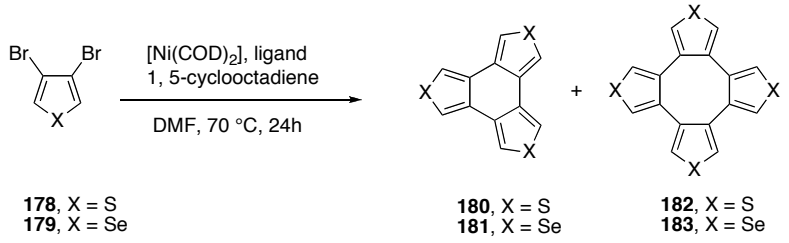

Scheme 1.26 Synthesis of planar [6]– and [8]radialenes

1.4 First generation of expanded radialenes and related derivatives

"Expanded radialenes" is the general term given to the cyclic compounds that originate by formal insertion of an unsaturated spacer between each pair of exo-methylene fragments in the cyclic framework of a radialene (Scheme **1.27**). This field was initiated in early 1990 and interest in radialenes and expanded radialenes has been growing steadily for years. This is not only for synthetic reasons (development of new preparative methods) but also because of structural and theoretical interest because radialenes are important reference structures in the developments of computational methods.[3] Radialenes carrying polarizing substituents are interesting substrates in materials science. The formation of expanded radialenes was pioneered by Diederich in 1994 via the insertion of a diacetylene moiety into the radialene framework. This general concept has been subsequently extended to encompass acetylene linkers, as well as hybrid radialenes with aryl moieties, heteroatoms, and transition metals introduced into the radialene core. (Scheme **1.27**)

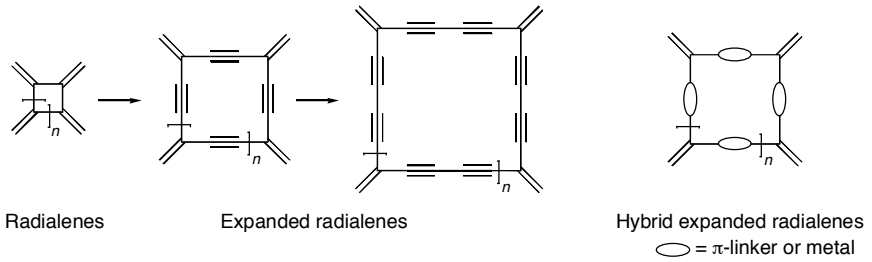

Scheme 1.27 Expanded radialenes

Expanded [4]–, [5]–, and [6]radialenes with diacetylene spacers were the first expanded radialenes to be reported and were introduced by Diederich and

co-workers in 1994 (Scheme **1.28**).[62-64] The even-numbered members of this series of expanded radialenes **(185a** and **185c)** resulted from oxidative coupling of a TEE dimer **184**. The odd-numbered expanded [5]radialene **185b** (Scheme **1.28**) required a somewhat more elaborate building block, trimeric **186**, which was then combined with dimer **184** under oxidative coupling conditions. The macrocycles **185a**–**c** were highly stable and yellow in color, despite the high degree of unsaturation. Based on UV-vis absorption analysis and AM1 calculations, there was little evidence for strong macrocyclic cross conjugation, which could be rationalized by the steric repulsion of the bulky TIPS groups that caused the macrocycles to adopt a nonplanar conformation particularly for hexameric **185c**. In addition to the bis(*tert*-butyl)aryl radialenes **187a-c (**Scheme **1.29**), the synthesis of donor end-capped expanded radialenes **188** has been reported via oxidative homocoupling reactions of the appropriate TEE precursor (Scheme **1.29**).[28,65] Amine end-capped expanded radialenes **188a**–**d** showed low-energy absorptions (λ_{max} = 609–646 nm) consistent with increased macrocyclic cross conjugation in these systems and also these derivatives showed large third-order nonlinear optical coefficients. The addition of mesogenic groups was accomplished as well, albeit the resulting radialenes **189** did not display good liquid crystalline properties.[28] Structure-function relationships for radialenes **185**, **187**, and **188** have been thoroughly explored with respect to their cross-conjugated core, particularly by UV-vis spectroscopy and electrochemical analysis. These studies confirmed the ability of the cyclic radialene core to act as

a better electron acceptor than acyclic analogues. Theoretical analysis of similar expanded radialenes has also been reported.[62,66]

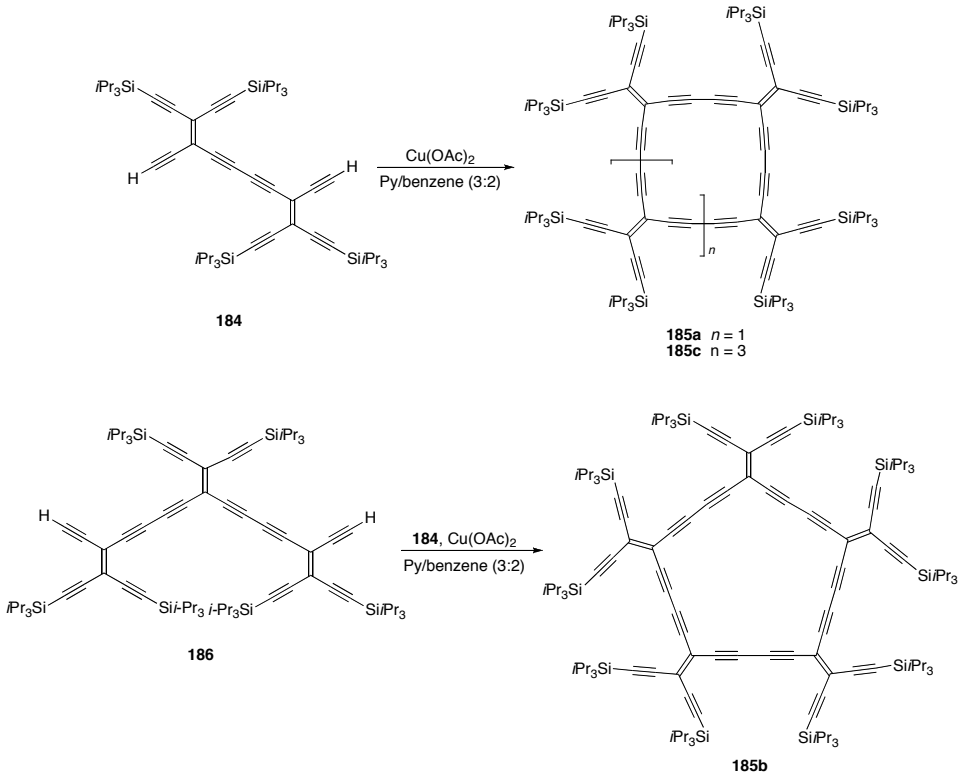

Scheme 1.28 Synthesis of the first expanded radialene series

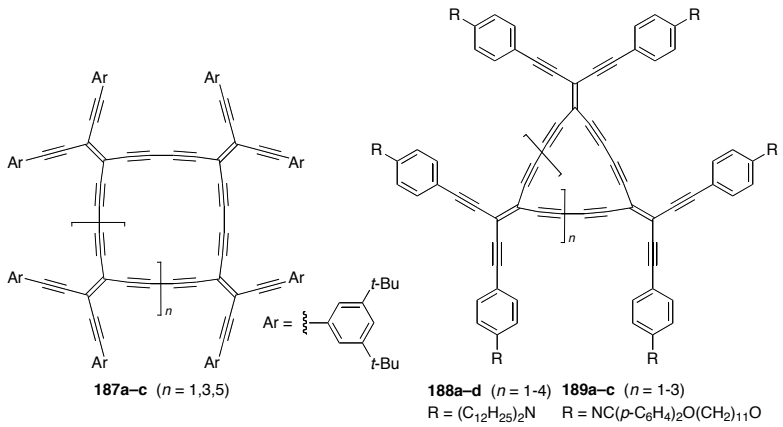

Scheme 1.29 Synthesis of functional expanded radialenes

Following the same one-pot approach established by Diederich, Tobe and

co-workers synthesized expanded radialenes **191a–d** (as a mixture of diastereomers) via the oxidative coupling of enediyne **190** (Scheme **1.30**).[67] UV-vis spectroscopic analysis of **191a–d** revealed that the smallest macrocycle **191a** (n = 1) showed the lowest energy absorption (λ_{max} = 344 nm), as well as the smallest molar absorptivity, in agreement with what is known for other radialenes of similar structure.[28,65] Expanded radialenes **191a-d** were then used as precursors to the cyclo[n]-carbons. [67]

Zhang and co-workers reported in the presence of a Ni-catalyst the one-pot synthesis of an expanded 1,3-dithiolane[5]radialene **193** from enediyne **192** (Scheme **1.31**).[68] Interesting was the fact that the use of the typical Cu-catalyzed homocoupling conditions was ineffective in the case of **193** → **192** and that reaction of dimer **194** (toward formation of the even-numbered analogues n = 0, 2, 4, ...) under the Ni-catalysis conditions was not successful. The UV-vis spectrum of **193** (λ_{max} = 443 nm) showed a slight bathochromic shift relative to that of **194** (λ_{max} = 421 nm). The shift was explained by the presence of macrocyclic cross conjugation, consistent with that reported by Diederich for electron-rich [5]radialene **188c**.[28] X-ray crystallography confirmed that the macrocycle **193** adopted a nonplanar, envelope conformation.

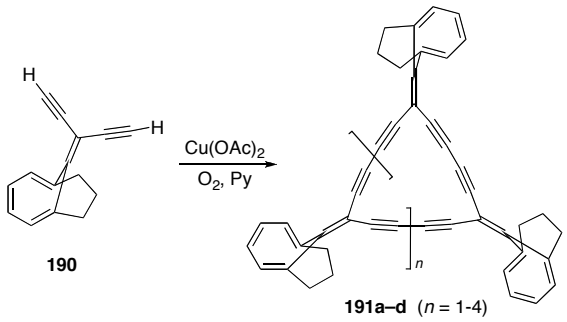

Scheme 1.30 Synthesis of expanded radialene series

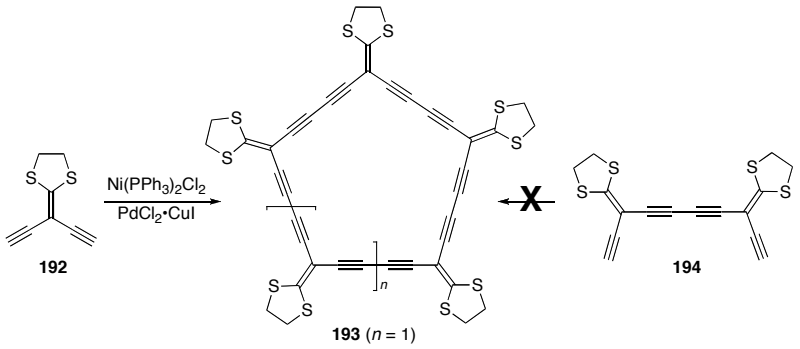

Scheme 1.31 Synthesis of **[5]**expanded radialene

Expanded radialenes have been formed based on the oxidative coupling of **195**, giving a mixture of the dimer **196** and trimer **197** (Scheme **1.32**).[69] Whereas **197** could be isolated and characterized, **196** was only detected by MS analysis. Radialene **197** contains a small cavity (2.6 Å) and formed a complex with either $AgOCOCF_3$ or $AgClO_4$, as characterized by ^1H NMR spectroscopy and MALDI- TOF MS analysis.

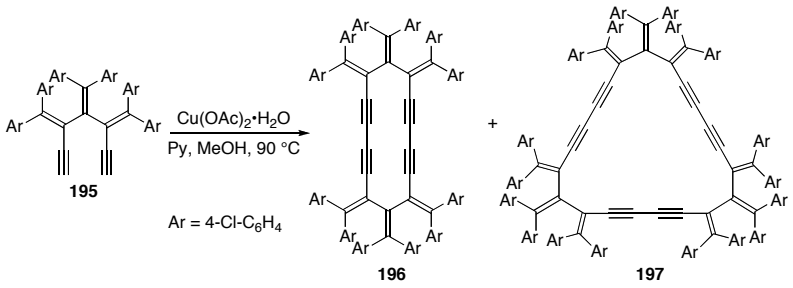

Scheme 1.32 Synthesis of hybrid expanded radialenes

1.5 Radiaannulenes

Diederich and co-workers developed a hybrid series of cross-conjugated macrocycles that marry the attributes of traditional annulenes with those of expanded radialenes, and christened them radiaannulenes (Scheme **1.33**).[70,71]

The first derivatives were formed from the corresponding trimeric TEE precursor via desilylation and intramolecular oxidative coupling to close the cycle at the bond shown in bold. Electrochemical analysis showed that the acetylenic cores of these molecules are powerful electron acceptors, and, in combination with peripheral donor and/or acceptor groups, intense intramolecular charge transfer results. Bicyclic radiaannulenes **199a** and **199b** were synthesized from a pentameric TEE precursor via an oxidative homocoupling reaction.[70,71]

Radiaannulene **199a** showed a remarkably low first reduction potential at – 0.81 V (vs. to Fc/Fc^+), making it a better electron acceptor than even C_{60} (under comparable conditions). The electronic absorption spectrum of **199b** confirmed a very strong intramolecular charge transfer with a lowest energy end-absorption at 850 nm, the lowest ever reported for a macrocyclic TEE derivative.

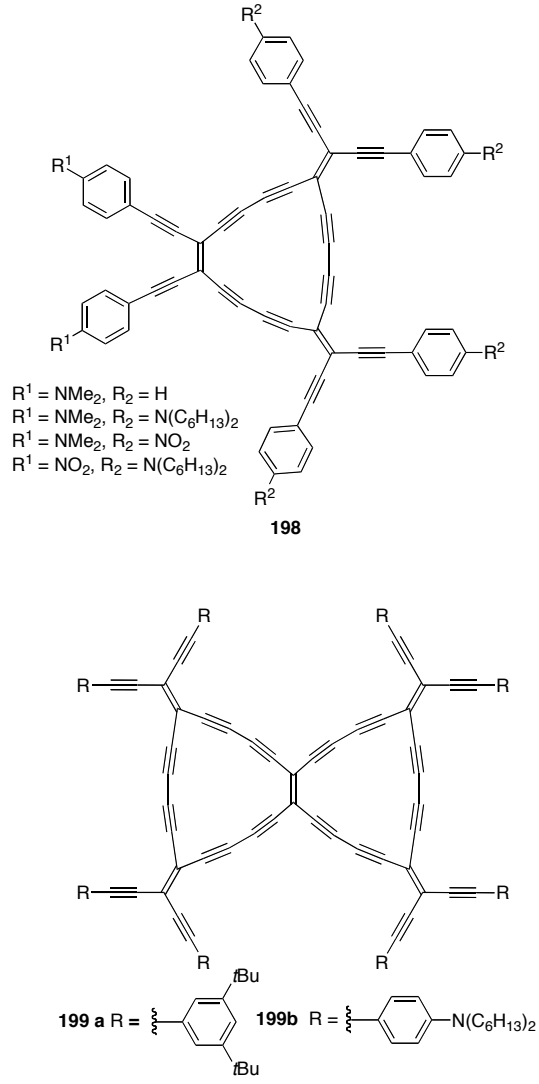

Scheme 1.33 Functional radiaannulenes

Diederich and co-workers synthesized the unique hybrid radialene **1102** by heating **1101** to 120 °C in *o*-dichlorobenzene in the presence of a catalytic amount of HI (Scheme **1.34**).[72] The highly strained, diastereomeric products were isolated as an inseparable 2:1 mixture that showed surprisingly high kinetic and thermal stability. The structure of **1102** could only be elucidated by X-ray analysis, which showed that the internal bond angles about the sp-hybridized carbons were significantly bent (157.4°) from the optimum of 180°.

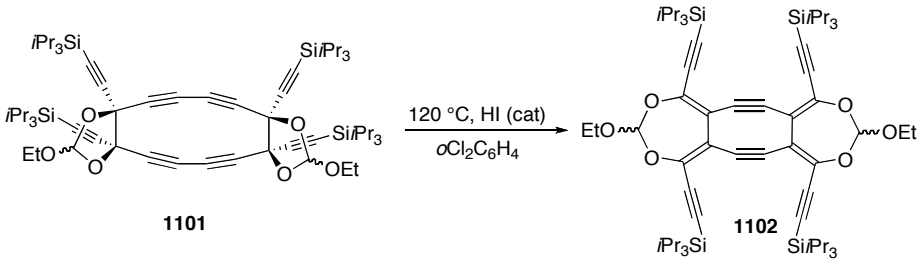

1101 **1102**

Scheme 1.34 Synthesis of hybrid expanded radialene

1.6 Second generation of expanded radialenes and related derivatives

The first example of an expanded radialene based on insertion of a single acetylene unit into the radialene skeleton (the second generation of expanded radialenes), was reported in 1999 (while in the first generation was developed before 1999) (Scheme **1.35**).[14] Sonogashira cross-coupling reaction of *iso*-PDA pentamer **1103** with a dibromoolefin **1104**, afforded radialene **1105**. Compound **1106** was also formed as a result of oxidative homocoupling of the *iso*-polydiacetylene moiety. A UV-vis spectroscopic comparison between **1103** and **1105** suggested that virtually the same extent of π--delocalization was present in each of the two molecules, that is, no evidence of macrocyclic cross conjugation was observed. A larger cousin of **1106**, radialene **1108**, was formed as a byproduct during the elongation of *iso*-PDA **1107**, likely due to the high dilution conditions used in the reaction that favored an intramolecular reaction (Scheme **1.36**).[13] Expanded radialene **1108** could be synthesized deliberately via the oxidative homocoupling of **1107** using the Hay catalyst in dry acetone. Iyoda and co-workers synthesized π-extended radialenes **1109a-b** from **195** using the

Sonogashira coupling protocol with *p*-diiodobenzene (Scheme **1.37**).[69] These macrocycles have calculated cavities with free space diameters of 5.4 and 9.1 Å, respectively, and hence were too large to form complexes with small cations such as Ag(I).

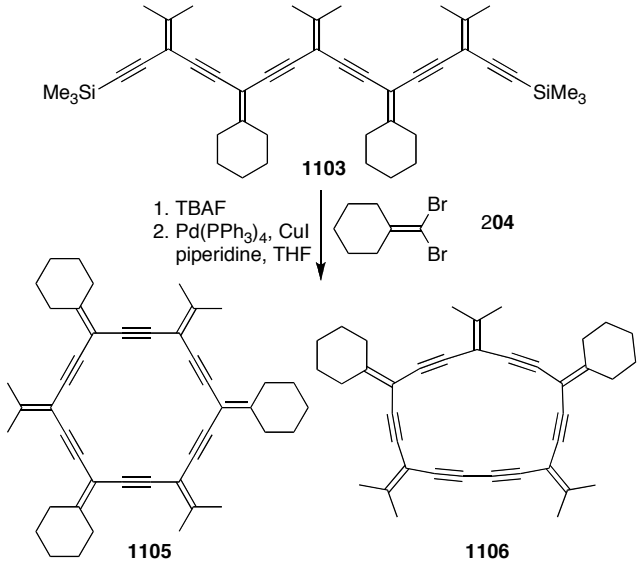

Scheme 1.35 First synthesis of second generation of expanded radialene

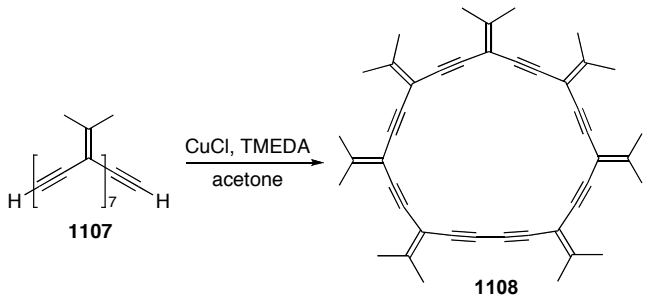

Scheme 1.36 Synthesis of a hybrid expanded radialene

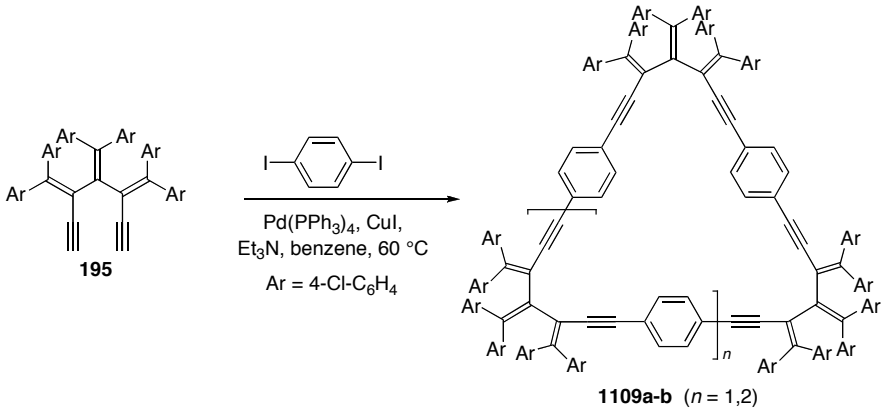

Scheme 1.37 Synthesis of hybrid expanded radialenes with 1,4-diethynylphenyl spacer

1.7 Potential applications of cross-conjugated skeletons

The radialenes that have been discussed in this chapter were tested for conductivity and magnetic properties however the results for these compounds were not promising and consequently the synthetic chemist had to re-evaluate the design of these compounds.[3] The synthesis of first generation of the expanded radialenes was one of the successful designs in terms of structural design and related properties. The physical studies of this series in particular with regards to NLO properties such as third-harmonic generation (THG) measurements were performed and the second hyperpolarizabilities γ obtained. For example, the introduction of donor or donor and acceptor groups led to an increase in the second hyperpolarizability.[28]

Also Tykwinski and coworkers performed the NLO studies for *iso*-polydiacetylene series. The main reason for NLO investigation was that the *iso*-polydiacetylene series have potential application as third-order NLO materials.

This is due to significant optical transparency of the *iso*-polydiacetylene series. Differential optical Kerr effect (DOKE) experiments obtained information with regards to NLO properties.[15] For example molecular second hyperpolarizabilities, γ_s, give a super-liners increase as a function of the *iso*-polydiacetylene chain length. Furthermore. Tykwinski and coworkers showed a relationship between structure and properties in third-order nonlinear optical chromophores. Their findings was that low symmetry and two-dimensional conjugation are likely the two most powerful tools for optimizing the second hyperpolarizability γ in small molecules.[73] It should be investigated whether such finding is applicable to larger molecules like the expanded radialenes.

In a bigger picture the expanded radialenes could be used for electronic materials due to the presence of the cross-conjugated π system. Such applications could be varied. They could be used in electronic circuits, transducers, memory micro-technology, displays, superconductors and optoelectronics.[74]

Further potential applications of the expanded radialenes may be in connection with their solid states. Their organized self assembly may produce channels or porous with right size for selective interactions and absorption of different compounds in solid or liquid phases like zeolites.[75]

1.8 Conclusion

The above brief historical review shows the fascination of the organic chemists with the cross-conjugated frameworks such as radialenes and

expanded radialenes not only in terms of their potential applications in materials science but also developing new synthetic methodologies for efficient syntheses that will be addressed and discussed more deeply through this thesis.

1.9 References

(1) (a) Meier, H. *Angew. Chem. Int. Ed.* **2005**, *44*, 2482-2506; (b) Martin, R. E.; Diederich, F. *Angew. Chem. Int. Ed.* **1999**, *38*, 1350–1377.

(2) (a) Klokkenburg, M.; Lutz, M.; Spek, A. L.; van der Maas, J. H.; van Walree, C. A. *Chem. Eur. J.* **2003**, *9*, 3544–3554; (b) Bryce, M. R.; Coffin, M.A.; Skabara, P. J. Moore, A. J.; Batsanov, A. S.; Howard, J. A. K. *Chem. Eur. J.* **2000**, *6*, 1955–1962; (c) Phelan, N. F.; Orchin, M. *J. Chem. Educ.* **1968**, *45*, 633–637.

(3) Hopf, H. *Classics in Hydrocarbon Chemistry*; Wiley-VCH, New York, **2000**, chapter 11.

(4) Suzuki, T.; Higuchi, H.; Ohkita, M.; Tsuji, T. *Chem. Commun.* **2001**, 1574–1575.

(5) Yamamoto, T.; Yasuda, T.; Kobayashi, K.; Yamaguchi, I.; Koizumi, T.; Ishii, D.; Nakagawa, M.; Mashiko, Y.; Shimizu, N. *Bull. Chem. Soc. Jpn.* **2006**, *79*, 498–500.

(6) Ikeda, Z.; Oshima, K.; Matsubara, S. *Org. Lett.* **2005**, *7*, 4859–4861.

(7) Halton, B.; Jones, C. S. *Eur. J. Org. Chem.* **2004**, 138–146.

(8) Gleiter, R.; Röckel, H.; Irngartinger, H.; Oeser, T. *Angew. Chem. Int. Ed. Engl.* **1994**, *33*, 1270–1272.

(9) Suzuki, N.; Tezuka, H.; Fukuda, Y.; Yoshida, H.; Iwasaki, M.; Saburi, M.; Tezuka, M.; Chihara, T.; Wakatsuki, Y. *Chem. Lett.* **2004**, *33*, 1466–1467.

(10) Fielder, S.; Rowan, D. D.; Sherburn, M. S. *Angew. Chem. Int. Ed.* **2000**, *39*, 4331–4333.

(11) Tykwinski, R. R.; Zhao, Y. *Synlett* **2002**, 1939–1953.

(12) Zhao, Y.; Tykwinski, R. R. *J. Am. Chem. Soc.* **1999**, *121*, 458–459.

(13) Zhao, Y.; Campbell, K.; Tykwinski, R. R. *J. Org. Chem.* **2002**, *67*, 336–344.

(14) Eisler, S.; Tykwinski, R. R. *Angew. Chem. Int. Ed.* **1999**, *38*, 1940–1943.

(15) Zhao, Y.; Slepkov, A. D.; Akoto, C. O.; McDonald, R.; Hegmann, F. A.; Tykwinski, R. R. *Chem. Eur. J.* **2005**, *11*, 321–329.

(16) Slepkov, A. D.; Hegmann, F. A.; Zhao, Y.; Tykwinski, R. R.; Kamada, K. *J. Chem. Phys.* **2002**, *116*, 3834–3840.

(17) Slepkov, A. D.; Hegmann, F. A.; Kamada, K.; Zhao, Y.; Tykwinski, R. R. *J. Opt. A: Pure Appl. Opt.* **2002**, *4*, S207–S211.

(18) Ciulei, S. C.; Tykwinski, R. R. *Org. Lett.* **2000**, *2*, 3607–3610.

(19) Boldi, A. M.; Anthony, J.; Gramlich, V.; Knobler, C. B.; Boudon, C.; Gisselbrecht, J. P.; Gross, M.; Diederich, F. *Helv. Chim. Acta* **1995**, *78*, 779–796.

(20) Zhao, Y.; McDonald, R.; Tykwinski, R. R. *Chem. Commun.* **2000**, 77–78.

(21) Zhao, Y.; McDonald, R.; Tykwinski, R. R. *J. Org. Chem.* **2002**, *67*, 2805–2812.

(22) Burri, E.; Diederich, F.; Nielsen, M. B. *Helv. Chim. Acta* **2002**, *85*, 2169–2182.

(23) (a) Solomon, G. C; Andrews, D. Q.; Goldsmith, R. H.; Hansen, T. Wasielewski, M. R.; Van Duyne, R. P.; Ratner, M. A. *J. Am. Chem. Soc.* **2008**, *130*, 17301–17308; (b) Brüschi, M.; Giuffreda, M. G.; Lüthi, H. P. *Chem. Phys. Chem.* **2005**, *6*, 511–519.
(24) Bruschi, M.; Giuffreda, M. G.; Lüthi, H. P. *Chem. Eur. J.* **2002**, *8*, 4216–4227.
(25) Eisler, S.; Slepkov, A. D.; Elliott, E.; Luu, T.; McDonald, R.; Hegmann, F. A.; Tykwinski, R. R. *J. Am. Chem. Soc.* **2005**, *127*, 2666–2676.
(26) Luu, T.; Elliott, E.; Slepkov, A. D.; Eisler, S.; McDonald, R.; Hegmann, F. A.; Tykwinski, R. R. *Org. Lett.* **2005**, *7*, 51–54.
(27) Zhao, Y.; Ciulei, S. C.; Tykwinski, R. R. *Tetrahedron Lett.* **2001**, *42*, 7721–7723.
(28) Nielsen, M. B.; Schreiber, M.; Baek, Y. G.; Seiler, P.; Lecomte, S.; Boudon, C.; Tykwinski, R. R.; Gisselbrecht, J. P.; Gramlich, V.; Skinner, P. J.; Bosshard, C.; Gunter, P.; Gross, M.; Diederich, F. *Chem. Eur. J.* **2001**, *7*, 3263–3280.
(29) Moonen, N. N. P.; Pomerantz, W. C.; Gist, R.; Boudon, C.; Gisselbrecht, J. P.; Kawai, T.; Kishioka, A.; Gross, M.; Irie, M.; Diederich, F. *Chem. Eur. J.* **2005**, *11*, 3325–3341.
(30) Ito, S.; Inabe, H.; Morita, N.; Tajiri, A. *Eur. J. Org. Chem.* **2004**, 1774–1780.
(31) Weltin, E.; Gerson, F.; Heilbronn, E.; Murrell, J. N. *Helv. Chim. Acta* **1961**, *44*, 1400–1413.
(32) Hopf, H.; Maas, G. *Angew. Chem. Int. Ed. Engl.* **1992**, *31*, 931–954.
(33) Gholami, M.; Tykwinski, R. R. *Chem. Rev*. **2006**, *106*, 4997–5027.
(34) Hopff, H.; Wick, A. K. *Helv. Chim. Acta* **1961**, *44*, 19–24.
(35) Kobrich, G.; Heineman, H. *Angew. Chem. Int. Ed.* **1965**, *4*, 594–595.
(36) Dorko, E. A. *J. Am. Chem. Soc.* **1965**, *87*, 5518–5520.
(37) Waitkus, P. A.; Sanders, E. B.; Peterson, L. I.; Griffin, G. W. *J. Am. Chem. Soc.* **1967**, *89*, 6318–6327;
(38) Griffin, G. W.; Peterson, L. I. *J. Am. Chem. Soc.* **1962**, *84*, 3398–3400.
(39) Iyoda, M.; Otani, H.; Oda, M.; Kai, Y.; Baba, Y.; Kasai, N. *J. Chem. Soc., Chem. Commun.* **1986**, 1794–1796.
(40) Fukunaga, T. *J. Am. Chem. Soc.* **1976**, *98*, 610–611.
(41) Lange, T.; Gramlich, V.; Amrein, W.; Diederich, F.; Gross, M.; Boudon, C.; Gisselbrecht, J. P. *Angew. Chem. Int. Ed. Engl.* **1995**, *34*, 805–809.
(42) Dunitz, J. D.; Mugnoli, A. *Helv. Chim. Acta* **1966**, *49*, 1680–1681.
(43) Dorko, E. A.; Hencher, J. L.; Bauer, S. H. *Tetrahedron* **1968**, *24*, 2425–2434.
(44) Dietrich, H.; Dierks, H. *Angew. Chem. Int. Ed.* **1968**, *7*, 465–465.
(45) Enomoto, T.; Nishigaki, N.; Kurata, H.; Kawase, T.; Oda, M. *Bull. Chem. Soc. Jpn.* **2000**, *73*, 2109–2114.
(46) Enomoto, T.; Kawase, T.; Kurata, H.; Oda, M. *Tetrahedron Lett.* **1997**, *38*, 2693–2696.

(47) Matsumoto, K.; Harada, Y.; Kawase, T.; Oda, M. *Chem. Commun.* **2002**, 324–325.
(48) Steel, P. J.; Sumby, C. J. *Chem. Commun.* **2002**, 322–323.
(49) Steel, P. J.; Sumby, C. J. *Inorg. Chem. Commun.* **2002**, *5*, 323–327.
(50) Uno, H.; Nibu, N.; Misobe, N. *Bull. Chem. Soc. Jpn.* **1999**, *72*, 1365–1375.
(51) Uno, H.; Kasahara, K.; Nibu, N.; Nagaoka, S.; Ono, N. *J. Org. Chem.* **2000**, *65*, 1615–1622.
(52) Iyoda, M.; Kuwatani, Y.; Oda, M. *J. Am. Chem. Soc.* **1989**, *111*, 3761–3762.
(53) Kuwatani, Y.; Yamamoto, G.; Oda, M.; Iyoda, M. *Bull. Chem. Soc. Jpn.* **2005**, *78*, 2188–2208.
(54) Kuwatani, Y.; Yamamoto, G.; Iyoda, M. *Org. Lett.* **2003**, *5*, 3371–3374.
(55) Matsuo, T.; Fure, H.; Sekiguchi, A. *Chem. Lett.* **1998**, 1101–1102.
(56) Matsuo, T.; Fure, H.; Sekiguchi, A. *Chem. Commun.* **1999**, 1981–1982.
(57) Matsuo, T.; Fure, H.; Sekiguchi, A. *Bull. Chem. Soc. Jpn.* **2000**, *73*, 2129–2137.
(58) Kano, K.; Sugimoto, T.; Misaki, Y.; Enoki, T.; Hatakeyama, H.; Oka, H.; Hosotani, Y.; Yoshida, Z. *J. Phys. Chem.* **1994**, *98*, 252–258.
(59) Höpfner, T.; Jones, P. G.; Ahrens, B.; Dix, I.; Ernst, L.; Hopf, H. *Eur. J. Org. Chem*. **2003**, 2596–2611; (B) Jones, P. G.; Bubenitschek, P.; Hopfner, T.; Hopf, H. *Acta Crystallogr., Sect. C* **1997**, *53*, 920–921.
(60) Stanger, A.; Ashkenazi, N.; Boese, R.; Bläser, D.; Stellberg, P. *Chem. Eur. J.* **1997**, *3*, 208–211.
(61) Patra, A.; Wijsboom, Y. H.; Shimon, L. J. W.; Bendikov, M. *Angew. Chem. Int. Ed.* **2007***, 46,* 8814–8818.
(62) Nielsen, M. B.; Diederich, F. *Chem. Rev.* **2005**, *105*, 1837–1867.
(63) Boldi, A. M.; Diederich, F. *Angew. Chem. Int. Ed. Engl.* **1994**, *33*, 468–471.
(64) Anthony, J.; Boldi, A. M.; Boudon, C.; Gisselbrecht, J. P.; Gross, M.; Seiler, P.; Knobler, C. B.; Diederich, F. *Helv. Chim. Acta* **1995**, *78*, 797–817.
(65) Schreiber, M.; Tykwinski, R. R.; Diederich, F.; Spreiter, R.; Gubler, U.; Bosshard, C.; Poberaj, I.; Gunter, P.; Boudon, C.; Gisselbrecht, J. P.; Gross, M.; Jonas, U.; Ringsdorf, H. *Adv. Mater.* **1997**, *9*, 339–343.
(66) Gisselbrecht, J. P.; Moonen, N. N. P.; Boudon, C.; Nielsen, M. B.; Diederich, F.; Gross, M. *Eur. J. Org. Chem.* **2004**, 2959–2972.
(67) Tobe, Y.; Umeda, R.; Iwasa, N.; Sonoda, M. *Chem. Eur. J.* **2003**, *9*, 5549–5559.
(68) Zhao, Y.-L.; Liu, Q.; Zhang, J.-P.; Liu, Z.-Q. *J. Org. Chem.* **2005**, *70*, 6913–6917.
(69) Iyoda, M.; Kuwatani, Y.; Yamagata, S.; Nakamura, N.; Todaka, M.; Yamamoto, G. *Org. Lett.* **2004**, *6*, 4667–4670.
(70) Mitzel, F.; Boudon, C.; Gisselbrecht, J. P.; Seiler, P.; Gross, M.; Diederich, F. *Helv. Chim. Acta* **2004**, *87*, 1130–1157.

(71) Mitzel, F.; Boudon, C.; Gisselbrecht, J. P.; Seiler, P.; Gross, M.; Diederich, F. *Chem. Commun.* **2003**, 1634–1635.
(72) Kammermeier, S.; Tykwinski, R. R.; Siemsen, P.; Seiler, P.; Diederich, F. *Chem. Commun.* **1998**, 1285–1286.
(73) Tykwinski, R. R.; Gubler, U.; Martin, R. E.; Diederich, F.; Bosshard, C.; Günter, P. *J. Phys. Chem. B* **1998**, *102*, 4451–4465.
(74) Braithwaite, N.; Weaver, G. *Electronic Materials*; The Open University: Milton Keynes, United Kingdom, **1998**.
(75) Campbell, K.; Ooms, K. J.; Wasylishen, R. E.; Tykwinski, R. R. *Org. Lett.* **2005**, *7*, 3397–3400.

Chapter 2:

Cyclic and Acyclic Skeletons Containing Metals

2.1 Cyclic conjugated and cross-conjugated skeletons containing metal center(s)

It is not surprising that there are no examples of inorganic or organometallic derivatives of the expanded radialenes available in the literature. The field of expanded radialenes is relatively young and derivatives that were previously synthesized are not particularly suitable for interaction(s) with metals in terms of their geometry and cavity size (Scheme **2.1**).[1-4] Also, it was not the intention of these researchers to synthesize expanded radialenes for use in inorganic and organometallic chemistry. Nevertheless, a series of conjugated cyclic compounds that are similar in terms of skeleton and proximity of alkyne units to expanded radialenes will be discussed in this chapter.

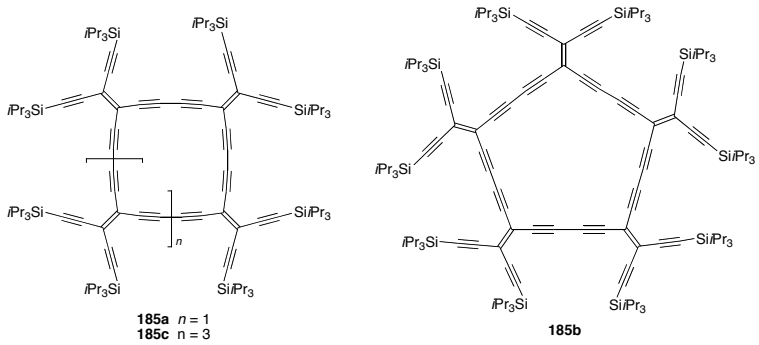

Scheme 2.1 Representative expanded radialene with unsuitable cavities

There are several examples of cyclic conjugated or cross-conjugated systems categorized as hybrids of the expanded radialenes that incorporate metal fragments as σ-acetylide linkages. Such hybrid expanded radialenes will also be discussed later in this chapter. In addition cobalt-mediated organic transformations, alkyne coordination with the group X transition metals at zero

oxidation state, titanium radialene, and platinum acetylide polymers are also considered in this chapter. The objective is to touch on some of the most relevant inorganic and organometallic chemistry to provide a basis for our exploratory study of expanded radialenes in Chapter **6**.

2.2 Cyclynes and their reactions with transition metals

A cyclyne is defined as any ring of atoms having one or more alkyne units.[5,6] Dehyroannulenes are a subset of cyclynes and are formed by dehydrogenating a ring of conjugated carbon-carbon double bonds (annulenes) (Scheme **2.2**).[7]

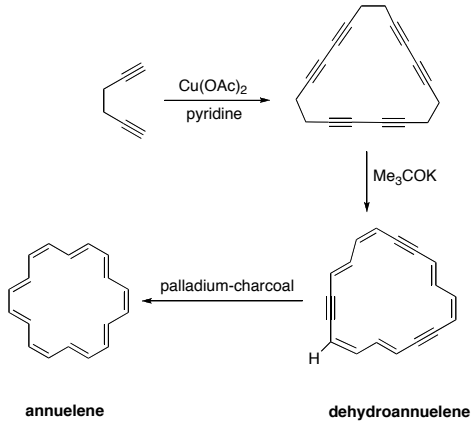

Scheme 2.2 Synthesis of an [18]annulene

Examples of cyclynes is compound **200a** (tribenzocyclyne or 1,2:5,6:9,10-tribenzocyclododeca-1,5,9-triene-3,7,-11-triyne) and its related derivatives, and their synthesis is outlined in Scheme **2.3**.[8,9] Structural features that allow such compounds to bind metals include planarity, the presence of an extended π-system, and, more importantly, the absence of any charge(s). These features allow cyclotriynes to bind a metal via three soft, polarizable alkyne donors.

Therefore, the organometallic chemistry of cyclotriynes might aid the design and predict the organometallic chemistry of expanded radialenes. The significant contributions of Youngs and co-workers including the reactions of cyclotriynes with suitable metallic-precursors such as $Ni(COD)_2$, $Co_2(CO)_8$, and $Cu_2(C_6H_6)(OTf)_2$ are discussed in this chapter.

Cyclynes such as **200a** are planar,[10-12] antiaromatic, conjugated molecules that have a suitable cavity to bind low-oxidation-state, first row[13,14] transition metals (the distance from the center of the cavity to the center of an alkyne is about 2.08 Å for **200a**). Also, these cyclynes are potential candidates for one-dimensional conductors[15-18] due to suitable stacking in their solid structures.

Compound **200a** reacts with $Ni(COD)_2$ in benzene to form a complex (**200c**) in which three alkynes are coordinated to Ni in an η^2-fashion (Scheme **2.4**). According to solid-state structural analysis, the nickel atom is located above the centre of the planar cyclotriyne (about 0.34 Å) with the average nickel to alkyne carbon distance being 1.958(5) Å.[19a,d]

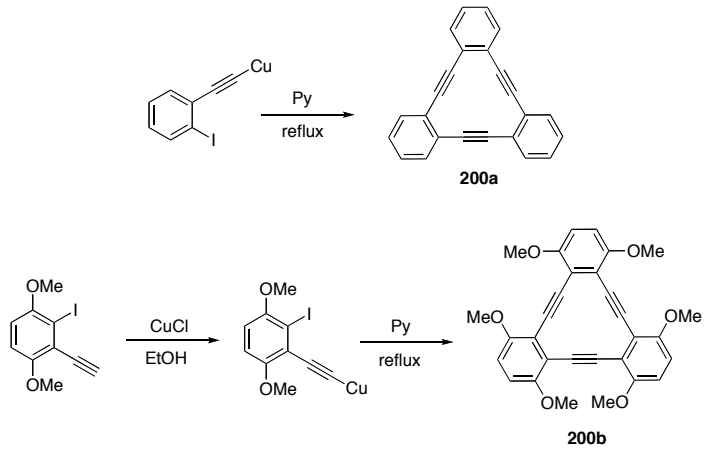

Scheme 2.3 Synthesis of cyclynes and functional cyclynes

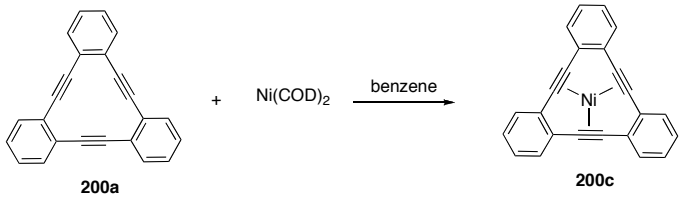

Scheme 2.4 Synthesis of a nickel cyclyne

Complex **200c** is a 16-electron complex because each alkyne donates two electrons and Ni(0) has 10 electrons. X-ray crystallography data confirms the geometry of compound **200c** and shows a distortion of about 6.2° from linear alkyne bond angle (180° natural angle of the alkyne). ^{13}C NMR spectroscopy revealed that the alkyne carbon signals are shifted downfield from 93.6 to 109.6 ppm and infrared spectroscopy showed the stretching frequency of the alkyne unit is shifted from 2208 to 1955 cm^{-1} upon complex formation. The evidence from ^{13}C NMR, IR, and X-ray data, and comparison of **200c** to typical four electron donor alkynes, confirms that there is only a limited back-donation of nickel electron density into the π^* orbitals of the alkynes.[19a.c] Cyclic voltammetry of **200c** shows two consecutive quasi-reversible waves at strongly reducing

potentials (no redox potentials reported) suggesting the formation of anion and di-anion. The reduction also was carried out with lithium, sodium or potassium as reducing agent.[19b]

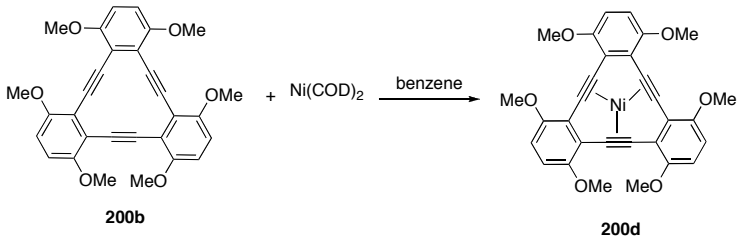

Scheme 2.5 Synthesis of a methoxy-nickel cyclyne

In a parallel concept, compound **200b** reacts in the same manner as compound **200a** with $Ni(COD)_2$, yielding compound **200d** as characterized by X-Ray crystallography (Scheme **2.5**).[20] ^{13}C NMR spectrum of **200d** shows a downfield shift (about 20 ppm) for the alkyne carbons compared to **200b**. This is accompanied by a shift to lower energy in the IR spectrum for the alkyne bond stretch from 2211 to 1968 cm^{-1}. The spectra and the spectral shifts for compound **200d** are comparable to those observed for compound **200a** and its nickel complex, compound **200c**.

The solid-state structure of compound **200d** has an intermolecular hydrogen-bonding interaction (C-H- - -O, from MeO group) and the first reported intermolecular C-H - - -Ni σ-donor interaction; these interactions may explain the differences in packing between **200c** and **200d**. The presence of the methoxy groups in compound **200d** changes the solid-structure packing versus compound **200c**. Youngs and co-workers have also investigated the reaction of cyclotriyne

200a with $Cu_2(C_6H_6)(OTf)_2$ in benzene at room temperature (molar ratio = 2:1, respectively). The X-ray crystallographic data shows that complex **200e** has trigonal pyramidal geometry with Cu(I) coordinated to the three alkyne units; Cu(I) is weakly bound to the oxygen of the triflate anion (Scheme **2.6**).[21] Also, the complex disproportionated to Cu(0) and Cu (II) in THF based on the EPR spectrum.

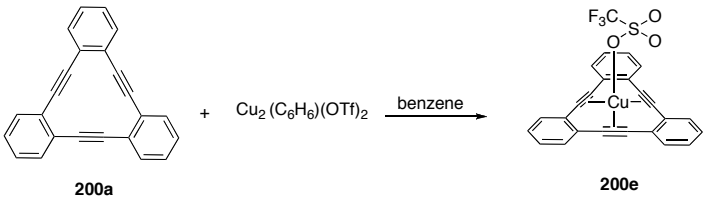

Scheme 2.6 Synthesis of a copper triflate cyclyne complex

The reaction of cyclotriyne **200a** with dicobalt octacarbonyl was also investigated by Youngs and co-workers. Compound **200a** reacted with $Co_2(CO)_8$ in ether to give compound **201**. Compound **201** is a cluster that, according to X-ray crystallography data, contains one cobalt in the cavity of **200a** that is coordinated to three alkyne units. Additionally, there were three cobalt atoms bound to the central cobalt and the alkynes (Scheme **2.7**).[22]

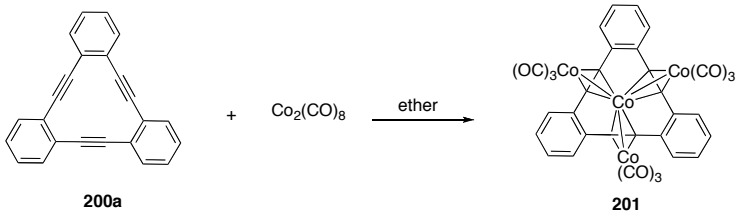

Scheme 2.7 Synthesis of a cobalt cluster cyclyne

Like compound **200a** compound **202** also affords the tetracobalt complex **202a** upon reaction with dicobaltoctacarbonyl (Scheme **2.8**). In the case of compound **202a**, The differences between **200a** and **202** with regard to their reactions with dicobalt octacarbonyl are explained based on differences in pocket sizes according to the solid state structures for compound **200a** and **202**.[23]

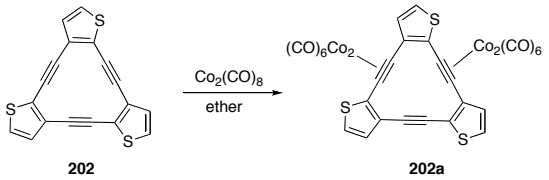

Scheme 2.8 Synthesis of an unsymmetrical cobalt cluster cyclyne

Coordination of alkynes with Ag(I) has been investigated by the reaction of compound **200a** with Ag(OTf) in benzene at room temperature forming complex **203** (Scheme **2.9**).[24]

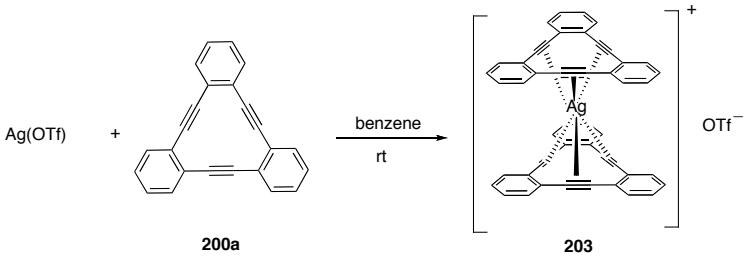

Scheme 2.9 Synthesis of a silver sandwich cyclyne

X-ray crystallography analysis of compound **203** revealed that the Ag(I) was not within the cavity of **200a**. This observation is not surprising because coordination of Ag(I) to the π-system of **200a** results in Ag–C bond lengths larger than the cavity size of **200a** (2.08 Å for the **200a** cavity compared to the range of 2.27–3.10 Å for Ag(I)–(C)alkyne bond length). The Ag(I) is sandwiched between

two macrocycles in both staggered and eclipsed conformations according to X-ray crystallographic data (Figure **2.1**). In the eclipsed conformation, only four of the six alkynes bind tightly to the Ag(I), contributing 8 electrons to the 18-electron complex. In contrast, the staggered conformation has higher symmetry and, formally, each alkyne contributes 1.333 electrons to achieve an 18-electron complex. An infrared spectrum shows two frequency stretches, at 2208 and 2180 cm^{-1}, corresponding to free and complexed alkyne units, respectively. The high energy of the alkyne absorption ($\nu_{C\equiv C}$) at 2180 cm^{-1} indicates a weak bond between the two-electron donor alkyne and Ag(I).[24]

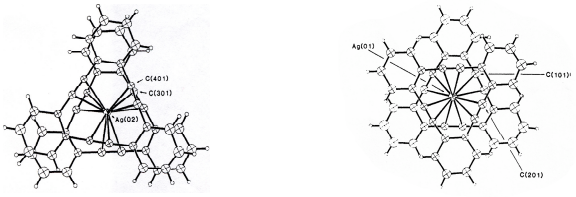

Figure 2.1 Eclipsed and staggered ORTEP plots for compound **203**

Larger annulenes, in particular tetradehydro[16]annulene, shows interesting reactions with Ag(I). Compound **204** reacted with Ag(OTf) or $Ag(SbF_6)$ in THF to form the silver cyclyne **205** (triflate) or **206** (hexafluoroantimonate) complexes (Scheme **2.10**).[25] X-ray crystallographic analysis showed that the Ag–C(alkyne) bond was in a range of 2.714(7)–2.863(7) Å for **205** and 2.52(1) –3.05(2) Å for **206**, comparable to bond lengths observed for the compound **203**, (2.47(2)–2.94(2) Å. Both infrared spectroscopy (alkyne stretch at 2155 cm^{-1} for **205** compared to 2251 and 2173 cm^{-1} for **204**) and ^{13}C NMR spectroscopy (small

shift for alkyne carbon in **205** compared to **204**) indicates weak Ag–alkyne interactions.[25]

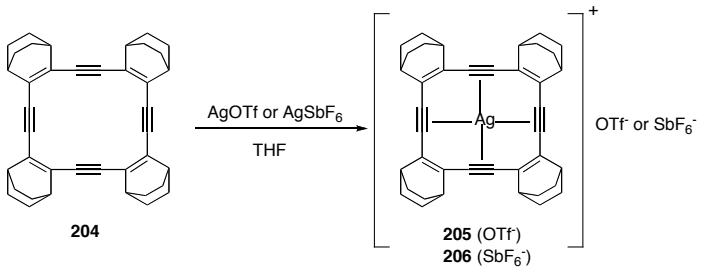

Scheme 2.10 Synthesis of silver cyclynes

2.3 Platinum and nickel alkyl and alkyne complexes (C–C bond activation)

Historically, the first investigation into the application of transition metals with regard to the activation of C–C bonds have been carried out by Tipper by allowing chloroplatinic acid (**207**) and cyclopropane to react in acetic anhydride. in the presence of pyridine, forming platina(IV)cyclobutane **208** (Scheme **2.11**).[26]

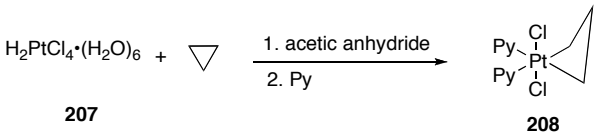

Scheme 2.11 Insertion of Pt(IV) in cyclopropane

Such methodology has been expanded to the use of low oxidation state transition metals, including Ni(0) and Pt(0). Atomic nickel, when reacted with cyclopropane in an argon matrix, inserts into the cyclopropane to form Ni(II) cyclobutane **209** (Scheme **2.12**).[27]

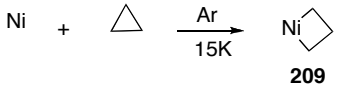

209

Scheme 2.12 Oxidative addition of Ni(0) to cyclopropane

Application of Pt(0) to C–C bond cleavage has been first demonstrated when $Pt(PPh_3)_4$ reacted with cyclopropenones to form platinum(II)cyclobutenones, as outlined in Scheme **2.13**.[28]

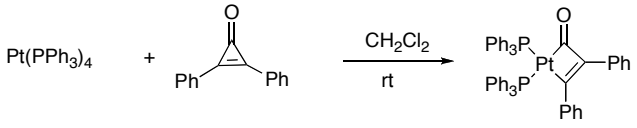

210

Scheme 2.13 Oxidative addition of Pt(0) to $C(sp^2)$–$C(sp^2)$ bond

Ni(0) reacts in the same manner as Pt(0) with strained cyclic compounds. In a typical example, $Ni(PPh_3)_4$ reacted with cyclopropabenzene in toluene at –20 °C. Other Ni(0) derivatives are also used in the C–C bond activation of strained cyclic compounds, including $Ni(PEt_3)_2(COD)_2$, $Ni(COD)_2$, and $Ni(C_2H_4)_3$ in toluene in the presence of TMEDA (Scheme **2.14**).[29]

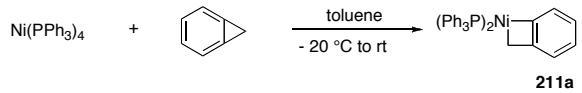

211a

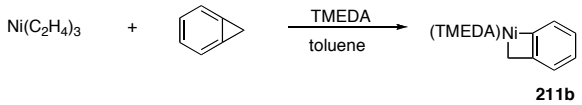

211b

Scheme 2.14 Oxidative addition of Ni(0) to $C(sp^3)$-$C(sp^3)$ bond

Highly strained cyclic alkynes such as cyclohexyne and cycloheptyne can be stabilized by complexation with transition metals, particularly Pt(0) derivatives.

In an example reported by Tanaka and co-workers, $Pt(CH_2{=}CH_2)(PPh_3)_2$ undergoes oxidative addition at the alkyne unit of dibenzocyclooctene in CH_2Cl_2 at room temperature to form a stable platinum-cyclopropene (**212**) (Scheme **2.15**).[30] Compound **212** was characterized by X-ray crystallographic analysis.

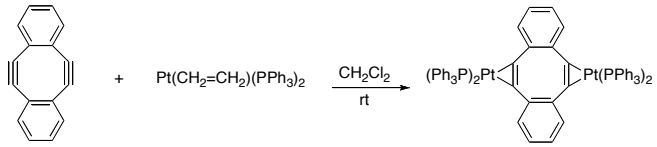

212

Scheme 2.15 Oxidative addition of Pt(0) to C(sp)–C(sp)

In contrast to platinacyclopropene **212**, a recent example reported by Ozawa and co-workers shows a series of platinum complexes; platinum remained at zero oxidation state[31] when forming the platinum-alkyne complex **213**, according to Scheme **2.16**.[31]

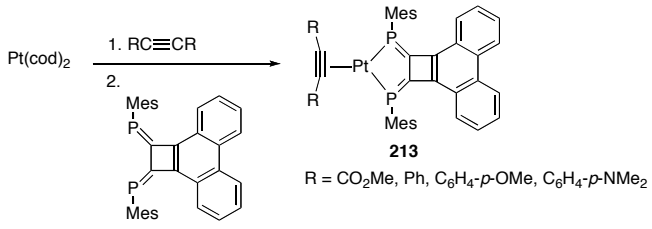

213

R = CO_2Me, Ph, C_6H_4-*p*-OMe, C_6H_4-*p*-NMe_2

Scheme 2.16 Synthesis of Pt(0) alkyne complex

It should be mentioned that the platinum oxidation state in Scheme **2.15** and **2.16** purely are quotations from the relevant literature for better and more comprehensive discussion here.

2.4 Cobalt mediated [2+2+2] cycloaddition

One of the most important applications of organometallic compounds is in the synthesis of complex organic molecules with the goal of improving and simplifying synthetic strategies. Such strategies are based on the application of versatile organometallic compounds to provide a new pathway for the synthesis of complex molecules more efficiently. One of the best known and classic reactions in organic synthesis is cycloaddition, in particular, [2+2+2] cycloaddition of three unsaturated moieties as outlined in general Scheme **2.17**.[32]

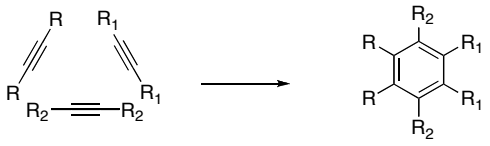

Scheme 2.17 Cyclotrimerization of alkynes

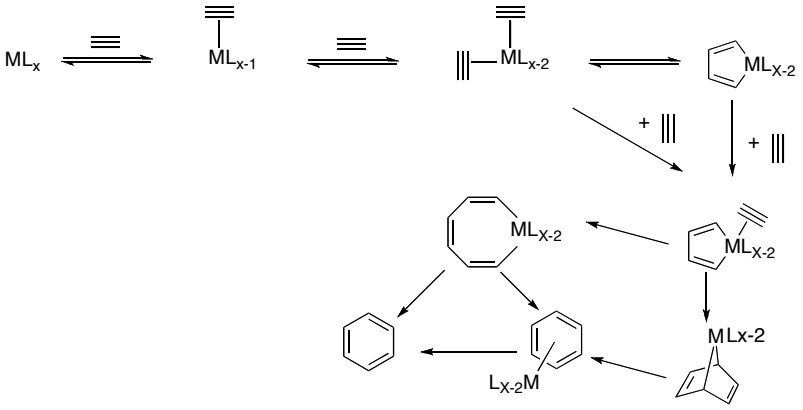

Scheme 2.18 General proposed mechanism for cyclotrimerization of alkynes

The proposed general mechanism for metal mediated [2+2+2] cyclotrimerization of alkynes is shown in Scheme **2.18**. The reaction is initiated by alkyne association, in two steps, that is followed by oxidative cyclization. The

oxidative addition product associates with a third alkyne unit and the resulting complex can be converted into product by two routes shown in the Scheme **2.18**. Vollhardt and co-workers have demonstrated the application of transition metals, particularly cobalt precursors in organic synthesis. [32,33] Schemes **2.19** and **2.20** show examples of these reactions.

An example of cobalt mediated [2+2+2] cyclotrimerization is outlined in Scheme **2.19**. Compound **214** reacts with $Cp^*Co(CH_2{=}CH_2)_2$ to form a cobalt (III) complex (**215**) that is converted thermally to **216**, which has been identified by X-ray crystallographic analysis. Compound **216** in hexamethylbenzene, heated in the presence of CO, resulted in the formation of compound **217**.[33]

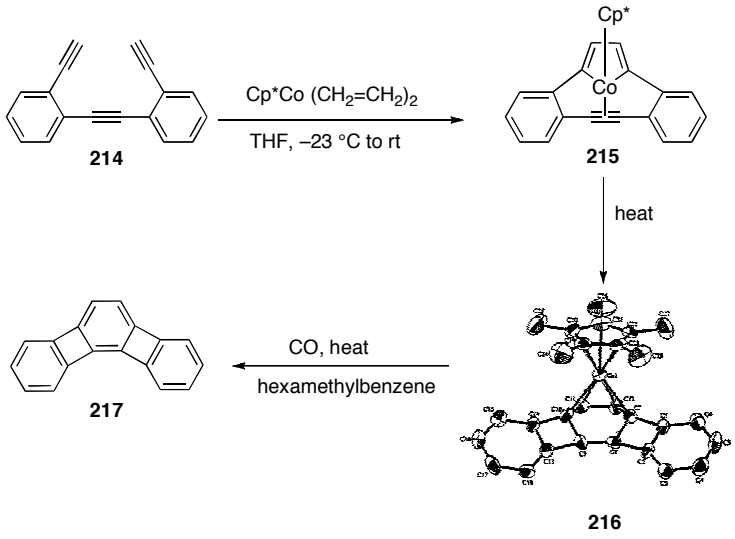

Scheme 2.19 Application of a cobalt complex in cyclotrimerization

The cobalt strategy has also been applied to the total synthesis of (±)-estrone by Vollhardt and co-workers as outlined in Scheme **2.20**.[34] The critical step in the synthesis is the reaction of $CpCo(CO)_2$ with **218** in the presence of bis-trimethylsilylacetylene to form the key intermediate **219,** which is subsequently converted to estrone in four additional steps. Also, it should be mentioned that the cobalt derivatives are used in stoichiometric, not catalytic, amounts with regard to the starting materials.

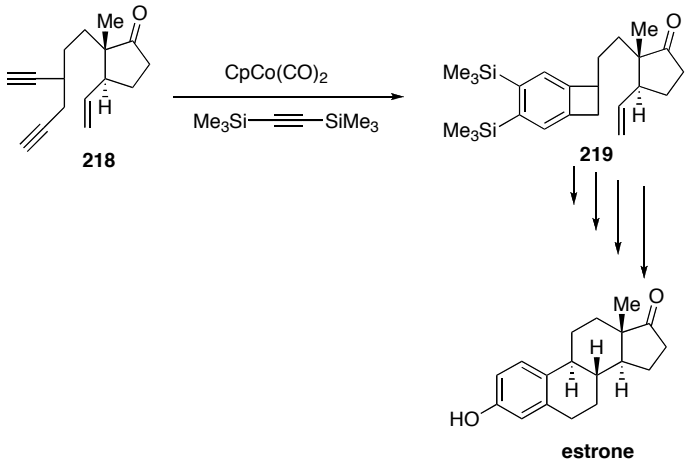

Scheme 2.20 Application of a cobalt complex in the synthesis of (±)-estrone

2.5 Cyclyne complexes (platinum acetylides)

Platinum acetylides have attracted the interest of synthetic chemists because they are possible candidates for nonlinear optical (NLO) and liquid-crystalline materials.[35c-f] Youngs and co-workers synthesized a series of cyclic platinum acetylides according to Hagihara's method. Lithium alkynide **220** reacts with a series of platinum precursors in diisopropylamine (used as solvent) in the presence of catalytic amounts of CuI according to Scheme **2.21**.[35a] All reactions

are performed under high-dilution conditions and the products were characterized by X-ray crystallography.

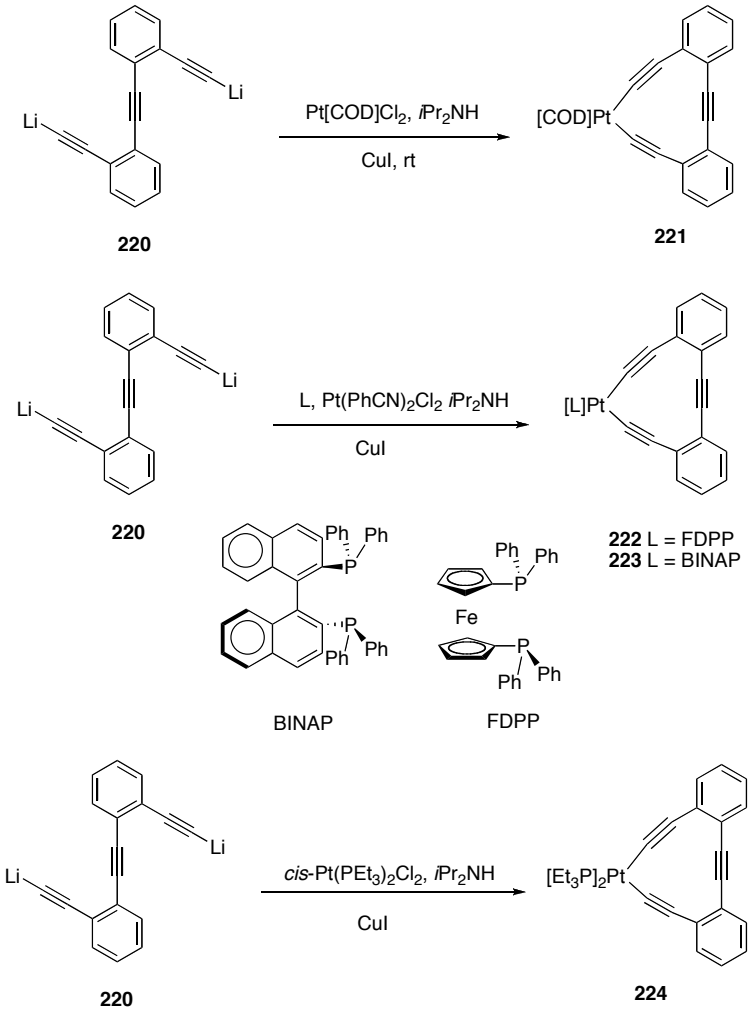

Scheme 2.21 Synthesis of platinum complexes

Bis-platinum species of cyclynes have been synthesized in the same manner, as outlined in Scheme **2.22**[35a] and the products characterized by X-ray crystallography.

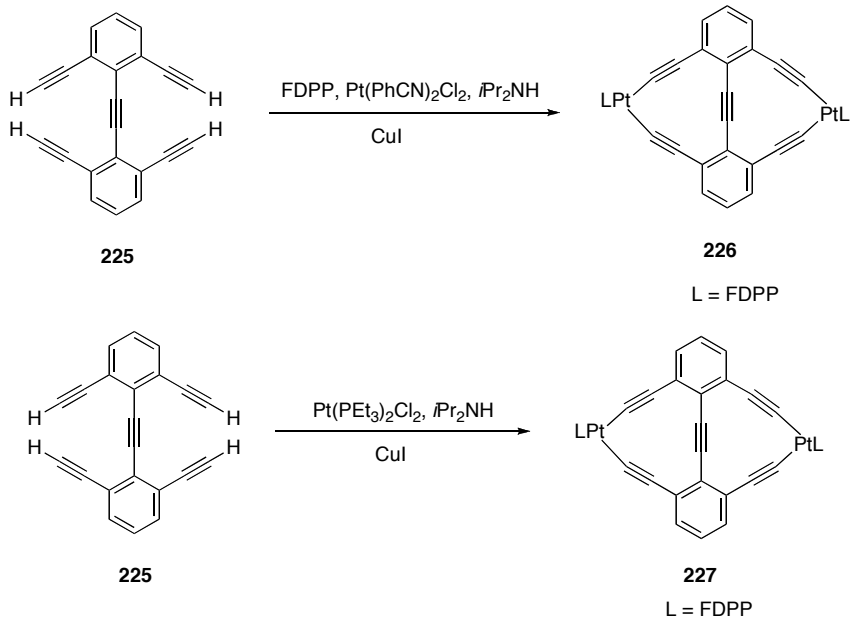

Scheme 2.22 Synthesis of platinum complexes

In related work, Youngs and co-workers explored the synthesis of compound **228** by reacting **220** with $PtCl_2(tht)_2$ in THF followed by reaction of the resulting mixture with NBu_4Br in *iso*-propylamine. Furthermore, complex **228** reacts with Hg_2Cl_2 in acetone to give compound **229**. Both compounds have been indentified by X-ray crsytallographic analysis (Scheme **2.23**).[35b] Compounds **228** has distorted square geometry at the platinum centre and its alkyne units deviate slightly from linearity (e.g., 174.1 (3)°). Complex **229** (double tweezer) also has distorted square geometry at the platinum centre and its alkyne units deviated from linearity (e.g., 179 (2)°). The geometry of the mercury in complex **229** is

distorted tetrahedral. Both compounds, **228** and **229** are among the first examples of tetraalkynyl-platinum complexes that have been characterized by solid-state X-ray analysis.

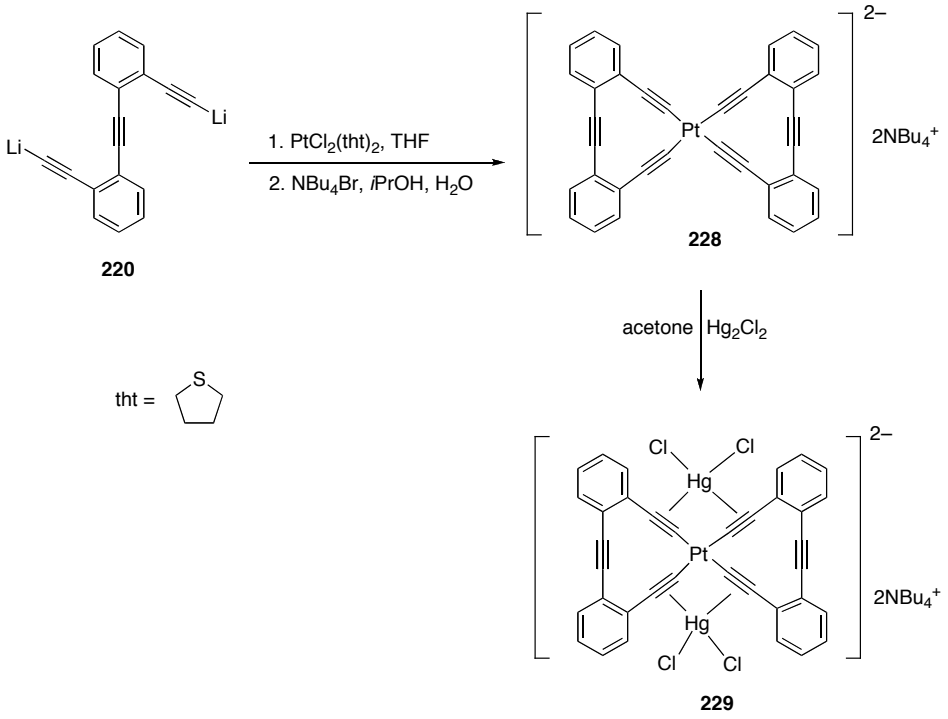

Scheme 2.23 Synthesis of complexes **228** and **229**

2.6 Cross-conjugated macrocycles containing metals

The only series of metal-contaning molecules with similar skeletons to expanded radialenes are “hybrid” expanded radialenes that contain framework metal centers (Scheme **2.24**). This catagory of compounds or metal complexes, contain metal σ-acetylide bonds. These compopunds are characterized by two factors; first, electronic interaction between the metal fragment and, second, alkynyl substrate and electronic delocalization across the metal centers.[36] This catagory of compounds may be considered either as linear or cyclic metal σ-acetylide complexes. Due to the presence of bridging polyyne units, these compounds exhibit enhanced non-linear optical behavior.[36] The role of the metal center is simply to serve as a spacer that effectively prevents proximal groups from sterically interfering with one another in both the solid and in solution state. In particular, the presence of repeating tetraethynylethene building blocks in the network, in which the metal centers bridge the building blocks, provides a clear picture and pattern for synthetic chemists (Scheme **2.24)**.[36]

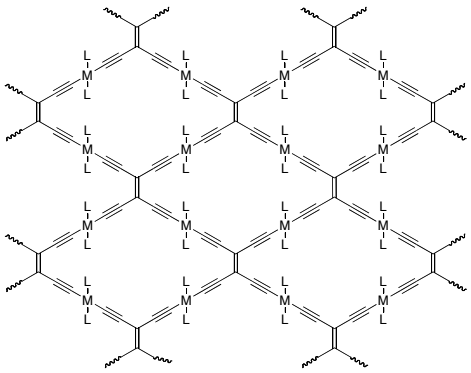

Scheme 2.24 Hypothetical transition metal-linked carbon networks

While the ligands (L) serve as spacers between potentially reactive carbon

layers, the metal centered d-orbitals may offer some electronic delocalization within the plane.

Diederich and co-workers have synthesized a series of linear compounds based on the tetraethynylethene building block containing *trans*-bis(triethylphosphine)platinum, as outlined in Scheme **2.25**.[36] Furthermore, platinum species **232** has been used under oxidative coupling conditions (after removing the TIPS protecting groups) in the synthesis of metalla-macrocycle **233,** presented in Scheme **2.26**.[36]

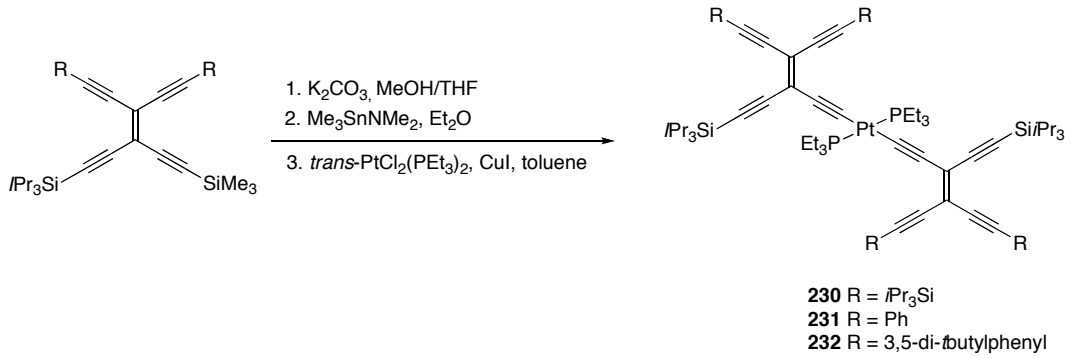

230 R = *i*Pr$_3$Si
231 R = Ph
232 R = 3,5-di-*t*butylphenyl

Scheme 2.25 Synthesis of platinum acetylide precursors

UV-vis spectroscpic analysis of compund **233** shows metal to ligand charge transfer (MLCT) that may result in transmission of electron density across the metal center. Due to its rigidity, the emission spectra of **233** shows a broad, featureless fluoresence band at 543 nm upon excitation at 450 nm.[36]

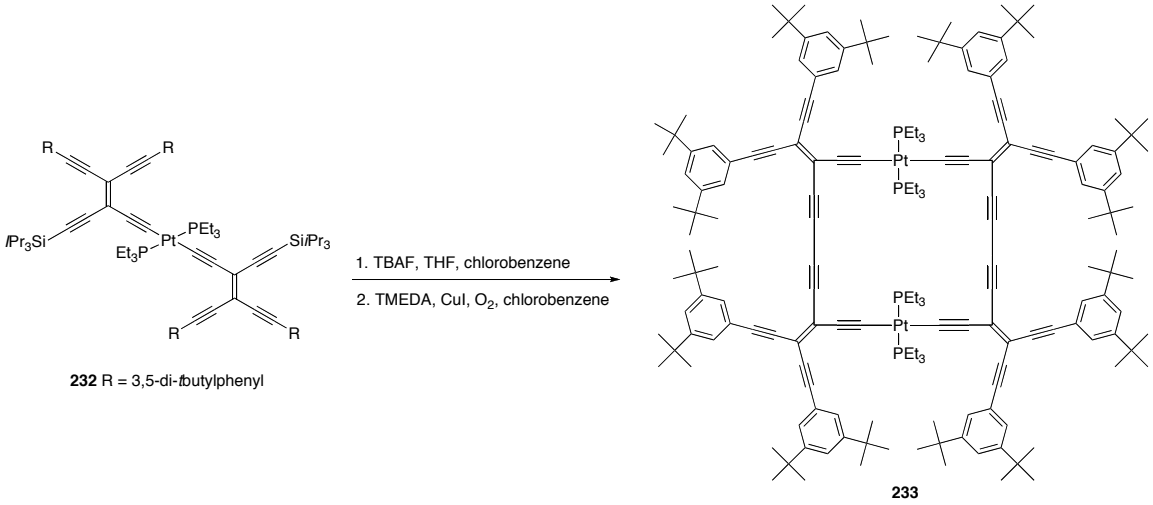

Scheme 2.26 Synthesis of a platinum macrocycle **233**

More recent contributions to this field have been carried out from Tykwinski and Campbell by the synthesis of new platinum containing macrocycles that carry functionality such as pyridyl groups. The design of the new macrocycles required the need of developing new synthetic strategy to achive the targeted macrocycles. The macrocycles exhibit enhanced optical and electronic properties due to the presence of tunable functional groups. With regard to the solid states, the macrocycles through self-assembly provide supramolecular building blocks for porous materials and consequently demonestrated their applicability in host-guest chemistry.[37a]

Two examples is presented in Scheme **2.27**. Compound **234** is protodesilylated and reacted with $PtCl_2(PR_3)_2$ to give compounds **235** and **236** (Scheme **2.27**).[37b,38] Both compounds have been characterized by X-ray crystallography, and most notable feature is that the platinum-phosphorous bonds are prependicular to the macrocyclic eyne core.

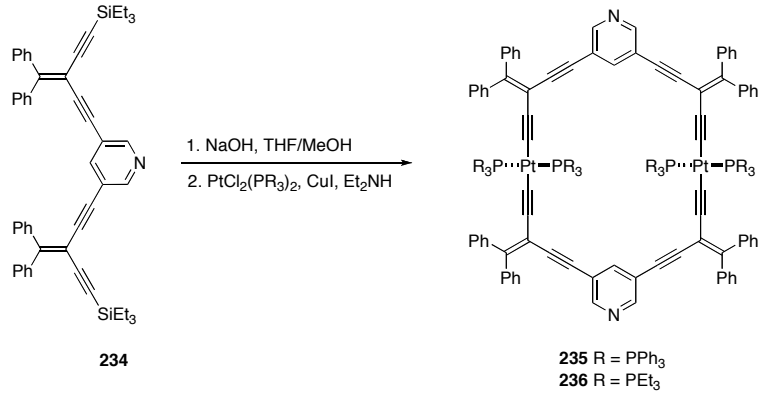

Scheme 2.27 Synthesis of platinum macrocycles

Furthermore, compound **235** reacts with *cis*-bis(diphenylphosphino)ethylene (dppee) in CH_2Cl_2 giving macrocyclic compound **237** as a result of exchange of triphenylphosphine with this bidentate phosphine ligands. (Scheme **2.28**).

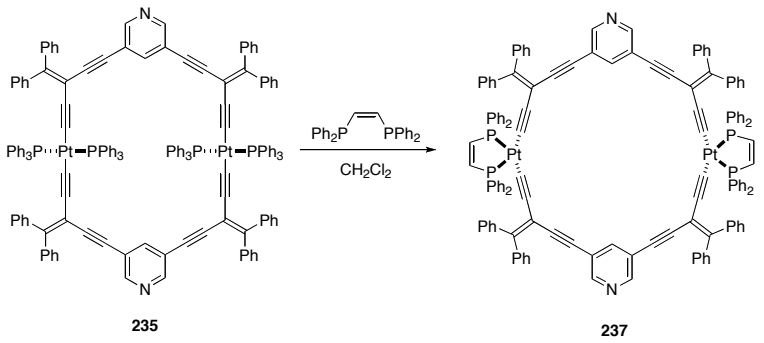

Scheme 2.28 Synthesis of a platinum macrocycle

Using acyclic precursor **238**, the Tykwinski group has synthesized a series of cross-conjugated macrocycles **239**–**242**, with and without embedded platinum acetylide linkages (Scheme **2.29**).[37,38]

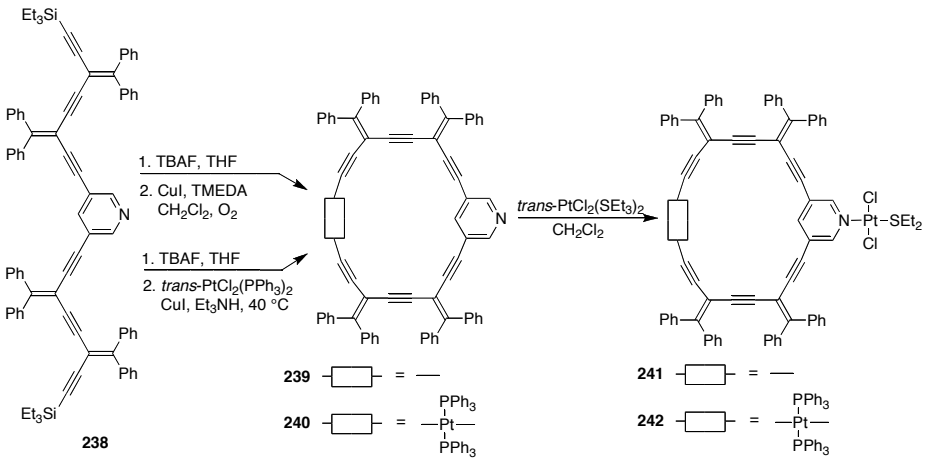

Scheme 2.29 Synthesis of platinum macrocycles

The exocyclic orientation of the pyridine moiety makes these systems suitable for metal coordination, as demonstrated by the formation of **241–242**. All four systems were characterized spectroscopically and crystallographically.

Chiral macrocyclic systems have been studied over the last decade, in particular due to their potential applications in areas such as asymmetric catalysis, chemical sensors, and enantioselective guest inclusion. In this regard, Tykwinski and coworkers have expanded on the ligand exchange protocol, demonstrating the formation of cross-conjugated macrocycles based on (*S*,*S*)-chiraphos and (*R*,*R*)-chiraphos ligands (Scheme **2.30)**. Starting with achiral **240**, reaction with (*S*,*S*)-chiraphos provides chiral product (*S*,*S*)-**243** in good yield. An analogous reaction afforded (*S*,*S*)-**244**, while both enantiomers of **245** were formed using either of (*S*,*S*)- or (*R*,*R*)-chiraphos.[39,40] Crystallographic analysis of (*S*,*S*)-**243** and CD studies of the series of macrocycles demonstrated unambiguously the ability of the chiraphos ligand to efficiently induce chirality in the conjugated molecular framework via the Pt-acetylide complex.[39,40]

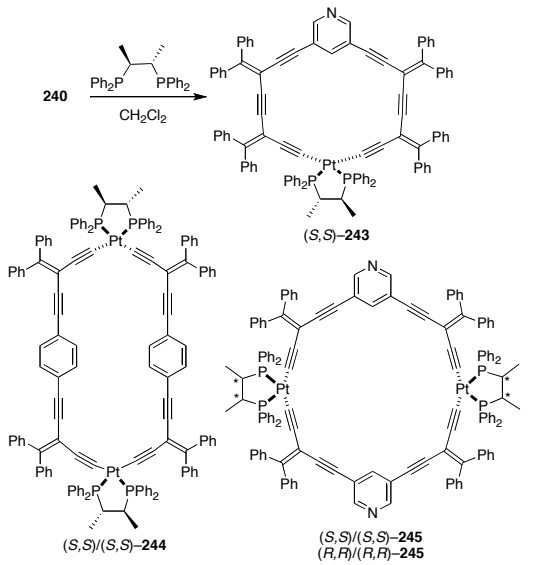

Scheme 2.30 Synthesis of chiral platinum macrocycles

2.7 Coordination chemistry of [3]radialenes

Coordination chemistry involving radialenes is very rare in the literature. The only examples available are contributions by the groups of Matsumoto and Steel, who have reported, at the same time, the synthesis of compounds **151**–**153** (Scheme **2. 31**).[41-45]

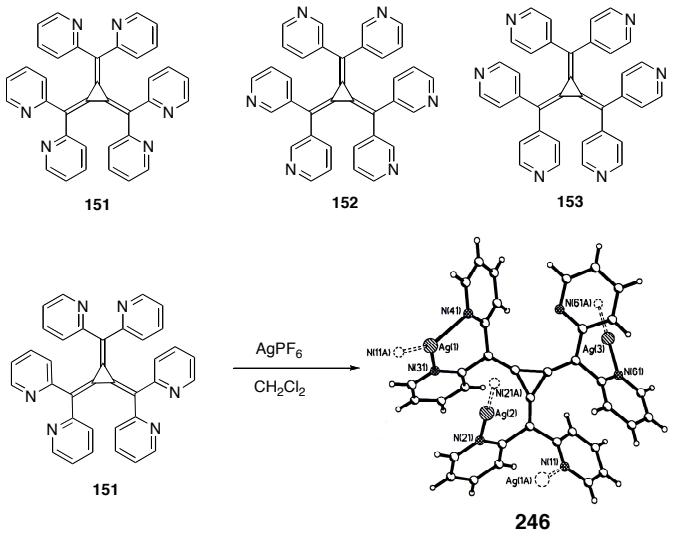

Scheme 2.31 Pyridyl radialene series

Silverhexafluorophosphate reacts with radialene **151** giving one dimensional coordination polymer **246** with a 2:1 metal to ligand ratio (Scheme **2.31**). The same reaction using $AgNO_3$ yielded a different one-dimesional polymer but with the same metal-ligand ratio. [42-44] Furthermore, the reaction of the radialene **152** with either $AgBF_4$ or $[Ru(byp)_2Cl_2]$, gave discrete coordination complexes.[44] The final member of this series of [3]radialenes incorporates the 4-pyridyl group and has been synthesized by Masumoto and co-workers.[45a] Upon reaction with silver perchlorate, radialene **153** assembles into a three-dimensional coordination polymer, based on X-ray crystallographic analysis. The

coordination polymer was the first such polymer to use a [3]radialene as a bridging ligand. Very recently a contribution by Sumby and co-workers has appeared in the literature that shows hexa(4-cyanophenyl)[3]radialene as a bridging ligand .[45b]

2.8 Coordination chemistry of hybrid expanded radialenes

In contrast to the radialenes, there have been extensive results from the Tykwinski group with regard to the coordination chemistry of hybrid expanded radialenes. Tykwinski and co-workers have synthesized cross-conjugated macrocycles **248**–**251** based on a copper catalyzed acetylenic dimerization strategy (Scheme **2.32**). Their work includes an unfunctionalized hydrocarbon skeleton (**248**) and examples in which a pyridyl moiety is oriented endocyclic (**249**) and exocyclic (**250** and **251**) with respect to the macrocyclic core.[46-48] X-ray analysis of **249** shows that the molecule adapted a nearly planar conformation in the solid state, essentially free of ring strain. Carbon rich macrocycles **250** and **251**, with nitrogens directed away from the cyclic periphery, function as equivalents to 4,4'-bipyridine and participate in self-assembly reactions and axial metal coordination in **252** and **253.** Both complexes are characterized by X-ray crystallography and show a planar macrocyclic framework for **252**, while **253** shows a chair-like conformation that likely results from steric repulsion between the diphenyl alkylidene moieties and the exocyclic porphyrin rings (Scheme **2.33**).[46-48]

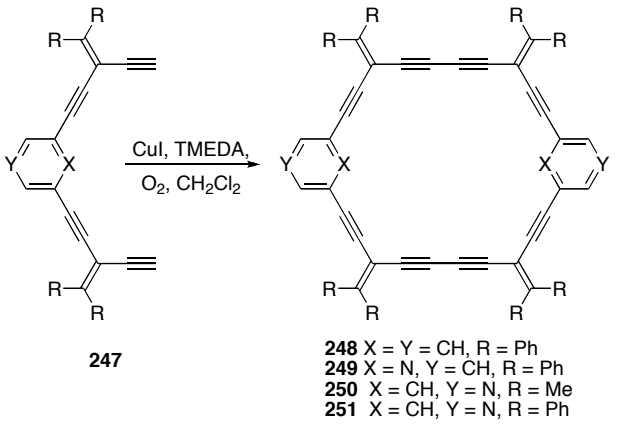

247

248 X = Y = CH, R = Ph
249 X = N, Y = CH, R = Ph
250 X = CH, Y = N, R = Me
251 X = CH, Y = N, R = Ph

Scheme 2.32 Synthesis of pyridyl macrocycles

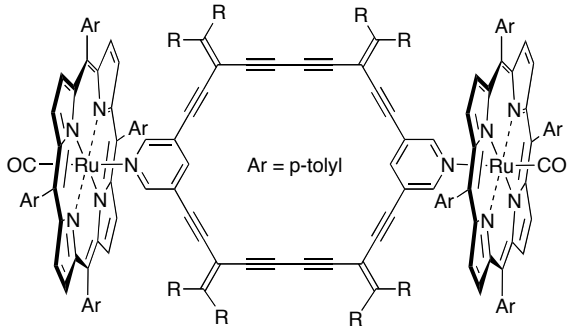

252 R = Me
253 R = Ph

Scheme 2.33 Synthesis of pyridyl-porphyrin macrocycles

Reaction of **251** with $Pt(PEt_3)_2(OTf)_2$ in CH_2Cl_2 gives the assembly **254**. X-ray crystallographic analysis has established that assembly **254** packs such that bidirectional channels are realized, and the incorporation of 1,2 dichloroethane (used in crystallization) into the channels demonstrates that the solid is suitable for the selective uptake of small organic guests (Scheme **2.34**). The displacement of this solvent and characterization of the resulting pores has been explored using hyperpolarized ^{129}Xe NMR spectroscopy.[37a,49]

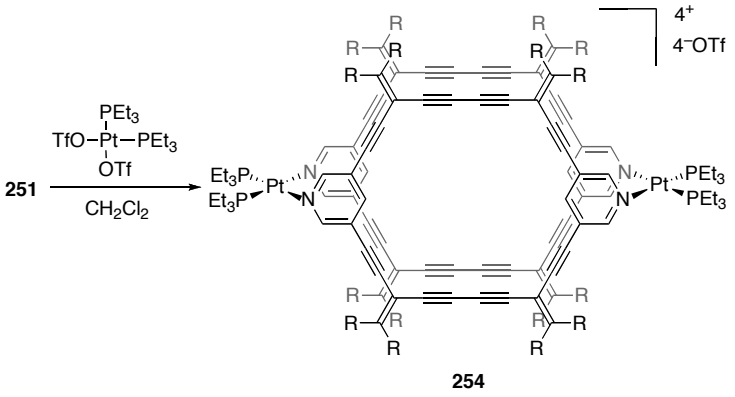

Scheme 2.34 Synthesis of a bis-platinum macrocycle

2.9 Titanium radialenes

In addition to platinum, an example of incorporation of titanium into a radialene framework comes from Rosenthal and co-workers[50]. This is due to potential applications of these compounds as building blocks in materials science.[51] The synthesis of the radialene-like fused titanacyclopentadienes **257** and **258** is accompanied by the reaction of **255** or **256** with diphenylbutadiyne in THF, as outlined in Scheme **2.35**.[50] X-ray crystallographic analysis of **257** confirms the proposed structure, but insolubility in organic solvents prevented full solution-state characterization.

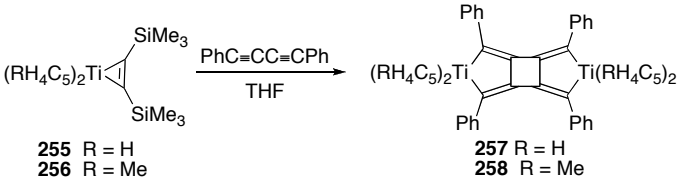

Scheme 2.35 Synthesis of titanium radialenes

2.10 Platinum σ-acetylide oligomers

Polymers and oligomers of platinum σ-actylides with π-cojugated skeletons have attracted interest because of their photophysical properties, including long-lived phosphorescent π, π*-excited states which can be applied to applications such as organic electroluminescent devices and for laser protection.[51a-c]

Two series of such oligomers have been synthesized based on platinum σ-actylides, as shown in Schemes **2.36** and **2.37**. In π-conjugated systems, Schanze and co-workers have reported the synthesis and photophysical characterization of linear Pt-acetylide oligomers (PAO, Scheme **2.36**).[52]

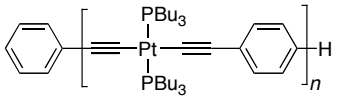

PAO series

(*n* = 1-5, 7)

Scheme 2.36 Platinum oligomers

In terms of cross-cojugated systems, Diederich and co-workers have synthesized a series of oligomers starting from **259** under Glaser-Hay conditions and in the presence of PhC≡CH, as an endcapping reagent.[36,53] (Scheme **2.37**). This reaction gives oligomers **260a**–**f**, which could be separated by GPC.[53] Executing the same polymerization reaction and waiting 20 min to introduce the end-capping reagent, resulted in polymer **261** (n_{avg} = 32), as an air-stable red solid that decomposes above 250 °C. UV-vis absorption and third-order NLO

characterization showed that the Pt centers function as an insulator toward π-electron delocalization in these oligomers.

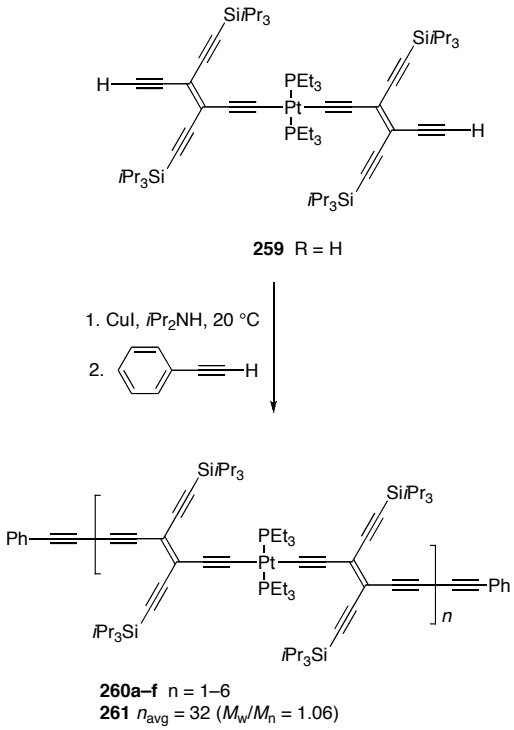

Scheme 2.37 Synthesis of platinum acetylide polymers

2.11 Conclusion

The above discussion has provided a brief background for the related inorganic and organometallic chemistry of the cyclic and acyclic frameworks that carry alkyne units. The discussion by no means covered all alkyne-metal chemistry, rather the focus has been limited to those concepts that are applicable to the chemistry of expanded radialenes for further discussion in Chapter **6**.

2.12 References

(1) (a) Nielsen, M. B.; Schreiber, M.; Baek, Y. G.; Seiler, P.; Lecomte, S.; Boudon, C.; Tykwinski, R. R.; Gisselbrecht, J. P.; Gramlich, V.; Skinner, P. J.; Bosshard, C.; Gunter, P.; Gross, M.; Diederich, F. *Chem. Eur. J.* **2001**, *7*, 3263–3280; (b) Boldi, A. M.; Diederich, F. *Angew. Chem., Int. Ed. Engl.* **1994**, *33*, 468–471.

(2) Tobe, Y.; Umeda, R.; Iwasa, N.; Sonoda, M. *Chem. Eur. J.* **2003**, *9*, 5549–5559.

(3) Zhao, Y.-L.; Liu, Q.; Zhang, J.-P.; Liu, Z.-Q. *J. Org. Chem.* **2005**, *70*, 6913–6917.

(4) Eisler, S.; Tykwinski, R. R. *Angew. Chem. Int. Ed.* **1999**, *38*, 1940–1943.

(5) Scott, L. T.; DeCicco, G. J.; Hyun, J. L.; Reinhardt, G. *J. Am. Chem. Soc.* **1985**, *107*, 6546–6555.

(6) Bennett, M. A.; Schwemlein, H. P. *Angew. Chem., Int. Ed. Engl*. **1989**, *28*, 1296–1320.

(7) (a) Nakagawa, M. *In The Chemistry of the Carbon–Carbon Triple Bond*; Patai, S., Ed.; Wiley: New York, **1978**; Part 2, pp 635–712 and references therein; (b) Sondheimer, F. *Acc. Chem. Res*. **1972**, *5*, 81–91.

(8) Stephens, R. D.; Castro, C. E. *J. Org. Chem.* **1963**, *28*, 3313–3315.

(9) Kinder, J. D.; Tessier, C. A.; Youngs, W. J. *Synlett* **1993**, 149–150.

(10) Joyner, R. D.; Kenney, M. E. *J. Am. Chem. Soc.* **1960**, *82*, 5790–5791.

(11) Nohr, R. S.; Kuznesof, P. M.; Wynne, K. J.; Kenney, M. E.; Siebenman, P. G. *J. Am. Chem. Soc.* **1981**, *103*, 4371–4377.

(12) Marks, T. J. *Science* **1985**, *227*, 881–889.

(13) Cotton, F. A. *Chemical Applications of Group Theory*, 3rd ed.; Wiley-Interscience: New York, **1990**.

(14) Cotton, F. A.; Wilkinson, G. *Advanced Inorganic Chemistry*, 5th ed.; Wiley: New York, **1988**; pp 353–357.

(15) Wudl, F. *Acc. Chem. Res.* **1984,** *17,* 227–232.

(16) Maugh, T. H. *Science* **1983,** *222*, 606–607.

(17) Williams, J. M.; Beno, M. A.; Wang, H.; Reed, P. E.; Azevedo, L. J. Schirber, J. F. *Inorg. Chem.* **1984,** *23***,** 1792–1793.

(18) Etemad, S.; Heeger, A. J.; MacDiarmid, A. G. *Annu. Rec. Phys. Chem* **1982**, *33***,** 443–470.

(19) (a) Ferrara, J. D.; Tanaka, A. A.; Flerro, C.; Tessier-Youngs, C. A.; Youngs, W. J. *Organometallics* **1989**, *8*, 2089–2098; (b) Ferrara, J. D.; Tessier-Youngs, C. A.; Youngs, W. J. *J. Am. Chem. Soc.* **1988**, *110*, 3326–332; (c) Mayer, J. M. *Inorg. Chem*. **1988**, *8*, 125–135. (d) Ferrara, J. D.; Tessier-Youngs, C. A.; Youngs, W. J. *J. Am. Chem. Soc.* **1985**, *107*, 6719–6721.

(20) Youngs, W. J.; Kinder, J. D.; Bradshaw, J. D.; Tessier, C. A. *Organometallics* **1993**, *12*, 2406–2407.

(21) Ferrara, J. D.; Tessier-Youngs, C. A.; Youngs, W. J. *Organometallics*

1987, *6*, 676–678.
(22) Djebli, A.; Ferrara, J. D.; Tessier-Youngs, C.; Youngs, W. J. *J. Chem. Soc., Chem. Commun.* **1988**, 548–549.
(23) Solooki, D.; Bradshaw, J. D.; Tessier, C. A.; Youngs, W. J. *Organometallics* **1994**, *13*, 451–455.
(24) Ferrara, J. D.; Djebli, A.; Tessier-Youngs, C.; Youngs, W. J. *J. Am. Chem. Soc.* **1988**, *110*, 647–649.
(25) Nishinaga, T.; Kawamura, T.; Komatsu, K. *J. Chem. Soc., Chem. Commun.* **1998**, 2263–2264.
(26) Tipper, C. F. H. *J. Chem. Soc*. **1955**, 2045.
(27) Kline, E. S.; Hauge, R. H.; Kafafi, Z. H.; Margrave, J. L. *Organometallics* **1988**, *7*, 1512–1516.
(28) Wong, W.; Singer, S. J.; Pitts, W. D.; Watkins, S. F.; Baddley W. H. *J . Chem. Soc., Chem. Commun.* **1972**, *6***,** 72–673.
(29) Neidlein, R.; Rufinska, A**.;** Schwager, H.; Wilke, G. *Angew. Chem., Int. Ed. Engl.* **1986**, *25*, 640–642.
(30) Shimada, S.; Tanaka, M.; Honda, K. *Inorganica Chem. Acta.* **1997***, 265,* 1–8.
(31) Hayashi, K.; Nakatani, M.; Hayashi, A.; Takano M.; Okazaki, M.; Toyota, K.; Yoshifuji, M.; Ozawa, F. *Organometallics* **2008**, *27*, 1970–1972.
(32) Vollhardt, K. P. C. *Angew. Chem., Int. Ed. Engl.* **1984,** *23*, 539–556.
(33) Diercks, R.; Eaton, B. E.; Gürtzgen, S.; Jalisatgi, S.; Matzger, A. J.; Radde, R. H.; Vollhardt, K. P. C.; *J. Am. Chem. Soc*. **1998**, *120*, 8247–8248
(34) Funk, R. L.; Vollhardt, K. P. C. *J. Am. Chem. Soc*. **1979**, *101*, 215–217.
(35) (a) Zhang, D.; McConville, D. B.; Tessier, C. A.; Youngs, W. J. *Organometallics* **1997**, *16*, 824–825 and references therein); (b) Bradshaw, J. D.; Guo, L.; Tessier, C. A.; Youngs, W. J. *Organometallics* **1996**, *15*, 2582–2584; (c) Long, N. J. *Angew. Chem. Int. Ed. Engl.* **1995**, *34*, 21–38; (d) Abe, A.; Kimura, N.; Tabata, S. *Macromolecules* **1991**, *24*, 6238–6243; (e) Marder, T. B.; Lesley, G.; Yuan, Z.; Fyfe, H. B.; Chow, P.; Stringer, G.; Jobe, I. R.; Taylor, N. J.; Williams, I. D.; Kurtz, S. K. In *Materials for Nonlinear Optics*; Marder, S. R., Sohn, J. E., Stucky, G. D., Eds.; ACS Symposium Series 455; American Chemical Society: Washington, DC, **1991**; Chapter 40; (f) Takahashi, S.; Takai, Y.; Morimoto, H.; Sonogashira, K*. J. Chem. Soc., Chem. Commun.* **1984**, 3–5; (g) Takahashi, S.; Takai, Y.; Morimoto, H.; Sonogashira, K. *Mol. Cryst. Liq. Cryst*. **1982**, *82*, 139–43.
(36) Faust, R.; Diederich, F.; Gramlich, V.; Seiler, P. *Chem. Eur. J.* **1995**, *1*, 111–117.
(37) (a) Campbell, K.; Ooms, K. J.; Wasylishen, R. E.; Tykwinski, R. R. *Org. Lett.* **2005**, *7*, 3397–3400; (b) Campbell, K.; McDonald, R.; Ferguson, M. J.; Tykwinski, R. R. *Organometallics* **2003**, *22*, 1353–1355.

(38) Campbell, K.; McDonald, R.; Ferguson, M. J.; Tykwinski, R. R. *J. Organomet. Chem.* **2003**, *683*, 379–387.
(39) Campbell, K.; Tykwinski, R. R. *In Carbon-Rich Compounds*; Haley, M. M.; Tykwinski R. R. ed.; Wiley-VCH, 2006.
(40) Campbell, K.; Johnson, C. A.; McDonald, R.; Ferguson, M. J.; Haley, M. M.; Tykwinski, R. R. *Angew. Chem. Int. Ed.* **2004**, *43*, 5967–5971.
(41) Matsumoto, K.; Harada, Y.; Kawase, T.; Oda, M. *Chem. Commun.* **2002**, 324–325.
(42) Steel, P. J.; Sumby, C. J. *Chem. Commun.* **2002**, 322–323.
(43) Steel, P. J.; Sumby, C. J. *Inorg. Chem. Commun.* **2002**, *5*, 323–327.
(44) D'Alessandro, D. M.; Keene, F. R.; Steel, P. J.; Sumby, C. J. *Aust. J. Chem.* **2003**, *56*, 657–664.
(45) (a) Hollis, C. A.; Hanton, L. R.; Morris, J. C.; Sumby, C. *J. Crystal Growth & Design*, **2009**, *9*, 2911–2916; (b) Matsumoto, K.; Harada, Y.; Yamada, N.; Kurata, H.; Kawase, T.; Oda, M. *Cryst. Growth Des.* **2006**, *6*, 1083–1085.
(46) Campbell, K.; Tiemstra, N. M.; Prepas-Strobeck, N. S.; McDonald, R.; Ferguson, M. J.; Tykwinski, R. R. *Synlett* **2004**, 182–186.
(47) Ooms, K. J.; Campbell, K.; Tykwinski, R. R.; Wasylishen, R. E. *J. Mater. Chem.* **2005**, *15*, 4318–4327.
(48) Campbell, K.; McDonald, R.; Tykwinski, R. R. *J. Org. Chem.* **2002**, 67, 1133–1140.
(49) Campbell, K.; Kuehl, C. J.; Ferguson, M. J.; Stang, P. J.; Tykwinski, R. R. *J. Am. Chem. Soc.* **2002**, *124*, 7266–7267.
(50) Pellny, P.-M.; Burlakov, V. V.; Peulecke, N.; Baumann, W.; Spannenberg, A.; Kempe, R.; Francke, V.; Rosenthal, U. *J. Organomet. Chem.* **1999**, *578*, 125–132.
(51) (a) Wilson, J. S.; Dhoot, A. S.; Seeley, A. J. A. B.; Khan, M. S.; Köhler, A.; Friend, R. H. *Nature* **2001**, *413*, 828–831; (b) Baldo, M. A.; O'Brien, D. F.; You, Y.; Shoustikov, A.; Sibley, S.; Thompson, M. E.; Forrest, S. R. *Nature* **1998**, *395*, 151–154; (c) Staromlynska, J.; McKay, T. J.; Bolger, J. A.; Davy, J. R. *J. Opt. Soc. Am. B* **1998**, *15*, 1731–1736.
(52) Liu, Y.; Jiang, S., Glusac, K.; Powell, D. H.; Anderson, D. F.; Schanze, K. S. *J. Am. Chem. Soc.* **2002***, 124,* 12412–12413*.*
(53) Siemsen, P.; Gubler, U.; Bosshard, C.; Günter, P.; Diederich, F. *Chem. Eur. J.* **2001**, *7*, 1333–1341.

Chapter 3:

Synthesis and Characterization of A New Generation of Expanded Radialenes

3.1 Synthesis and characterization of cross-conjugated macrocycles: The expanded radialenes

Investigation of the synthesis of expanded radialenes was undertaken for two reasons; first, to establish a reliable protocol to synthesize different compounds based on an expanded radialene skeleton, and second to synthesize stable compounds for physical studies in order to reveal their potential for applications in materials science (e.g., electronic devices, optoelectronics).[1] The first generation of expanded radialenes, or butadiyne expanded radialenes, were synthesized according to the availability of starting materials, using oxidative coupling to achieve the targeted molecules. Both the Diederich[2] and Tobe[3] groups have synthesized expanded radialenes using the corresponding terminal alkyne(s) and $Cu(OAc)_2$ in an organic solvent, like pyridine, in the presence of oxygen. This strategy did not provide much selectivity because a variety of products can be formed when terminal alkynes react under homocoupling conditions in a single vessel; some examples are [4]–, [5]–, and [6]expanded radialenes. Furthermore, other unwanted side products are formed under these conditions due to oxidative coupling and polymerization during the reaction. Improved outcomes can be achieved by controlling the concentration of reactants and the execution of the reaction, but selectivity is still a problem. The first generation of expanded radialenes in which two alkyne units are inserted between two double bonds is schematically depicted in Schemes **3.1** and **3.2**.[2]

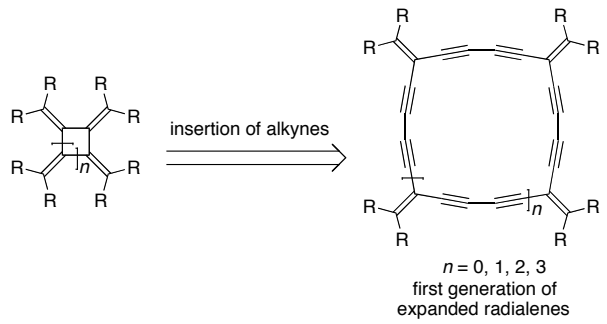

Scheme 3.1 Transformation from radialenes to expanded radialenes

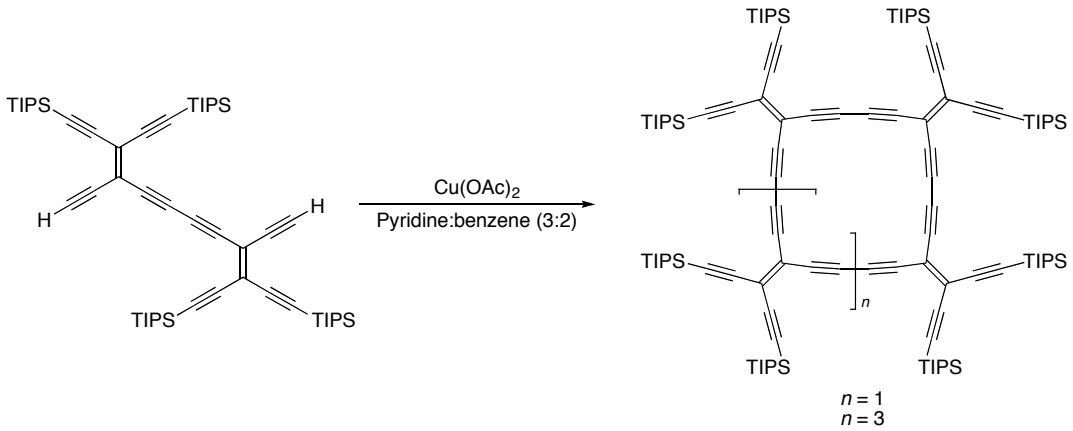

Scheme 3.2 Example of first generation of expanded radialenes

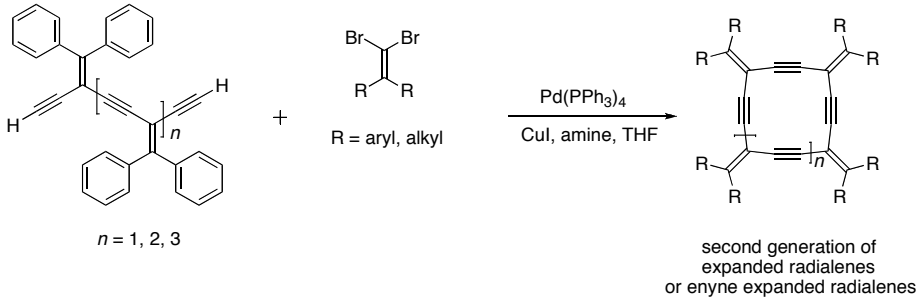

Scheme 3.3 Sonogashira cross coupling reaction protocol toward radialenes

To define the new format for expanded radialenes, it was proposed to investigate the synthesis of expanded radialenes that carry only one alkyne unit

between two exocyclic double bonds, as depicted in Scheme **3.3**. For synthesis of the proposed skeletons shown in Scheme **3.3**, preparation of a new series of precursors was essential. The adopted strategy in this project is based on the existence of the *iso*-polydiacetylene series developed in the Tykwinski group.[4] The expanded radialenes were synthesized in an inert atmosphere in a reaction containing a terminal acetylene, a dibromoolefin, a catalytic amount of palladium catalyst, usually $Pd(PPh_3)_4$, a co-catalyst such as CuI, and a base such as diisopropylamine. The reactants were mixed in an organic medium, typically THF, and heated under reflux (Scheme **3.3**). The protocol shown in Scheme **3.3**, the Sonogashira cross coupling reaction, should be carried out very carefully to successfully synthesize highly strained cross-conjugated macrocycles in reasonable yields. This strategy has provided a set of conditions that selectively produce a single expanded radialene during the cross coupling reaction; the size of the macrocycle depends on the length of *iso*-polydiactetylene oligomer used in the reaction. Many variables are involved in the reaction that could be optimized for a more efficient conversion. The most important variables include preventing the presence of oxygen in the reaction vessel, the purity of the starting materials, and the execution of the reaction. In particular special attention should be given to handling $Pd(PPh_3)_4$ under an inert atmosphere because oxidization of this pre-catalyst could hinder the cyclization reaction. The optimization of all the aspects of radialene synthesis played a major role in the research presented in this chapter.

3.2 Synthesis of *iso*-polydiacetylene series

The first synthesis of the new generation of expanded radialenes was accomplished by Eisler and Tykwinski[5a,b] as mentioned in Chapter **1**. Initial problem encountered in the synthesis was low stability of the macrocycle carrying alkyl groups as exocyclic substituents and low yield of the reaction. In the second generation of expanded radialenes, aryl groups replaced the alkyl groups. Aryl groups may prevent oxidation of the macrocycles, but may lead to lower solubility and consequently more challenging and tedious separations during purification, as well as time-consuming characterization. The above challenges are characteristic of this series of compounds and generally of the chemistry of expanded radialenes. It was quickly realized that incorporating functional groups such as TIPS or CF_3 would significantly increase the solubility of their corresponding macrocycles.

The synthesis begins with the preparation of vinyl triflate **300** as a yellowish oil through a two–step synthesis from the corresponding acyl chloride and bis-silylacetylene, as outlined in Scheme **3.4**.[4] Triflate **300** was reacted with trimethylsilylacetylene in the presence of Pd(II) pre-catalyst to give the monomer **301** as a pale yellow solid in 95% yield (Scheme **3.5**).

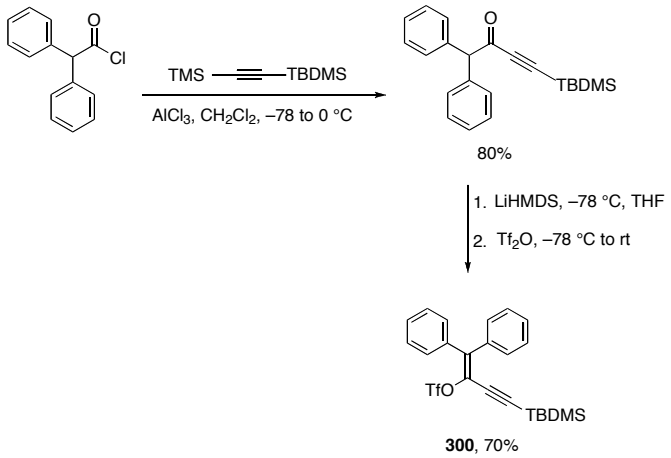

Scheme 3.4 Synthesis of triflate **300**

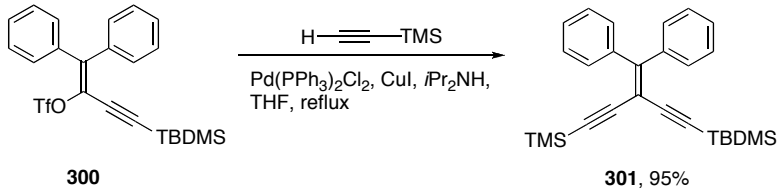

Scheme 3.5 Synthesis of monomer **301**

The presence of two different protecting groups, TMS and TBDMS, provides an opportunity for selective protodesilylation of the monomer to expand its length toward the *iso*-polydiacetylene series (oligomers) including dimer (**303**), trimer (**305**), tetramer (**304**), and pentamer (**306**).

The synthesis of the dimer is initiated by protodesilylation of monomer **301** by K_2CO_3 in THF/MeOH (1:1) at room temperature. The resulting terminal alkyne **302** was reacted with **300** in the presence of $Pd(PPh_3)_4$ at reflux in THF. Separation and purification gave dimer **303** as a yellow solid in 95% yield (Scheme **3.6**).

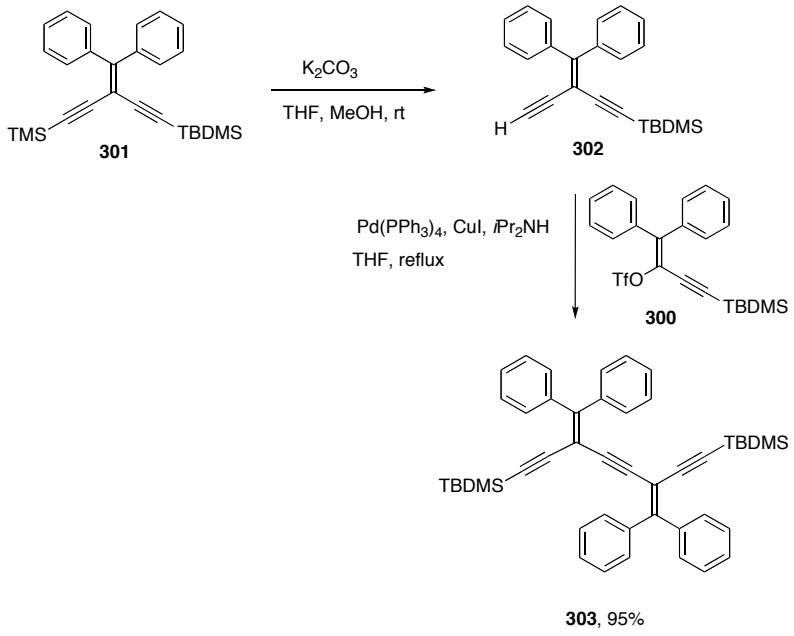

Scheme 3.6 Synthesis of dimer **303**

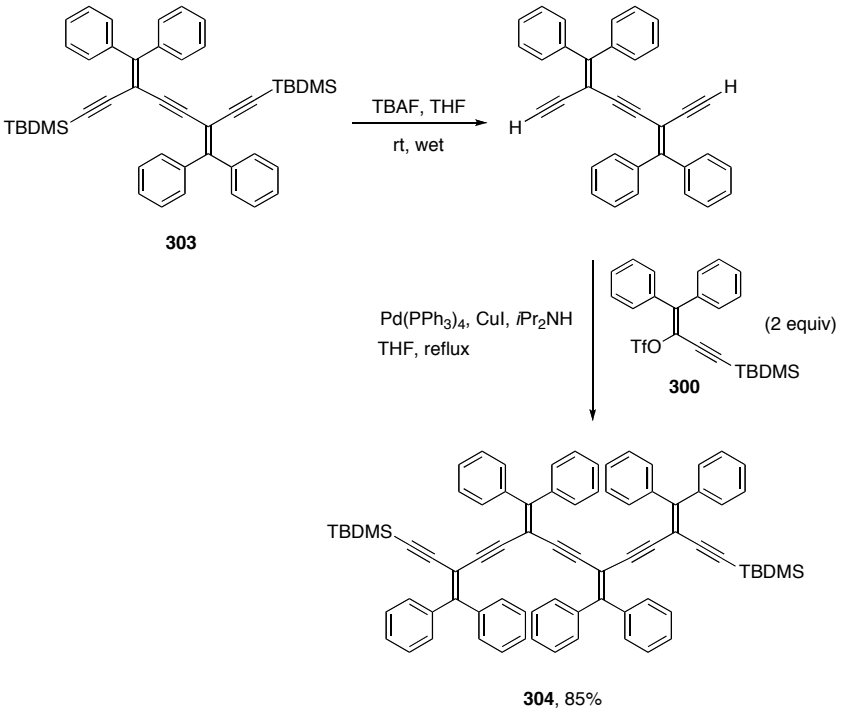

Scheme 3.7 Synthesis of tetramer **304**

Compound **303** was fully characterized and used for synthesis of a higher oligomer. Dimer **303** was protodesilylated with TBAF in THF at room temperature, and the product reacted with two equivalents of **300** in the presence of $Pd(PPh_3)_4$ in THF at reflux to give tetramer **304** as a yellow solid in 85% yield (Scheme **3.7**).

The oligomer series was completed with the synthesis of trimer (**305**) and pentamer (**306**). For the synthesis of the trimer, monomer **301** could be used. However, synthesis of an alternate monomer was developed where TMS has been used instead of TBDMS. The synthetic route started with synthesis of dibromoolefin **308** according to the reaction in Scheme **3.9**. Benzophenone **307** was added to a mixture of PPh_3 and CBr_4 in benzene and the resulting mixture was refluxed for 7 days to produce **308** as an off-white solid in 21% yield.[6] Compound **308** was reacted with an excess of trimethylsilylacetylene under the Sonogashira protocol to give monomer **309** as a pale yellow solid in 80% yield (Scheme **3.8**).

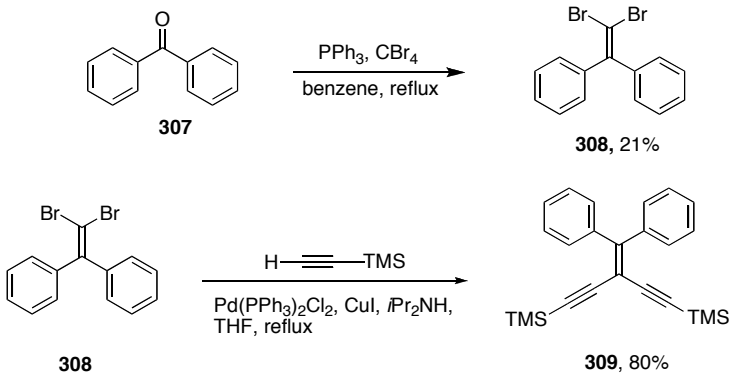

Scheme 3.8 Synthesis of monomer **309**

Compound **309** can be used instead of **301** for the synthesis of trimer **305**. Compound **309**, obtained via a two-step synthesis, is cheaper than monomer **301**, which requires a five-step synthesis. Compound **309** was protodesilylated by K_2CO_3 in THF/MeOH (1:1) at room temperature and the product then reacted with triflate **300** in THF under the standard Sonogashira protocol to give **310** as a yellow solid in 85% yield (Scheme **3.9**). Trimer **305** was protodesilylated in THF in the presence of TBAF at room temperature and the desilylated trimer reacted with two equivalents of triflate **300** to give pentamer **306** as a yellow solid in 65% yield (Scheme **3.10**).

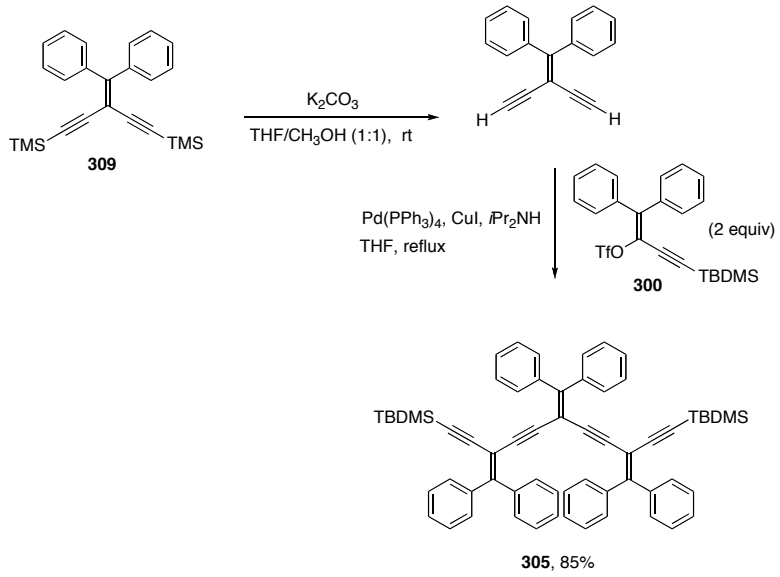

Scheme 3.9 Synthesis of trimer **305**

Electrochemical behavior of **303**, **304**, **305,** and **309** were measured in CH_2Cl_2 at room temperature in collaboration with professor Luis Echegoyen group at Clemson University, South Carolina, USA.

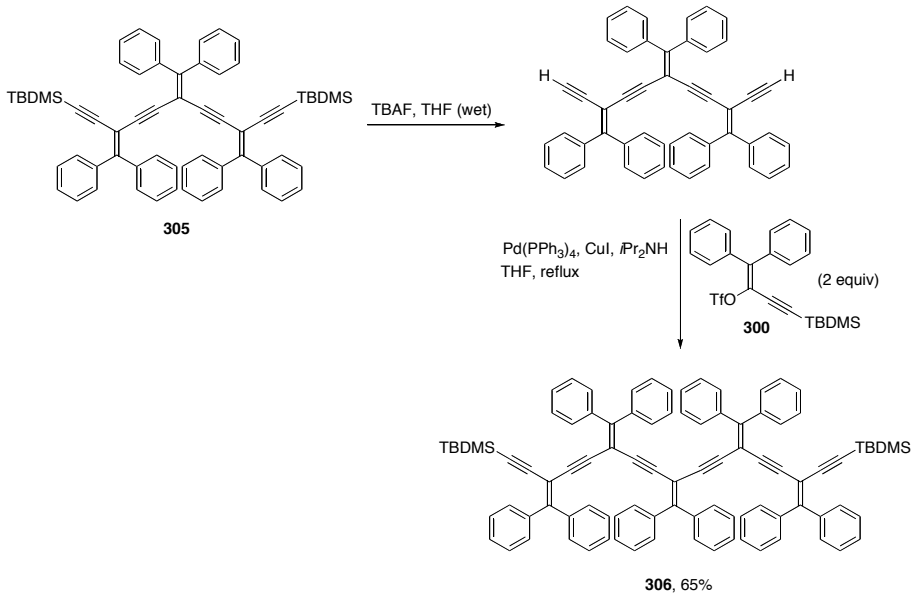

Scheme 3.10 Synthesis of pentamer **306**

Compound **303**–**305** present similar cathodic behavior with a first irreversible reduction potential around 2.15–2.22 V and at least two more one electron irreversible reductive processes, and apparently a multi-electron oxidation. Compound **309** shows a single reduction and it does not exhibit any oxidative behavior within the solvent window (Table **3.1**). For *iso*-polydiacetylene series **303**–**305**, there is good agreement between optical and electronic gaps (see Table **A.1** and **A.2** in the appendix) regardless of the size of the oligomers (n = 1–3).

Table 3.1 Redox potentials of compounds **303**–**305** and **309**[†]

Compounds	E_p, ox_1	E_p, red_1	E_p, red_2	E_p, red_3	ΔE_{gap} [V]
309	-	–2.23	-	-	**-**
303	1.14	–2.09	–2.22	–2.38	3.23
305	0.99	–2.22	–2.38	-	3.21
304	1.08	–2.15	–2.28	–2.45	3.23

[†]Cyclic voltammetry measured in CH_2Cl_2 + 0.1 M nBu_4NPF_6 at a scan rate 100 mV s^{-1}. All potentials are reported versus the ferrocenium/ferrocene (Fc^+/Fc) couple.

3.3 Synthesis and characterization of expanded radialene series

Synthesis of the second generation of expanded radialenes was based on phenyl rings outside the cyclic core in order to increase the macrocycle stability. In considering the synthesis of the expanded radialenes two types of strains have to be discussed.

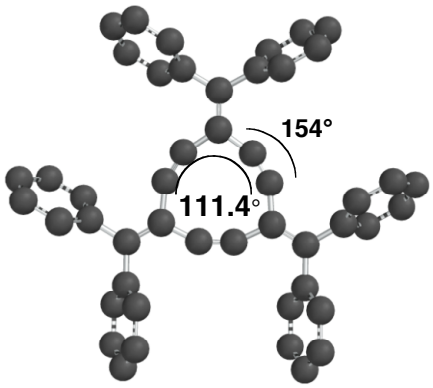

Figure 3.1 Spartan modeling (MMFF94 force field) for [3]expanded radialene **310**

Exocyclic strain increases as the macrocycle becomes larger because there are more substituents outside the cyclic core repelling one another. Conversely, internal strain becomes more significant as the macrocycle becomes smaller. The endocyclic vinylidene carbon with sp^2 hybridization deviates from 120° to a smaller value in concert with a deviation from 180° for the alkyne bond angle. A ball–stick model of [3]expanded radialene is shown in Figure **3.1** generated by Spartan modeling software from Wavefunction, Inc, Irvine, California. The calculation model (molecular mechanics, MMFF94 force field) predicts a vinylidene carbon angle (endocyclic) of 111.4°, that is, 8.6° smaller

than its natural angle of 120° (about 116° observed for *iso*-podiacetylenes series[4]); the alkyne bond angle is predicted to be 154°, a decrease of 26° from the normal linear structure.

In the view of the significant level of strain, radialene **310** is the most interesting member of the radialene series. Initially, it was imagined to be difficult to synthesize [3]expanded radialene. Based on Spartan modeling, the [3]expanded radialene is very strained internally and the synthesis is dependent predominantly on whether intramolecular cyclization can occur to close the radialene core. The synthesis is initiated with protodesilylation of dimer **303** in the presence of TBAF in wet THF at room temperature. The resulting terminal alkyne was added to a degassed solution of **308** and reacted under the standard Sonogashira protocol (Scheme **3.11**).

During the syntheses of this series of radialenes and subsequent radialenes, the reaction mixtures were refluxed under positive pressure of argon gas and the reaction progress was monitored by low resolution MALDI-TOF mass spectrometry at intervals of 6 h. Although, the MALDI technique is not quantitative, it is a good qualitative method for detecting what compounds are present in a mixture (e.g., a reaction crude) if a suitable matrix is used. Also, all the ^{13}C NMR experiments were obtained with d1 = 5 (delay time) in order to achieve higher quality spectra (higher signal to noise ratio) because of long relaxation times for quaternary carbons in the cyclic core of the radialenes.

Following work up, the crude reaction product was separated on silica gel, and gave **310** as a yellow solid in 32% yield. This was a very promising yield for the highly strained macrocycle **310** (Scheme **3.11**). The ^{13}C NMR spectrum shows 7 signals in accordance with the proposed structure for radialene **310**. High resolution electron impact (EI) mass spectrometry shows a molecular ion at m/z 606.2354 while the calculated value for $C_{48}H_{30}$ is m/z 606.2347. Characteristic alkyne carbons show a resonance at 92.5 ppm while the vinylidene carbons resonate at 107.2 and 146.2 ppm.

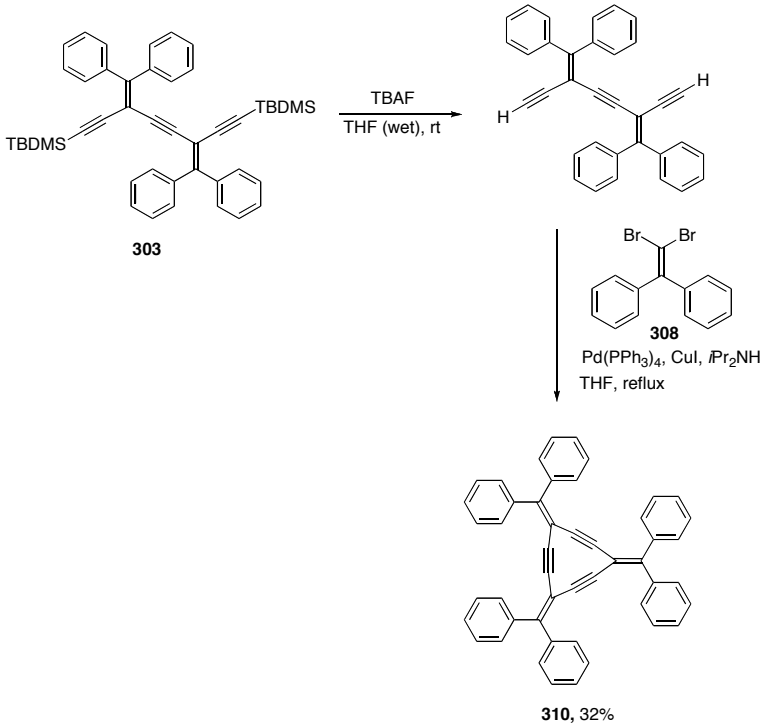

Scheme **3.11** Synthesis of [3]expended radialene **310**

The second member of the series is [4]expanded radialene **311**. Trimer **305** was protodesilylated with TBAF in wet THF at room temperature. After work-

up, the product was added to a degassed solution of **308** and the resulting mixture was reacted under the standard Sonogashira coupling protocol (Scheme **3.12)**. The crude reaction product was separated on silica gel to give radialene **311** as a yellow solid in 75% yield. The solubility of **311** is relatively low compared to **310** in solvent like CH_2Cl_2. Like radialene **310**, however, **311** was reasonably soluble in four solvents including dichloromethane, chloroform, benzene, and toluene; dichloromethane was the best choice.

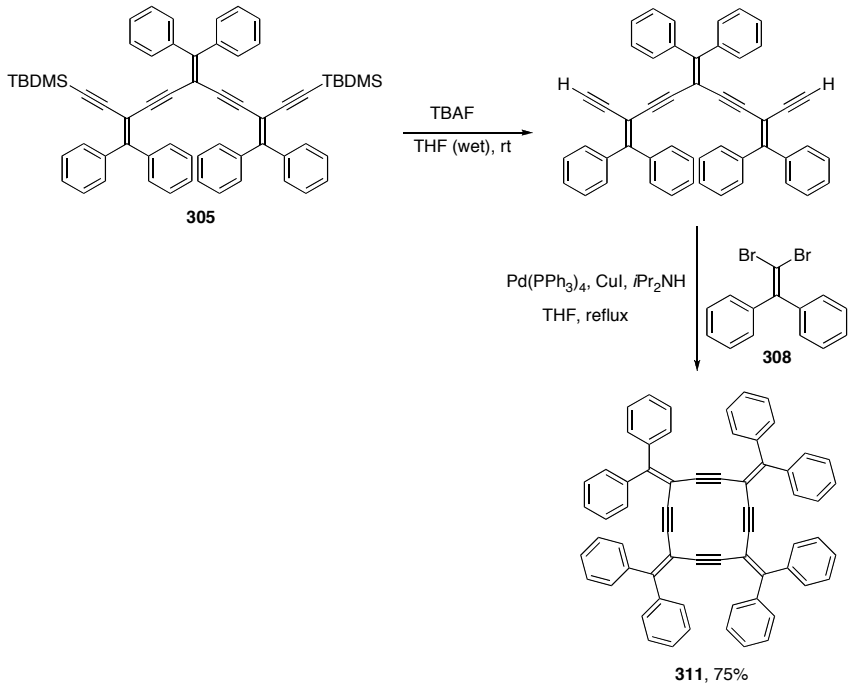

Scheme 3.12 Synthesis of [4]expanded radialene **311**

An overnight ^{13}C NMR experiment gave a quality spectrum for radialene **311**. Compound **311** shows 7 unique peaks as expected and supported the proposed structure. The most characteristic signals are those of alkyne carbons at 97.1 ppm and vinylidene carbons that resonate at 102.6 and 151.8 ppm.

Based on the success of the synthesis of **310** and **311** formation of the next member of the series, [5]expanded radialene was attempted. Compound **304** was protodesilylated with TBAF in THF at room temperature. Following work-up the resulting ether solution of desilylated **304** was added to a degassed solution of **308** and reacted under the standard Sonogashira protocol. The crude reaction product was separated on silica gel to give radialene **312** as a yellow solid in 45% yield (Scheme **3.13**).

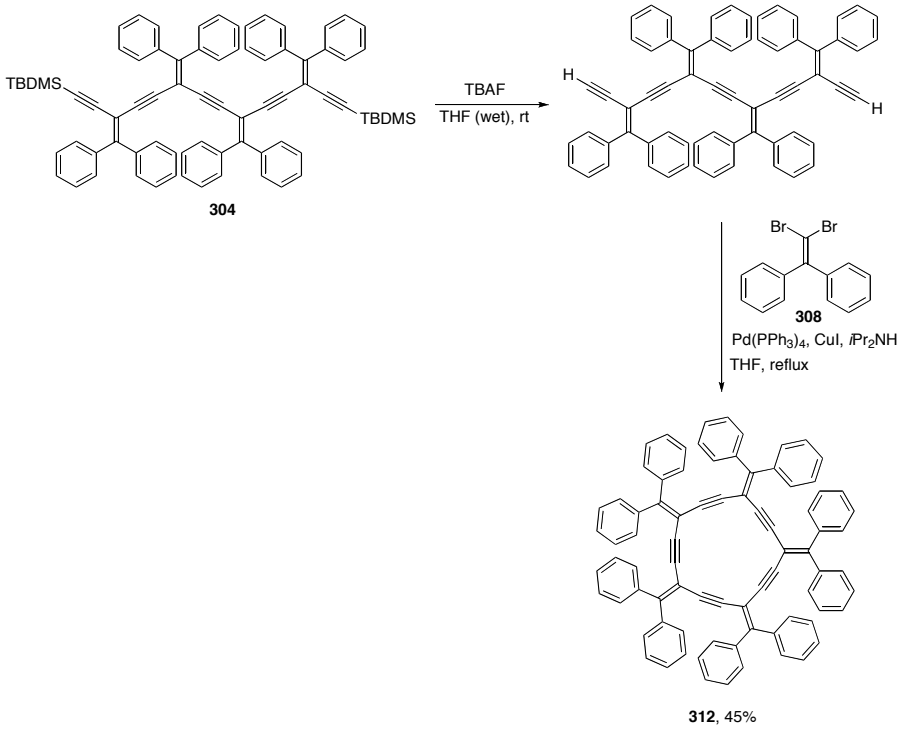

Scheme 3.13 Synthesis of [5]expanded radialene **312**

It is not necessarily surprising that the yield was lower for **312** than that for **311**, as the higher external strain might hinder the cyclization. Radialene **312** was

slightly more soluble than **311** and CH_2Cl_2 was also the best solvent for obtaining a ^{13}C NMR spectrum of radialene **312**. ^{13}C NMR spectroscopy of radialene **312** was run with the same protocol as radialene **311** and as expected, radialene **312** shows 7 unique resonances.

The most characteristic features of the ^{13}C NMR spectrum of **312** were the alkyne carbons that resonate at 90.8 ppm and the vinylidene carbons peaks appear at 101.9 and 155.2 ppm.

3.4 UV-vis spectroscopy, electrochemistry, and solid-state studies of the expanded radialene series

The UV-vis spectrum of **310** shows an absorption is at λ_{max} = 364 nm (ε = 105300 L mol^{-1} cm^{-1}) and a second absorption at λ_{max} = 415 nm (ε = 107500 L mol^{-1} cm^{-1}). λ_{max} is defined here as the lowest energy absorbance observed in the spectrum. Cyclic voltammetry (CV) of the radialene **310** shows two reductions, the first reversible at –1.96 V and the second less defined at –1.99 V as well as a one-electron oxidation at 0.8 V (all the CV experiments were referenced versus the Fc/Fc^+ couple, page 113). The UV-vis spectrum of **311** shows a single absorption at λ_{max} = 377 nm (ε = 99300 L mol^{-1} cm^{-1}) with a much weaker shoulder absorption at approximately at 420 nm. Cyclic voltammetry of **311** in CH_2Cl_2 shows two reductions, the first reversible at –2.0 V and the second less well defined at –2.2 V (refer to page 113 for CV voltammograms). A single, one-electron, reversible oxidation step at 0.8 V has been also observed. The UV-vis spectrum of **312** also shows a single absorption at λ_{max} = 374 nm (ε = 51300 L

$mol^{-1}\ cm^{-1}$). Cyclic voltammetry of **312** shows two reductions, the first reversible at –1.94 V and second irreversible at –1.98 V; both reductions are one-electron event (refer to page 113 for CV voltammograms). Radialene **310**, in contrast to **311** and **312** shows two absorptions in the UV-vis range. At present, the origin of the more significant lower energy absorption for **310** is not yet understood (Figure **3.2**). It may be the result of an augmentation of the shoulder signal observed for **311** as a result of the decreased conformational flexibility in the more strained structure of **310**. Conversely, it may arise from an increase in macrocyclic cross-conjugation, which has been invoked to account for the red shift in the λ_{max} values observed for trimeric derivatives of the larger expanded radialenes belonging to the first generation**.**

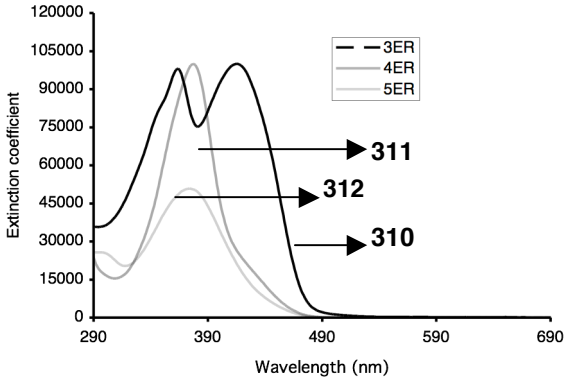

Figure 3.2 UV-vis spectra of extended radialenes (ER): 3ER = **310,** 4ER = **311,** 5ER = **312** measured in THF

Cyclic voltammetry of compounds **310–312** show very similar behavior regardless of difference in macrocycle sizes. No significant lowering of the electrochemical HOMO–LUMO gap was observed for compound **310**, despite

its lower energy absorption in the UV-vis region. The same trend was found for the larger expanded radialenes of the first generation, as described by Diederich and co-workers, where similar redox potentials were observed irrespective of the size of the macrocycle (n = 1–3).[7] The smaller radialenes **310**, **311**, and **312** are considerably more difficult to reduce than any of the reported radialenes of the first generation (Scheme **3.2**).[7,8] The difficult reduction of compound **310** may substantiate the prediction of Chauvin and co-workers[8] that a one-electron reduction of a [3]radialene analogue of **310** (where Ph is replaced by H for a simpler calculation) should lead to an antiaromatic molecule, although this premise inspires the analysis of additional substitution patterns. Some such derivatives have been synthesized and they will be discussed in the next chapter. No single crystal for X-ray analysis was achieved for **310** despite numerous attempts. Single crystals of compound **312** suitable for X-ray crystallographic of **311** were grown from slow evaporation of a THF solution at 4–5 °C (CCDC #, 652658, Figure **3.3**). Macrocycle **311** shows a planar cyclic core with the pendent phenyl groups twisted from this plane in a manner that facilitates π-π stacking interactions (Figure **3.4**). Table **3.2** summarizes selected bond lengths and bond angles from X-ray analysis for radialene **311**.

Table 3.2 Selected bond lengths and bond angles for radialenes **311**

C2–C3–C5 angle	110.4(12)°
C1–C2–C3 angle	166.65(14)°
C4–C3–C5 angle	123.66(13)°
C5–C3–C4–C11 torsion angle	173.17(14)°
C1–C2 bond length	1.200(19) Å
C2–C3 bond length	1.439(2) Å

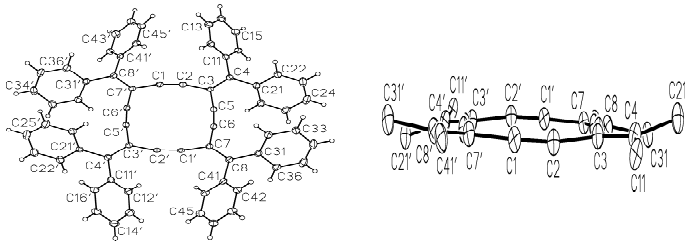

Figure 3.3 ORTEP plots for radialene **311** (only ipso carbons of pendent phenyl rings are shown for clarity in the structure to the right)

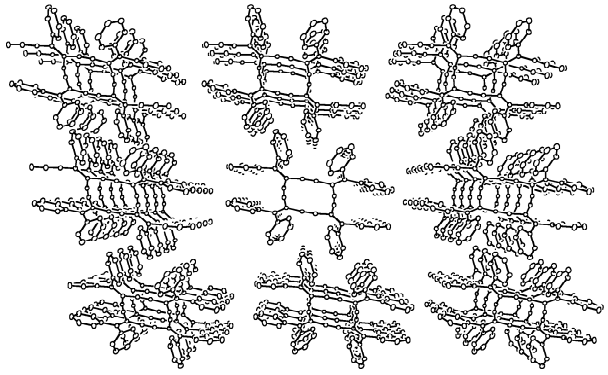

Figure 3.4 Solid-state packing for radialene **311** (hydrogen removed for clarity)

Single crystals of compound **312** suitable for X-ray crystallographic analysis were grown from slow evaporation of a THF solution at 4–5 °C (CCDC #, 652686). The structure of the radialene **312** is not planar, and its cyclic core resembles an envelope conformation, which likely arises from increased steric interactions between the pendent phenyl rings. Table **3.3** summarizes selected bond lengths and bond angles from X-ray analysis for radialene **312**. Figure **3.5** shows ORTEP plots and solid-state packing of compound **312.**

Table 3.3 Selected bond lengths and bond angles for radialene **312**

C5–C6–C7 bond angle	111.65(15)°
C4–C5–C6 bond angle	170.97(19)°
C7–C6–C17 bond angle	123.70(17)°
C7–C6–C17–C41 torsion angle	173.52(18)°
C4–C5 bond length	1.193(3) Å
C1–C2 bond length	1.200(3) Å
C6–C17 bond length	1.368(3) Å
C3–C16 bond length	1.362(3) Å

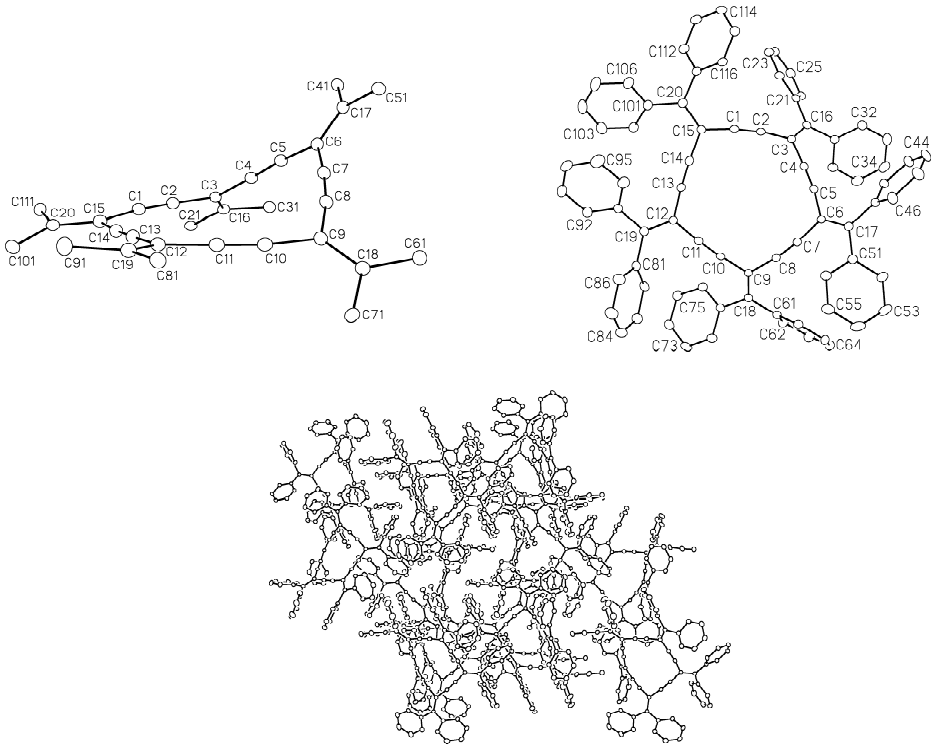

Figure 3.5 ORETP plots and solid-state packing of radialene **312** (hydrogens removed for clarity and only ipso carbons of pendent phenyl rings are shown for the top left structure, for clarity)

Having synthesized the first three members of the series, it was logical to expand this protocol to synthesize different skeletons based on the expanded

radialenes or novel derivatives of expanded radialenes that have not been seen before.

3.5 Synthesis and characterization of bisexpanded radialenes and radiaannulenes

Diederich and co-workers,[10-12] reported a synthesis for tetraethynylethene (**313**) that could be used as a building block for synthesis of two-dimensional all-C networks and novel C-rich nanoarchitectures with unusual structural and electronic properties. Some examples for these compounds are perethynylated expanded radialenes, or molecular wires and polymers with the novel polytriacetylene backbone.[10-12] If it is assumed that the four terminal alkynes of tetraethynylethene are free for a coupling reaction, there should be no selectivity and two pathways for a reaction are plausible (Scheme **3.14**).[10-12] Potentially useful staring material however, **313** decomposes in solution, therefore the usage of **313** has been limited due to its lack of stability.

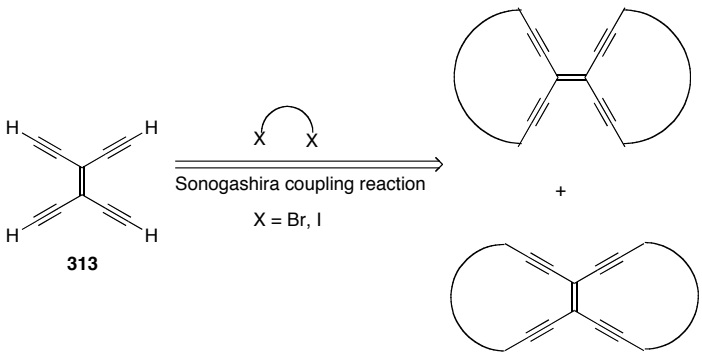

Scheme 3.14 Two possible routes for a tetraethynylethene coupling reaction

Since our synthetic strategy is the coupling reaction of a given terminal

alkyne with a dibromoolefin, we looked for a compound that carries four bromides in place of the terminal alkynes, considering that it could be used as a major building block for the synthesis of cross-conjugated macrocycles that are essentially derivatives of the expanded radialenes. Tetrabromoethene **314** (Scheme **3.15**) was the best choice for the coupling reaction shown in Scheme **3.15**.

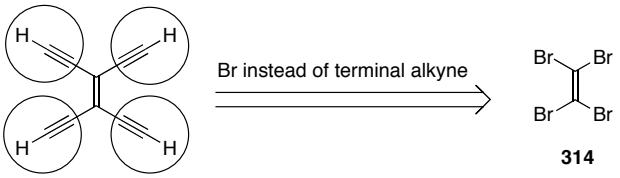

313 **314**

3.15 Tetrabromoethene **314** building block instead of **313**

Thus, compound **314** was chosen for the coupling reaction with the *iso*-polydiacetylene series and a one-pot synthesis seemed to be the best choice for the synthesis of bisradialenes. The first member synthesized was the corresponding bis[4]expanded radialene.

Compound **305** was protodesilylated in the presence of TBAF at room temperature in THF. The resulting terminal alkyne was reacted with **314** under the standard Sonogashira coupling reaction conditions. The reaction mixture turned red immediately upon the addition of the terminal alkyne. The crude reaction product was subjected to column chromatography using silica gel. The collected fractions, assumed to contain product(s), were further purified by separation on pre-coated silica gel TLC plates. The red solid product **315** was

isolated in 24% yield as a mixture of two isomers **315a** (the first bisexpanded radialene) and **315b** (radiaannulene)[13] (Scheme **3.16**). It was believed initially that the product was only **315a**, but the ^{13}C NMR spectrum of the red solid revealed extra peaks that confirmed the presence of a second compound, **315b,** which differed in only a few peaks from its isomer **315a**. Finally, X-ray analysis confirmed the identity of both isomers **315a** and **315b**. High performance liquid chromatographic (HLPC) analysis also clearly showed two peaks, confirming the presence of two isomers of very close retention times. HPLC confirmed that the separation of the isomers was not possible at that time (Figure **3.6**).

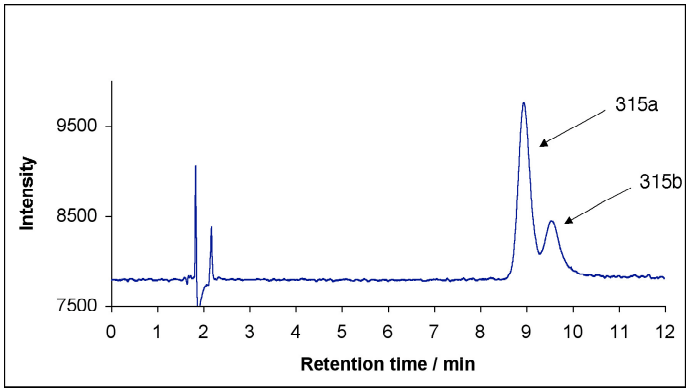

Figure 3.6 HPLC chromatogram for separation of **315a** and **315b** mixture (hexanes/ethyl acetate, 95:5)

LR MALDI-TOF mass spectrometry shows molecular mass signal (M^+) at m/z 1285.5 while the calculated for $C_{102}H_{60}$ is m/z 1285.5. UV-vis spectroscopic analysis of the **315a** and **315b** mixture shows two absorptions, the first absorption at 387 nm (ε = 139400 L mol^{-1} cm^{-1}), and the second absorption at 509 nm (ε = 38900 L mol^{-1} cm^{-1}). Thus, the mixture of **315a** and **315b** seems to exhibit

unique electronic characteristics resulting from the macrocyclic structures of the components.

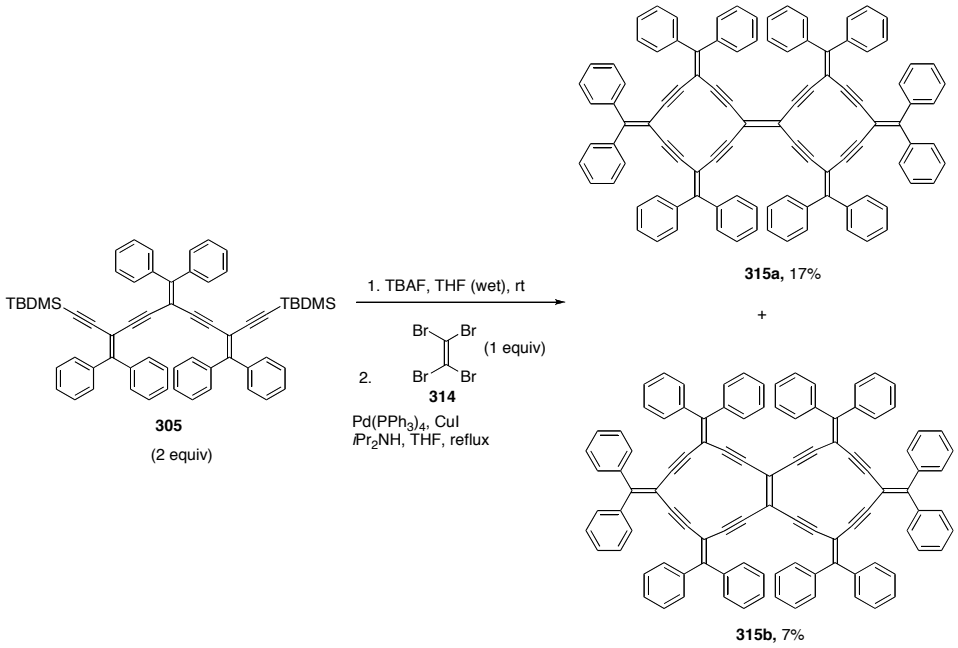

Scheme 3.16 A one-pot synthesis of **315a** and **315b**

Synthesis of the **315** mixture cleared doubt about the application of **314** to other members of this series, in particular bis[3]expanded radialene that was considered to be more strained and challenging. Thus, compound **303** was protodesilylated by TBAF in wet THF and the resulting terminal alkyne was added to a degassed solution of **314** and reacted under the standard Sonogashira protocol (Scheme **3.17**). The reaction mixture immediately turned dark red upon addition of the terminal alkyne. Separation of the crude reaction product on silica gel gave a red solid (the crude product of the reaction gave complicated preliminary TLC pattern). At least 8 spots were observed from TLC

analysis, one of which was expected to be the target molecule.

The red solid was subjected to separation on pre-coated silica gel plate (hexanes/CH_2Cl_2, 1:1) to give compound **316**, as a red-purple solid in 18% yield. The initial confirmation (molecular formula) came from LR MALDI-TOF mass spectrometry analysis. The product had very low solubility and it was difficult to get a quality ^{13}C NMR spectrum. After several attempts, however a relatively good quality spectrum was obtained; but one carbon still was missing in the spectrum due to the low solubility of the sample. Thus, the ^{13}C NMR spectrum shows 13 signals out of 14 expected signals. The most notable peaks are the alkyne carbons that resonate at 102.9, 101.5, and 96.1 ppm.

A trace amount of **316b** was separated from the product but it was not substantial enough for full characterization. Formation of **316a** rather than **316b** can also be explained by the higher strain in **316b** than **316a.** The synthesis of **316b** was not achieved through the mentioned synthetic route.

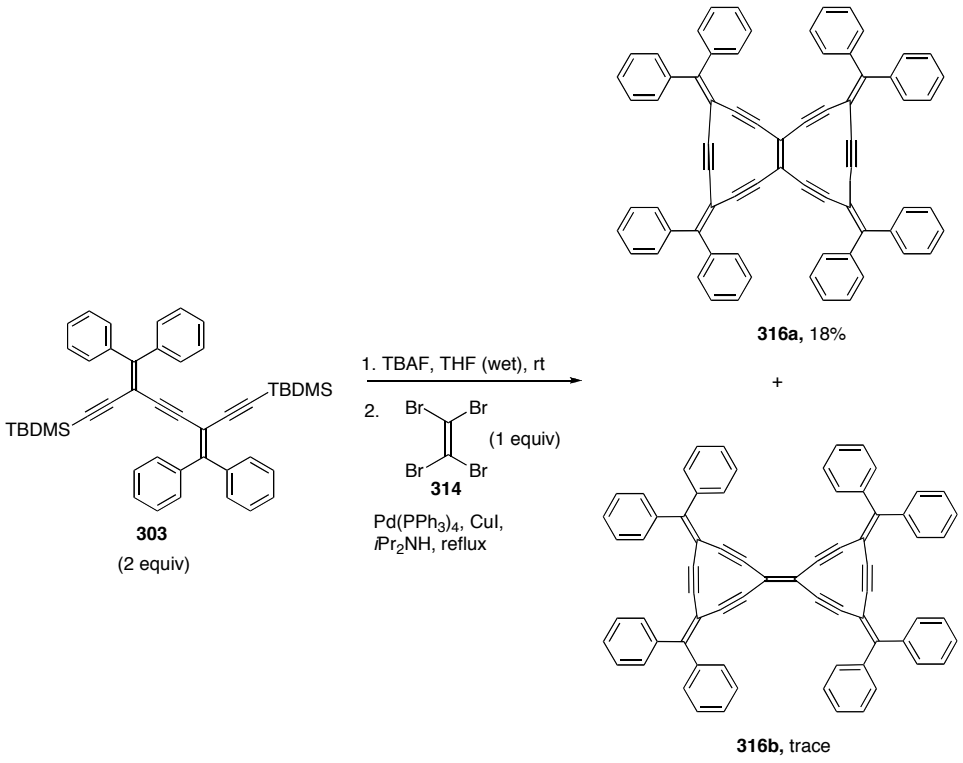

Scheme 3.17 Synthesis of **316a** and **316b**

According to the UV-vis spectroscopic analysis the high-energy region of the absorption spectrum of radiaannulene **316a** shows an absorption similar to that of radialenes **310, 311,** and **313** (λ_{max} = 381 nm, ε = 63000 L mol^{-1} cm^{-1}). λ_{max} is defined here as the lowest energy absorbance observed in the spectrum. The low-energy region was quite dissimilar from that of the other expanded radialenes mentioned above. Compound **316a** show two more absorptions, first at λ_{max} = 534 nm (ε = 19500 L mol^{-1} cm^{-1}) and second at λ_{max} = 572 nm (ε = 31700 L mol^{-1} cm^{-1}), which signifies a substantial lowering of the HOMO–LUMO gap. It is unlikely that this lowering of the HOMO–LUMO gap derives simply from an extension of the linearly conjugated segment of **316a**, since the absorption spectrum of oligodiacetylene **317** synthesized by Giesa and Schulz[14] showed a

λ_{max} = 418 nm, over 100 nm higher in energy than that of radiaannulene **316a**, despite the longer linear conjugated segment in **317**. Thus, it seems clear that the constrained, cross-conjugated framework of **316a** plays a major role in the electronic makeup of compound **316a**.[14a,b]

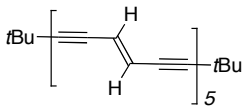

317

A cyclic voltammetry study of **316a** contrasts that of the expanded radialenes **310–312**, in that **316a** is more easily reduced and oxidized. This is consistent with the UV-vis absorption data that showed a smaller HOMO–LUMO gap for **316a**. More specifically compound **316a** shows a reversible one-electron reduction at –1.36 V and –1.71 V and a reversible one-electron oxidation event at 0.68 V (refer to page 113 for CV voltammograms).

Single crystals of compound **316a** suitable for X-ray crystallographic analysis were grown from diffusion of pentane to a THF solution at 4–5 °C. (CCDC #, 652688). X-ray analysis shows that the cyclic core of this molecule adopts a planar geometry (Figure **3.7**). The endocyclic alkylidene bond angles C7–C8–C10 at 105.7(3)° and C3–C4–C6 at 106.9(3)° are significantly smaller than those observed for either **310** or **311** and reflect the significant ring strain in the framework of **316a**. The alkyne bond angles of **316a** are also substantially reduced from optimal values, and ranged from 158.1(3)° to 173.6(4)° (average of 164.68°). Single crystals of compounds **315a** and **315b** suitable for X-ray

crystallographic analysis were grown from slow evaporation of a $CHCl_3$ solution at 4–5 °C (isomers were co-crystallized, CCDC #, 652687). The X-ray data revealed some interesting aspects of **315a** and **315b** solid structures. Neither **315a** nor **315b** is planar, both have a stretched chair conformation. The structure of **315a** shares many similarities to that of **311**, including C≡C–C bond angles that average 167.6° (range from 160.4° to 172.7°). Radiaannulene **315b**, is the next higher analogue of **316a**, and shows substantially less ring strain than **316a** with an average bond angle of 172.3° (range from 165.5 to 178.9°) and also internal alkylidene bond angles that were between 110 and 118°. A comparison of bond angles for structures **315a** and **315b** show that the bisradialene is clearly the more strained of the two (Figure **3.8**).[14a]

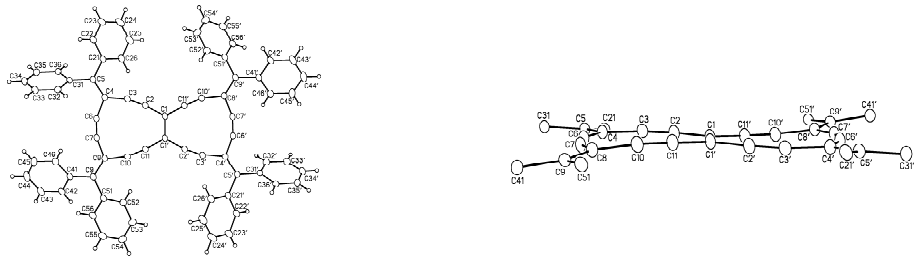

Figure 3.7 ORTEP plots for compound **316a** (only ipso carbons of pendent phenyl rings are shown for clarity, right structure)

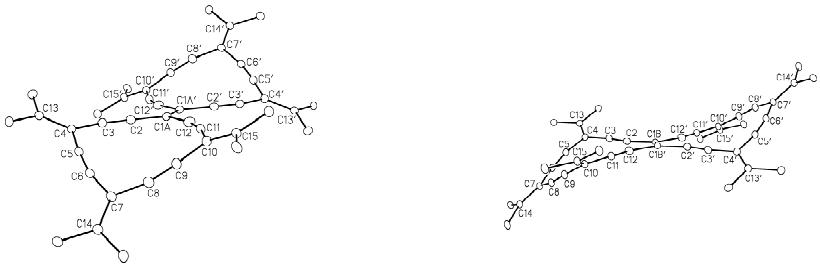

Figure 3.8 ORETP pots of compound **315a** and **315b** (only ipso carbons of pendent phenyl rings are shown for clarity)

3.6 Coupling reactions and possible side reactions

A deeper look into the coupling reactions toward formation of the expanded radialenes may help us to understand how these reactions work and what their obstacles are.

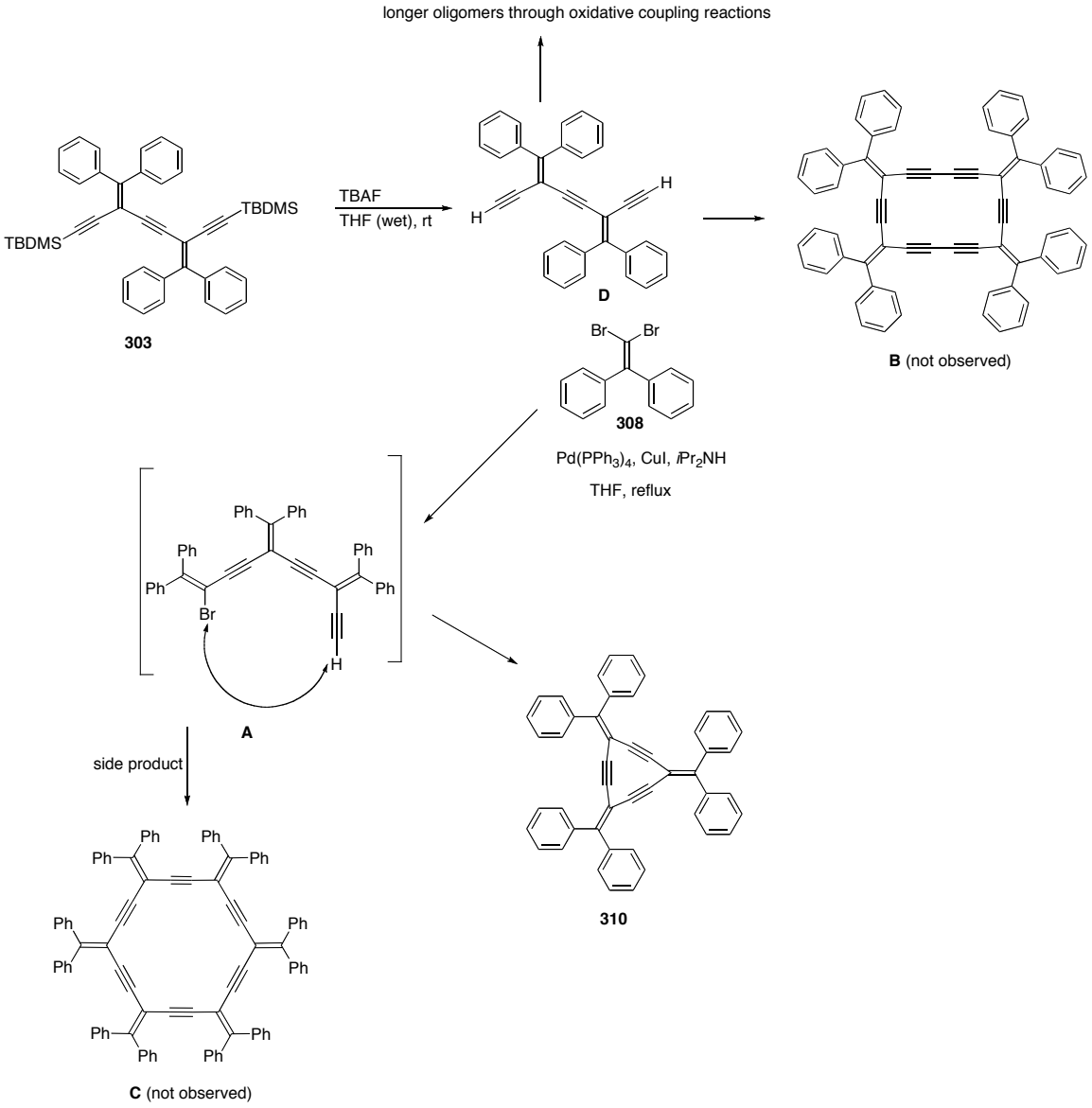

Scheme 3.18 Some possible parallel reactions during the synthesis of **310**

In particular, for the more strained expanded radialenes, the first step should be a single coupling between one of the terminal alkynes and one bromide of the dibromoolefin; that is, an intermolecular coupling as outlined by Scheme **3.18** for the synthesis of **310**.

Based on Scheme **3.18**, and for the sake of simplicity, three major side reactions are at least possible to occur in a parallel fashion. The major evidence for side reactions are side products that are recovered for all the Sonogashira cross coupling reactions. The terminal alkynes undergo oxidative coupling reactions to form higher oligomers; this side reaction is promoted by the presence of even a trace of O_2. While other factors could contribute to the oxidative coupling, O_2 is thought to be the main cause. Also, the terminal alkyne **D** could react to form compound **B**, as a result of dimerization (observed and characterized in Chapter **6**). Furthermore, the intermediate **A** has the opportunity to form a dimer **C** via cross coupling (not observed) rather than the formation of **310**.

The formation of [3]expanded radialene is the hardest among all these reactions because of the difficulty of the terminal alkyne and bromide to reach one another for the intramolecular cyclization reaction. The presence of two phenyl rings that are not in the same plane (twisted) apparently affects the outcome of this reaction significantly. It will be realized in the synthesis of [3]expanded radialene of fluorenylidene skeleton in Chapter **4**, how a planar dibromoolefin leads to a higher yield.

Use of the above discussion toward the synthesis of **316a** is summarized in Scheme **3.19**.

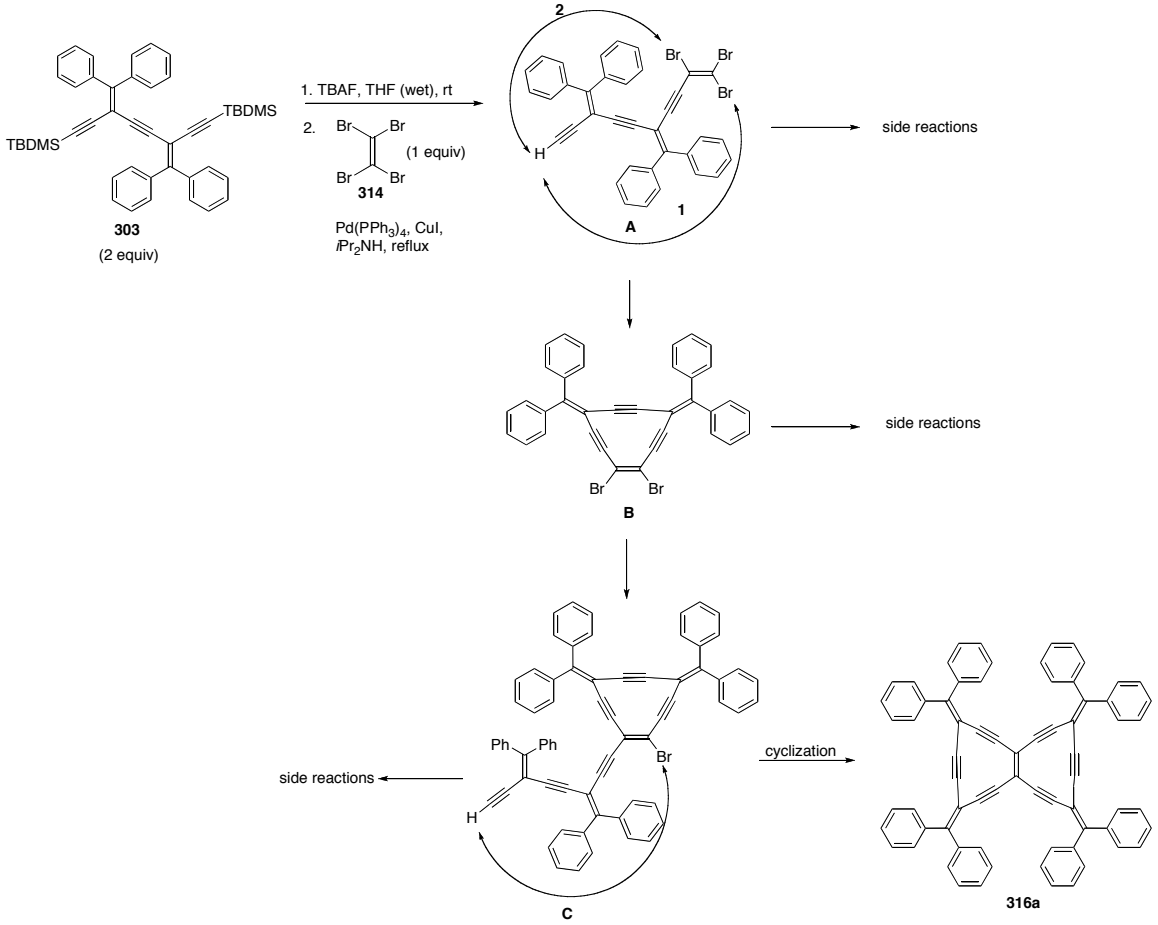

Scheme 3.19 Possible parallel reactions in the synthesis of **316a**

It is very simple to appreciate from Scheme **3.20** (simplified) how difficult it could be to synthesize **316a** in view of the many parallel reactions that might take place with higher or lower rates than the target reaction pathway. These side reactions, plus the side reactions from the terminal alkynes, could decrease the yield of the target molecule. As a rule of thumb, the coupling reaction of **314** with terminal alkynes, creates more side reactions than a coupling reaction of **308**

(four bromides versus two bromides). Therefore, for the synthesis of **316** and the coupling reaction in general, purification and characterization become more difficult and challenging when the products are present as mixtures of two isomers.

In general, the synthesis of highly strained cross-conjugated macrocycles such as **310** or **316a** is difficult to execute. The best ways to decrease the side reactions are to increase the purity of starting materials, optimize the activity of the palladium pre-catalyst, deoxygenate the reaction mixture thoroughly, and control the sequence in which reactants are added to the reaction vessel.

3.7 Synthesis of [6]expanded radialene

The synthesis of [6]expanded radialene **319** was carried out in a way similar to other radialenes as outlined in Scheme **3.20**. Unfortunately the major product was the result of the oxidative coupling (intramolecular cyclization)[5a] that gave macrocycle **318.** The yield of compound **319** was very low compared to **318**, and separation became very challenging due to similar R_f values of **318** and **319**. The **319** low yield is likely explained by the significant steric crowding originating from the 12 pendent phenyl rings that would reduce the ability of this macrocycle to approach the approximately planar conformation that would favor ring closure. Compound **319** was detected only via LR MALDI-TOF mass spectrometry while **318** was fully characterized, including X-ray crystallographic analysis. Single crystals of compound **318** suitable for X-ray crystallographic analysis were grown from slow evaporation of a THF solution at 4–5 °C. The

ORTEP plot of compound **318** is very similar to the [5]expanded radialene **312** that is an envelop shape (Figure **3.9**).

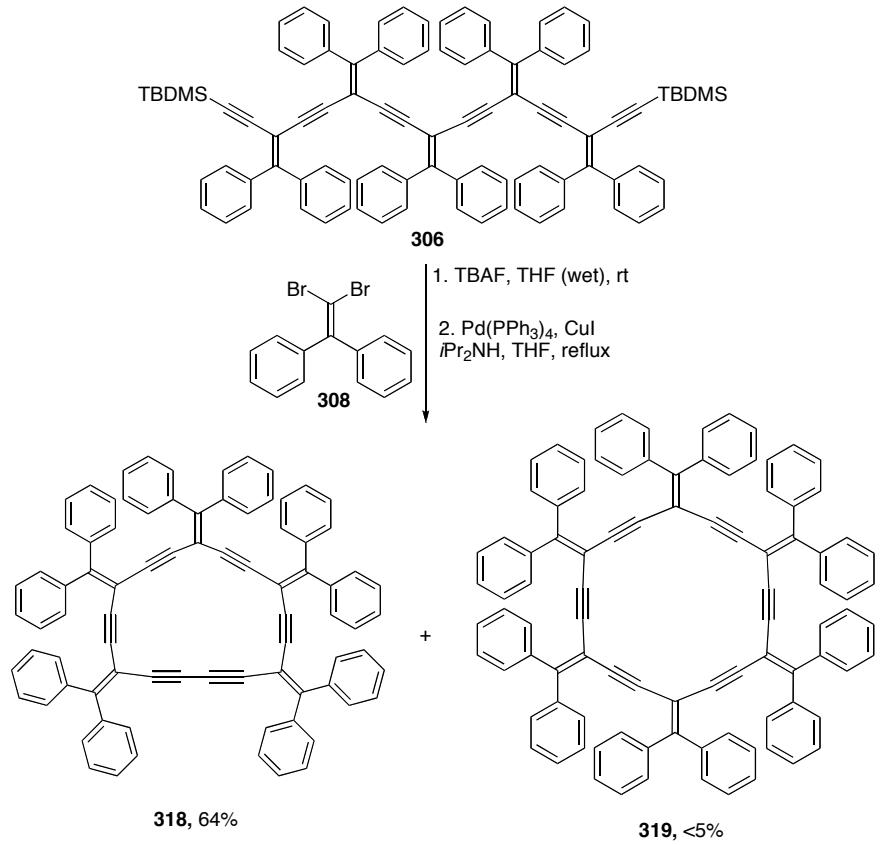

Scheme 3.20 Synthesis of compounds **318** and **319**

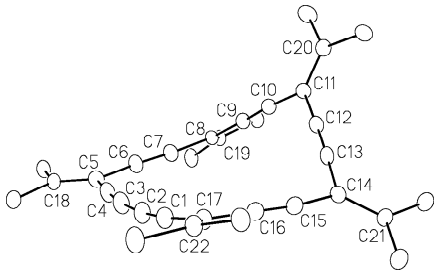

Figure 3.9 ORTEP plot of compound **318** (only ipso carbons of pendent phenyl rings are shown for clarity).

3.8 Synthesis of bis[5]expanded radialene (radiaannulene)

The last members of the bisradialene series, bis[5]expanded radialene **320a** and radiaannulene **320b**, were synthesized according to Scheme **3.21**. The dark orange solid compound was isolated in 16% yield.

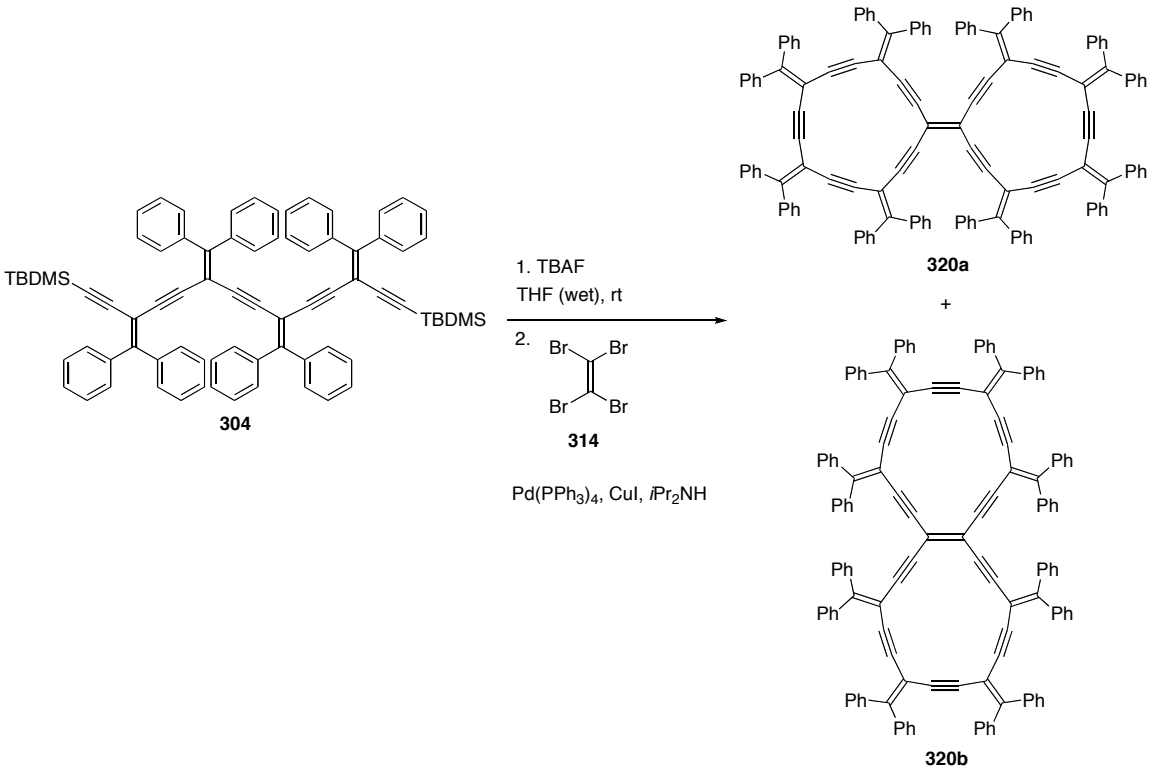

Scheme 3.21 Synthesis of **320a** and **320b**

The solubility of **320** was higher than the other bisradialenes, consequently, the characteristic alkyne carbons appeared more clearly in the NMR spectrum; they resonate at 98.8, 91.3, 90.8, 90.5, and 90.4 ppm. UV-vis spectroscopy shows an absorption at λ_{max} = 380 nm (ε = 82500 L mol^{-1} cm^{-1}). Single crystals of compound **320** were grown from slow evaporation of a $CHCl_3$ at

solution at 4–5 °C, but X-ray crystallographic analysis could not determine the identity of the compound, i.e., whether the product was **320a**, **320b**, or a mixture of the two isomers (the crystal was not quality for X-ray analysis). ^{13}C NMR spectrum of compound **320** showed only one compound due to the absence of extra peaks; however, there could be a small amount of a second isomer present that did not appear in the spectrum.

With regard to identity of **320** there will be discussed further in Chapter **5** where derivatization of the expanded radialenes through a stepwise approach is considered for the synthesis of a single isomer of a bisradialene such as **315a**. This approach could lead to more information about the structure of **320**.

3.9 Summary and comparisons for radialenes, bisradialenes, and radiaannulenes

This chapter focused on the synthesis and characterization of the second generation of the expanded radialenes (enyne radialenes). The basic radialenes can be summarized in terms of spectroscopic properties such as UV-vis that is shown in Figure **3.2**. The ^{13}C NMR spectra of **310**–**312** are exhibited in Figure **3.10**. Figure **3.10** shows how the chemical shifts change from [5]radialene to [3]radialene. As a result of their symmetry, the three radialenes **310**, **311**, and **312** each have only seven unique resonances in their ^{13}C NMR spectra. Of note is the consistent shift of particular resonances as a result of increased ring strain; this has been observed for other acetylenic macrocycles.[15] For example, the resonance of the exocyclic vinylidene carbon atom is the most diagnostic, and

this signal shifts upfield from 155 ppm for [5]radialene **312** to 146 ppm for the most strained [3]radialene **310**.[15]

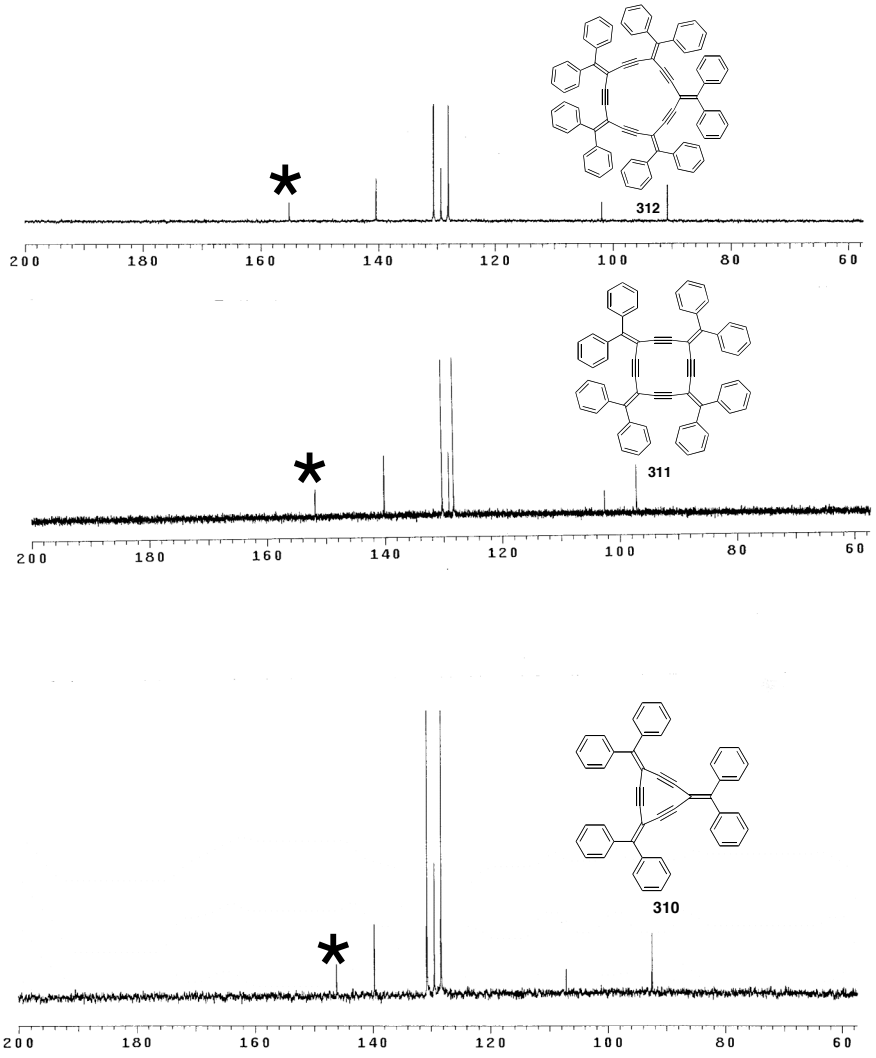

Figure 3.10 ^{13}C NMR spectra of the expanded radialenes **310**–**312** from bottom to top respectively (the shift of the relevant carbons alkylidene carbons are labeled with *, see text for discussion)

The use of tetrabromoethene was a breakthrough in the synthesis of bisradialenes. While the tetrabromoethene building block presented a very useful fragment toward the synthesis of both bisexpanded radialenes and

radiaannulenes, the lack of selectivity was a barrier to higher yields. As well the challenging separation of the isomers should not be forgotten. Nevertheless, the use of tetrabromoethene showed that it is possible to execute four coupling reactions simultaneously in a one-pot reaction for the synthesis of highly strained cross-conjugated macrocycles although as discussed before there are side reactions present to compete with the target reaction. The synthesis of **315a**, **315b**, and **316a** was accomplished and their identities confirmed by solid states X-ray analysis. In terms of UV-vis study of these compounds **316a** showed very interesting absorptions in the UV-vis range, particularly in the low energy region (Figure **3.11**). This was confirmed also by the electrochemistry measurement. Figure **3.12** shows cyclic voltammograms of **310**–**312**, and **316a** and Table **3.4** shows the redox potentials of these compounds.

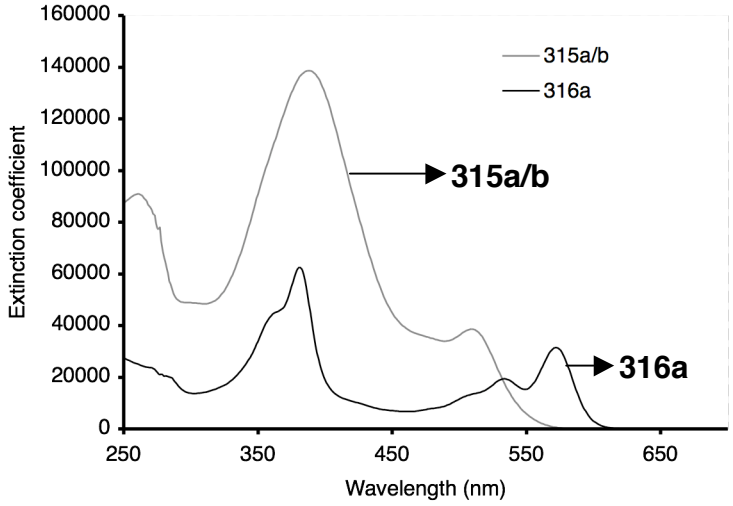

Figure 3.11 UV-vis spectra of compounds **315a/b** and **316a** measured in

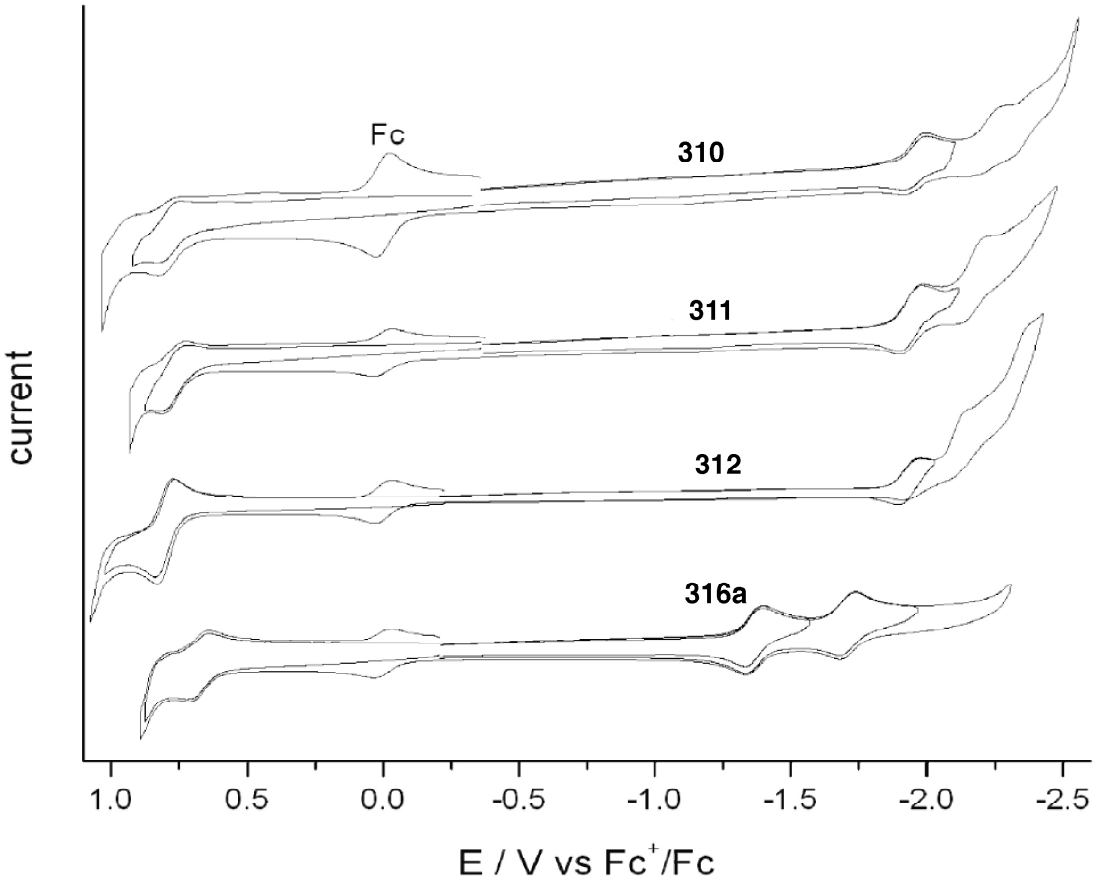

THF

Figure 3.12 Cyclic voltammograms of expanded radialenes **310–312** and **316a** Cyclic voltammetry measured in CH_2Cl_2 + 0.1 M nBu_4NPF_6 at a scan rate 100 mV s^{-1}. All potentials are reported versus the ferrocenium/ferrocene (Fc^+/Fc) couple.

As mentioned before, Figure **3.12** and Table **3.4** show compound **316a** is reduced and oxidized more easily than the radialene series **310**–**312** and also the UV-vis spectrum of compound **316a** in Figure **3.11** confirms this finding.[14a]

Table 3.4 Redox potentials of selected expanded radialenes[†]

Compound	Ep_c red_1	Ep_a red_1	$E_{1/2}$ red_1	Ep_a ox_1	Ep_c ox_1	$E_{1/2}$ ox_1
310	–1.99	–1.92	–1.96	0.82	0.75	0.79
311	–1.98	–1.91	–1.94	0.81	0.75	0.78
312	–1.98	–1.91	–1.94	0.83	0.76	0.80
316a	–1.40	–1.33	–1.36	0.71	0.64	0.68

[†]Cyclic voltammetry measured in CH_2Cl_2 + 0.1 M nBu_4NPF_6 at a scan rate 100 mV s^{-1}. All potentials are reported versus the ferrocenium/ferrocene (Fc^+/Fc) couple.

3.10 Conclusion

The synthesis of a new class of expanded radialenes and radiaannulenes has been demonstrated in this chapter. Macrocycles with incredibly strained conjugated enyne structures were synthesized by Sonogashira cross coupling reactions. UV-vis absorption spectroscopy indicates that the electronic characteristics of the expanded radialenes are related to their macrocyclic cross-conjugated framework, and that the more strained the structure, the more interesting the electronic properties. The new radialenes have been used without any concerns with regard to their stability in solid or solution phase for physical studies.

3.11 References

(1) (a) Zhang, W.; Moore, J. S. *Angew. Chem. Int. Ed.* **2006**, *45*, 4416–4439; (b) Tahara, K.; Tobe, Y. *Chem. Rev*. 2006, *106*, 5274–5290; (c) Gholami, M.; Tykwinski, R. R. *Chem. Rev.* **2006**, *106*, 4997–5027; (d) Spitler, E. L.; Johnson II, C. A.; Haley, M. M. *Chem. Rev*. **2006**,*106*, 5344–5386; (e) Meier, H. *Angew. Chem. Int. Ed.* **2005**, *44*, 2482–2506; (f) Höger, S. in Acetylene Chemistry (Eds.: Diederich, F. ; Stang, P. J.; Tykwinski, R. R.), Wiley-VCH, Weinheim, **2005**, Chapter 10; (g) Nielsen, M. B.; Diederich, F. *Chem. Rev.* **2005**, *105*, 1837–1867; (h) Yamaguchi, Y.; Yoshida, Z. *Chem. Eur. J.* **2003**, *9*, 5430–5440; (i) Bunz, U. H. F. *J. Organomet. Chem.* **2003**, *683*, 269–2876; (j) Grave, C.; Schlüter, A. D. *Eur. J. Org. Chem*. **2002**,

3075-3098; (k) Hopf, H. *Classics in Hydrocarbon Chemistry;* Wiley-VCH, **2000**; (l) Martin, R. E.; Diederich, F. *Angew. Chem. Int. Ed.* **1999**, *38*, 1350–1377.

(2) (a) Nielsen, M. B.; Schreiber, M.; Baek, Y. G.; Seiler, P.; Lecomte, S.; Boudon, C.; Tykwinski, R. R.; Gisselbrecht, J. P.; Gramlich, V.; Skinner, P. J.; Bosshard, C.; Günter, P.; Gross, M.; Diederich, F. *Chem. Eur. J.* **2001**, *7*, 3263–3280; (b) Boldi, A. M.; Diederich, F. *Angew. Chem. Int. Ed. Engl.* **1994**, *33*, 468–471.

(3) Tobe, Y.; Umeda, R.; Iwasa, N.; Sonoda, M. *Chem. Eur. J.* **2003**, *9*, 5549–5559.

(4) Zhao, Y.; Slepkov, A. D.; Akoto, C. O.; McDonald, R.; Hegmann, F. A.; Tykwinski, R. R. *Chem. Eur. J.* **2005**, *11*, 321–329.

(5) (a) Tykwinski, R. R.; Zhao, Y. *Synlett* **2002**, 1939–1953; (b) Eisler, S.; Tykwinski, R. R. *Angew. Chem. Int. Ed.* **1999**, *38*, 1940–1943.

(6) (a) Neidlein, R.; Winter, M. *Synthesis* **1998**, 1362–1366; (b) Corey, E. J.; Fuchs, P. L. *Tetrahedron Lett.* **1972**, *13*, 3769–3772; (c) Ramirez, F.; Desai, N. B.; McKelvie, N. *J. Am. Chem. Soc*. **1962**, *84*, 1745–1747.

(7) Gisselbrecht, J. P.; Moonen, N. N. P.; Boudon, C.; Nielsen, M. B.; Diederich, F.; Gross, M*. Eur. J. Org. Chem.* **2004**, 2959–2972.

(8) Lepetit, C.; Nielsen, M. B.; Diederich, F.; Chauvin, R. *Chem. Eur. J.* **2003**, *9*, 5056–5066.

(9) Rubin, Y.; Knobler, C. B.; Diederich, F. *Angew. Chem., Int. Ed. Engl*. **1991**, *30*, 698–700.

(10) Anthony, J.; Boldi, A. M.; Rubin, Y.; Hobi, M.; Gramlich, V.; Knobler, C. B.; Seiler, P.; Diederich, F*. Helv. Chim. Acta* **1995***, 78*, 13–45.

(11) Anthony, J.; Boldi, A. M.; Boudon, C. ;Gisselbrecht, J. P. ;Gross, M. Seiler, P.; Knobler, C. B.; Diederich, F. *Helv. Chim. Acta* **1995**, *78*, 797–817.

(12) Mitzel, F.; Boudon, C.; Gisselbrecht, J.-P.; Seiler, P.; Gross, M.; Diederich, F. *Helv. Chim. Acta* **2004**, *87*, 1130–1157.

(13) Mitzel, F.; Boudon, C.; Gisselbrecht, J.-P.; Seiler, P.; Gross, M.; Diederich, F. *Chem. Commun.* **2003**,1634–635.

(14) (a) Gholami, M.; Melin, F.; McDonald, R.; Ferguson, M. J.; Echegoyen, L.; Tykwinski, R. R. *Angew. Chem. Int. Ed.* **2007**, *46*, 9081–9085; (b) Giesa, R.; Schulz, R. C. *Polym. Int.* ***1994***, *33*, 43–60.

(15) Eisler, S.; McDonald, R.; Loppnow, G. R.; Tykwinski, R. R. *J. Am. Chem. Soc*. **2000**,*122*, 6917–6928.

Chapter 4:

Synthesis and Characterization of Functionalized Expanded Radialenes

4.1 Functionalized expanded radialenes: objectives and targets

The synthesis and characterization of the second generation of expanded radialenes (enyne radialenes), and the synthesis of bisexpanded radialenes and the radiaannulenes has been discussed in Chapter **3**. The strategy for synthesis of the expanded radialenes is based on the reaction of an *iso*-polydiacetylene and a dibromoolefin under the Sonogashira coupling protocol. The incorporation of either functionalized *iso*-polydiacetylenes or functionalized dibromoolefins in the coupling reaction can afford functionalized expanded radialenes. First a new series of dibromoolefins has been synthesized that carry functional groups and used in the synthesis of functionalized expanded radialenes. The presence of the functional groups provides a new focus in the chemistry of expanded radialenes. Whether the expanded radialenes containing functional groups are stable and suitable for further physical studies are addressed in this chapter. The functional groups effects on the reaction yields and how their presence might change the electronic and optical properties of the radialenes also have been investigated. These are the main questions that are addressed in this chapter.

These studies are based on the synthesis of [3]–, and [4]expanded radialenes that incorporate six functional groups: CF_3, triisopropylsilylethynyl, fluorenylidene, tetraphenylcyclopentadienylidene, MeO, and NO_2.

4.2 Synthesis of the functional expanded radialenes incorporating the CF_3

The synthesis of dibromoolefins has been discussed in Chapter **1** and it is based on the reaction of a mixture of PPh_3 and CBr_4 with a ketone in solvents such as benzene or dichloromethane either at room temperature or at elevated temperature (under reflux).[1] Some ketones are available commercially, such as benzophenone and benzophenone substituted with CF_3 or NO_2 groups in the meta position. The synthesis of functionalized expanded radialenes began with the synthesis of dibromoolefin with a meta CF_3 group. Ketone **400** (commercially available) reacted with PPh_3 and CBr_4 in benzene at reflux yielding **401** as an off-white solid according to Scheme **4.1.**[1]

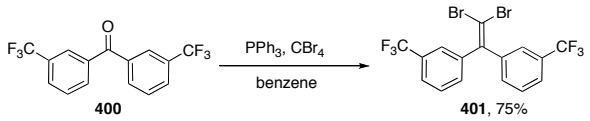

400 **401**, 75%

Scheme 4.1 Synthesis of dibromoolefin **401**

Compound **401** then reacted with trimethylsilylacetylene in the presence of $Pd(PPh_3)_2Cl_2$ giving **402** in 90% yield as a white solid. (Scheme **4.2**)

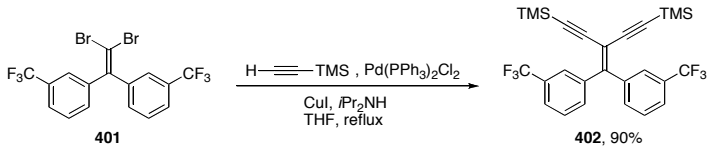

401 **402**, 90%

Scheme 4.2 Synthesis of compound **402**

Compound **402** was protodesilylated in the presence of K_2CO_3 in THF/MeOH (1:1) and reacted with two equivalents of triflate **300** in the presence of $Pd(PPh_3)_4$ in THF at reflux giving trimer **403** in 75% as a yellow solid (Scheme **4.3**).

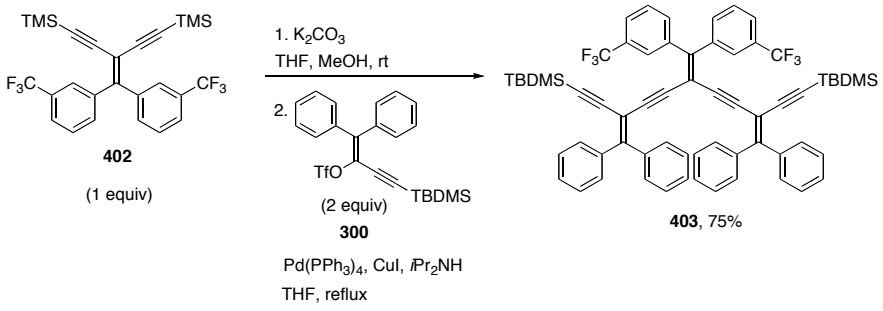

Scheme 4.3 Synthesis of trimer **403**

Compound **403** was protodesilylated by TBAF in wet THF at room temperature and reacted with **401** under the Sonogashira protocol to give the first synthesized functionalized [4]expanded radialene of the new series, **404**, in 65% yield as a yellow solid (Scheme **4.4**).

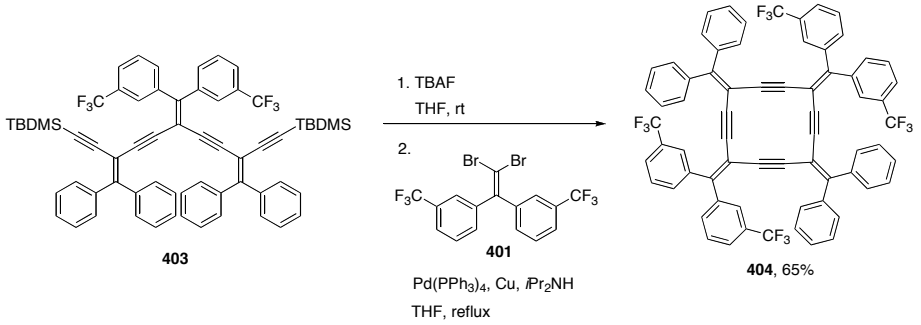

Scheme 4.4 Synthesis of radialene **404**

Compound **404** is more soluble than **311** because of the presence of CF_3 substituents; this is an advantage for separation and characterization. ^{13}C NMR spectroscopy shows how the radialene **404** is less symmetrical compared to **311**

due to the presence of CF_3 substituents. The ^{13}C NMR spectrum shows characteristic alkyne carbons at 98.4 and 96.1 ppm for radialene **404** due to the presence of C2 axis of symmetry. Finally, the^{13}C NMR spectra also show characteristic patterns of coupling to carbon due to the presence of fluorine (^{19}F is NMR active with nuclear spin = 1/2; it has a natural abundance of 100%). The coupling constants $^1J_{C\text{-}F}$ is about 272 Hz, $^2J_{C\text{-}F}$ is about 34 Hz and $^3J_{C\text{-}F}$ is in the range of 3 to 6 Hz, and is similar for all the fluorinated compounds that are discussed in this chapter. ^{19}F NMR spectrum of compound **404** shows a singlet at –63.5 ppm in CD_2Cl_2.

Single crystals of compound **404** suitable for crystallography were grown as a result of pentane diffusion to a chloroform solution of the compound **404** at 4–5 °C (Figure **4.1**). X-ray data for **311** and **404** were compared with regard to the cyclic core of these molecules that are summarized in Table **1**. The analysis from solid-state structures reveals the effects of CF_3 substituents on the bond length and bond angles of radialene **404** compared to radialene **311** (Figure **4.1**).

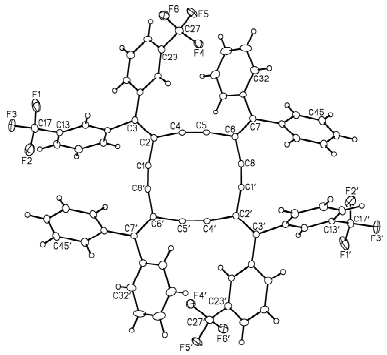

Figure 4.1 ORTEP plot for radialene **404**

Table 4.1 Selected bond lengths and angles for radialenes **311** and **404**

	311	**404**
C5–C6–C8 angle	110.40(12)°	110.10(14)°
C4–C5–C6 angle	166.65(14)°	170.63(18)°
C7–C6–C8 angle	124.99(13)°	126.45(16)°
C1–C2–C4 angle	----------	111.08(15) °
C8–C6–C7–C31 torsion angle	172.11(14)°	169.97(17)°
C1–C2–C3–C21 torsion angle	----------	177.75(17)°
C4–C5 bond length	1.2000(19) Å	1.201(2) Å

Based on the above table, the alkyne bond angle is more contracted in radialene **311** compared to radialene **404** but the vinylidene angle is smaller in radialene **404.** The alkyne bond length is the same for both radialenes **404** and **311**. The synthesis of **404** encouraged us to synthesize other derivatives of this series. Also, one of our interests was to know whether different substituents could affect the reaction yield or not.

Compound **305** was desilylated by TBAF in THF at room temperature and reacted with **401** in a one to one ratio according to the general Sonogashira cross coupling protocol to give radialene **405** as a yellow solid in 75% yield, outlined in Scheme **4.5**.

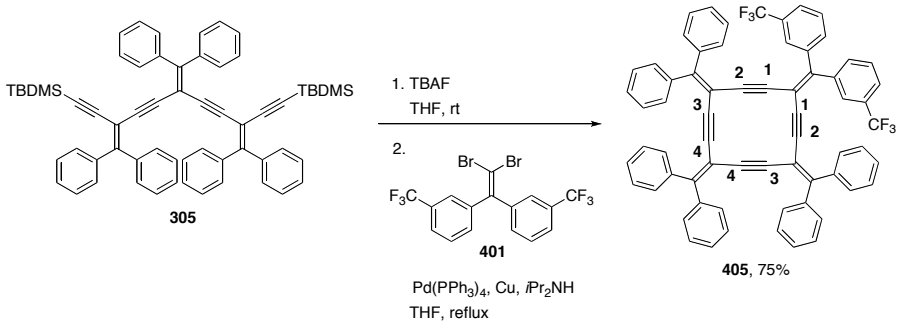

Scheme 4.5 Synthesis of radialene **405**

Compound **405** carries CF_3 only at one corner of the macrocycle making it unsymmetrical compared to radialenes **311** and **404** with regard to the number of alkyne carbons but the radialene **405** still has C2-axis of symmetry. ^{13}C NMR spectrum of compound **405** shows characteristic alkyne carbons at 98.8, 97.4, 96.7, and 95.8 ppm that matches the expected number of alkyne carbons according to symmetry (Scheme **4.5**). ^{19}F NMR spectrum shows a signal at –63.4 ppm as a result of fluorine atoms. HR MALDI-TOF mass spectrometry confirms a molecular ion (M^+) at m/z 944.28598 while the calculated molecular ion is m/z 944.28777.

No crystals were obtained for X-ray crystallography despite many efforts to grow single crystals in different solvents and conditions.

The synthesis of **404** and **405** provided a reason to complete the series with a focus on the more strained, [3] expanded radialene.

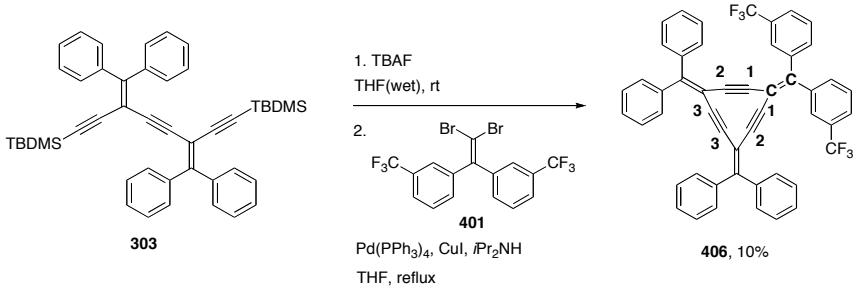

Scheme 4.6 Synthesis of radialene **406**

Oligomer **303** was protodesilylated in the presence of TBAF in THF at room temperature and reacted with **401** in the presence of $Pd(PPh_3)_4$ giving **406** in low yield of 10% as a yellow solid (Scheme **4.6**).

^{13}C NMR spectrum of **406** in CD_2Cl_2 shows characteristic alkyne carbons at 94.3, 92.2, and 91.1 ppm with approximately the same relative intensities (1:1:1); consistent with the symmetry of radialene **406**. ^{19}F NMR spectroscopy in $C_2D_2Cl_4$ shows a fluorine signal at –63.1 ppm. Based on the intensity of peaks and chemical shifts (refer to radialenes **310**–**312**) two characteristic carbons belonging to the vinylidene fragment (bold carbons) that carry the CF_3 rings resonate at 142.3 (exocyclic) and 110.2 (endocyclic) ppm compared to the other vinylidene carbons that resonated at 147.2 and 106.5 ppm. Electron impact mass spectrometry (HR) confirms a molecular ion (M^+) at m/z 742.2104 while that calculated for $C_{50}H_{28}F_6$ is m/z 742.2095.

So far a series of CF_3 radialenes has been synthesized and the yields are reasonable for the [4]radialenes. Apparently, the presence of the CF_3 groups has caused a dramatic change and therefore low yield for [3]radialene **406**.

4.3 UV-vis and electrochemical studies of the CF_3 radialenes

Uv-vis spectroscopy of **404** in THF did not show any change in terms of λ_{max} at 376 nm (ε = 120400 L mol^{-1} cm^{-1}) compared to radialene **311**. λ_{max} is defined here and through this chapter as the lowest energy absorbance observed in the spectrum. Cyclic voltammetry of **404** was measured in CH_2Cl_2. Radialene **404** shows three reductions, first at –1.80, second at –2.01 and the third reduction at –2.42 V. Also it shows two oxidations the first at 0.93 and the second at 1.14 V. The presence of CF_3 causes **404** to be reduced more easily compared

to **311**. Radialene **404** is harder to be oxidized than **311**; **404** shows oxidation at 0.93 and 1.14 V compared to 0.8 V for **311**.

UV-vis spectroscopy of **405** as measured in THF shows λ_{max} at 376 nm (ε = 81800 L mol^{-1} cm^{-1}). Cyclic voltammetry of **405** in CH_2Cl_2 shows two reductions, the first at –1.79 and second at –2.02 V as well as a single oxidation at 0.79 V (refer to page 151 for CV voltammograms).

Radialenes **404** and **405** are similar in terms of redox properties (**404** has one more reduction). A cyclic voltammerty comparison among [4]expanded radialenes **404**, **405**, and **311**(reduction at –2.0 V) reveal that **404** and **405** are reduced more easily than **311** due to the presence of CF_3 groups as electron acceptor (refer to page 151 for CV voltammograms). Figure **4.2** shows UV-vis spectra of radialenes **404** and **405** measured in THF.

UV-vis spectroscopy of radialene **406** shows a λ_{max} = 363 nm (ε = 19200 $Lmol^{-1}cm^{-1}$) and a λ_{max} = 412 nm (ε = 18800 L mol^{-1} cm^{-1}). Compounds **406** and **310** absorb at relatively similar wavelengths. Cyclic voltammetry of the radialene **406** shows one-electron reduction at –2.15 and –2.28 and –2.45 V. The first reduction is reversible, the second reduction is quasi-irreversible, and the third reduction is irreversible and not well defined. Compound **406** shows an oxidation at 1.08 V (refer to page 152 for CV voltammograms). The cyclic voltammetry study of **406** shows one-electron reductions, similar to **310** (–1.99, –2.12 and –2.25 V). However, it is clearly harder to reduce **406** relative to **310**, the first reduction is at –2.15 V for **406** and at –1.99 V for **310**. While the CF_3 is electron

withdrawing group and it should be easier to reduce **406** compared to **310** but this is not the case and the origin of this contrast is unclear.

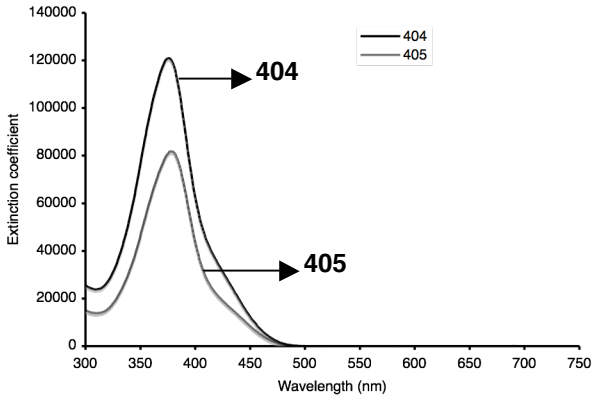

Figure 4.2 UV-vis spectra of radialenes **404** and **405** measured in THF

4.4 Synthesis and characterization of fluorenylidene expanded radialenes

To extend the scope of the radialene synthesis, incorporation of the fluorenylidene unit into the framework of expanded radialenes is logical because fluorenylidene framework is planner compared to diphenylalkylidene framework. This planarity should consequently reduce the steric influence of twisted diphenyl rings during cyclization. Also, a fluorenylidene expanded radialene is anticipated to have a longer linear cross-conjugated fragment and therefore its UV-vis absorption should exhibit a bathochromic shift.

The commercially available ketone 9-fluorenone reacts with PPh_3 and CBr_4 in heptanes under reflux to give dibromoolefin **407** in 50% yield as a pale yellow solid (Scheme **4.7**).[2]

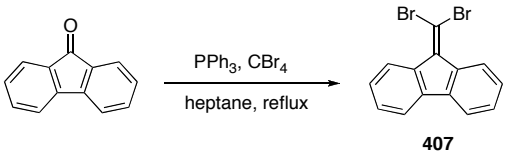

Scheme 4.7 Synthesis of dibromoolefin **407**

A major difference between **407** and **308** is that **308** has twisted phenyl rings while dibromoolefin **407** is entirely planar. Figure **4.3** shows two views of solid-state structure of the dibromoolefin **407**.

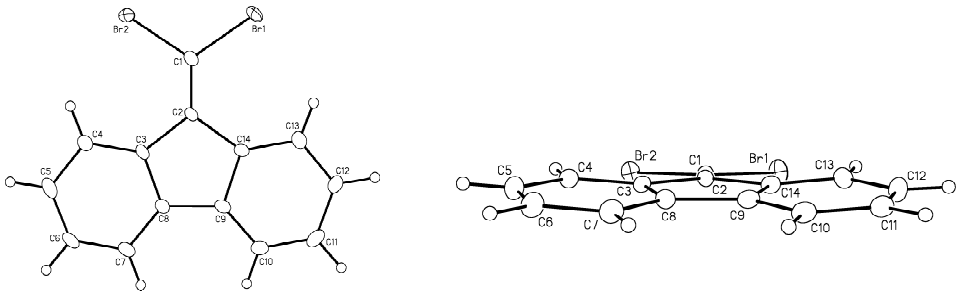

Figure 4.3 Two ORTEP plots of compound **407**

The synthesis of a [4]expanded radialene incorporating **407** was initiated by adding protodesilylated **305** to a degassed mixture of **407** under the Sonogashira protocol to give radialene **408** as a yellow solid in 79% yield (Scheme **4.8**).

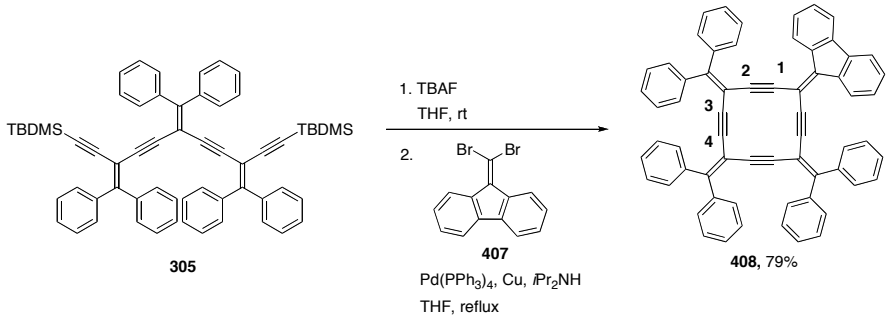

Scheme 4.8 Synthesis of radialene **408**

^{13}C NMR spectrum of compound **408** reveals alkyne carbons at 104.3, 102.8, 97.4 and 96.7 ppm (carbons **1**–**4**). HR MALDI-TOF mass spectrometry shows a molecular ion at m/z 806.29551 while that calculated molecular ion for $C_{64}H_{38}$ is m/z 806.29580.

The synthesis of another member of the [3]expanded radialene series with the fluorenylidene framework is discussed here. Dimer **303** was protodesilylated in the presence of TBAF in wet THF at room temperature and added to a degassed mixture of **407** under the Sonogashira cross coupling protocol, giving **409** as a yellow solid in 45% yield (Scheme **4.9**). The radialene **409** reaction yield has been the highest among the discussed [3]expanded radialenes so far; this clearly shows the effect of the planner fluorenylidene fragment. ^{13}C NMR spectrum of compound **409** shows characteristic alkyne carbons at 99.9, 92.4 and 90.6 ppm (carbon **1**–**3**). Electron impact mass spectrometry (HR) shows a molecular ion (M^+) at m/z 604.21912 while the calculated value for $C_{48}H_{28}$ is 604.21912.

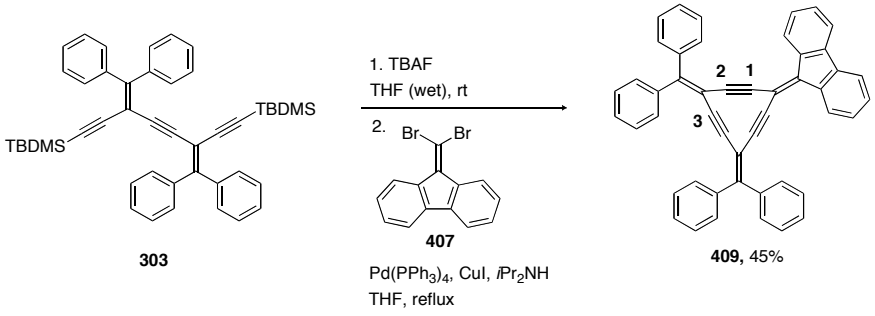

Scheme 4.9 Synthesis of [3]expanded radialene **409**

4.5 UV-vis and electrochemical studies of fluorenylidene radialenes

A UV-vis spectroscopic study of **408** in THF shows one absorption at λ_{max} = 393 nm (ε = 86500 L mol^{-1} cm^{-1}) with a shoulder around 468 nm. The absorption of radialene **408** shifted toward lower energy compared to **311**, mainly because of extension of the linear cross-conjugated fragment of the macrocycle **408**. Cyclic voltammetry of compound **408** shows reductions at –1.51, –1.81, and –2.37 V, the first two reversible and the third one irreversible. Oxidation events are observed at 0.83 and 1.01 V similar to that found for **311** (refer to page 151 for CV voltammograms). However, the radialene **408** is reduced more easily compared to **311**. Efforts to grow single crystals did not succeed.

A UV-vis spectroscopic study of radialene **409** shows absorptions at λ_{max} = 383 nm (ε = 16100 L mol^{-1} cm^{-1}), λ_{max} = 447 nm (ε = 14100 L mol^{-1} cm^{-1}), and λ_{max} = 474 nm (ε = 12000 L mol^{-1} cm^{-1}). This is the first [3]radialene that show three absorptions, The presence of the fluorenylidene is clearly responsible for extra absorption but the nature of this phenomenon is not clear yet.

Cyclic voltammetry of radialene **409** shows reductions at –1.55, –1.88, and –2.03 V, all are one-electron reductions (refer to page 152 for CV voltammograms). Thus, **409** is reduced at lower potential than **310**. It is worth mentioning that the third reduction of **409** (–2.03 V) is close the first reduction of **310** (–1.99, –2.12 and –2.25 V). Radialene **409** shows first oxidation at 0.88 and the second oxidation at 1.13 V that are very similar to those of [3]radialene **310**. Figure **4.4** shows the UV-vis spectra of [3]radialenes of **406** and **409** that

measured in THF.

Generally, the fluorenylidene radialenes were synthesized in higher yields than the radialenes with diphenyl rings (45% and 32% for **409** and **310**, respectively, and 79% and 75% for **408** and **311**, respectively).

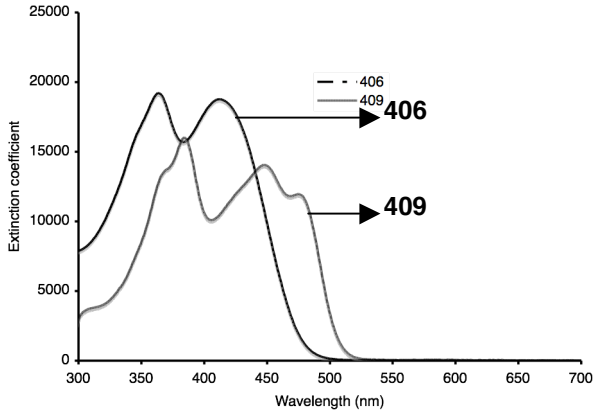

Figure 4.4 UV-vis spectra of [3]radialenes **406** and **409** measured in THF

4.6 Synthesis of functional expanded radialenes (triisopropylsilylethynyl groups)

The study of the optical and electronic properties of the functionalized expanded radialenes that carry CF_3 or fluorenylidene functionalities has provided new insight into the ability to alter HOMO–LUMO gaps for these marcorocyclic compounds from a synthetic perspective. One of the most desirable functional groups would be triisopropylsilylethynyl as an exocyclic substituent in the expanded radialene framework. The presence of the TIPS group could provide a new series of radialenes for the synthesis of new expanded radialene derivatives through protodesilylation and further cross coupling reactions.

For this target it is required to have dibromoolefin **410** with the triisopropylsilylethynyl groups which was synthesized according to the method reported by Diederich and coworkers (Scheme **4.10**).[3]

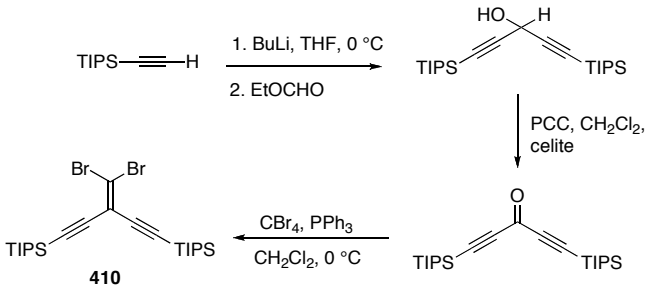

Scheme 4.10 Synthesis of dibromoolefin **410**

The first target was [4]expanded radialene **411**. Oligomer **305** was protodesilylated in the presence of TBAF in wet THF at room temperature. The resulting product was added to a degassed mixture of **410** and reacted under the Sonogashira coupling protocol to give **411** as a yellow solid in 78% yield (initial attempt, the yield was 70%, Scheme **4.11**). The presence of the trialkylsilylethynyl end-capped groups makes **411** more soluble in common organic solvents relative to the other [4]expanded radialenes. ^{13}C NMR spectrum of compound **411** shows characteristic alkyne carbons at 103.8, 102.1, 102.0, 96.6, 96.5 and 96.3 ppm (Scheme **4.11**). HR MALDI-TOF mass spectrometry of radialene **411** shows a molecular ion (M^+) at m/z 1016.51562, while the mass to charge ratio calculated for $C_{74}H_{72}Si_2$ is 1016.51671.

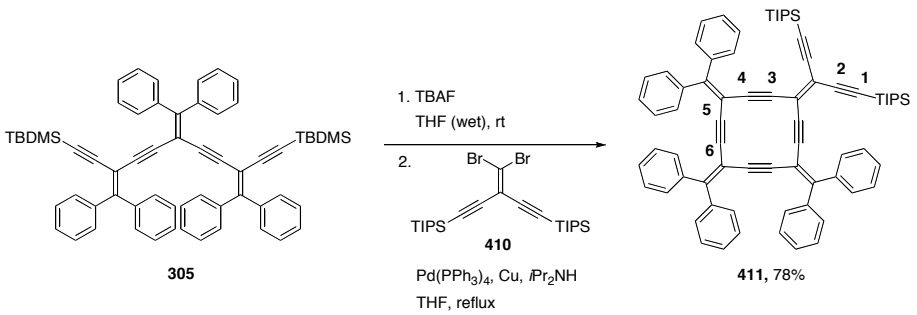

Scheme 4.11 Synthesis of radialene **411**

The [3]expanded radialene, was synthesized according to Scheme **4.1**. Dimer **303** was protodesilylated in the presence of TBAF in wet THF at room temperature. The resulting terminal alkyne moiety was added to a degassed mixture of **410** and reacted under the general Sonogashira protocol. Purification of the crude reaction product by chromatography gave **412** as a yellow solid in 33% (initial attempt, the yield was 18%, Scheme **4.12**). ^{13}C NMR spectrum shows characteristic carbons at 103.7, 102.7, 99.9, 92.0, and 91.6 ppm as well as two peaks of the vinylidene carbons (that carry the TIPS-ethynyl groups, carbons **1** and **2**), appear at 107.2 and 123.5 ppm (Scheme **4.12**).

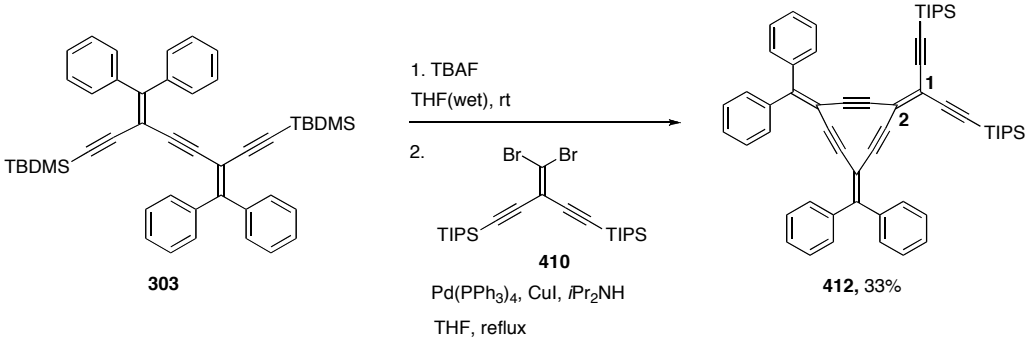

Scheme 4.12 Synthesis of radialene **412**

4.7 UV-vis and electrochemical studies of the triisopropylsilylethynyl radialenes

The UV-vis spectrum of radialene **411** (in THF) shows one absorption at λ_{max} = 388 nm (ε = 47500 L mol^{-1} cm^{-1}). Cyclic voltammetry of radialene **411** was carried out in CH_2Cl_2 and shows reductions at –1.58 and –1.88 V (refer to page 192 for CV voltammograms). The first reduction is reversible, and also there is a unique and surprisingly multi-electron oxidation at 0.92 V.

The UV-vis spectrum of radialene **412** measured in THF shows an absorption at λ_{max} = 378 nm (ε = 42800 L mol^{-1} cm^{-1}) and a second absorption at λ_{max} = 430 nm (ε = 31800 L mol^{-1} cm^{-1}). Cyclic voltammetry of radialene **412** in CH_2Cl_2 exhibits reductions at –1.59, –1.98, and –2.2 V and also oxidations at 0.94 and 1.19 V (refer to page 152 for CV voltammograms).

4.8 Synthesis of [3]expanded radialene containing phenylethynyl groups and its related cycloaddition product

We were interested in exploring the expansion of the π-electron system or increasing the length of the linear conjugated fragment of the expanded radialenes. This could accomplished either via incorporation of a planner fragment like radialene **408** and **409** or via insertion of alkyne units outside the cyclic core of expanded radialene. Here we describe using a new dibromoolefin, **413**, in the synthesis of an expanded radialene framework; **413** was synthesized according to Scheme **4.13**.[4]

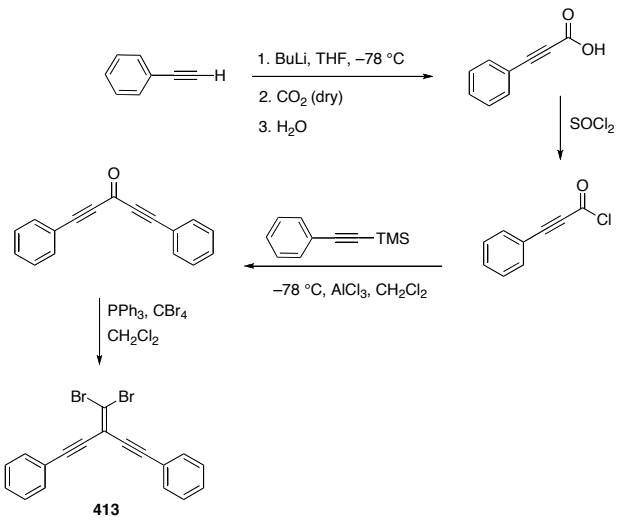

Scheme 4.13 Synthesis of dibromoolefin **413**

Dimer **303** was protodesilylated in the presence of TBAF in wet THF at room temperature. The resulting product was added to a degassed mixture of **413** and the mixture was subjected to the Sonogashira protocol. Purification of the crude reaction product by chromatography gave two products; radialene **414** as an orange solid in 40%, yield, and a radialene derivative **415** as a yellow solid in 8% yield, the result of two-fold [2+2] cycloaddition reaction of the radialene **414** and the dibromoolefin **413** (Scheme **4.14**).

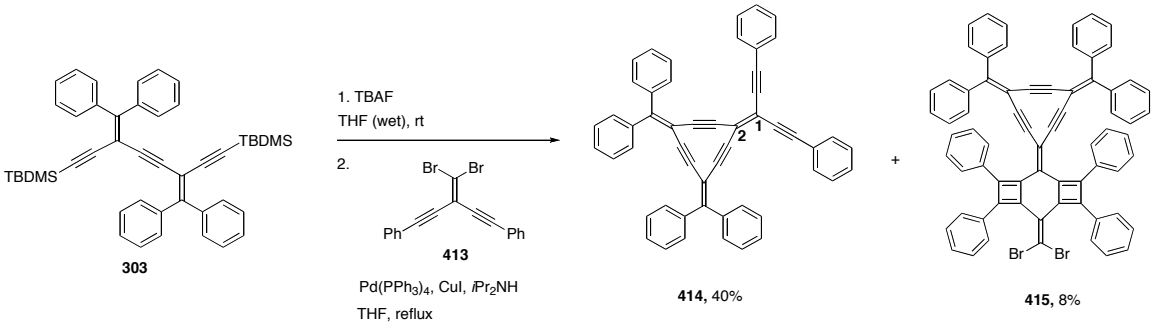

Scheme 4.14 Synthesis of radialene **414** and **415**

The ^{13}C NMR spectrum of **414** exhibits the characteristic alkyne carbons at

100.1, 99.2, 92.2, 91.8, and 87.2 ppm and two peaks belonging to the vinylidene carbons (carrying the phenylethynyl group) at 123.8 and 106.8 ppm (Scheme **4.14**, carbons **1** and **2**). The chemical shifts and intensity of the two peaks are very similar to peaks belonging to **412**, therefore, they might be considered as important evidence for the identity of unsymmetrical [3]expanded radialenes in general. HR MALDI-TOF mass spectrometry shows a molecular ion (M^+) at m/z 654.23448 while the mass to charge ratio calculated for $C_{52}H_{30}$ is 654.23420. UV-vis spectroscopic study of **414** measured in THF shows absorptions at λ_{max} = 388 nm (ε = 35100 L mol^{-1} cm^{-1}), λ_{max} = 457 nm (ε = 29500 L mol^{-1} cm^{-1}), and λ_{max} = 482 nm (ε = 27000 L mol^{-1} cm^{-1}). As discussed above, the presence of alkyne units extends the π-system and consequently the absorptions of **414** are shifted to longer wavelengths. Cyclic voltammetry of radialene **414** in CH_2Cl_2 shows reductions at –1.42, –1.80, and –1.89 V and oxidations at 0.92 and 1.16 V (refer to page 152 for CV voltammograms). Generally, radialene **414** is easier to reduce and harder to oxidize than radialene **310**. Also, radialene **414** is reduced more easily than **412**, with the first reduction of **414** at –1.42 compared to –1.55 for **412**.

Single crystals of compound **414** suitable for X-ray crystallographic analysis were grown from slow evaporation of a mixture of acetone and CH_2Cl_2 at 4–5 °C. The crystal structure of **414** is the first solid-state structure among the [3]expanded radialenes, a long awaited achievement. ORTEP plot of compound **414** and its packing are shown in Figure **4.5**.

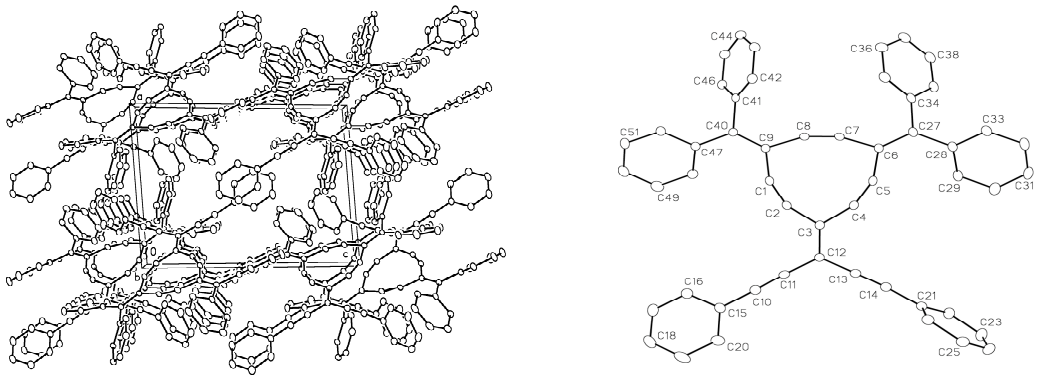

Figure 4.5 Solid-state packing and ORTEP plot for **414** (hydrogens removed for clarity)

The most notable parameters from the solid-state structure of **414** is alkyne bond angle C6–C5–C4 at 155.59(14)° or C3–C2–C1 at 156.20(15)° is one of the most contracted alkyne angles reported to date.[5] Also, the endocyclic vinylidene angles are for C7–C6–C5 103.73(12)° and for C2–C3–C4 107.68(12)°. The alkyne bond length of **414** is 1.210(2) Å in the cyclic core, basically it is very close to the alkyne bond length in the radialene **311**.

The cycloaddition reaction observed for compound **414** was not the first such observation. The first cycloaddition reaction observed was for the reaction of [3]expanded radialene **310** with xylene (refluxing xylene), however, these products were confirmed by mass spectrometry only. Throughout this research, the cycloaddition reaction was observed only and exclusively for [3]expanded radialenes. The first confirmation of the formula of the byproduct compound **415** came from HR MALDI-TOF mass spectrometry that showed a molecular ion (M^+) at m/z 1038.14853 while the mass to charge ratio calculated for $C_{70}H_{40}Br_2$ is

1038.14913. The first fragmentation came from a loss of a bromide at m/z 959.22963 while the calculated mass to charge ratio for $C_{70}H_{40}Br$ is 959.23079. The second fragmentation came from the loss of two bromides at m/z 880.31191 while the mass to charge ratio calculated for $C_{70}H_{40}$ is 880.31245. ^{13}C NMR and ^{1}H NMR spectra showed no peaks in the region of sp^3 type carbon chemical shifts, thus basically eliminating the involvement of the double bond of compound **413** in the cycloaddition reaction because the final product should have peak(s) belonging to the sp^3 carbons at high field chemical shifts. The ^{13} C NMR spectrum shows 28 peaks out of 29 theoretical counts for the proposed structure with regard to the carbon atoms (one carbon may overlap with others). While the proposed structure is the best match with the available data however the anti aromatic character of the proposed structure makes it hard to consider the structure. Only X-ray crystallographic study could establish the actual structure for compound **415**. UV-vis spectrum of compound **415** in THF showed an absorption at λ_{max} = 410 nm (ε = 51200 L mol^{-1} cm^{-1}). Figure **4.6** shows the UV-vis spectra of radialenes **412**, **414** and **415** in THF.

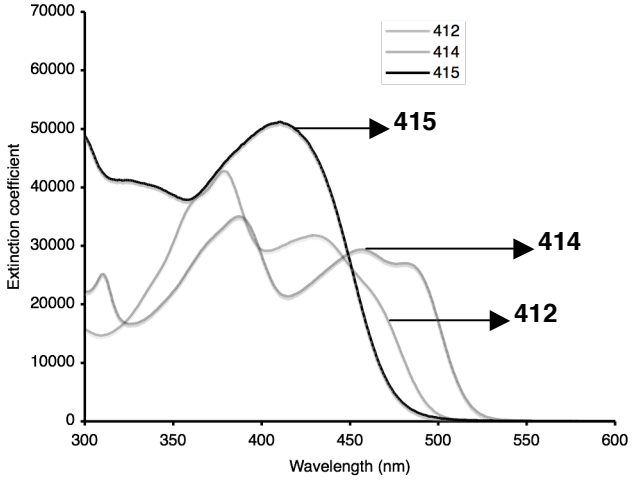

Figure 4.6 UV-vis spectra for compounds **412**, **414** and **415** measured in THF

4.9 Synthesis of functionalized [3]expanded radialenes (para: NO_2, MeO, and CF_3)

An important electronic factor is the presence of substituents (donor or acceptor) in the phenyl rings. In the beginning of this chapter it was demonstrated that substituents at the meta position did not change the UV-vis absorptions of the radialenes because there was no electronic communication between the substituents and the cyclic core of the expanded radialenes. Only inductive effect was present which was not significant for a CF_3 group in the meta position. Based on these observations, the effects of placing CF_3, NO_2, or MeO in the para position of the phenyl ring will be addressed. First the corresponding dibromoolefins were synthesized. The synthesis of **416** is outlined in Scheme **4.15**. There were no ketones commercially available for the synthesis of dibromoolefins **418** and **419** with CF_3 or NO_2 substituents. Synthesis of the required ketones was accomplished by applying microwave technology. In this method, an aryl-iodide or aryl-bromide derivative such as 1-iodo-4-nitrobenzene

or 4-iodobenzotrifluride were reacted with dicobalt octacarbonyl in a polar solvent under microwave radiation for a period of time (normally from 30 min to a few hours). Usually, iodide derivatives give higher yields than bromide derivatives (Scheme **4.16**).[6]

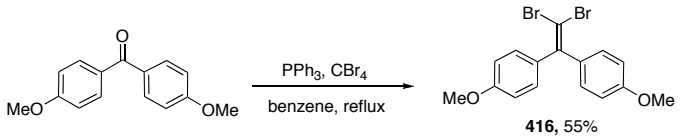

Scheme 4.15 Synthesis of dibromoolefin **416**

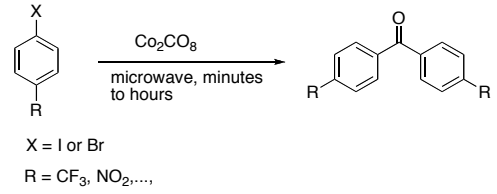

Scheme 4.16 Application of microwave technology in the synthesis of ketones

Scheme **4.17** shows the synthesis of ketone **418** with para CF_3 groups from compound **417**; its characterization was in agreement with the reported data.[6] Ketone **418** was used as shown in Scheme **4.25** to synthesize dibromoolefin **419** as a colorless solid in 60% yield.

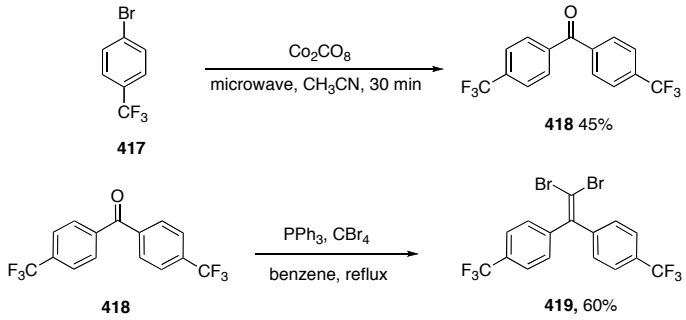

Scheme 4.17 Syntheses of ketone **418** and dibromoolefin **419**

Dibromoolefin **419** was used to synthesize [3]expanded radialene **420** according to the Scheme **4.18**. The reaction yield was very low and there was insufficient amount of materials for ^{13}C NMR spectroscopic analysis.

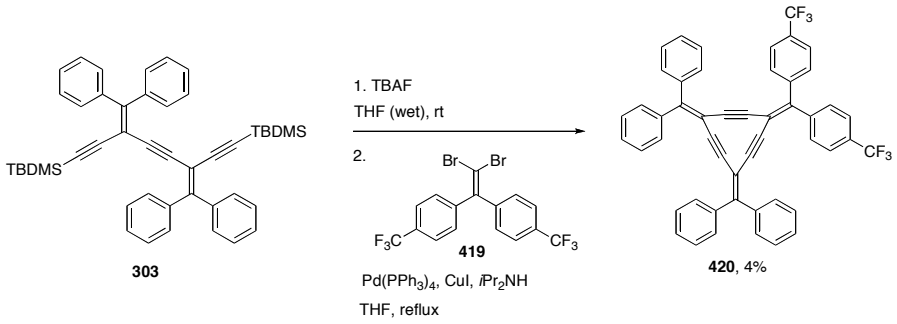

Scheme 4.18 Synthesis of [3]expanded radialene **420**

High resolution MALDI TOF mass spectrometry for **420** shows a molecular ion (M^+) at m/z 742.20878 while the mass to charge ratio calculated for $C_{50}H_{28}F_6$ is 742.20897. The UV-vis spectrum of radialene **420** in THF shows an absorption at λ_{max} = 365 nm and another lower energy absorption at λ_{max} = 413 nm. The UV-vis absorption of radialenes **420** and **406** are similar within the range of instrument error. Apparently, the presence of two CF_3 groups in para positions did not change the electronic properties compared to the meta positions. This observation raised the question: What effects would be observed with stronger acceptors and donors such as NO_2 or MeO? The dibromoolefin **421** was synthesized according to Scheme **4.19**.

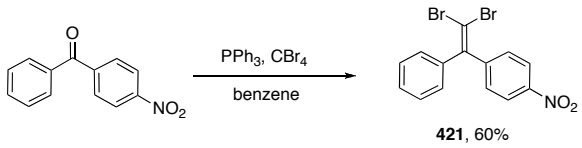

Scheme 4.19 Synthesis of dibromoolefin **421**

Dibromoolefins **416** and **421** were utilized for the synthesis of the corresponding [3]expanded radialenes **422** and **423** as outlined in Scheme **4.20**.

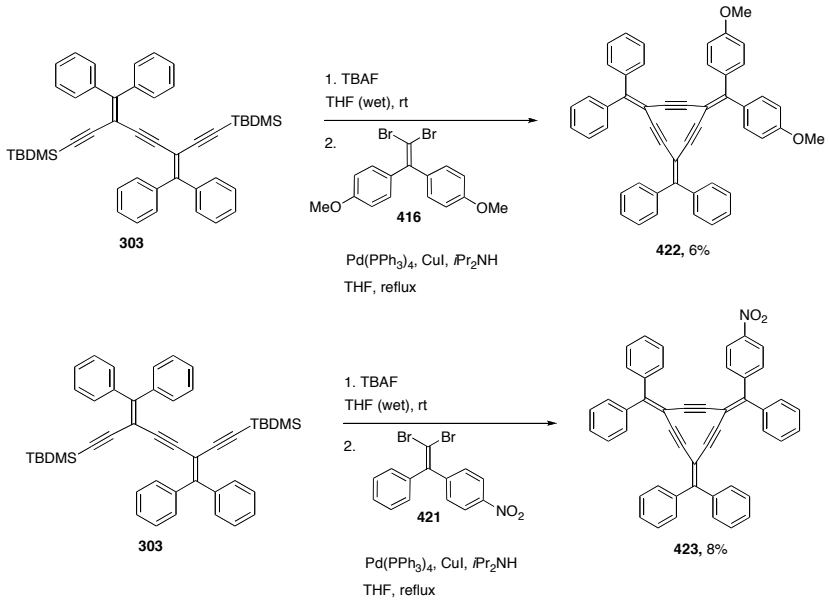

Scheme 4.20 Synthesis for [3]expanded radialenes **422** and **423**

Radialenes **422** and **423** were obtained in low yields making full characterization difficult, particularly for ^{13}C NMR spectroscopy. Based on the appearance of the solutions for both radialenes **422** and **423** it was assumed they are not stable for long periods of time. Confirmation for the structure of radialenes **422** and **423** constitutional formulas came from HR MALDI-TOF mass spectrometry. For radialene **422**, the MALDI-TOF shows a molecular ion (M^+) at

m/z 666.25551 while the mass to charge ratio calculated for $C_{50}H_{34}O_2$ is 666.25533. For compound **423**, the HR MALDI-TOF shows a molecular ion (M^+) at m/z 651.21929 while the mass to charge ratio calculated for $C_{48}H_{29}NO_2$ is 651.21928. Radialene **422** has two absorptions in the UV-vis, the first at 370 nm and the second at 421 nm. The UV-vis spectrum of radialene **423** shows an absorption at 365 nm and second absorption at 418 nm. Radialene **422** and **423** show two absorptions that are characteristics of the [3]radialenes in general. Both compounds also show shifts in λ_{max} to lower energy in the UV-vis region with regard to **310,** in particular the presence of two methoxy groups caused a shift of 6 nm for both absorptions for radialene **422** in comparison to radialene **310.** For radialene **423** the shift toward lower energy absorption was only around 3 nm. Figure **4.7** shows the UV-vis spectra of radialenes **420**, **422**, and **423**.

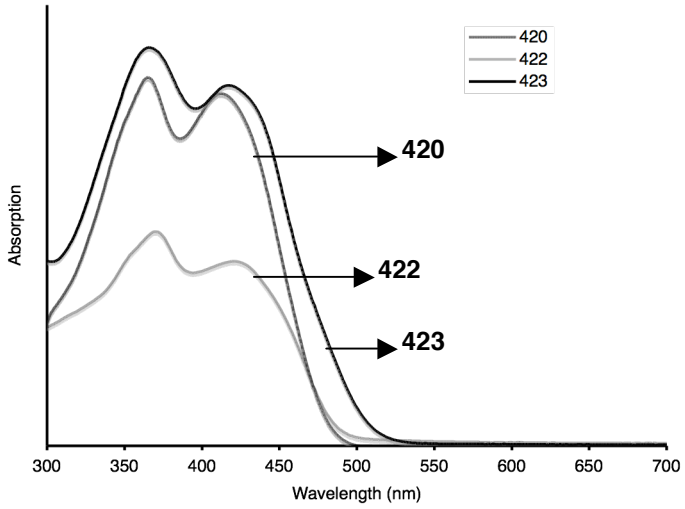

Figure 4.7 UV-vis spectra of radialenes **420**, **422**, and **423** measured in THF

4.10 Synthesis of [4]expanded radialenes (NO_2 and pyridyl groups)

The availability of commercial ketones provided more opportunities to look at the synthesis of dibromoolefins, **424** and **425**, shown in Scheme **4.21**.

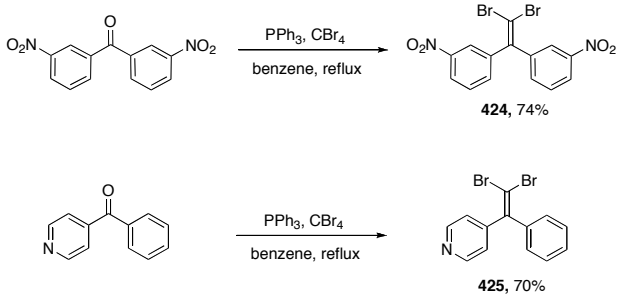

Scheme 4.21 Synthesis of dibromoolefins **424** and **425**

Compound **424** was used to synthesize the corresponding [4]expanded radialene in three consecutive steps as shown in Scheme **4.22**.

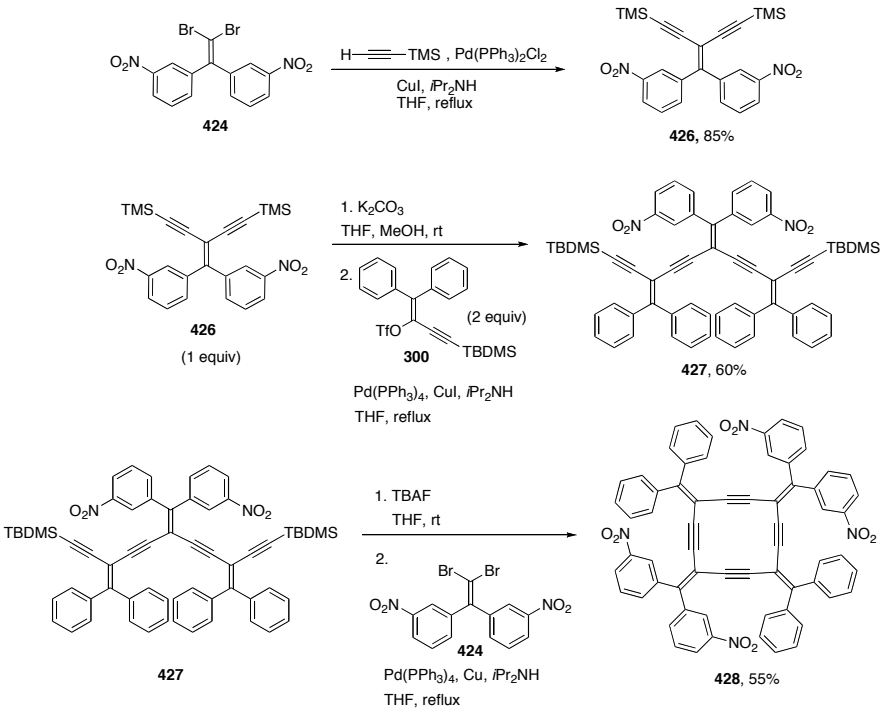

Scheme 4.22 Synthesis of radialene **428**

Radialene **428** showed very low solubility in common organic solvents so it was very difficult to proceed with the ^{13}C NMR analysis. Even attempts in deuterated 1,1,2,2 tetrachloroethane at 65 °C, as had been successful in other cases (see Chapter **5**, compound **528**), were not helpful with the radialene **428**.

HR MALDI-TOF mass spectrometry of radialene **428** shows a molecular ion (M^+) at m/z 988.25233 while the mass to charge ratio calculated for $C_{64}H_{36}N_4O_8$ is 988.25277. UV-vis spectroscopy for **428** shows an absorption at λ_{max} = 376 nm. Radialene **428** does not show any change in λ_{max} compared to **311** so the presence of NO_2 in a meta position did not affect the absorption energy for radialene **428** compared to **311** (Figure **4.8**).

Dibromoolefin **425** was used to synthesize [4]expanded radialene **431** as outlined in Scheme **4.23**. The product was a mixture of cis and trans isomers (based on HPLC analysis) that were difficult to separate due to the presence of the pyridyl groups. In addition, the low solubility of the mixture made it hard to obtain a ^{13}C NMR spectrum. HR MALDI-TOF mass spectrometry shows a molecular ion (M^+) of radialene **431** at m/z 810.30263 while the mass to charge ratio calculated for $C_{62}H_{38}N_2$ is 810.30295. Despite the fact that two of the phenyl rings in **431** are replaced with 4-pyridyl, non-quantitative UV-vis study of the radialene **431** in THF shows an absorption at 376 nm, very close to the absorption of compound **311** (Figure **4.8**).

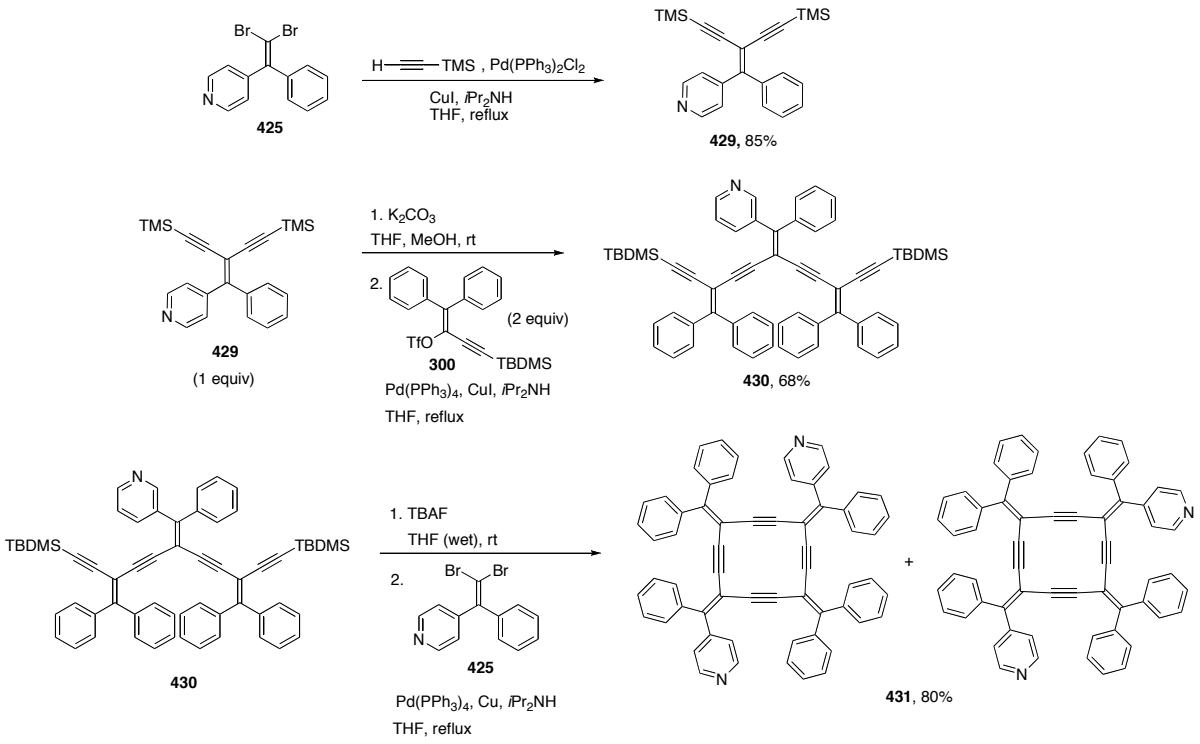

Scheme 4.23 Synthesis of radialene **431**

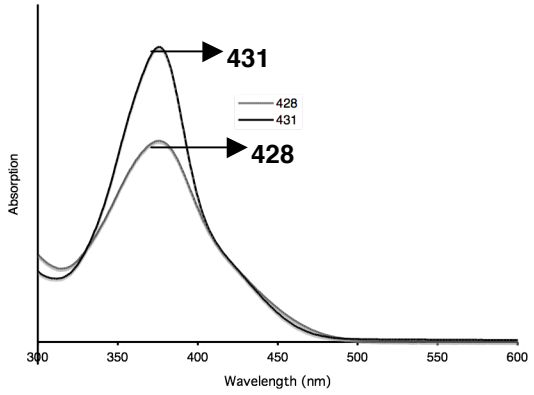

Figure 4.8 UV-vis spectra of radialene **428** and **431** measured in THF

In conclusion, in order to see more significant electronic effects from substituents that affect the optical properties of the radialenes, there is a need for stronger donor or acceptor groups.

4.11 Synthesis of tetraphenylcyclopentadienylidene [4]expanded radialene

Dibromoolefin **432**, was synthesized in the same manner as other dibromoolefin reagents (Scheme **4.24)**. It is expected the incorporation of new dibromoolefin increases the π-system territory over a longer linear fragment. Also the core of cyclpendiene could potentially be considered as a cyclopentadienyl anion (Cp^-) that carries a negative charge and therefore creates a dipole moment across the molecule.

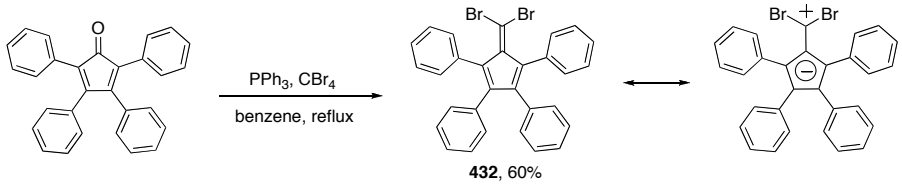

Scheme 4.24 Synthesis of dibromoolefin **432**

Compound **432** was fully characterized, including the solid-state structure. The ORTEP plot of **432** is shown in Figure **4.9**. The presence of two phenyl rings around the dibromide may cause steric hindrance for cyclization reaction of **432** with *iso*-polydiacetylene oligomers compared to compound **308**.

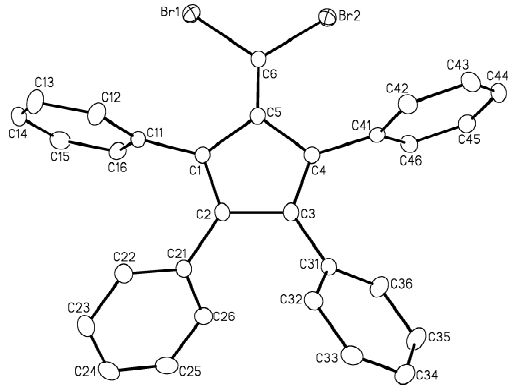

Figure 4.9 ORTEP plot of compound **432** (hydrogens removed for clarity)

The ORTEP plot in Figure **4.9** shows that access to the dibromide from the phenyl-ring side is blocked. Dibromoolefin **432** was reacted with desilylated trimer **305** to give [4]expanded radialene **433** as a brown solid, in 65% yield, as outlined in Scheme **4.25**.

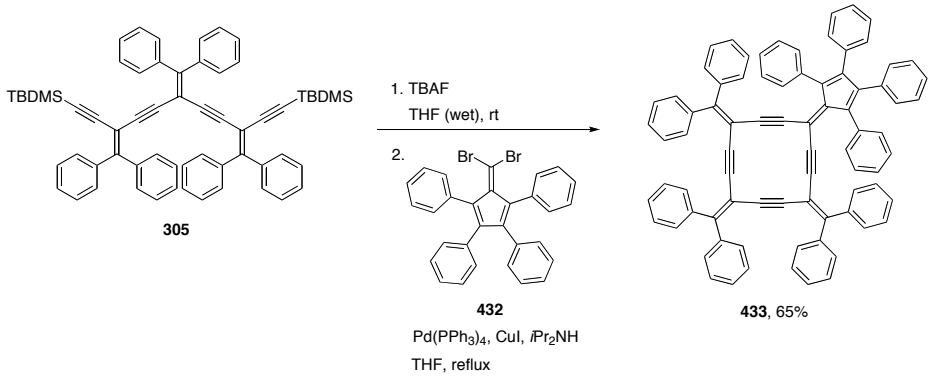

Scheme 4.25 Synthesis of radialene **433**

^{13}C NMR spectroscopic analysis for **433** in CD_2Cl_2 shows characteristic alkyne carbons at 101.8, 98.1, 97.6, and 95.5 ppm. The vinylidene carbons carrying the tetraphenylcyclopentadienylidene group resonate at 150.6 and 102.5 ppm compared with the same carbons in **432** that appeared at 146.3 and 104.1 ppm (in $CDCl_3$). Both carbons in **433** are shifted to lower field as a result of the cyclization. The UV-vis spectrum of **433** in THF shows one absorption at λ_{max} = 403 nm (ε = 20600 L mol^{-1} cm^{-1}). The λ_{max} shifted from 377 nm for compound **311** to 403 nm for compound **433** as a result of replacement of the phenyl rings with tetraphenylcyclopentadienylidene functional group. Expansion of the π-system through the tetraphenylcyclopentadienylidene functional group caused the UV-vis absorption to shift to lower energy. Figure **4.10** shows UV-vis spectra of radialenes **408**, **411**, and **433** in THF.

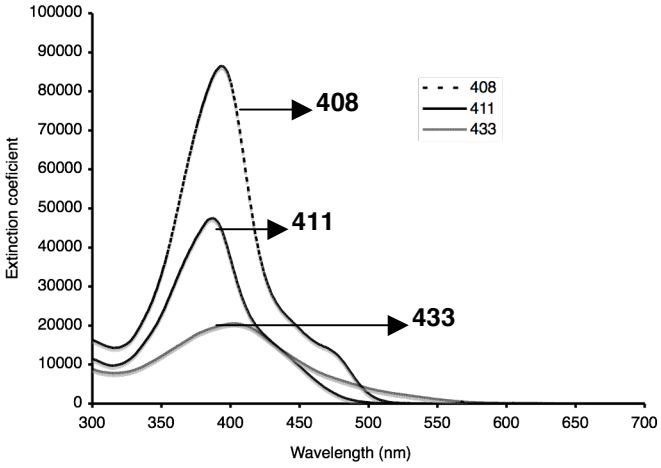

Figure 4.10 UV-vis spectra of radialenes **408**, **411**, and **433** measured in THF

Single crystals of radialene **433** suitable for X-ray crystallographic analysis was grown from slow evaporation of a THF solution at 4-5 °C. ORTEP plot of radialene **433** is shown in Figure **4.11** and Table **4.2** contains selected bond angles and bond lengths for **433** and **311.**

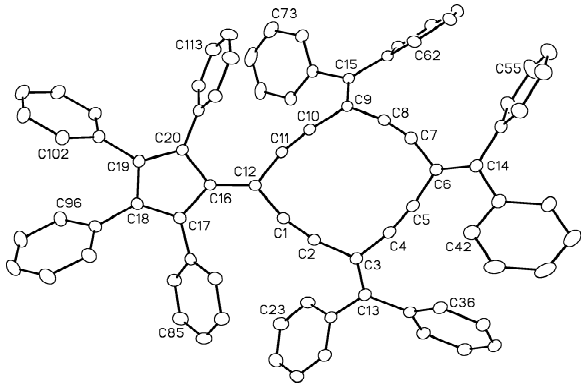

Figure 4.11 ORTEP plot of radialene **433** (hydrogens removed for clarity)

Table 4.2 Selected bond lengths and bond angles for radialene **311** and **433**

	311	**433**
C5–C6–C7 angle	110.40(12)°	109.09(14)°
C4–C5–C6 angle	166.65(14)°	170.11(18)°
C1–C12–C11 angle	----------	108.76(11)°
C14–C6–C7–C8 torsion angle	159.8(6)°	–180(100)°
C11–C12–C16–C17 torsion angle	----------	175.98(16)°
C4–C5 bond length	1.2000(19) Å	1.201(2) Å
C1–C2 bond length	----------	1.200(2) Å

Based on Table **4.2**, while the alkyne bond angle is smaller in radialene **311** compared to **433,** the vinylidene bond angle is more contracted in radialene **433** compared to **311**.

Cyclic voltammetry of **433** measured in CH_2Cl_2 shows at least three reductions, all reversible, the first at –1.26, the second at –1.54, and the third at –1.69 V. The radialene **433** shows oxidation event at 0.65 and 0.83 V (refer to page 151 for CV voltammograms). Compound **433** is reduced and oxidized more easily than **310**–**312**. In fact, radialene **433** shows behavior similar to the compound **316a**. To better understand the electrochemical behavior of **433**, compound **434** was synthesized for electrochemical analysis. The dibromoolefin **432** was reacted with an excess of trimethylsilylacetylene in the presence of $Pd(PPh_3)_2Cl_2$ yielding **434** (55%) as outlined in Scheme **4.26**.

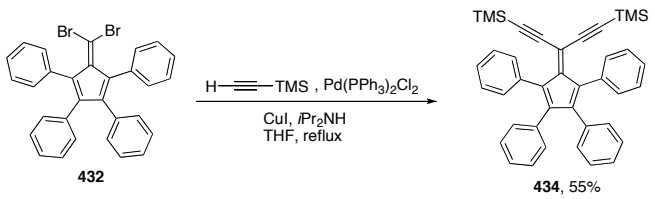

Scheme 4.26 Synthesis of compound **434**

Cyclic voltammetry of **434** shows a reversible reduction at –1.58 V and a second irreversible reduction at –2.05 V. It also shows one-electron reversible oxidation event at 0.81 V and a second irreversible oxidation event at 1.21 V. Comparing **434** with **433** shows that **433** is reduced and oxidized more readily.

4.12 Summary and comparisons of the functional radialenes

The presence of substituents like MeO or NO_2 on the radialene framework shifted UV-vis absorptions to lower energy in comparison to unsubstituted radialene **310**. The π-electron system through the cross-conjugation was extended by incorporation of the fluorenylidene or tetraphenylcyclopentadienylidene functionality. Cyclic voltammetry experiment showed the presence of functional groups like CF_3 or TIPS-ethynyl could change the redox potentials compared to radialenes **310** and **311**. For example, compound **404** is reduced and oxidized more easily than **311**. In contrast to the [4]radialenes, it is harder to reduce and oxidize [3]radialene **406** compared to **310**. On the other hand, radialenes **411** and **412** that carry TIPS-ethynyl groups are more easily reduced and more difficult to oxidize than radialenes **311** and **310** respectively. Figures **4.12** and **4.13** show cyclic voltammetry and Osteryoung square wave voltammetry (OSWV) for the [4]– and [3]expanded radialenes

discussed in this chapter with regard to basic radialene **311** and **310** respectively. (refer to page 192 for radialene **411** CV voltammograms).

A general comparison among the radialenes synthesized by Diederich and coworkers and the new series of radialenes reveals that the later series is reduced at higher potentials, suggesting the new series is more electron rich compared to the previous generation.[7] Consequently, the new series of radialenes should behave differently. Already, it has been shown that the radialene **414** undergoes cycloaddition reaction and as we will observe later in Chapter **6**, the [3]radialenes in particular, react readily with selected organometallic precursors. This suggests, the new series of radialenes has special structural and electronic makeup. The most notable feature that could explain this participation in the selected chemical reactions may be associated with macrocyclic strain particularly for [3]radialene series. The [3]radialenes may react more readily in order to release their strain.

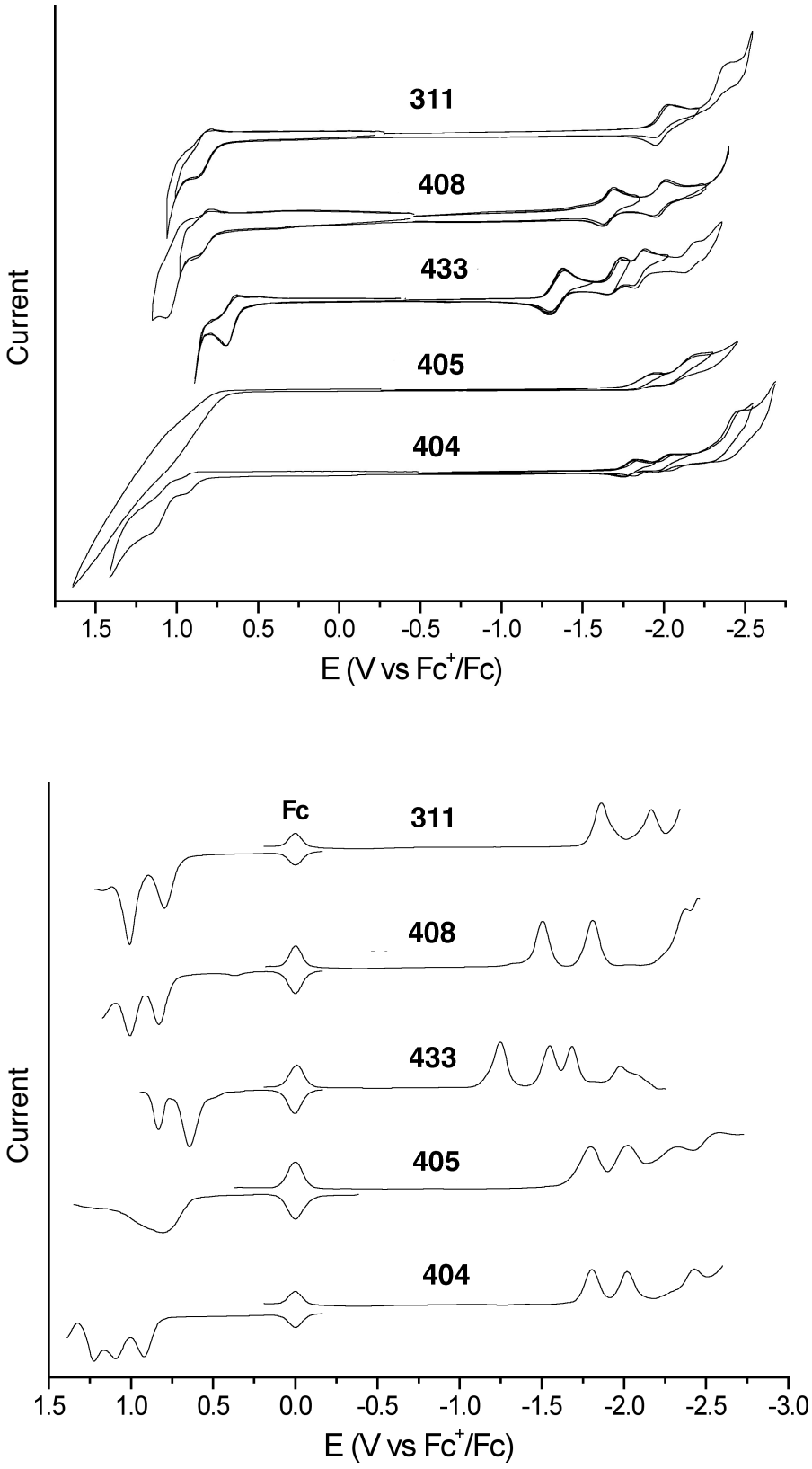

Figure 4.12 CV and OSWV voltammograms for [4]radialenes measured in CH_2Cl_2

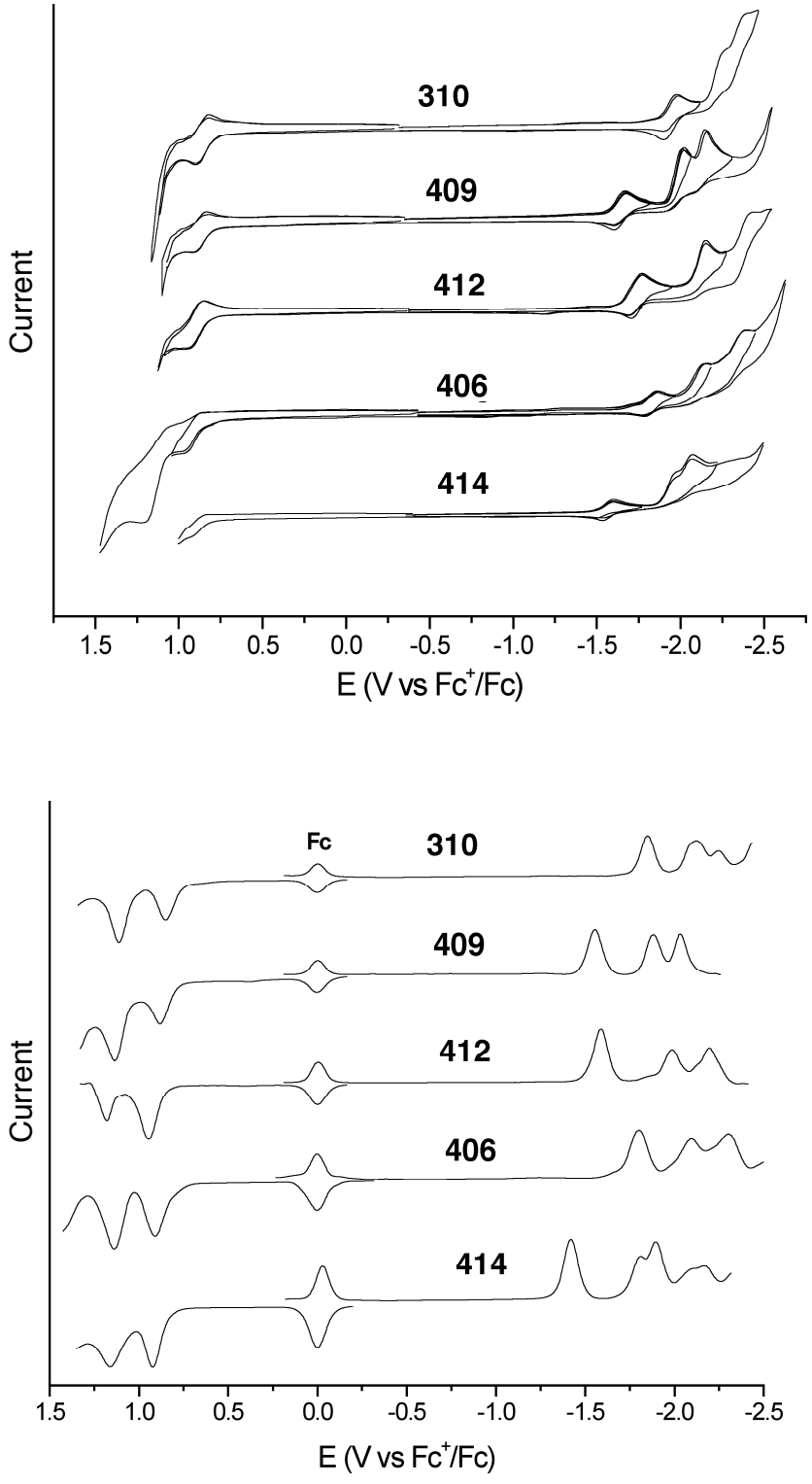

Figure 4.13 CV and OSWV voltammograms for [3]radialenes measured in CH_2Cl_2

4.13 Conclusion

Synthesis of the first series of functional expanded radialenes was accomplished in reasonable yields. Solubility of the [4]radialenes with NO_2 and pyridyl groups hindered full characterization of these compounds. Generally, those [3]–, and [4]radialenes that were fully characterized did not show any sign of decompositions in solution or in the solid state, and the macrocycles could be used for physical studies such as UV-vis or cyclic voltammetry. The first crystal structure of a [3]expanded radialene **414** has reported that confirmed this strained macrocyclic compound. Also, the first convincing evidence regarding [3]radialenes undergoing cycloaddition reaction has been observed. This chapter shows that the functional expanded radialenes can be synthesized and studied but there is a need for stronger functional groups that can influence more intensely the physical properties of the radialenes, in particular the UV-vis absorptions toward lower energies.

4.14 References

(1) Neidlein, R.; Winter, M. *Synthesis* **1998**, 1362–1366.
(2) Paul, G. C.; Gajewski, J. J. *Synthesis* **1997**, 524–526.
(3) (a) Lange, T.; van Loon, J.-D.; Tykwinski, R. R.; Schreiber, M.; Diederich, F. *Synthesis*, **1996**, 537–550; (b) Anthony, J.; Boldi, A. M.; Rubin, Y.; Hobi, M.; Gramlich, V.; Knobler, C. B.; Seiler, P.; Diederich, F. *Helv. Chim. Acta* **1995**, *78*, 13–45.
(4) (a) Jamie Kendall, University of Alberta, **2004–2006**; (b) Diederich, F.; Philp, D.; Seiler, P. *J. Chem. Soc.*, *Chem. Comm.* **1994**, 205–208.
(5) Collins, S. K.; Yap, G. P. A.; Fallis, A. G. *Org. Lett*. **2002**, *4*, 11–14.
(6) Enquist, P.-A.; Nilsson, P.; Larhed, M. *Org. Lett*. **2003***, 5*, 4875–4878.
(7) (a) Gisselbrecht, J.-P.; Moonen, N. N. P.; Bouden, C.; Nielsen, M. B.; Diederich, F.; Gross M. *Eur. J. Org. Chem.* **2004**, 2959–2972; (b) Nielsen, M. B.; Schreiber, M.; Baek, Y. G.; Seiler, P.; Lecomte, S.; Boudon, C.; Tykwinski, R. R.; Gisselbrecht, J. P.; Gramlich, V.; Skinner, P. J.;

Bosshard, C.; Günter, P.; Gross, M.; Diederich, F. *Chem. Eur. J.* **2001**, *7*, 3263–3280.

Chapter 5

Synthesis and Characterization of Expanded Radialene Derivatives

5.1 Expanded radialene derivatives: one-pot and stepwise syntheses

Derivatizations of the expanded radialenes could be accomplished by usage of tetrabromide derivatives of anthracene–, and pentacenequinone for building up expanded radialene skeletons in one-pot reaction. With suitable precursors, it is plausible also to derivatize the expanded radialenes, particularly where the framework contains trialkylsilylethynyl groups (e,g., TIPS-ethynyl). Protodesilylation of the radialenes containing trialkylsilylethynyl groups readily provides terminal alkynes for further Sonogashira cross coupling reactions and therefore derivatization of the radialene framework. In terms of physical properties, the targeted molecules are unknown, but it is anticipated that they would exhibit electronic and optical properties similar to the smaller expanded radialenes. These expanded radialene derivatives are potentially useful as receptors[1] for large molecules such as C_{60} or its analogues, and they have the potential to undergo cycloaddition reactions.

This chapter focuses on the synthesis of expanded radialenes using tetrabromide derivatives that carry skeletons such as adamantyl, anthracenylidene, and pentacenylidene. Also, this chapter explores strategies for derivatizing the expanded radialene skeleton, where an expanded radialene is used as starting material for the synthesis of higher radialene analogues (Scheme **5.1**). For example Scheme **5.1** shows two pathways toward the synthesis of new radialenes as a result of coupling reactions of desilylated radialene **411** (stepwise approach). Compound **A** results from coupling with aryl

halides and compound **B** can lead to larger derivatives of expanded radialenes such as bisradialene or trisradialene via protodesilylation followed by Sonogashira cross coupling reaction. Two examples of such reactions leading to **A** and **B** will be discussed in this chapter.

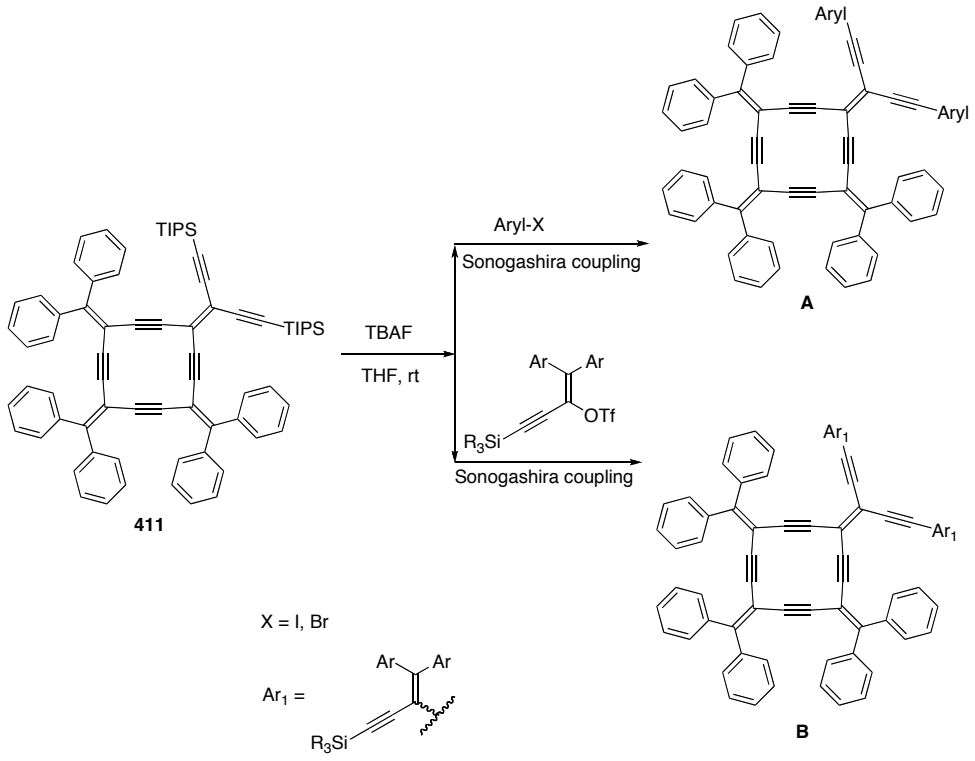

Scheme 5.1 Strategy for derivatization of expanded radialenes: **A** has no further capacity for higher radialene derivatives, **B** allows for higher radialene derivatives

Parallel to the larger radialene derivatives described above, there has been interest in the synthesis of radiaannulene derivatives, not only for the synthetic aspects or physical studies but also for their applications in organometallic chemistry, which has not been yet explored.

5.2 Synthesis and characterization of expanded radialene (radiaannulene) derivative of anthracenylidene framework

Anthraquinone **500** was used to synthesize tetrabromide **501** (Scheme **5.2**) according to the procedure reported by Neidlein and coworkers.[2]

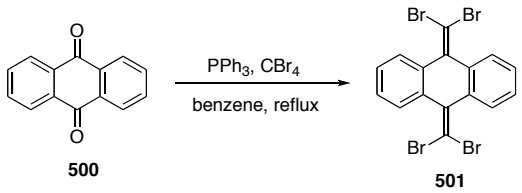

500 **501**

Scheme 5.2 Synthesis of tetrabromide **501**

Like tetrabromoethene **314** in Chapter **3**, compound **501** is considered a useful starting material. However, in terms of steric hindrance **501** is quite different from **314** due to the presence of fused phenyl rings that can insert a significant steric influence during the palladium mediated cross coupling reaction. To investigate steric factors single crystals of compound **501** for X-ray crystallographic analysis were grown by slow evaporation of a $CHCl_3$ solution at 4–5 °C. The data from X-ray analysis showed the fused rings are not in the same plane as the dibromoalkylidene moieties, as shown in Figure **5.1**.

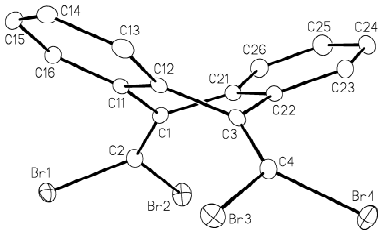

Figure 5.1 ORTEP plot of compound **501** (hydrogens removed for clarity)

The geometry of compound **501** suggests, two coupling reaction routes are possible. In the coupling with an *iso*-polydiacetylene oligomer, the first would occur at the geminal bromides Br1 to Br2 and Br3 to Br4 affording anthracenylidene-expanded radialene (**502a**). Second coupling of the *iso*-polydiacetylene oligomer with further away bromides, Br1 to Br3 and Br2 to Br4 would afford anthracenylidene-radiaannulene (**502b**) (Scheme **5.3**).[3]

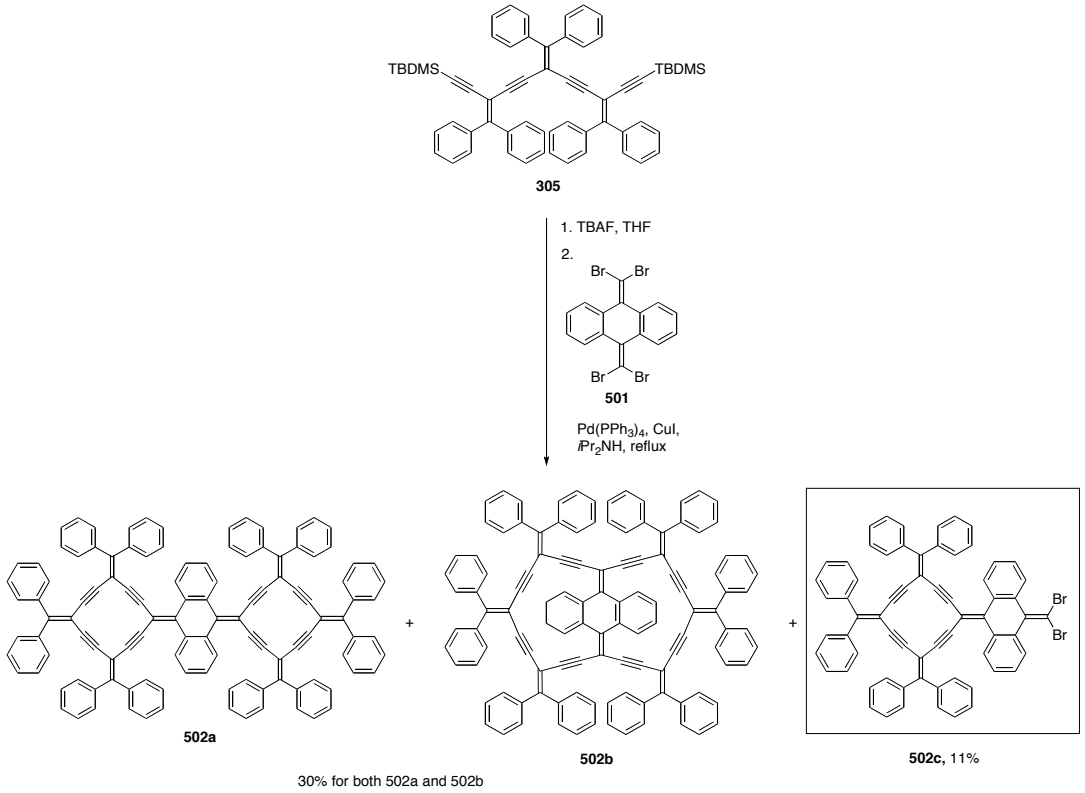

Scheme 5.3 Synthesis of anthracenylidene–expanded radialene and radiaannulene

Compound **501** reacted with the desilylated **305** under the standard Sonogashira protocol according to Scheme **5.3**. The crude reaction product mixture was initially separated using silica gel chromatography (hexanes/CH_2Cl_2,

5:1 to 2:1) and the resulting fractions were further purified on pre-coated silica gel TLC plates (hexanes/CH_2Cl_2, 1:1), yielding a red solid. HR MALDI-TOF mass spectrometry confirmed a molecular ion consistent with the proposed structure(s) in Scheme **5.3**. The red solid was subjected to HPLC (silica gel column) using hexanes/ethyl acetate (100:0 to 80:20) yielding a yellow solid (minor) and a red solid (major) as products. Both products show an identical molecular ion (M^+) in HR MALDI-TOF mass spectrometry. The minor isomer shows a molecular ion at m/z 1460.53079, while the calculated mass to charge ratio for $C_{116}H_{68}$ is 1460.53155. The major isomer also shows a molecular ion (M^+) at m/z 1460.53155. A chromatogram for the HPLC separation is shown in Figure **5.2**.

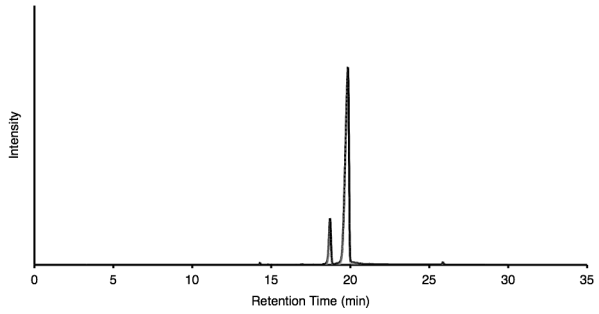

Figure 5.2 HPLC chromatogram from the separation of compounds **502a** and **502b** (hexanes:ethyl acetate, 100:0 to 80:20)

^{13}C NMR and UV-vis spectroscopic data of the yellow and red solids were used to see if they had different characteristic patterns. Unfortunately, the yield of the yellow solid was too low for the ^{13}C NMR spectroscopy. ^{13}C NMR spectrum of the red solid shows 25 peaks overall which is consistent with the theoretical

count for carbons of the compound **502**. ^{13}C NMR spectrum shows characteristic alkyne carbons (**C1**–**C4**) at 98.8, 97.0, 96.8, and 96.7 ppm (Scheme **5.3**).

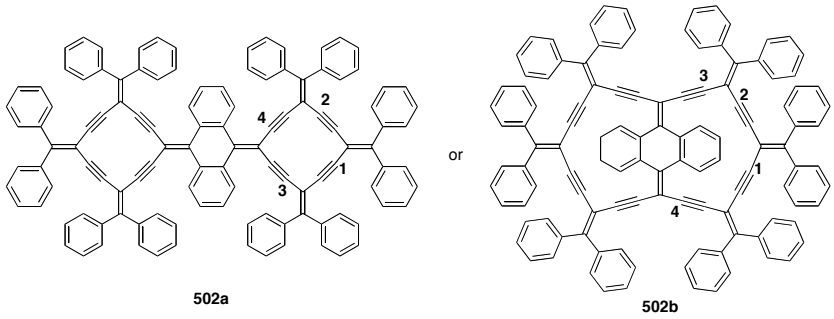

Scheme 5.4 Alkyne carbons for compounds **502a** and **502b**

UV-vis spectroscopy of the yellow solid (minor isomer, Figure **5.3**) in THF shows an absorption at λ_{max} = 381 nm (ε = 57200 L mol^{-1} cm^{-1}). λ_{max} is defined here as the lowest energy absorbance observed in the spectrum. UV-vis of the major isomer (red solid) in THF shows absorptions at λ_{max} = 377 nm (ε = 75100 L mol^{-1} cm^{-1}) and λ_{max} = 513 nm (ε =16500 L mol^{-1} cm^{-1}). Thus, the major and minor isomers are very different in terms of UV-vis absorptions. The identities of the major and minor isomers will be discussed with regard to compounds **502a** and **502b** later in this chapter. Cyclic voltammetry of the major isomer in CH_2Cl_2 shows a single reduction at –1.48 V and oxidation events at 0.66 and at 0.8 V (refer to page 191 for CV voltammograms).

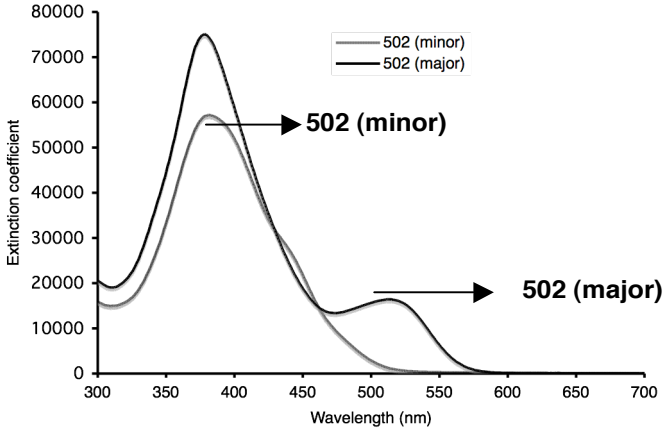

Figure 5.3 UV-vis spectra of compounds **502a** and **502b** measured in THF

5.3 Synthesis and characterization of pentacenylidene expanded radialene (radiaannulene)

Pentacenequinone[4a,b] was synthesized according to Scheme **5.5** in a 4-fold aldol condensation reaction as a yellow solid with very low solubility in common organic solvents. Pentacenequinone was used to synthesize tetrabromide **503** as shown in Scheme **5.6**.

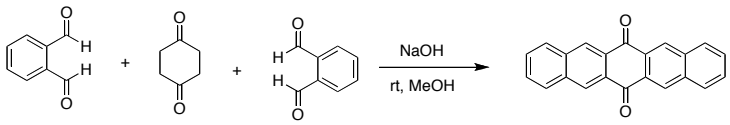

Scheme 5.5 Synthesis of pentacenequinone

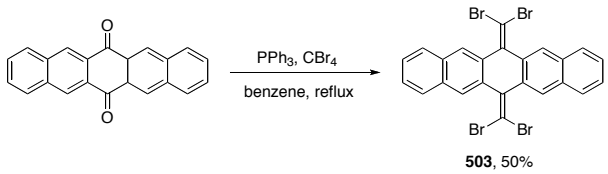

Scheme 5.6 Synthesis of tetrabromide **503**

Single crystals of compound **503** suitable for crystallographic analysis were grown from slow evaporation of a $CHCl_3$ solution show structural features similar to compound **501** (Figure **5.4**).

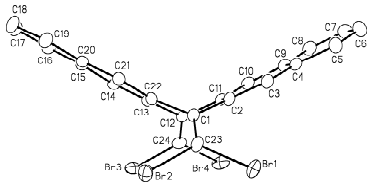

Figure 5.4 ORTEP plot of compound **503 (**hydrogens removed for clarity)

Compound **503** has been used according to Scheme **5.7** toward the synthesis of the pentacenylidene-expanded radialene **504a** or pentacenylidene-radiaannulene **504b**. Two isomers were isolated by HPLC separation procedure similar to that employed to separate compounds **502a** and **502b,** resulting in two compounds, a yellow solid (minor product) and a red solid (major product).

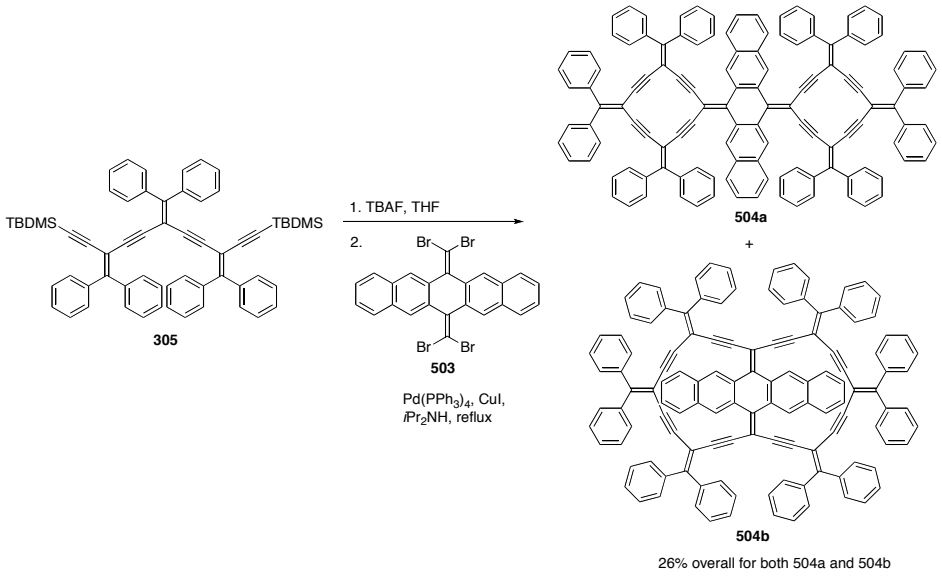

Scheme 5.7 Synthesis of compounds **504a** and **504b**

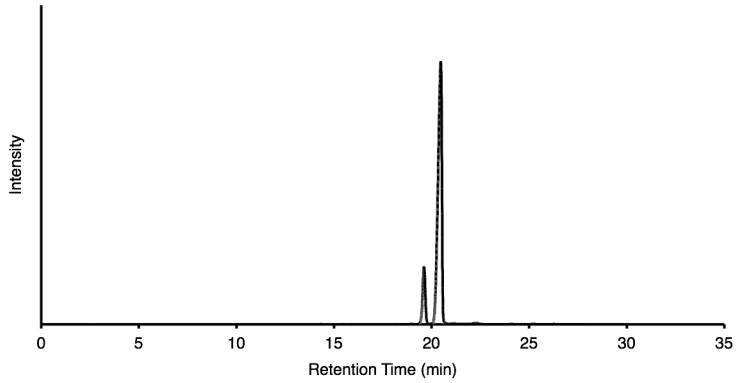

Figure 5.5 HPLC chromatogram for the separation of compounds **504a** and **504b** (hexanes:ethyl acetate,100:0 to 80:20)

Both products showed identical masses in HR MALDI-TOF mass spectrometry. The first isomer shows (M^+) at m/z 1560.56237 while the mass to charge ratio calculated for $C_{124}H_{72}$ is 1560.56285. The major product shows (M^+) at m/z 1560.56261 while the calculated value for $C_{124}H_{72}$ is 1560.56285. Only the major isomer has been produced in sufficient amount for full characterization by NMR spectroscopy. The ^{13}C NMR spectrum of major isomer **504** shows overall 25 signals out of 27 expected this including those of alkyne carbons at 98.8, 97.5, 97.4, and 96.8 ppm (**C1**–**C4**, Scheme **5.8**).

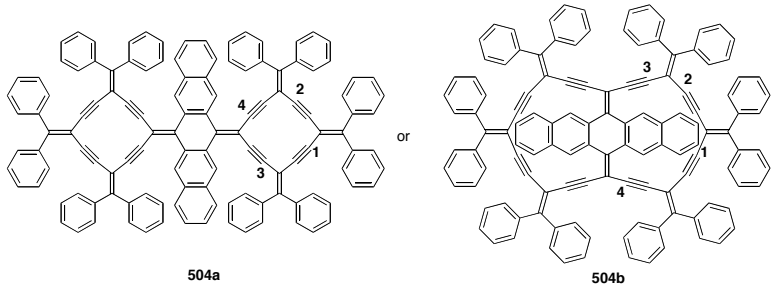

Scheme 5.8 Alkyne carbons for compounds **504a** and **504b**

A UV-vis spectroscopic study of both isomers has been performed in THF. The minor isomer shows at λ_{max} = 382 nm (ε = 82700 L mol^{-1} cm^{-1}); the major isomer shows at λ_{max} = 385 nm (ε = 120400 L mol^{-1} cm^{-1}). The minor isomer shows a shoulder around 440 nm, while the major isomer shows a shoulder around 480 nm (Figure **5.6**).

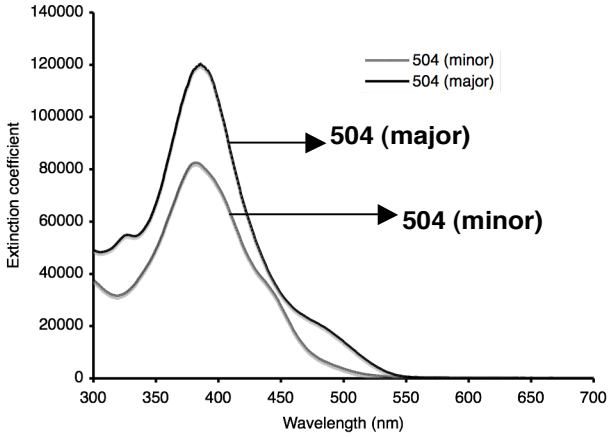

Figure 5.6 UV-vis spectra of compounds **504a** and **504b** measured in THF

Cyclic voltammetry of the major isomer of the compound **504** in CH_2Cl_2 shows a reduction at –1.54 and –2.09 V and an oxidation event at 0.69 and 0.85 V (refer to page 191 for CV voltammograms). Assignments of the major and minor isomer with regard to **504a** and **504b** are discussed later in this chapter.

5.4 Synthesis of adamantyl and phenyl-alkoxy bisexpanded radialenes

Two additional tetrabromide derivatives **505** and **506** were synthesized according to Schemes **5.9** and **5.10**.[5,6] The tetrabromide derivatives were then incorporated in the synthesis of expanded radialenes. Due to the presence of adamantyl and phenyl-alkoxy group that are diverse from other previously used functional groups and it is difficult to predict physical properties of these new compounds.

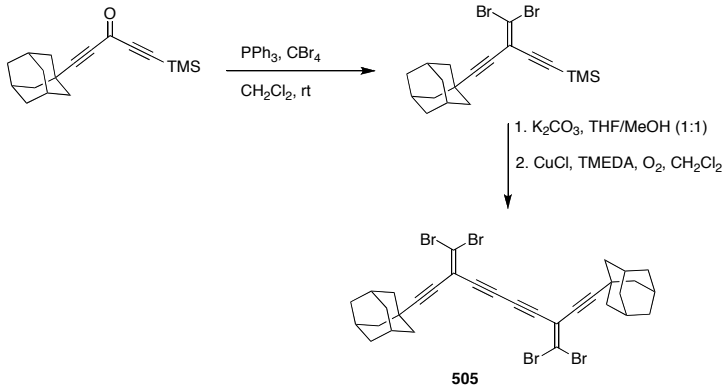

Scheme 5.9 Synthesis of tetrabromide derivative **505**

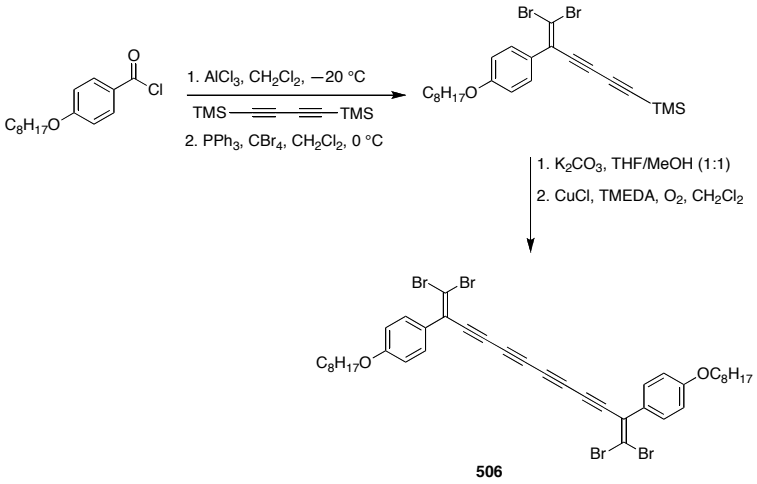

Scheme 5.10 Synthesis of tetrabromide derivative **506**

Compound **505** was reacted with the desilylated trimer according to Scheme **5.11** to give compound **507** as a red solid in 29% yield.

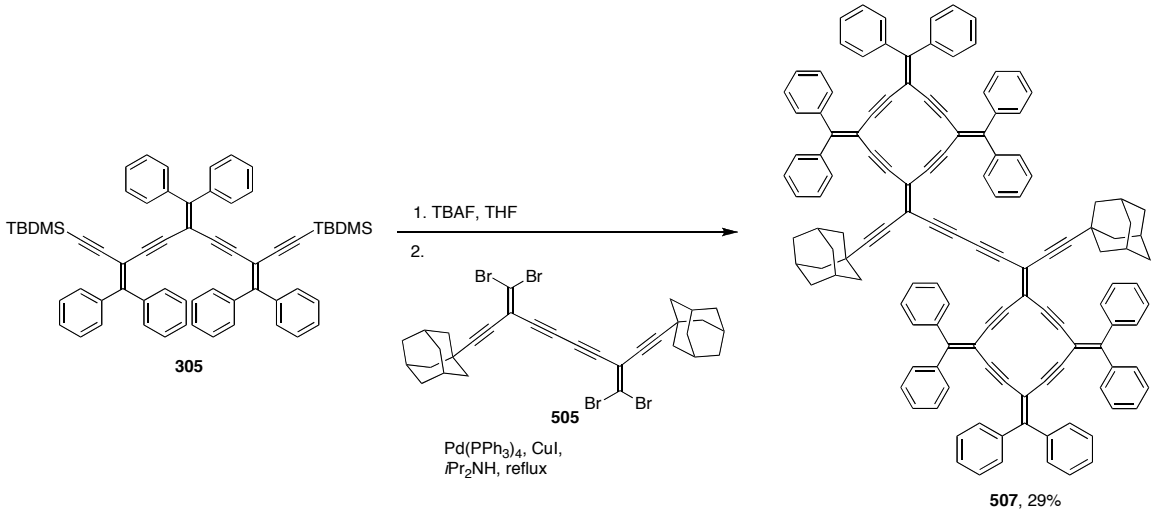

Scheme 5.11 Synthesis of adamantyl expanded radialene **507**

Confirmation of the composition of compound **507** (constitution formula) came from HR MALDI-TOF mass spectrometry that showed a molecular ion (M^+) at m/z 1674.70060 while the mass to charge ratio calculated for $C_{132}H_{90}$ is 1674.70370. The ^{13}C NMR spectrum shows signals characteristic of alkyne carbons at 97.9, 96.8, 96.7, 96.6, 96.0, 84.5, 82.3, and 76.4 ppm.

Incorporating the tetrabromide **506** in the Sonogashira coupling reaction with desilylated trimer **305** gave compound **508** in 15% yield as a red solid (Scheme **5.12**). HR MALDI-TOF mass spectrometry shows a molecular ion (M^+) 1814.78610 m/z while the mass to charge ratio calculated for $C_{140}H_{102}O_2$ is 1814.78743. The ^{13}C NMR spectrum of compound **508** in CD_2Cl_2 shows characteristic alkyne carbon signals at 97.5, 97.4, 97.0, 96.4, 96.1, 72.4, 70.9, 68.6, and 67.0 ppm.

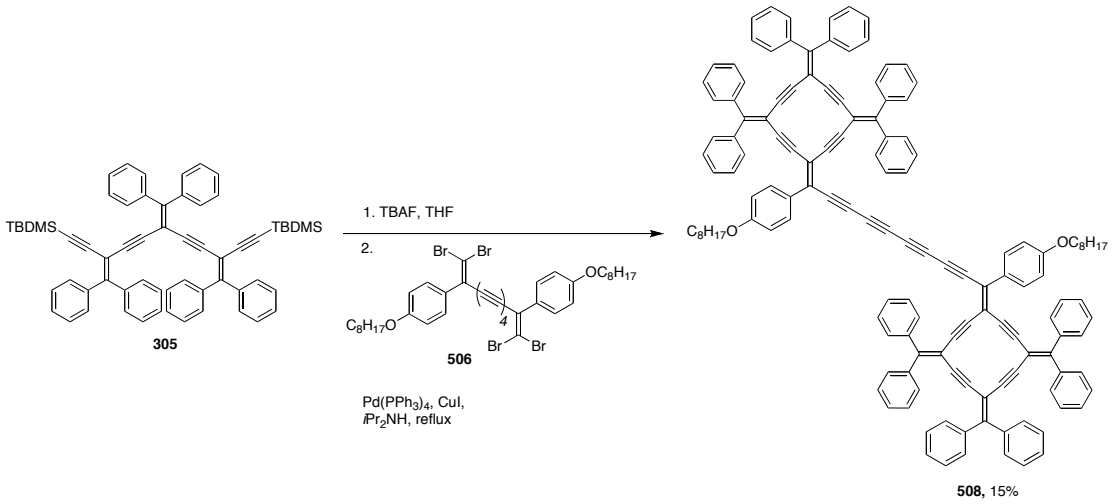

Scheme 5.12 Synthesis of radialene **508**

The UV-vis spectrum of **507** in THF shows an absorption at λ_{max} = 393 nm (ε = 61800 L mol^{-1} cm^{-1}) and a shoulder around 530 nm (Figure **5.7**). Cyclic voltammetry of the macrocycle **507** shows a reduction at –1.29, –1.43, –2.03, and – 2.14 V. Compound **507** shows an oxidation event at 0.85 and 1.05 V (page 180).

UV-vis spectroscopy of the macrocycle **508** in THF shows an absorption at λ_{max} = 388 nm (ε = 131200 L mol^{-1} cm^{-1}) and a shoulder around 540 nm (Figure **5.7**). Cylic voltammetry of compound **508** shows a reduction at –1.40, –1.88, –1.99, and –2.19 V and two oxidation events the first at 0.77 and the second at 0.93 V (refer to page 191 for CV voltammograms).

From the UV-vis studies, surprisingly there is no significant difference between the phenyl-alkoxy functional group in **508** compared to the adamantyl functional group in **507**, the only difference is the lower energy absorption for **508** is more intense than **507** while the higher energy absorption of the **507** is at 393

nm compared to 388 nm for radialene **508**. It is assumed that the para donating group is not communicating with the cyclic core of the radialene. This is due to the repulsion of the phenyl rings with the adjacent radialene framework that consequently decreases the overall electronic effect of the phenyl-alkoxy fragment on the molecule.

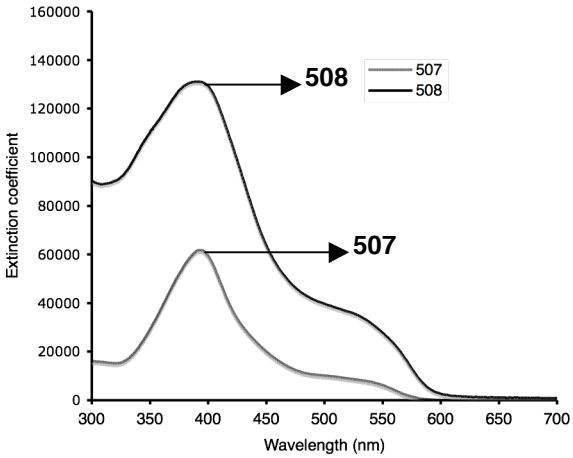

Figure 5.7 UV-vis spectra of compounds **507** and **508** measured in THF

5.5 Synthesis of bis-[4]expanded radialene through a stepwise route (B)

The synthesis of bis-expanded radialene **315a** and **315b** in a one pot reaction was discussed in Chapter **3**.[7] It was not possible to separate the mixture by HPLC, so a new way of synthesizing **315a** and **315b** or a new way for separating these compounds was necessary in order to obtain single isomers sufficiently pure for full characterization. The synthesis was addressed through incorporation of the expanded radialene **411** which was used for the first time in our experiments as a starting material for further coupling reactions. Radialene **411** was protodesilyated with TBAF and reacted with vinyl triflate **300** under the

standard Sonogashira protocol to afford compound **509** as an orange solid in 78% yield. Compound **509**, an intermediate, has been confirmed its identity only by HR MALDI-TOF mass spectrometry and infrared spectroscopy and used for the synthesis of radialene **315a**. Compound **509** was protodesilylated and reacted with dibromoolefin **308** to afford bis-expanded radialene **315a** in 50% yield as a red solid (Scheme **5.13**).

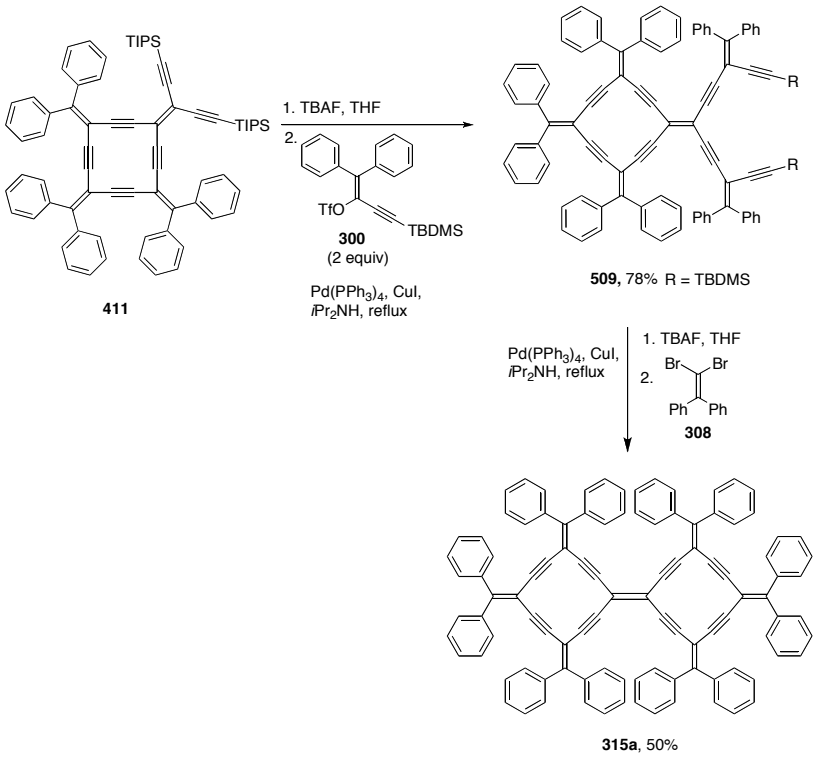

Scheme 5.13 Stepwise synthesis of radialene **315a**

Initial experimental confirmation came from TLC comparison (co-spot) of the product of the stepwise synthesis and the one-pot synthesis of compound **315a**. The constitution formula of compound **315a** has been confirmed by HR MALDI-TOF mass spectrometry. The solubility of compound **315a** is low,

however, a relatively reasonable ^{13}C NMR spectrum was obtained after several attempts. The ^{13}C NMR spectrum of radialene **315a** shows alkyne carbons at 102.1, 97.1, and 96.7 ppm but still one carbon is absent. Also, the bridged double bond may resonate at 111.9 ppm. UV-vis spectroscopy of radialene **315a**, measured in THF, shows an absorption at 389 nm and a less intensive absorption at 509 nm. At the time of the stepwise reaction, a final effort was made to separate the mixture of **315a** and **315b**. The mixture was subjected to chromatography using aluminum oxide (activity 2, pre-coated plate) in hexanes/CH_2Cl_2, 1.5:1 and resulted in both isomers.

The chromatography afforded compound **315b** ($R_{f315b} > R_{f315a}$) as a red solid, and, like radialene **315a**, it had very low solubility and there was not sufficient amount of material for ^{13}C NMR spectroscopy. UV-vis spectroscopic analysis of compound **315b** in THF shows absorptions at 370 nm and less intensively absorption at 509 nm. Due to the low solubility, extinction coefficients (ε) are not reported for either isomer (Figure **5.8**). Cyclic voltammetry of **315a** has been measured in CH_2Cl_2 and shows a reduction at –1.29 and –1.59 V as well as oxidations at 0.78 and 0.86 V (refer to page 191 for CV voltammograms).

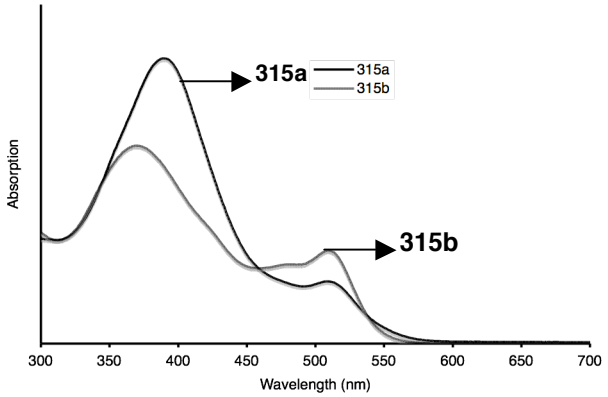

Figure 5.8 UV-vis spectra of compounds **315a** and **315b** measured in THF

5.6 Discussion regarding the identities of pentacenylidene and anthracenylidene derivatives

Without X-ray analysis it is difficult to clearly establish the identities of **502a**, **502b**, **504a**, and **504b**. Based on the X-ray data for tetrabromide derivatives **501** and **503**, cyclization is more likely to be geminal (Br1 to Br2 and Br3 to Br4) than further away (Br1 to Br3 and Br2 to Br4) because there is less steric hindrance from fused rings. In other words, the formation of expanded radialene is more favored than radiaannulene (for example Figures **5.1** or **5.4**).

The ^{13}C NMR spectra of the major isomers for compounds **502** and **504** are quite similar in terms of the chemical shifts of the alkyne carbons and similar to compound **315a**. UV-vis spectroscopic studies of the relevant compounds measured in THF show that compound **315a** is very similar to the major isomer of the compound **502**, both have two absorptions that are very close in terms of wavelengths and the spectral pattern and less similar to the major isomer of compound **504**. Because of the spectral similarities to compound **315a** and the

fact that radialene **315a** is the major isomer of compound **315** in the one-pot formation of **315a** and **315b**, the best possible prediction is that the major isomer of compounds **502** and **504** are expanded radialenes **502a** and **504a,** respectively.

5.7 Synthesis of [4]expanded radialene derivative incorporating para methoxy-phenylethynyl functional group (route A)

The use of suitably functionalized expanded radialenes for synthesis of other derivatives of radialenes is based on the protodesilylation of the trialkylsilylethynyl end-capped groups and further coupling with vinyl triflate or aryl halides (Scheme **5.14**). The stepwise synthesis of compound **315a** is an example of triflate coupling or route **B** shown in the Scheme **5.1**. Alternatively, 4-iodoanisole reacted with desilylated radialene **411** under the Sonogashira coupling protocol as outlined in Scheme **5.14 (**route **A,** Scheme **5.1)**. The reaction afforded compound **510** as an orange solid in 70% yield and compound **511** as a dark red solid in 15% yield.

The constitutional formula of radialene **510** has been confirmed by HR MALDI-TOF mass spectrum that shows a molecular ion (M^+) at m/z 916.33410 while the mass to charge ratio calculated for $C_{70}H_{44}O_2$ is 916.33358. Compound **511** HR MALDI-TOF mass spectrum shows a molecular ion (M^+) at m/z 1618.57789 while the mass to charge ratio calculated for $C_{126}H_{74}O_2$ is 1618.56833.

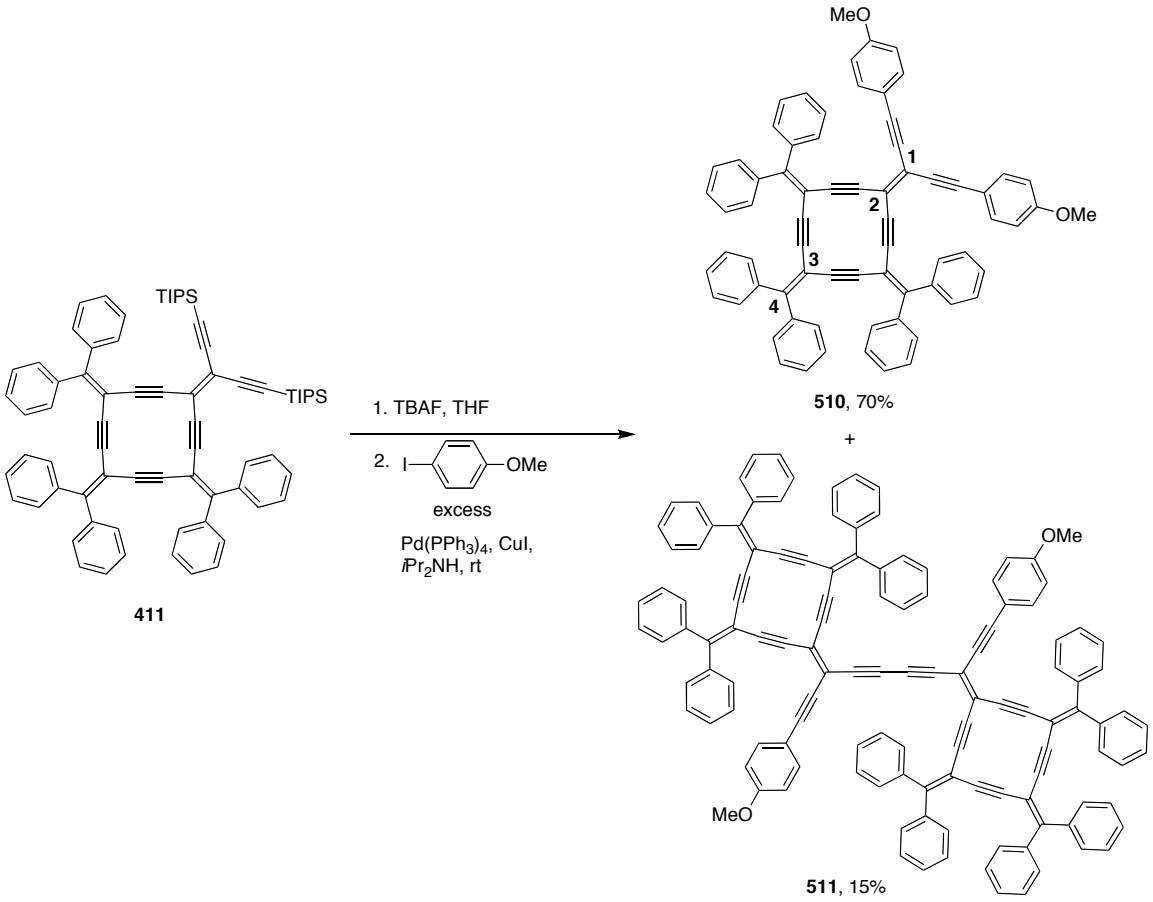

Scheme 5.14 Synthesis of radialene **510** and radialene-oligomer **511**

The ^{13}C NMR spectrum of radialene **510** shows 27 signals out of 29 expected. The alkyne carbon signals are at 102.3, 99.1, 97.1, 96.9, 96.8, and 86.3 ppm. The vinylidene carbons, as shown for the labeled carbons (**C1**–**C4**), resonated at 152.5, 115.7, 112.0, and 102.5 ppm (Scheme **5.14**). The yield of radialene-oligomer **511** was low and there was not sufficient amount of compound **511** available for ^{13}C NMR spectroscopy.

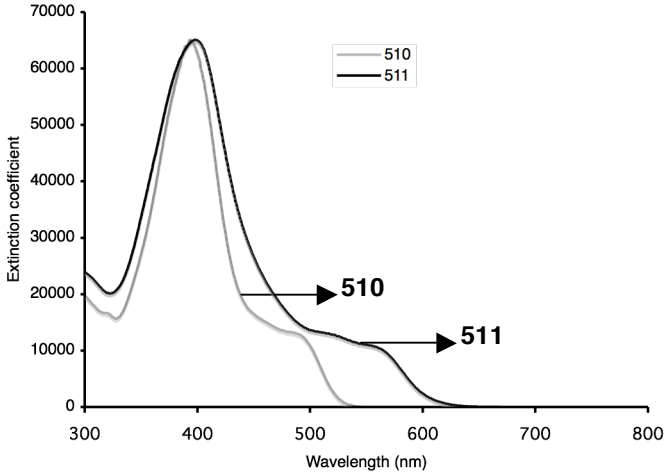

Figure 5.9 UV-vis spectrum of radialenes **510** and radialene oligomer **511** measured in THF

The UV-vis spectra of radialenes **510** and **511** were obtained in THF. Radialene **510** shows an absorption at λ_{max} = 393 nm (ε = 65200 L mol^{-1} cm^{-1}) with a shoulder around 490 nm. Radialene **511** shows an absorption at λ_{max} = 399 nm (ε = 65100 L mol^{-1} cm^{-1}) and a shoulder at 560 nm. Radialene **511** shifted more to lower energy due to an increase in the linear cross-conjugated fragment of the molecule (Figure **5.9**).

5.8 Stepwise synthesis of [4]expanded radialene incorporating triisopropylsilylethynyl functional group

Synthesis of a bisexpanded radialene **315a** through a stepwise pathway was discussed in this chapter. In this section, the concept of derivatizing the expanded radialene structure is considered in more detail. In order to synthesize our target in Scheme **5.15**, a stepwise approach is designed. The plan is to have

two different trialkylsilylethynyl functional groups, one of which can be selectively protodesilylated. The best groups are TES and TIPS because the TES is desilylated selectively than TIPS and both groups are stable during the coupling reactions compared to TMS group. Dibromoolefin **410**[8] was treated with **513**[9] under the general Sonogashira coupling protocol giving compound **514a** as a yellow oil in 50% yield. Compound **514a** was selectively protodesilylated and reacted with **410** under the Sonogashira protocol affording radialene **515** as a yellow solid in 78% yield (improved yield from initial attempt of 70% yield)(Scheme **5.15**).

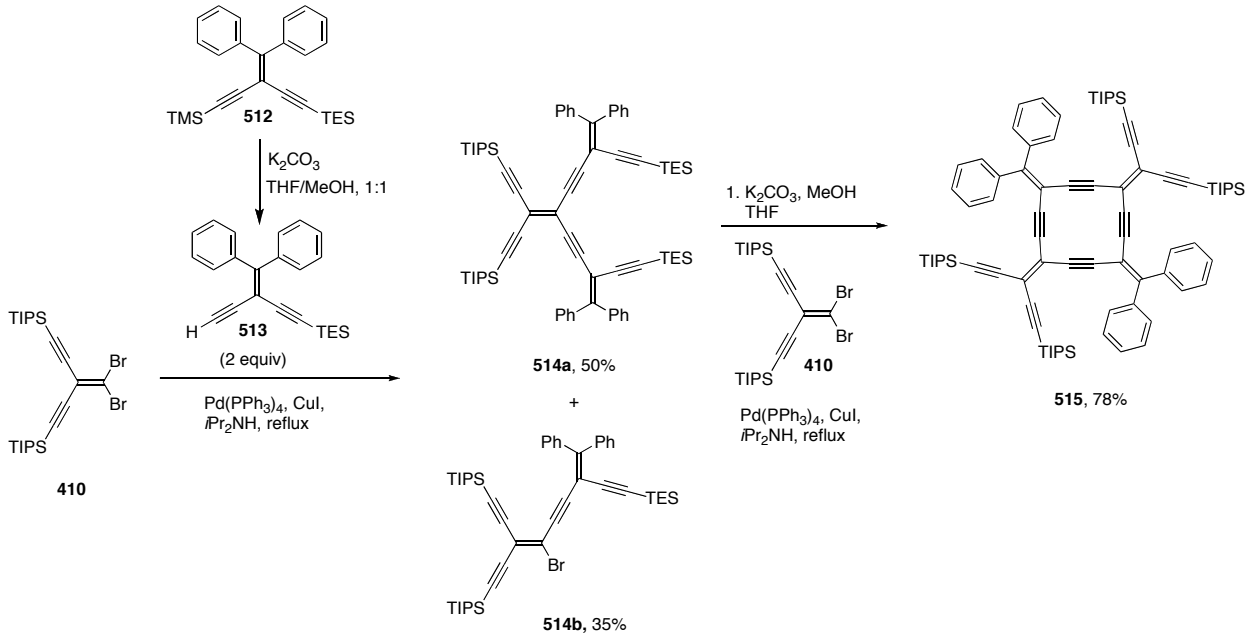

Scheme 5.15 Stepwise synthesis of radialene **515**

The constitution formula of radialene **515** has been confirmed initially by HR MALDI-TOF mass spectrometry which shows a molecular ion (M^+) at m/z 1244.72033 while the mass to charge ratio calculated for $C_{84}H_{104}Si_4$ is

1224.72096. The ^{13}C NMR spectrum shows 14 signals in accordance with the expected number of carbons in the radialene **515**. In this regard, the ^{13}C NMR spectrum shows characteristic alkyne carbons at 104.1, 103.9, 102.3, and 95.8 ppm. The vinylidene carbons resonate at 153.0, 116.9, 111.5, and 101.8 ppm.

A UV-vis spectroscopic study of radialene **515** in THF shows an absorption at λ_{max} = 399 nm (ε = 25500 L mol^{-1} cm^{-1}) (Figure **5.13**). Cyclic voltammetry of compound **515** shows a reduction at –1.61, –1.85, and –2.11 V and an oxidation event at 0.95 V (refer to page 192 for CV voltammograms). Radialene **515** is a very useful starting material that can be used for the synthesis of higher derivatives of the expanded radialenes via desilylation and Sonogashira coupling (refer to appendix for further discussion).

Single crystals of compound **515** suitable for X-ray crystallographic analysis were grown by slow evaporation of a $CHCl_3$ solution at 4–5 °C. The ORTEP plot of radialene **515** is shown in two views in Figure **5.10**.

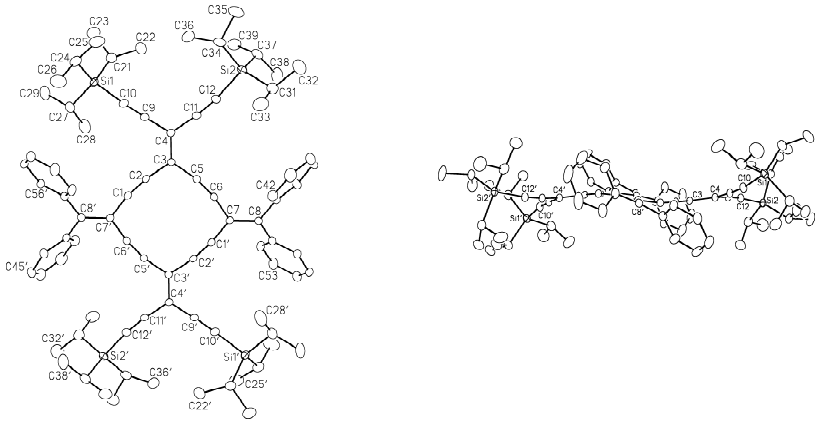

Figure 5.10 ORTEP plots of compound **515** (hydrogens removed for clarity)

The most notable solid-state feature is that the cyclic core is quite planner and the planarity it is extended by the alkyne units outside the cyclic periphery. The alkyne bond angle for C3–C5–C6 is 165.2(3)° and for C5–C6–C7 is 166.8(3)° (Figure **5.12**). The alkyne bond length for C5–C6 is 1.199(4) Å and for C9–C10 is 1.199(5) Å. Also, the vinylidene bond angle for C2–C3–C5 is 112.3(2)° and for C6–C7–C1' is 111.4(3)°. For the radialene **311,** the alkyne bond angle is C5–C6–C7 is 171.30(15)° and the vinylidene bond angle C6–C7–C1' is 110.40(11)° and the alkyne bond length is 1.2018(19) Å. Therefore, the alkyne bond angle and bond length are larger for radialene **311** but the vinylidene bond angle is more contracted for the radialene **311** than the radialene **515**.

5.9 Synthesis of triisopropylsilylethynyl [4]expanded radialene and radialene oligomer

Radialenes **411** and **515** have been discussed with regard to the proposal to elaborate the structures of the expanded radialenes. In a related issue, a new strategy has been formulated to design an expanded radialene that has a phenyl ring outside the cyclic core of the expanded radialene, which carries a triisopropylsilylethynyl group. Based on this plan Scheme **5.16** has been proposed and executed.

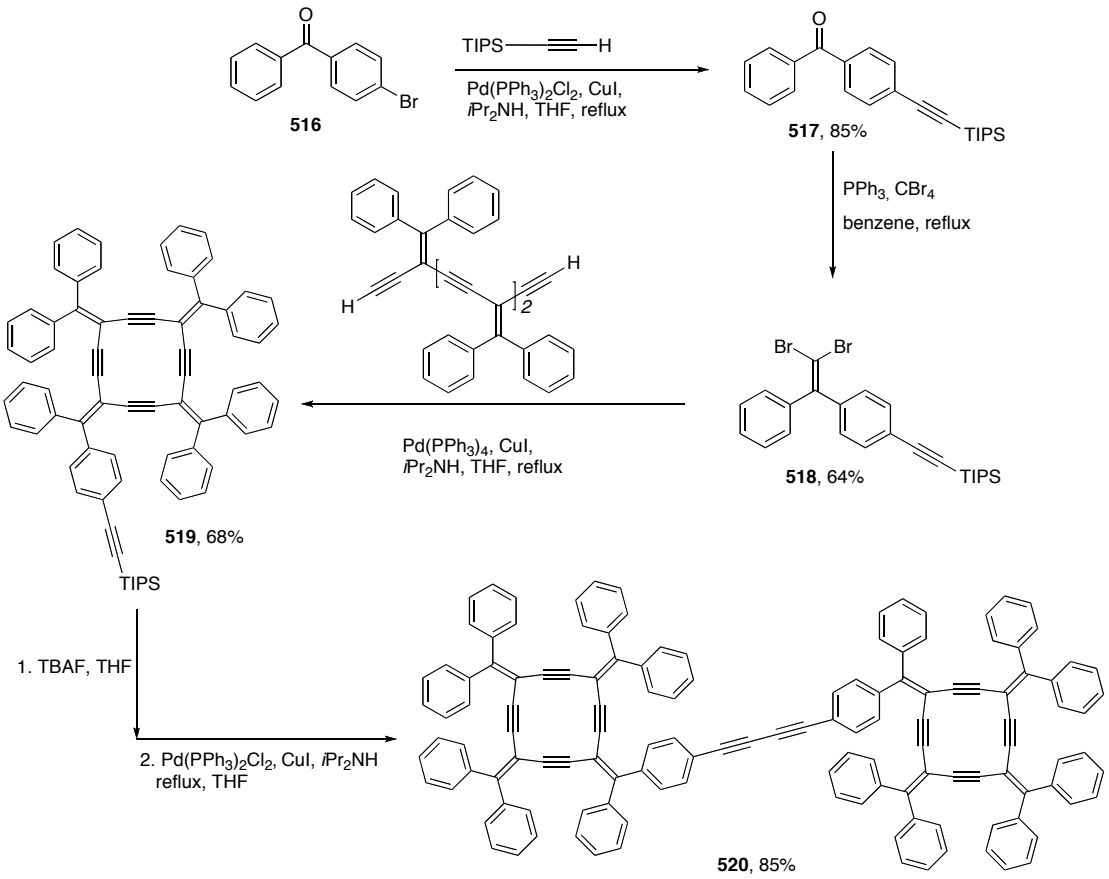

Scheme 5.16 Synthesis of radialene oligomer **520**

The ketone **516** (commercially available) is reacted with triisopropylsilyl-acetylene to give compound **517** as a pale yellow oil. Compound **517** was converted to dibromoolefin **518** as an off-white solid in 64% yield. Dibromoolefin **518** reacted with the desilylated trimer **305** under the Sonogashira coupling protocol giving a yellow solid **519** in 68% yield. The constitutional formula of compound **519** has been confirmed initially by HR MALDI-TOF mass spectrometry, which shows a molecular ion (M^+) at m/z 988.4611 while the calculated mass to charge ratio for $C_{75}H_{60}Si$ is 988.44588. Due to the presence of the TIPS-ethynyl group, the lack of symmetry of molecule is clear in the ^{13}C

spectrum with the presence of 10 alkyne carbons at 102.5, 97.7, 97.4, 97.2, 97.0, 96.9, 96.84, 96.77, 96.7, and 91.7 ppm. Infrared spectroscopy shows an alkyne bond stretch at 2153 cm^{-1}. UV-vis spectroscopy of radialene **519** shows one absorption at λ_{max} = 381 nm (ε = 70300 L mol^{-1} cm^{-1}). Figure **5.11** shows a comparison of the UV-vis spectra of radialenes **515** and **519** in THF. Cyclic voltammetry of radialene **519** shows a reduction at –1.87 and –2.19 V and two oxidations the first at 0.81 and the second at 1.03 V (refer to page 192 for CV voltammograms).

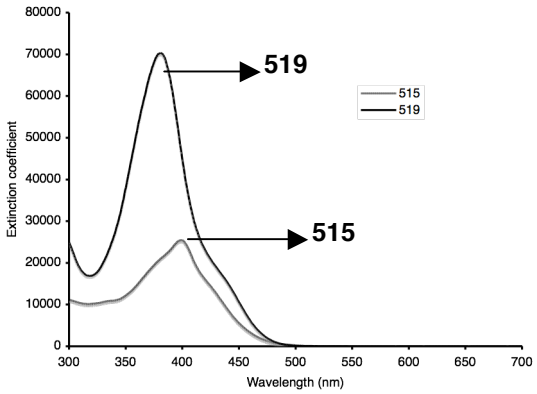

Figure 5.11 UV-vis of radialenes **515** and **519** measured in THF

In a manner similar to that described in **5.16**, the radialene **519** is desilylated and refluxed in the presence of Pd(II) (Sonogashira protocol) to give radialene-oligomer **520**, a yellow solid at an excellent yield of 85% (Hay oxidative coupling protocol: TMEDA, CuCl, in the presence of O_2 in CH_2Cl_2 afforded a 60% yield for **520**).[10] The radialene-oligomer **520** does not show significant solubility in organic solvents, making ^{13}C NMR spectroscopy impossible for now. Initial confirmation of the proposed structure of the radialene-oligomer **520**

(constitutional formula) comes from HR MALDI-TOF mass spectrometry that shows a molecular ion at m/z 1662.61079 while the calculated mass to charge ratio for $C_{132}H_{78}$ is 1662.60980 (Figure **5.12**).

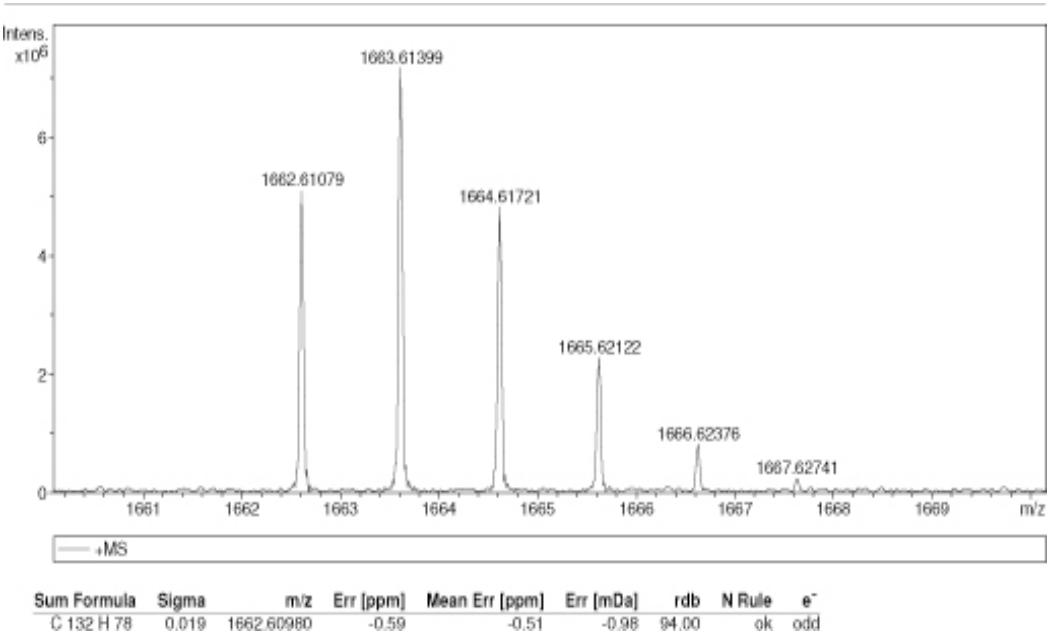

Sum Formula	Sigma	m/z	Err [ppm]	Mean Err [ppm]	Err [mDa]	rdb	N Rule	e⁻
C 132 H 78	0.019	1662.60980	-0.59	-0.51	-0.98	94.00	ok	odd

Figure 5.12 HR MALDI-TOF mass spectrum of radialene-oligomer **520**

The UV-vis spectrum of compound **520** in THF shows an absorption at 385 nm, and a shoulder around 450 nm, as shown in Figure **5.13**.

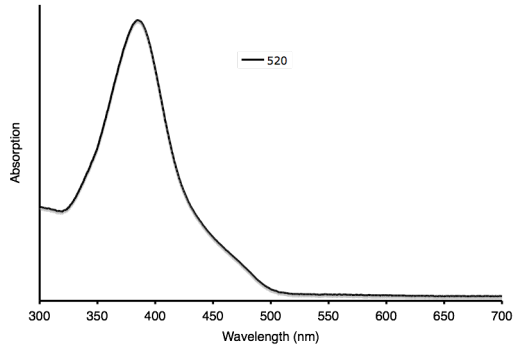

Figure 5.13 UV-vis spectrum of compound **520** measured in THF

5.10 Synthesis of [4]expanded radialene derivatives incorporating ferrocenyl functional group

Synthesis of anthracenylidene [4]radialene in Scheme **5.3** also gave a side product **502c** in 11% yield, a yellow solid that was useful for further coupling reactions (Scheme **5.17**).

Compound **502c** was fully characterized and reacted with ferrocenyl derivative **521**[11] in the presence of a catalytic amount of $Pd(PPh_3)_2Cl_2$ at reflux, resulting in the first ferrocenyl expanded radialene **522** as a dark red-brown solid in 98% yield (Scheme **5.17**). The reaction also gave a trace amount of compound **523** that has been confirmed by ^1H NMR spectroscopy and HR MALDI-TOF mass spectrometry.

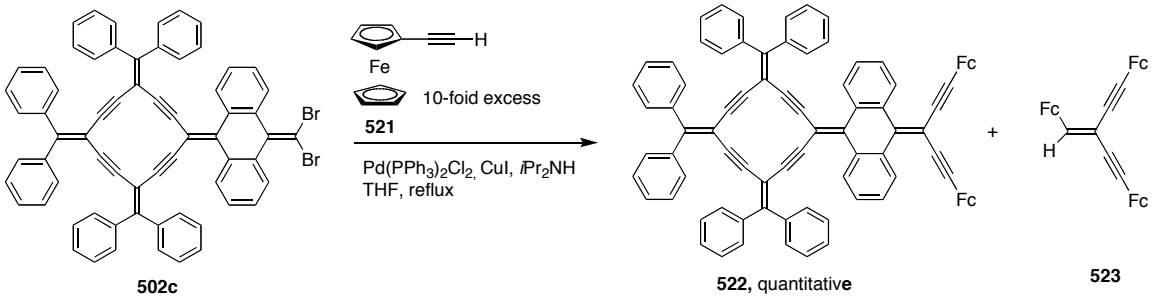

Scheme 5.17 Synthesis of compounds **522** and **523**

Confirmation of compound **522** (constitutional formula) initially comes from HR MALDI-TOF mass spectrometry with a molecular ion (M^+) is at m/z 1248.30646 while the calculated mass to charge ratio for $C_{90}H_{56}Fe_2$ is 1248.30754. The ^{13}C NMR spectrum shows characteristic alkyne carbons at

99.1, 97.1, 97.0, 96.9, 94.1, and 85.8 ppm. The signals belonging to the ferrocenyl fragments resonate at 71.8, 70.4, 69.7, and 65.3 ppm.

In a related concept of ferrocenyl radialene chemistry compound **514b** from Scheme **5.16** reacted in the same fashion with compound **521** according to Scheme **5.18**. The resulting product, compound **524** is a red-brown oil in 80% yield. Its composition has been confirmed by HR MALDI-TOF mass spectrometry and ^{13}C NMR spectroscopy. The MALDI-TOF data shows a molecular ion (M^+) at m/z 936.46002 while the calculated mass to charge ratio for $C_{60}H_{76}FeSi_3$ is 936.45988. The ^{13}C NMR spectrum shows signals of ferrocenyl framework at 71.8, 70.2, 69.5, and 64.2 ppm and alkyne carbons at 101.9, 101.01, 100.95, 99.5, 96.4, 95.7, 89.0 and 83.9 ppm.

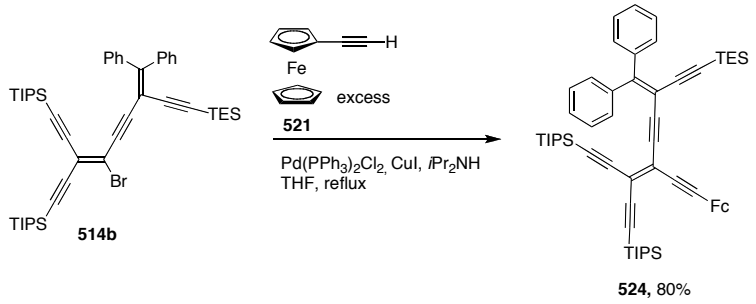

Scheme 5.18 Synthesis of compound **524**

The UV-vis spectra of compounds **522** and **524** were measured in THF. Radialene **522** shows an absorption at λ_{max} = 392 nm (ε = 30000 L mol^{-1} cm^{-1}) and a shoulder around 530 nm. The compound **524** shows an absorption at λ_{max} = 353 nm (ε = 27600 L mol^{-1} cm^{-1}), a shoulder around 380 nm, and a second

absorption at λ_{max} = 510 nm (ε = 3400 L mol^{-1} cm^{-1}) (Figure **5.14**). Compound **524** also could be considered for its potential usage in organometallic chemistry. (refer to Chapter **6**)

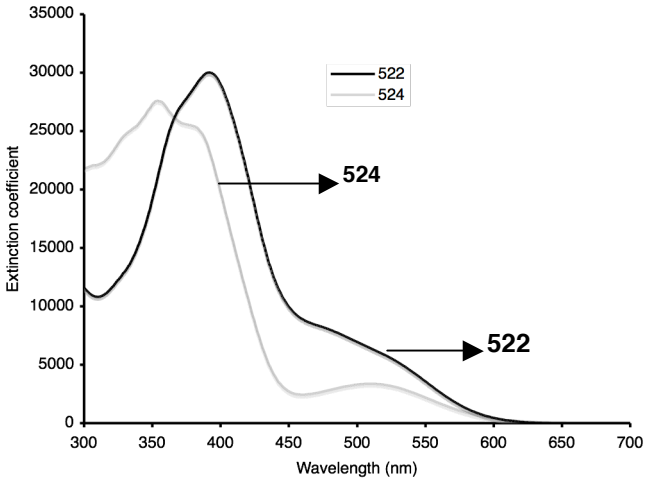

Figure 5.14 UV-vis spectra of compounds **522** and **524** measured in THF

5.11 Synthesis of radiaannulenes in stepwise and one-pot reactions[12]

In regard to expanded radialenes and related derivatives of expanded radialenes that carry radialene skeletons, a variety of conjugated cyclic topologies can be accessed on the basis of enyne building blocks, including linearly-conjugated dehydroannulenes/dehydrobenzannulenes **A** and cross-conjugated radialenes **B**. Intermediate between these two limiting structures are the radiaannulenes **C** and the *meta*-substituted aryl analogues **D.** Several molecules based on the general structure of **D** have been described, while only a single report of radiaannulenes appeared recently by Zhao and coworkers who incorporated *p*-extended tetrathiafulvalene moieties at the alkylidene positions and their related derivatives.[13] Moreover, the formation of macrocycles **C** with a

minimalistic all carbon structure in comparison to radialenes **B** is a logical target in terms of synthesis and physical properties (Scheme **5.19**).

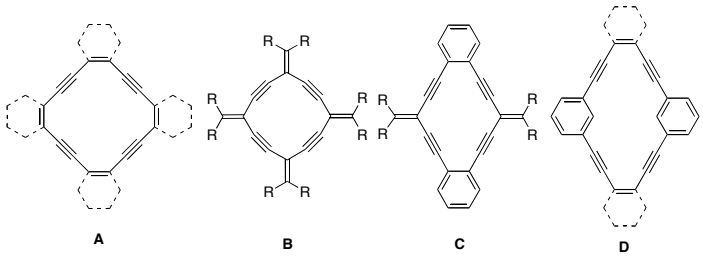

Scheme 5.19 General structures for carbon-rich macrocycles

The strategy for the synthesis of **C** is based on incorporation of the desilylated monomer where it is reacted with diiodobenzene in a one-pot reaction under the Sonogashira coupling protocol (Scheme **5.20**). The reaction gave radiaannulene **526** as a pale yellow solid in a very reasonable yield of 31%. The radiaannulene **526** has been confirmed by ^{13}C NMR spectroscopy and mass spectrometry. HR MALDI-TOF mass spectrometry shows a molecular ion (M^+) at m/z 604.21854 while the calculated mass to charge ratio for $C_{48}H_{28}$ is 604.21855. The ^{13}C NMR spectrum shows the expected 11 unique resonances as expected. The synthesis of **526** invited the use of **527** in the synthesis of an analogue, radiaannulene **528**, where the phenyl rings are joined. First, the synthesis was attempted by a one-pot strategy, but due to the low yield of product under these conditions, the reaction was not followed up (Scheme **5.21**).

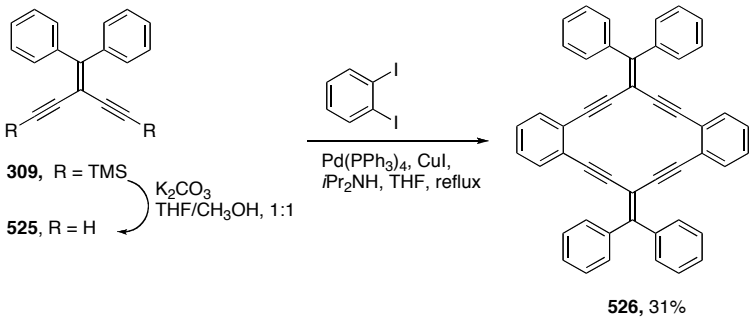

Scheme 5.20 Synthesis of radiaannulene **526**

A stepwise strategy was designed according to Scheme **5.21**. The synthesis was based on the selective desilylation of compound **530**[14] and a coupling reaction with the dibromoolefin **407**.[15] Compound **531** was desilylated by TBAF giving compound **532**. Compound **532** reacted with the dibromoolefin **407** to give compound **528** in an excellent yield of 90% as a red solid.

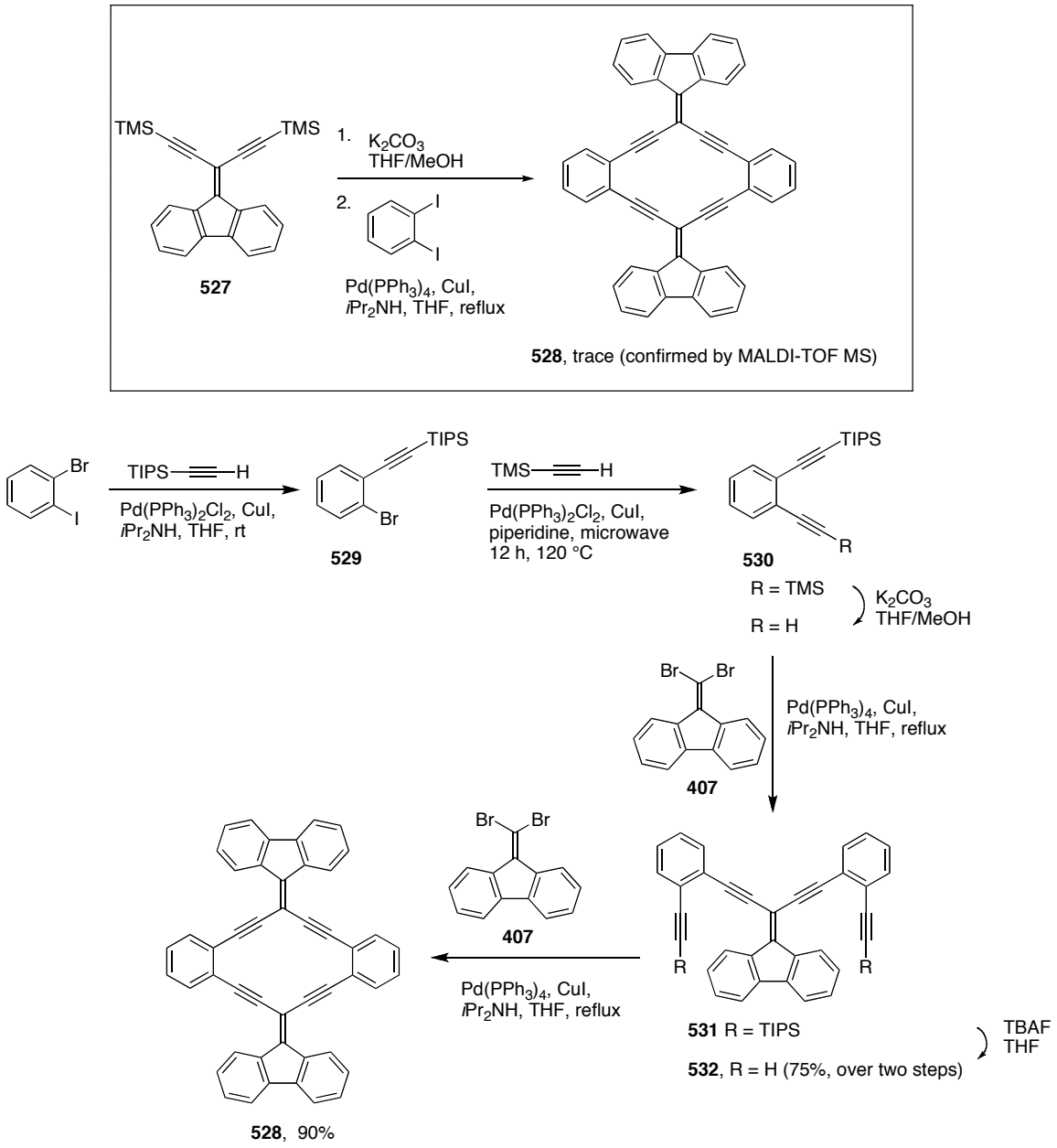

Scheme 5.21 Synthesis of compound **528** from a one-pot and stepwise route

The solubility of **528** is very low in most organic solvents and it has been a big challenge to obtain a good quality carbon NMR spectrum. The ^{13}C NMR experiment was executed at 65 °C using $C_2D_2Cl_4$ to dissolve compound **528**. The carbon NMR spectrum shows 13 peaks corresponding to the expected number.

Furthermore, the HR MALDI-TOF mass spectroscopy of compound **528** shows a molecular ion at m/z 600.18698 while the calculated mass to charge ratio for $C_{48}H_{24}$ is 600.18725.

5.12 UV-vis, solid state, and electrochemical studies of radiaannulenes [12a,b]

UV-Vis spectroscopic analysis of **526** and **528** begins with a comparison of the absorption spectra of the basic building blocks, represented by enediynes **309** (λ_{max} = 328 nm) and **527** (λ_{max} = 374 nm).[12b] Thus, there is a bathochromic shift for λ_{max} of 46 nm (in CH_3CN) upon the transformation from pendent diphenylalkylidene unit to that of the fluorenylidene. Comparing the absorption spectra of macrocycles **526** (λ_{max} = 413 nm) and **528** (λ_{max} = 472 nm) shows that the bathochromic shift arising from fluorenylidene versus diphenylalkylidene substitution is increased slightly to 59 nm, as a result of incorporation into the macrocyclic framework. Within the series of molecules **A**–**C** (Scheme **5.19**, page 175), the fully cross-conjugated radialene **311** (R =Ph) shows a blue shifted λ_{max} = 377 nm (in THF) in comparison to **526**, while the tetrabenzo[16]annulene **A** shows $\lambda_{max} \approx$ 405 nm (in cyclohexane). Thus, the longer linearly-conjugated segments of annulene **A** and radiaannulenes **C** afford reduced HOMO–LUMO gaps in comparison to radialene **B**, as would be expected.

The structures of **526** and **528** were confirmed by single crystal X-ray crystallographic analysis. Single crystals of compound **526** suitable for X-ray crystallographic analysis were grown by slow evaporation of a $CHCl_3$ solution at 4–5 °C (CCDC #, 721525) (for compound **528** from a solution of 1,2

dichloroethane, CCDC #, 721526). The radiaannulene framework of both molecules is nearly planar, although the diphenylalkylidene moieties of **526** project slightly above and below the plane of the macrocycle, imparting an overall flattened chair conformation to the molecule. The major structural feature in both **526** and **528** is the deviation of alkyne units from linearity, resulting in a tendency of the endocyclic alkylidene angles to be slightly less than 120° (i.e., C(10)–C(11)–C(13) = 114.07(15)°, C(22)–C(23)–C(1) = 114.37(16)° as observed for numerous similar systems (Figures **5.15** and **5.16**).[12a]

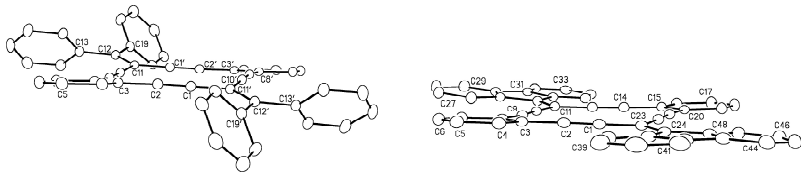

Figure 5.15 Edge on view of radiaannulenes **526** (left) and **528** (right) (hydrogens removed for clarity)

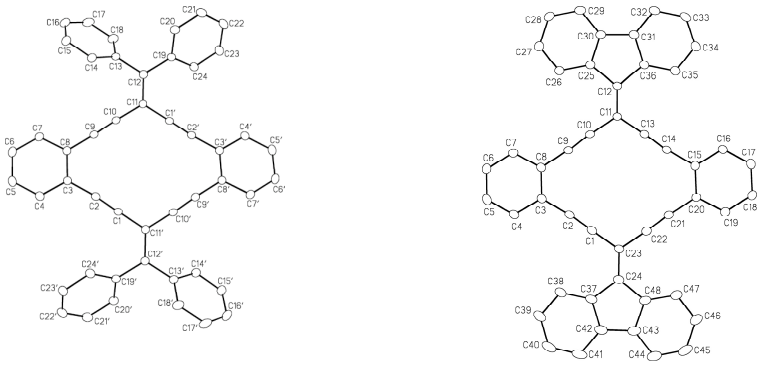

Figure 5.16 ORTEP plots for compound **526** and **528** (hydrogens removed for clarity)

Cyclic voltammetry (CV) shows that macrocycles **526** and **528** both exhibit three one-electron reductions. In each case, the first two reductions are reversible, while the third is quasireversible. Fluorenylidene substitution provides a much more facile first reduction, which occurs at –1.50 V for **528** versus –1.97 V for the diphenylalkylidene counterpart **526**. Two very closely spaced oxidation processes are observed for **526** and this is confirmed by Osteryoung square wave voltammetry (OSWV). Conversely, compound **528** does not exhibit any appreciable anodic behavior. Table **5.1** shows the redox potentials and the electrochemical HOMO–LUMO gaps for **526** and **528.**[12a]

Table 5.1 Redox potentials for radiaannulenes **526** and **528**[†]

Compounds	Ep ox1 [V]	$E_{1/2}$ red_1 [V]	E_p red_3 [V]	E_p red_3 [V]	$\Delta E_{elec\ gap}$ [V]
526	0.75	–1.97	–2.15	–2.41	2.72
528	0.88	–1.50	–1.65	–2.30	2.38

[†]Cyclic voltammetry measured in CH_2Cl_2 + 0.1 M nBu_4NPF_6 at a scan rate 100 mV s^{-1}. All potentials are reported versus the ferrocenium/ferrocene (Fc^+/Fc) couple (refer to appendix for definition and discussion of $\Delta E_{elec\ gap}$)

5.13 Summary and comparison of the radialene derivatives

Cyclic voltammetry voltammograms of the radialene derivatives measured in CH_2Cl_2 are shown in Figures **5.17.** Comparing the redox potentials of large [4]radialenes with compound **311** with regard to general Table **A.1** (appendix), clearly shows that these compounds are reduced more easily than [4]radialene **311**. Also, these compounds are more easily oxidized compared to **311**. Basically, for all the radialenes in Figure **5.17** there is a good agreement between

the optical gaps and the electrochemical gaps according to the general Table **A.2** (appendix). Also, cyclic voltammetry voltammograms for the [4]radialenes carrying TIPS groups is shown in Figure **5.18**, again there is a good agreement between the optical gaps and the electrochemical gaps of these compounds according to the general Table **A**.**2** (appendix).

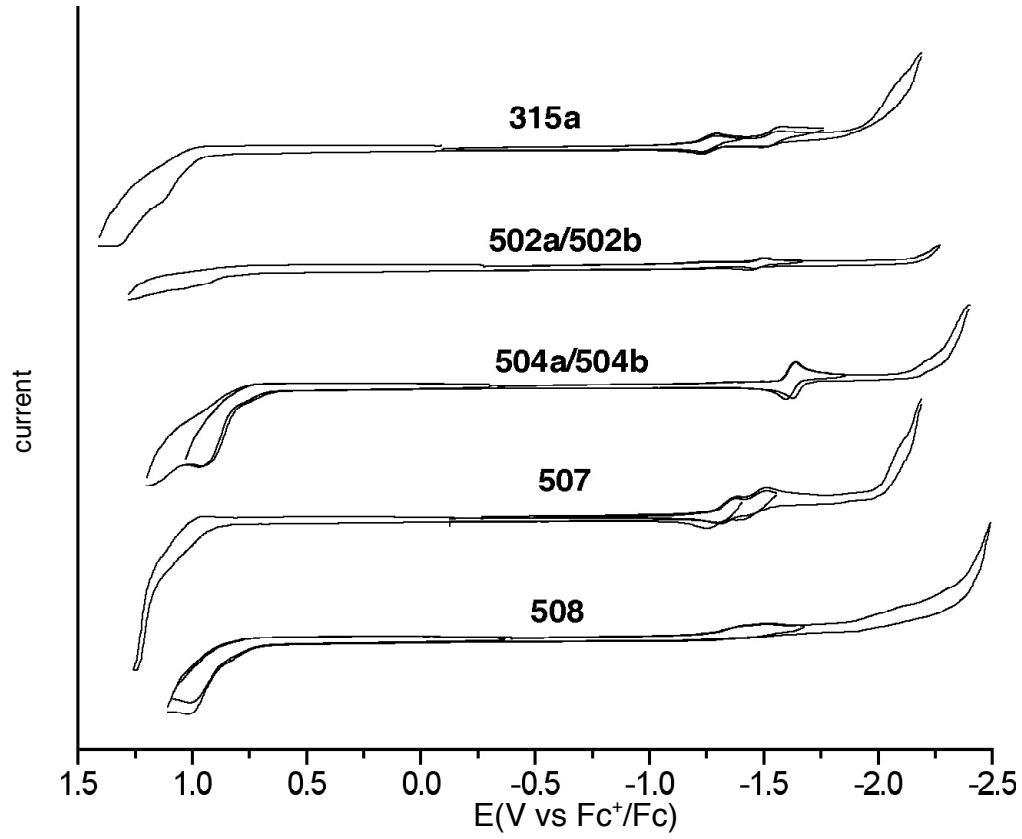

Figure 5.17 CV voltammograms of the radialene derivatives measured in CH_2Cl_2 Cyclic voltammetry measured in CH_2Cl_2 + 0.1 M nBu_4NPF_6 at a scan rate 100 mV s^{-1}. All potentials are reported versus the ferrocenium/ferrocene (Fc^+/Fc)

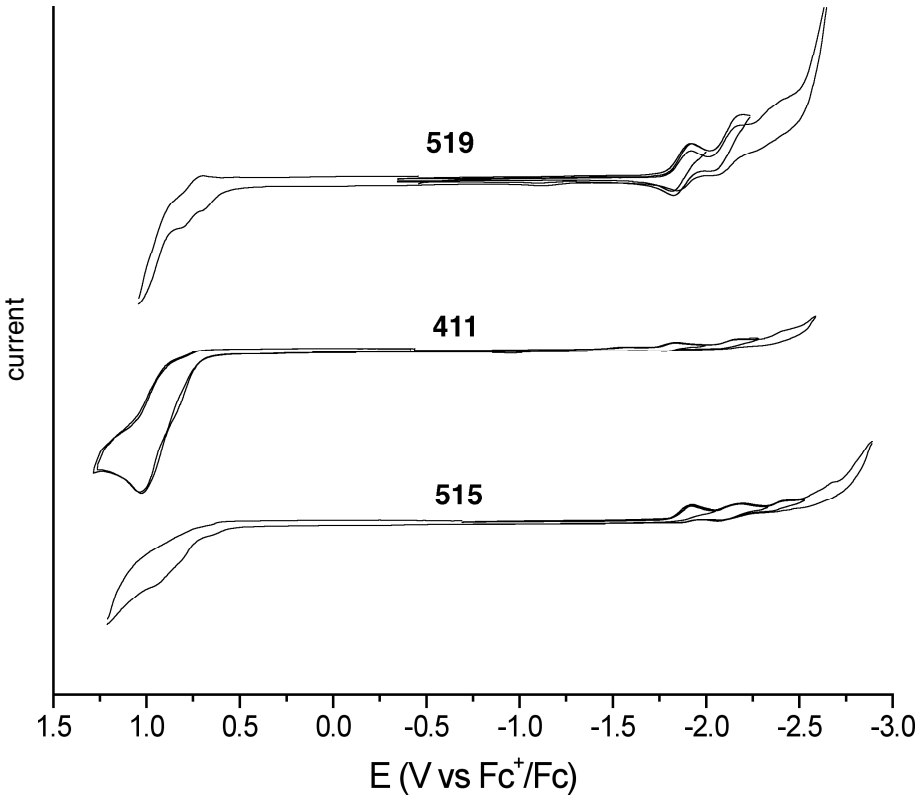

Figure 5.18 CV voltammograms of the TIPS-[4]radialenes measured in CH_2Cl_2 Cyclic voltammetry measured in CH_2Cl_2 + 0.1 M nBu_4NPF_6 at a scan rate 100 mV s^{-1}. All potentials are reported versus the ferrocenium/ferrocene (Fc^+/Fc)

The use of expanded radialenes carrying trialkylsilylethynyl groups as a synthetic strategy for the derivatization of the expanded radialenes has been demonstrated. The first stepwise synthesis of compound **315a** confirms the proposed strategy. Also, the synthesis of compound **510** is the first example for the reaction of desilylated radialene **411** with an aryliodide. This method is an efficient method for synthesizing the functional radialenes. However, if the corresponding dibromoolefin of the aryliodide is available, it is wiser to use the methodology discussed in Chapter **4** because it is shorter by one step.

The synthesis of compounds **515** and **519** is a further testimony to the concept of derivatization of the expanded radialenes. Through the desilylation of

compound **519** and its reaction under the Sonogashira protocol, compound **520** has been synthesized.

Compound **522** is the first radialene derivative that carries the ferrocenyl, anthracenylidene and radialene frameworks in one molecule. The π-system is expanded from the radialene to the ferrocenyl framework bridged by the anthracenylidene framework. A cyclic voltammetry study could potentially explore how the different frameworks influence one another in terms of communication in compound **522**.

Based on the synthesis of radiaannulenes **526** and **528**, both strategies that have been developed are applicable to other derivatives that carry functional groups, either through a one-pot or stepwise synthesis (Scheme **5.22**).[7] The presence of suitable functional groups may increase the solubility that has been the major obstacle for the characterization of compounds **526** and **528**. Also, compound **528** may be a suitable candidate for organometallic and cycloaddition reactions, because the solid-state analysis for compound **528** shows, that it is approximately planner with a suitable cavity for potential metal interaction(s).

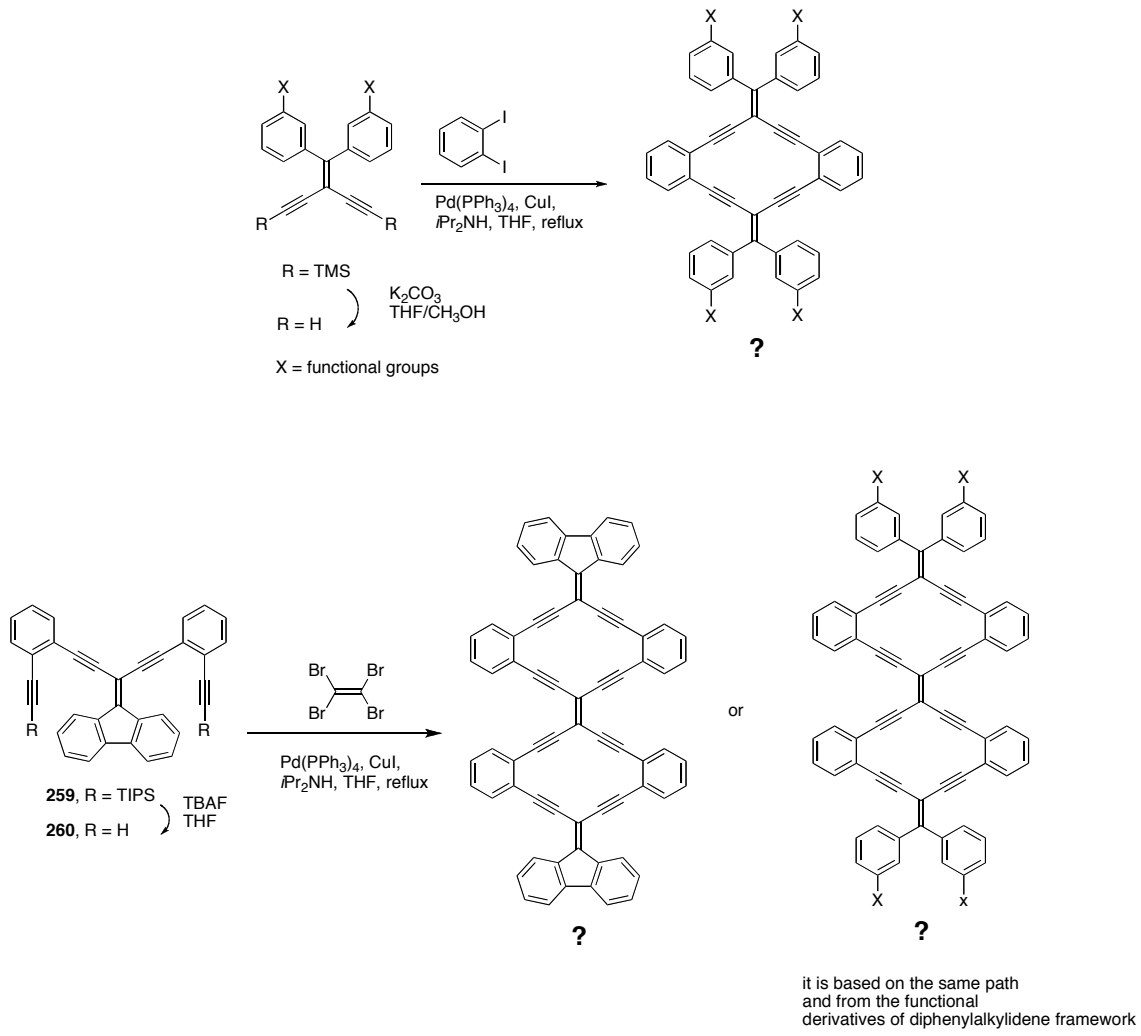

Scheme 5.22 Proposal for synthesis of functional radiaannulenes

5.14 Conclusion

The usage of a series of tetrabromide derivatives in the synthesis of the expanded radialene derivatives has established. The characterization of these compounds provided new information with regard to physical properties of these frameworks. The UV-vis spectroscopic properties of these compounds are similar to the bisexpanded radialene because of the similarity in the size of π-system that

is expanded over the molecule. Also, the differences between anthracenylidene and pentacenylidene frameworks are clearly shown in the UV-vis absorptions and electrochemical properties of their corresponding compounds.

Furthermore, the derivatization of the expanded radialenes has been established by the synthesis of compounds **315a**, **510**, and **520**.

The physical studies of the radiaannulenes **526** and **528** have shown how different are the optical and electronic properties of the fluorenylidene moiety compared to diphenylalkylidene moiety.

5.15 References

(1) (a) Campbell, K.; Ooms, K. J.; Wasylishen, R. E.; Tykwinski, R. R. *Org. Lett.* **2005**, *7*, 3397–3400; (b) Campbell, K.; Kuehl, C. J.; Ferguson, M. J.; Stang, P. J.; Tykwinski, R. R. *J. Am. Chem. Soc.* **2002**, *124*, 7266–7267.

(2) Neidlein, R.; Winter, M. *Synthesis* **1998**, 1362–1366.

(3) Bandyopadhyay, A.; Varghese, B.; Hopf, H.; Sankararaman, S. *Chem. Eur. J.* **2007**, *13,* 3813–3821.

(4) (a) Dan Lehnherr, **2005**–present, Department of Chemistry, University of Alberta; (b) Allen, C. F. H.; Bell, A. *J. Am. Chem. Soc.* **1942**, *64*, 1253–1260.

(5) Wesly Chalifoux, **2004**–present, Department of Chemistry, University of Alberta.

(6) Thanh Luu, **2002–2007**, Department of Chemistry, University of Alberta.

(7) Gholami, M.; Melin, F.; McDonald, R.; Ferguson, M. J.; Echegoyen, L.; Tykwinski, R. R. *Angew. Chem. Int. Ed.* **2007**, *46*, 9081–9085.

(8) Anthony, J.; Boldi, A. M.; Rubin, Y.; Hobi, M.; Gramlich, V.; Knobler, C. B.; Seiler, P.; Diederich, F. *Helv. Chim. Acta* **1995**, *78*, 13–45.

(9) Zhao, Y.; Slepkov, A. D.; Akoto, C. O.; McDonald, R.; Hegmann, F. A.; Tykwinski, R. R. *Chem. Eur. J.* **2005**, *11*, 321–329.

(10) Gibtner, T.; Hampel, F.; Gisselbrecht, J.-P.; Hirsch, A. *Chem. Eur. J.* **2002**, *8*, 408–432.

(11) Doisneau, G. ; Balavoine, G. ; Fillebeen-Khan, T. *J. Organomet. Chem*. **1992**, *425*, 113–17.

(12) (a) Gholami, M.; Chaur, M. N.; Wilde, M.; Ferguson, M. J.; McDonald, R.; Echegoyen, L.; Tykwinski, R. R. *Chem. Comm*. **2009,** 3038–3040; (b) Treitel, N.; Eshdat, L.; Sheradsky, T.; Donovan, P. M.; Tykwinski, R. R.; Scott, L. T.; Hopf, H.; Rabinovitz, M. *J. Am. Chem. Soc*. **2006**, *128*, 4703–

4709.
(13) (a) Chen, G.; Dawe, L.; Wang, L.; Zhao, Y. *Org. Lett.* **2009**, *11*, 2736–2739; (b) Chen, G.; Wang, L.; Thompson, D. W.; Zhao, Y. *Org. Lett*. **2008**, *10*, 657–660.
(14) Bell, M. L.; Chiechi, R. C.; Johnson, C. A.; Kimball, D. B.; Matzger, A. J.; Brad Wan, W.; Weakley, T. J. R.; Haley, M. M. *Tetrahedron* **2001**, *57*, 3507–3520.
(15) Paul, G. C.; Gajewski, J. J. *Synthesis* **1997**, 524–5260.

Chapter 6:

Exploratory Studies of Inorganic and Organometallic Chemistry of the Expanded Radialenes

6.1 Inorganic and organometallic chemistry of the expanded radialenes: objectives

A preliminary overview of organometallic and inorganic skeletons that resemble the expanded radialenes was given in Chapter **2**. The synthesis of organometallic derivatives of the cyclynes was based on their potential applications in materials science such as one dimensional conducting compounds.[1a,b] These compounds also have a cavity suitable to interact with transition metals in different oxidation states for the synthesis of new organometallic compounds that could be used as catalysts as well as functional compounds which provide path(s) toward further organic transformations.[2]

The chemistry of expanded radialenes with regard to their interactions with metal(s) has not yet been explored. In this chapter suitable precursors are used to explore reactions of the expanded radialenes with metal complexes in different oxidation states.

6.2 Coordination chemistry of the expanded radialenes

This study began with looking at the coordination chemistry of the expanded radialenes. The concept of coordination becomes valid when expanded radialenes carry electron-pair donor atoms that are able to share electrons with unsaturated metals. In the design of such ligands, with regard to the skeleton of the expanded radialenes, aryl groups such as pyridyl are more functional than phenyl rings. The previous synthesis of expanded radialenes was based on the coupling reaction of the *iso*-polydiacetylenes with dibromoolefins

under the Sonogashira protocol. Each of the two components could be altered to behave as ligands in the presence of donor atoms. A dibromoolefin with a pyridyl group is a good choice, and if it carries two 2-pyridyl groups it has the potential to form a strong bidentate ligand. One the most suitable candidates is the dibromoolefin of 2-pyridyl, **600**.

It was pointed out that the presence of lone electron pairs on nitrogen prevented the synthesis of [4]expanded radialene. Electron pairs of nitrogen atoms bond to the palladium catalyst and stop the coupling reaction. Therefore, it was required to design a strategy to tackle the issue and the following strategy could address this issue. Based on this strategy, the nitrogen lone pairs are first coordinated to a metal like Pt(II) and the resulting complex is then employed in a Sonogashira cross coupling reaction to form the target macrocycle. The concept of protecting groups is regularly used in organic chemistry and here also this method provides a metal complex prior to the formation of macrocycle.

The first example of the coordination ability of compound **600**–was the reaction of $Co(acac)_2(H_2O)_2$[3] which gave compound **601** as a red solid in 85% yield (Scheme **6.1**). X-ray crystallography showed that the product adopted octahedral geometry. The reaction demonstrated that **600** can act as a bidentate ligand and its behavior in principal is very similar to 2,2-bipyridyl. According to X-ray analysis, the bite angle of N–Co–N is 83.80° (measured as angle of N–Co–N) while the acetylacetonate (acac) bite angle is 88.24° (Mercury Crystal Structure Visualization Software version 1.4.1).

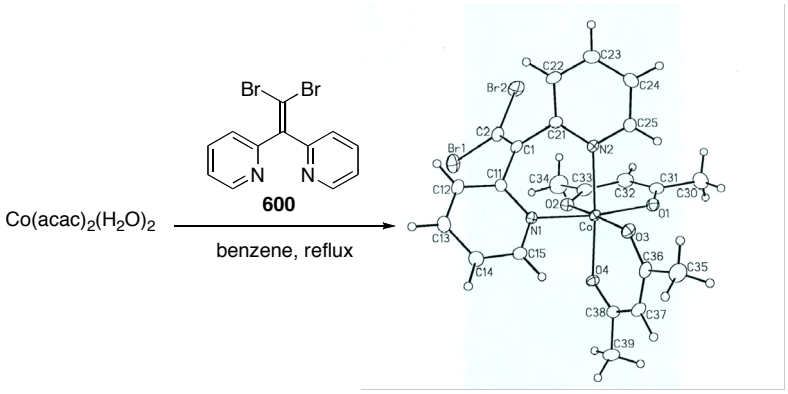

Scheme 6.1 Synthesis of a cobalt pyridyl complex **601**

The second example of the ability of compound **600** to coordinate to transition metals is the reaction of $Ru(bipy)_2Cl_2$[4] with **600** in a mixture of ethanol and water under reflux as outlined in Scheme **6.2**.

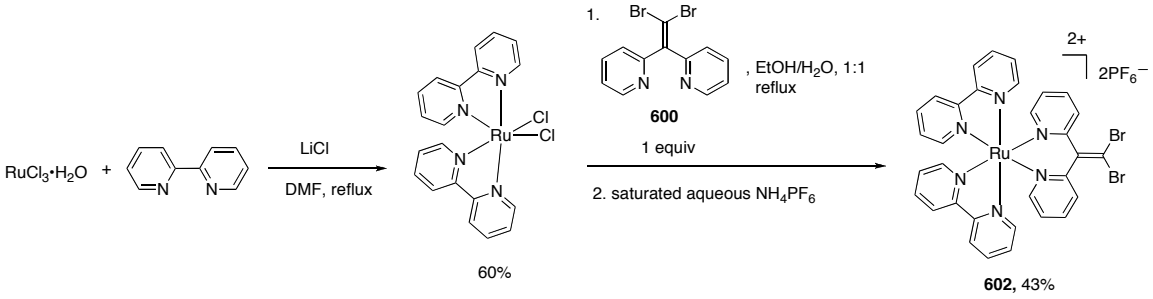

Scheme 6.2 Synthesis of a ruthenium pyridyl complex **602**

Complex **602** is insoluble in most common organic solvents, and it was very difficult to characterize. Compound **602** is partially soluble in dichloromethane but attempts to grow suitable single crystals for X-ray analysis failed. Confirmation of the product's stoichiometry (molecular composition) was obtained only by mass spectrometry, using electrospray technique (low resolution) that showed molecular ion (M^{2+}) for $C_{32}H_{24}Br_2N_6Ru$ at m/z 377. Based

on the two reactions described so far, compound **600** acts as a strong ligand and could potentially interrupt catalytic reactions where the catalyst is trapped with compound **600.** In order to prevent the nitrogen lone pairs from interrupting the Sonogashira coupling reaction, they could be protected through coordination with metal(s) such as Pt(II). The objective of the synthesis of [4]expanded radialene with a pyridyl ring was to use the expanded radialene product as a ligand for coordination chemistry. As mentioned before the strategy initiates first with metal coordination reaction and then the resulted complex is then used in the Sonogashira cross coupling reaction to form the targeted expanded radialene complex, as outlined in Scheme **6.3**.

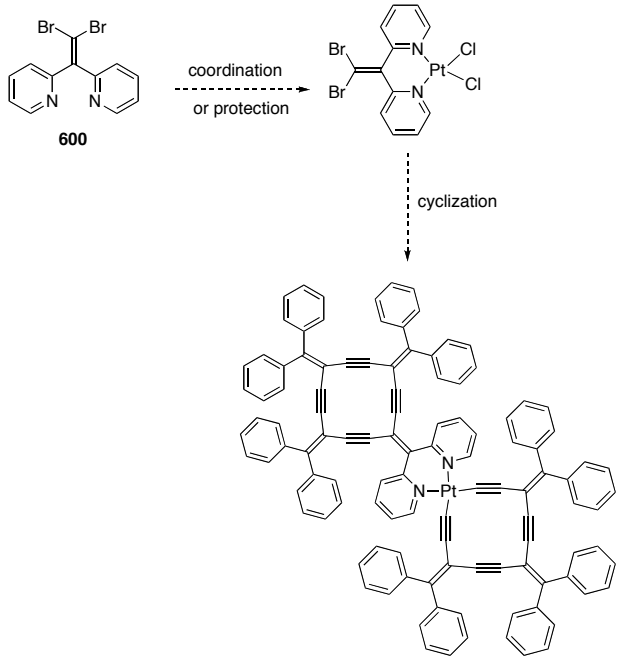

Scheme 6.3 Synthesis of a platinum radialene complex

Scheme **6.4** shows platinum complex **603** is obtained from **600** as a creamy solid in 85% yield according to the procedure of Newkome and coworkers .[5]

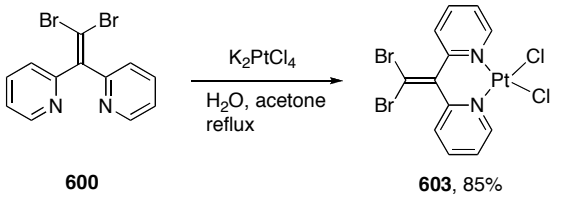

600 **603**, 85%

Scheme 6.4 Synthesis of complex **603**

Complex **603** carries two bromides suitable for the Sonogashira cross coupling reaction and the nitrogen lone electron pairs are protected via coordination to platinum. Complex **603** was mixed with CuI, *i*Pr_2NH, and $Pd(PPh_3)_4$ in deoxygenated THF and oligomer **305** (excess) was protodesilylated and reacted with the mixture under reflux. After purification using aluminum oxide and re-crystallization, a brown solid was collected in 25% yield (Scheme **6.5**). HR MALDI-TOF mass spectrometry showed the molecular mass of the product was in accordance with the targeted radialene complex **604** (Figure **6.1**).

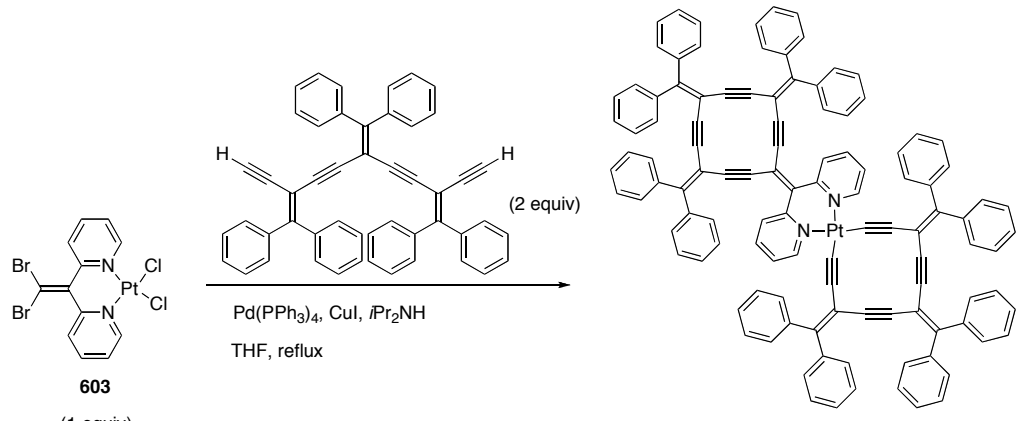

603
(1 equiv)

604, 25%

Scheme 6.5 Synthesis of platinum radialene complex **604**

According to the high resolution MALDI-TOF mass spectrometry spectrum of complex **604**, not only the molecular ion is present (m/z 1636.5) but also major

peaks due to fragmentation of the complex **604**. The most important peaks that are observable in the spectrum of complex **604** are: 1) a peak at m/z 1004.3 due to the loss of oligomer fragment from the complex **604** and 2) a peak at m/z 811 due to the loss of oligomer fragment and platinum from the complex **604** (see Figure **6.1**). The latter peak indeed belongs to the protonated [4]expanded radialene and confirms the formation of the macrocycle upon the Sonogashira cross coupling reaction. Also, there are two peaks that come from combination of the matrix (DCTB) with either complex **604** (m/z 1886.6) or the complex **604** that has lost the oligomer fragment.

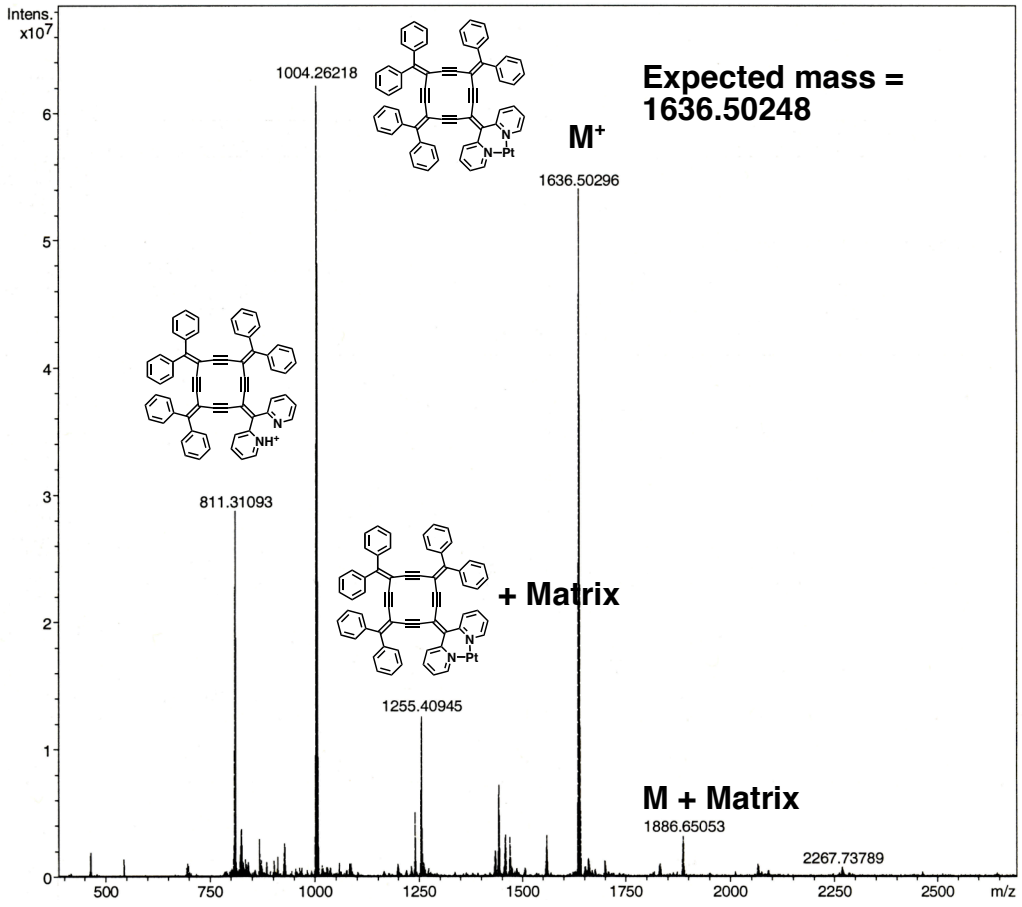

Figure 6.1 HR MALDI-TOF mass spectrometry for radialene complex **604**

Complex **604** was very insoluble and all attempts for obtaining ^{13}C NMR and ^{195}Pt NMR spectra failed.

Other similar starting materials with different metals were used to synthesize their corresponding dibromide complexes including the salt of Co(II), Ni(II), and Fe(II). But, all the corresponding products also were too insoluble in common organic solvents for further characterization or for the use in the cyclization reaction. Scheme **6.6** shows an example, the synthesis of cobalt complex **605** from $CoCl_2$.[6]

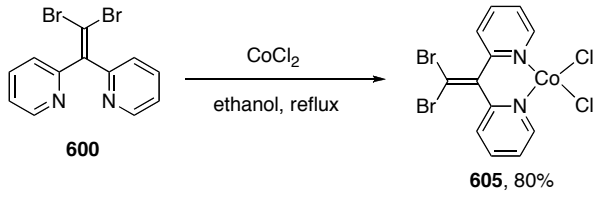

Scheme 6.6 Synthesis of complex **605**

Single crystals suitable for X-ray analysis were finally obtained from a solution of **605** in a mixture of 1,2-dichloroethane and dichloromethane at room temperature (Figure. **6.2**). The ORTEP plot of **605** shows the cobalt center is tetrahedral and all the four halogen atoms (bromides and chlorides) are positioned above the two phenyl rings.

Due to the low solubility of **605** and based on the results for complex **604** regarding its solubility no attempt was made to use **605** in the Sonogashira cross coupling reaction.

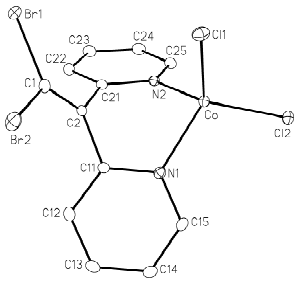

Figure 6.2 ORTEP plot of cobalt complex **605** (hydrogens removed for clarity)

In conclusion, the proposed strategy of protection through metal coordination followed by cyclization to form the expanded radialene succeeded in providing the targeted molecule **604**, as a general approach but the solubility of the products is too low for further manipulation and full characterization.

6.3 Synthesis of hybrid expanded radialenes

The Diederich and Tykwinski groups synthesized a series of cross-conjugated macrocycles with platinum acetylides that carry the skeletons of the first and second generation of the expanded radialenes.[7-9] Two examples of their macrocycles are shown in Scheme **6.7** and discussed in Chapter **2**. For example**,** macrocycles with pyridyl groups are highly ordered in the solid-state and will participate in self- assembly processes and they are excellent building block for supramolecular assemblies.[7a, 8, 9]

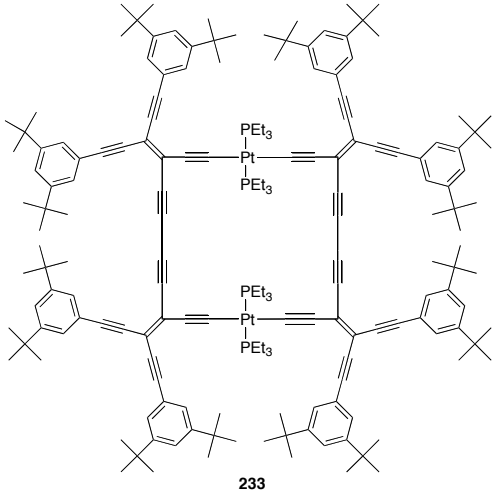

233

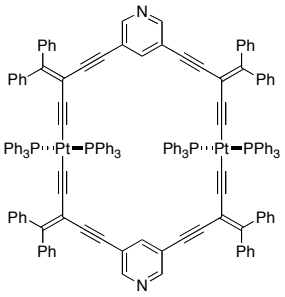

235

Scheme 6.7 Two examples of the platinum macrocycle

Among the hybrid series, two new macrocycles related to [3]expanded radialenes were proposed, both are more strained than **233** and **235** and are challenging to synthesize. These target molecules are shown in Scheme **6.8**. The synthesis could proceed via a Pt(II) derivative such as $Pt(PPh_3)_2Cl_2$ or $Pt(PEt_3)_2Cl_2$. Due to the low solubility of the triphenylphosphine macrocycles and also the presence of bulky triphenylphosphine group that may decrease the

chance of cyclization, (presumably because of steric hindrance), the triethylphosphine platinum derivative was used for the targeted reaction.

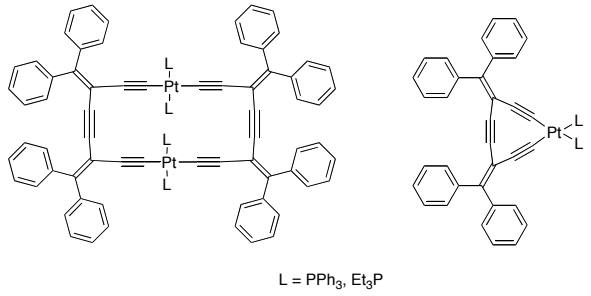

Scheme 6.8 Target platinum complexes

The synthetic approach to both macrocycles is similar in terms of starting materials and conditions. In principle the reaction could lead to both products, depending on concentration of reactants and execution of the reaction. Assume in the first step a desilylated dimer replaced one of the chlorides and the second terminal alkyne arm is available for further chloride replacement. Two predominant pathways exist: an intramolecular reaction that replaces the second chloride from the same molecule or an intermolecular reaction with another fragment. The two possibilities are shown in Scheme **6.9**. Also, as discussed in Chapter **3**, side reactions that form higher oligomers and larger macrocycles could make separation and purification of the targeted macrocycle very difficult. These side reactions are not shown in Scheme **6.9** for simplification.

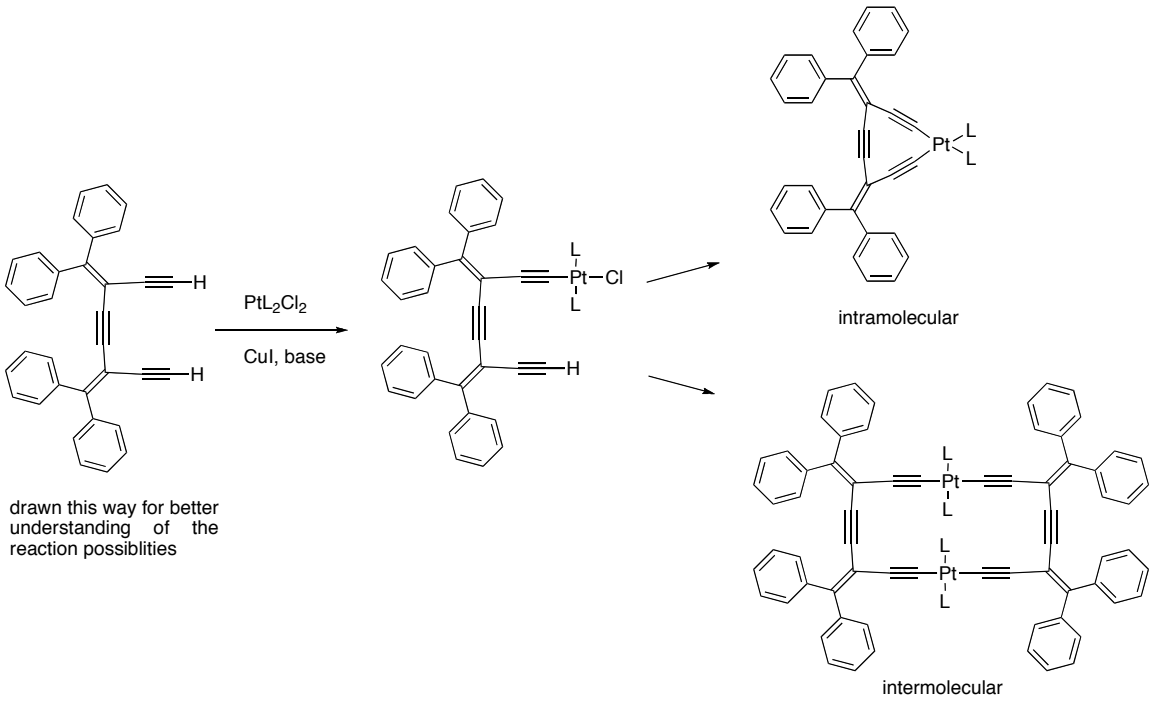

Scheme 6.9 A general scheme for synthesis of strained platinum macrocycles

In the first trial, dimer **303** was desilylated by TBAF in THF and added to $Pt(PEt_3)_2Cl_2$ in iPr_2NH under reflux. Analysis of the crude reaction product revealed that there was a series of side products, mainly higher oligomers and larger macrocycles with no evidence of the desired product(s). In the second trial, the reaction was left at room temperature stirring for 3 days at very low concentration ($\approx 10^{-4}$ M) using triethylamine as solvent. Separation carried out on silica-gel, gave the platinum macrocycle **606** in 20% yield as a yellow solid with low solubility (Scheme **6.10**). HR MALDI-TOF mass spectrometry showed a molecular ion (M^+) at m/z 1718.60806, while the calculated value for $C_{92}H_{100}P_4Pt_2$ is m/z 1718.60655. The product **606** showed low solubility in common organic solvents but was soluble enough in CD_2Cl_2 to obtain a ^{13}C NMR spectrum. The

characteristic alkyne carbons resonated at 108.4, 108, and 92.1 ppm, however, theoretically there should be overall 15 carbons including the ethyl group while the ^{13}C NMR spectrum shows 18 signals. ^{31}P NMR spectroscopy confirmed the presence of the second compound. The ^{31}P NMR spectrum showed a singlet at 8.9 ppm with $J_{P\text{-}Pt}$ = 2360 Hz and the presence of a second compound as a singlet at 11.3 ppm with $J_{P\text{-}Pt}$ = 2355 Hz (Figure **6.3**). ^{195}Pt NMR spectroscopy showed a triplet at –135.9 ppm with $J_{P\text{-}Pt}$ = 2364 Hz as a result of coupling of the two phosphorus atoms with the platinum (Figure **6.4**). The coupling constants from platinum and phosphorus NMR spectra match and confirm one another. More importantly the $J_{P\text{-}Pt}$ = 2360 Hz is very similar to the coupling constant that has been reported by Haley and coworkers which is consistent with trans-acetylide linkage.[10a] Also, the ^{13}C NMR spectrum shows a triplet for the methyl group as a result of its coupling with the phosphorus but theoretically the C–P coupling should lead to a doublet. Such triplet signal is called “virtual coupling” that confirms the ethylphosphine groups are trans (not cis) as shown in Scheme **6.10** and this is in agreement with the $J_{P\text{-}Pt}$ from the ^{31}P NMR spectroscopy.[10b]

In order to explore whether the second compound is the isomer of compound **606** a series of ^{31}P NMR experiments performed at different temperatures. It is possible that the ethylphosphine groups are rotating in and out with regard to the macrocyclic plane core in compound **606** due to the strained nature of the compound **606**. The ratio of compounds in this study as a function of temperature remained unchanged, thus, the presence of the second isomer

has not been confirmed. Interestingly, the coupling constant of platinum and phosphorus of the second product is very close to the main product, 2355 Hz compared to 2360 Hz. The only way to establish the identity of the second product is likely to obtain X-ray data.

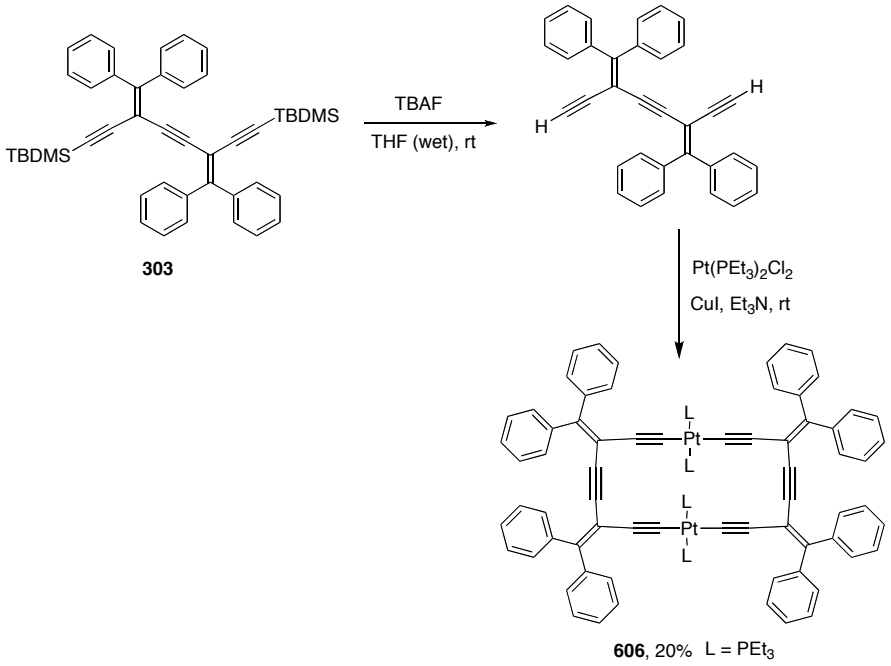

Scheme 6.10 Synthesis of complex **606**

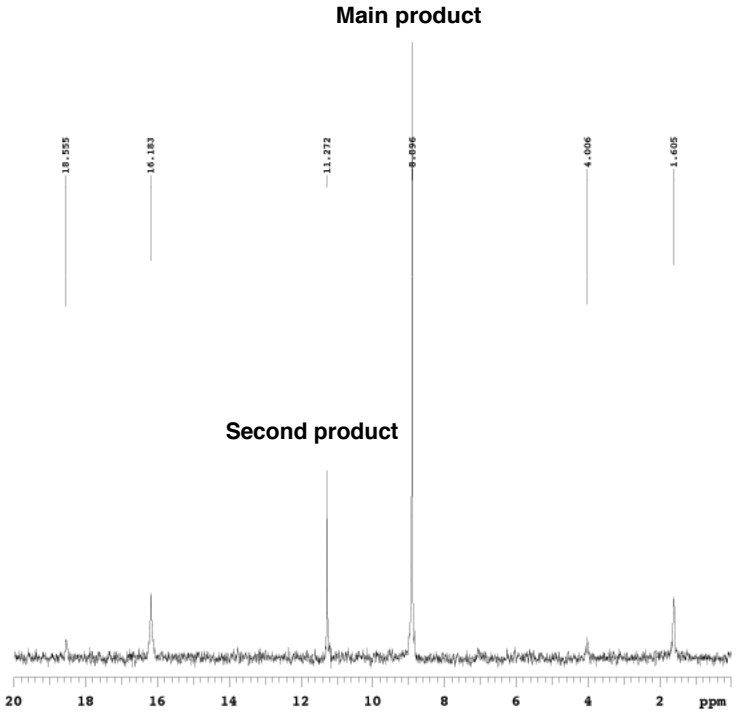

Figure 6.3 ^{31}P NMR spectrum of **606** at room temperature in CD_2Cl_2

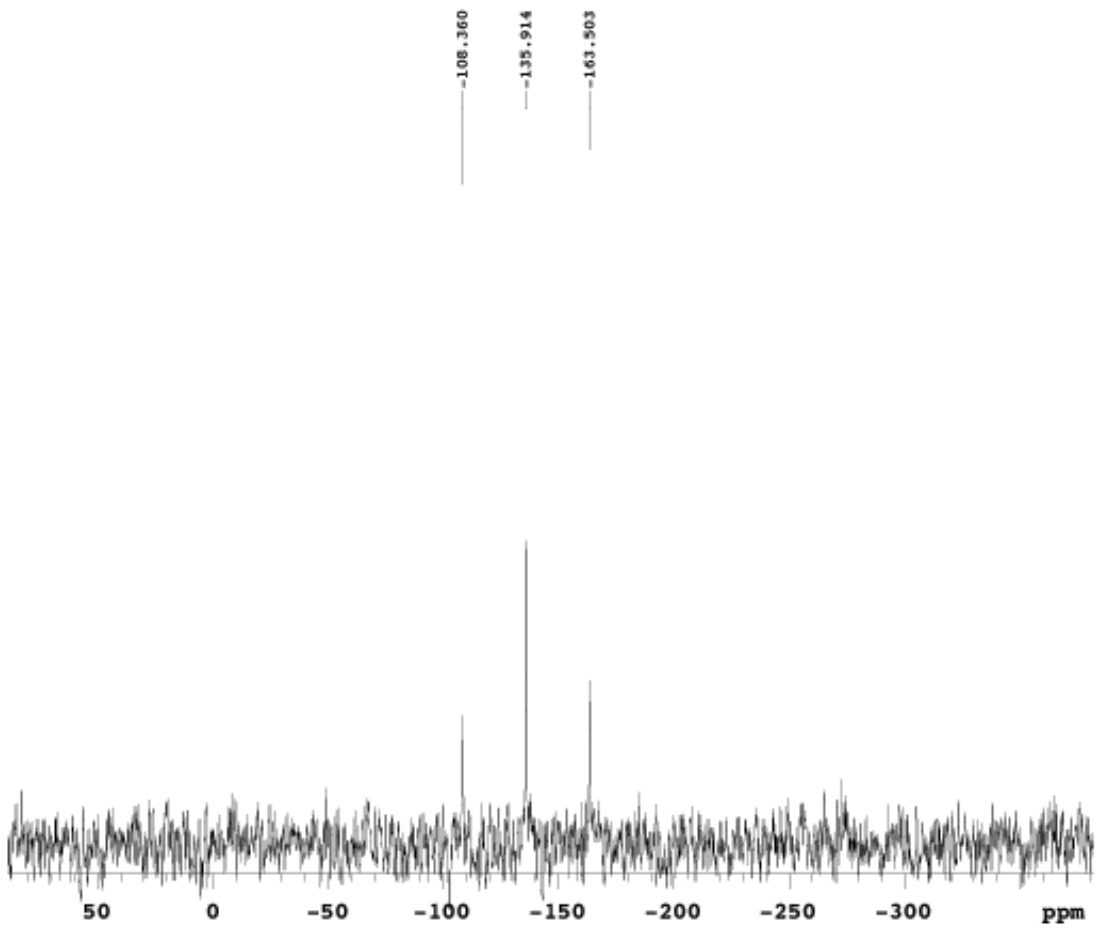

Figure 6.4 ^{195}Pt spectrum of platinum-macrocycle **606** in CD_2Cl_2

6.4 Reaction of [3]–, and [4]expanded radialenes with group X transition metals in zero oxidation states

The organometallic chemistry of expanded radialenes is relatively unexplored. One strategy is to test expanded radialene interactions with different metals in different oxidation states. Alkynes have been shown to react with transition metals in zero oxidation states, for instance, the oxidative addition of Pt(0) to alkyne bonds of compound **212** that gave complex **213** (Scheme **6.11**).[11] Also, the association of Pt(0) with the alkyne bonds in compound **214** shows the

tendency of transition metals in low oxidation states to react with alkyne bonds (Scheme **6.11**).[12] It is logical to explore reactions of the expanded radialenes with suitable candidates, in particular with Pt(0), Ni(0), and Pd(0). Because the expanded radialenes have different sizes and structures, different behaviors may be expected and the following exploratory study testifies to these assumptions. It should be mentioned that the platinum oxidation states in Scheme **6.11** purely are quotations from the relevant literature.[11,12]

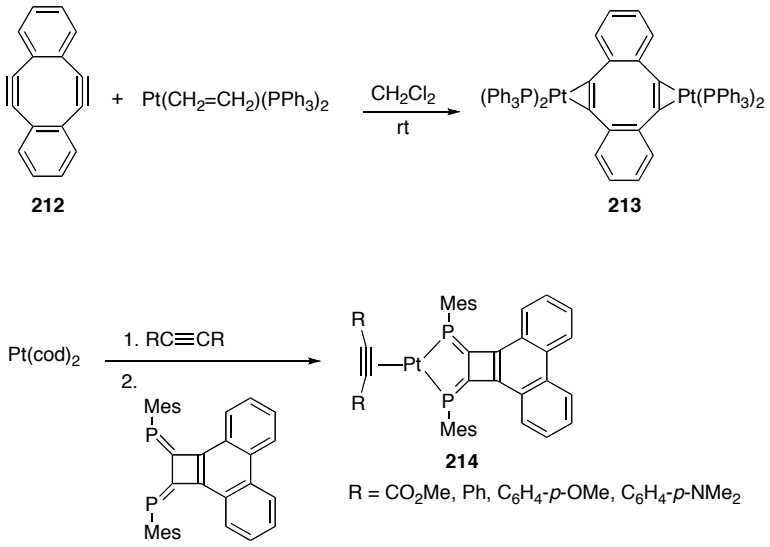

Scheme 6.11 Alkyne interactions with Pt(0) precursors

Complexes $Pt(PPh_3)_4$, $Ni(PPh_3)_4$ and $Pd(PPh_3)_4$ reacted with [4]expanded radialene **311** in a glove box (nitrogen atmosphere) at room temperature but only the starting material, **311**, was recovered.

A more reactive form of Ni(0), $Ni(COD)_2$, was reacted with the series of radialene compounds **310**–**312** in toluene. Radialene **311** reacted with $Ni(COD)_2$ at about –43 °C to give a red solid (Scheme **6.12**). The toluene solution of red

solid was left in the freezer but did not give any crystals suitable for X-ray analysis. THF was also used to grow single crystals but these attempts were also not successful. The reaction was repeated at room temperature and the same result was obtained. The red solid was very air sensitive and decomposed immediately upon exposure to air.

^{1}H NMR spectroscopy of the product showed the presence of COD ligand at 4.19 and 2.09 ppm as shown in Figure **6.5**. ^{13}C NMR spectrum also showed two peaks belonging to the COD group at 97.9 and 29.7 ppm. Olefinic carbons of coordinated COD appears at 97.9 ppm, therefore there has been an up-field shift about 30 ppm, because for free COD, the olefinic carbons appear at 128 ppm (Figure **6.6**).[13] The NMR spectra suggests that the red solid is a nickel complex with a 1:1 ratio of [4]radialene (**311**) to COD (Scheme **6.12**). The product may contain either a double bond and an alkyne coordinated to Ni(0) or two alkyne units associated with Ni(0). As well, it could be something else entirely different. Again, X-ray crystallographic analysis is required to establish the identity of this compound.

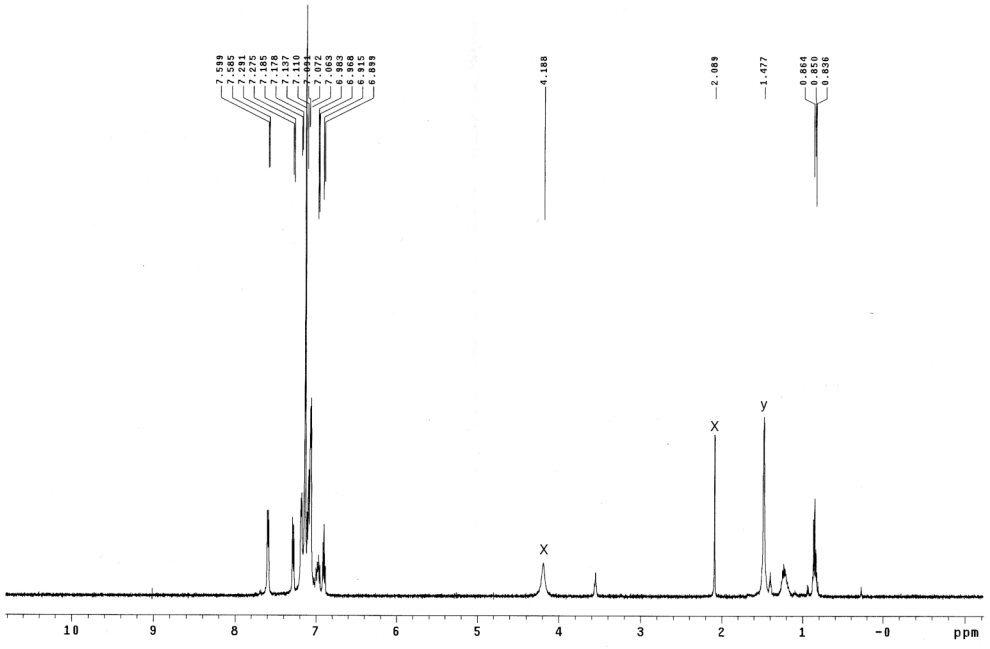

Figure 6.5 ^{1}H NMR spectrum of compound **607**: X is coordinated COD, Y is H_2O

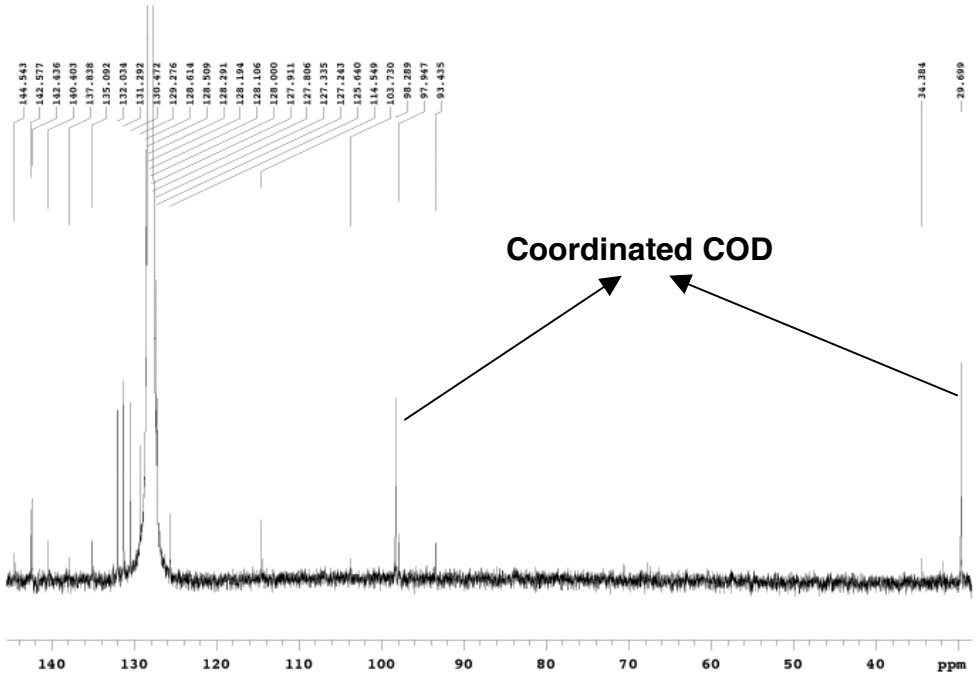

Figure 6.6 Expanded ^{13}C NMR spectrum of proposed compound **607**

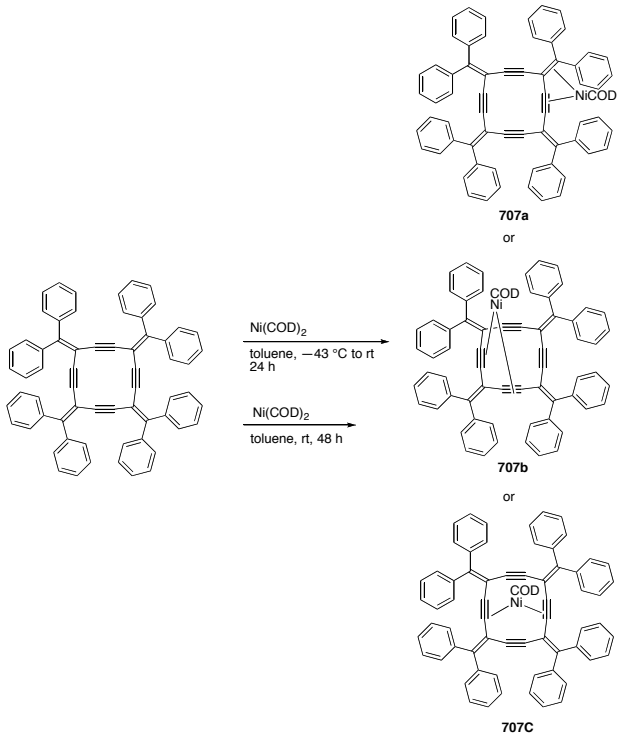

Scheme 6.12 Reaction of compound **311** with $Ni(COD)_2$, proposed products

The coordination of $Ni(COD)_2$ was explored also for [3]–, and [5]expanded radialenes. For [3]expanded radialene **310**, reaction with $Ni(COD)_2$ gave a red-brown solid. A toluene solution of the solid was prepared and left at low temperature but did not give any crystals. Most of the product decomposed in solution during the crystal growing period. The reaction of [5]expanded radialene **312** with $Ni(COD)_2$ at room temperature in toluene gave only a trace of product, and most of the starting materials were recovered.

While [4]expanded radialene **311** did not react with $Pt(PPh_3)_4$, compound **310** reacted with $Pt(PPh_3)_4$ in 1:1 ratio in toluene at room temperature. The crude reaction product separated on aluminum oxide and showed some decomposition during the separation. The first TLC spot is un-reacted [3]expanded radialene **310**. The next two spots corresponded to compounds **608a** and **608b**,

respectively (see Scheme **6.13**). HR MALDI-TOF mass spectrometry shows a molecular ion at m/z 1325.38191 corresponding to a molecular formula of $C_{84}H_{60}P_2Pt$ (the exact mass is m/z 1325.38125). Both isomers showed very similar fragmentation patterns in HR MALDI-TOF mass spectrometry. ^{31}P NMR spectroscopy of compound **608a** (the major product) showed phosphorous signal (singlet) at 23.1 ppm, $J_{P\text{-}Pt}$ = 1802 Hz (Figure **6.7**).[14] The ^{31}P NMR results point to the **608a** structure because there is only one type of phosphorus atom due to the symmetry. The proposed compound **608b** (the minor product) is not a symmetrical molecule, and there are two different phosphorus atoms in terms of symmetry and chemical environments. The ^{31}P NMR spectrum (CD_2Cl_2) is in agreement with one of the proposed structures showing two doublets, each doublet carrying its related Pt satellites: the first doublet at 21.5 ppm, $J_{P\text{-}P}$ = 16.2 Hz and $J_{P\text{-}Pt}$ = 2812 Hz; the second doublet at 15.1 ppm, $J_{P\text{-}P}$ = 15.8 Hz, $J_{P\text{-}Pt}$ = 1789 Hz (Figure **6.8**).[14]

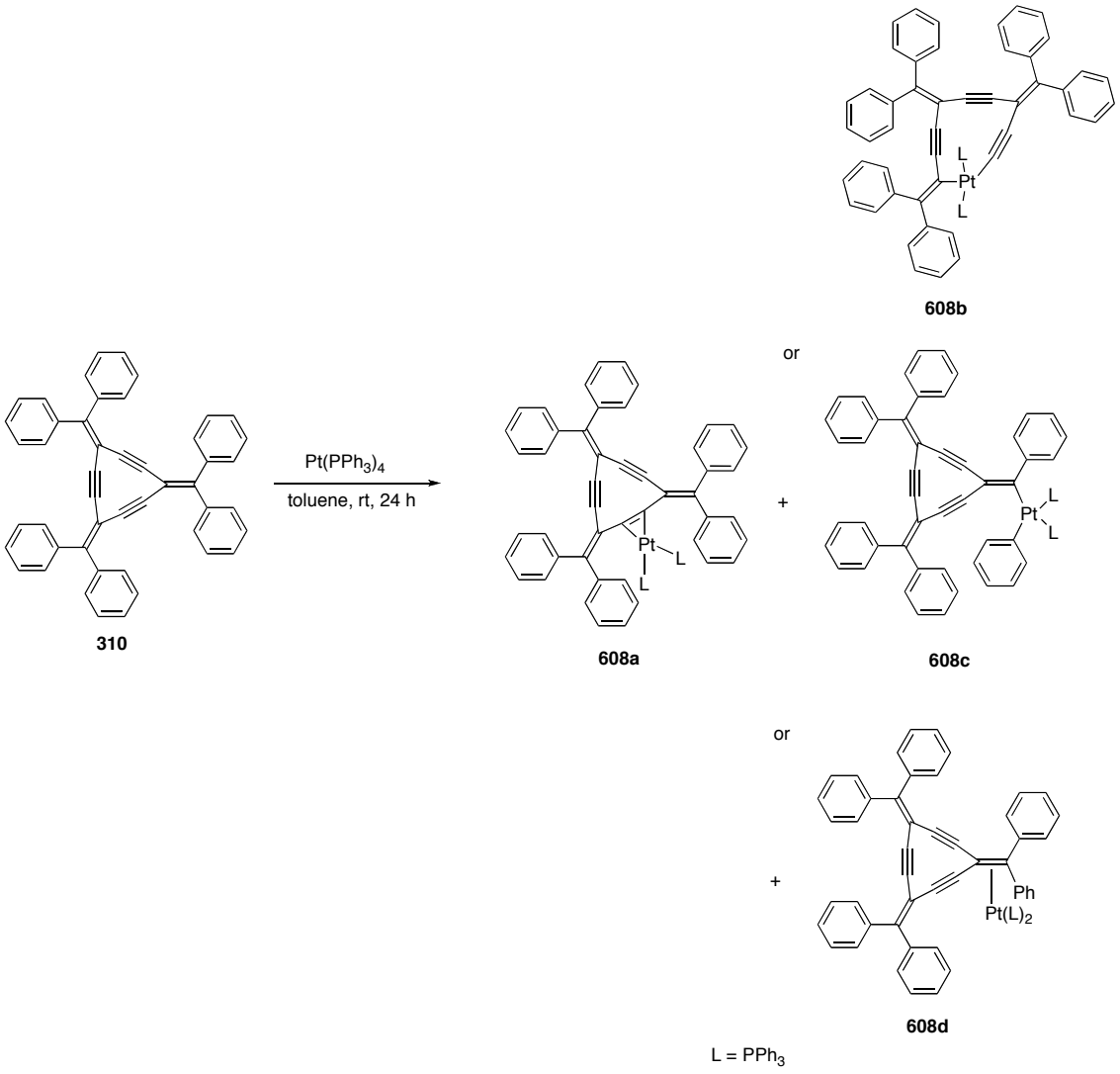

Scheme 6.13 Possible products of the reaction of **310** with $Pt(PPh_3)_4$

^{31}P NMR spectroscopy confirms the different chemical environments of the phosphorus atoms and one of the structures that matches with the data is the proposed **608b**. The complex **608b** could be the first compound afforded due to $C(sp^2)–C(sp)$ bond activation. Interestingly, neither $Ni(PPh_3)_4$ nor $Pd(PPh_3)_4$ could activate the $C(sp^2)–C(sp)$ bond. Apparently, the strained radialene **310** in the presence of $Pt(PPh_3)_4$ is the best condition to break the sigma bond. The above

reaction is very important if it is true with regard to application of catalysts in the selective activation of the sigma C–C bond rather than simple coordination to the alkyne bond. Also, there are other possibilities that are shown in Scheme 6.13 and Figure **6.8** such as **608c** or **608d**. Nevertheless, final confirmation for the proposed structures must come from X-ray analysis. Despite many attempts, no crystals have been obtained so far. Attempts to grow crystals are still underway.

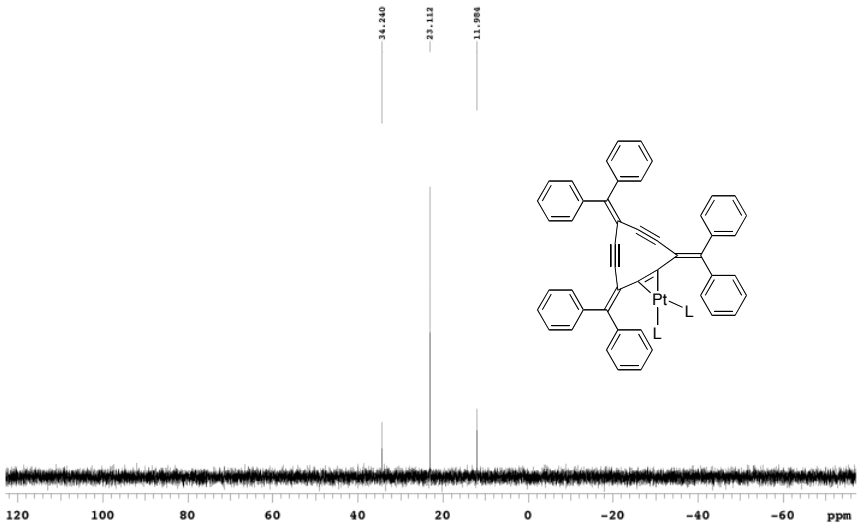

Figure 6.7 ^{31}P NMR spectrum of major product isomer from **310** reaction with $Pt(PPh_3)_4$ in CD_2Cl_2

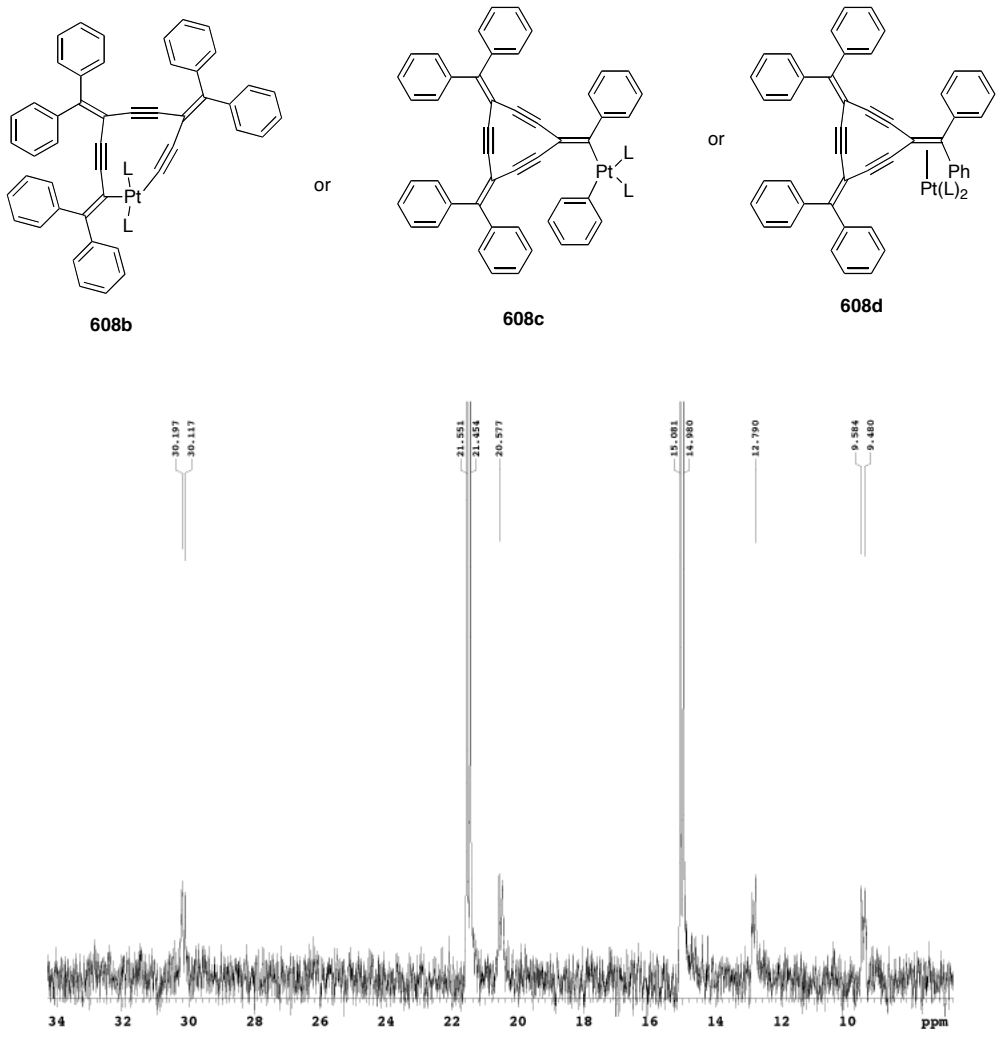

Figure 6.8 ^{31}P NMR spectrum of minor isomer from **310** reaction with $Pt(PPh_3)_4$ (CD_2Cl_2)

To get more understanding into reactions of [3]expanded radialenes with $Pt(PPh_3)_4$, [3]expanded radialene **409** was chosen because it has a fluorenylidene group that is basically planner. The partial planarity of **409** may reduce the steric hindrance compared to the twisted diphenyl rings in the radialene **310** for reaction with suitable transition metals.

Radialene **409** and $Pt(PPh_3)_4$ were mixed in a 1:1 ratio in toluene at room temperature in a glove box. The reaction yielded a series of compounds that

decomposed on aluminum oxide during separation. Scheme **6.14** shows two possible isomers that could arise from the reaction of **409** and $Pt(PPh_3)_4$.

The phosphorus atoms in **609a** and **609b** are different in terms of symmetry. Product **609a** is expected to be a singlet; and product **609b** has two different phosphorus atoms coupled to each other and further coupled with the platinum like compound **608b**. Separation of the crude reaction product was tedious and not really successful due to decomposition and streaking of the compounds on the aluminum oxide. The separation gave two bands.

Both chromatographic bands showed identical molecular ion according to the HR MALDI-TOF mass spectrometry results. The major compound had the lowest R_f and it was an orange solid. ^{195}Pt NMR spectroscopy (in CD_2Cl_2) confirms the presence of two magnetically different phosphorus atoms via a doublet of doublets at 33.1 ppm, $J_{P\text{-}Pt}$ = 2813, 1790 Hz (Figure **6.9**). ^{31}P NMR spectrum (in acetone-d6) showed a doublet at 21.4 ppm $J_{P\text{-}P}$ = 16.7 Hz, $J_{P\text{-}Pt}$ = 2817 Hz and a second doublet at 14.3 ppm, $J_{P\text{-}P}$ = 16.8 Hz, $J_{P\text{-}Pt}$ = 1792 Hz (Figure **6.10**) and the ^{31}P NMR spectrum was in agreement with ^{195}Pt NMR.[14] The ^{31}P spectrum also showed a small amount of a second product that again is not symmetrical with regard to the phosphorus atoms, with two doublets at 21.7 and 15.1 ppm, $J_{P\text{-}P}$ = 16.4 Hz, $J_{P\text{-}P}$ = 16.4 Hz**.** A mass spectrum (HR MALDI-TOF) of the major product showed a molecular ion (M^+) at m/z 1323.36560 while the calculated mass of $C_{84}H_{58}P_2Pt$ is m/z 1323.36560. ^{13}C NMR spectroscopy of the major compounds in CD_2Cl_2 showed 45 peaks, the most notable being the alkyne

carbons at 119.5, 119.1, 108.9, 108.4, 106.4, and 101.6 ppm. It is hard to use the ^{13}C NMR spectrum to determine the structure of the major compound due to lack of symmetry in the molecules. It is clear, however, that upon complex formation the alkyne shifted downfield, particularly the peaks that are at 119.6 and 119.1 ppm. Infrared spectroscopy showed absorptions at 2108 and 2057 cm^{-1} for the alkyne bonds.[14]

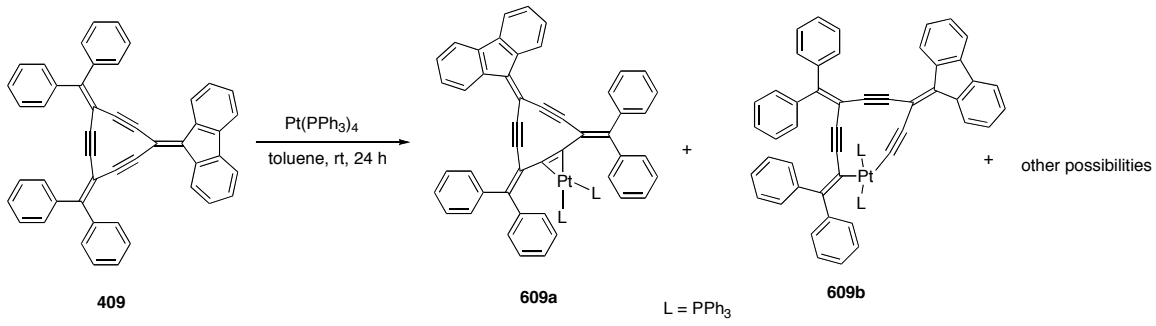

Scheme 6.14 Proposed products from reaction of **409** with $Pt(PPh_3)_4$

The presence of at least three additional compounds observed by several close TLC spots from the second band of chromatography with higher R_f values. ^{31}P NMR spectroscopy showed a singlet at 22.9 ppm with $J_{P\text{-}Pt}$ = 2893 Hz and another singlet at 21.2 ppm with $J_{P\text{-}Pt}$ = 2530 Hz, suggesting third and fourth compounds. A fifth compounds shows a peak at 25.7 ppm but it was not a strong peak and its platinum satellites were not observed (Figure **6.11**). Some of the compounds were lost due to their lack of stability and this complicated the separation and analysis. Based on the results of the spectroscopic analysis, three compounds in Figure **6.11** are present that theoretically each of them could

match with the symmetrical product in Scheme **6.14**. Once again it is likely only that solid-state analyses can establish identities of the products**.**

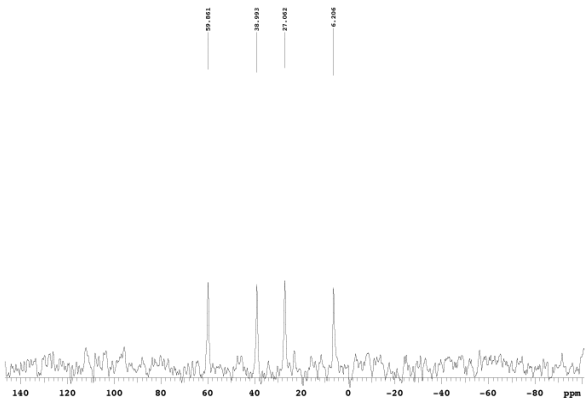

Figure 6.9 ^{195}Pt NMR spectrum of major product from reaction of radialene **409** and $Pt(PPh_3)_4$ (CD_2Cl_2)

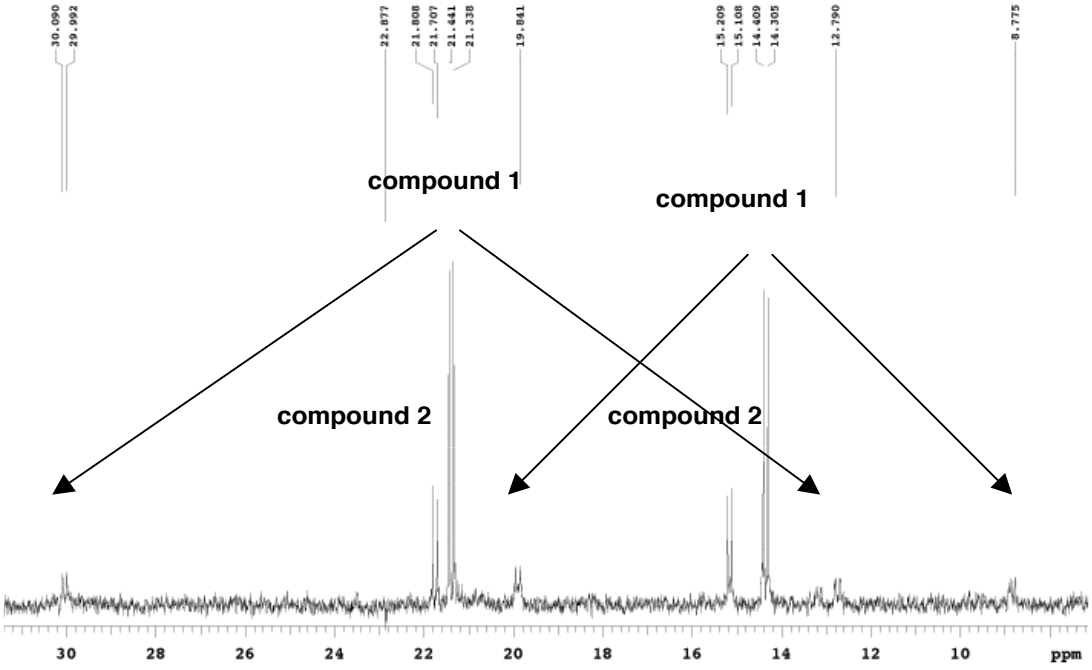

Figure 6.10 ^{31}P NMR spectrum of major product and a second product from reaction of radialene **409** and $Pt(PPh_3)_4$ (acetone-d6)

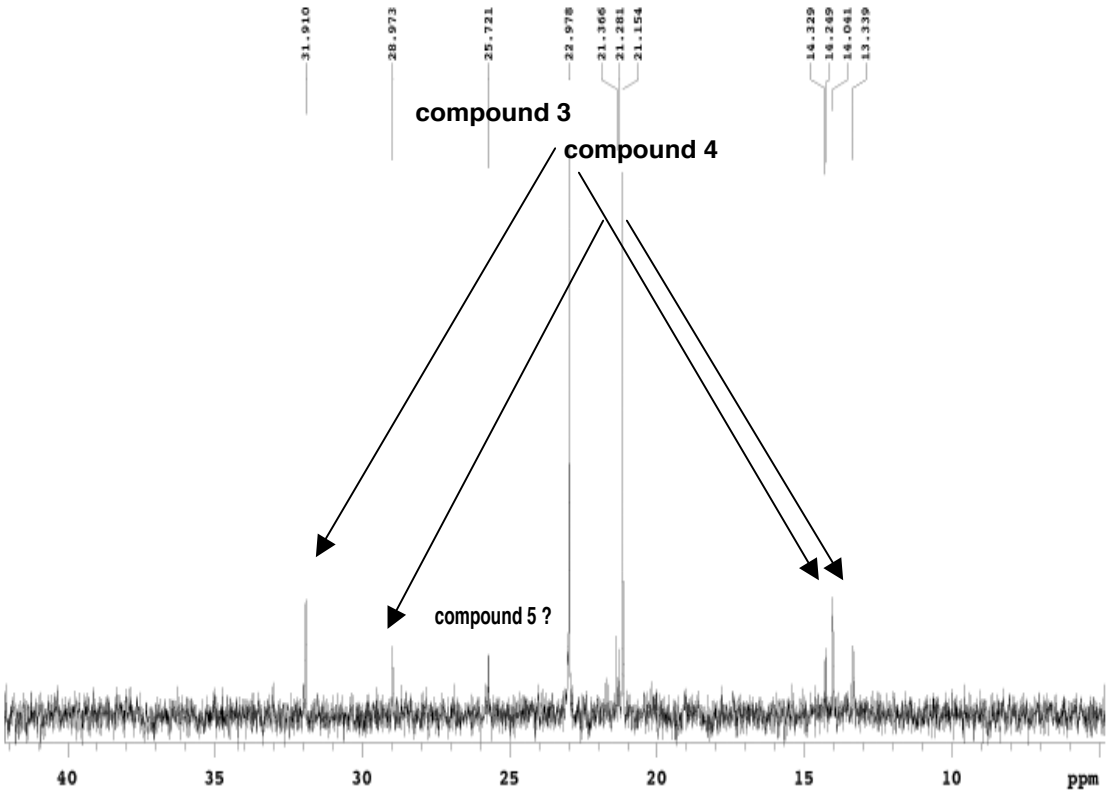

Figure 6.11 ^{31}P NMR of isomers for reaction of **409** with $Pt(PPh_3)_4$ (acetone-d6)

In conclusion, while the reaction of the [3]radialenes with $Pt(PPh_3)_4$ has been successful but the tedious separation, decomposition of the products during separation and the lack of X-ray analysis data have made this discussion a little speculative but there are ways to improve the results which will be discussed later in the chapter.

6.5 Reactions of the expanded radialene series with dicobaltoctacarbonyl

The reaction of alkyne with dicobaltoctacarbonyl were discussed in Chapter **2**. Two products of cyclyne reactions with dicobaltoctacarbonyl ($Co_2(CO)_8$), **201** and **203,** are shown in Scheme **6.15**.[15-17]

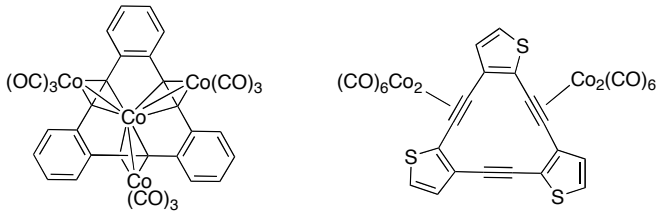

201 **203**

Scheme 6.15 Cyclyne cobaltcarbonyl derivatives

Radialene **310** reacted with $Co_2(CO)_8$ in THF at room temperature giving a purple solid in 70% yield after separation of the crude reaction product on aluminum oxide. The purple solid shows three absorptions in the infrared spectrum at 2092, 2057, and 2031 cm^{-1} (Figure **6.12**). ^1H NMR spectroscopy showed three multiplets for the product at 7.60–7.58, 7.43–7.37, and 7.36–7.09 ppm. ^{13}C NMR spectroscopy shows 14 peaks and one peak at 200 ppm for the carbonyl group indicating that the compound is symmetrical. The alkyne carbons appear at 91.4, 88.5, and 76.8 ppm.[17] Comparing the results of the **310**- and **203**-$Co_2(CO)_8$ reactions in terms of the number of alkyne peaks and carbonyl signal suggests the structure consistent with Scheme **6.16**.

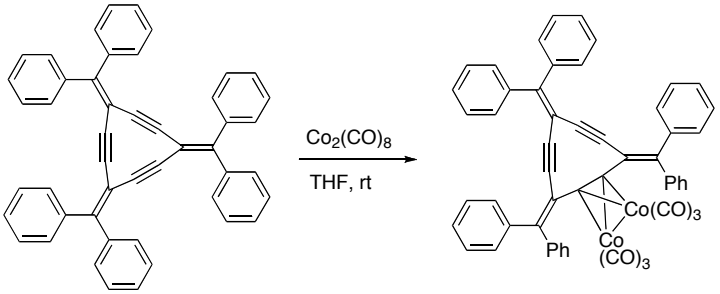

310 **610**, 70%

Scheme 6.16 Proposed product for a reaction between **310** and $Co_2(CO)_8$

Products of the reactions of radialenes **311** and **312** with dicobaltoctacarbonyl afforded green solids in very low yields (unstable products). The product of **311** with $Co_2(CO)_8$ shows four absorptions in the infrared region at 2086, 2052, 2030, and 2022 cm^{-1} (Figure **6.12)**. Despite the low solubility of the product, a reasonable ^{13}C NMR spectrum was obtained showing two alkyne peaks at 96.1 and 94.1 ppm and two peaks for CO at 198.9 and 240.9 ppm.[16] Two possible structures that match the data is shown in Scheme **6.17**. The product decomposed during attempts to grow single crystals for X-ray analysis.

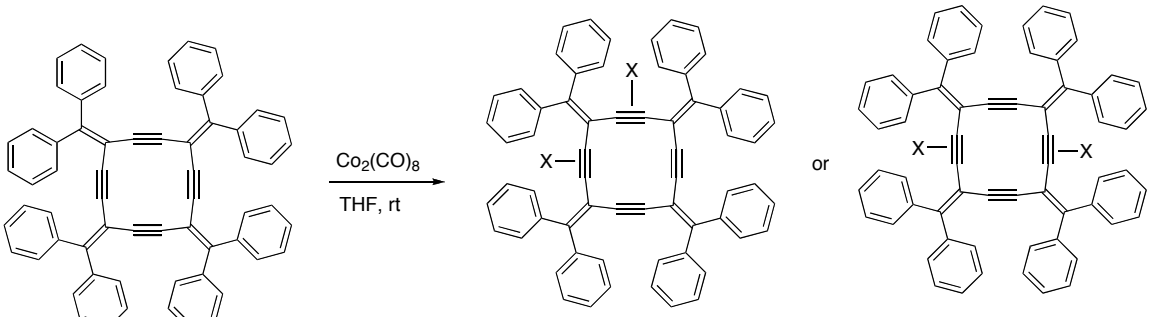

311 **611**, < 10%, X = $Co_2(CO)_6$

Scheme 6.17 Proposed products for a reaction between **311** and $Co_2(CO)_8$

The reaction of radialene **312** with $Co_2(CO)_8$ also afforded a sparingly soluble green solid that decomposed during attempts to grow crystals for X-ray analysis. ^{13}C NMR spectroscopy of the green solid exhibited about 10 alkyne peaks from 103.1 to 90.8 ppm and one peak at 198.9 ppm corresponding to the CO group stretching shown in Figure **6.12**. The best guess based on the NMR spectrum from the reaction of **312** with $Co_2(CO)_8$ is shown in Scheme **6.18** based on the pattern of ^{13}C NMR spectrum.

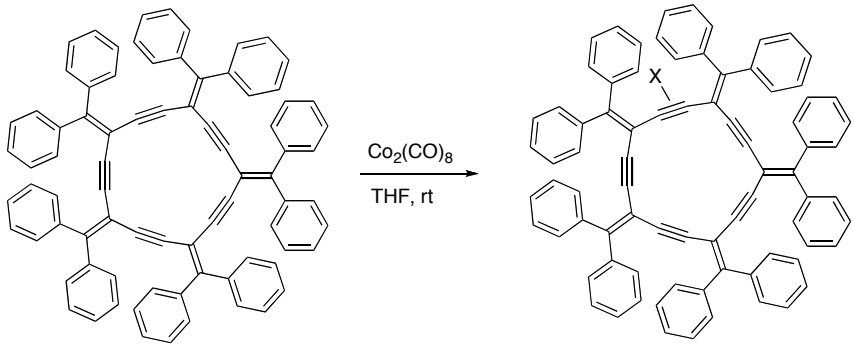

312 **612**, < 10%, X = $Co_2(CO)_6$

Scheme 6.18 Proposed product for a reaction between **312** and $Co_2(CO)_8$

With respect to cobalt complexes, only radialene **310** with $Co_2(CO)_8$ gave a product of reasonable yield and stability. Possible structures of products from radialene reactions with $Co_2(CO)_8$ were estimated with information from spectroscopic techniques and could not be verified with X-ray analysis. It is important to note that in all the organometallic reactions described here, the radialene starting materials were recovered after products decomposed. This indicates that association of he radialenes with metal centers, presumably

through alkyne units, did not appreciably change the integrity of the radialene frameworks.

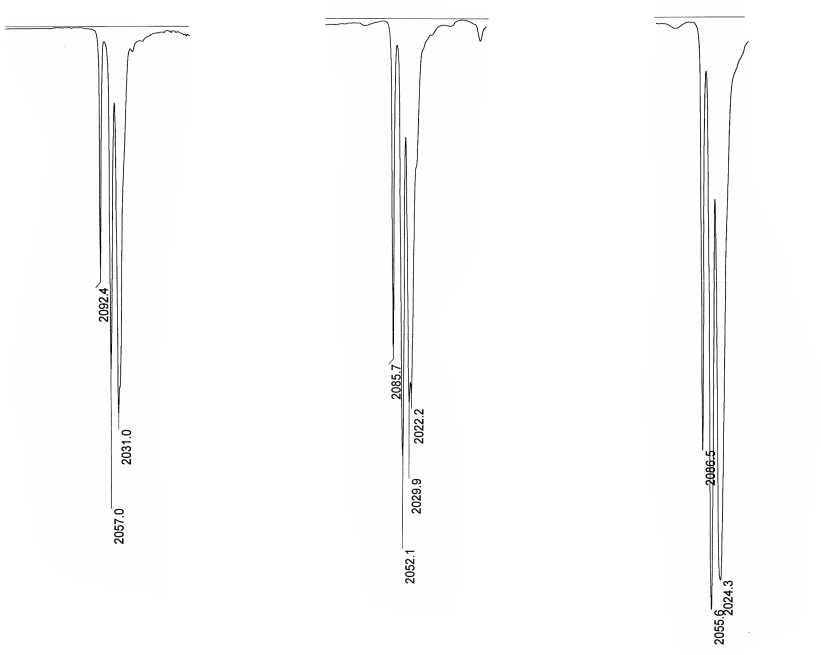

Figure 6.12 Infrared spectra of reactions of radialenes **310–312** (from left to right) with $Co_2(CO)_8$ (only CO absorption is shown, measured in CH_2Cl_2 cast)

6.6 Reaction of [4]radialene with $Ru_3(CO)_{12}$

The synthesis of compound **433** in Chapter **2**, created an opportunity to explore whether its cyclopentadiene group is able to react with suitable metal precursors. In this regard, during the last few decades, ruthenium carbonyl has attracted interests in the field of organometallic chemistry.[18] One example is the reaction of $Ru_3(CO)_{12}$ with cyclopentadienone in benzene by Bruce and colleagues[19] that resulted in a ruthenium complex as shown in Scheme **6.19**. Also, Bäckvall and colleagues showed the application of a Ru(II) complex

(Scheme **6.19**) in the racemization of secondary alcohols at ambient temperature.[20] Radialene **433** was reacted with $Ru_3(CO)_{12}$ under reflux in benzene. A brown solid separated as a product with limited solubility in common organic solvents. Infrared spectroscopy showed CO stretching at 2055, 2013, and 1985 cm^{-1}. HR MALDI-TOF mass spectrometry showed a molecular ion (M^+) at m/z 1212.40665, while the mass calculated for $C_{83}H_{66}O_3Ru$ is m/z 1212.40500 (very weak signal). ^{13}C NMR spectrum in CD_2Cl_2 showed a very weak peak at 194.9 ppm. The identity of the product is not easy to predict but the ruthenium is expected to remain in the zero oxidation state similar to that of Bruce compound that fulfills the 18-electron rule. The proposed compound could carry three CO groups as shown in Scheme **6.20**. All attempts to grow crystals suitable for X-ray analysis have so far failed.

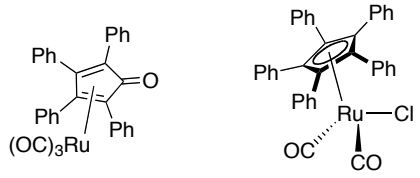

Bruce Backvall

Scheme 6.19 Organometallic derivatives of ruthenium

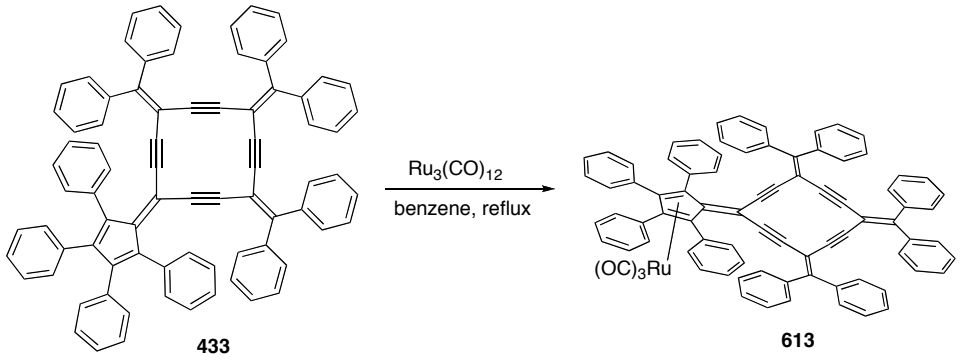

433 613

Scheme 6.20 Proposed product from a reaction of radialene **433** with $Ru_3(CO)_{12}$

6.7 Discussion of the results

In this chapter two aspects of the chemistry of the expanded radialenes in reactions with transition metals have been explored. First investigation was the coordination chemistry in which the low solubility of the products did not allow for their full characterization. The best way to resolve this issue would be to look at the expanded radialenes that carry functional groups such as TIPS-ethynyl, CF_3, and OR in order to increase their solubility (Scheme **6.21**). Nevertheless, the exploratory study was successful with regard to the protection of nitrogen lone pairs with Pt(II) and employment of the resulting platinum complex in the cyclization reaction.

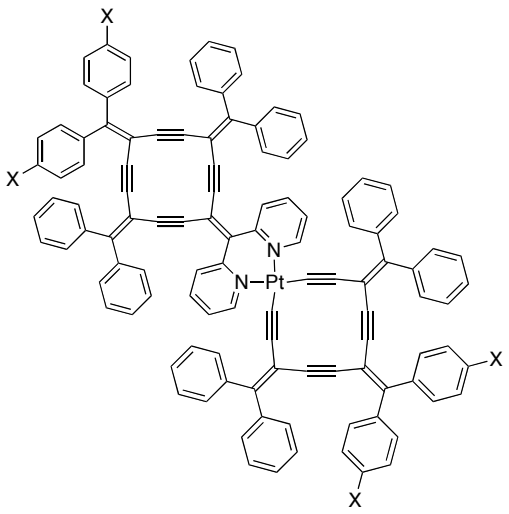

X = TIPS-ethynyl, CF_3, OR

Scheme 6.21 Platinum complexes with solubilizing groups

In a study of the expanded radialenes, the [3]expanded radialenes **310** and **409** showed more promise toward attractive organometallic chemistry than compounds **311** and **312**. The differences could arise from solubility and strain.

The higher solubility of the [3]expanded radialenes could also help in terms of reaction rates. In terms of strain, as discuss in Chapter **3**, the [3]radialenes have higher internal train, therefore to release their strain particularly at the alkyne bonds, they react more readily with suitable organometallic precursors. For example reaction of [3]expanded radialenes with transition metals such as $Co_2(CO)_8$ and $Pt(PPh_3)_4$ have shown high reactivity and higher yields compared to larger radialenes such as **311** or **312**. In particular, the reaction with $Pt(PPh_3)_4$ presented a very interesting and unexpected result that illustrates a chemical difference between [3]expanded radialene and [4]expanded radialene.

Oxidative addition reactions of $Pt(PPh_3)_4$ with the [3]radialenes appear favorable. Thus, both factors, the strained macrocycles and the tendency of platinum to be oxidized could contribute to the success of the reaction. In contrast, $Ni(PPh_3)_4$ did not react with either **310** nor **409,** so in this case, it is clear that Ni(0) is not as strong as Pt(0) for the reaction with strained [3]radialenes.

The reaction of [3]radialenes with $Pt(PPh_3)_4$ yielded unexpected products that require a deeper look to understand this chemistry. X-ray data could only help the investigation but single crystals from organometallic derivatives of [3]radialenes have not yet been obtained for X-ray analysis.

A few steps that could be taken to understand the reaction of group X transition metals with radialenes are outlined here. First, the reactions should be repeated with $Pt(PPh_3)_4$ and $Ni(PPh_3)_4$ for both [3]–, and [4]radialenes at elevated temperatures (lack of stability should be considered at high temperatures). Reactions of $Pt(PPh_3)_4$ with radialenes that have different exocyclic substituents (in terms of functionality and size), should be tested as well.

In Chapter **5**, the synthesis of compound **525** was discussed. It is possible that compound **525** could be used for C–H activation (cyclometallation) according to Scheme **6.22**.[21] This idea arises from the work of Robinson and colleagues who activated the C–H bond through a cyclometallation reaction according to Scheme **6.22**.[22] The difference in our case is that a terminal alkyne is involved rather than a dimethylamine ligand that has been reported in the literature.[21] While Robinson and coworkers synthesized and tested a series of platinum

complex (*cis*-platin) as anti tumors but one issue that was mentioned is about low solubility of the complexes for delivery. The new compound in Scheme **6.22** carries two TIPS groups that would enhance the solubility.[22]

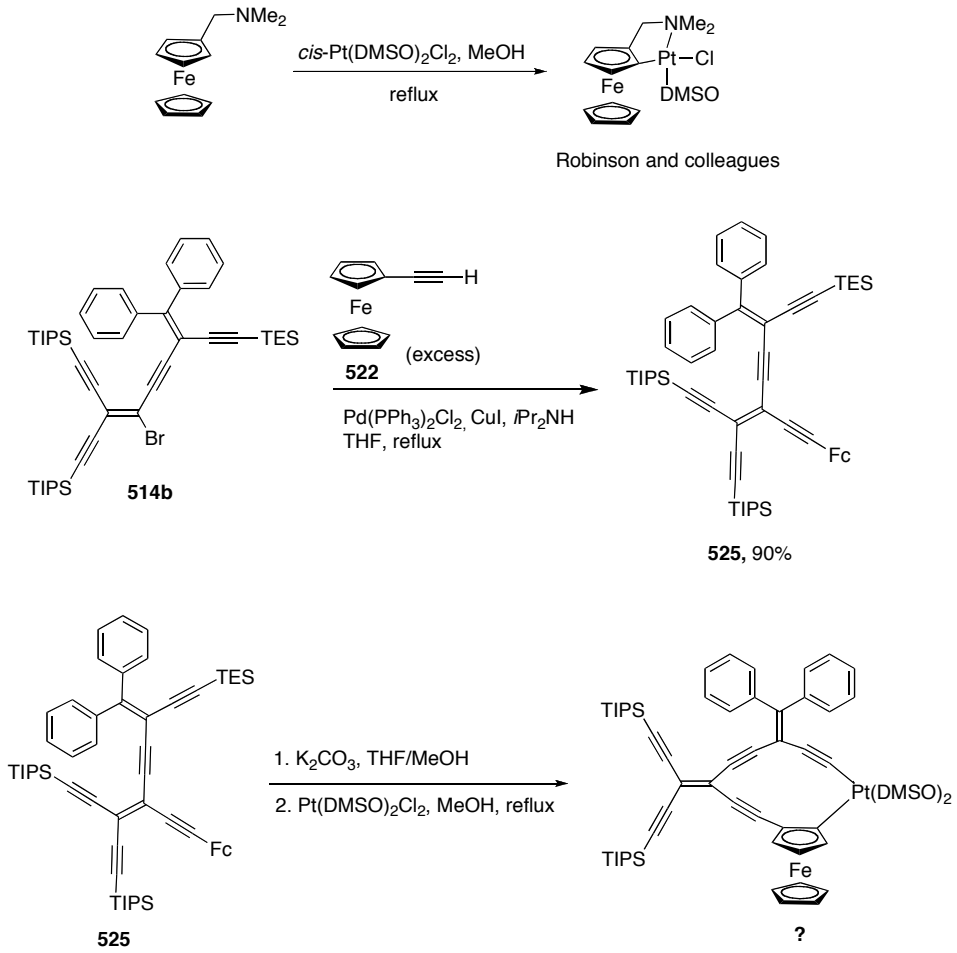

Scheme 6.22 C–H bond activation through coordination

6.8 Conclusion

The organometallic chemistry of [3]expanded radialenes exhibited very revealing results compared to the larger radialenes at this stage. This exploratory study shows through several examples that it would be worthwhile to further

investigate the organometallic chemistry of [3]expanded radialenes as a continuous effort to follow this thesis.

6.9 References

(1) (a) Wudl, F. *Acc. Chem. Res.* **1984**, *17,* 227–232; (b) Maugh, T. H. *Science* **1983**, *222*, 606–607.

(2) Diercks, R.; Eaton, B. E.; Gürtzgen, S.; Jalisatgi, S.; Matzger, A. J.; Radde, R. H.; Vollhardt, K. P. C.; *J. Am. Chem. Soc*. **1998**, *120*, 8247–8248.

(3) Ellern, J. B.; Ragsdale, R. O. *Inorg. Synth.* **1978***, 18,* 82–87.

(4) Sullivan, B. P.; Salmon, D. J.; Meyer, T. J. *Inorg. Chem*. **1978**, *17*, 3334–3341.

(5) Newkome, G. R.; Theriot, K. J.; Fronczek, F. R.; Villar, B. *Organometallics* **1989**, *8*, 2513–2523.

(6) Brewer, B.; Brooks, N. R.; Abdul-Halim, S.; Skyes*,* A. G. *J. Chem. Crystallogr*. **2003**, *33*, 651–662.

(7) (a) Campbell, K.; McDonald, R.; Ferguson, M. J.; Tykwinski, R. R. *Organometallics* **2003**, *22*, 1353–1355; (b) Faust, R.; Diederich, F.; Gramlich, V.; Seiler, P. *Chem. Eur. J.* **1995**, *1*, 111–117.

(8) Campbell, K.; McDonald, R.; Ferguson, M. J.; Tykwinski, R. R. *J. Organomet. Chem.* **2003**, *683*, 379–387.

(9) Campbell, K.; Tykwinski, R. R. In *Carbon-Rich Compounds*; Haley, M.M.; Tykwinski R. R. ed.; Wiley-VCH, **2006**.

(10) (a) Johnson, C. A.; Baker, B. A.; Berryman, O. B.; Zakharov, L. N.; O'Connor, M. J.; Haley, M. M.; *J. Organomet. Chem.* **2006**, *691*, 413–421; (b) Crabtree, R. H. *The Organometallic Chemistry of the Transition Metals*; Wiley Interscience, **2005**, chapter 9.

(11) Shimada, S.; Tanaka, M.; Honda, K. *Inorg. Chem. Acta* **1997***, 265,* 1–8.

(12) Hayashi, K.; Nakatani, M.; Hayashi, A.; Takano M.; Okazaki, M.; Toyota, K.; Yoshifuji, M.; Ozawa, F. *Organometallics* **2008**, *27*, 1970–1972.

(13) Spectral Database for Organic Compounds (SDBS), the spectrum obtained by SDBS (25.16 MHz, 0.5 mL: 1.5 mL $CDCl_3$).

(14) (a) Still, B. M.; Anil Kumar, P. G.; Aldrich-Wright, J. R.; Price, W. S. *Chem. Soc. Rev*. **2007**, *36*, 665–686; (b) Kalberer, E. W.; Roddick, D. M. Organoemyallics **2004**, *23*, 4209–4214; (c) Belluco, U.; Bertani, R.; Michelin, R. A.; Mozzon, M. *J. Organomet. Chem.* **2000**, *600*, 37–55; (d) Bennett, M. A.; Dirnberger, T.; Hockless, D. C. R.; Weger, E.; Willis, A. C. *J. Chem. Soc. Dalton Trans.* **1998**, 271–277; (e) Boag, N. M.; Green, M.; Grove, D. M.; Howard, J. A. K.; Spencer, J. L.; Stone, F. G. A. *J. Chem. Soc. Dalton Trans.* **1980**, 2170–2181.

(15) Djebli, A.; Ferrara, J. D.; Tessier-Youngs, C.; Youngs, W. J. *J. Chem. Soc., Chem. Commun.* **1988**, 548–549.
(16) Solooki, D.; Bradshaw, J. D.; Tessier, C. A.; Youngs, W. J. *Organometallics* **1994**, *13*, 451–455.
(17) Marshall, J. A.; Konicek, T. R.; Flynn, K. E. *J. Am. Chem. Soc*. **1980**, *102*, 3288–3290.
(18) Huerta, F. F.; Minidis, A. B. E.; Bäckvall, J.-E. *Chem. Soc. Re*v. **2001**, *30*, 321–331.
(19) Bruce, M. I.; Knight, J. R. *J. Organomet. Chem*. **1968**, *12*, 411–413.
(20) Martin-Matute, B.; Edin, M.; Bogár, K.; Betül Kaynak, F.; Bäckvall, J.-E. *J. Am. Chem. Soc*. **2005**, *127*, 8817–8825.
(21) Newkome, G. R.; Puckett, W. E.; Gupta, V. K. E.; Kiefer, G. *E. Chem. Rev.* **1986**, *86*, 451–489.
(22) Ranatunge-Bandarage, P. R. R.; Robinson, B. H.; Simpson, J. *Organoemtallics* **1994**, *13*, 500–510.

Chapter 7:

Experimental

7.1 General experimental

Column chromatography: Aluminum oxide, neutral, Brockman 1, 150 mesh from Aldrich Chemical Company, Inc. (5% water) or silica gel-60 (230–400 mesh) from *General Intermediates of Canada* or *Silicycle*. Thin Layer Chromatography (TLC): Aluminum sheets coated with aluminum oxide N/UV_{254} from *Macherey-Nagel* or plastic sheets coated with silica gel UV_{254} from *Macherey-Nagel*. Visualization by UV light. Mp: *Gallenkamp* or *Fischer-Johns* apparatus; uncorrected. UV-vis spectra: *Varian Cary 400* at room temperature; λ_{max} in nm (ε in L mol^{-1} cm^{-1}). Fluorescence spectra: *Photon Technology International* instrument at room temperature, degassed THF. IR spectra: *Nic–Plan IR Microscope* (as solids or cast from CH_2Cl_2 as noted). ^{1}H–, ^{13}C–, ^{31}P–, ^{195}Pt, ^{19}F– NMR: Varian –300, 400 and 500 MHz instruments at room temperature or elevated temperature (as noted) in CD_2Cl_2, $CDCl_3$, or $C_2D_2Cl_4$; solvent peaks (5.32, 7.24 and 6.0 ppm for ^{1}H NMR and 53.8, 77.23 and 73.78 for ^{13}C NMR, respectively) and internal instrument references for ^{31}P, ^{195}Pt, ^{19}F NMR. EI MS (70 eV): Kratos MS 50 instrument. ESI MS (m/z): *Micromass Zabspec oαTOF or PE Biosystems Mariner TOF instruments.* Solvents as noted. Low resolution MALDI MS (m/z): PE Voyager Elite instruments in reflection mode with delayed extraction; matrices as noted, solvent: toluene/CH_2Cl_2. High resolution MALDI TOF mass spectrometry (m/z): Bruker 9.4 T Apex-Qe FTICR (Fourier Transform Ion Cyclotron Resonance Mass Spectrometry). In both the low resolution and high resolution MALDI TOF DCTB ({2E)-3-[4-(tert-butyl)phenyl]-2-methylprop-2-

enylidene}malononitrile) as matrix (50 mM in 1:1 mixture of CH_2Cl_2/toluene) (Scheme **8.1**). Microwave technology: Biotage initiator synthesizer microwave. HPLC: Hewlett-Packard/Agilent 1100 MSD (UV-vis, diode array detector, light source: deuterium or tungsten lamp, range of 190–950 nm, column, Agilent Prep-Sil 9.4 X 250 mm, 5 microns). Elemental analyses were performed by analytical and instrumentation laboratory, department of Chemistry, University of Alberta. Crystallographic data for unpublished compounds is available from the X-ray Crystallographic Laboratory, Department of Chemistry, University of Alberta.

7.2 High resolution MALDI-TOF mass spectrometry sample preparation (MALDI–FTICR)[1]

MALDI was done on the Bruker 9.4T APEX–QeFTICR mass spectrometer. Samples were prepared on a stainless steel target by mixing 1 part sample dissolved in CH_2Cl_2 with 10 parts matrix prepared at 30 mg/mL in dichloromethane. (DCTB), *trans*-2-[3-(4-*tert*-butylphenyl)-2-methyl-2-propenylidene]malononitrile was used as the matrix (Scheme **8.1**). 1 μL of the mixture was loaded to the target. Samples were desorbed/ionized using a pulsed nitrogen laser (337 nm), cooled in a storage hexapole with pulsed cooling gas and then transformed through the quadrupole and other ion optics to the infinity cell. Ion accumulation time was set to 1 s. External calibration was done over the mass range from m/z 500 to 2000 using sodium cationized polyethylene glycol.

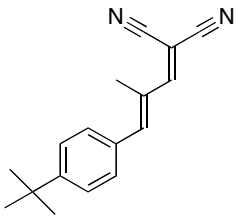

DCTB

Scheme 8.1 DCTB structure

Mass spectrometric results are reported based on the most abundant isotope of a given element for example, for bromine that has two isotopes ^{79}Br and ^{81}Br, the data is reported based on ^{79}Br and for other elements are as follows: carbon (^{12}C), hydrogen (^{1}H), silicon (^{28}Si), fluorine (^{19}F), oxygen (^{16}O), nitrogen (^{14}N), phosphorous (^{31}P), platinum (^{195}Pt), iodine (^{127}I), cobalt (^{59}Co), nickel (^{58}Ni), ruthenium (^{102}Ru), chlorine (^{35}Cl), iron (^{56}Fe).

7.3 Electrochemistry procedure[2]

Cyclic voltammetry and Osteryoung square wave voltammetry (OSWV) were carried out in a one-compartment cell connected to a BAS 100B workstation in CH_2Cl_2 containing 0.1M of NBu_4PF_6 as the supporting electrolyte. The concentration of analyte was about 5 x 10^{-4} M. A 2 mm diameter glassy carbon disk was used as the working electrode (The surface of the disk was polished with diamond paste (0.25 micron), sonicated for 1 minute in water and then rinsed copiously with water, acetonitrile and dichloromethane before use) and a platinum wire as the counter electrode. A silver wire served as a pseudo reference electrode. A small amount of ferrocene was added at the end of each experiment and used as a reference for measuring the potentials.

Typically error during the CV or OSWV experiments with regard to the redox potential is +/- 1 mV. However, it could vary since for example in CV and OSWV the value of the peak is taken where the derivative of the curve is zero and this measurement is taken by the person running the experiment by zooming the graph so most likely two different people would have a slightly different perception of which is the maxima or minima of the curve. But this error usually does not vary for more than 5 mV at the most. On the other hand, from experiment to experiment (even running the same sample) the values of a peak potential could vary but that depends highly on the cleanness of the electrodes and the amount of electrolyte in the solution. This error is about 5mV but again also depends on how cautious the person running the experiment is.

Also some of the most notable experimental errors during the electrochemical measurements are as follows:

- Low current could be attributed to low concentration of electrolyte and/or sample.
- Adsorption over the working electrode which may generate fake signals and/or hide the sample potentials.
- Presence of oxygen. Applying a flow of argon or nitrogen gas throughout the sample eliminates the oxygen. Oxygen peaks appear around 1.0 V.

- Since usually electrochemical methods are very sensitive, purity should be a requirement, so all the electrodes must be cleaned and polished before experiment.

The electrochemical measurements in this thesis were done through collaboration with the professor Luis Echegoyan group at Clemson University, SC, USA.

7.4 General experimental methods

Reagents were purchased from commercial suppliers and used without further purification. THF, benzene, and toluene were distilled from sodium/benzophenone ketyl, and hexanes and CH_2Cl_2 from CaH_2 immediately prior to use. All the Pd–catalyzed cross–coupling, inorganic and organometallic reactions were performed in standard, dry glassware under inert atmosphere of argon. A positive pressure of argon was essential for the success of all Pd–mediated cross–coupling reactions. Degassing of the reaction mixtures was accomplished by vigorously bubbling Argon through the mixtures for at least two hours. Anhydrous $MgSO_4$ was used as the drying agent when it was needed after aqueous workup. Evaporation and concentration in vacuo was achieved at H_2O–aspirator pressure (water or dry-ice cooling).

The following compounds are synthesized according to previously published literature: $Co(acac)_2(H_2O)_2$,[3] *cis*-$Ru(bpy)_2Cl_2$[4], **605**,[5] **603**,[6] **527**,[7] **521**,[8] **512**,[9] **501**,[7] **418**,[14] **416**,[13] **407**,[10] **410**,[11] **309**,[12] **308**,[7] **300**[9].

7.5 References

(1) Dr. Randy Whittal, mass spectrometry laboratory, University of Alberta.

(2) Manuel N. Chaur, Fredric Melin, Luis Echegoyen, Department of Chemistry, Clemson University, SC, USA.

(3) Ellern, J. B.; Ragsdale, R. O. *Inorg. Synth.* **1978***, 18,* 82–87.

(4) Sullivan, B. P., Salmon, D. J.; Meyer, T. J. *Inorg. Chem*. **1978**, *17*, 3334–3341.

(5) Brewer, B.; Brooks, N. R.; Abdul-Halim, S.; Skyes*,* A. G. *J. Chem. Crystallogr*. **2003**, *33*, 651–662.

(6) Newkome, G. R.; Theriot, K. J.; Fronczek, F. R.; Villar, B. *Organometallics* **1989**, *8*, 2513–2523.

(7) Neidlein, R.; Winter, M. *Synthesis* **1998**, 1362–1366

(8) Doisneau, G. Balavonie, G. Fillebeen-Khan, T. *J. Organomet. Chem*. **1992**, *425*, 113–17.

(9) Zhao, Y.; Slepkov, A. D.; Akoto, C. O.; McDonald, R.; Hegmann, F. A.; Tykwinski, R. R. *Chem. Eur. J.* **2005**, *11*, 321–329.

(10) Paul, G. C.; Gajewski, J. J. *Synthesis* **1997**, 524–526.

(11) (a) Lange, T.; van Loon, J.-D.; Tykwinski, R. R.; Schreiber, M.; Diederich, F. *Synthesis*, **1996**, 537–550; (b) Anthony, J.; Boldi, A. M.; Rubin, Y.; Hobi, M.; Gramlich, V.; Knobler, C. B.; Seiler, P.; Diederich, F. *Helv. Chim. Acta* **1995**, *78*, 13–45.

(12) Donovan, P. M.; Scott, L. T. *J. Am. Chem. Soc.* **2004**, *126*, 3108–3112.

(13) (a) Buck, H. M.; Oldenburg, S. J.; Oosterhoff, L. J.; Rijksuniv, L. N. *Chimia* **1966**, *20*, 324–326; (b) Harris, E. E.; Frankforter, G. B. *J. Am. Chem. Soc.* **1926**, *48*, 3144–3150.

(14) Enquist, P.–A.; Nilsson, P.; Larhed, M. *Org. Lett*. **2003***, 5*, 4875–4878.

Experimental Details

Compound **301**

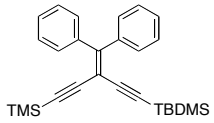

To a degassed mixture of triflate **300** (1 g, 2 mmol), CuI (38.8 mg, 0.203 mmol), $Pd(PPh_3)_2Cl_2$ (80.0 mg, 0.114 mmol), iPr$_2$NH (3 mL) and dry THF (10 mL) was added trimethylsilylacetylene (1.69 g, 17.2 mmol, 2.41 mL). The resulting mixture was refluxed for 18 h. Et_2O and H_2O were added, the organic phase separated, washed with saturated NH_4Cl (2 x 20 mL), dried ($MgSO_4$). Solvent removal and purification by column chromatography (silica gel, hexanes/CH_2Cl_2, 10:1) afforded **301** (0.84 g, 94%) as a pale yellow solid. Mp 53 °C. R_f = 0.58 (hexanes/CH_2Cl_2, 2:1). IR (CH_2Cl_2, cast) 3056, 2955, 2928, 2856, 2151 cm^{-1}; ^{1}H NMR ($CDCl_3$, 400 MHz) δ 7.42–7.38 (m, 4H), 7.28–7.26 (m, 6H), 0.82 (s, 9H), 0.85 (s, 9H), 0.03 (s, 6H); ^{13}C NMR (125 MHz, $CDCl_3$) δ 157.7, 140.2, 140.1, 130.3, 130.2, 128.4, 128.3, 127.6, 127.5, 103.7, 103.4, 102.1, 97.7, 96.4, 26.1, 16.8, –0.43, –4.9. EI HRMS calcd. for $C_{27}H_{34}Si_2$ 414.2199 (M^+), found 414.2203.

Compound **303**

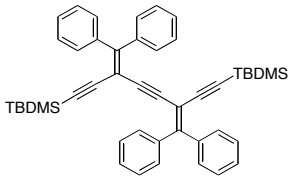

A mixture of **301** (200.0 mg, 0.4820 mmol), K_2CO_3 (13 mg, 0.096 mmol) in wet THF (1 mL) and MeOH (1 mL) was stirred for 2 h. Et_2O and H_2O were added, the organic phase separated, washed with saturated NH_4Cl (2 x 20 mL), dried ($MgSO_4$) and reduced to 2 mL. The Et_2O solution was added to a degassed mixture of triflate **300** (225 mg, 0.483 mmol), CuI (11 mg, 0.057 mmol), $Pd(PPh_3)_4$ (2.3 mg, 0.0019 mmol), *i*Pr_2NH (3 mL) and dry THF (5 mL). The resulting mixture was refluxed for 18 h. Solvent removal and purification by column chromatography (silica gel, hexanes/CH_2Cl_2, 10:1 to 5:1) afforded **303** (302 mg, 95%) as a bright yellow solid. Mp 73 °C. R_f = 0.5 (hexanes/CH_2Cl_2, 2:1). IR (CH_2Cl_2, cast) 3081, 3055, 3030, 2954, 2928, 2884, 2856, 2144 cm^{-1}; ^1H NMR ($CDCl_3$, 400 MHz) δ 7.37–7.34 (m, 8H), 7.27–7.20 (m, 12H), 0.79 (s, 18H), 0.01 (s, 12H); ^{13}C NMR (125 MHz, $CDCl_3$) δ 156.5, 140.4, 139.8, 130.4, 130.2, 128.5, 128.2, 127.7, 127.6, 103.4, 102.1, 95.8, 90.5, 26.1, 16.7, –4.8. EI HRMS calcd. for $C_{46}H_{50}Si_2$ 658.3451 (M^+), found 658.3475. CV.

Compound **304**

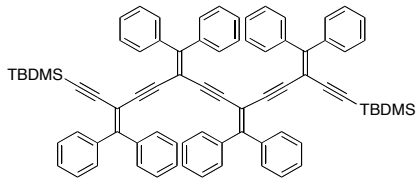

A mixture of dimer **303** (220 mg, 0.33 mmol) and TBAF (0.75 mL, 0.75 mmol, 1M in THF) in wet THF (2 mL) was stirred for 1 h. Et_2O and H_2O were added, the organic phase separated, washed with saturated NH_4Cl (2 x 20 mL), dried ($MgSO_4$) and reduced to 2 mL. The Et_2O solution was added to a degassed mixture of triflate **300** (312 mg, 0.666 mmol), CuI (20 mg, 0.1 mmol), $Pd(PPh_3)_4$ (21 mg, 0.018 mmol), iPr$_2$NH (3 mL) and dry THF (5 mL). The resulting mixture was refluxed for 18 h. Solvent removal and purification by column chromatography (silica gel, hexanes/CH_2Cl_2, 10:1 to 5:1) afforded **304** (302 mg, 85%) as a bright yellow solid. Mp 75 °C. R_f = 0.15 (hexanes/CH_2Cl_2, 2:1). IR (CH_2Cl_2, cast) 3054, 3028, 2933, 2911, 2873, 2190, 2140, 2090 cm^{-1}; ^{1}H NMR ($CDCl_3$, 400 MHz) δ 7.45–7.41 (m, 8H), 7.36–7.24 (m, 32H), 0.88 (s, 18H), 0.10 (s, 12H); ^{13}C NMR (125 MHz, $CDCl_3$) δ 156.9, 154.8, 140.5, 140.07, 140.03, 139.8, 130.40, 130.37, 130.2, 128.7, 128.5, 128.2, 127.8, 127.7, 127.6, 103.5, 102.1, 95.8, 90.8, 90.3, 89.9, 26.1, 16.7, –4.8. MALDI-TOF HRMS (DCTB) calcd. for $C_{78}H_{70}Si_2$ 1062.50106 (M^+), found 1062.50080. CV.

Compound **305**

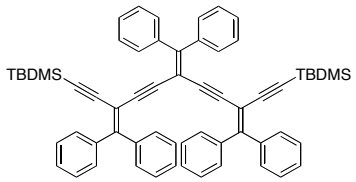

A mixture of **309** (247 mg, 0.663 mmol) and K_2CO_3 (18.3 mg, 0.132 mmol) in wet THF (1 mL) and MeOH (1 mL) was stirred for 1 h. Et_2O and H_2O were added, the organic phase separated, washed with saturated NH_4Cl (2 x 20 mL), dried ($MgSO_4$) and reduced to 2 mL. The Et_2O solution was added to a degassed mixture of **300** (617 mg, 1.32 mmol), CuI (42 mg, 0.22 mmol), $Pd(PPh_3)_4$ (52 mg, 0.045 mmol), *i*Pr_2NH (3 mL) and dry THF (5 mL). The resulting mixture was refluxed for 18 h. Solvent removal and purification by column chromatography (silica gel, hexanes/CH_2Cl_2, 1:10 to 5:1) afforded **305** (485 mg, 85%) as a bright yellow solid. Mp 60 °C. R_f = 0.42 (hexanes/CH_2Cl_2, 2:1). IR (CH_2Cl_2, cast) 3081, 3055, 3030, 2953, 2927, 2856, 2193, 2144, 2094, cm^{-1}; ^1H NMR ($CDCl_3$, 400 MHz) δ 7.42-7.40 (m, 4H), 7.34–7.26 (m, 26H), 0.85 (m, 18H), –0.07 (m, 12H); ^{13}C NMR (125 MHz, $CDCl_3$) δ 156.7, 154.9, 140.4, 140.1, 139.8, 130.4, 130.3, 130.2, 128.6, 128.5, 128.2, 127.7, 127.64, 127.61, 103.5, 102.1, 95.9, 90.6, 90.1, 26.1, 16.7, –4.8. MALDI-TOF HRMS (DCTB) calcd. for $C_{62}H_{60}Si_2$ 860.42281 (M^+), found 860.42278. CV.

Compound **310**

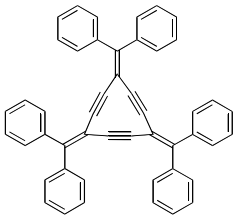

A mixture of **303** (68 mg, 0.10 mmol) and TBAF (0.23 mL, 0.23 mmol, 1 M in THF) in wet THF (5 mL) was stirred for 2 h. Et_2O and H_2O were added, the organic phase separated, washed with saturated NH_4Cl (2 x 20 mL), dried ($MgSO_4$) and reduced to 2 mL. The Et_2O solution was added to a degassed mixture of dibromoolefin **308** (34.8 mg, 0.103 mmol), CuI (6.1 mg, 0.032 mmol), $Pd(PPh_3)_4$ (6 mg, 0.005 mmol), *i*Pr_2NH (3 mL) and dry THF (10 mL). The resulting mixture was refluxed for 18h. Solvent removal and purification by column chromatography (silica gel, hexanes/CH_2Cl_2, 4:1) afforded **310** (20 mg, 32%) as a yellow solid. Mp 185–186 ˚C. R_f = 0.63 (hexane/CH_2Cl_2, 1:1). UV-vis (THF) λ_{max} (ε) 364 (105300), 415 (107500) nm; IR (CH_2Cl_2, cast) 2956, 2923, 2853, 1651, 1455, 1441 cm^{-1}; ^1H NMR (CD_2Cl_2, 300 MHz) δ 7.60–7.39 (m, 30H); ^{13}C NMR (125 MHz, CD_2Cl_2) δ 146.2, 139.7, 130.7, 129.5, 128.3, 107.2, 92.5. EI HRMS calcd. for $C_{48}H_{30}$ 606.2347 (M^+), found 606.2353. CV.

Compound **311**

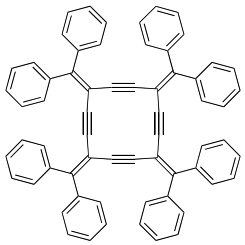

A mixture of trimer **305** (150.0 mg, 0.1750 mmol) and TBAF (0.39 mL, 0.39 mmol, 1M in THF) in wet THF (5 mL) was stirred for 2 h. Et_2O and H_2O were added, the organic phase separated, washed with saturated NH_4Cl (2 x 20 mL), dried ($MgSO_4$) and reduced to 2 mL. The Et_2O solution was added to a degassed mixture of dibromoolefin **308** (59.2 mg, 0.175 mmol), CuI (10.0 mg, 0.0520 mmol), $Pd(PPh_3)_4$ (10.0 mg, 0.00890 mmol), *i*Pr_2NH (3 mL) and dry THF (10 mL). The resulting mixture was refluxed for 18 h. Solvent removal and purification by column chromatography (silica gel, hexanes/CH_2Cl_2, 4:1) afforded **311** (105.6 mg, 75%) after re-crystallization from (hexane/CH_2Cl_2, 2:1) as a bright yellow solid. Mp 305-306 ˚C (decomp.). R_f = 0.56 (hexane/CH_2Cl_2, 1:1). UV-vis (THF) λ_{max} (ε) 377 (99300) nm; IR (CH_2Cl_2, cast) 3050, 1651, 1574, 1486, 1440 cm^{-1}; ^1H NMR (300 MHz, $CDCl_3$) δ 7.22–7.05 (m, 40H); ^{13}C NMR (125 MHz, CD_2Cl_2) δ 151.8, 140.1, 130.2, 129.1, 128.3, 102.6, 97.1. MALDI-TOF LRMS (DCTB) calcd. for $C_{64}H_{40}$ 808.4 (M^+), found 808.3. CV. X-ray.

Compound **312**

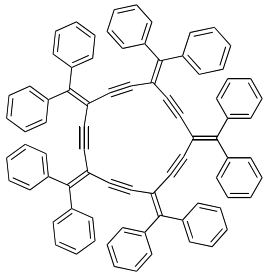

A mixture of tetramer **304** (75.5 mg, 0.0709 mmol) and TBAF (0.16 mL, 0.16 mmol, 1M in THF) in wet THF (5 mL) was stirred for 2 h. Et_2O and H_2O were added, the organic phase separated, washed with saturated NH_4Cl (2 x 20 mL), dried ($MgSO_4$) and reduced to 2 mL. The Et_2O solution was added to a degassed mixture of dibromoolefin **308** (24 mg, 0.071 mmol), CuI (4.2 mg, 0.022 mmol), $Pd(PPh_3)_4$ (4 mg, 0.003 mmol), *i*Pr_2NH (3 mL) and dry THF (10 mL). The resulting mixture was refluxed for 18h. Solvent removal and purification by column chromatography (silica gel, hexanes/CH_2Cl_2, 4:1) afforded **312** (28.7 mg, 40%) as a yellow solid. Mp 300–301 ˚C (decomp.). R_f = 0.66 (hexane/CH_2Cl_2, 1:1). UV-vis (THF) λ_{max} (ε) 374 (51300) nm; IR (CH_2Cl_2, cast) 3051, 2960, 2923, 2853, 2229, 1739, 1574, 1490, 1441, 1417 cm^{-1}; ^1H NMR (300 MHz, $CDCl_3$) δ 7.23–7.00 (m, 50H); ^{13}C NMR (125 MHz, CD_2Cl_2) δ 155.2, 140.4, 130.6, 129.3, 128.1, 101.9, 90.8. MALDI-TOF LRMS (DCTB) calcd. for $C_{80}H_{50}$ 1010.4 (M^+), found 1010.4. CV. X-ray.

Compound **315a** and **315b**

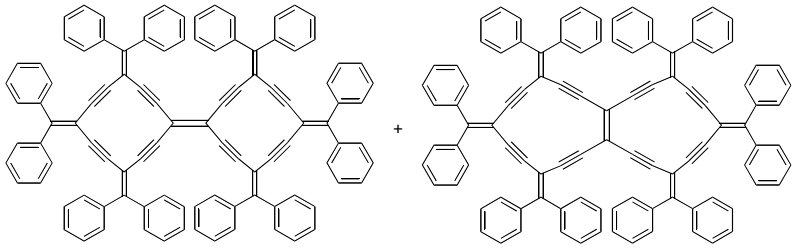

315a **315b**

A mixture of trimer **305** (90.0 mg, 0.104 mmol) and TBAF (0.23 mL, 0.23 mmol, 1M in THF) in wet THF (5 mL) was stirred for 2 h. Et_2O and H_2O were added, the organic phase separated, washed with saturated NH_4Cl (2 x 20 mL), dried ($MgSO_4$) and reduced to 2 mL. The Et_2O solution was added to a degassed mixture of tetrabromoethylene **314** (18 mg, 0.052 mmol), CuI (6.1 mg, 0.032 mmol), $Pd(PPh_3)_4$ (6 mg, 0.005 mmol), *i*Pr_2NH (3 mL) and dry THF (10 mL). The resulting mixture was refluxed for 18 h. Solvent removal and purification by column chromatography (silica gel, hexanes/CH_2Cl_2 5:1) and further separation by preparative TLC preparative plate (hexanes/CH_2Cl_2, 2:1) afforded **315a** and **315b** as red-orange solid (16.1mg, 24%, a mixture of two isomers). Mp 295–296 ˚C (decomp.). R_f = 0.43 (hexane/CH_2Cl_2 1:1). UV-vis (THF) λ_{max} (ε) 387 (139400), 509 (38900) nm; IR (CH_2Cl_2, cast) 3051, 2923, 2853, 2152 cm^{-1}. MALDI-TOF LRMS (DCTB) calcd. for $C_{102}H_{60}$ 1285.5 (M^+), found 1285.5. X-ray.

Compound **316a**

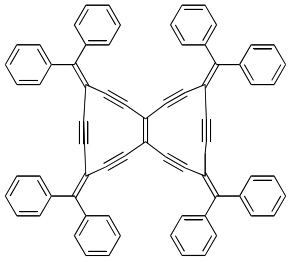

A mixture of dimer **303** (60.0 mg, 0.0910 mmol) and TBAF (0.2 mL, 0.2 mmol, 1M in THF) in wet THF (5 mL) was stirred for 2 h. Et_2O and H_2O were added, the organic phase separated, washed with saturated NH_4Cl (2 x 20 mL), dried ($MgSO_4$) and reduced to 2 mL. The Et_2O solution was added to a degassed mixture of tetrabromoethylene **314** (15.7 mg, 0.0457 mmol), CuI (5.3 mg, 0.027 mmol), $Pd(PPh_3)_4$ (6 mg, 0.005 mmol), *i*Pr_2NH (3 mL) and dry THF (10 mL). The resulting mixture was refluxed for 18 h. Solvent removal and purification by column chromatography (silica gel, hexanes/CH_2Cl_2, 5:1) and further separation by preparative TLC plate (hexanes/CH_2Cl_2, 2:1) afforded **316a** as a red-purple solid (7 mg, 18%). Mp 250–251 ˚C (decomp.). R_f = 0.53 (hexane/CH_2Cl_2 1:1). UV-vis (THF) λ_{max} (ε) 381 (63000), 534 (19500) nm, 572 (31700); IR (CH_2Cl_2, cast) 3056, 2923, 2853, 2141, 1721, 1649.7, 1547, 1462, 1441 cm^{-1}; ^1H NMR (300 MHz, $CDCl_3$) δ 7.54–7.30 (m, 40H); ^{13}C NMR (125 MHz, CD_2Cl_2) δ 149.0, 139.7, 139.4, 131.9, 130.8, 130.6, 129.8, 129.7, 128.4, 128.3, 119.9, 104.4, 102.9, 101.5, 96.0, 70.8. MALDI-TOF LRMS (DCTB) calcd. for $C_{70}H_{40}$ 880.3 (M^+), found 880.3. CV. X-ray.

Compound **318** and **319**

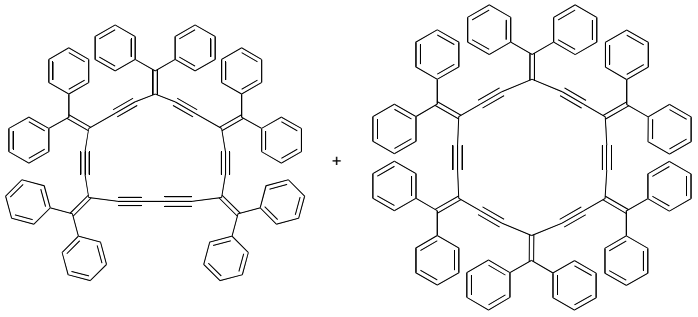

318 **319**

A mixture of **306** (90. mg, 0.071 mmol) and TBAF (0.16 mL, 0.16 mmol, 1 M in THF) in wet THF (5 mL) was stirred for 2 h. Et_2O and H_2O were added, the organic phase separated, washed with saturated NH_4Cl (2 x 20 mL), dried ($MgSO_4$) and reduced to 2 mL. The Et_2O solution was added to a degassed mixture of dibromoolefin **308** (23.7 mg, 0.0701 mmol), CuI (4.1 mg, 0.021 mmol), $Pd(PPh_3)_4$ (4 mg, 0.003 mmol), *i*Pr_2NH (3 mL) and dry THF (10 mL). The resulting mixture was refluxed for 24h. Solvent removal and purification by column chromatography (silica gel, hexane/CH_2Cl_2 5:1 to 2:1) afforded the first band as compound **319** as a yellow solid (2.5 mg, 2.9%) according to LR MALDI-TOF MS (DCTB) calcd. for $C_{96}H_{60}$ 1213.5 (M^+), found 1213.5. (Not sufficient for further characterization).

The second band afforded intramolecular homo-coupled compound **318** (47 mg, 64%) as yellow solid. Mp 160 ˚C. R_f = 0.8 (hexane/CH_2Cl_2, 1:1). UV-vis (THF) λ_{max} (ε) 370 (47100) nm; IR (CH_2Cl_2, cast) 3052, 2924, 1491, 1441, 1261 cm^{-1}; ^1H NMR (300 MHz, CD_2Cl_2) δ 7.36–7.05 (m, 50H); ^{13}C NMR (125 MHz, CD_2Cl_2) δ 157.8, 156.7, 155.5, 140.8, 140.6, 140.4, 140.3, 139.6, 130.6, 130.5, 130.4,

129.6, 129.5, 129.3, 129.1, 129.0, 128.4, 128.3, 128.2, 128.1, 128.0, 101.6, 101.5, 91.7, 90.8, 89.6, 89.1, 84.9, 77.9. MALDI-TOF LRMS (DCTB) calcd. for $C_{82}H_{50}$ 1034.4 (M^+), found 1034.4. CV. X-ray.

Compound **320a/b** and **A56**

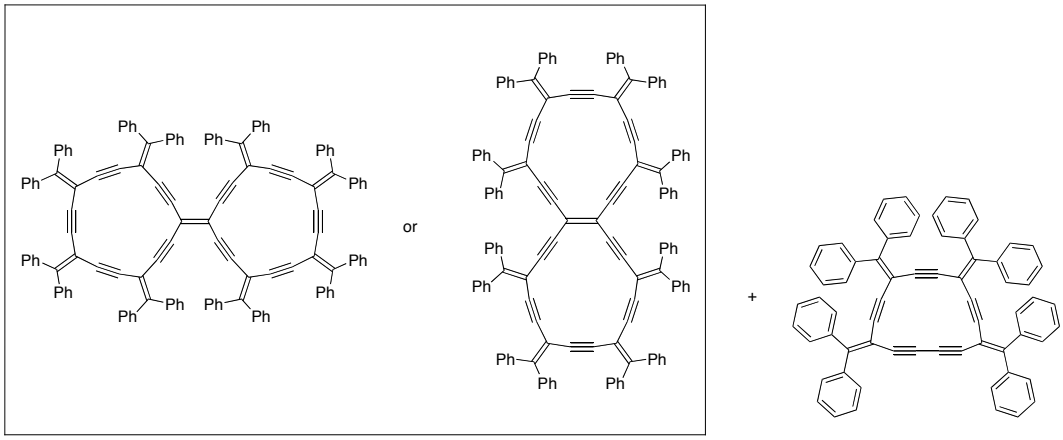

320a/b **A56**

A mixture of tetramer **304** (104 mg, 0.0977 mmol) and TBAF (0.23 mL, 0.23 mmol, 1M in THF) in wet THF (5 mL) was stirred for 2 h. Et_2O and H_2O were added, the organic phase separated, washed with saturated NH_4Cl (2 x 20 mL), dried ($MgSO_4$) and reduced to 2 mL. The Et_2O solution was added to a degassed mixture of tetrabromoethylene **314** (17 mg, 0.048 mmol), CuI (4 mg, 0.02 mmol), $Pd(PPh_3)_4$ (11 mg, 0.0095 mmol), *i*Pr_2NH (3 mL) and dry THF (10 mL). The resulting mixture was refluxed for 18 h. Solvent removal and purification by column chromatography (silica gel, hexanes/CH_2Cl_2, 5:1) first afforded compound **A56** (8 mg, 10%) as a yellow solid and second an orange solid that was further subjected to preparative TLC separation (hexanes/CH_2Cl_2, 2:1) and gave compound **320/b** (13 mg, 16%) as an orange solid.

Compound **320a/b**: Mp 165–166 ˚C (decomp.). R_f = 0.65 (hexane/CH_2Cl_2, 1:2). UV-vis (THF) λ_{max} (ε) 380 (82500) nm; IR (CH_2Cl_2, cast) 2941, 2854, 1667, 1647 cm^{-1}; ^1H NMR (CD_2Cl_2, 500 MHz) δ 7.34–7.04 (m, 76H), 6.97–6.94 (m, 4H); ^{13}C

NMR (125 MHz, CD_2Cl_2) δ 155.5, 155.2, 147.7, 140.5, 140.3, 140.2, 139.4, 131.1, 130.8, 130.6, 130.5, 130.4, 129.7, 129.4, 129.3, 129.2, 128.3, 128.13, 128.11, 128.01, 127.9, 115.4, 102.7, 102.1, 101.6, 101.4, 98.7, 91.3, 90.7, 90.5, 90.4. MALDI-TOF HRMS (DCTB) calcd. for $C_{134}H_{80}$ (M^+) 1688.62545, found 1688.62264.

Compound **A56**: Mp 165 ˚C. R_f = 0.8 (hexane/CH_2Cl_2 1:1). UV-vis (THF) λ_{max} 397 nm; IR (CH_2Cl_2, cast) 3053, 3030, 2923, 2851, 2179 cm^{-1}; ^1H NMR (CD_2Cl_2, 500 MHz) δ 7.37–7.07 (m, 40H); ^{13}C NMR (125 MHz, CD_2Cl_2) δ 156.0, 151.9, 140.5, 140.3, 140.2, 139.2, 130.5, 130.46, 130.41, 130.4, 129.58, 129.55, 129.3, 129.2, 128.43, 128.35, 128.1, 102.5, 102.1, 92.3, 91.5, 91.2, 88.4, 81.6. MALDI-TOF HRMS (DCTB) calcd. for $C_{66}H_{40}$ (M^+) 832.31245, found 832.31261. CV. (refer to appendix for more discussion)

Compound 401

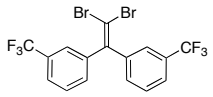

To a mixture of PPh_3 (17 g, 0.065 mol) in dry benzene (60 mL), was added CBr_4 (10.9 g, 0.0329 mol) and the resulting mixture was stirred at room temperature for 30 min. Compound **400** (4.0 g, 0.013 mol) was added in one portion and the resulting mixture was refluxed for 48 h. The crude reaction product was filtered and washed with benzene (2 x 40 mL). Solvent removal and purification by column chromatography (silica gel, hexanes/CH_2Cl_2, 10:1 to 5:1) afforded **401** (4.5 g, 75 %) as an off white solid. Mp 51–52 °C. R_f = 0.66 (hexanes/CH_2Cl_2, 2:1). IR (CH_2Cl_2, cast) 3071, 3042 cm^{-1}; ^1H NMR ($CDCl_3$, 300 MHz) δ 7.59–7.56 (m, 4H), 7.50–7.43 (m, 4H); ^{13}C NMR (125 MHz, $CDCl_3$) δ 144.9, 141.3, 132.2, 131.2 (q, $^2J_{C\text{-}F}$ = 33 Hz), 129.2, 125.7 (q, $^3J_{C\text{-}F}$ = 3.9 Hz), 125.2 (q, $^3J_{C\text{-}F}$ = 3.3 Hz), 123.7 (q, $^1J_{C\text{-}F}$ = 272 Hz), 93.5. EI HRMS calcd. for $C_{16}H_8F_6{}^{79}Br_2$ 471.8897 (M^+), found 471.8887.

Compound **402**

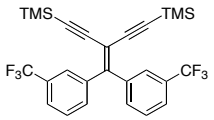

To a degassed mixture of **401** (79 mg, 0.17 mmol), CuI (3.2 mg, 0.016 mmol), $Pd(PPh_3)_2Cl_2$ (5.8 mg, 0.0082 mmol), *i*Pr_2NH (3 mL) and dry THF (10 mL) was added trimethylsilylacetylene (331 mg, 3.38 mmol, 0.476 mL). The resulting mixture was refluxed for 18 h. Et_2O and H_2O were added, the organic phase separated, washed with saturated NH_4Cl (2 x 20 mL), and dried ($MgSO_4$). Solvent removal and purification by column chromatography (silica gel, hexanes/CH_2Cl_2, 10:1) afforded **402** (76 mg, 90%) as a white solid. Mp 120 °C. R_f = 0.7 (hexanes/CH_2Cl_2, 2:1). IR (CH_2Cl_2, cast) 3071, 2961, 2901, 2150, 2132 cm^{-1}; ^1H NMR ($CDCl_3$, 500 MHz) δ 7.84 (s, 2H), 7.58–7.57 (m, 2H), 7.42–7.41 (m, 4H), 0.08 (s, 18H); ^{13}C NMR (125 MHz, $CDCl_3$) δ 153.7, 140.1, 133.4, 130.3 (q, $^2J_{C\text{-}F}$ = 32.3 Hz), 128.4, 127.0 (q, $^3J_{C\text{-}F}$ = 3.8 Hz), 125.3 (q, $^3J_{C\text{-}F}$ = 3.8 Hz), 124.0 (q, $^1J_{C\text{-}F}$ = 271 Hz), 104.7, 101.8, 99.9, –0.65. EI HRMS calcd. for $C_{26}H_{26}F_6Si_2$ 508.1477 (M^+), found 508.1490.

Compound **403**

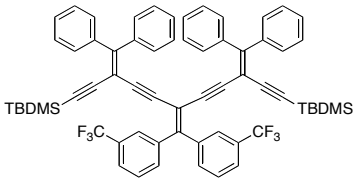

A mixture of **402** (55 mg, 0.11 mmol) and K_2CO_3 (2.9 mg, 0.020 mmol) in wet THF (1 mL) and MeOH (1 mL) was stirred for 1 h. Et_2O and H_2O were added, the organic phase separated, washed with saturated NH_4Cl (2 x 20 mL), dried ($MgSO_4$) and reduced to 2 mL. The Et_2O solution was added to a degassed mixture of triflate **300** (101 mg, 0.206 mmol), CuI (6.4 mg, 0.33 mmol), $Pd(PPh_3)_4$ (7 mg, 0.006 mmol), *i*Pr_2NH (3 mL) and dry THF (5 mL). The resulting mixture was refluxed for 18 h. Solvent removal and purification by column chromatography (silica gel, hexanes/CH_2Cl_2, 1:10 to 5:1) afforded **403** (81 mg, 75%) as a bright yellow solid. Mp 85 °C. R_f = 0.5 (hexanes/CH_2Cl_2, 2:1). UV-vis (THF) λ_{max} 304, 366 nm; IR (CH_2Cl_2, cast) 3056, 2954, 2928, 2856, 2192, 2097, 2143 cm^{-1}; ^1H NMR ($CDCl_3$, 400 MHz) δ 7.57–7.55 (m, 2H), 7.50–7.40 (m, 2H), 7.39-7.19 (m, 24H), 0.79 (s, 18H), 0.01 (s, 12H); ^{13}C NMR (100.6 MHz, $CDCl_3$) δ 157.8, 150.8, 140.2, 140.0, 139.6, 133.5, 130.5, 130.3, 130.2, 128.7, 128.5, 128.3, 127.7, 127.6, 126.9 (q, $^3J_{C\text{-}F}$ = 4 Hz), 125.4 (q, $^3J_{C\text{-}F}$ = 3.2 Hz), 123.9 (q, $^1J_{C\text{-}F}$ = 273 Hz), 104.8, 103.1, 101.5, 96.3, 92.2, 88.6, 26.1, 16.7, –4.9. MALDI-TOF HRMS (DCTB) calcd. for $C_{64}H_{58}F_6Si_2$ 996.39758 (M^+), found 996.39787.

Compound **404**

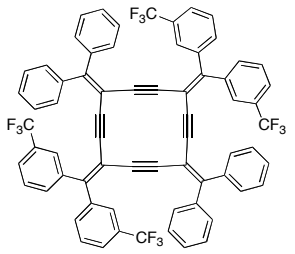

A mixture of trimer **403** (32 mg, 0.031 mmol) and TBAF (0.03 mL, 0.03 mmol, 1M in THF) in wet THF (2 mL) was stirred for 1 h. Et_2O and H_2O were added, the organic phase separated, washed with saturated NH_4Cl (2 x 20 mL), dried ($MgSO_4$) and reduced to 2 mL. The degassed Et_2O solution was added to a degassed mixture of dibromoolefin **401** (15 mg, 0.031 mmol), CuI (1 mg, 0.005 mmol), $Pd(PPh_3)_4$ (1.8 mg, 0.0015 mmol), *i*Pr_2NH (3 mL) and dry THF (5 mL). The resulting mixture was refluxed for 18 h. Solvent removal and purification by column chromatography (silica gel, hexanes/CH_2Cl_2, 5:1 to 3:1) afforded **404** (22 mg, 65%) as a bright yellow solid. Mp >205 °C (decomp.). R_f = 0.63 (hexanes/CH_2Cl_2 1.5:1). UV-vis (THF) λ_{max} (ε) 376 (122000) nm; IR (CH_2Cl_2, cast) 3081, 3056, 3030, 2151 cm^{-1}; ^1H NMR (CD_2Cl_2, 500 MHz) δ 7.66 (d, J = 8 Hz, 4H), 7.51 (d, J = 8 Hz, 4H), 7.25–7.19 (m, 20H), 7.09–7.07 (m, 8H); ^{19}F NMR (376 MHz, $CDCl_3$) δ –63.4; ^{13}C NMR (125 MHz, CD_2Cl_2) δ 153.8, 147.9, 140.1, 139.7, 133.5, 130.7 (q, $^2J_{C\text{-}F}$ = 32.4 Hz) 130.3, 129.5, 129.3, 128.2, 127.0 (q, $^3J_{C\text{-}F}$ = 4 Hz), 126.1 (q, $^3J_{C\text{-}F}$ = 3.8 Hz) 124.3 (q, $^1J_{C\text{-}F}$ = 272 Hz) 105.40, 101.8, 98.4, 96.1. MALDI-TOF HRMS (DCTB) calcd. for $C_{68}H_{36}F_{12}$ 1080.26199 (M^+), found 1080.26221. X-ray. CV.

Compound **405**

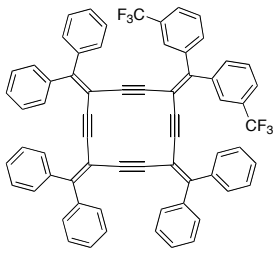

A mixture of trimer **305** (75 mg, 0.087 mmol) and TBAF (0.198 mL, 0.198 mmol, 1M in THF) in wet THF (2 mL) was stirred for 1 h. Et_2O and H_2O were added, the organic phase separated, washed with saturated NH_4Cl (2 x 20 mL), dried ($MgSO_4$) and reduced to 2 mL. The Et_2O solution was added to a degassed mixture of dibromoolefin **401** (38 mg, 0.08 mmol), CuI (5.5 mg, 0.028 mmol), $Pd(PPh_3)_4$ (4 mg, 0.003 mmol), *i*Pr_2NH (3 mL) and dry THF (5 mL). The resulting mixture was refluxed for 18 h. Solvent removal and purification by column chromatography (silica gel, hexanes/CH_2Cl_2, 5:1 to 4:1) afforded **405** (56 mg, 75%) as a bright yellow solid. Mp 244–245 °C. R_f = 0.7 (hexanes/CH_2Cl_2, 1:1). UV-vis (THF) λ_{max} 376 (81800) nm; IR (CH_2Cl_2, cast) 3055, 2925, 2170, 1684 cm^{-1}; ^1H NMR ($CDCl_3$, 400 MHz) δ 7.60 (d, J = 7.6 Hz, 2H), 7.42 (d, J = 8 Hz, 2H), 7.27–7.02 (m, 34H); ^{19}F NMR (376 MHz, $CDCl_3$) δ –63.4; ^{13}C NMR (125 MHz, CD_2Cl_2) δ 152.8, 152.4, 147.4, 140.1, 140.1, 140.0, 139.7, 133.4, 130.6 (q, $^2J_{C\text{-}F}$ = 31.5 Hz) 130.3, 130.2, 129.4, 129.3, 129.22, 129.20, 128.4, 128.3, 128.2, 126.9 (q, $^3J_{C\text{-}F}$ = 3.6 Hz), 125.9 (q, $^3J_{C\text{-}F}$ = 3.6 Hz) 124.3 (q, $^1J_{C\text{-}F}$ = 272 Hz), 105.5, 102.4, 102.2, 98.8, 97.4, 96.7, 95.8. MALDI-TOF HRMS (DCTB) calcd. for $C_{66}H_{38}F_6$ 944.28722 (M^+), found 944.28598. CV.

Compound **406**

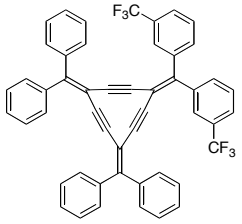

A mixture of dimer **303 (**53 mg, 0.081 mmol) and TBAF (0.07 mL, 0.07 mmol, 1M in THF) in wet THF (2 mL) was stirred for 1 h. Et_2O and H_2O were added, the organic phase separated, washed with saturated NH_4Cl (2 x 20 mL), dried ($MgSO_4$) and reduced to 2 mL. The Et_2O solution was added to a degassed mixture of dibromoolefin **401** (38 mg, 0.081 mmol), CuI (5.0 mg, 0.025 mmol), $Pd(PPh_3)_4$ (4.5 mg, 0.0039 mmol), *i*Pr_2NH (3 mL) and dry THF (5 mL). The resulting mixture was refluxed for 18 h. Solvent removal and purification by column chromatography (silica gel, hexanes/CH_2Cl_2, 5:1 to 2:1) afforded **406** (5.9 mg, 10%) as a bright yellow solid. Mp 200 °C (decomp.). R_f = 0.65 (hexanes/CH_2Cl_2, 1:1). UV-vis (THF) λ_{max} (ε) 363 (19200), 412 (18800) nm; IR (CH_2Cl_2, cast) 3058 cm^{-1}; ^1H NMR ($C_2D_2Cl_4$, 400 MHz) δ 8.00 (s, 2H), 7.69–7.52 (m, 14H), 7.44–7.39 (m, 12H); ^{19}F NMR (376 MHz, $C_2D_2Cl_4$) δ –63.1; ^{13}C NMR (125 MHz, CD_2Cl_2) δ 147.2, 142.3, 140.0, 139.7, 139.4, 133.9, 131.1, 130.8, 130.6, 129.7, 129.3, 128.5, 128.1, 127.2 (q, $^3J_{C\text{-}F}$ = 3.7 Hz), 126.2 (q, $^3J_{C\text{-}F}$ = 4 Hz) ,125.6, 123.4, 110.2, 106.5, 94.3, 92.2, 91.1. EI HRMS calcd. for $C_{50}H_{28}F_6$ 742.20953 (M^+), found 742.21041. CV.

Compound **408**

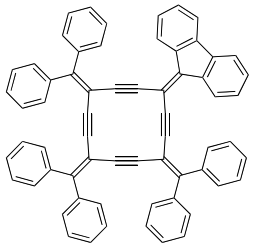

A mixture of **305** (60 mg, 0.069 mmol) and TBAF (0.2 mL, 0.2 mmol, 1M in THF) in wet THF (2 mL) was stirred for 1 h. Et_2O and H_2O were added, the organic phase separated, washed with saturated NH_4Cl (2 x 20 mL), dried ($MgSO_4$) and reduced to 2 mL. The Et_2O solution was added to a degassed mixture of dibromoolefin **407** (24 mg, 0.071 mmol), CuI (6 mg, 0.03 mmol), $Pd(PPh_3)_4$ (5 mg, 0.004 mmol), *i*Pr_2NH (3 mL) and dry THF (5 mL). The resulting mixture was refluxed for 18 h. Solvent removal and purification by column chromatography (silica gel, hexanes/CH_2Cl_2, 5:1 to 2:1) afforded **408** (44.4 mg, 79%) as a bright yellow solid. Mp >300 °C (decomp.). R_f = 0.7 (hexanes/CH_2Cl_2, 1:1). UV-vis (THF) λ_{max} (ε) 393 (86500) nm; IR (CH_2Cl_2, cast) 3053, 2921, 2849, 2153, 1941, 1880, 1814, 1600 cm^{-1}; ^1H NMR ($CDCl_3$, 400 MHz) δ 7.54–7.39 (m, 10H), 7.34–7.30 (m, 8H), 7.24–7.08 (m, 18H), 6.77–6.73 (m, 2H); ^{13}C NMR (125 MHz, CD_2Cl_2) δ 153.4, 152.6, 141.5, 140.9, 140.0, 139.6, 137.0, 130.4, 130.34, 130.27, 129.8, 129.52, 129.50, 129.3, 129.0, 128.4, 128.1, 124.9, 119.7, 104.3, 102.8, 102.5, 100.7, 97.4, 96.7. MALDI-TOF HRMS (DCTB) calcd. for $C_{64}H_{38}$ 806.29680 (M^+), found 806.29551. CV.

Compound **409**

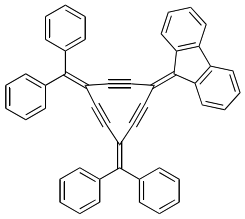

A mixture of dimer **303** (65 mg, 0.098 mmol) and TBAF (0.1 mL, 0.1 mmol, 1M in THF) in wet THF (2 mL) was stirred for 1 h. Et_2O and H_2O were added, the organic phase separated, washed with saturated NH_4Cl (2 x 20 mL), dried ($MgSO_4$) and reduced to 2 mL. The Et_2O solution was added to a degassed mixture of dibromoolefin **407** (33 mg, 0.098 mmol), CuI (6 mg, 0.03 mmol), $Pd(PPh_3)_4$ (6 mg, 0.005 mmol), *i*Pr_2NH (3 mL) and dry THF (5 mL). The resulting mixture was refluxed for 20 h. Solvent removal and purification by column chromatography (silica gel, hexanes/CH_2Cl_2, 5:1) afforded **409** (26.8 mg, 45%) as a bright yellow solid. Mp >300°C (decomp.). R_f = 0.6 (hexanes/CH_2Cl_2, 1:1). UV-vis (THF) λ_{max} 383 (16100), 447 (14100), 474 (12000) nm; IR (CH_2Cl_2, cast) 3085, 3054, 3019, 2111, 1616, 1598, 1577, 1544 cm^{-1}; ^1H NMR (CD_2Cl_2, 400MHz) δ 8.44 (d, *J* = 7.6 Hz, 2H), 7.73–7.65 (m, 10H), 7.55–7.53 (m, 6H), 7.46–7.43 (m, 6H), 7.39 (td, *J* = 6.8, 0.8 Hz, 2H), 7.31 (td, *J* = 6.8, 1.2 Hz, 2H); ^{13}C NMR (125 Hz, CD_2Cl_2) δ 147.5, 140.8, 139.8, 139.5, 137.4, 137.3, 130.9, 130.8, 130.1, 129.9, 129.8, 128.6, 128.4, 127.9, 124.9, 120.3, 107.0, 103.7, 99.9, 92.4, 90.6. EI HRMS calc. for $C_{48}H_{28}$ 604.2191 (M^+), found 604.2191. CV.

Compound **411**

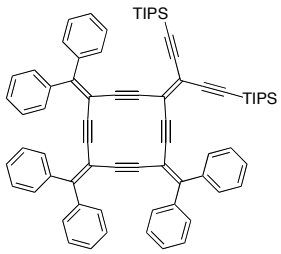

A mixture of timer **305** (90.0 mg, 0.104 mmol) and TBAF (0.3 mL, 0.3 mmol, 1M in THF) in wet THF (2 mL) was stirred for 1 h. Et_2O and H_2O were added, the organic phase separated, washed with saturated NH_4Cl (2 x 20 mL), dried ($MgSO_4$) and reduced to 2 mL. The Et_2O solution was added to a degassed mixture of dibromoolefin **410** (57.2 mg, 0.104 mmol), CuI (6 mg, 0.03 mmol), $Pd(PPh_3)_4$ (6.5 mg, 0.0056 mmol), *i*Pr_2NH (3 mL) and dry THF (5 mL). The resulting mixture was refluxed for 18 h. Solvent removal and purification by column chromatography (silica gel, hexanes/CH_2Cl_2, 5:1 to 2:1) afforded radialene **411** (82 mg, 78%) as a yellow solid. Mp >250 °C (decomp.). R_f = 0.62 (hexanes/CH_2Cl_2, 1:1). UV-vis (THF) λ_{max} (ε) 388 (47500) nm; IR (CH_2Cl_2, cast) 3054, 2925, 2863, 2137, 1741 cm^{-1}; ^1H NMR ($CDCl_3$, 500 MHz) δ 7.39–7.37 (m, 4H), 7.27–7.13 (m, 22H), 7.06–7.03 (m, 4H), 0.89–0.83 (m, 42H); ^{13}C NMR (125 MHz, $CDCl_3$) δ 151.8, 151.6, 140.0, 139.9, 139.8, 130.5, 130.2, 130.1, 128.9, 128.7, 128.5, 127.9, 127.8, 127.7, 117.6, 110.9, 104.0, 103.8, 102.6, 102.1, 102.0, 96.6, 96.5, 96.3, 18.5, 11.1. MALDI-TOF HRMS (DCTB) calcd. for $C_{74}H_{72}Si_2$ 1016.51671 (M^+), found 1016.51720. CV.

Compound **412**

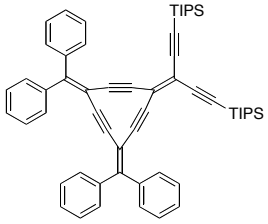

A mixture of **303** (60.0 mg, 0.0910 mmol) and TBAF (0.1 mL, 0.1 mmol, 1M in THF) in wet THF (2 mL) was stirred for 1 h. Et_2O and H_2O were added, the organic phase separated, washed with saturated NH_4Cl (2 x 20 mL), dried ($MgSO_4$) and reduced to 2 mL. The Et_2O solution was added to a degassed mixture of dibromoolefin **410** (50. mg, 0.091 mmol), CuI (6.0 mg, 0.030 mmol), $Pd(PPh_3)_4$ (5.0 mg, 0.0040 mmol), *i*Pr_2NH (3 mL) and dry THF (5 mL). The resulting mixture was refluxed for 18 h. Solvent removal and purification by column chromatography (silica gel, hexanes/CH_2Cl_2, 5:1 to 2:1) afforded **412** (24.6 mg, 33%) as a yellow solid. Mp 195 °C (decomp.). R_f = 0.75 (hexanes/CH_2Cl_2, 1:1). UV-vis (THF) λ_{max} 378 (42800), 430 (31800) nm; IR (CH_2Cl_2, cast) 3058, 2995, 2941, 2925, 2864, 2100, 1737, cm^{-1}; ^1H NMR (CD_2Cl_2, 400 MHz) δ 7.59–7.53 (m, 8H), 4.71–7.39 (m, 12H), 1.10–1.08 (m, 42H); ^{13}C NMR (125 Hz, CD_2Cl_2) δ 147.7, 139.7, 139.5, 130.8, 130.7, 129.7, 129.6, 128.6, 128.4, 123.5, 107.2, 106.5, 103.7, 102.7, 99.9, 92.0, 91.6, 18.8, 11.6; $^{29}Si\{1H\}$ NMR (79.5 MHz, CD_2Cl_2) δ –0.8. MALDI-TOF HRMS (DCTB) calcd. for $C_{58}H_{62}Si_2$ 814.43846 (M^+), found 814.43868. CV.

Compound **414** and **415**

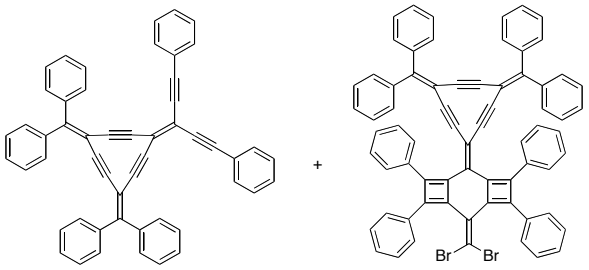

414 **415**

A mixture of **303** (85 mg, 0.13 mmol) and TBAF (0.3 mL, 0.3 mmol, 1M in THF) in wet THF (2 mL) was stirred for 1 h. Et_2O and H_2O were added, the organic phase separated, washed with saturated NH_4Cl (2 x 20 mL), dried ($MgSO_4$) and reduced to 2 mL. The Et_2O solution was added to a degassed mixture of dibromoolefin **413** (50.2 mg, 0.130 mmol), CuI (7.5 mg, 0.040 mmol), $Pd(PPh_3)_4$ (7.5 mg, 0.0060 mmol), iPr$_2$NH (3 mL) and dry THF (5 mL). The resulting mixture was refluxed for 20 h. Solvent removal and purification by column chromatography (silica gel, hexanes/CH_2Cl_2, 5:1) afforded first compound **414** (34 mg, 40%) as an orange solid and second compound **415** (5.4 mg, 8%) as a yellow solid.

Compound **414**: Mp 220 °C. R_f = 0.45 (hexanes/CH_2Cl_2, 1:1). UV-vis (THF) λ_{max} 388 (35100), 457 (29400), 482 (27000) nm; IR (CH_2Cl_2, cast) 3079, 3057, 3032, 3019, 2208, 2188, 2109, 1596 cm^{-1}; ^{1}H NMR (CD_2Cl_2, 400 MHz) δ 7.65–7.63 (m, 8H), 7.53–7.40 (m, 22H); ^{13}C NMR (125 MHz, CD_2Cl_2) δ 147.8, 139.8, 139.5, 132.3, 131.0, 130.8, 129.9, 129.73, 129.68, 128.9, 128.6, 128.4, 123.8, 122.6, 106.8, 106.6, 100.1, 99.2, 92.2, 91.8, 87.2. MALDI-TOF HRMS (DCTB) calcd. for $C_{52}H_{30}$ 654.23420 (M^+), found 654.23448. CV. X-ray.

Compound **415**: Mp 185 °C (decomp.). R_f = 0.45 (hexanes/CH_2Cl_2, 1:1); UV-vis (THF) λ_{max} 410 (51200) nm; IR (CH_2Cl_2, cast) 3055, 3032, 2213, 2192, 2161, 1713, 1597, 1572 cm^{-1}; ^1H NMR ($CDCl_3$, 400 MHz) δ 7.58–7.55 (m, 10H), 7.48–7.45 (m, 10H), 7.36–7.21 (m, 20H); ^{13}C NMR (125 MHz, $CDCl_3$) δ 158.4, 139.5, 139.3, 132.0, 131.8, 130.5, 130.4, 129.3, 129.2, 129.1, 129.0, 128.4, 128.3, 127.78, 127.76, 122.4, 122.2, 113.8, 113.7, 101.9, 100.6, 99.3, 95.8, 90.3, 90.0, 87.5, 86.1. MALDI-TOF HRMS (DCTB) calcd. for $C_{70}H_{40}{}^{79}Br_2$ 1038.14913 (M^+), found 1038.14854; $C_{70}H_{40}{}^{79}Br$ 959.23079 ($[M–Br]^+$), found 959.22963; $C_{70}H_{40}$ 880.31245 ($[M–2Br]^+$), found 880.31191.

Compound **416**

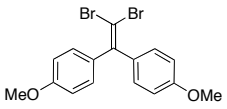

To a mixture of PPh_3 (16.3 g, 62.1 mmol) in dry benzene (20 mL), was added CBr_4 (9.5 g, 29 mmol) and the resulting mixture was stirred at room temperature for 30 min. 4,4'-Dimethoxybenzophenone (3.0 g, 12 mmol) was added in one portion and the resulting mixture was stirred at room temperature for 1 h and followed by reflux for 20 h. The crude reaction product was filtered and washed with benzene (2 x 40 mL). Solvent removal and purification by column chromatography (silica gel, hexanes/CH_2Cl_2, 5:1) afforded **416** (2.7 g, 55%) as an off-white solid. Mp 81 °C. R_f = 0.64 (hexanes/ethyl acetate, 3:1). IR (CH_2Cl_2, cast) 3034, 3001, 2956, 2932, 2907, 2836, 2053, 1605, 1509 cm^{-1}; ^1H NMR ($CDCl_3$, 400 MHz) δ 7.24 (d, J = 8.8 Hz, 4H), 6.89 (d, J = 8.8 Hz, 4H), 3.83 (s, 6H); ^{13}C NMR (125 MHz, $CDCl_3$) δ 159.2, 147.0, 133.9, 130.4, 113.6, 88.5, 55.2. EI HRMS calcd. for $C_{16}H_{14}O_2{}^{79}Br_2$ 395.9361 (M^+), found 395.9370.

Compound **419**

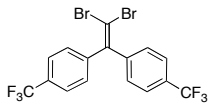

To a mixture of PPh_3 (5.5 g, 21 mmol) in dry benzene (50 mL), was added CBr_4 (3.5 g, 11 mmol) and the resulting mixture was stirred at room temperature for 30 min. Ketone **418** (1.34 g, 4.21 mmol) was added in one portion and the resulting mixture was refluxed for 18 h. The crude reaction product was filtered and washed with benzene (2 x 40 mL). Solvent removal and purification by column chromatography (silica gel, hexanes/CH_2Cl_2 10:1) afforded **419** (1.2 g, 60%) as a colorless solid. Mp 100 °C. R_f = 0.65 (hexanes/CH_2Cl_2, 10:1). IR (CH_2Cl_2, cast) 2923, 2853 cm^{-1}; ^1H NMR ($CDCl_3$, 300 MHz) δ 7.64–7.61 (m, 4H), 7.44–7.42 (m, 4H); ^{13}C NMR (125 MHz, $CDCl_3$) δ 145.3, 144.1, 130.4 (q, $^2J_{C\text{-}F}$ = 34 Hz), 129.2, 125.6 (q, $^3J_{C\text{-}F}$ = 4 Hz), 124.8 (q, $^1J_{C\text{-}F}$ = 272 Hz), 93.1. EI HRMS calcd. for $C_{16}H_8{}^{79}Br_2F_6$ 471.8897 (M^+), found 471.8898.

Compound **420**

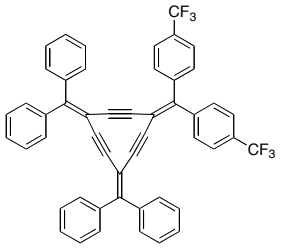

A mixture of dimer **303** (60.0 mg, 0.0910 mmol) and TBAF (0.2 mL, 0.2 mmol, 1M in THF) in wet THF (2 mL) was stirred for 1 h. Et_2O and H_2O were added, the organic phase separated, washed with saturated NH_4Cl (2 x 20 mL), dried ($MgSO_4$) and reduced to 2 mL. The Et_2O solution was added to a degassed mixture of dibromoolefin **419** (42.7 mg, 0.09 mmol), CuI (6.70 mg, 0.035 mmol), $Pd(PPh_3)_4$ (5 mg, 0.004 mmol), *i*Pr_2NH (3 mL) and dry THF (5 mL). The resulting mixture was refluxed for 18 h. Solvent removal and purification by column chromatography (silica gel, hexanes/CH_2Cl_2, 5:1 to 2:1) afforded **420** (2.7 mg, 4%) as a bright yellow solid. R_f = 0.65 (hexanes/CH_2Cl_2, 1:1). UV-vis (THF) λ_{max} 365, 413 nm; ^{1}H NMR ($CDCl_3$, 400 MHz) δ 7.68–7.35 (m, 4H), 7.61–7.35 (m, 20H), 6.54–6.53 (m, 4H). MALDI-TOF HRMS (DCTB) calcd. for $C_{50}H_{28}F_6$ 742.20897 (M^+), found 742.20878.

Note: also, it is worth mentioning that the first product collected from the column was compound **A59** (3.4 mg, 10%).

Compound **421**

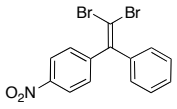

To a mixture of PPh_3 (17.3 g, 65.9 mmol) in dry benzene (30 mL), was added CBr_4 (11 g, 33 mmol) and the resulting mixture was stirred at room temperature for 30 min. 4-Nitrobenzophenone (3 g, 10 mmol) was added in one portion and the resulting mixture was refluxed for 4 h followed by stirring at room temperature for 12 h. The crude reaction product was filtered and washed with benzene (40 mL). Solvent removal and purification by column chromatography (silica gel, hexanes/CH_2Cl_2, 4:1) afforded **421** (3 g, 60%) as a white solid. Mp 65–66 °C. R_f = 0.72 (hexanes/ethyl acetate, 3:1). IR (CH_2Cl_2, cast) 3103, 3077, 3059, 3029, 2851, 1600, 1518 cm^{-1}; ^1H NMR ($CDCl_3$, 300 MHz) δ 8.19–8.17 (m, 2H), 7.49–7.46 (m, 2H), 7.36–7.32 (m, 3H), 7.28–7.25 (m, 2H); ^{13}C NMR (125 MHz, $CDCl_3$) δ 198.7, 147.7, 147.2, 145.9, 140.2, 129.9, 128.7, 128.6, 123.7, 92.5. EI HRMS calcd. for $C_{14}H_9NO_2{}^{79}Br_2$ 380.8999 (M^+), found 380.9003.

Compound **422**

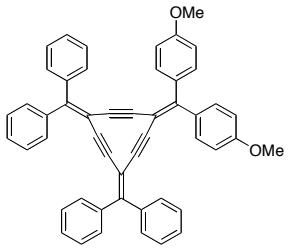

A mixture of oligomer **303** (65 mg, 0.098 mmol) and TBAF (0.1 mL, 0.1 mmol, 1M in THF) in wet THF (2 mL) was stirred for 1 h. Et_2O and H_2O were added, the organic phase separated, washed with saturated NH_4Cl (2 x 20 mL), dried ($MgSO_4$) and reduced to 2 mL. The Et_2O solution was added to a degassed mixture of dibromoolefin **416** (40.0 mg, 0.0980 mmol), CuI (6.5 mg, 0.030 mmol), $Pd(PPh_3)_4$ (6.0 mg, 0.0050 mmol), *i*Pr_2NH (3 mL) and dry THF (5 mL). The resulting mixture was refluxed for 20 h. Solvent removal and purification by column chromatography (silica gel, hexanes/CH_2Cl_2, 4:1) afforded radialene **422** (4 mg, 6%) as a yellow solid. R_f = 0.65 (hexanes/CH_2Cl_2, 1:1). UV-vis (THF) λ_{max} 370, 421nm; IR (CH_2Cl_2, cast) 3054, 2954, 2924, 2854, 1730, 1603 cm^{-1}. MALDI-TOF HRMS (DCTB) calcd. for $C_{50}H_{34}O_2$, 666.25533 (M^+), found 666.25551.

Compound **423** and **A59**

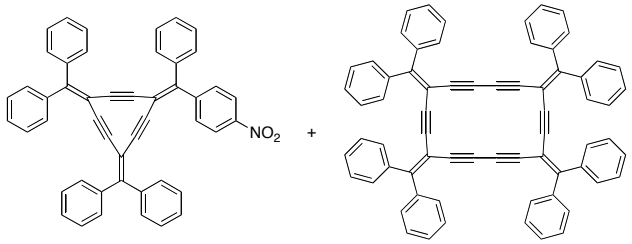

423 **A59**

A mixture of dimer **303** (60.0 mg, 0.0910 mmol) and TBAF (0.1 mL, 0.1 mmol, 1M in THF) in wet THF (2 mL) was stirred for 1 h. Et_2O and H_2O were added, the organic phase separated, washed with saturated NH_4Cl (2 x 20 mL), dried ($MgSO_4$) and reduced to 2 mL. The Et_2O solution was added to a degassed mixture of dibromoolefin **421** (34 mg, 0.088 mmol), CuI (6.0 mg, 0.030 mmol), $Pd(PPh_3)_4$ (5.0 mg, 0.0040 mmol), *i*Pr_2NH (3 mL) and dry THF (5 mL). The resulting mixture was refluxed for 20 h. Solvent removal and purification by column chromatography (silica gel, hexanes/CH_2Cl_2, 4:1 to 1:1) afforded first compound **A59** as a yellow solid (3.9 mg, 10%) and second radialene **421** (4.6 mg, 8%) as an orange solid.

Compound **423**: R_f = 0.6 (hexanes/CH_2Cl_2, 1:1). UV-vis (THF) λ_{max} 365, 418 nm; IR (CH_2Cl_2, cast) 3053, 1728 cm^{-1}; MALDI-TOF HRMS (DCTB) calcd. for $C_{48}H_{29}NO_2$, found 651.21928 (M^+), found 651.21929.

Compound **A59**: Mp >300 °C. R_f = 0.6 (hexanes/CH_2Cl_2, 1:1). UV-vis (THF) λ_{max} 392 nm; IR (CH_2Cl_2, cast) 3083, 3051, 3033 cm^{-1}; ^1H NMR (CD_2Cl_2, 400 MHz) δ 7.37–7.13 (m, 40H); ^{13}C NMR (125 MHz, CD_2Cl_2) δ 155.4, 140.1, 139.6, 130.6, 130.3, 129.7, 128.5, 128.3, 101.5, 94.1, 85.3, 77.2. MALDI-TOF HRMS (DCTB)

calcd. for $C_{68}H_{40}$ 856.31245 (M^+), found, 856.31243. CV. (refer to appendix for more discussion)

Compound 424

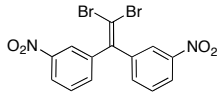

To a mixture of PPh_3 (19.7 g, 75.1 mmol) in dry benzene (60 mL), was added CBr_4 (12.5 g, 37.6 mmol) and the resulting mixture was stirred at room temperature for 30 min. 3,3'-Dinitrobenzophenone (4 g, 10 mmol) was added in one portion and the resulting mixture was refluxed for 48 h. The crude reaction product was filtered and washed with benzene (2 x 40 mL). Solvent removal and purification by column chromatography (silica gel, hexanes/ethyl acetate, 9:1 to 5:1) afforded **424** (4.6 g, 73%) as a white solid. Mp 146–147 °C; R_f = 0.27 (hexanes/CH_2Cl_2, 1:2). IR (CH_2Cl_2, cast) 3085, 1529 cm^{-1}; ^1H NMR ($CDCl_3$, 500 MHz) δ 8.22–8.17 (m, 4H), 7.66–7.64 (m, 2H), 7.57 (t, J = 8 Hz, 2H); ^{13}C NMR (125 MHz, $CDCl_3$) δ 148.4, 143.2, 141.6, 134.9, 129.9, 124.0, 123.5, 95.3. EI HRMS calcd. for $C_{14}H_8{}^{79}Br_2N_2O_4$ 425.8851 (M^+), found 425.8854.

Compound **425**

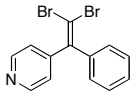

To a mixture of PPh_3 (40.0 g, 160 mmol) in dry benzene (70 mL), was added CBr_4 (25 g, 75 mmol) and the resulting mixture was stirred at room temperature for 30 min. 2-Benzoylpyridine (4 g, 20 mmol) was added in one portion and the resulting mixture was stirred at room temperature for 2 days. The crude reaction product was filtered and washed with benzene (2 x 40 mL). Solvent removal and purification by column chromatography (silica gel, hexanes/CH_2Cl_2, 5:1) afforded dibromoolefin **425** (5.1 g, 69%) as a white solid. Mp 112 °C. R_f = 0.3 (hexanes/ethyl acetate, 3:1); IR (CH_2Cl_2, cast) 3081, 3059, 3031, 3021, 1593, 1541, cm^{-1}; ^1H NMR (400 MHz, $CDCl_3$) δ 8.49 (d, J = 3.6 Hz, 2H), 7.26–7.23 (m, 3H), 7.18–7.15 (m, 2H), 7.11 (d, J = 3.6 Hz, 2H); ^{13}C NMR (125 MHz, $CDCl_3$) δ 150.1, 148.9, 145.3, 140.1, 128.7, 128.6, 128.5, 132.4, 92.3; EI HRMS calcd. for $C_{13}H_9N^{79}Br_2$ 336.9102 (M^+), found 336.9102.

Compound **426**

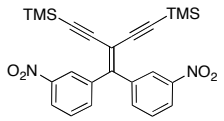

To a degassed mixture of **424** (181 mg, 0.423 mmol), CuI (8 mg, 0.04 mmol), $Pd(PPh_3)_2Cl_2$ (15 mg, 0.021 mmol), *i*Pr_2NH (3 mL) and dry THF (10 mL) was added trimethylsilylacetylene (331 mg, 3.38 mmol, 0.476 mL). The resulting mixture was refluxed for 24 h. Et_2O and H_2O were added, the organic phase separated, washed with saturated NH_4Cl (2 x 20 mL), and dried ($MgSO_4$). Solvent removal and purification by column chromatography (silica gel, hexanes/ethyl acetate, 10:1) afforded **426** (162 mg, 83%) as an off white solid. Mp 100 °C. R_f = 0.4 (hexanes/CH_2Cl_2, 1:1). IR (CH_2Cl_2, cast) 3084, 2961, 2900, 2148, 1532 cm^{-1}; ^1H NMR ($CDCl_3$, 500 MHz) δ 8.14–8.40 (m, 2H), 8.21–8.19 (m, 2H), 7.65–7.63 (m, 2H), 7.52–7.49 (m, 2H), 0.08 (s, 18H); ^{13}C NMR (125 MHz, $CDCl_3$) δ 151.3, 147.9, 140.5, 136.0, 129.1, 125.2, 123.6, 106.3, 101.4, 101.1, –0.65. EI HRMS calcd. for $C_{24}H_{26}O_4N_2Si_2$ 462.1431 (M^+), found 462.1426.

Compound **427**

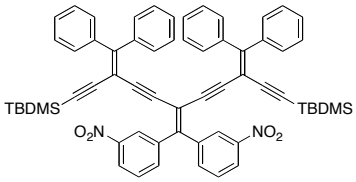

A mixture of **426** (100 mg, 0.2 mmol) and K_2CO_3 (5.9 mg, 0.043 mmol) in wet THF (1 mL) and MeOH (1 mL) was stirred for 1 h. Et_2O and H_2O were added, the organic phase separated, washed with saturated NH_4Cl (2 x 20 mL), dried ($MgSO_4$) and reduced to 2 mL. The Et_2O solution was added to a degassed mixture of triflate **300** (201 mg, 0.430 mmol), CuI (8 mg, 0.04 mmol), $Pd(PPh_3)_4$ (13 mg, 0.011 mmol), *i*Pr_2NH (3 mL) and dry THF (5 mL). The resulting mixture was refluxed for 18 h. Solvent removal and purification by column chromatography (silica gel, hexanes/CH_2Cl_2, 1:10 to 3:1) afforded **427** (123 mg, 60%) as a bright yellow solid. Mp 140 °C. R_f = 0.4 (hexanes/CH_2Cl_2, 1:1). UV-vis (THF) λ_{max} 321, 367 nm; IR (CH_2Cl_2, cast) 3082, 3056, 2953, 2927, 2884, 2856, 2185, 2144 cm^{-1}; ^1H NMR ($CDCl_3$, 400 MHz) δ 8.09–8.06 (m, 2H), 8.00–7.99 (m, 2H), 7.69–7.67 (m, 2H), 7.39–7.30 (m, 6H), 7.30–7.21 (m, 16H), 0.08 (s, 18H), 0.02 (s, 12H); ^{13}C NMR (125 MHz, $CDCl_3$) δ 158.5, 148.4, 147.9, 140.4, 134.0, 139.6, 136.1, 130.3, 130.2, 129.0, 128.9, 128.7, 127.8, 127.7, 124.8, 123.7, 106.4, 102.9, 101.1, 96.6, 93.5, 87.9, 26.1, 16.7, –4.9. MALDI-TOF HRMS (DCTB) calcd. for $C_{62}H_{58}N_2O_4Si_2$ 950.39296 (M^+), found 950.39290.

Compound **428**

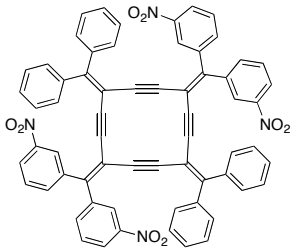

A mixture of trimer **427** (46 mg, 0.050 mmol) and TBAF (0.1 mL, 0.1 mmol, 1M in THF) in wet THF (2 mL) was stirred for 1 h. Et_2O and H_2O were added, the organic phase separated, washed with saturated NH_4Cl (2 x 20 mL), dried ($MgSO_4$) and reduced to 2 mL. The Et_2O solution was added to a degassed mixture of dibromoolefin **424** (20.7 mg, 0.0480 mmol), CuI (3.7 mg, 0.020 mmol), $Pd(PPh_3)_4$ (3.8 mg, 0.0030 mmol), *i*Pr_2NH (3 mL) and dry THF (5 mL). The resulting mixture was refluxed for 18 h. Solvent removal and purification by column chromatography (silica gel, hexanes/CH_2Cl_2, 5:1 to 1:1) afforded radialene **428** (26 mg, 55%) as a bright yellow solid. Mp >300 °C. R_f = 0.55 (hexanes/CH_2Cl_2, 1:1). UV-vis (THF) λ_{max} 376 nm; ^{1}H NMR ($C_2D_2Cl_4$, 400 MHz) δ 8.12–8.07 (m, 8H), 7.59–7.57 (m, 4H), 7.31 (t, *J* = 7.6 Hz, 4H), 7.20–7.16 (m, 12H), 7.02 (t, *J* = 7.6 Hz, 8H). MALDI-TOF HRMS (DCTB) calc. for $C_{64}H_{36}N_4O_8$ 988.25277 (M^+), found 988.25233.

Compound **429**

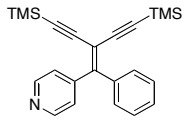

To a degassed mixture of **425** (201 mg, 0.592 mmol), CuI (11.3 mg, 0.0593 mmol), $Pd(PPh_3)_2Cl_2$ (20.8 mg, 0.0296 mmol), iPr$_2$NH (3 mL) and dry THF (10 mL) was added trimethylsilylacetylene (316 mg, 3.22 mmol, 0.45 mL). The resulting mixture was refluxed for 18h. Et_2O and H_2O were added, the organic phase separated, washed with saturated NH_4Cl (2 x 20 mL), and dried ($MgSO_4$). Solvent removal and purification by column chromatography (silica gel, hexanes/ethyl acetate, 6:1) afforded **429** (188 mg, 85%) as an off white solid. Mp 100 °C. R_f = 0.5 (hexanes/CH_2Cl_2, 1:1). IR (CH_2Cl_2, cast) 2958, 2898, 2152, 2132, 1590 cm^{-1}; ^{1}H NMR ($CDCl_3$, 400 MHz) δ 8.56 (s, 2H), 7.39–7.33 (m, 2H), 7.32–7.27 (m, 5H), 0.095 (s, 9H), 0.093 (s, 9H); ^{13}C NMR (125 MHz, $CDCl_3$) δ 154.6, 149.4, 147.7, 138.5, 130.0, 128.9, 127.7, 124.4, 104.1, 102.2, 102.0, 99.69, 99.67, –0.59, –0.62. EI HRMS calcd. for $C_{23}H_{27}NSi_2$ 373.1682 (M^+), found 373.1687.

Compound **430**

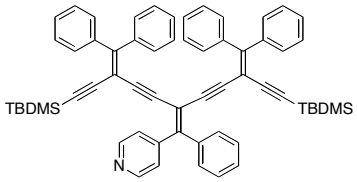

A mixture of **429** (107 mg, 0.288 mmol) and K_2CO_3 (7.9 mg, 0.057 mmol) in wet THF (1 mL) and MeOH (1 mL) was stirred for 1 h. Et_2O and H_2O were added, the organic phase separated, washed with saturated NH_4Cl (2 x 20 mL), and dried ($MgSO_4$) and reduced to 2 mL. The Et_2O solution was added to a degassed mixture of triflate **300** (260 mg, 0.209 mmol), CuI (16 mg, 0.084 mmol), $Pd(PPh_3)_4$ (17.9 mg, 0.0154 mmol), *i*Pr_2NH (3 mL) and dry THF (5 mL). The resulting mixture was refluxed for 18 h. Solvent removal and purification by column chromatography (silica gel, hexanes/CH_2Cl_2 8:1 to 2:1) afforded **430** (156 mg, 63%) as a bright yellow solid. Mp 160 °C. R_f = 0.5 (hexanes/CH_2Cl_2, 1:1). UV-vis (THF) λ_{max} 323, 368 nm; IR (CH_2Cl_2, cast) 3055, 3029, 2954, 2926, 2855, 2144 cm^{-1}; ^1H NMR ($CDCl_3$, 500 MHz) δ 8.41 (bs, 2H), 7.40–7.37 (m, 5H), 7.29–7.23 (m, 20H), 7.11 (bs, 2H), 1.20 (s, 9H), 0.81 (s, 9H), 0.05 (s, 6H), 0.03 (s, 6H); ^{13}C NMR (125 MHz, $CDCl_3$) δ 157.6, 157.5, 151.2, 149.3, 140.2, 140.1, 139.8, 139.7, 138.6, 130.4, 130.3, 130.1, 128.9, 128.8, 128.7, 128.5, 128.4, 127.9, 127.82, 127.77, 127.69, 124.4, 104.4, 103.2, 103.1, 101.7, 101.6, 96.5, 96.3, 92.2, 89.2, 88.9, 26.1, 16.7, –4.8. MALDI-TOF HRMS (DCTB) calcd. for $C_{62}H_{59}NSi_2$ 861.41806 (M^+), found 861.41836.

Compound **431**(cis/trans)

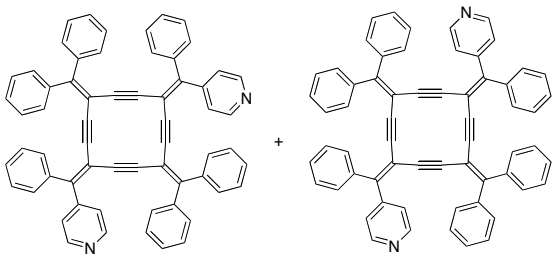

A mixture of trimer **430** (55 mg, 0.063 mmol) and TBAF (0.1 mL, 0.1 mmol, 1M in THF) in wet THF (2 mL) was stirred for 1 h. Et_2O and H_2O were added, the organic phase separated, washed with saturated NH_4Cl (2 x 20 mL), dried ($MgSO_4$) and reduced to 2 mL. The Et_2O solution was added to a degassed mixture of dibromoolefin **425** (21.5 mg, 0.0634 mmol), CuI (3.7 mg, 0.019 mmol), $Pd(PPh_3)_4$ (4.2 mg, 0.0036 mmol), iPr$_2$NH (3 mL) and dry THF (5 mL). The resulting mixture was refluxed for 18 h. Solvent removal and purification by column chromatography (aluminum oxide, hexanes/ethyl acetate, 5:1) afforded **431** (41 mg, 80%) as a yellow solid (a mixture of two isomers). R_f = 0.5 (hexanes/CH_2Cl_2, 1:1.5). UV-vis (THF) λ_{max} 376 nm; IR (CH_2Cl_2, cast) 3057, 3028, 2954, 2924, 2853, 1732 cm^{-1}. MALDI-TOF HRMS (DCTB) calc. for $C_{62}H_{38}N_2$ 810.30295 (M^+), found 810.30263.

Compound **432**

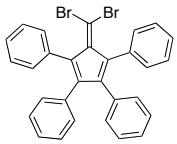

To a mixture of PPh_3 (6.8 g, 26 mmol) in dry benzene (30 mL), was added CBr_4 (4.4 g, 13 mmol) and the resulting mixture was stirred at room temperature for 4 days. Tetraphenylcyclopentadienone (2 g, 4 mmol) was added in one portion and the resulting mixture was refluxed for 4 h followed by stirring at room temperature for 2 days. The crude reaction product was filtered and the residue washed with benzene (40 mL). Solvent removal and purification by column chromatography (aluminum oxide, activity 2, hexanes) afforded **432** (1.7 g, 60.5 %) as an orange solid. Mp 73 °C. R_f = 0.23 (hexanes/CH_2Cl_2, 8:1). IR (CH_2Cl_2, cast) 3076, 3059, 3024, 1520 cm^{-1}; ^1H NMR (400 MHz, $CDCl_3$) δ 7.26–7.18 (m, 10H), 6.98–6.93 (m, 6H), 6.81–6.79 (m, 4H); ^{13}C NMR (125 MHz, $CDCl_3$) δ 146.3, 146.2, 136.56, 134.6, 134.5, 131.5, 129.8, 127.9, 127.1, 126.9, 126.6, 104.1; EI HRMS calcd. for $C_{30}H_{20}{}^{79}Br_2$ 537.9931 (M^+), found 537.9929. X ray.

Compound **433**

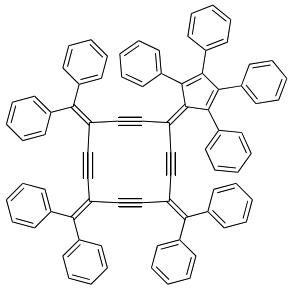

A mixture of trimer **305** (70.0 mg, 0.0810 mmol) and TBAF (0.3 mL, 0.3 mmol, 1M in THF) in wet THF (2 mL) was stirred for 1 h. Et_2O and H_2O were added, the organic phase separated, washed with saturated NH_4Cl (2 x 20 mL), dried ($MgSO_4$) and reduced to 2 mL. The Et_2O solution was added to a degassed mixture of dibromoolefin **432** (43 mg, 0.079 mmol), CuI (6.0 mg, 0.031 mmol), $Pd(PPh_3)_4$ (6.5 mg, 0.0056 mmol), *i*Pr_2NH (3 mL) and dry THF (5 mL). The resulting mixture was refluxed for 18 h. Solvent removal and purification by column chromatography (silica gel, hexanes/CH_2Cl_2, 5:1 to 3:1) afforded radialene **433** (52 mg, 65%) as a brown solid. Mp >300 °C (decomp.). R_f = 0.7 (hexanes/CH_2Cl_2, 1:1). UV-vis (THF) λ_{max} (ε) 403 (20600) nm; IR (CH_2Cl_2, cast) 3080, 3053, 3028, 2953, 2924, 2853, 2157, 2139, 1947, 1884, 1801, 1734 cm^{-1}; ^1H NMR (CD_2Cl_2, 500 MHz) δ 7.35–6.96 (m, 42H), 6.76–6.59 (m, 8H); ^{13}C NMR (125 MHz, CD_2Cl_2) δ 153.9, 151.6, 150.6, 145.3, 140.6, 140.1, 139.9, 135.7, 134.7, 133.3, 131.3, 131.0, 130.6, 130.5, 130.3, 129.6, 129.3, 129.0, 128.5, 128.3, 128.1, 127.5, 127.4, 126.9, 126.3, 113.5, 108.8, 102.5, 101.8, 98.1, 97.6,

95.5. MALDI-TOF HRMS (DCTB) calcd. for $C_{80}H_{50}$ 1010.39070 (M^+), found 1010.38941. CV. X-ray.

Compound **434**

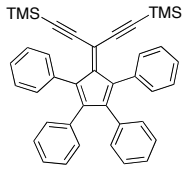

To a degassed mixture of **432** (13 mg, 0.24 mmol), CuI (9 mg, 0.05 mmol), $Pd(PPh_3)_2Cl_2$ (13 mg, 0.018 mmol), iPr_2NH (3 ml) and dry THF (10 mL) was added trimethylsilylacetylene (98 mg, 1.0 mmol, 0.15 mL). The resulting mixture was refluxed for 18 h. Et_2O and H_2O were added, the organic phase separated, washed with saturated NH_4Cl (2 x 20 mL), and dried ($MgSO_4$). Solvent removal and purification by column chromatography (silica gel, hexanes/CH_2Cl_2, 10:1) afforded **434** (69 mg, 50%) as a brown solid. Mp 100 °C (decomp.). R_f = 0.65 (hexanes/CH_2Cl_2, 2:1). IR (CH_2Cl_2, cast) 3081, 3055, 3027, 2957, 2989, 2143 cm^{-1}; ^1H NMR ($CDCl_3$, 500 MHz) δ 7.30–7.28 (m, 4H), 7.25–7.22 (m, 6H), 7.03–6.99 (m, 6H), 6.84–6.81 (m, 4H) 0.03 (s, 18H); ^{13}C NMR (125 MHz, $CDCl_3$) δ 153.3, 145.2, 136.3, 134.9, 133.1, 131.5, 130.1, 127.5, 127.0, 126.9, 126.5, 111.8, 109.9, 102.9, –0.55. EI HRMS calcd. for $C_{40}H_{38}Si_2$ 574.2512 (M^+), found 574.2511.

Compound **502a/b** and **502c**

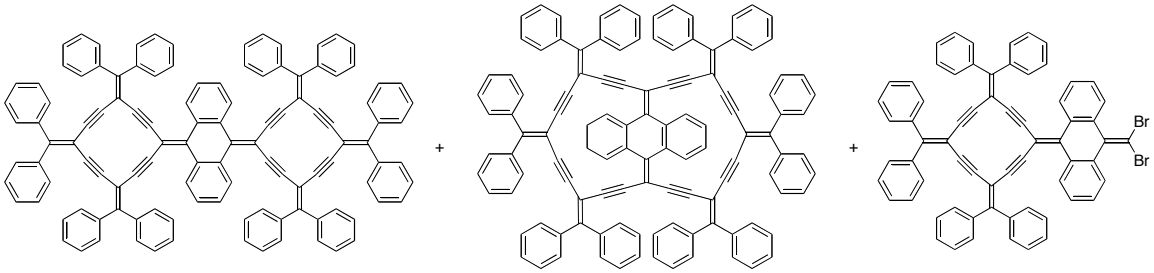

502a/b **502c**

A mixture of **305** (120.0 mg, 0.1390 mmol) and TBAF (0.14 mL, 0.14 mmol, 1M in THF) in wet THF (5 mL) was stirred for 2 h. Et_2O and H_2O were added, the organic phase separated, washed with saturated NH_4Cl (2 x 20 mL), dried ($MgSO_4$) and reduced to 2 mL. The Et_2O solution was added to a degassed mixture of tetrabromide **501** (37 mg, 0.071 mmol), CuI (4.3 mg, 0.022 mmol), $Pd(PPh_3)_4$ (8.7 mg, 0.0075 mmol), *i*Pr_2NH (3 mL) and dry THF (10 mL). The resulting mixture was refluxed for 18 h. Solvent removal and purification by column chromatography (silica gel, hexanes/CH_2Cl_2, 5:1 to 2:1) first afforded compound **502c** as a yellow solid (15 mg, 11%) and second a red solid that subjected to pre-coated silica gel TLC plates (hexanes/CH_2Cl_2, 1:1) for further purification and afforded a mixture of two isomers **502a** and **502b** at (30 mg, 29%) yields as a red solid. The mixture of two isomers was subjected to the HPLC separation (silica gel, hexanes/ethyl acetate, 100:0 to 80:20) and gave two isomers, the first a yellow solid (1 mg) and the second isomers as a red solid (10 mg). (note: some of the mixture did not dissolved and left on the top of HPLC column).

Compound **502c**: Mp 200 °C. R_f = 0.65 (hexanes/CH_2Cl_2 1:1). IR (CH_2Cl_2, cast) 3054, 3031, 2924, 2854, 2160 cm^{-1}; ^1H NMR ($CDCl_3$, 500 MHz,) δ 7.77–7.76 (m, 2H), 7.61–7.59 (m, 2H), 7.42–7.35 (m, 6H), 7.30–7.19 (m, 12H), 7.15–7.06 (m, 12H), 6.75–6.72 (m, 4H); ^{13}C NMR (125 MHz, $CDCl_3$) δ 151.9, 151.5, 141.1, 140.3, 139.9, 139.5, 139.3, 134.5, 134.2, 130.4, 130.1, 130.0, 128.8, 128.7, 128.6, 128.0, 127.93, 127.89, 127.5, 127.3, 126.7, 126.3, 102.63, 102.55, 101.4, 99.2, 96.9, 96.5, 96.4, 89.9. MALDI-TOF HRMS (DCTB) calcd. for $C_{66}H_{38}{}^{79}Br_2$ 988.13348 (M^+), found 988.13376.

Compound **502** yellow isomer (minor): R_f = 0.5 (hexanes/CH_2Cl_2 1:1). UV-vis (THF) λ_{max} (ε) 381 (57200) nm; IR (CH_2Cl_2, cast) 3055, 3030, 2954, 2924, 2854 cm^{-1}. MALDI-TOF HRMS (DCTB) calc. for $C_{116}H_{68}$ 1460.53155 (M^+), found 1460.53079.

Compound **502** red isomer (major): Mp >300 °C (decomp.). R_f = 0.5 (hexanes/CH_2Cl_2, 1:1). UV-vis (THF) λ_{max} (ε) 377 (57100), 513 (16500) nm; IR (CH_2Cl_2, cast) 3053, 3031, 2955, 2918, 2849 cm^{-1}; ^1H NMR ($CDCl_3$, 500 MHz) δ 7.59–7.57 (m, 4H), 7.39–7.04 (m, 60H), 6.50–6.49 (m 4H); ^{13}C NMR (125 MHz, $CDCl_3$) δ 151.6, 151.2, 141.3, 140.5, 139.9, 139.7, 132.9, 130.5, 130.1, 130.0, 128.7, 128.6, 128.5, 128.1, 127.9, 127.8, 127.5, 125.9, 102.8, 102.7, 101.3, 98.8, 97.0, 96.8, 96.7. MALDI-TOF HRMS (DCTB) calcd. for $C_{116}H_{68}$ 1460.53155 (M^+), found 1460.53071. CV.

Compound **503**

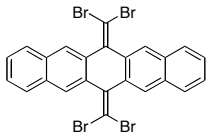

To a mixture of PPh_3 (2 g, 7 mmol) in dry benzene (20 mL), was added CBr_4 (1.2 g, 3.6 mmol) and the resulting mixture was stirred at room temperature for 30 min. Pentacenequinone (0.5 g, 1 mmol) was added in one portion and the resulting mixture was stirred at room temperature for 1 h followed by reflux for 20 h. The crude reaction product was filtered and washed with benzene (40 mL). Solvent removal and purification by column chromatography (silica gel, hexanes/CH_2Cl_2, 19:1) afforded tetrabromide **503** (0.5 g, 50%) as a white solid. Mp 270 °C. R_f = 0.44 (hexanes/CH_2Cl_2, 3:1). IR (CH_2Cl_2, cast) 3056, 2926, 1599, 1583, 1569 cm^{-1}; ^1H NMR ($CDCl_3$, 500 MHz) δ 8.24 (d, J = 1Hz, 4H), 7.84–7.82 (m, 4H), 7.50–7.49 (m, 4H); ^{13}C NMR (125 MHz, $CDCl_3$) δ 139.6, 133.3, 131.8, 128.1, 127.1, 90.5 (one coincident peak not observed); EI HRMS calcd. for $C_{24}H_{12}{}^{79}Br_4$ 615.7673 (M^+), found 615.7687. X ray.

Compound **504a/b** and **A19**

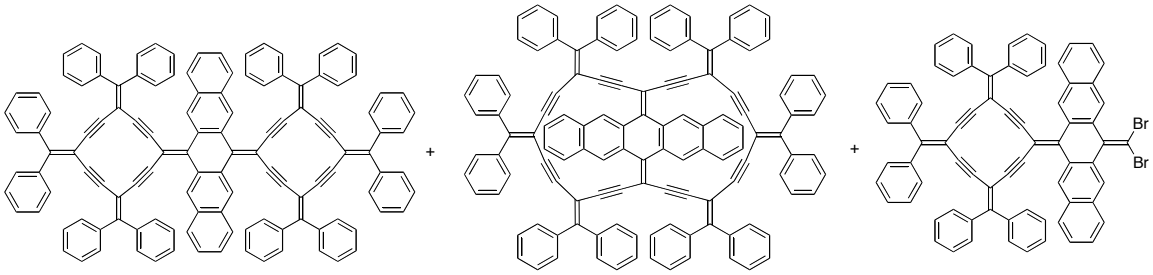

504a/b **A19**

A mixture of **305** (100 mg, 0.116 mmol) and TBAF (0.12 mL, 0.12 mmol, 1M in THF) in wet THF (5 mL) was stirred for 2 h. Et_2O and H_2O were added, the organic phase separated, washed with saturated NH_4Cl (2 x 20 mL), dried ($MgSO_4$) and reduced to 2 mL. The Et_2O solution was added to a degassed mixture of tetrabromide **503** (35 mg, 0.056 mmol), CuI (6.8 mg, 0.035 mmol), $Pd(PPh_3)_4$ (7.2 mg, 0.0062 mmol), *i*Pr_2NH (3 mL) and dry THF (10 mL). The resulting mixture was refluxed for 18 h. Solvent removal and purification by column chromatography (silica gel, hexanes: CH_2Cl_2 5:1 to 2:1) afforded first compound **A19** (5 mg, 4%) as an orange solid and second a red solid that was subjected to separation in pre-coated silica gel TLC plates (hexanes/CH_2Cl_2, 1:1) for further purification. This afforded a mixture of two isomers of **504a** and **504b** (23.6 mg, 26%). The mixture of two isomers was subjected to the HPLC (silica gel, hexanes/ethyl acetate 100:0 to 80:20) and gave two isomers, first an isomer as a yellow solid (minor isomer, 1.5 mg) and second was a red solid (major isomer, 8 mg) (note: some of the mixture did not dissolved and left on the top of column).

Compound **A19**: Mp 220 °C. R_f = 0.65 (hexanes/CH_2Cl_2 1:1). IR (CH_2Cl_2, cast) 3080, 3054, 3030, 2954, 2924, 2853 cm^{-1}; ^1H NMR (CD_2Cl_2, 500 MHz) δ 8.26 (m, 4H), 7.84 (d, J = 8.5 Hz, 2H), 7.49–7.12 (m, 30H), 6.77–6.69 (m, 6H); ^{13}C NMR (125 MHz, CD_2Cl_2) δ 152.4, 152.2, 143.0, 140.2, 140.0, 139.9, 132.6, 132.4, 132.2, 130.35, 130.28, 129.3, 129.2, 129.1, 129.0, 128.4, 128.3, 128.0, 127.9, 127.5, 127.0, 126.5. 102.6, 102.4, 101.7, 98.8, 97.2, 97.1, 90.8. MALDI-TOF HRMS (DCTB) calcd. for $C_{74}H_{42}{}^{79}Br_2$ 1088.16478 (M^+), found 1088.16428. (refer to appendix for more discussion)

Compound **504** yellow isomer (minor): R_f = 0.5 (hexanes/CH_2Cl_2 1:1). UV-vis (THF) λ_{max} (ε) 382 (82700) nm; IR (CH_2Cl_2, cast) 3054, 3031, 2954, 2924, 2854, cm^{-1}. MALDI-TOF HRMS (DCTB) calc. for $C_{124}H_{72}$ 1560.56285 (M^+), found 1560.56237.

Compound **504** red isomer (major): Mp >300 °C (decomp.). R_f = 0.5 (hexanes/CH_2Cl_2 1:1). UV-vis (THF) λ_{max} (ε) 385 (120400) nm; IR (CH_2Cl_2, cast) 3081, 3053, 3030, 2921, 2850 cm^{-1}; ^1H NMR (CD_2Cl_2, 400 MHz) δ 8.38 (d, J = 1.2 Hz, 4H), 7.38–7.14 (m, 60H), 6.96–6.89 (m, 8H); ^{13}C NMR (125 MHz, CD_2Cl_2) δ 152.3, 151.6, 143.1, 140.4, 140.1, 132.5, 131.9, 130.5, 130.4, 130.3, 129.21, 129.2, 129.1, 128.30, 128.26, 128.2, 127.0, 126.5, 102.6, 102.6, 101.4, 98.8, 97.5, 97.4, 96.8. MALDI-TOF HRMS (DCTB) calc. for $C_{124}H_{72}$ 1560.56285 (M^+), found 1560.56261. CV.

Compound **507** and **A20**

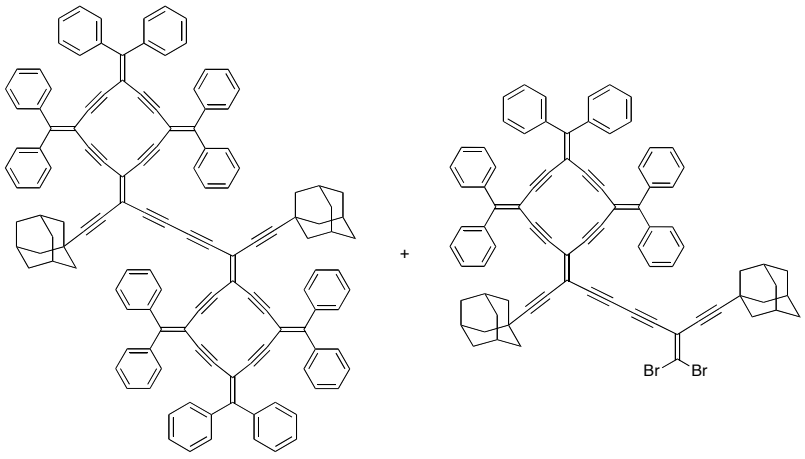

506 **A20**

A mixture of **305** (83 mg, 0.096 mmol) and TBAF (0.2 mL, 0.2 mmol, 1M in THF) in wet THF (2 mL) was stirred for 1 h. Et_2O and H_2O were added, the organic phase separated, washed with saturated NH_4Cl (2 x 20 mL), dried ($MgSO_4$) and reduced to 2 mL. The Et_2O solution was added to a degassed mixture of tetrabromide **505** (33.0 mg, 0.045 mmol), CuI (7.1 mg, 0.037 mmol), $Pd(PPh_3)_4$ (6.2 mg, 0.0053 mmol), *i*Pr_2NH (3 mL) and dry THF (5 mL). The resulting mixture was refluxed for 20 h. Solvent removal and purification by column chromatography (silica gel, hexanes/CH_2Cl_2, 5:1 to 2:1) afforded first **A20** (only trace amount) and second compound **507** (23.4 mg, 29%) as a red solid.

Compound **A20**: MALDI-TOF HRMS (DCTB) calcd. for $C_{82}H_{60}{}^{79}Br_2$ 1202.30563 (M^+), found 1202.30541. (refer to appendix for more discussion)

Compound **507**: Mp >300 °C (decomp.). R_f = 0.4 (hexanes/CH_2Cl_2, 1:1). UV-vis (THF) λ_{max} (ε) 393 (61800) nm; IR (CH_2Cl_2, cast) 2963, 2867, 2214, 1591 cm^{-1}; ^1H NMR (CD_2Cl_2, 400MHz) δ 7.38–7.11 (m, 60H), 1.88 (bs, 6H), 1.64 (bs, 18H), 1.27

(bs, 6H); ^{13}C NMR (125 MHz, CD_2Cl_2) δ 153.9, 153.4, 152.5, 140.4, 140.1, 139.7, 139.5, 130.9, 130.5, 130.4, 130.3, 130.2, 129.7, 129.6, 129.4, 129.2, 128.6, 128.5, 128.4, 128.3, 119.2, 110.4, 110.1, 106.5, 104.7, 102.4, 102.1, 102.0, 97.9, 96.8, 96.7, 96.6, 96.0, 84.5, 82.3, 76.4, 42.3, 36.5, 31.1, 28.3. MALDI-TOF HRMS (DCTB) calc. for $C_{132}H_{90}$ 1674.70370 (M^+), found 1674.70256. CV.

Compound **508** and **A21**

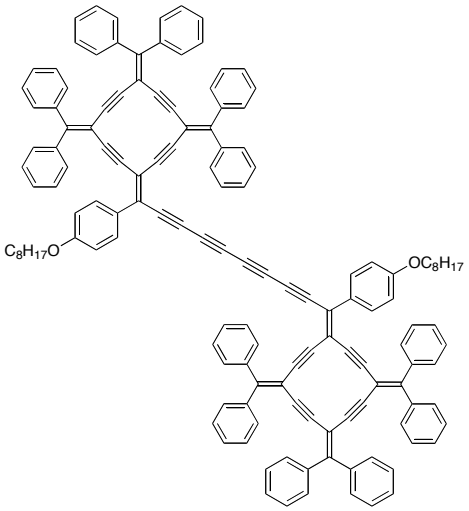

508

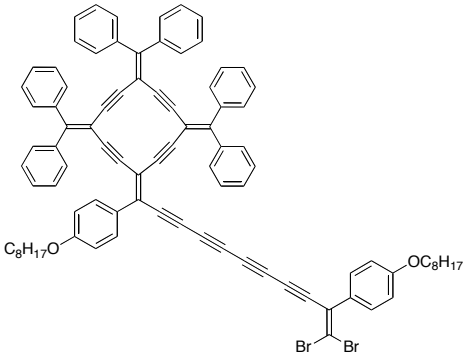

A21

A mixture of **305** (99.0 mg, 0.115 mmol) and TBAF (0.3 mL, 0.3 mmol, 1M in THF) in wet THF (2 mL) was stirred for 1 h. Et_2O and H_2O were added, the organic phase separated, washed with saturated NH_4Cl (2 x 20 mL), dried ($MgSO_4$) and reduced to 2 mL. The Et_2O solution was added to a degassed mixture of tetrabromide compound **506** (50.0 mg, 0.0570 mmol), CuI (5.0 mg, 0.026 mmol), $Pd(PPh_3)_4$ (7.5 mg, 0.0064 mmol), *i*Pr_2NH (3 mL) and dry THF (5 mL). The resulting mixture was refluxed for 20 h. Solvent removal and purification by column chromatography (silica gel, hexanes/CH_2Cl_2 5:1 to 2:1) afforded first product compound **A21** (1 mg, 2.4 %) as an orange solid and second red solid **508** (16.9 mg, 15%).

Compound **A21**: R_f = 0.4 (hexanes/CH_2Cl_2 1:1). IR (CH_2Cl_2, cast) 3054, 2923, 2853, 2169, 2099, 1734, 1602 cm^{-1}; ^1H NMR (400 MHz, $CDCl_3$) δ 7.50 (d, J = 8.8 Hz 2H), 7.42–7.07 (m, 30H), 6.88 (d, J = 8.8 Hz, 2H), 6.53 (d, J = 8.8 Hz, 2H), 3.94–3.90 (m, 4H), 1.78–1.74 (m, 4H), 1.45–1.23 (m, 20H), 0.87–0.86 (m, 6H);

MALDI-TOF HRMS (DCTB) calcd. for $C_{90}H_{72}O_2{}^{79}Br_2$ 1342.38936 (M^+), found 1342.38769. (refer to appendix for more discussion)

Compound **508**: Mp >300 °C. R_f = 0.3 (hexanes: CH_2Cl_2 1:1). UV-vis (THF) λ_{max} (ε) 388 (131200) nm; IR (CH_2Cl_2, cast) 2954, 2925, 2853 cm^{-1}; ^1H NMR ($CDCl_3$, 500 MHz) δ 7.54 (d, J = 8 Hz, 4H), 7.45–7.03 (m, 60H), 6.55 (d, J = 8.5 Hz, 4H), 3.97–3.89 (m, 2H), 3.62–3.57 (m, 4), 1.78–1.58 (m, 2H), 1.36–0.84 (m, 26H); ^{13}C NMR (125MHz, CD_2Cl_2) δ 160.6, 153.7, 153.1, 152.5, 140.6, 140.1, 140.0, 139.9, 139.6, 131.3, 130.7, 130.6, 130.4, 130.30, 130.25, 130.0, 129.7, 129.6, 129.4, 129.2, 128.6, 128.5, 128.4, 127.3, 127.2, 114.6, 111.7, 106.3, 102.4, 102.4, 102.2, 102.0, 97.5, 97.4, 97.0, 96.4, 96.1, 84.9, 79.3, 72.4, 70.9, 68.6, 67.0, 32.3, 32.2, 29.7, 29.6, 29.5, 26.4, 23.1,14.2. MALDI-TOF HRMS (DCTB) calcd. for $C_{140}H_{102}O_2$ 1814.78743 (M^+), found 1814.78610.

Compound **509**

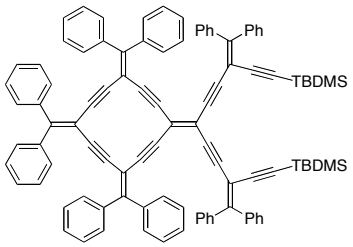

A mixture of radialene **411** (35 mg, 0.034 mmol) and TBAF (0.2 mL, 0.3 mmol, 1M in THF) in wet THF (2 mL) was stirred for 1 h. Et_2O and H_2O were added, the organic phase separated, washed with saturated NH_4Cl (2 x 20 mL), dried ($MgSO_4$) and reduced to 2 mL. The Et_2O solution was added to a degassed mixture of **300** (32 mg, 0.07 mmol), CuI (2.0 mg, 0.010 mmol), $Pd(PPh_3)_4$ (4.3 mg, 0.0037 mmol), *i*Pr_2NH (3 mL) and dry THF (5 mL). The resulting mixture was refluxed for 18 h. Solvent removal and purification by column chromatography (silica gel, hexanes/CH_2Cl_2 5:1to 2:1) afforded radialene **509** (36 mg, 78%) as an orange solid. R_f = 0.7 (hexanes/CH_2Cl_2, 1:1). IR (CH_2Cl_2, cast) 3055, 2955, 2924, 2873, 2854, 2150 cm^{-1}. MALDI-TOF HRMS (DCTB) calcd. for $C_{100}H_{80}Si_2$ (M^+) 1336.57931, found 1336.57893.

Compound **315a** (stepwise route)

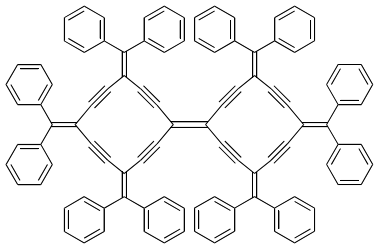

A mixture of radialene **509** (25 mg, 0.018 mmol) and TBAF (0.1 mL, 0.1 mmol, 1M in THF) in wet THF (2 mL) was stirred for 1 h. Et_2O and H_2O were added, the organic phase separated, washed with saturated NH_4Cl (2 x 20 mL), dried ($MgSO_4$) and reduced to 2 mL. The Et_2O solution was added to a degassed mixture of dibromoolefin **308** (6.1 mg, 0.018 mmol), CuI (1.0 mg, 0.0052 mmol), $Pd(PPh_3)_4$ (2.0 mg, 0.0017 mmol), *i*Pr_2NH (3 mL) and dry THF (5 mL). The resulting mixture was refluxed for 18 h. Solvent removal and purification by column chromatography (silica gel, hexanes/CH_2Cl_2, 5:1 to 2:1) afforded radialene **315a** (11.1 mg, 50%) as a red solid. Mp >300 °C (decomp.). R_f = 0.45 (hexanes/CH_2Cl_2, 1:1). UV-vis (THF) λ_{max} 389, 509 nm; IR (CH_2Cl_2, cast) 3081, 3052, 3024, 2953, 2924, 2853, 2171, 2155, 1949, 1855, 1801, 1728 cm^{-1}; ^1H NMR ($CDCl_3$, 500 MHz) δ 7.27–6.92 (m, 60H); ^{13}C NMR (125 Hz, CD_2Cl_2) δ 152.5, 152.1, 140.2, 140.1, 139.3, 130.7, 130.4, 129.6, 129.2, 129.1, 128.3, 128.2, 128.1, 111.9, 104.6, 102.1, 97.1, 96.7. MALDI-TOF HRMS (DCTB) calcd. for $C_{102}H_{60}$ 1284.46895 (M^+), found 1284.46796.

Compound **510** and **511**

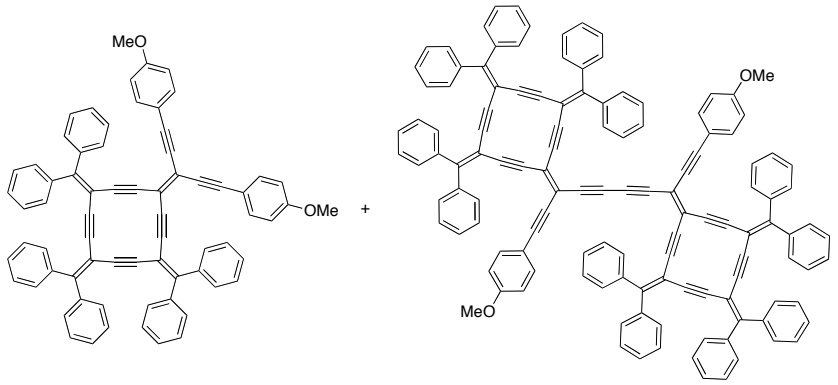

510 **511**

A mixture of compound **411** (14 mg, 0.014 mmol) and TBAF (0.1 mL, 0.1 mmol, 1M in THF) in wet THF (1 mL) was stirred for 1 h. CH_2Cl_2 and H_2O were added, the organic phase separated, washed with saturated NH_4Cl (2 x 20 mL), dried ($MgSO_4$) and reduced to 1 mL. The CH_2Cl_2 solution was added to a degassed mixture of 4-iodoanisole (27.0 mg, 0.116 mmol), CuI (1.4 mg, 0.073 mmol), $Pd(PPh_3)_4$ (1.0 mg, 0.0086 mmol), iPr$_2$NH (3 mL) and dry THF (2 mL). The resulting mixture was stirred for 18 h at room temperature. Solvent removal and purification by column chromatography (silica gel, hexanes/CH_2Cl_2, 4:1) afforded first radialene **510** (8.9 mg, 70%) as an orange solid and second radialene oligomer **511** (1.7 mg, 15%) as a red solid.

Compound **510**: Mp >300 °C (decomp.). R_f = 0.3 (hexanes/CH_2Cl_2, 1:1). UV-vis (THF) λ_{max} 393 (65200) nm; IR (CH_2Cl_2, cast) 3081, 3053, 2961, 2927, 2854, 2838, 2210, 2189, 1604 cm^{-1}; ^{1}H NMR (CD_2Cl_2, 400 MHz) δ 7.46–7.43 (m, 4H), 7.28–7.07 (m, 30H), 6.81–6.79 (d, 4H), 3.84 (s, 6H); ^{13}C NMR (100 MHz, CD_2Cl_2) δ 160.9, 152.7, 152.5, 140.1, 140.0, 134.0, 130.8, 130.4, 130.3, 129.4, 129.3,

129.2, 128.33, 128.25, 115.7, 114.5, 114.3, 112.0, 104.1, 102.5, 102.3, 99.1, 97.1, 96.9, 96.8, 86.3, 55.8. MALDI-TOF HRMS (DCTB) calc. for $C_{70}H_{44}O_2$ 916.33358 (M^+), found 916.33140.

Compound **511**: IR (CH_2Cl_2, cast) 3053, 2955, 2925, 2854, 2200, 2175, 2153, 603, 1511 cm^{-1}; UV-vis (THF) λ_{max} 399 (65100) nm. MALDI-TOF HRMS (DCTB) calc. for $C_{126}H_{74}O_2$ 1618.56833 (M^+), found 1618.56789.

Compound **514a** and **514b**

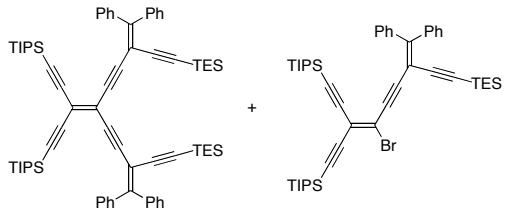

514a **514b**

A mixture of **512** (150 mg, 0.361 mmol), K_2CO_3 (10 mg, 0.07 mmol) in wet THF (1 mL) and MeOH (1 mL) was stirred for 2 h. Et_2O and H_2O were added, the organic phase separated, washed with saturated NH_4Cl (2 x 20 mL), dried ($MgSO_4$) and reduced to 2 mL. The Et_2O solution was added to a degassed mixture of dibromoolefin **410** (98 mg, 0.18 mmol), CuI (21 mg, 0.11 mmol), $Pd(PPh_3)_4$ (20.8 mg, 0.0179 mmol), *i*Pr_2NH (3 mL) and dry THF (5 mL). The resulting mixture was refluxed for 18 h. Solvent removal and purification by column chromatography (silica gel, hexanes/CH_2Cl_2, 10:1 to 5:1) afforded **514b** (51 mg, 35%) as a yellow oil (solidified when stored at 4 °C) and then **514a** (95 mg, 50%) as a yellow oil (solidified when stored at 4 °C).

Compound **514a**: R_f = 0.3 (hexanes/CH_2Cl_2 5:1). IR (CH_2Cl_2, cast) 3082, 3056, 2956, 2890, 2866, 2182, 2143 cm^{-1}; ^1H NMR (300 MHz, $CDCl_3$) δ 7.39–7.35 (m, 8H), 7.30–7.28 (m, 6H), 7.25–7.23 (m, 6H), 1.09–105 (m, 42H), 0.87 (t, *J* = 7.8 Hz, 18H), 0.50 (q, *J* = 7.8 Hz, 12H); ^{13}C NMR (125 Hz, $CDCl_3$) δ 158.0, 140.6, 139.6, 130.33, 130.29, 128.7, 128.4, 127.7, 127.6, 118.1, 116.5, 103.7, 103.6, 101.79, 101.77, 97.3, 95.6, 88.3, 18.6, 11.2, 7.3, 4.2. MALDI-TOF HRMS (DCTB) calcd. for $C_{72}H_{92}Si_4$ 1068.62706 (M^+), found 1068.62743.

Compound **514b**: R_f = 0.45 (hexanes/CH_2Cl_2 5:1). IR (CH_2Cl_2, cast) 3056, 2956, 2944, 2890, 2860, 2179, 2143 cm^{-1}; ^1H NMR (300 MHz, $CDCl_3$) δ 7.40–7.37 (m, 4H), 7.30–7.28 (m, 6H), 1.09–1.07 (m, 21H), 1.07–1.05 (m, 21H), 0.87 (t, J = 8.4 Hz, 9H), 0.49 (q, J = 8.4 Hz, 6H); ^{13}C NMR (125 Hz, $CDCl_3$) δ 159.4, 140.1, 139.5, 130.4, 130.3, 129.0, 128.7, 127.8, 127.6, 115.1, 114.1, 103.5, 103.1, 102.8, 102.5, 102.0, 101.2, 98.6, 96.2, 88.9, 18.6, 18.5, 11.19, 11.17, 7.3, 4.1. MALDI-TOF HRMS (DCTB) calcd. for $C_{48}H_{67}Si_3{}^{79}Br$ 806.37285 (M^+), found 806.37265.

Compound **515**

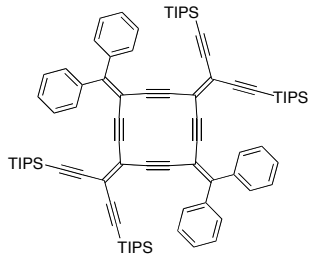

A mixture of **514a** (45 mg, 0.042 mmol), K_2CO_3 (8.1 mg, 0.21 mmol) in wet THF (1 mL) and MeOH (2 mL) was stirred for 2 h. Et_2O and H_2O were added, the organic phase separated, washed with saturated NH_4Cl (2 x 20 mL), dried ($MgSO_4$) and reduced to 2 mL. The Et_2O solution was added to a degassed mixture of dibromoolefin **410** (23 mg, 0.042 mmol), CuI (6.0 mg, 0.031 mmol), $Pd(PPh_3)_4$ (4.4 mg, 0.0038 mmol), *i*Pr_2NH (3 mL) and dry THF (5 mL). The resulting mixture was refluxed for 18 h. Solvent removal and purification by column chromatography (silica gel, hexanes/CH_2Cl_2, 5:1 to 2:1) afforded **515** (40 mg, 78 %) as a yellow solid. Mp 235 °C. R_f = 0.6 (hexanes/CH_2Cl_2 1:1). UV-vis (THF) λ_{max} (ε) 399 (25500) nm; IR (CH_2Cl_2, cast) 2941, 2924, 2890, 2863, 2165, 2134 cm^{-1}; ^1H NMR ($CDCl_3$, 400 MHz,) δ 7.38–7.36 (m, 8H), 7.26–7.23 (m, 12H), 0.95–0.93 (m, 84H); ^{13}C NMR (125 Hz, $CDCl_3$) δ 153.0, 139.9, 130.7, 129.1, 127.7, 116.9, 111.5, 104.1, 103.9, 102.3, 101.8, 95.8, 18.6, 11.2. MALDI-TOF HRMS (DCTB) calc. for $C_{84}H_{104}Si_4$ 1224.72096 (M^+), found 1224.72033. CV. X-ray.

Note: also a series of side products are collected from the crude reaction product that is as follows (refer to appendix for more discussion):

Compound **A22**: MALDI-TOF HRMS (DCTB) calcd. for $C_{75}H_{84}Si_3$ 1068.58753 (M^+), found 1068.58705.

Compound **A23**: MALDI-TOF HRMS (DCTB) calcd. for $C_{99}H_{125}BrSi_5$ 1532.78055 (M^+), found 1532.78108.

Compound **A24**: MALDI-TOF HRMS (DCTB) calcd. for $C_{90}H_{105}BrSi_4$ 1376.64712 (M^+), found 1376.64707.

Compound **A25**: MALDI-TOF HRMS (DCTB) calcd. for $C_{135}H_{146}Si_5$ 1907.02654 (M^+), found 1907.02740.

Compound **A26**: MALDI-TOF HRMS (DCTB) calcd. for $C_{159}H_{188}Si_7$ 2293.30904 (M^+), found 2293.31081.

Compound 517

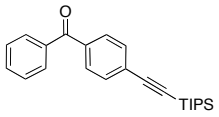

A mixture of bromoketone **516** (1 g, 4 mmol), CuI (73.0 mg, 383 mmol), $Pd(PPh_3)_2Cl_2$ (135 mg, 0.192 mmol) and *i*Pr_2NH (5 mL) in dry THF (10 mL) was degassed for 30 min. Triisopropylsilylacetylene (1.3 g, 6.7 mmol, 1.5 mL) was added in one portion and the resulting mixture refluxed for 4 h. Solvent removal and purification by column chromatography (silica gel, hexanes/CH_2Cl_2, 7:1 to 2:1) afforded ketone **517** (1.2 g, 86%) as a colorless oil. R_f = 0.77 (hexanes/ethyl acetate, 10:1). IR (CH_2Cl_2, cast) 3063, 2943, 2891, 2865, 2156, 1662, 1601, 1578 cm^{-1}; ^1H NMR (300 MHz, $CDCl_3$) δ 7.46-7.72 (m, 4H), 7.57-7.54 (m, 3H), 7.48–7.45 (m, 2H), 1.14–1.13 (m, 21H); ^{13}C NMR (125 MHz, $CDCl_3$) δ 195.8, 137.4, 136.8, 132.5, 131.8, 129.93, 129.86, 128.3, 127.7, 106.1, 94.4 18.6, 11.3. EI HRMS calcd. for $C_{24}H_{30}OSi$ 362.2066 (M^+), found 362.2061.

Compound **518**

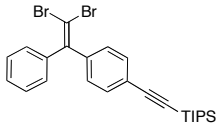

To a mixture of PPh_3 (4.9 g, 18 mmol) in dry benzene (30 mL), was added CBr_4 (2.8 g, 8.4 mmol) and the resulting mixture was stirred at room temperature for 30 min. Ketone **517** (1.2 g, 3.3 mmol) was added in one portion and the resulting mixture was stirred at room temperature for 12 h. The crude reaction product was filtered and washed with benzene (2 x 40 mL). Solvent removal and purification by column chromatography (silica gel, hexanes/CH_2Cl_2, 10:1) afforded dibromoolefin **518** (1 g, 64%) as a white crystalline solid. Mp 46 °C. R_f = 0.4 (hexanes). IR (CH_2Cl_2, cast) 3059, 3032, 2942, 2890, 2865, 2156, 1503 cm^{-1}; ^1H NMR (300 MHz, $CDCl_3$) δ 7.46–7.44 (m, 2H), 7.36–7.23 (m, 7H), 1.31 (s, 21H); ^{13}C NMR (125 MHz, $CDCl_3$) δ 147.2, 141.2, 141.0, 132.0, 128.79, 128.77, 128.4, 128.1, 123.2, 106.6, 91.7, 90.6, 18.7, 11.3. EI HRMS calcd. for $C_{25}H_{30}Si^{79}Br_2$ 516.0483 (M^+), found 516.0487.

Compound **519**

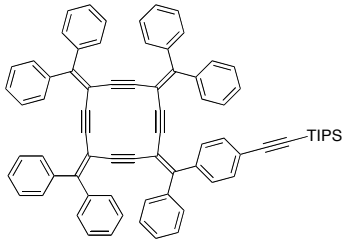

A mixture of **305** (70.0 mg, 0.0812 mmol) and TBAF (0.3 mL, 0.3 mmol, 1M in THF) in wet THF (2 mL) was stirred for 1 h. Et_2O and H_2O were added, the organic phase separated, washed with saturated NH_4Cl (2 x 20 mL), dried ($MgSO_4$) and reduced to 2 mL. The Et_2O solution was added to a degassed mixture of dibromoolefin **518** (42 mg, 0.081 mmol), CuI (4.8 mg, 0.025 mmol), $Pd(PPh_3)_4$ (9.2 mg, 0.0079 mmol), *i*Pr_2NH (3 mL) and dry THF (5 mL). The resulting mixture was refluxed for 18 h. Solvent removal and purification by column chromatography (silica gel, hexanes/CH_2Cl_2, 5:1) afforded **519** (54 mg, 68%) as a yellow solid. Mp >300 °C (decomp.). R_f = 0.6 (hexanes/CH_2Cl_2, 1:1). UV-vis (THF) λ_{max} 381 (70300) nm; IR (CH_2Cl_2, cast) 3056, 2924, 2865, 2153 cm^{-1}; ^1H NMR ($CDCl_3$, 500 MHz,) δ 7.35–7.28 (m, 24H), 7.19–7.16 (m, 15H), 1.26–1.24 (m, 21H); ^{13}C NMR (125 MHz, $CDCl_3$) δ 151.1, 151.0, 149.8, 139.85, 139.80, 139.75, 139.69, 139.64, 139.2, 131.5, 129.96, 129.93, 129.91, 129.8, 128.6, 128.5, 127.9, 127.8, 123.4, 107.3, 103.1, 102.6, 102.5, 97.7, 97.4, 97.2, 97.0, 96.9, 96.84, 96.77, 96.7, 91.7, 18.7, 11.4. MALDI-TOF HRMS (DCTB) calcd. for $C_{75}H_{60}Si$ 988.44588 (M^+), found 988.44611. CV.

Compound **520**

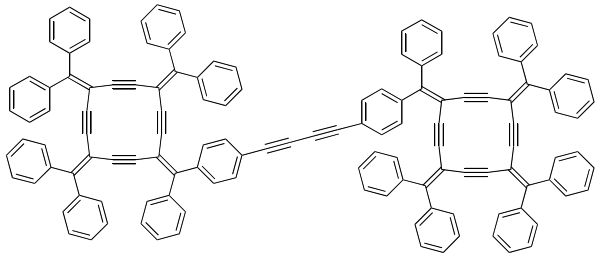

A mixture of compound **519** (10.0 mg, 0.0101 mmol) and TBAF (0.5 mL, 0.5 mmol, 1M in THF) in wet THF (2 mL) was stirred for 1 h. CH_2Cl_2 and H_2O were added, the organic phase separated, washed with saturated NH_4Cl (2 x 20 mL), dried ($MgSO_4$) and reduced to 0.5 mL. The CH_2Cl_2 solution was added to a mixture of $Pd(PPh_3)_2Cl_2$ (1 mg, 0.001 mmol), CuI (0.5 mg, 0.002 mmol), *i*Pr_2NH (1 mL) and dry THF (2 mL). The resulting mixture was refluxed for 4h. Solvent taken and the crdue reaction product re-dissolved in mixture of (hexanes/CH_2Cl_2, 1:1) and filtered through a fritted funnel (a 10–20 microns), and washed with hexanes (~ 250 mL) on the frit, and then allowed to air dry that afforded radialene oligomer **520** (7 mg, 85%) as a yellow solid. Mp >300 °C (decomp.). IR (CH_2Cl_2, cast) 3055, 3029, 2959, 2924, 2853 cm^{-1}; ^1H NMR (CD_2Cl_2, 500 MHz) δ 7.70 (bs, 8H), 7.56–7.54 (m, 8H), 7.25–7.23 (m, 42H), 7.16–7.15 (m, 20H). MALDI-TOF HRMS (DCTB) calcd. for $C_{132}H_{78}$ 1662.60980 (M^+), found 1662.61079.

Compound **522** and **523**

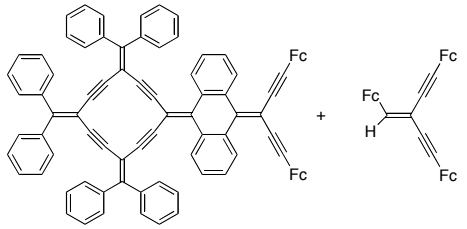

522 **523**

Compound **521** (30.0 mg, 0.142 mmol) was added to a degassed mixture of compound **502c** (14.5 mg, 0.0146 mmol), CuI (0.8 mg, 0.004 mmol), $Pd(PPh_3)_2Cl_2$ (1.5 mg, 0.0021 mmol) iPr_2NH (2 mL) and dry THF (3 mL). The resulting mixture refluxed for 18 h. Solvent removal and purification by column chromatography (silica gel, hexanes/CH_2Cl_2, 3:1) afforded first compound **523** (1 mg, 3.5 %) as a red solid and second compound **522** (17.9 mg, 98%) as a red-brown solid.

Compound **523**: IR (CH_2Cl_2, cast) 3095, 2923, 2852, 2200, 1728 cm^{-1}; ^1H NMR ($CDCl_3$, 500 MHz) δ 6.82 (s, 1H), 4.90–4.89 (m, 2H), 4.56–4.55 (m, 2H), 4.48–4.47 (m, 2H), 4.39–4.38 (m, 2H), 4.30–4.28 (m, 5H), 4.27–4.25 (m, 2H), 4.25–4.22 (m, 5H), 4.22–4.20 (m, 5H), 4.20–4.19 (m, 2H). MALDI-TOF HRMS (DCTB) calcd. for $C_{36}H_{28}Fe_3$ 628.02338 (M^+), found 628.02321.

Compound **522**: Mp 190 °C. R_f = 0.7 (hexanes/CH_2Cl_2, 1:1). UV-vis (THF) λ_{max} 392 (30000) nm; IR (CH_2Cl_2, cast) 3083, 3054, 3030, 2956, 2924, 2853, 2190, 1729cm^{-1}; ^1H NMR (CD_2Cl_2, 500 MHz,) δ 8.29 (d, J = 8 Hz, 2H), 7.74 (d, J = 8 Hz, 2H), 7.45–7.11 (m, 32H), 6.81 (t, J = 8 Hz, 2H), 4.49 (s, 4H), 4.28–4.25 (m, 14H); ^{13}C NMR (125 MHz, CD_2Cl_2) δ 152.7, 152.1, 143.0, 142.3, 140.7, 140.2, 140.0,

134.6, 133.8, 130.7, 130.32, 130.29, 129.4, 129.2, 129.1, 128.6, 128.4, 128.3, 127.9, 127.3, 126.4, 102.7, 102.6, 101.1, 99.1, 97.1, 97.0, 96.9, 94.1, 85.8, 71.8, 70.4, 69.7, 65.3. MALDI-TOF HRMS (DCTB) calcd. for $C_{90}H_{56}Fe_2$ 1248.30754 (M^+), found 1248.30646.

Compound **524**

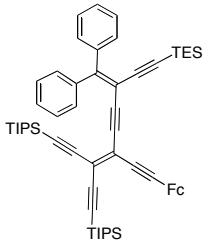

Compound **521** (32 mg, 0.15 mmol) was added to a degassed mixture of compound **514b** (73 mg, 0.090 mmol), CuI (1.8 mg, 0.0094 mmol), $Pd(PPh_3)_2Cl_2$ (3.2 mg, 0.0045 mmol), *i*Pr_2NH (2 mL) and dry THF (3 mL). The resulting mixture was refluxed for 12h. Solvent removal and purification by column chromatography (silica gel, hexanes/CH_2Cl_2, 12:1) afforded **525** (68 mg, 80%) as a red solid (solidified under refrigeration at 4 °C). Mp 25 °C. R_f = 0.45 (hexanes/CH_2Cl_2, 5:1). UV-vis (THF) λ_{max} (ε) 353 (27600), 510 (3400) nm IR (CH_2Cl_2, cast) 3084, 3056, 2956, 2944, 2890, 2866, 2203, 2188, 2141 cm^{-1}; ^1H NMR ($CDCl_3$, 400 MHz) δ 7.48–7.46 (m, 2H), 7.38–7.36 (m, 2H), 7.29–7.27 (m, 6H), 4.43 (s, 2H), 4.26 (s, 2H), 4.19 (s, 5H), 1.13–1.11 (m, 21H), 1.08–1.05 (m, 21H), 0.86 (t, *J* = 8 Hz, 9H), 0.49 (q, *J* = 8 Hz, 6H); ^{13}C NMR (125 Hz, $CDCl_3$) δ 157.7, 140.6, 139.7, 130.35, 130.33, 128.7, 128.3, 127.7, 127.6, 118.3, 115.0, 103.4, 104.1, 103.8, 101.9, 101.01, 100.95, 99.5, 96.4, 95.7, 89.0, 83.9, 71.8, 70.2, 69.5, 64.2, 18.7, 18.6, 11.3, 11.2, 7.3, 4.2. MALDI-TOF HRMS (DCTB) calcd. for $C_{60}H_{76}Si_3Fe$ 936.45988 (M^+), found 936.46002.

Compound **526**

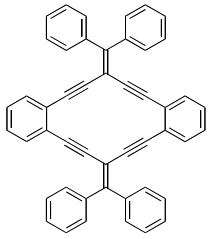

A mixture of compound **309** (107 mg, 0.288 mmol) and K_2CO_3 (8 mg, 0.06 mmol) in THF (1 mL) and MeOH (1 mL) was stirred for 1 h. Et_2O and H_2O were added, the organic phase separated, washed with saturated NH_4Cl (2 x 20 mL), dried ($MgSO_4$) and reduced to 2 mL. The degassed Et_2O solution was added to a degassed mixture of 1,2 diiodobenzene (95.0 mg, 0.288 mmol), CuI (15 mg, 0.078 mmol), $Pd(PPh_3)_4$ (17 mg, 0.015 mmol), iPr$_2$NH (3 mL) and dry THF (5 mL). The resulting mixture was refluxed for 18 h. Solvent removal and purification by column chromatography (silica gel, hexanes/CH_2Cl_2, 7:1 to 3:1) after re-crystallization from hexanes/CH_2Cl_2 (1:1) afforded **526** (27 mg, 31%) as a pale yellow solid. Mp >300 °C (decomp.). R_f = 0.43 (hexanes/CH_2Cl_2, 1:1). UV-vis (THF) λ_{max} 413 nm; IR (CH_2Cl_2, cast) 3078, 3050, 3021, 2923, 2851, 2193, 1960, 1733, 1617, 1591 cm^{-1}; ^{1}H NMR (500 MHz, CD2Cl$_2$) δ 7.59–7.57 (m, 8H), 7.45–7.43 (m, 12H), 7.23–7.21 (m, 4H), 7.08–7.06 (m, 4H); ^{13}C NMR (125 MHz, CD_2Cl_2) δ 157.6, 140.7, 132.3, 131.1, 129.3, 128.6, 128.1, 125.4, 102.2, 92.9, 90.7. EI HRMS calcd. for $C_{48}H_{28}$ (M^+) 604.2191, found 604.2185. MALDI-TOF HRMS (DCTB) for $C_{48}H_{28}$ 604.2186 (M^+), found 604.2185.

Compound **528**

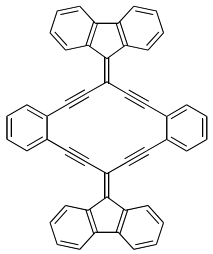

Compound **532** (64 mg, 0.15 mmol) was dissolved in Et_2O (8 mL) and the solution deoxygenated. The degassed Et_2O solution was added to a degassed mixture of **407** (50.0 mg, 0.140 mmol), CuI (9.0 mg, 0.047 mmol), $Pd(PPh_3)_4$ (9.0 mg, 0.0077 mmol), *i*Pr_2NH (3 mL) and dry THF (5 mL). The resulting mixture was refluxed for 20 h. The reaction crude was cooled and washed with saturated NH_4Cl (2 X 20 mL), H_2O (40 mL) and extracted with CH_2Cl_2. After removing the solvent, a solution of hexanes/CH_2Cl_2 (50 mL, 1:1) was added resulting in dispersed red solid. The solid was filtered on a fritted funnel (a 10–20 microns), the solid washed with hexanes (~500 mL) on the frit, and then allowed to air dry. Compound **528** (81 mg, 90%) as a highly insoluble red solid. Mp >300 °C (decomp.). R_f = 0.4 (hexanes/CH_2Cl_2, 1:1). UV-vis (THF) λ_{max} 345, 446, and 472 nm; IR (CH_2Cl_2, cast) 3055, 2960, 2925, 2856, 1727 cm^{-1}; ^1H NMR (500 MHz, $C_2D_2Cl_4$) δ 8.85–8.33 (m, 4H), 7.80–7.79 (m, 4H), 7.75–7.74 (m, 4H), 7.56–7.54 (m, 4H), 7.47–7.45 (m, 4H); ^{13}C NMR (125 MHz, $C_2D_2Cl_4$, 65 °C) δ 146.08, 140.3, 137.4, 131.8, 129.8, 128.9, 127.5, 125.6, 125.5, 119.7, 101.1, 96.1, 93.2. MALDI-TOF HRMS (DCTB) calcd. for $C_{48}H_{24}$ 600.18725 (M^+), found 600.18698.

Compound **532**

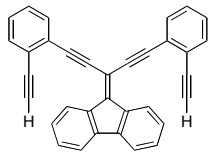

A mixture of compound **530** (150.0 mg, 0.4230 mmol) and K_2CO_3 (13 mg, 0.090 mmol) in THF (2 mL), CH_3OH (2 mL) was stirred for 1 h. Et_2O and H_2O were added, the organic phase separated, washed with saturated NH_4Cl (2 x 20 mL), dried ($MgSO_4$) and reduced to 2 mL. The degassed Et_2O solution was added to a degassed mixture of **407** (71 mg, 0.21 mmol), CuI (12 mg, 0.063 mmol), $Pd(PPh_3)_4$ (24 mg, 0.020 mmol), *i*Pr_2NH (3 mL) and dry THF (5 mL). The resulting mixture was refluxed for 20 h. Solvent removal and purification by column chromatography (silica gel, hexanes/CH_2Cl_2, 5:1) afforded **531** as an orange liquid. To a solution of **531** in THF (2 mL) was added TBAF (0.2 mL, 0.2 mmol, 1M in THF) and the mixture stirred at rt for 30 min. Et_2O and H_2O were added, the organic phase separated, washed with saturated NH_4Cl (2 x 20 mL), and dried ($MgSO_4$). Solvent removal and column chromatography (silica gel, hexanes/ CH_2Cl_2, 4:1) gave **532** (68 mg, 75%) as a yellow solid. Mp >300 °C (decomp.). R_f = 0.6 (hexanes/CH_2Cl_2, 1:1). UV-vis (THF) λ_{max} 396, 414 nm; IR (CH_2Cl_2, cast) 3289, 3058, 2925, 2181, 2108, 1918, 1718, 1601, 1580, 1560 cm^{-1}; ^1H NMR (400 MHz, CD_2Cl_2) δ 8.34–8.32 (d, 2H), 7.03–7.00 (m, 4H), 6.96–6.94 (m, 2H), 6.79–7.70 (m, 6H), 6.67–6.63 (m, 2H), 2.78 (s, 2H); ^{13}C NMR (125 MHz, CD_2Cl_2) δ 145.8, 140.7, 137.6, 133.4, 132.9, 130.3, 129.4, 129.3, 127.8, 126.4, 126.1,

124.8, 120.9, 110.9, 97.1, 92.6, 82.5, 82.1. MALDI-TOF HRMS (DCTB) calcd. for $C_{34}H_{18}$ 426.1403 (M^+), found 426.1403.

Compound 601

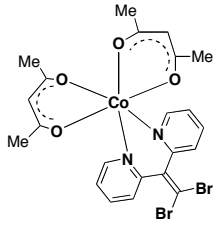

A mixture of **600** (59 mg, 0.17 mmol), $Co(acac)_2(H_2O)_2$ (400 mg, 0.130 mmol) in dry benzene (5 mL) and $CHCl_3$ (5 mL) was stirred and heated for 5 min. The mixture color changed from purple to red. The crude reaction product was filtered and an orange solid was collected and washed with cold benzene (30 mL). This afforded **601** as an organe soild (69 mg, 85%). ES LRMS calc. for $C_{22}H_{22}{}^{79}Br_2N_2O_4Co$ 596.9 (M^+), found 596.9. IR (CH_2Cl_2, cast) 3145, 3098, 3073, 3055, 2991, 2963, 2916, 1655, 1570, 1507 cm^{-1}. X-ray. (refer to Chapter **6** for discussion).

Compound **602**

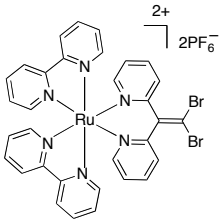

A mixture of *cis*-Ru(bpy)$_2$Cl$_2$ (31 mg, 0.059 mmol), MeOH/H$_2$O (5 mL, 1:1) and dibromoolefin **600** (30.0 mg, 0.0882 mmol) degassed for 15 min and the mixture refluxed for 5h. After cooling the mixture treated with a saturated aqueous solution of NH_4PF_6 (3 mL) that caused an orange solid to precipitate. The mixture filtered and the orange solid washed with H_2O (30 mL) and Et_2O (20 mL) and air-dried that afforded **602** as an orange solid (23 mg, 43%). ES LRMS calc. for $C_{32}H_{24}Br_2N_6Ru$ (M^{2+}) 376, found 377; calc. for $C_{32}H_{24}{}^{79}Br_2N_6F_6PRu$ ($[MPF_6]^+$) 898.9, found 898.9. (refer to Chapter **6** for discussion).

Compound **603**

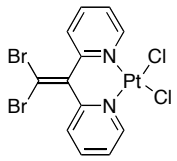

Complex K_2PtCl_4 (122 mg, 0.294 mmol) was stirred in H_2O (3 mL) for 30 min. Dibromoolefin **600** (100.0 mg, 0.2940 mmol) was dissolved in 3 mL acetone and was added in one portion to the aqueous solution. The resulting mixture was refluxed for 18 h. After cooling the reaction to room temperature, the crude reaction product was filtered and washed with H_2O (2 x 20 mL), Et_2O (3 x 20 mL) and CH_2Cl_2 (3 x 20 mL) to give compound **603** (151 mg, 85%) as a creamy solid. Mp < 200 °C (decomp.). IR (solid) 3108, 3077, 3066. 3041, 1644 cm^{-1}. ES HRMS calcd. for $C_{12}H_{12}N_3Cl_2{}^{79}Br_2Pt$ ($[M + NH_4]^+$) 620.84174, found 620.84220. Anal. calc. for $C_{12}H_8N_2Br_2Cl_2Pt$: C, 23.79, H,1.33, N, 4.62, found C, 23.90, H, 1.35, N, 4.43. (refer to Chapter **6** for discussion).

Compound **604**

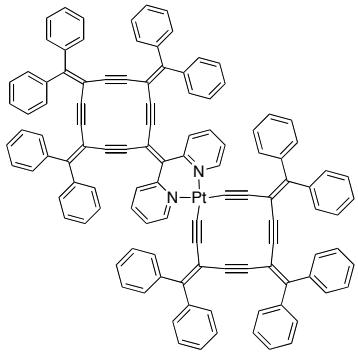

A mixture of trimer **305** (157 mg, 0.182 mmol) and TBAF (0.2 mL, 0.2 mmol, 1M in THF) in wet THF (4 mL) was stirred for 1 h. Et_2O and H_2O were added, the organic phase separated, washed with saturated NH_4Cl (2 x 20 mL), dried ($MgSO_4$) and reduced to 2 mL. The Et_2O solution was added drop-wise to a degassed mixture of platinum complex **603** (50.0 mg, 0.0820 mmol), CuI (5.0 mg, 0.026 mmol), $Pd(PPh_3)_4$ (5.3 mg, 0.0045 mmol) and dry THF (10 mL) that was under reflux as the Et_2O solution being added. The resulting mixture was refluxed for 18 h. The crude reaction product was filtered and washed with NH_4Cl (20 mL), H_2O (2 x 40 mL) extracted with CH_2Cl_2, and dried ($MgSO_4$). The crude reaction product was subjected to column chromatography (aluminum oxide, activity 2, hexanes/ethyl acetate, 10:1 to 3:1) that was followed with two consecutive re-crystallizations (hexanes/CH_2Cl_2 1:1) which afforded a brown solid **604** (34 mg, 25%). MALDI-TOF HRMS (DCTB) calc. for $C_{112}H_{68}N_2Pt$ 1635.50248 (M^+), found 1635.50394. (refer to Chapter **6** for discussion).

Fragmentations: $C_{79}H_{55}N_4Pt$ 1254.40690 (M^+), found 1254.40690; $C_{62}H_{37}N_2Pt$ 1004.25990 (M^+), found 1004.26218; $C_{62}H_{38}N_2$ 811.31078 (M^+), found 811.31093; $C_{62}H_{38}N_2$ 810.30295 (M^+), found 810.30319. (refer to Chapter **6** for discussion).

Compound **605**

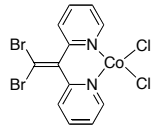

A mixture of dibromoolefin **600** (50.0 mg, 0.147 mmol), $CoCl_2$ (28 mg, 0.21 mmol, anhydrous) and absolute ethanol (5 mL) was refluxed for 5 h. The crude reaction product was washed with cold ethanol (2 x 20 mL) and air dried which afforded compound **605** as a blue solid (55 mg, 80%). X-ray. (refer to Chapter **6** for discussion).

Compound **606**

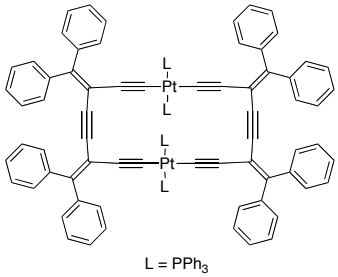

A mixture of dimer **303** (20.0 mg, 0.0303 mmol) and TBAF (0.1 mL, 0.1 mmol, 1M in THF) in wet THF (2 mL) was stirred for 1 h. Et_2O and H_2O were added, the organic phase separated, washed with saturated NH_4Cl (2 x 20 mL), dried ($MgSO_4$) and reduced to 2 mL. The Et_2O solution was added to a degassed mixture of $Pt(PEt_3)_2Cl_2$ (15.0 mg, 0.0310 mmol), Et_3N (250 mL), and CuI (1 mg, 0.005 mmol) and the resulting mixture was stirred for 3 days at room temperature. The crude reaction product was treated with NH_4Cl (400 mL) and extracted with CH_2Cl_2 (100 mL). The solvent was removed and the crude reaction product was subjected to column chromatography (silica gel plate, hexanes/CH_2Cl_2, 1:1) to give compound **606** as a yellow solid (5 mg, 20%, low solubility solid). Mp >300 °C (decomp.). R_f = 0.2 (hexanes/CH_2Cl_2, 1:1). IR (CH_2Cl_2, cast) 2957, 2925, 2872, 2856, 2080 cm^{-1}; ^1H NMR (CD_2Cl_2, 400 MHz) δ 7.37–6.97 (m, 40H), 1.98–1.95 (m, 24H), 1.10–1.01 (m, 36H); ^{13}C NMR (125 MHz, CD_2Cl_2) δ 146.2, 143.0, 141.6, 130.8, 130.6, 130.4, 130.3, 128.1, 127.8, 127.8, 127.6, 127.1, 116.1, 108.4, 107.9, 97.7, 92.1, 17.1 (virtual t, J_{C-P} = 17 Hz), 8.8 (app. d, J_{C-P} = 23 Hz) ; $^{31}P\{^1H\}$ NMR (161.9 MHz, CD_2Cl_2) δ 8.9 (s, J_{P-Pt} = 2360

Hz); ^{195}Pt NMR (85.8 Hz, CD_2Cl_2) δ –135.4 ($J_{P\text{-}Pt}$ = 2364 Hz). MALDI-TOF HRMS calcd. for $C_{92}H_{100}P_4Pt_2$ (M^+) 1718.60655, found 1718.60806. (refer to Chapter **6** for discussion).

Compound **607**

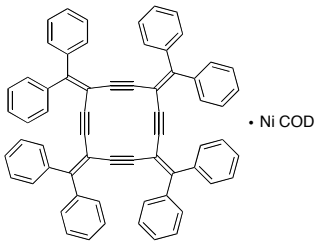

To a solution of **311** (29 mg, 0.035 mmol) in toluene (4 mL), was added $Ni(COD)_2$ (10.0 mg, 0.0360 mmol) in glove box. The mixture stirred at room temperature for 18 h. The solvent was removed by high vacuum pump that gave a red solid. The red solid dissolved in THF and some residue formed that was filtered. After taking removing the solvent, the resulting red solid was analyzed: ^{1}H NMR (benzene-d6, 500 MHz) δ 7.59 (d, J = 5 Hz, 8H), 7.28 (d, J = 8 Hz, 4H), 7.18–6.96 (m, 24H), 6.89 (d, J = 8 Hz, 4H), 4.19 (s, 4H), 2.10 (s, 8H); ^{13}C NMR (125 MHz, benzene-d6) 144.6, 142.6, 142.5, 140.4, 137.8, 135.1, 132.1, 131.3, 130.5, 129.3, 128.6, 128.5, 128.3, 128.2, 128.1, 128.0, 127.9, 127.8, 127.4, 127.3, 125.6, 114.6, 103.7, 98.3, 97.9, 93.5, 31.9. (refer to Chapter **6** for discussion).

Compound **608a** and **608b**

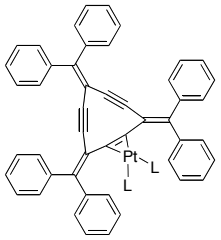

Complex $Pt(PPh_3)_4$ (20.0 mg, 0.0160 mmol) was added to a solution of **310** (10 mg, 0.016 mmol) in dry toluene (3 mL) in glove box. The mixture stirred at room temperature for 24 h in glove box. The solvent was taken by high vacuum pump and the resulting crude reaction product was subjected to the chromatography on aluminum oxide (activity 2, hexanes/ethyl acetate, 10:1) and gave two products as yellow solids **608a** and **608b** respectively (due to decomposition on the aluminum oxide no yield is reported).

608a: ^1H NMR (CD_2Cl_2, 400 MHz) δ 7.55–6.75 (m, 60H); ^{31}P $\{^1H\}$ NMR (161.9 MHz, CD_2Cl_2) δ 23.1 ppm (s, $^1J_{P\text{-}Pt}$ = 1802 Hz). HR MALDI TOF MS Calcd. for $C_{84}H_{60}P_2Pt$ (M^+) 1325.38125, found very weak, 1063.29220 ($[M–PPh_3]^+$)

608b: ^1H NMR (CD_2Cl_2, 500 MHz) δ 7.70–6.63 (m, 60H); ^{31}P $\{^1H\}$ NMR (161.9 Hz, CD_2Cl_2) δ 21.5 (d, $J_{P\text{-}P}$ = 16.2 Hz, $J_{P\text{-}Pt}$ = 2812 Hz), 15.1 (d, $J_{P\text{-}P}$ = 15.8 Hz, $J_{P\text{-}Pt}$ = 1789 Hz). HR MALDI TOF MS Calcd. for $C_{84}H_{60}P_2Pt$ (M^+) 1325.38125, found 1325.38191, 1063.29115 ($[M–PPh_3]^+$). (refer to Chapter **6** for discussion).

Compound **609** (related compounds)

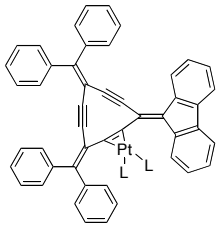

L = PPh_3

Complex $Pt(PPh_3)_4$ (31 mg, 0.025 mmol) was added to a solution of **409** (15 mg, 0.025 mmol) in dry toluene (3 mL) in glove box. The mixture stirred at room temperature for 24 h in glove box. The mixture stirred at room temperature for 24h glove box. The solvent was removed by high vacuum pump and the resulting crude was subjected to the chromatography on aluminum oxide (activity 2, hexanes/ethyl acetate 10:1) that gave two different bands (major decomposition observed). The major band as orange solid contains two compounds.

Isomer with the lowest R_f (major product): IR (CH_2Cl_2, cast) 3058, 2924, 2853, 2109, 2057 cm^{-1}; $^{31}P\{^1H\}$ NMR (161.9 MHz, Ac-d6) δ 21.4 (d, $J_{P\text{-}P}$ = 16.7 Hz, Hz $J_{P\text{-}Pt}$ = 2817 Hz), 14.3 (d, $J_{P\text{-}P}$ = 16.8 Hz, $J_{P\text{-}Pt}$ = 1792 Hz); ^{13}C NMR (500 MHz, CD_2Cl_2) δ 147.6, 142.7, 141.2, 140.7, 139.3, 139.1, 138.4, 137.8, 135.5, 135.4, 134.8, 134.7, 132.6, 132.4, 132.1, 131.8, 131.4, 130.5, 130.4, 130.3, 130.2, 129.9, 128.5, 128.4, 128.3, 128.2, 128.1, 128.0, 127.9, 127.7, 127.5, 127.4, 127.3, 127.2, 127.1, 126.8, 126.2, 124.6, 123.9, 119.5, 119.1, 108.9, 108.4, 106.4, 101.6; ^{195} Pt NMR (85.8 MHz, CD_2Cl_2) δ 33.1 (dd $J_{P\text{-}Pt}$ = 2813, 1790 Hz). HR MALDI TOF calc. for $C_{84}H_{58}P_2Pt$ (M^+) 1323.36560, found 1323.36622. The

second isomer: ^{31}P {^{1}H} NMR (161.9 MHz, Ac-d6,) δ 21.7 (d, J_{P-P} = 16.4 Hz), 15.2 (d, J_{P-P} = 16.4 Hz).

Second band: the third compound: ^{31}P {^{1}H} NMR (161.9 MHz, Ac-d6) δ 22.9 (s, J_{P-Pt} = 2893 Hz); the forth compound: δ 21.1 (s, J_{P-Pt} = 2530 Hz); the fifth compound: δ 25.7 (its satellites are not clear). (refer to Chapter **6** for discussion).

Compound **610**

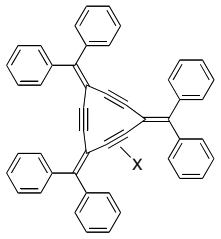

X = $Co_2(CO)_6$

To a solution of radialene **310** (8 mg, 0.01 mmol) in THF (3 mL), was added $Co_2(CO)_8$ (23.4 mg, 0.0684 mmol). The resulting mixture was stirred at room temperature for 12 h. The crude reaction product was filtered and the solvent was removed. The crude reaction product dissolved in CH_2Cl_2 and subjected to column chromatography on aluminum oxide (neutral, activity 2, hexanes/ethyl acetate, 10:1) that gave **610** (7.5 mg, 60%) as purple solid. IR (CH_2Cl_2, cast) 2963, 2926, 2855, 2092, 2057, 2031 cm^{-1}; ^1H NMR (400 MHz CD_2Cl_2) δ 7.60–7.57 (m, 4H), 7.42–7.36 (m, 22H), 7.36–7.08 (m, 4H); ^{13}C NMR (125 MHz, CD_2Cl_2) δ 200.1, 151.2, 142.8, 141.2, 136.3, 130.0, 129.1, 129.0, 128.8, 128.3, 128.1, 118.9, 91.4, 88.5, 76.8. (refer to Chapter **6** for discussion).

Note: The mass spectrometric analysis usually does not work for the carbonyl clusters because under laser or electron beam, these compounds are decomposed or eject CO(s) therefore, it is not possible to find accurate molecular ion for them.

Compound **611**

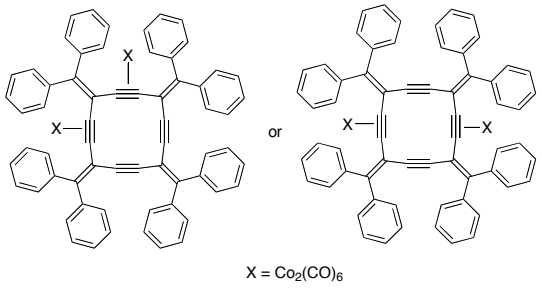

To a solution of radialene **311** (15 mg, 0.18 mmol) in THF (3 mL), was added $Co_2(CO)_8$ (28.3 mg, 0.0827 mmol) in one portion. The resulting mixture was stirred at room temperature for 12 h. The crude reaction product was filtered and the solvent was taken. The crude reaction product dissolved in CH_2Cl_2 and subjected to column chromatography on aluminum oxide (neutral, activity 2, hexanes/ethyl acetate, 10:1) that gave **611** as a green solid in low yield <10% (decomposition through the separation). IR (CH_2Cl_2, cast) 2957, 2924, 2854, 2086, 2052, 2030, 2022 cm^{-1}; ^{13}C NMR (125 MHz, CD_2Cl_2) δ 240.9, 198.9, 152.2, 143.9, 142.3, 140.9, 139.7, 131.5, 130.9, 130.7, 130.3, 130.0, 129.1, 128.9, 128.6, 128.4, 128.3, 128.1, 127.9, 120.4, 96.1, 94.1. (refer to Chapter **6** for discussion).

Compound **612**

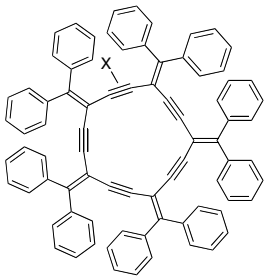

X = $Co_2(CO)_6$

To a solution of radialene **312** (13 mg, 0.013 mmol) in THF (3 mL), was added $Co_2(CO)_8$ (23.4 mg, 0.0684 mmol) in one portion. The resulting mixture was stirred at room temperature for 12 h. The crude reaction product was filtered and the solvent was taken. The crude reaction product dissolved in CH_2Cl_2 and subjected to column chromatography on aluminum oxide (neutral, activity 2, hexanes/ethyl acetate, 10:1) that gave **612** as a green solid in low yield (decomposition through separation). IR (CH_2Cl_2, cast) 3054, 2925, 2087, 2056, 2024 cm^{-1}; ^{13}C NMR (125 MHz, CD_2Cl_2) δ 198.7 (it is very weak), 154.6, 152.9, 151.3, 151.2, 144.3, 142.9, 142.7, 142.2, 141.6, 141.2, 140.9, 140.5, 140.1, 131.1, 130.9, 130.6, 130.4, 130.3, 130.1, 130.0, 129.4, 129.2, 128.9, 128.8, 128.7, 128.6, 128.5, 128.4, 128.2, 128.1, 127.7, 120.5, 120.2, 119.7, 103.1, 102.7, 96.9, 95.2, 94.9, 93.9, 93.2, 92.7, 91.6, 90.7. (refer to Chapter **6** for discussion).

Compound **613**

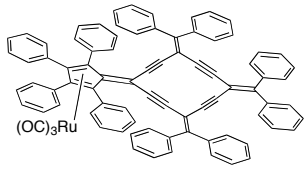

To a degassed solution of radialene **433** (18 mg, 0.018) in dry benzene (5 mL) was added $Ru_3(CO)_{12}$ (4mg, 0.006) and the mixture refluxed for 4h. The crude was cooled to room temperature, solvent taken and the mixture was treated with a solution of (hexanes/CH_2Cl_2, 10 mL, 1:1) that caused product crushed out as a brown solid **613** (7.6 mg, 40% yield). IR (CH_2Cl_2 cast) 2158, 2183, 2055.7, 2013.8, 1984.8 cm^{-1}; ^{13}C NMR (125 MHz, CD_2Cl_2) 194.9, 153.9, 151.6, 150.6, 145.3, 140.6, 140.1, 139.9, 135.7, 134.7, 133.3, 131.3, 131.1, 130.6, 130.5, 130.3, 129.6, 129.3, 128.9, 128.5, 128.3, 128.1, 127.5, 127.4, 126.9, 126.3, 125.7, 113.5, 110.3, 108.8, 102.5, 101.8, 98.1, 97.6, 95.5, 95.3. MALDI-TOF HRMS calc. for $C_{83}H_{66}O_3Ru$ 1212.40500 (M^+, very weak), found 1212.40665. (refer to Chapter **6** for discussion).

Selected ^{13}C NMR Spectra

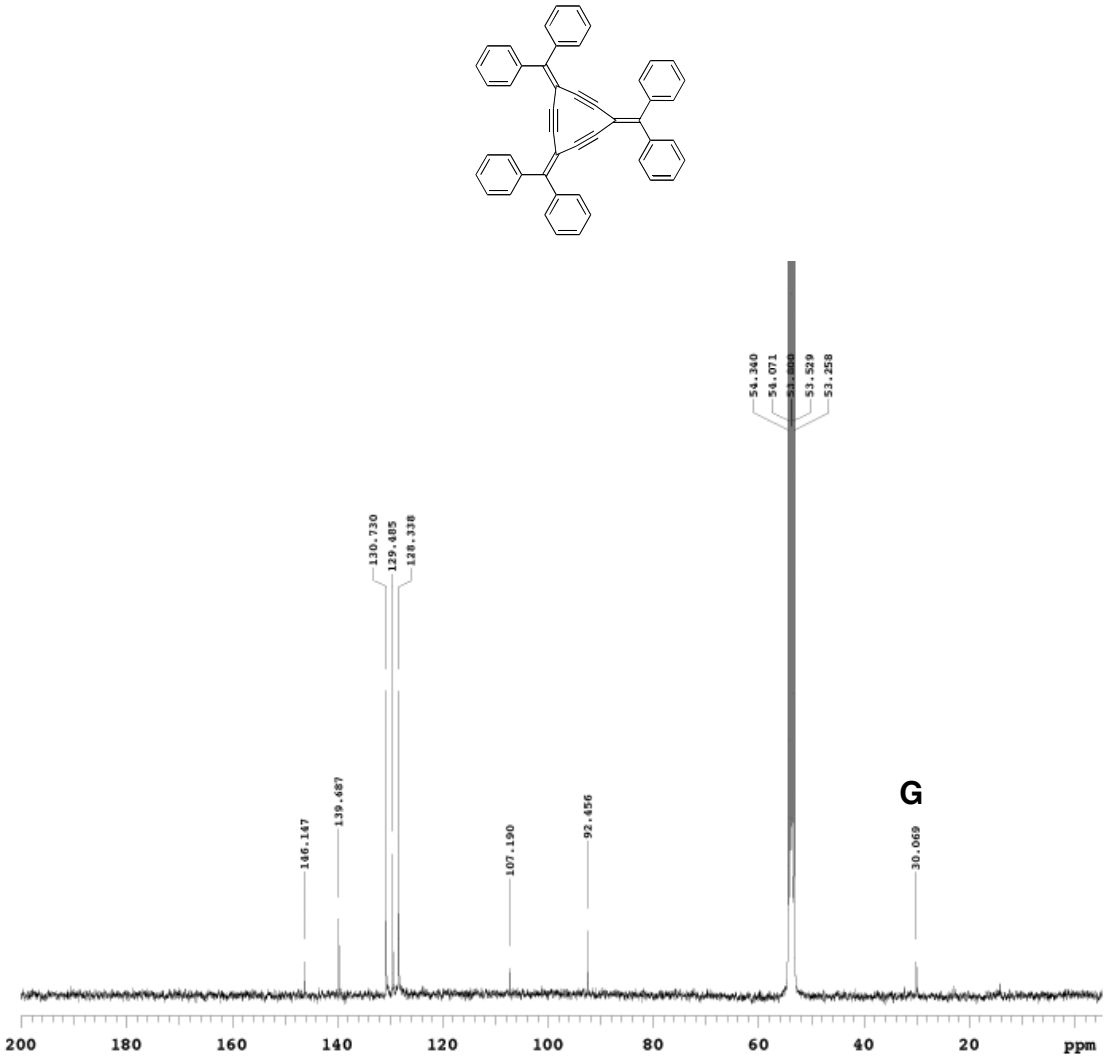

Figure A.1 ^{13}C NMR spectrum of compound **310** (CD_2Cl_2)

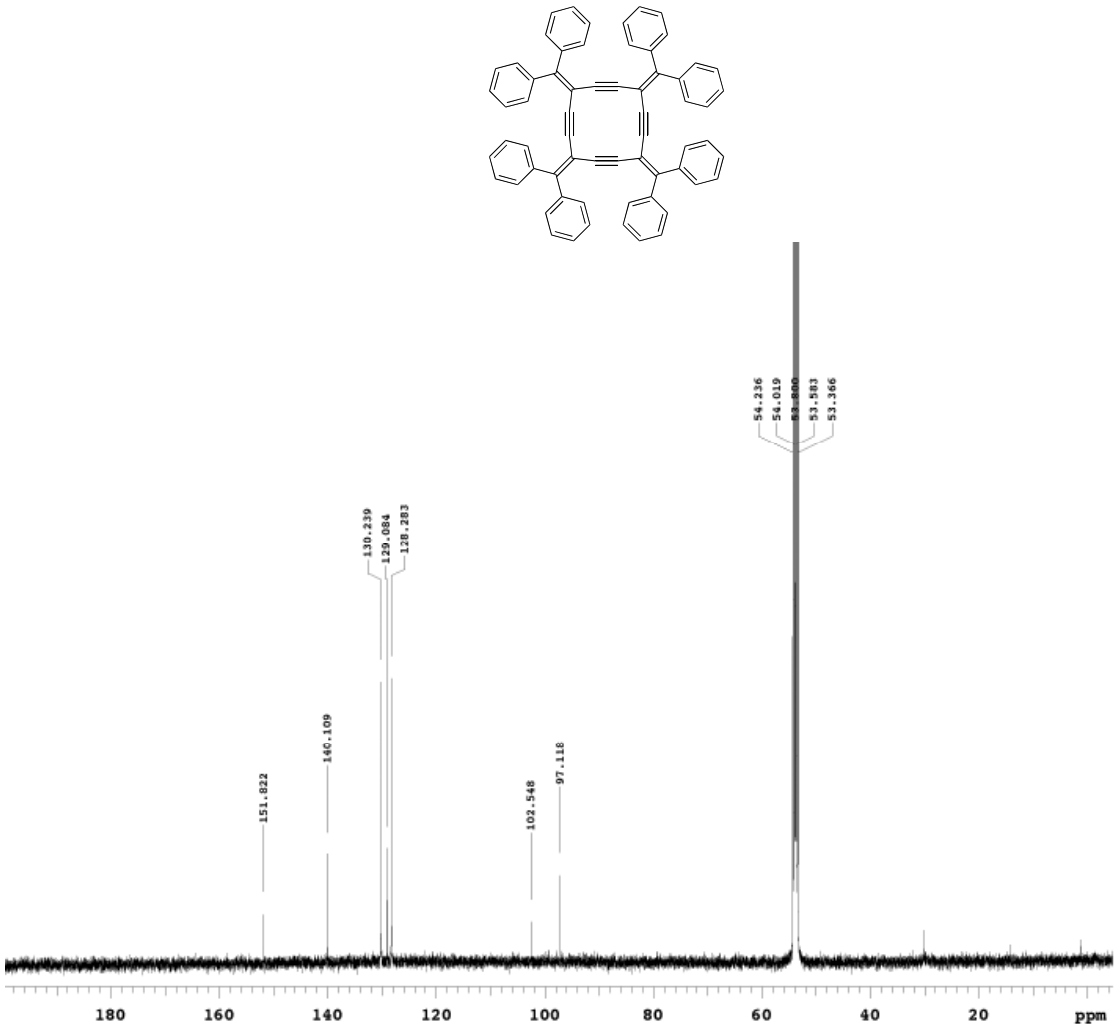

Figure A.2 ^{13}C NMR spectrum of compound **311** (CD_2Cl_2)

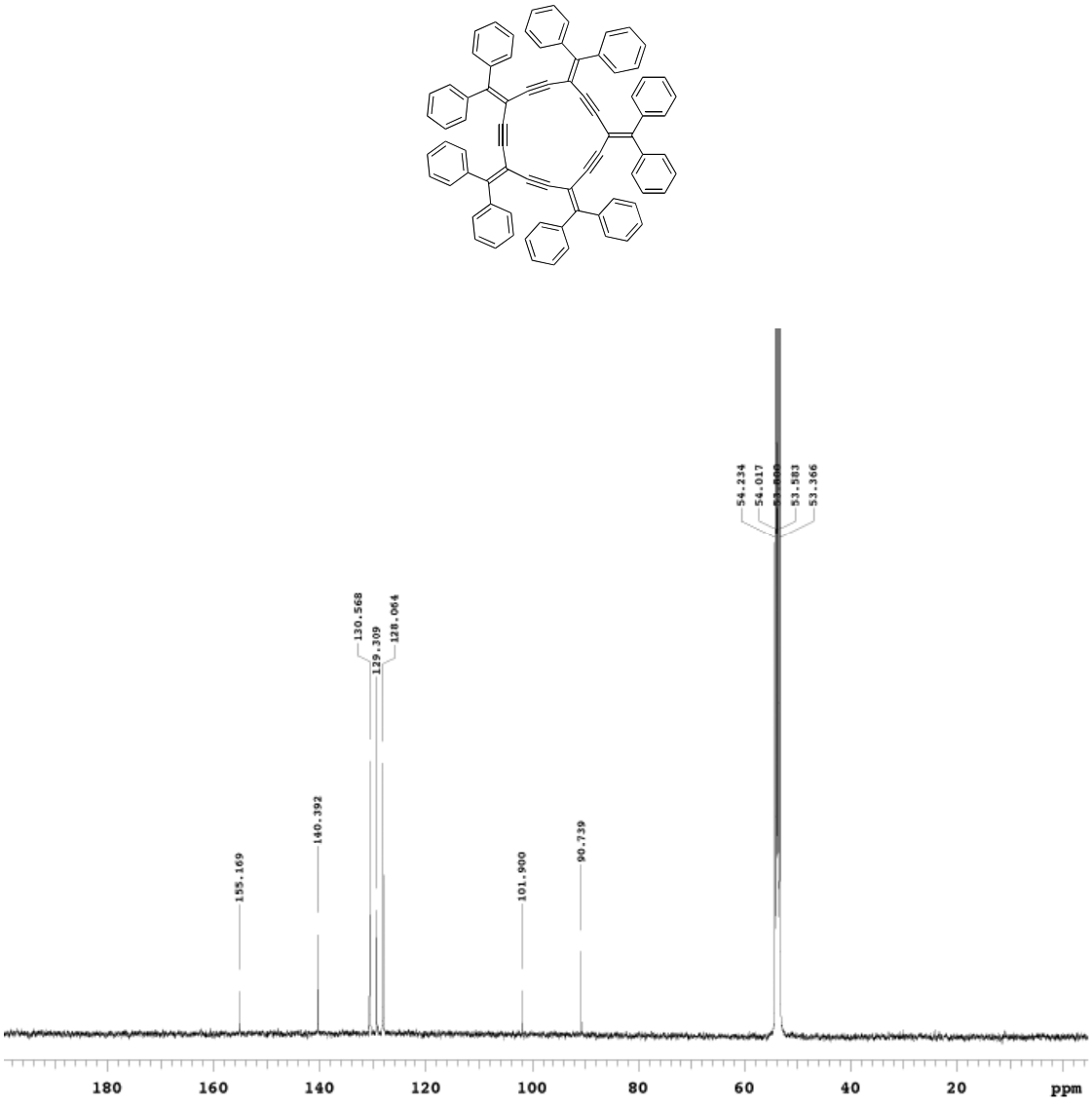

Figure A.3 ^{13}C NMR spectrum of compound **312** (CD_2Cl_2)

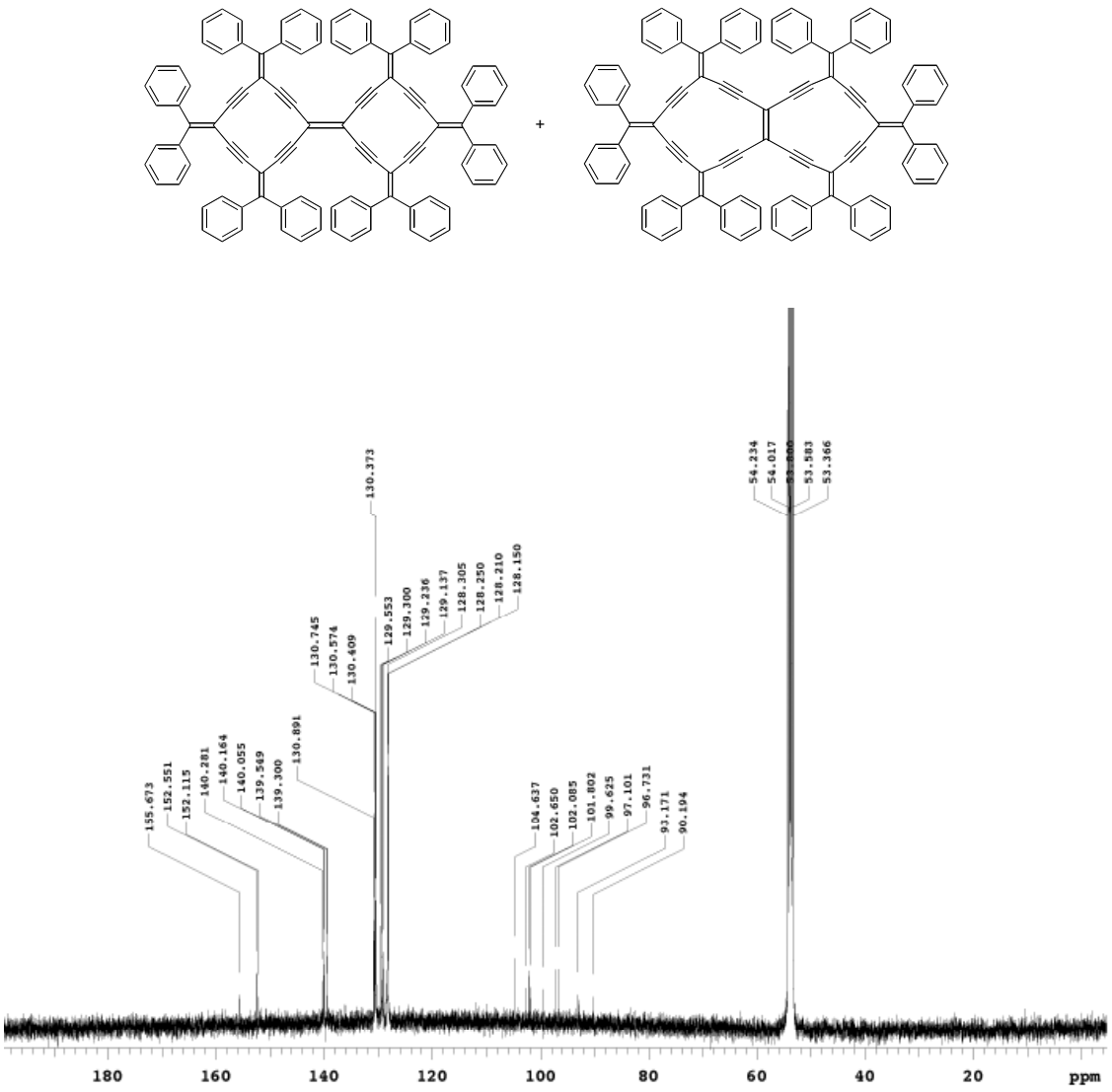

Figure A.4 ^{13}C NMR spectrum of compound **315a** and **315b** (CD_2Cl_2)

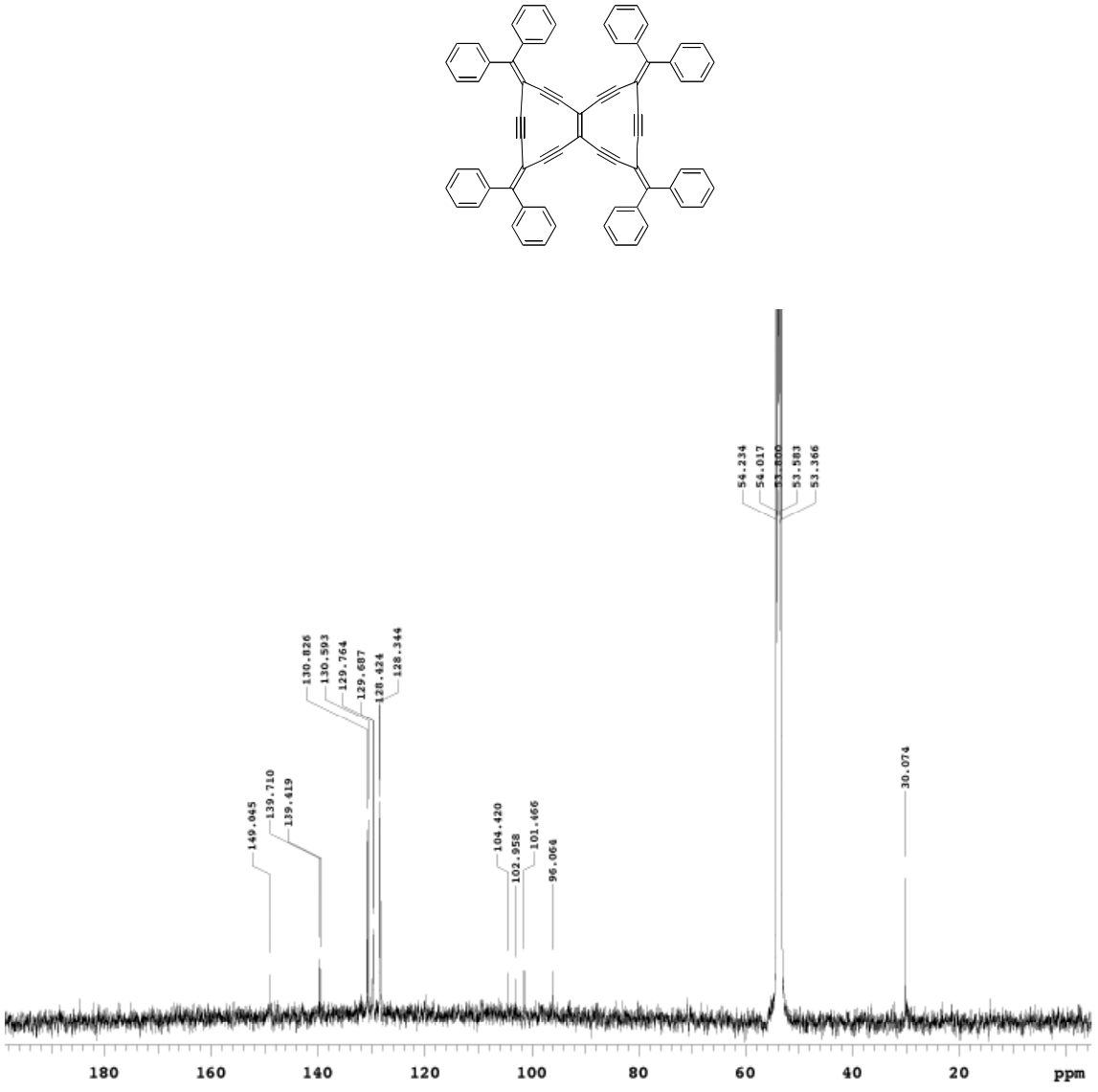

Figure A.5 ^{13}C NMR spectrum of compound **316a** (CD_2Cl_2)

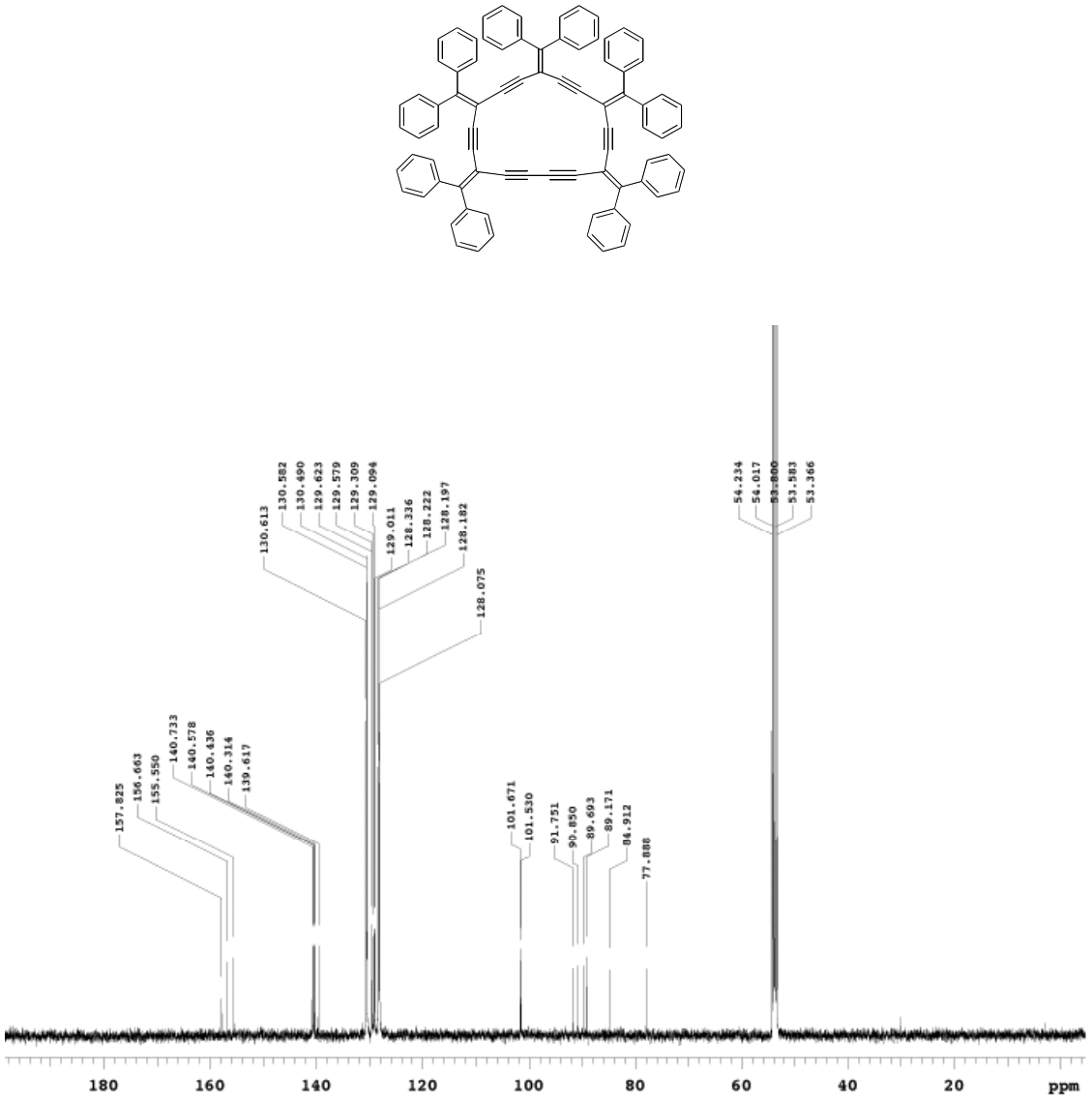

Figure A.6 ^{13}C NMR spectrum of compound **318** (CD_2Cl_2)

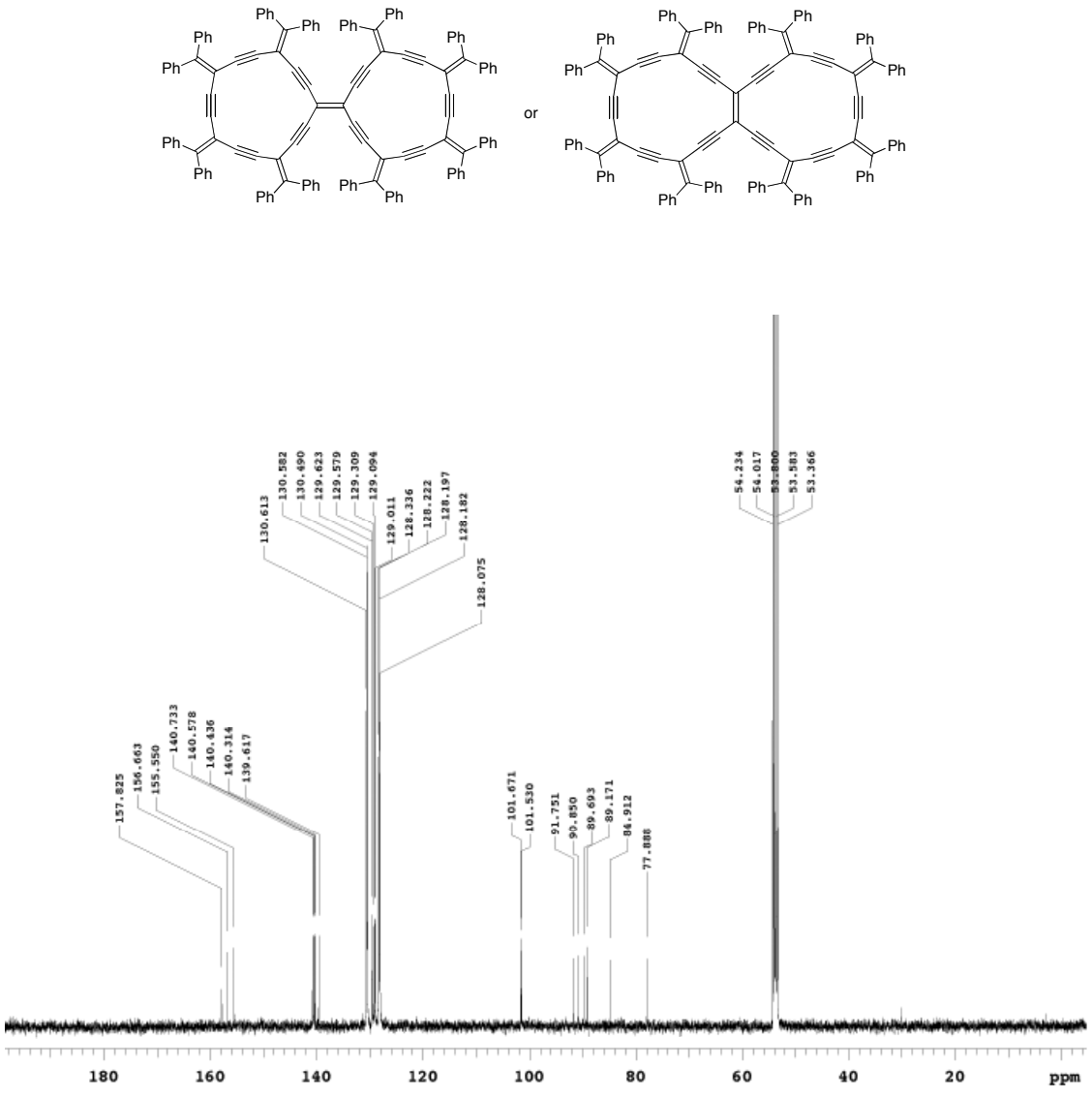

Figure A.6 ^{13}C NMR spectrum of compound **320a** or **320b** (CD_2Cl_2)

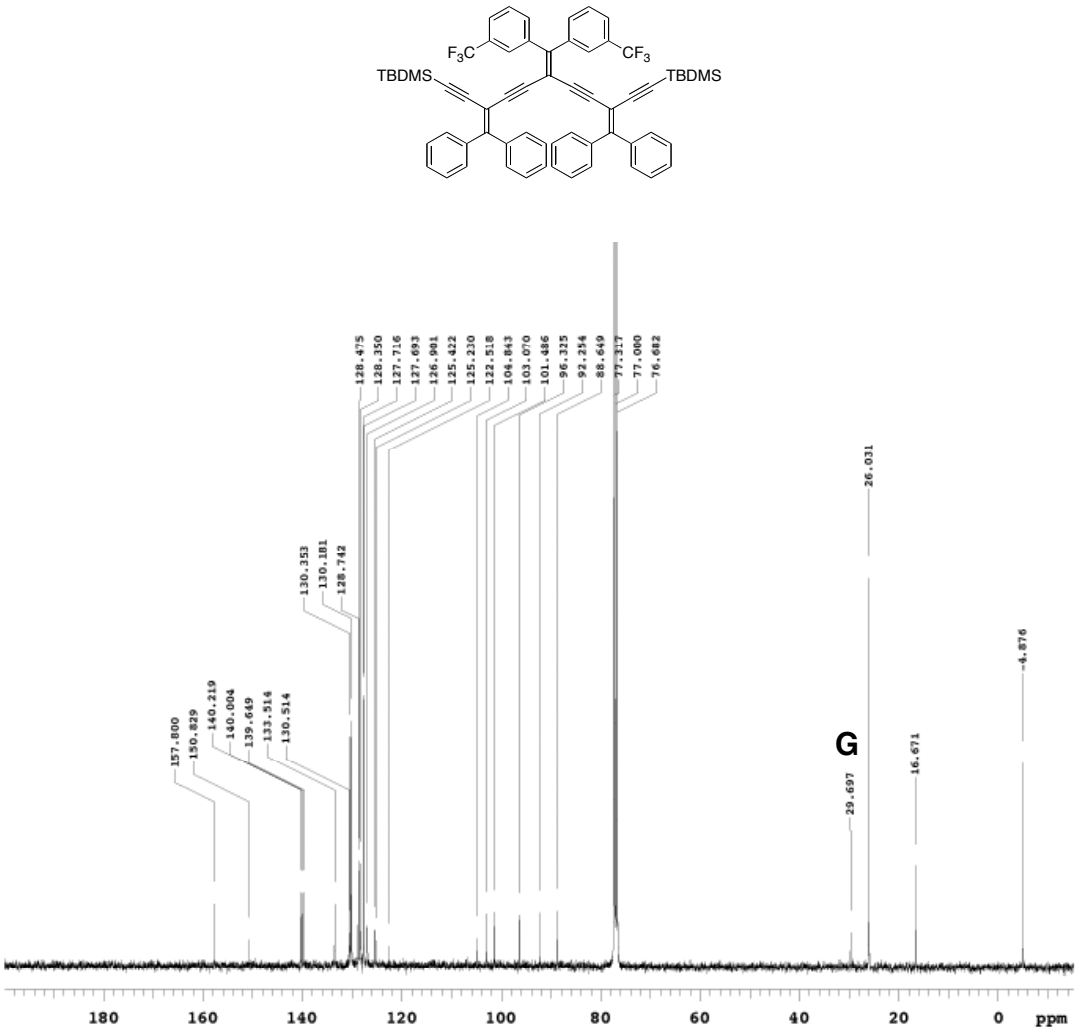

Figure A.7 ^{13}C NMR spectrum of compound **403** ($CDCl_3$)

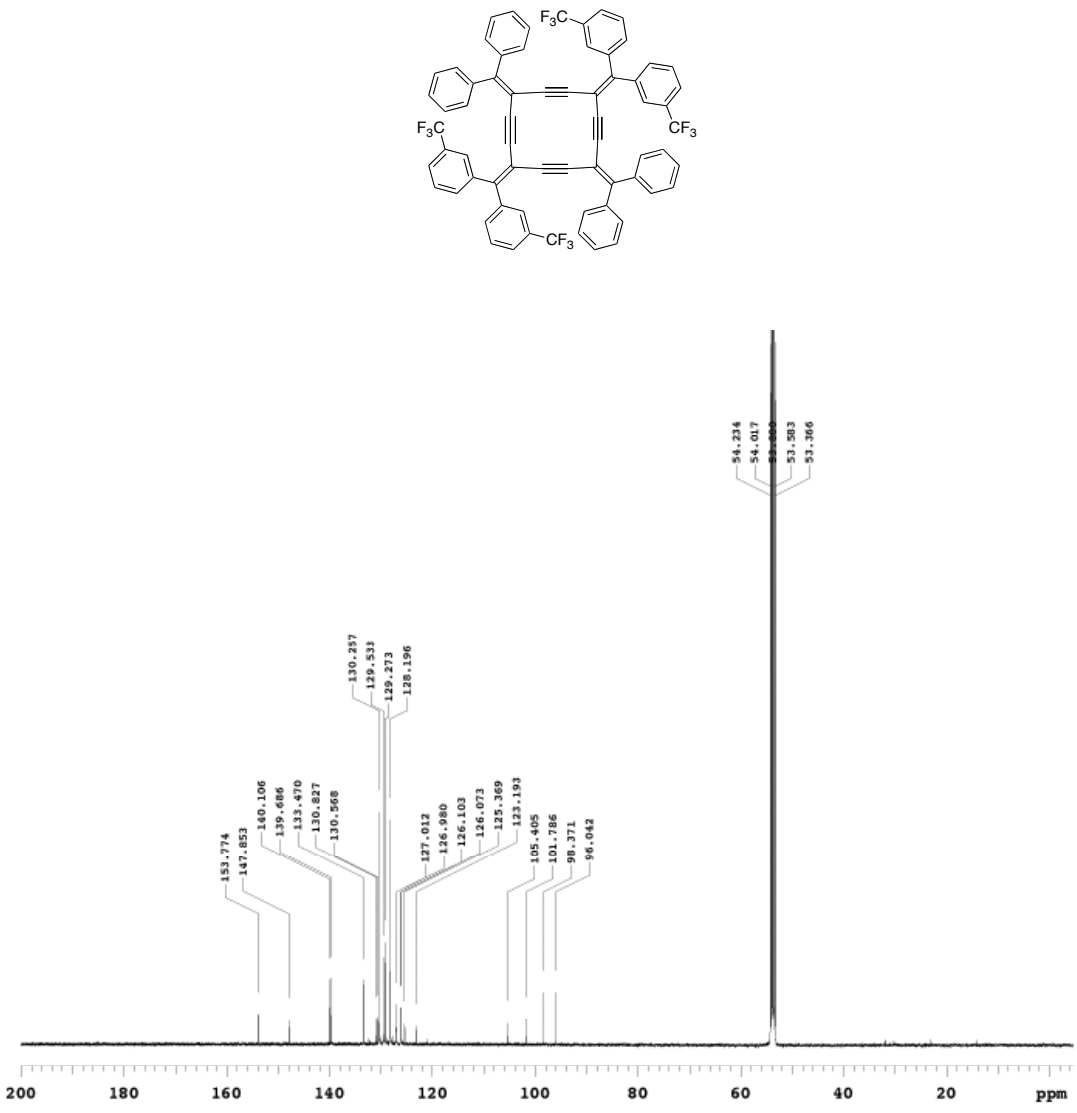

Figure A.8 ^{13}C NMR spectrum of compound **404** (CD_2Cl_2)

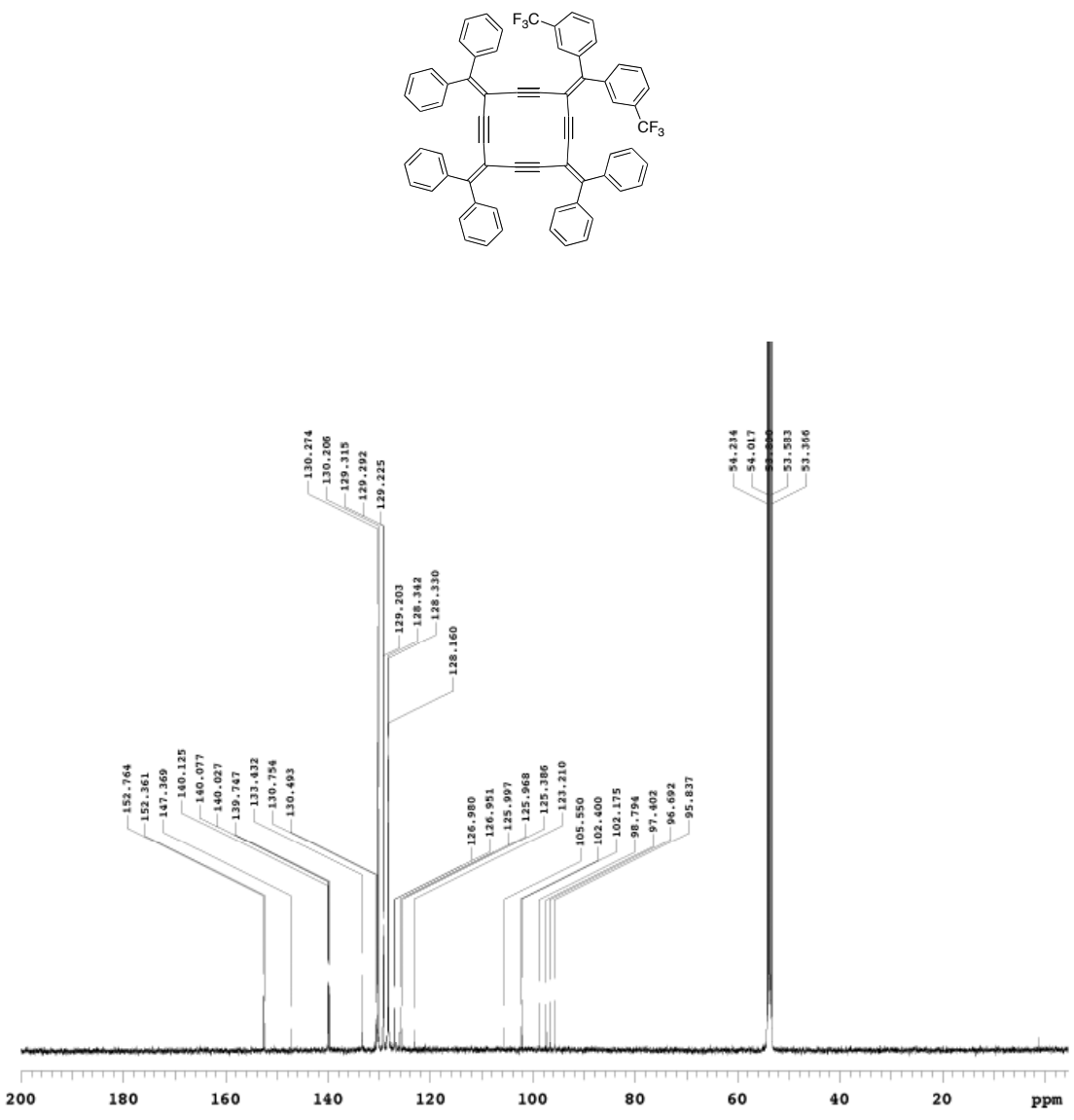

Figure A.9 ^{13}C NMR spectrum of compound **405** (CD_2Cl_2)

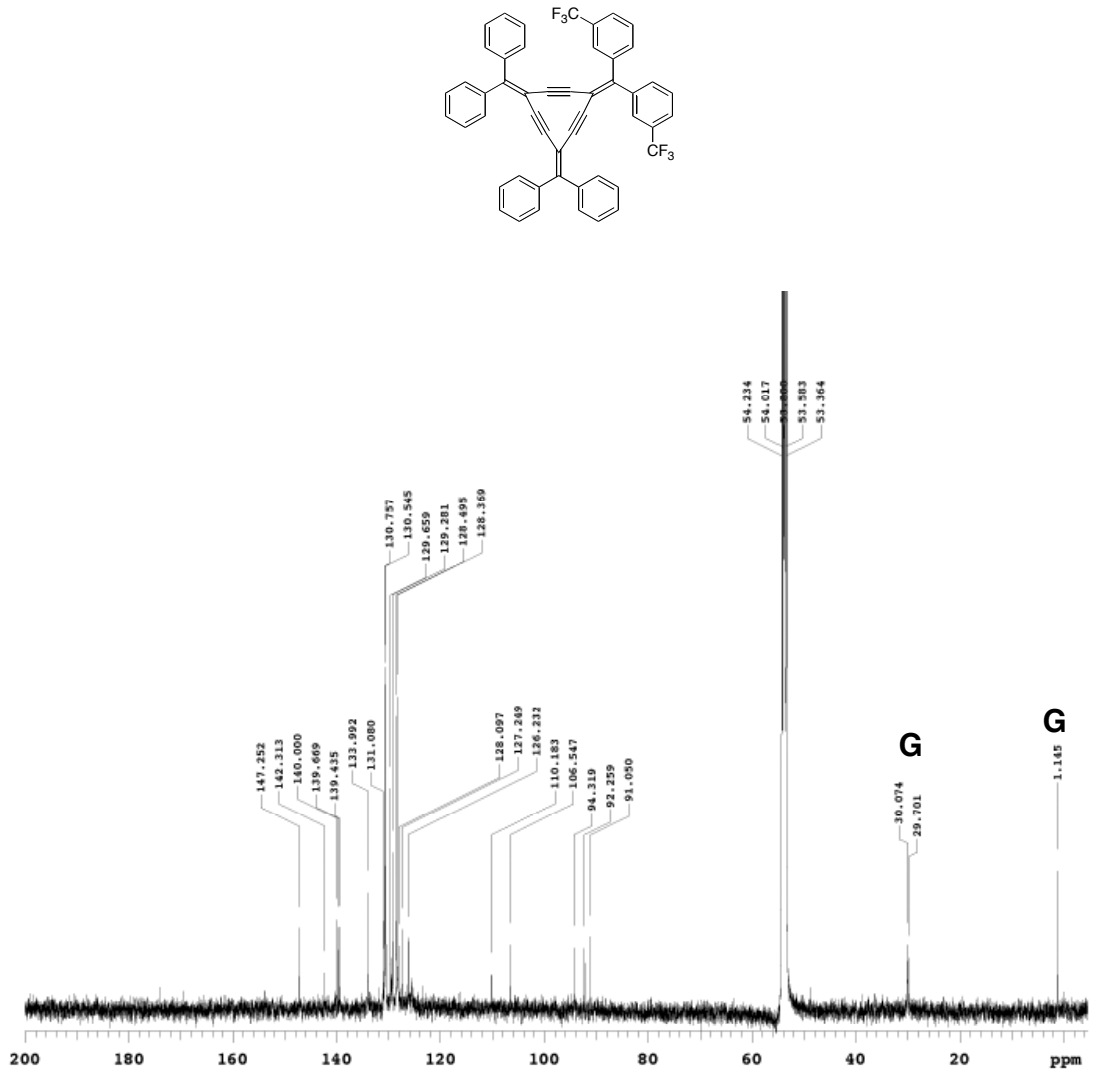

Figure A.10 ^{13}C NMR spectrum of compound **406** (CD_2Cl_2)

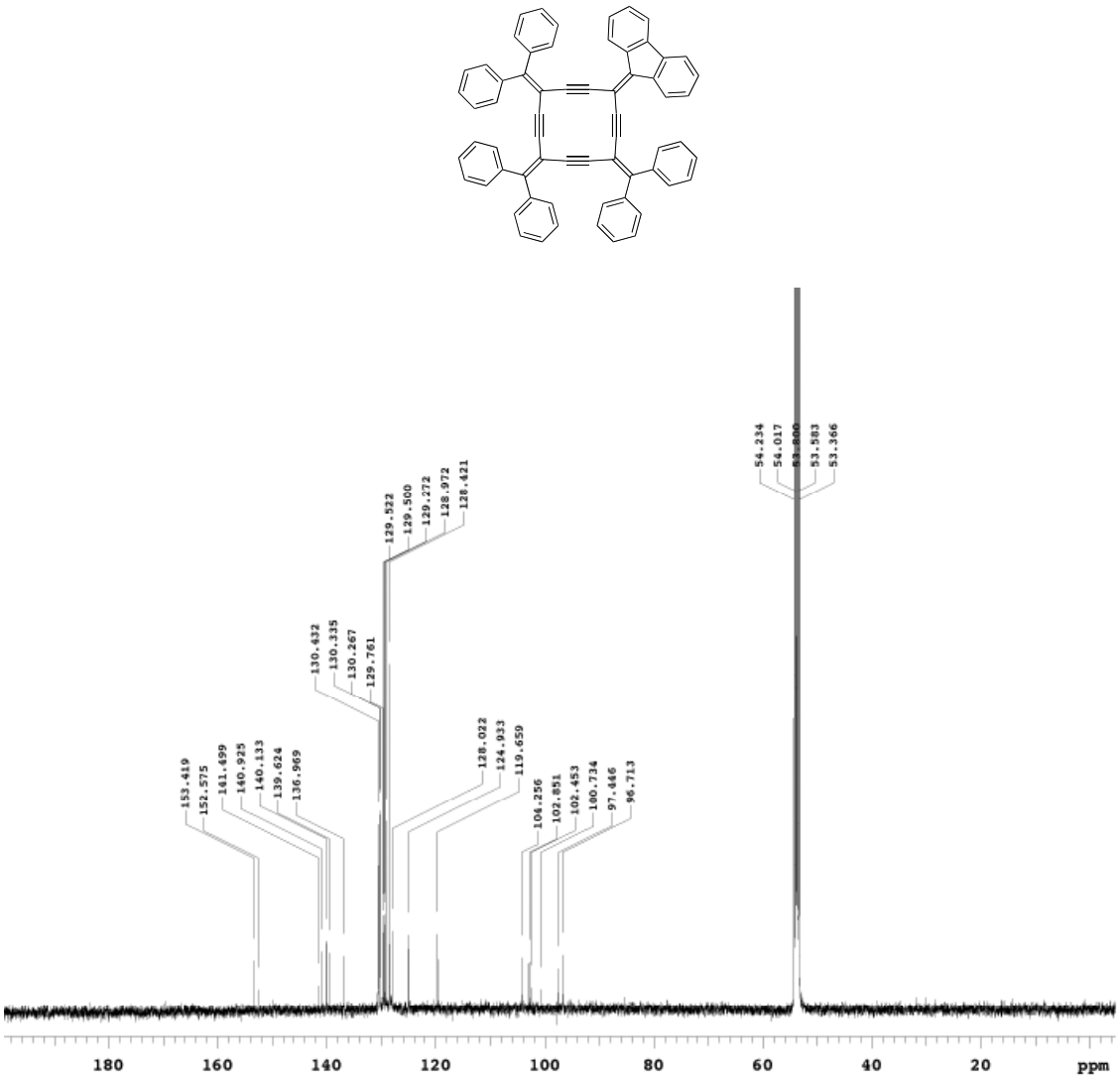

Figure A.11 ^{13}C NMR spectrum of compound **408** (CD_2Cl_2)

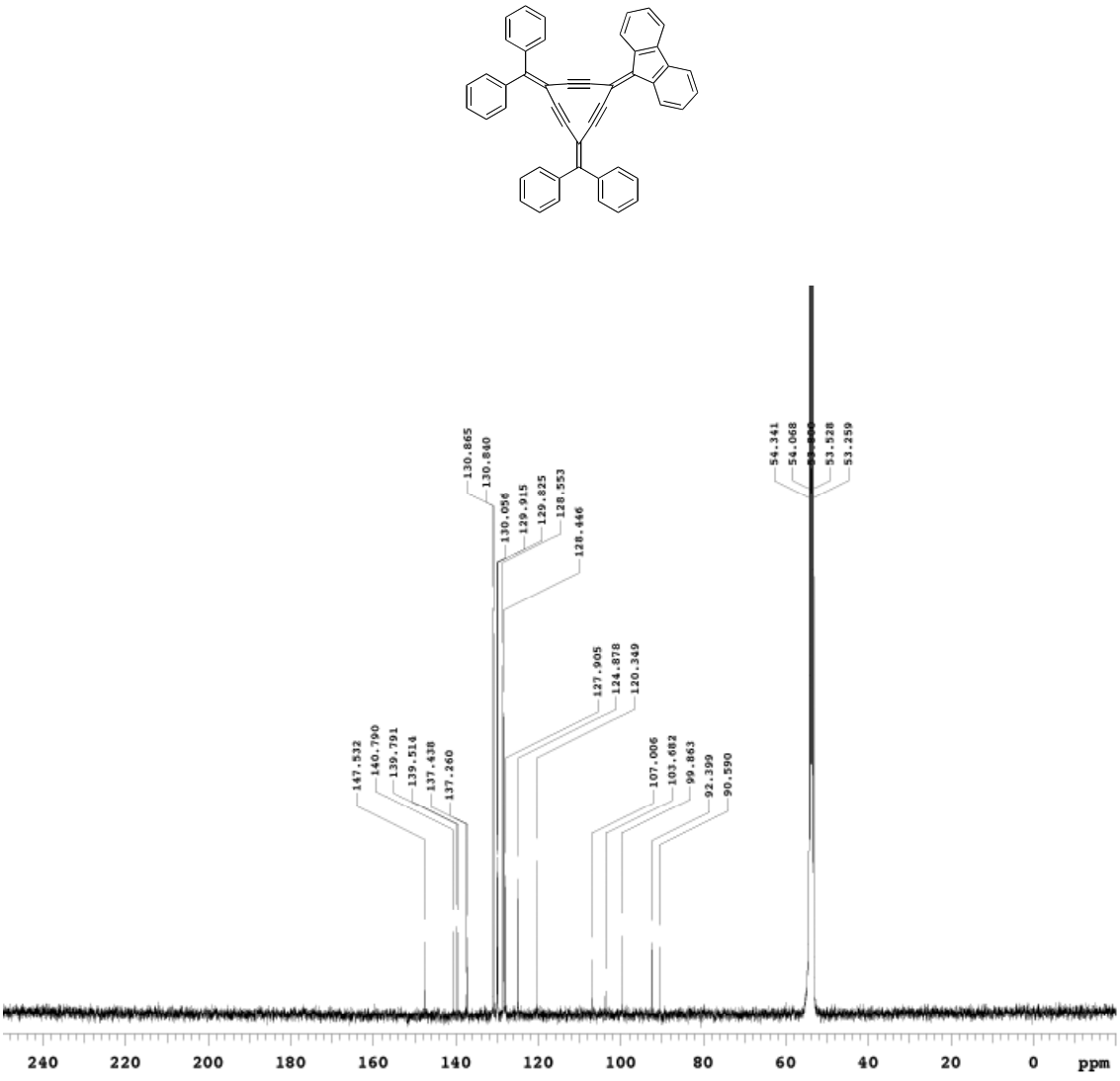

Figure A.12 ^{13}C NMR spectrum of compound **409** (CD_2Cl_2)

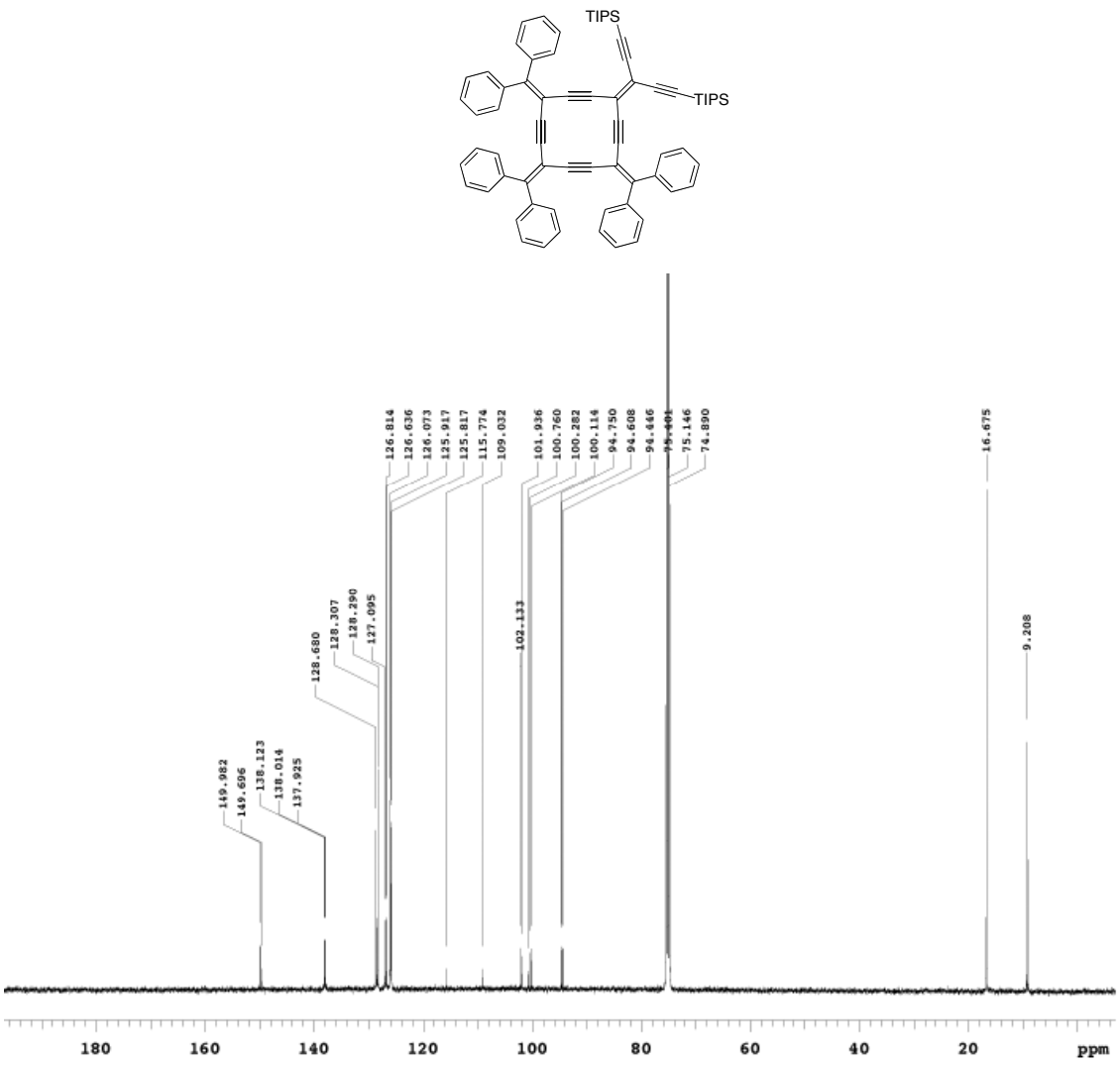

Figure A.13 ^{13}C NMR spectrum of compound **411** ($CDCl_3$)

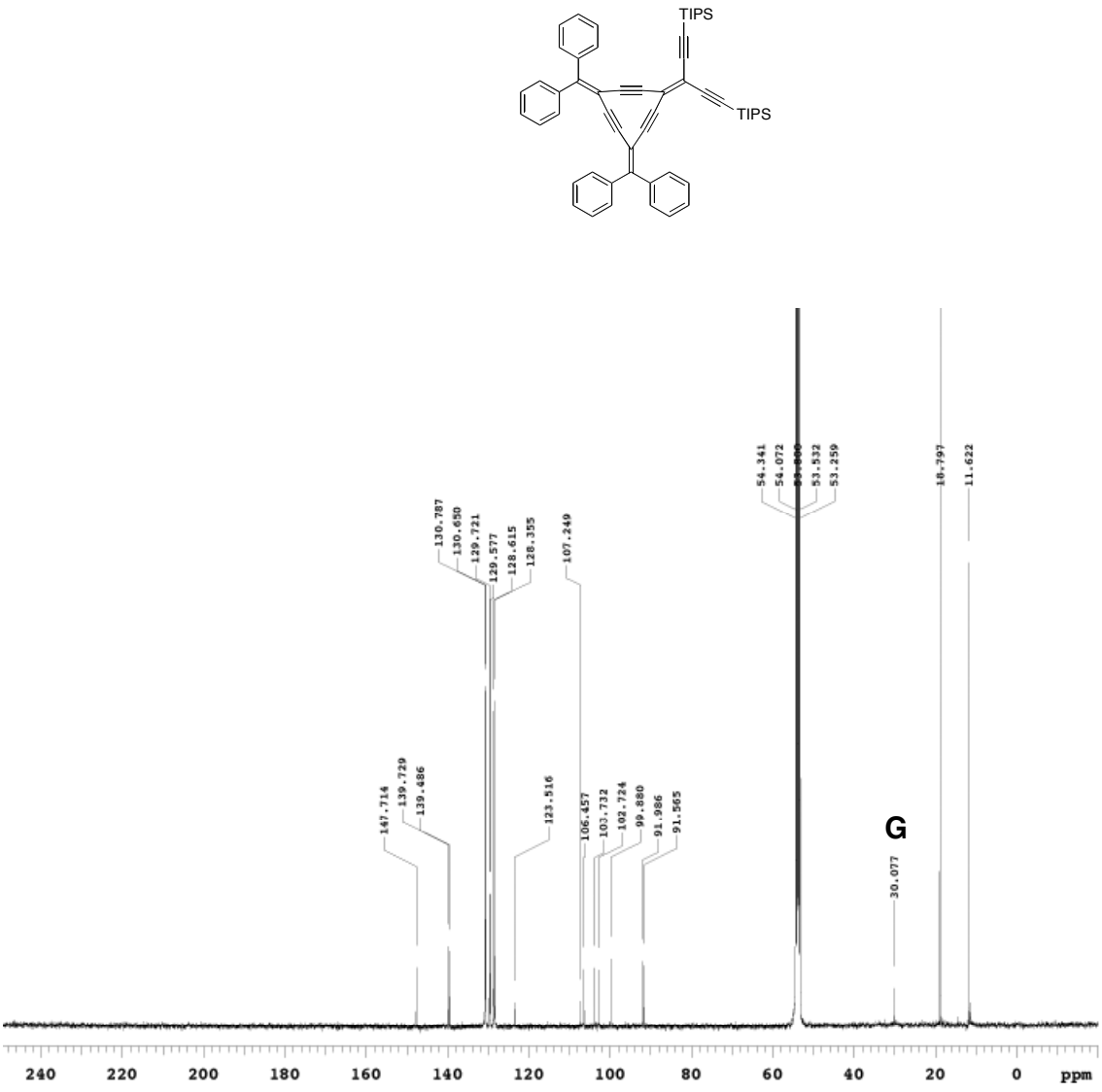

Figure A.14 ^{13}C NMR spectrum of compound **412** (CD_2Cl_2)

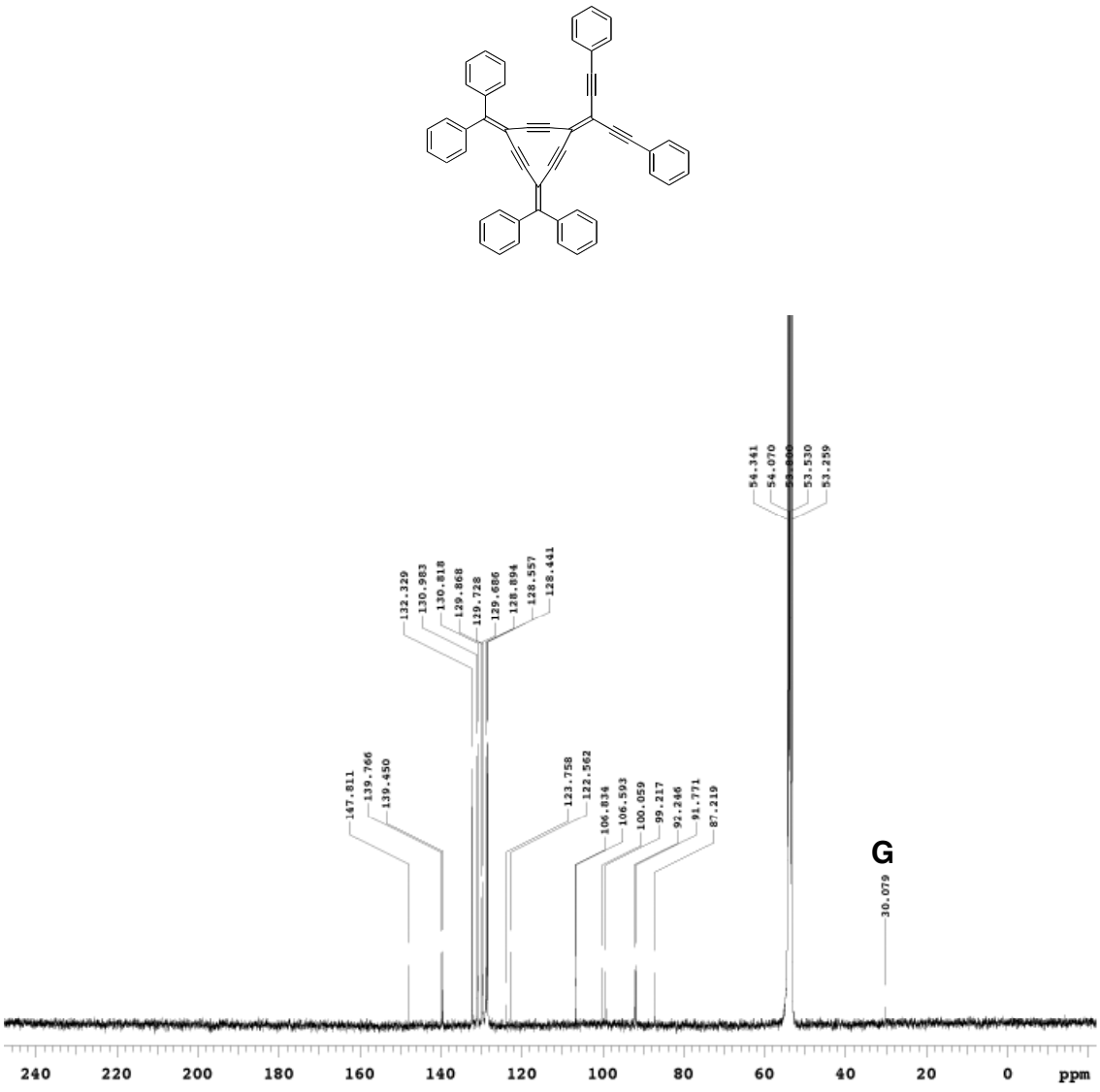

Figure A.15 ^{13}C NMR spectrum of compound **414** (CD_2Cl_2)

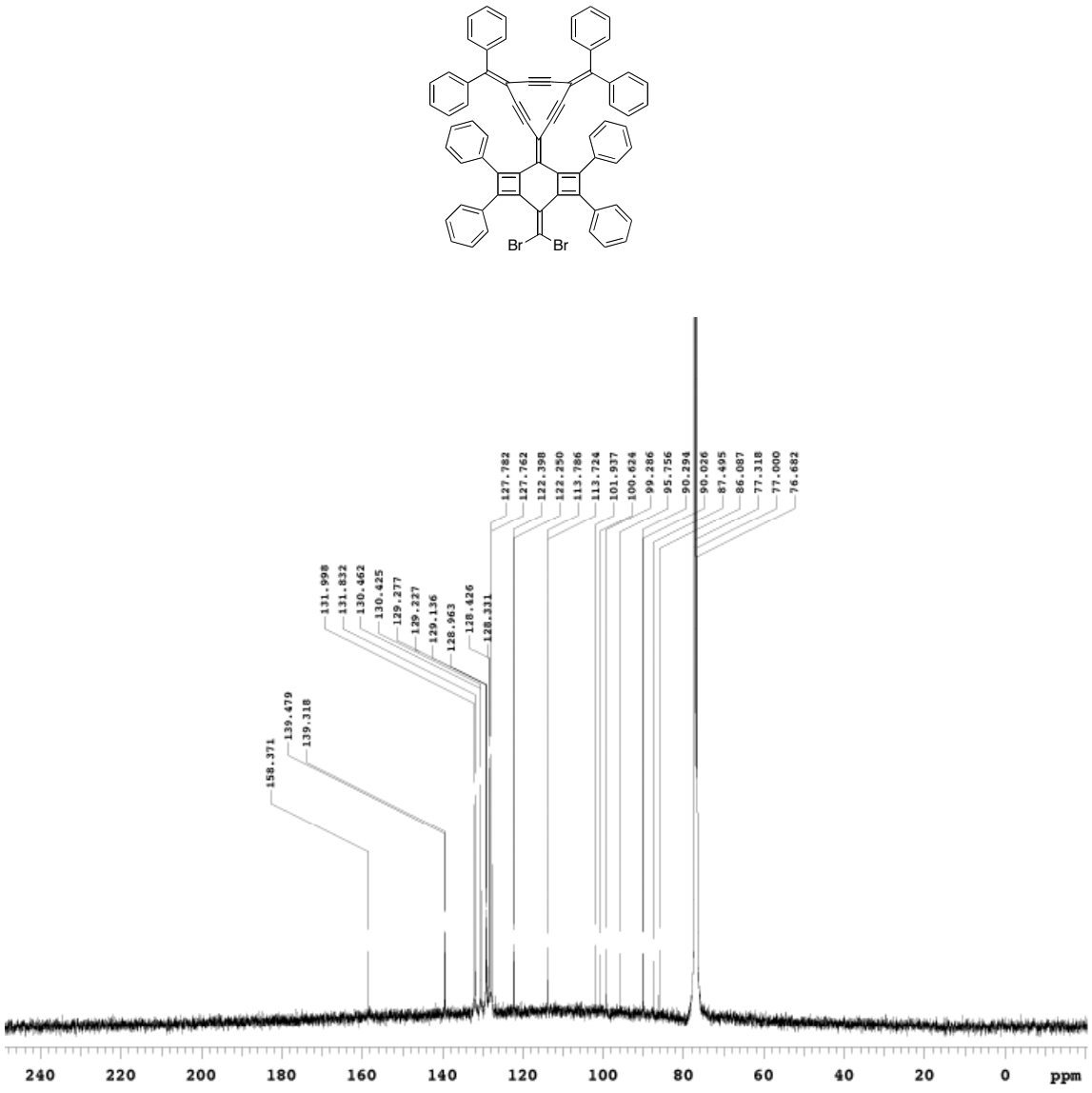

Figure A.16 ^{13}C NMR spectrum of compound **415** ($CDCl_3$)

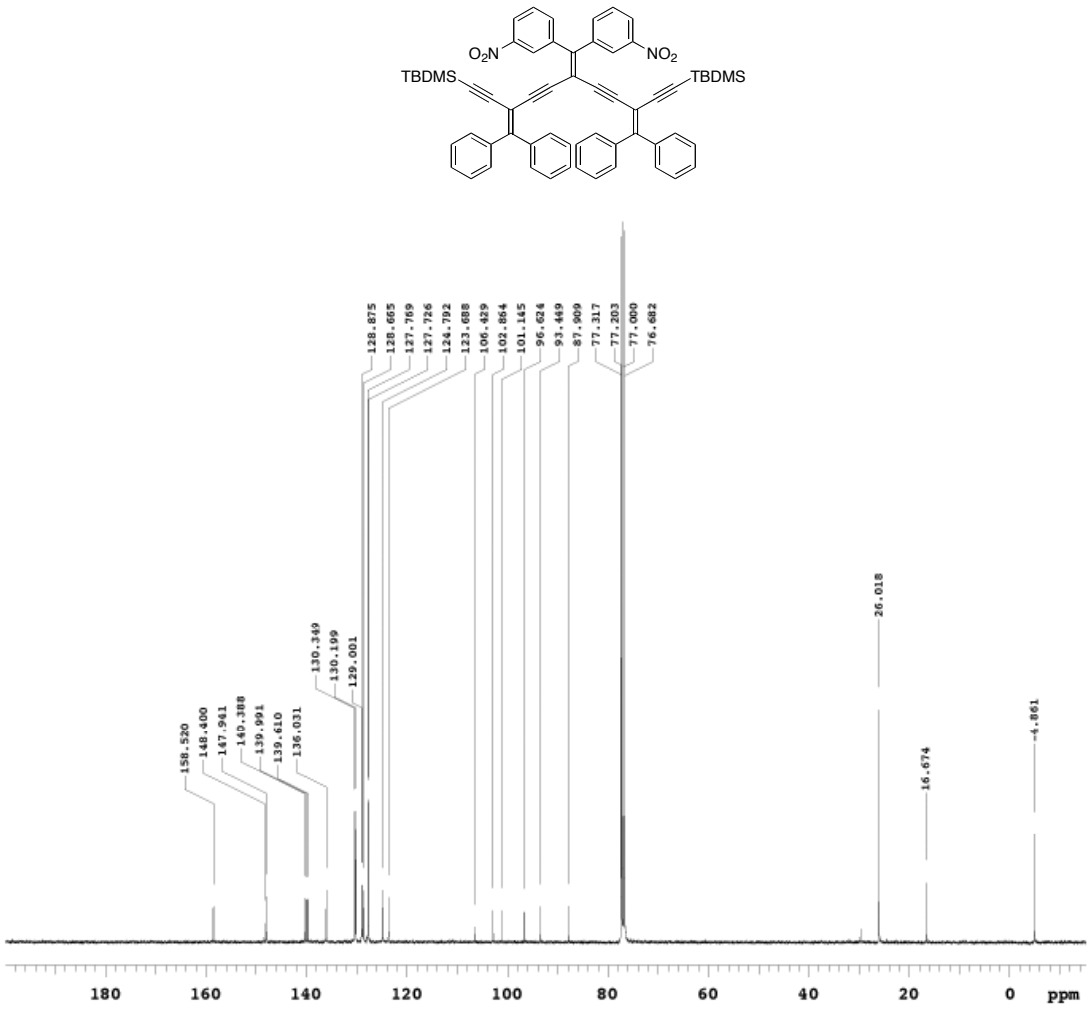

Figure A.17 ^{13}C NMR spectrum of compound **427** ($CDCl_3$)

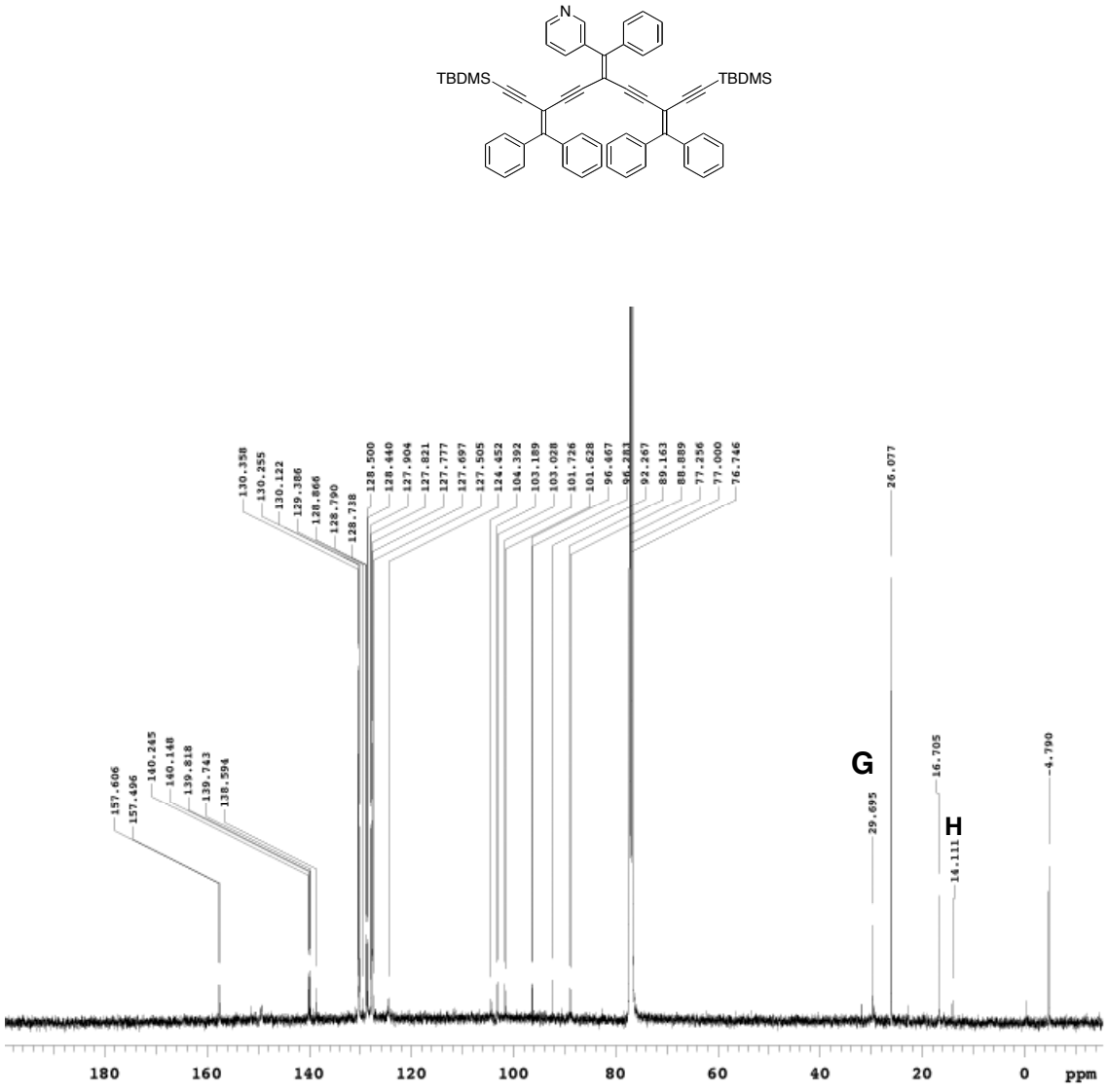

Figure A.18 ^{13}C NMR spectrum of compound **430** ($CDCl_3$)

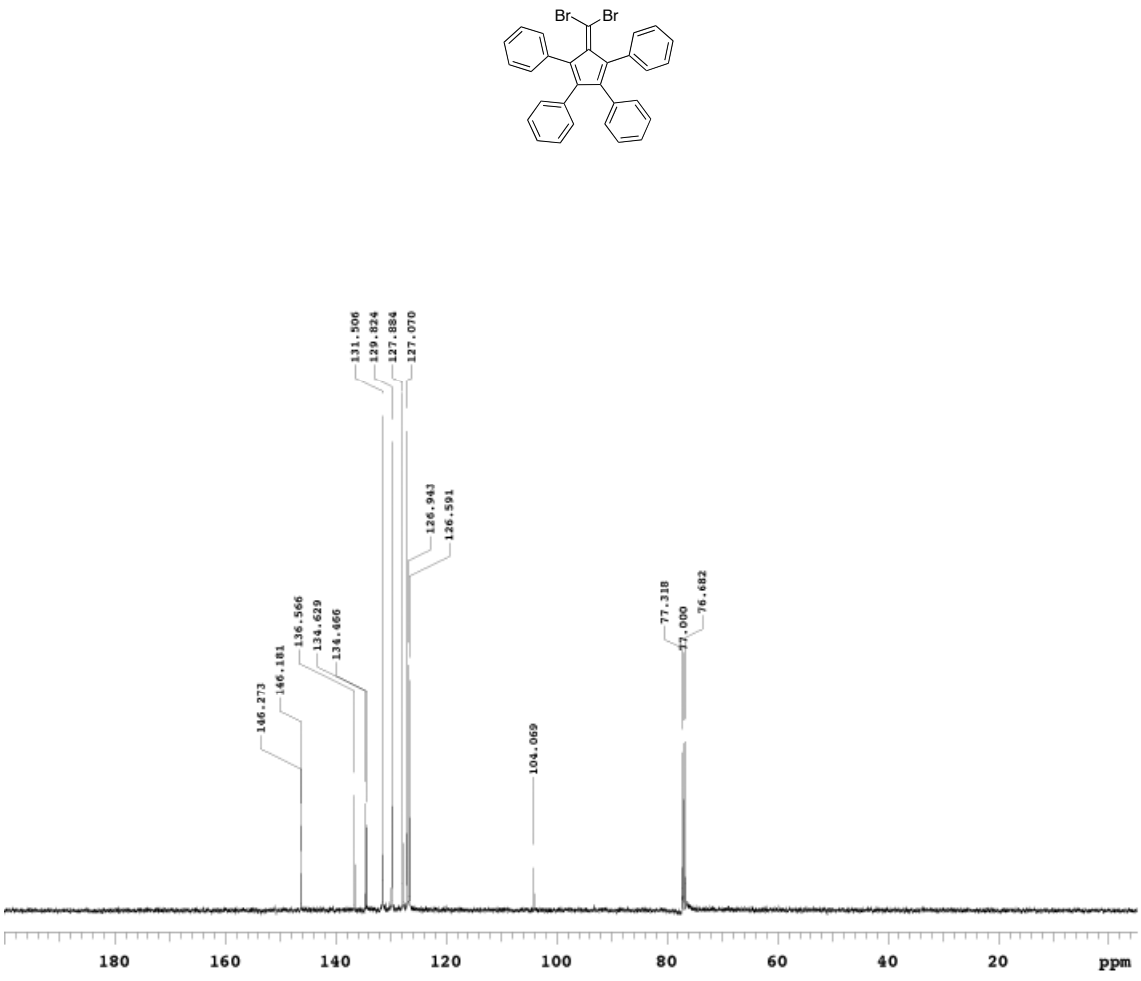

Figure A.19 ^{13}C NMR spectrum of compound **432** ($CDCl_3$)

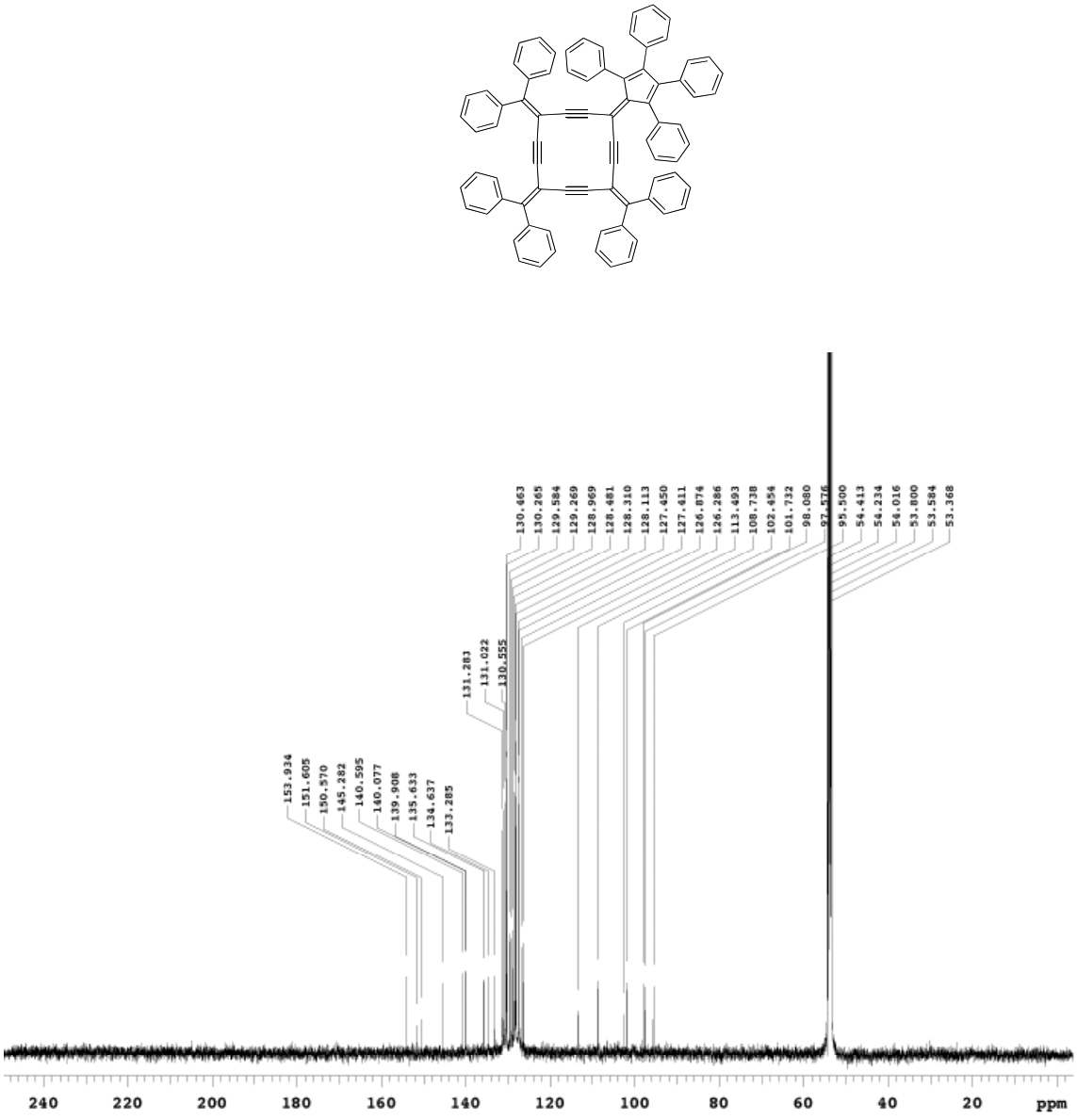

Figure A.20 ^{13}C NMR spectrum of compound **433** (CD_2Cl_2)

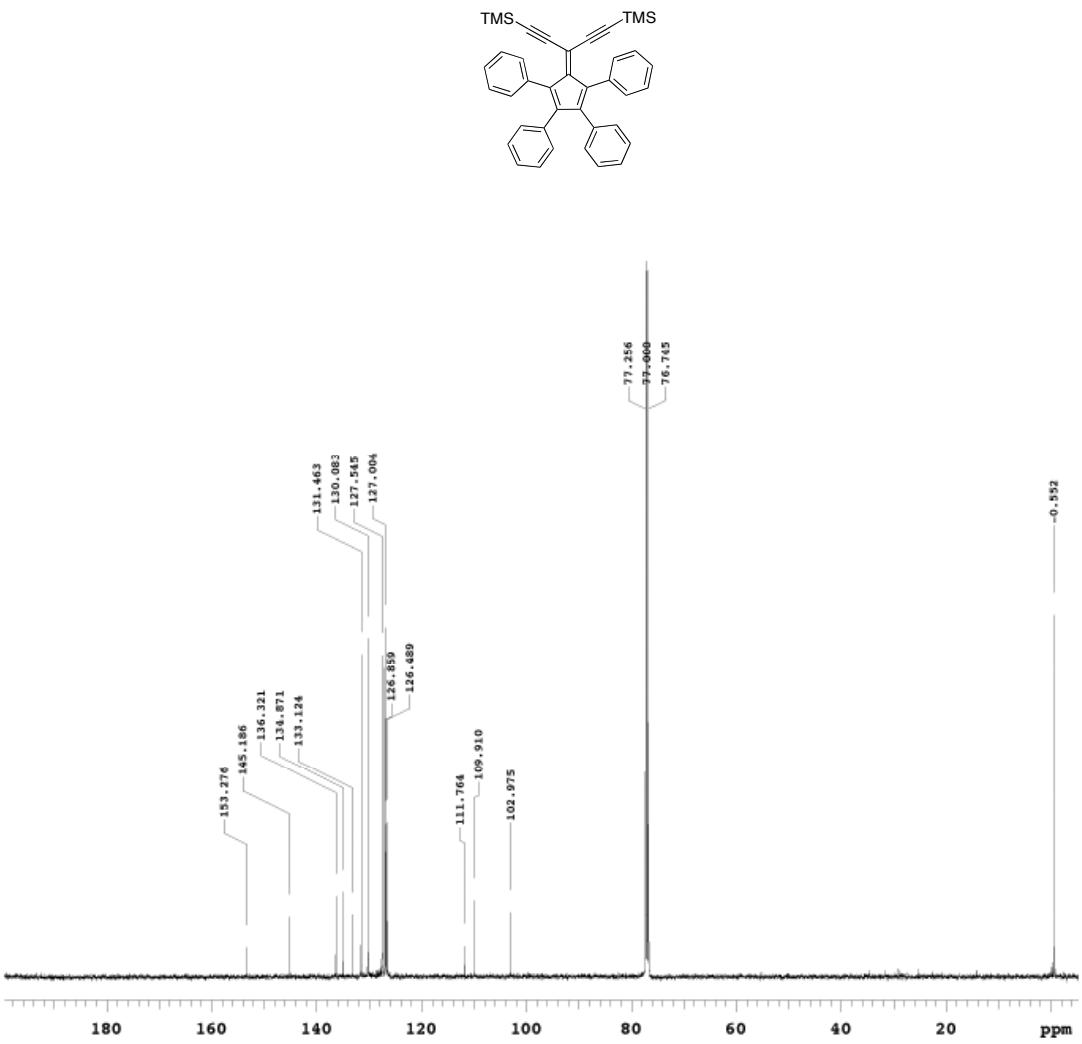

Figure A.21 ^{13}C NMR spectrum of compound **434** ($CDCl_3$)

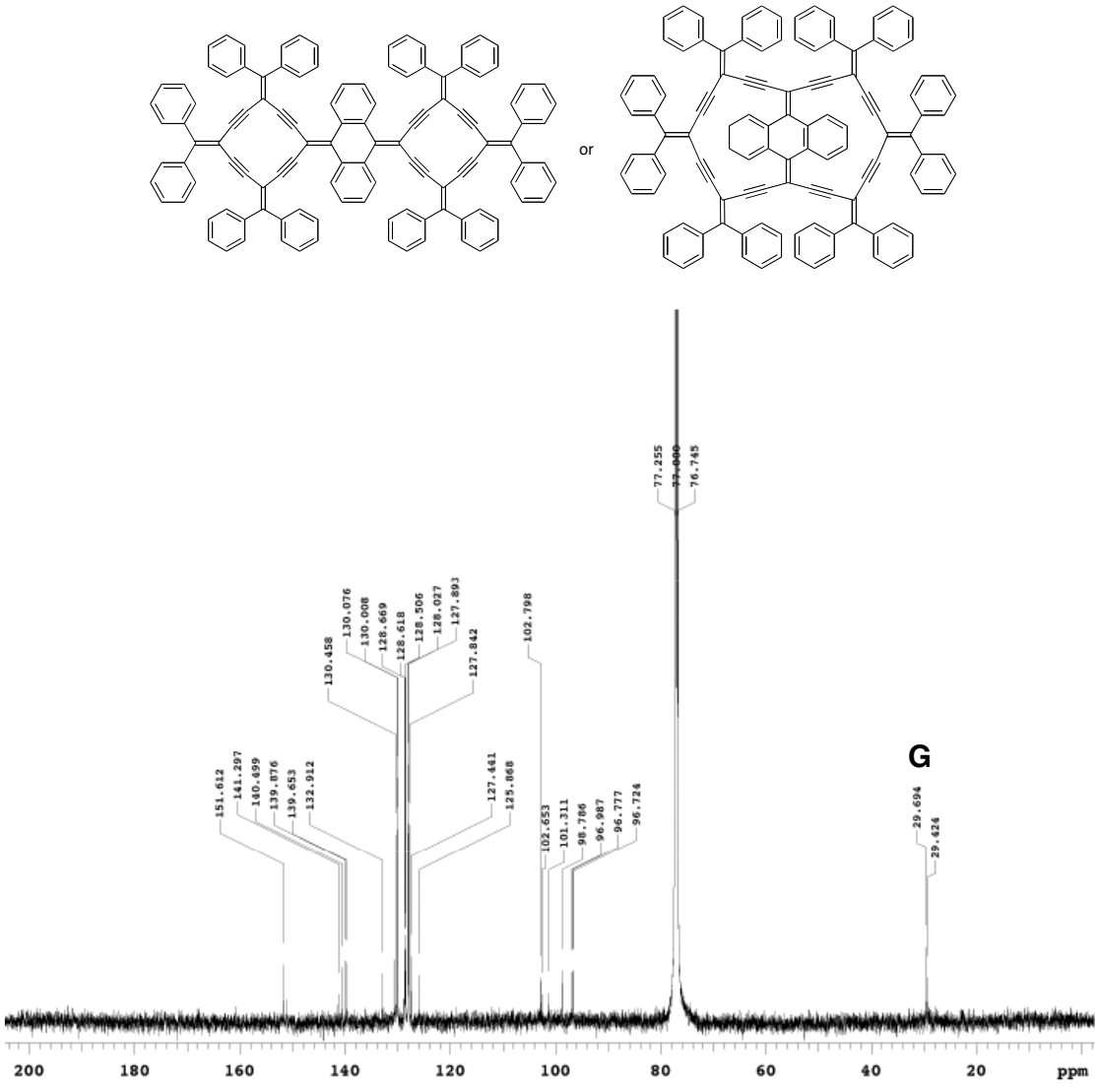

Figure A.22 ^{13}C NMR spectrum of compound **502a** or **502b** ($CDCl_3$)

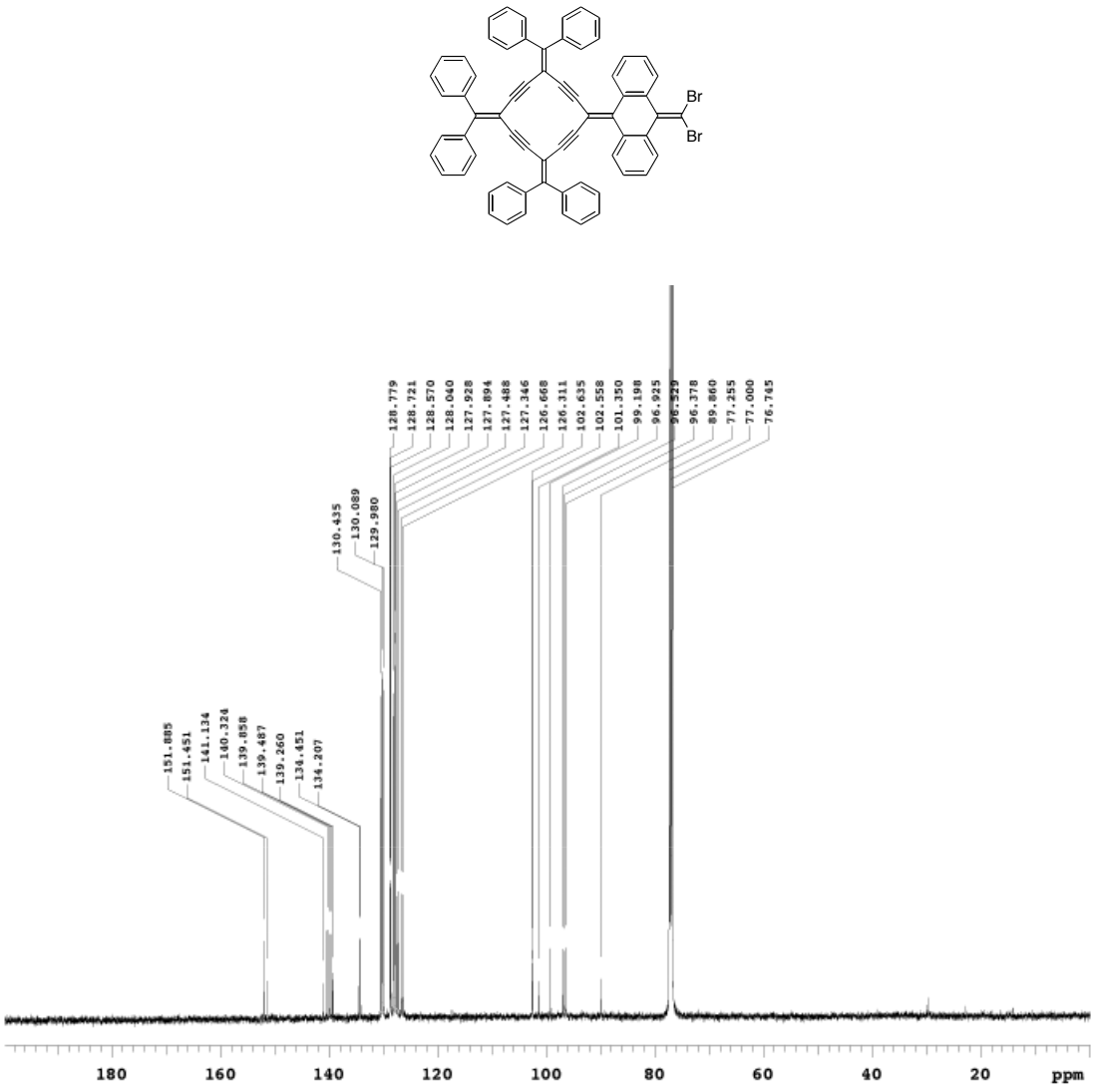

Figure A.23 ^{13}C NMR spectrum of compound **502C** ($CDCl_3$)

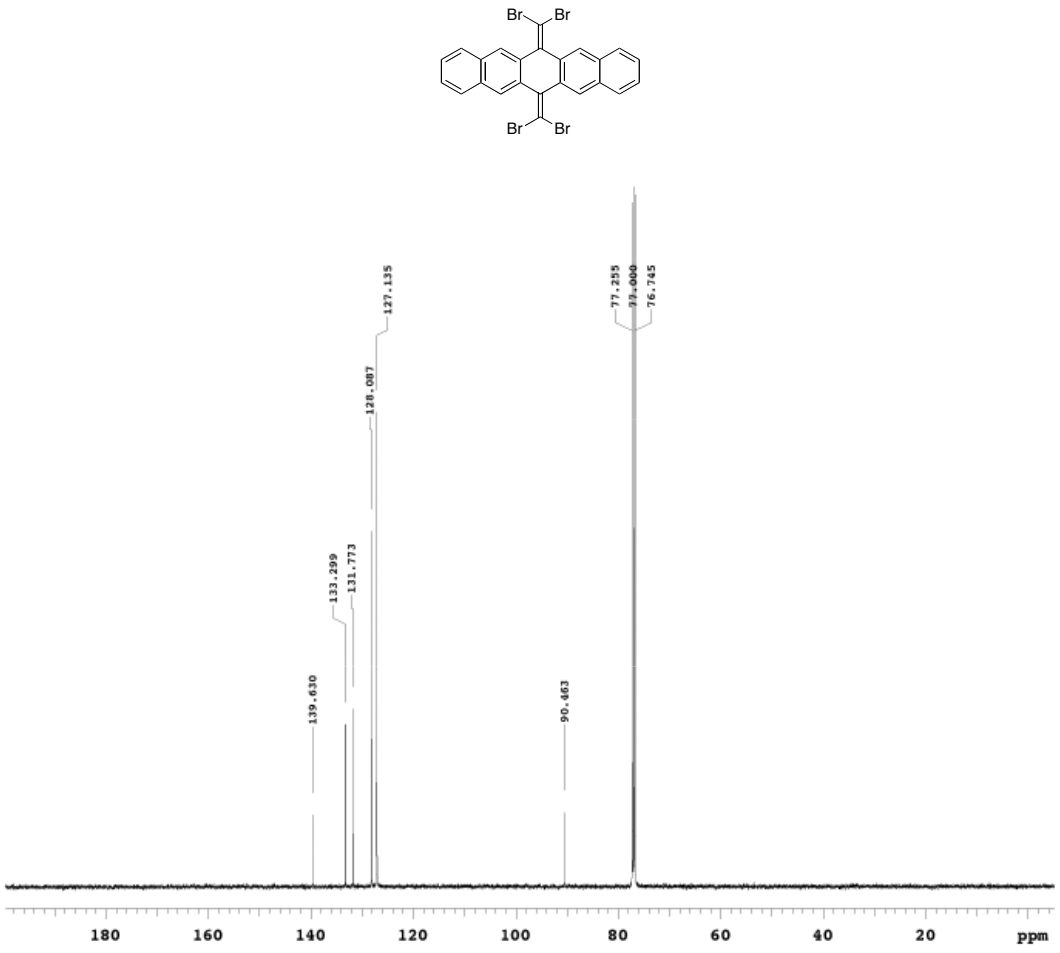

Figure A.24 ^{13}C NMR spectrum of compound **503** ($CDCl_3$)

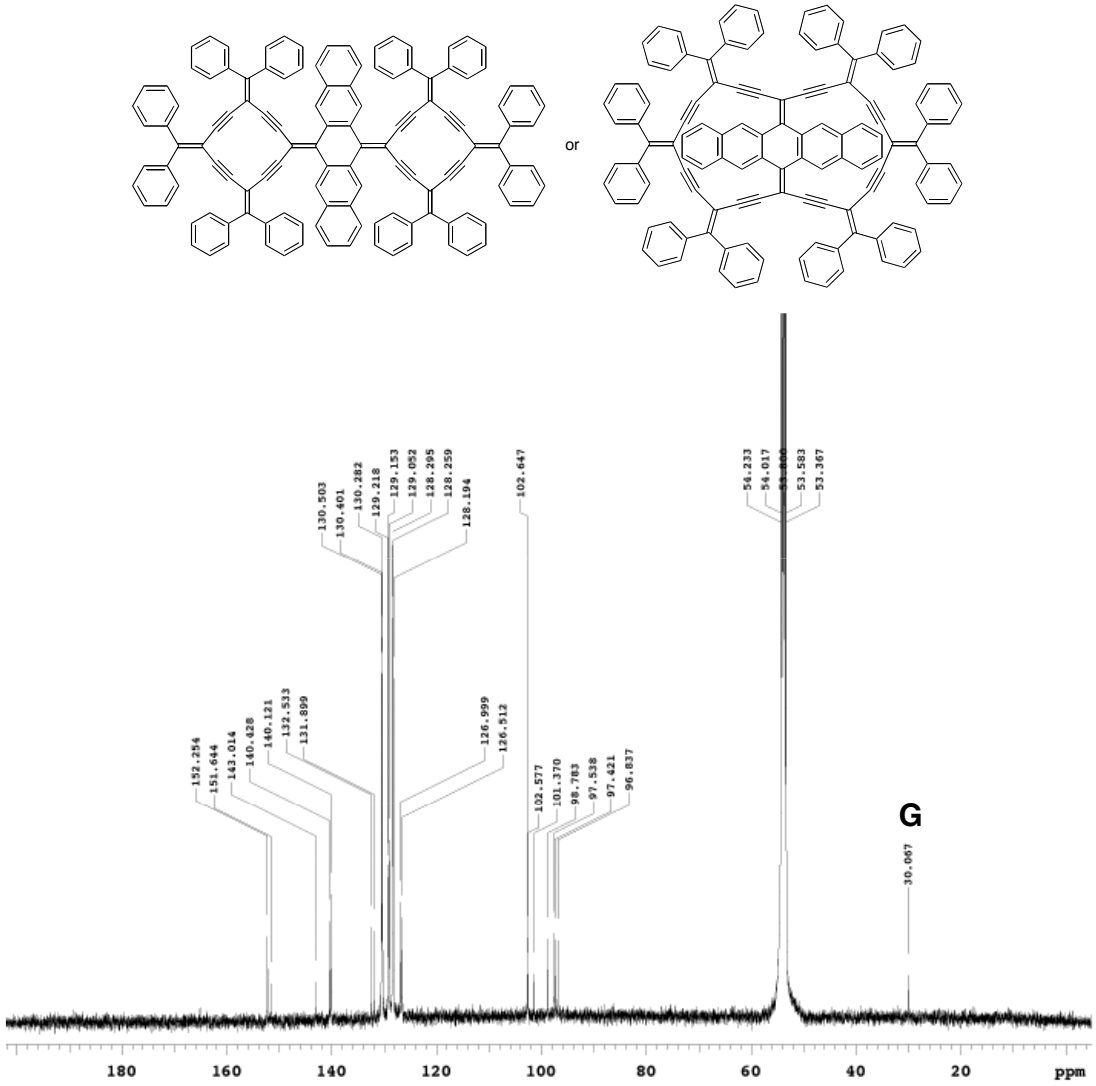

Figure A.25 ^{13}C NMR spectrum of compound **504** (CD_2Cl_2)

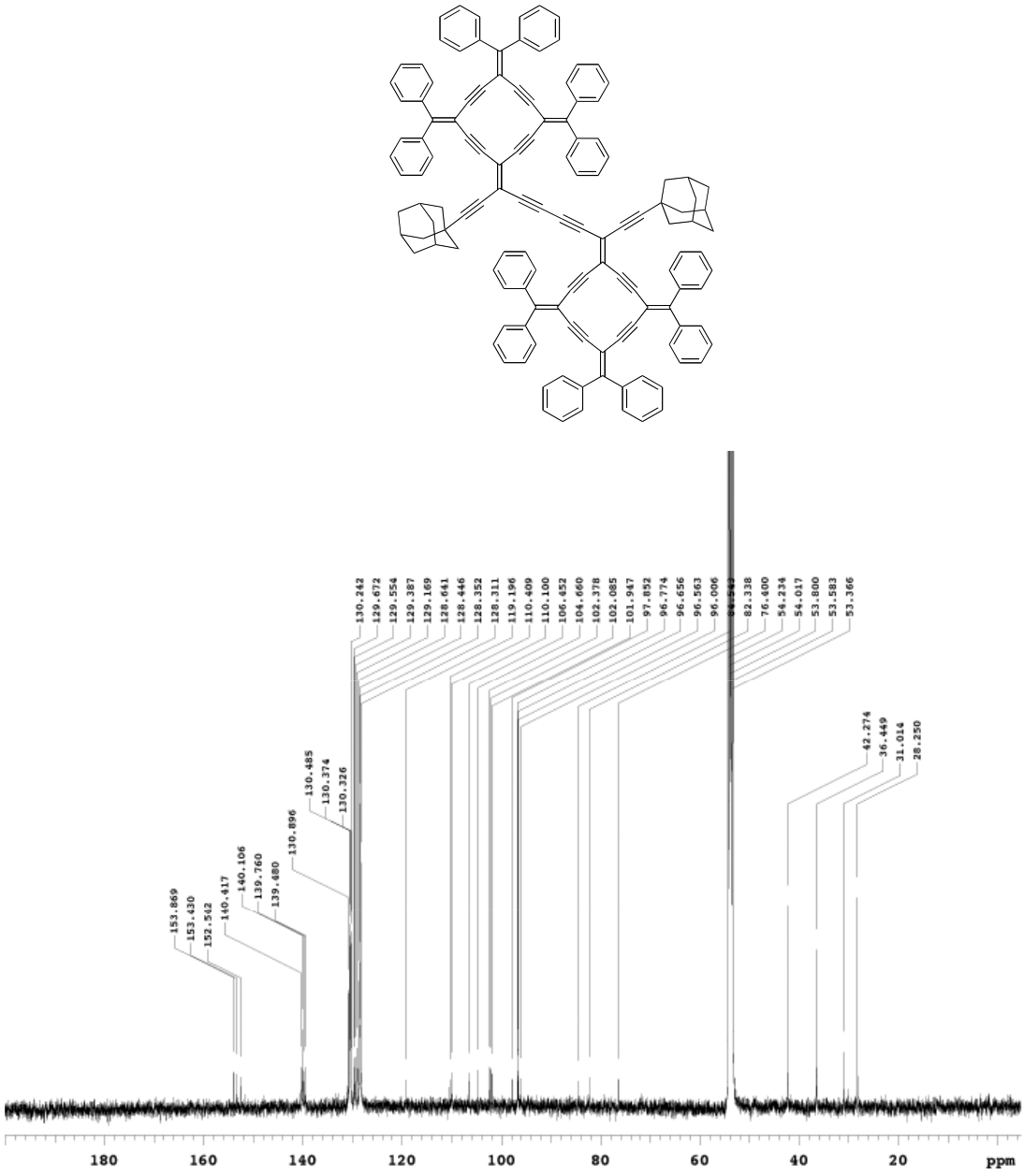

Figure A.26 ^{13}C NMR spectrum of compound **507** (CD_2Cl_2)

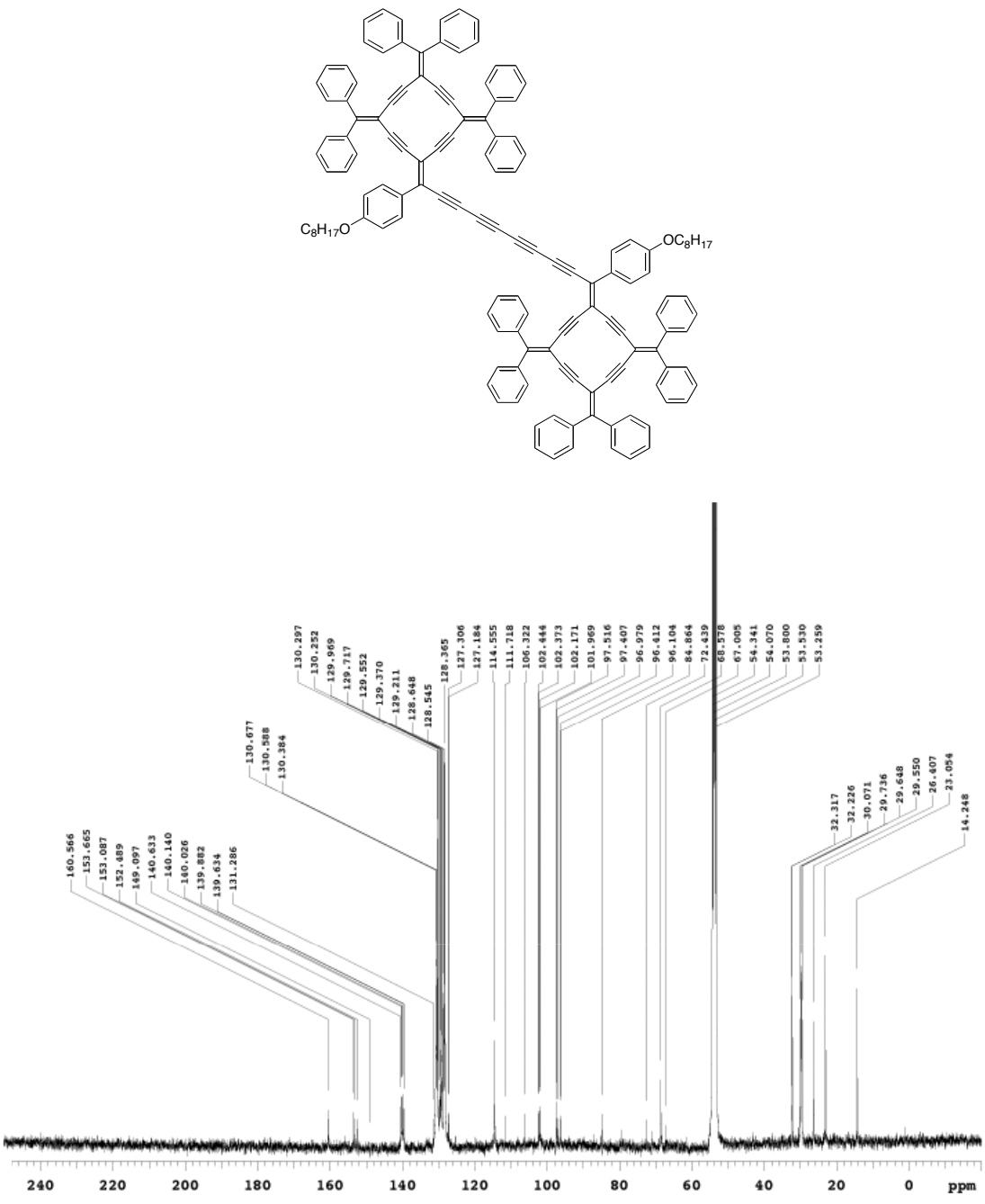

Figure A.27 ^{13}C NMR spectrum of compound **508** (CD_2Cl_2)

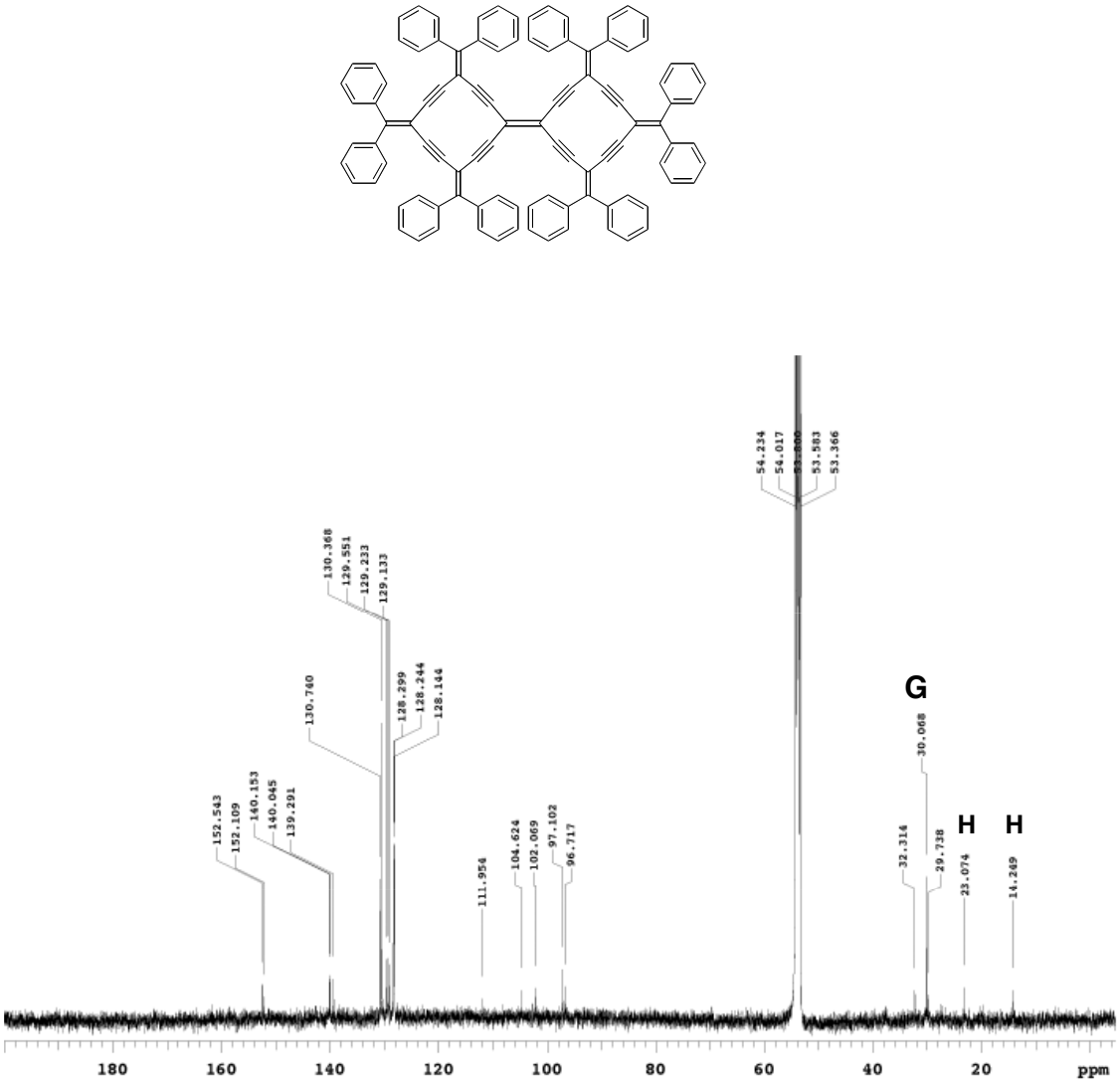

Figure A.28 ^{13}C NMR spectrum of compound **315a** (CD_2Cl_2)

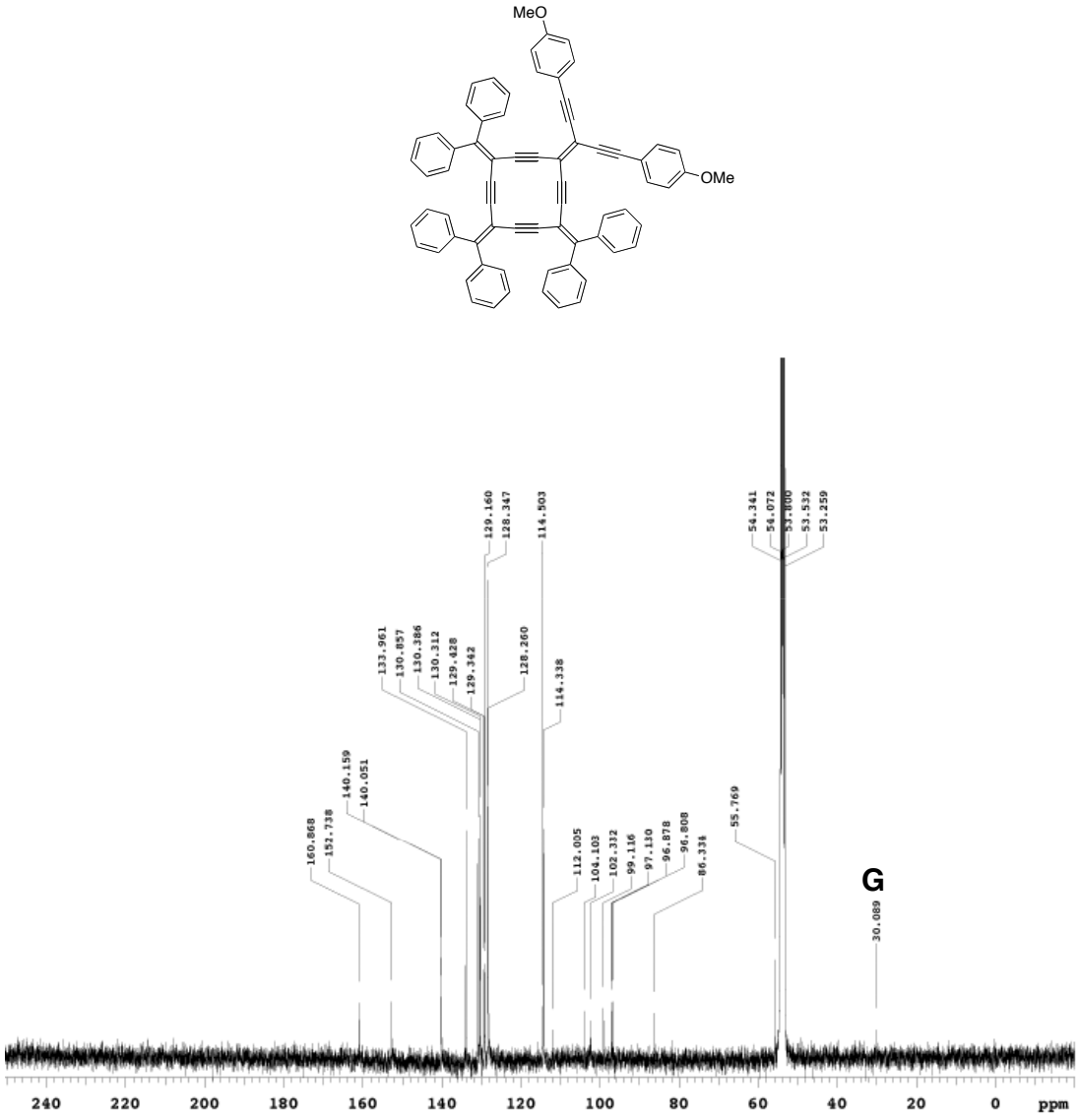

Figure A.29 ^{13}C NMR spectrum of compound **510** (CD_2Cl_2)

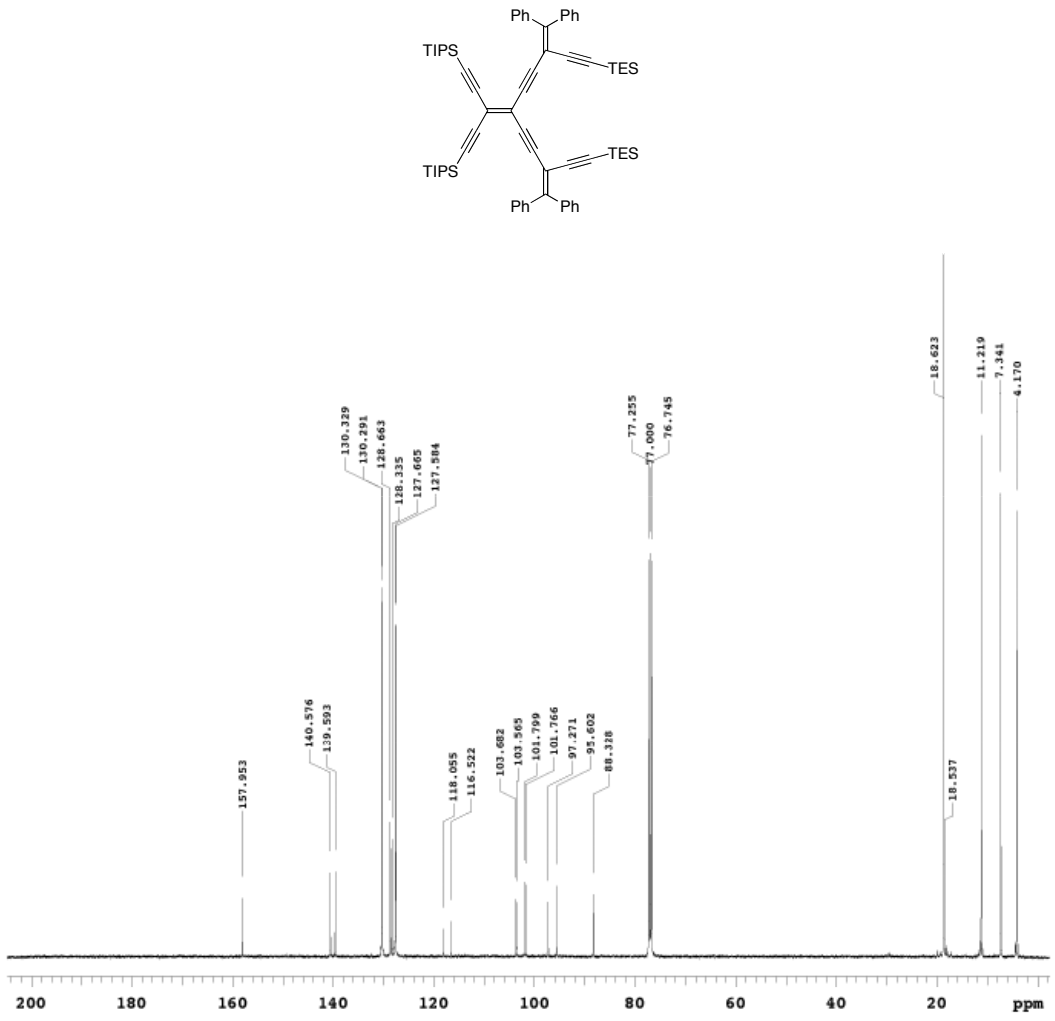

Figure A.30 ^{13}C NMR spectrum of compound **514a** ($CDCl_3$)

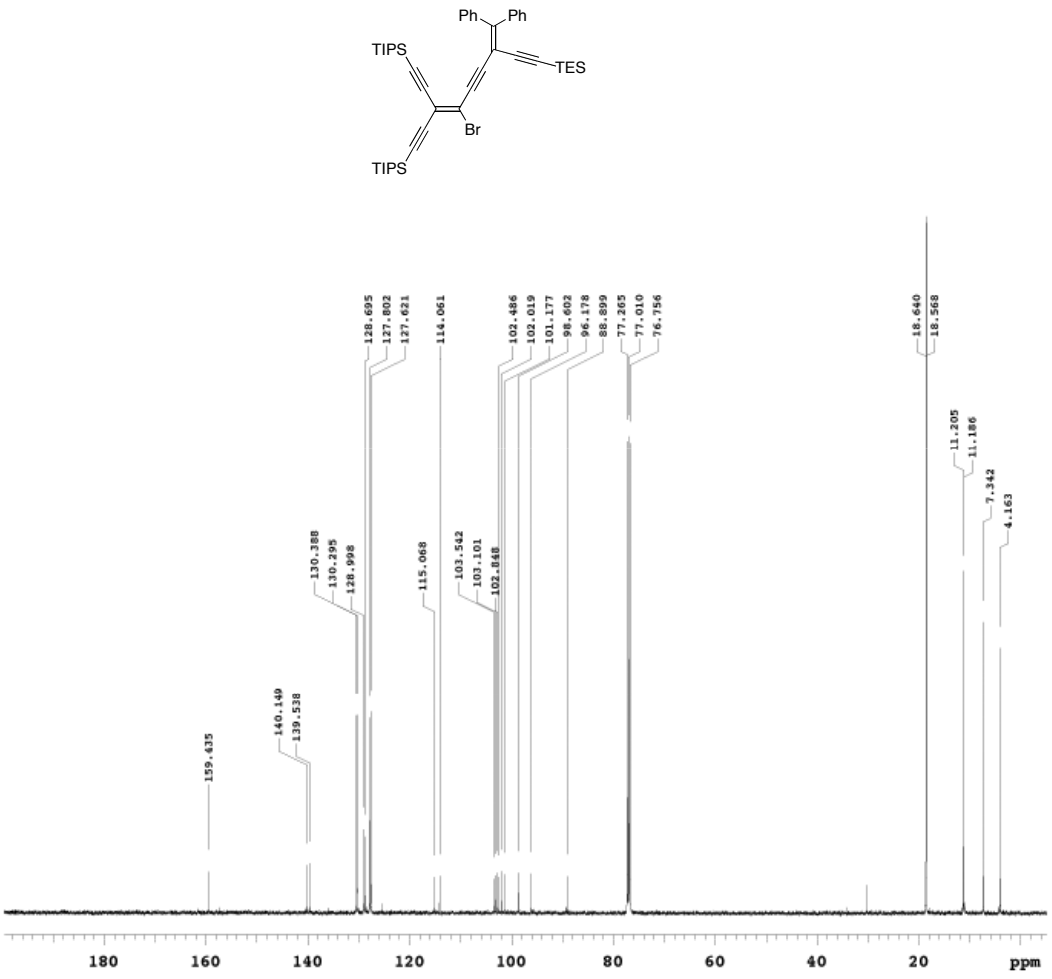

Figure A.31 ^{13}C NMR spectrum of compound **514b** ($CDCl_3$)

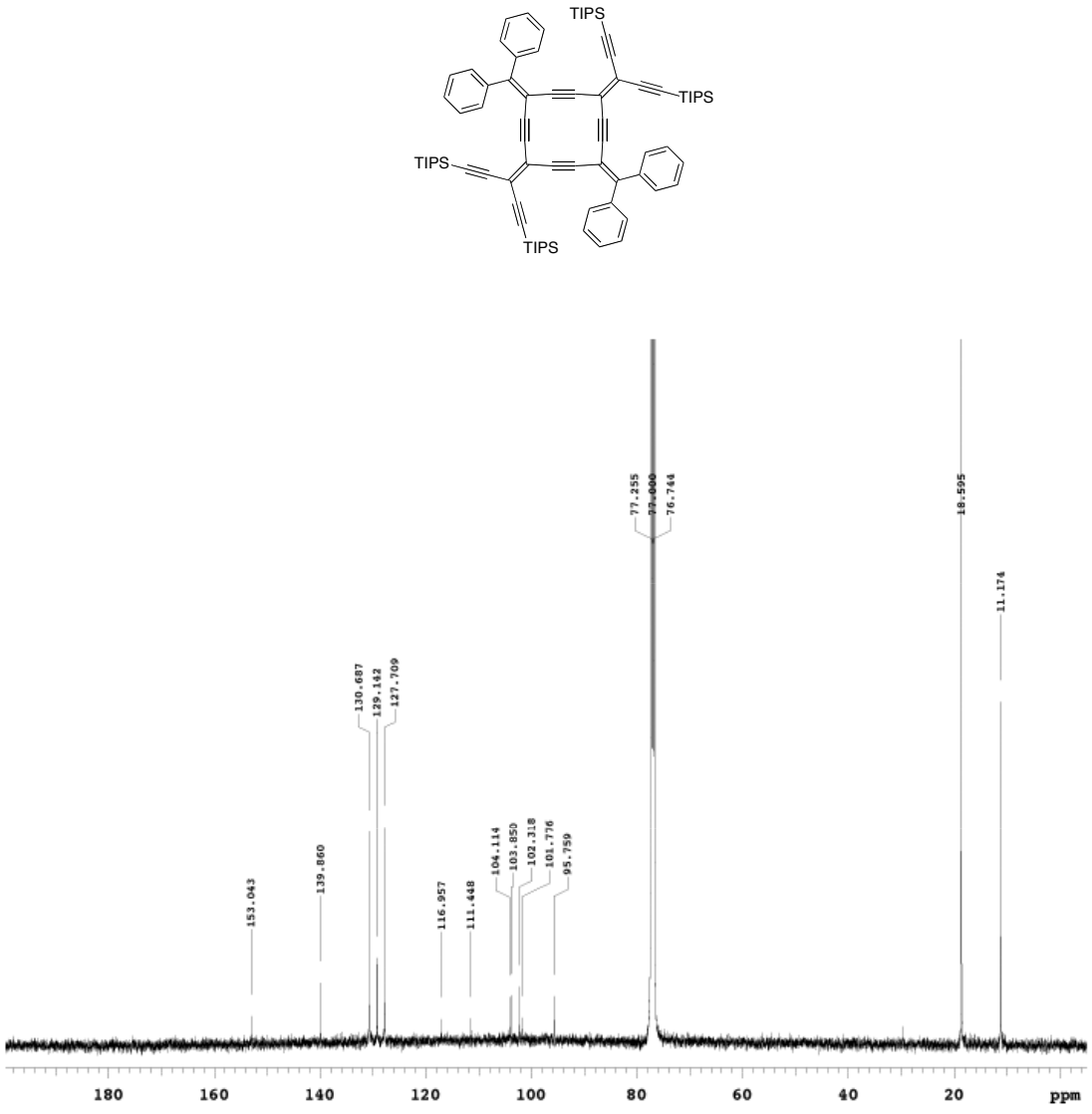

Figure A.32 ^{13}C NMR spectrum of compound **515** ($CDCl_3$)

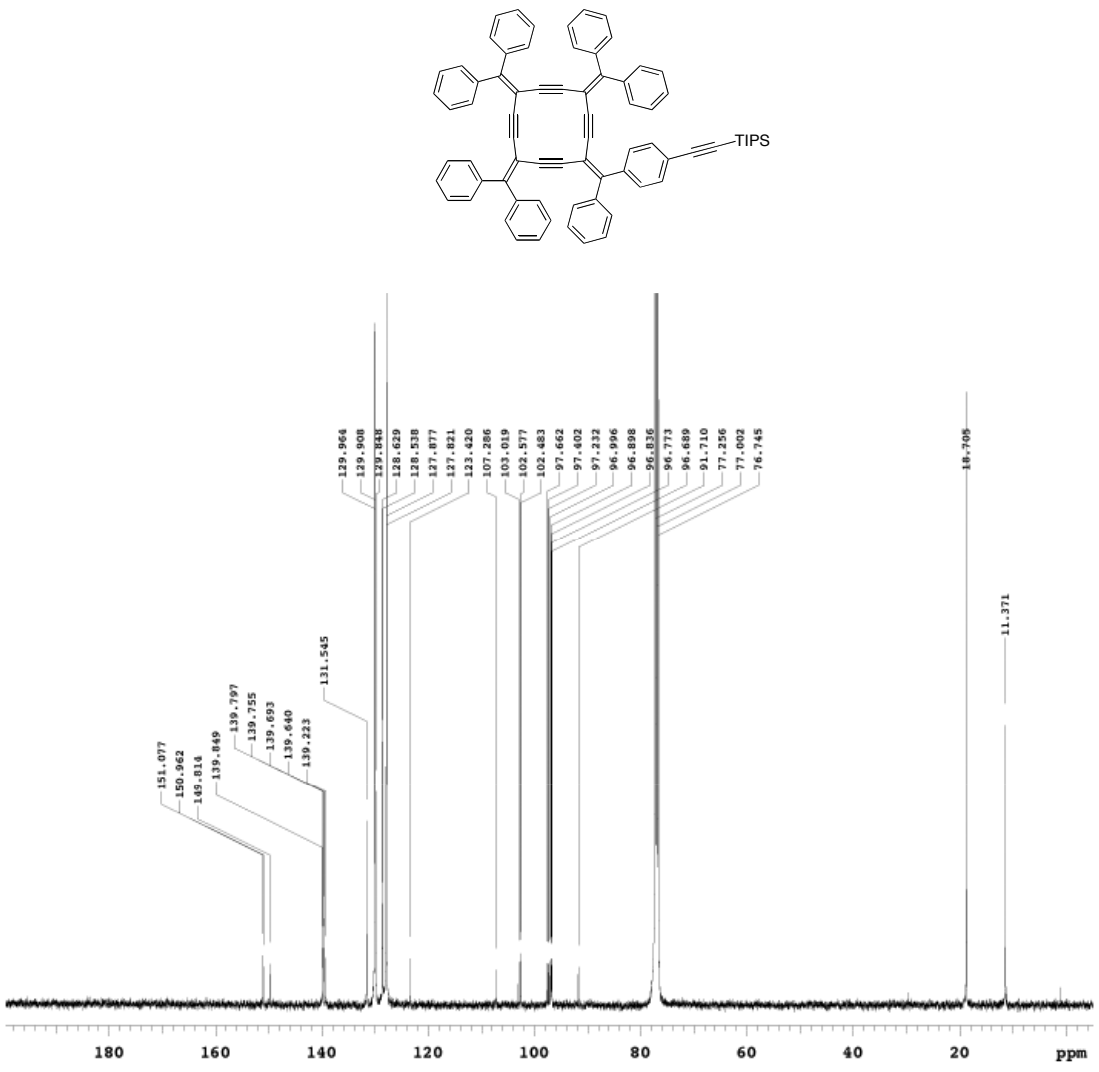

Figure A.33 ^{13}C NMR spectrum of compound **519** ($CDCl_3$)

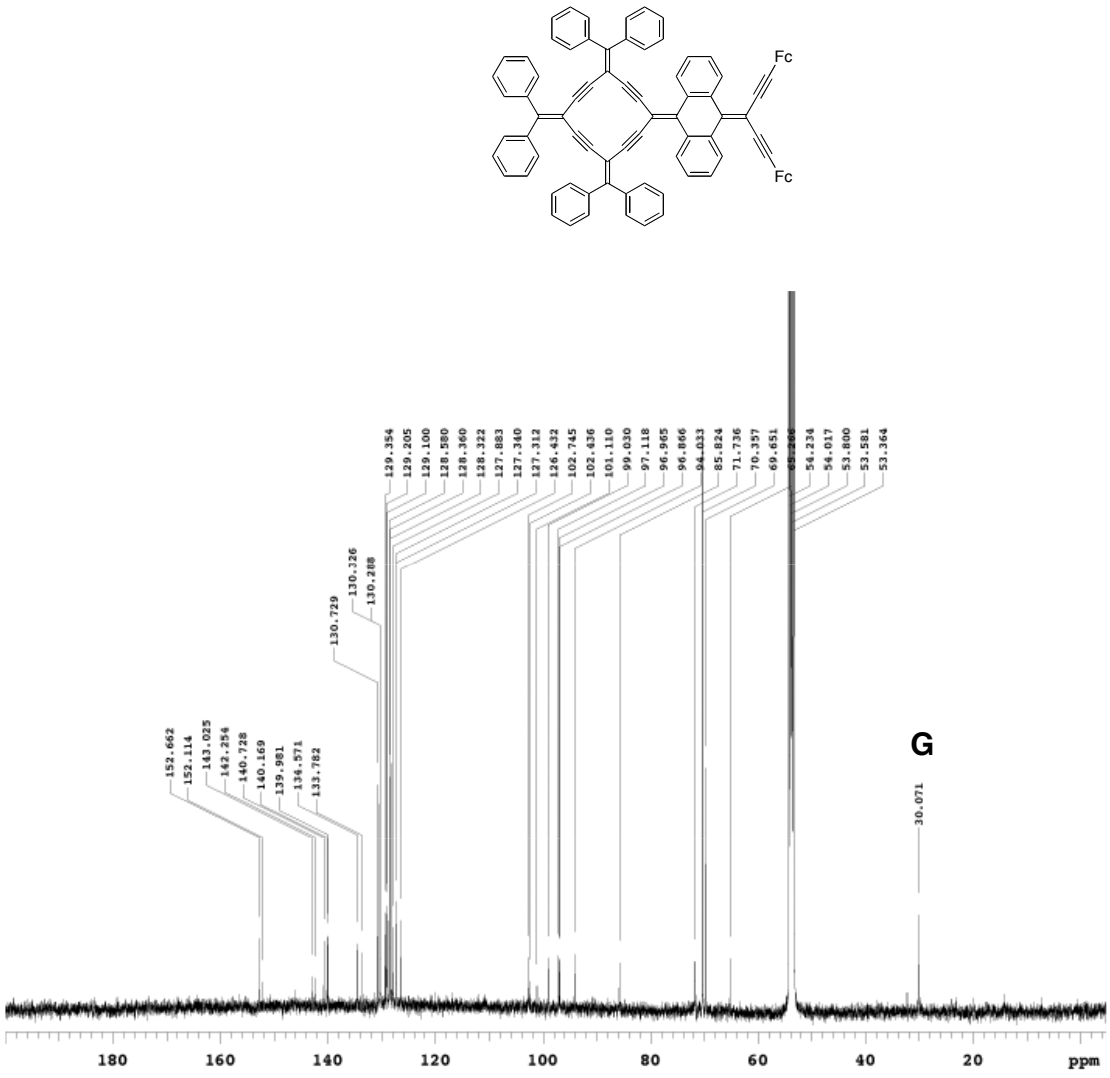

Figure A.34 ^{13}C NMR spectrum of compound **522** (CD_2Cl_2)

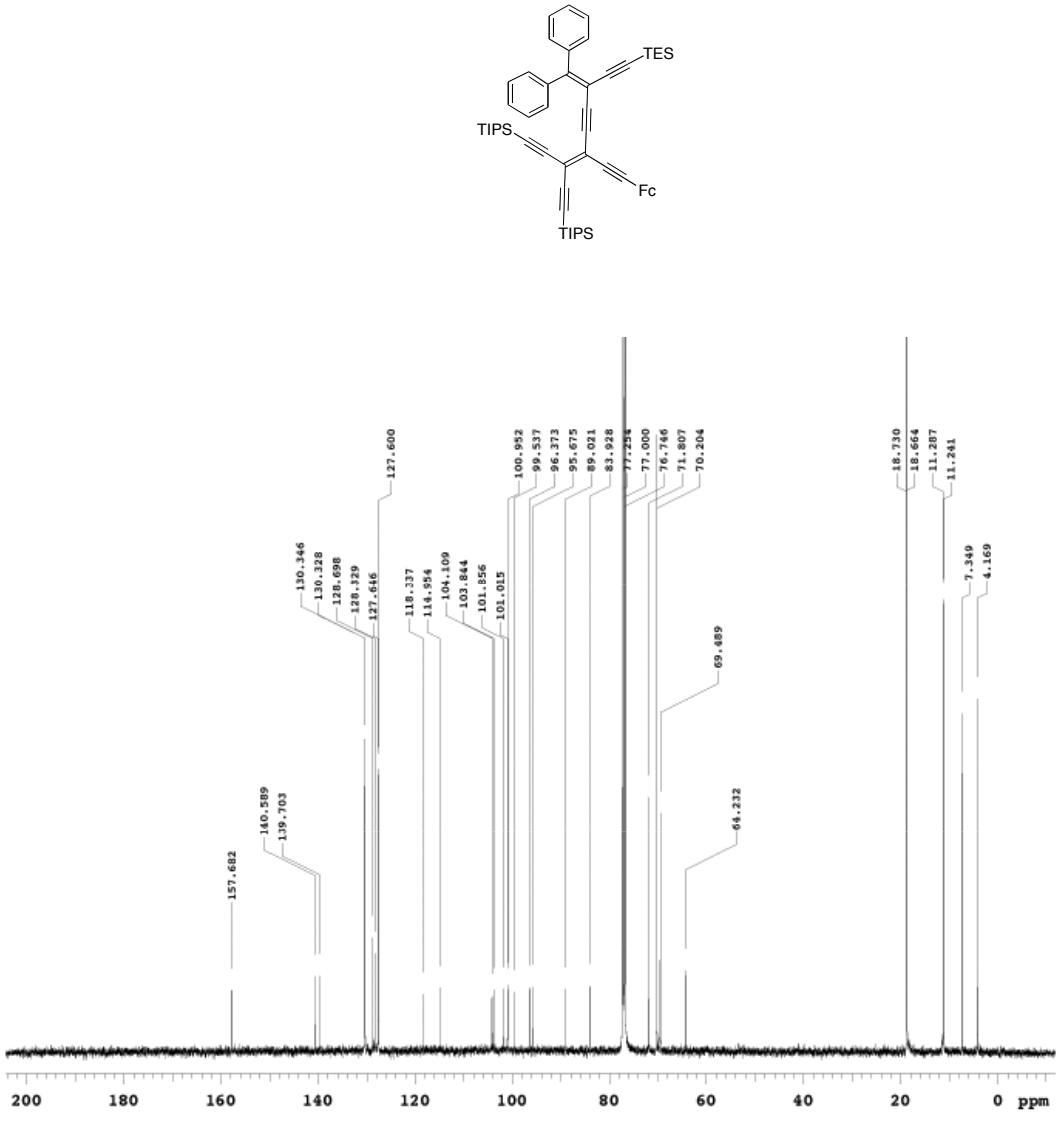

Figure A.35 ^{13}C NMR spectrum of compound **524** ($CDCl_3$)

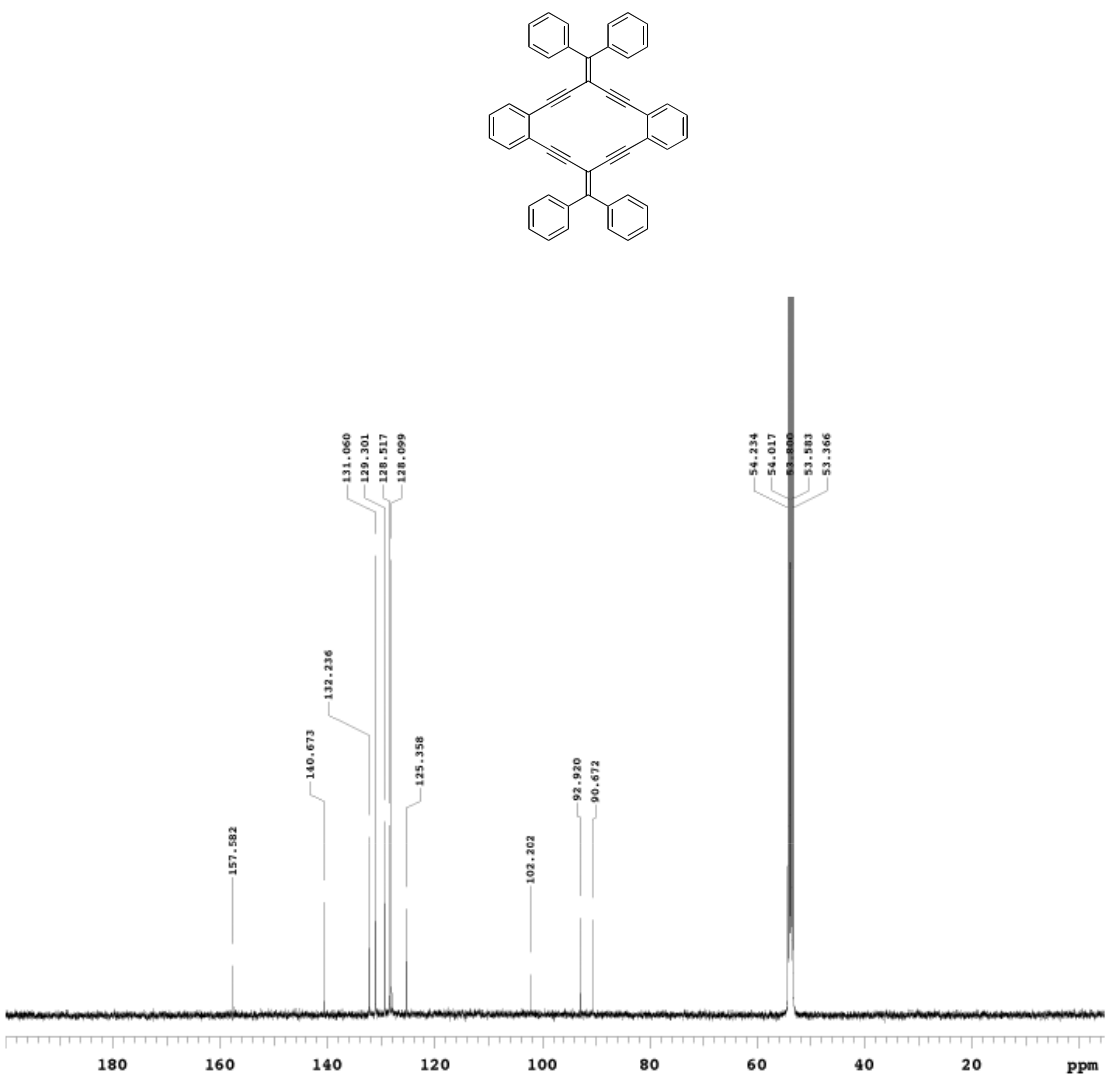

Figure A.35 ^{13}C NMR spectrum of compound **526** (CD_2Cl_2)

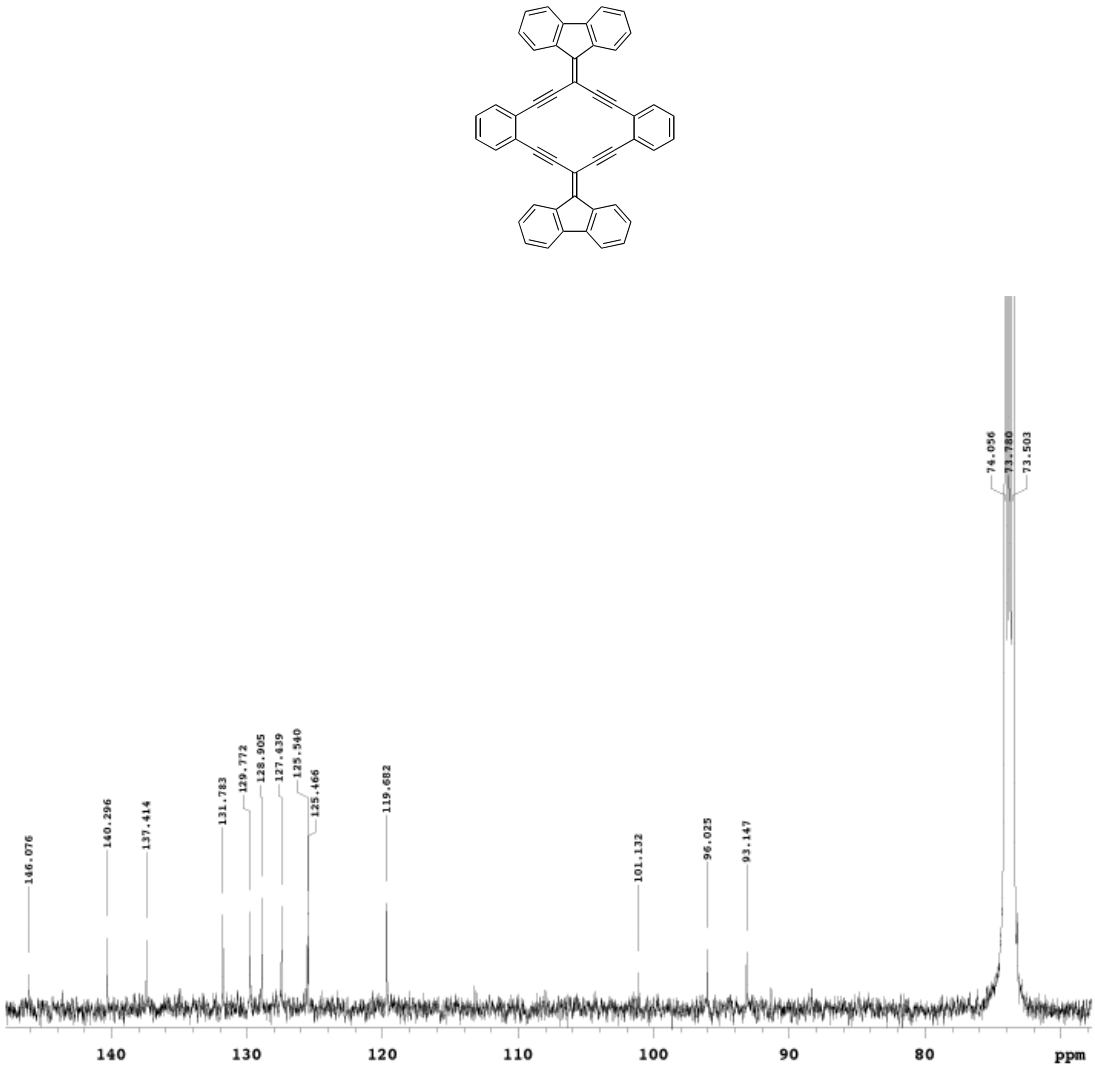

Figure A.36 Expanded ^{13}C NMR spectrum of compound **528** ($C_2D_2Cl_4$ at 65 °C)

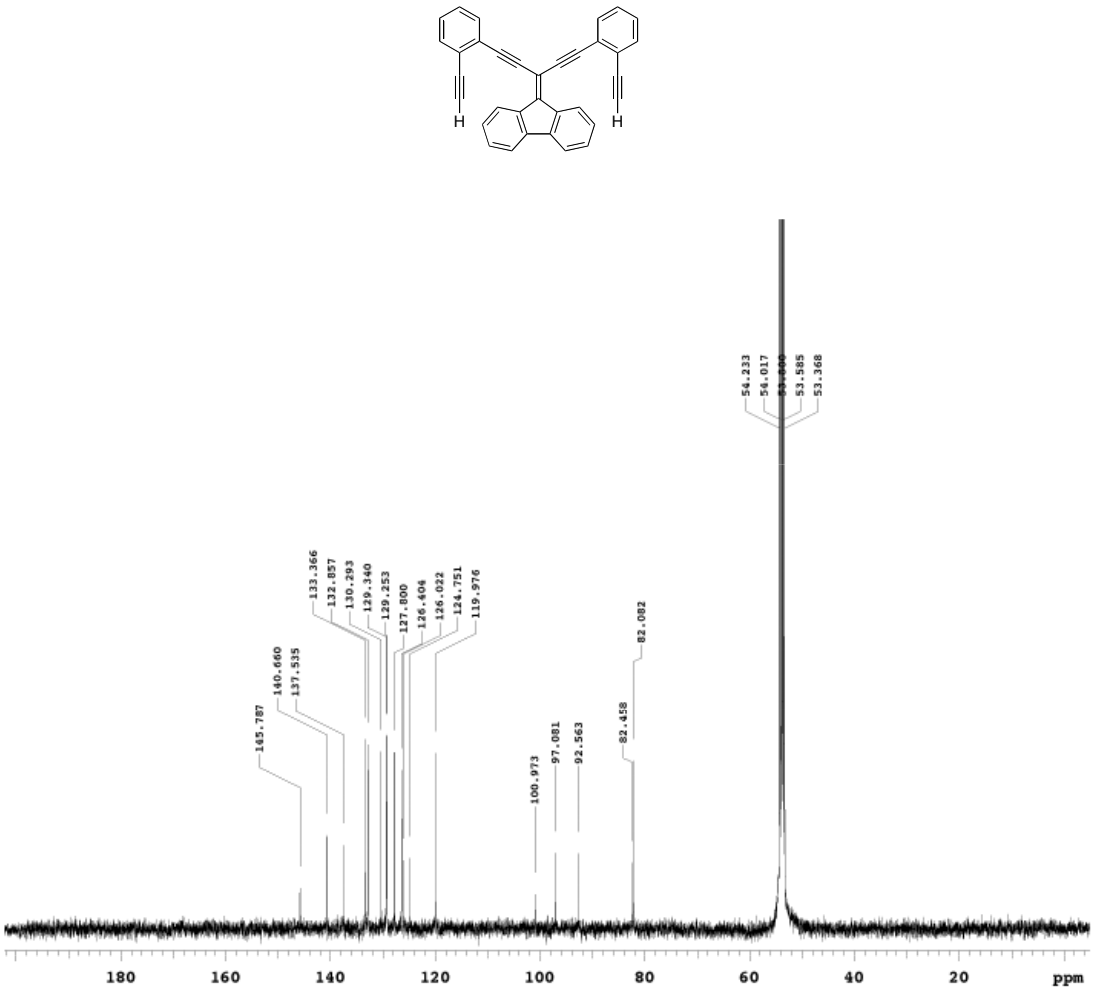

Figure A.36 ^{13}C NMR spectrum of compound **532** (CD_2Cl_2)

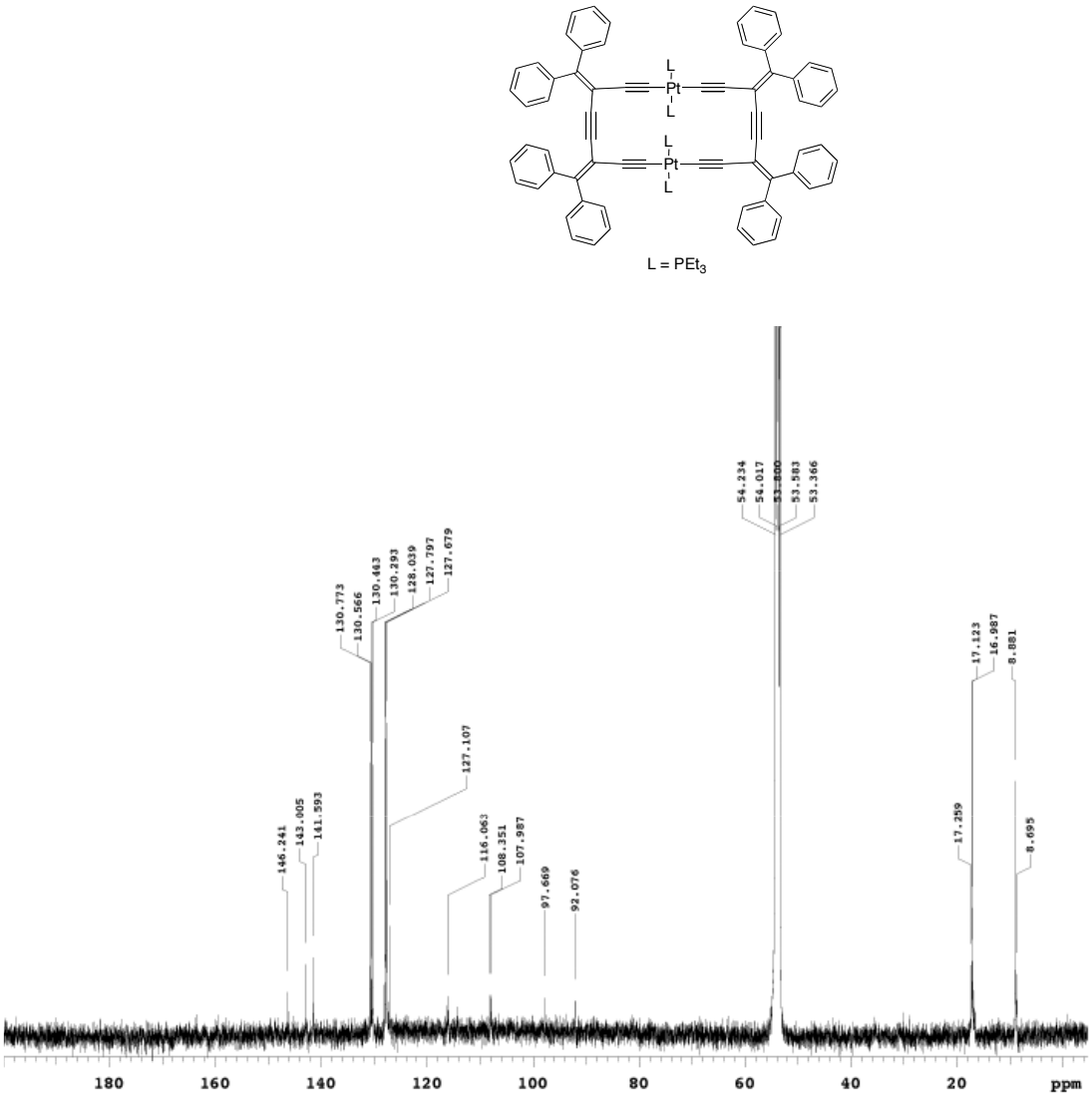

Figure A.37 ^{13}C NMR spectrum for compound **606** (CD_2Cl_2)

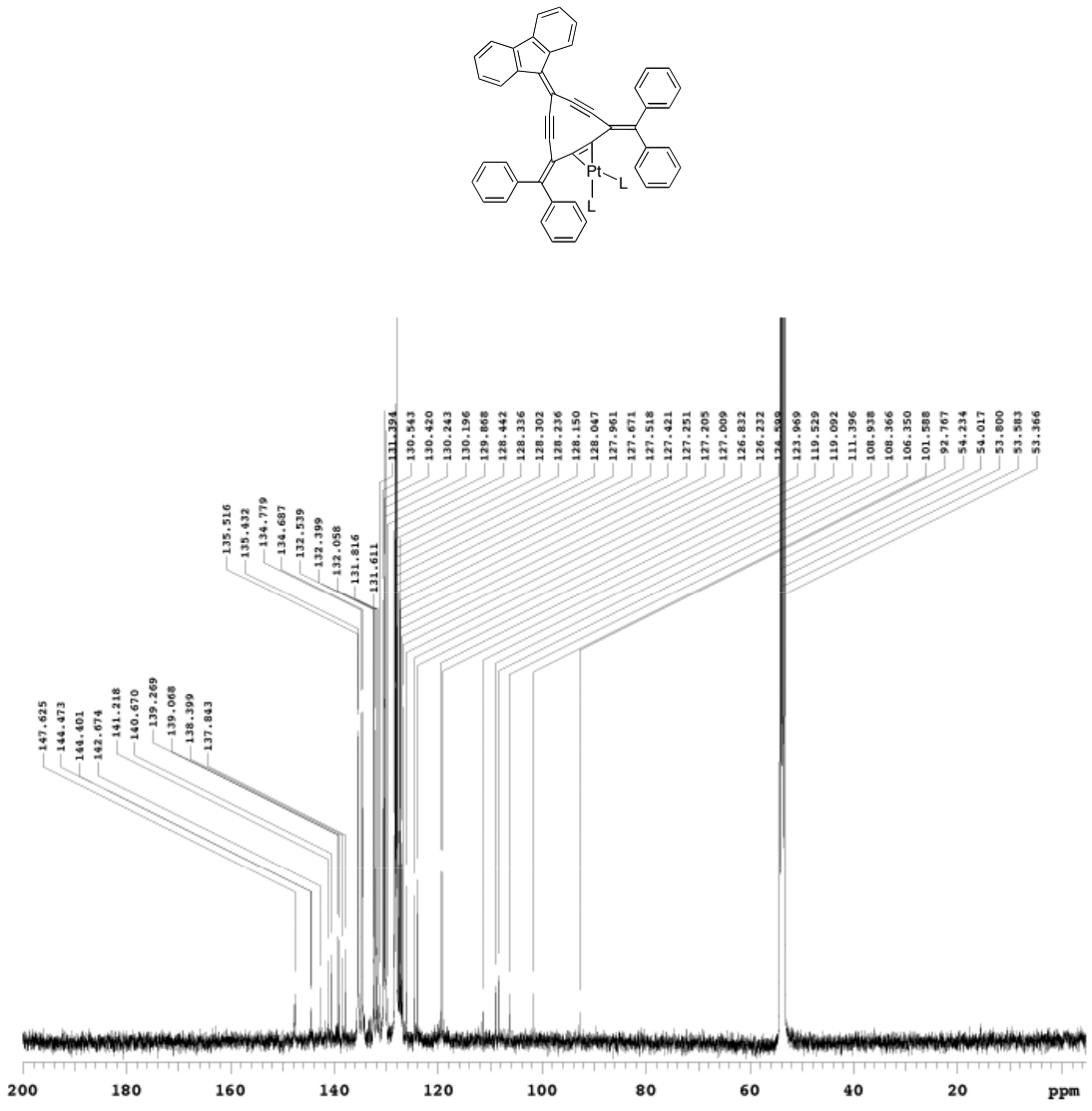

Figure A.38a ^{13}C NMR spectrum for proposed structure **609** (CD_2Cl_2)

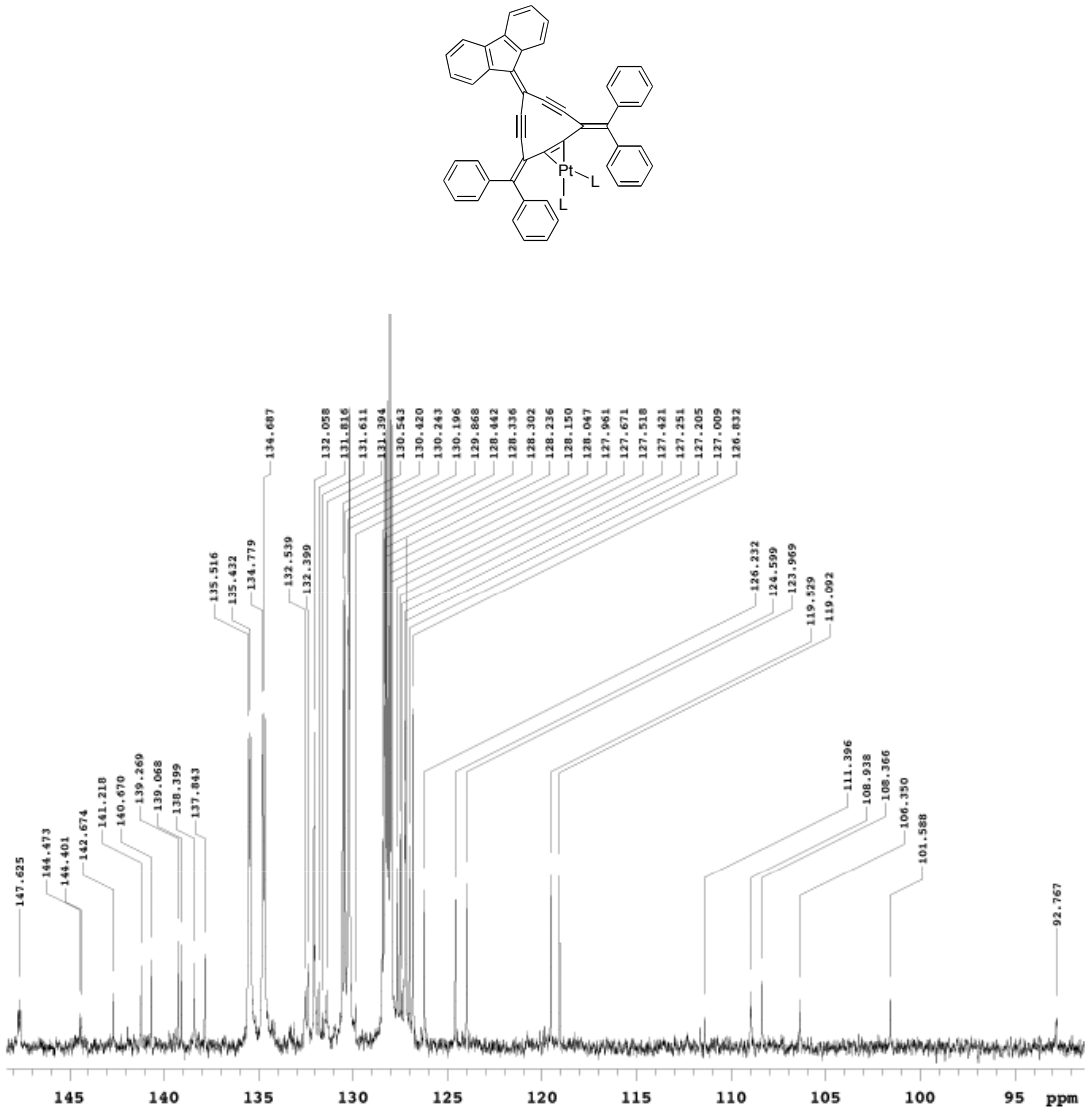

Figure A.38b Expanded ^{13}C NMR spectrum for proposed structure **609** (CD_2Cl_2)

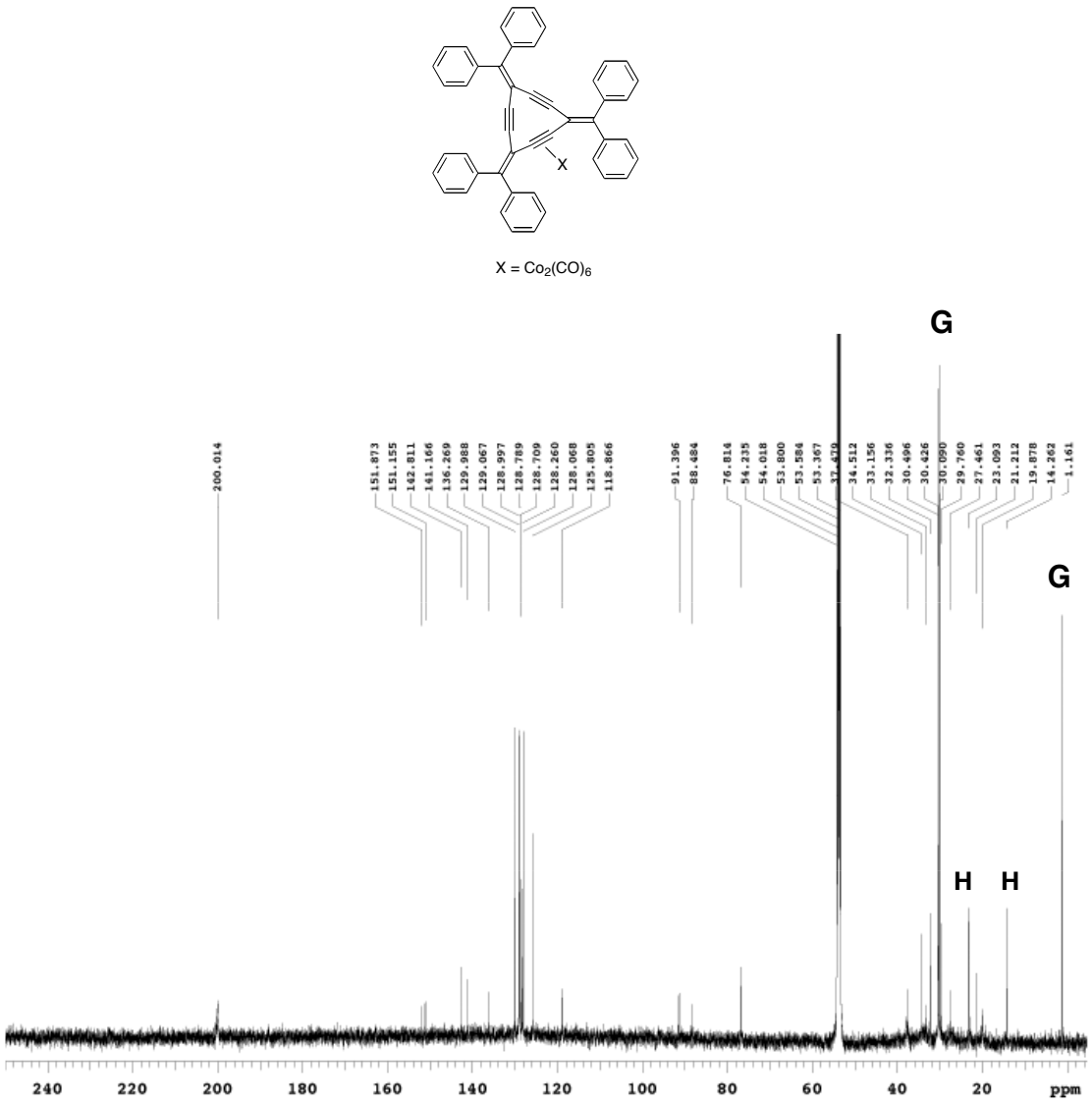

Figure A.39a ^{13}C NMR spectrum for proposed structure **610** (CD_2Cl_2)

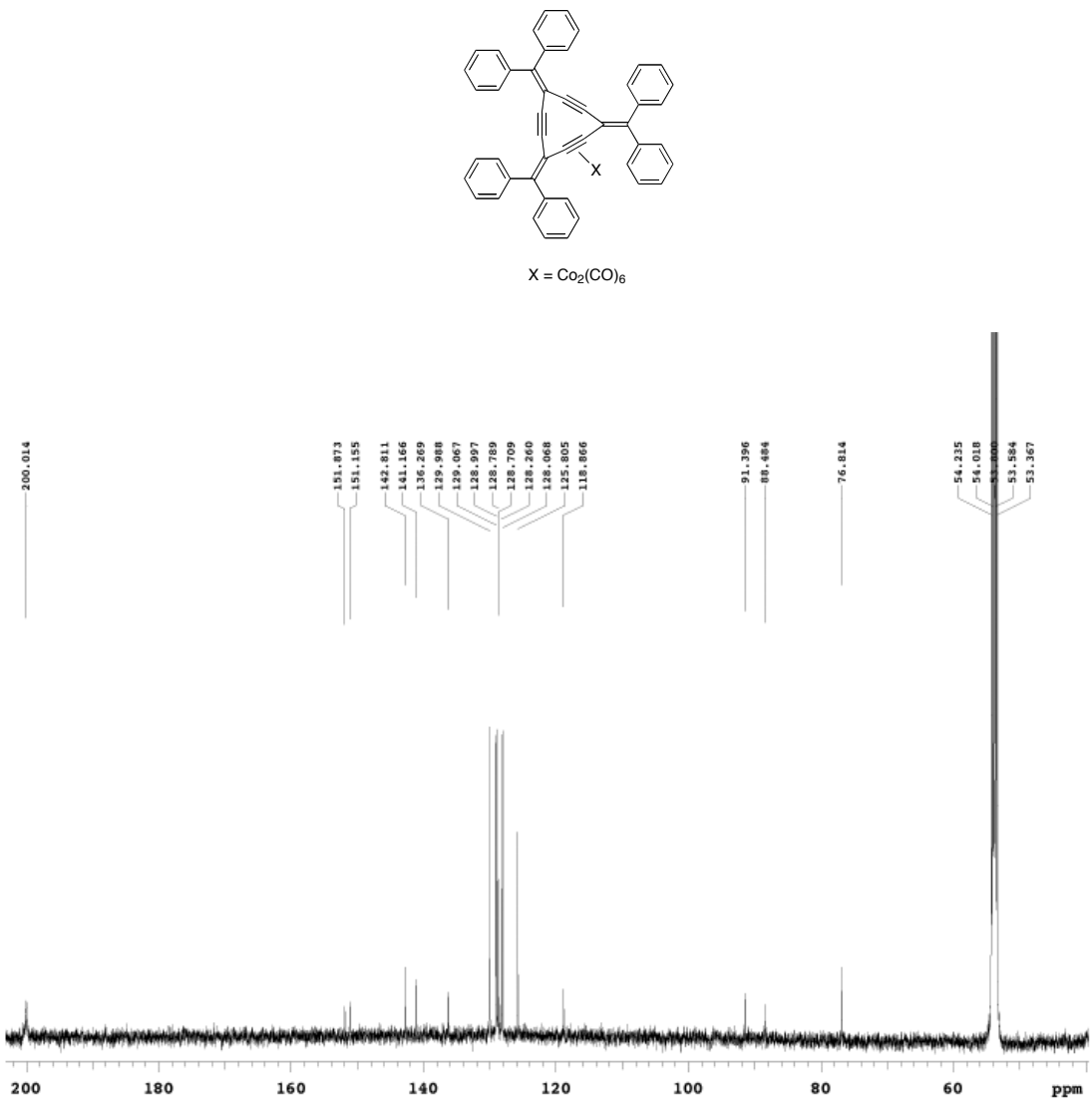

Figure A.39b Expanded ^{13}C NMR spectrum for proposed structure **610** (CD_2Cl_2)

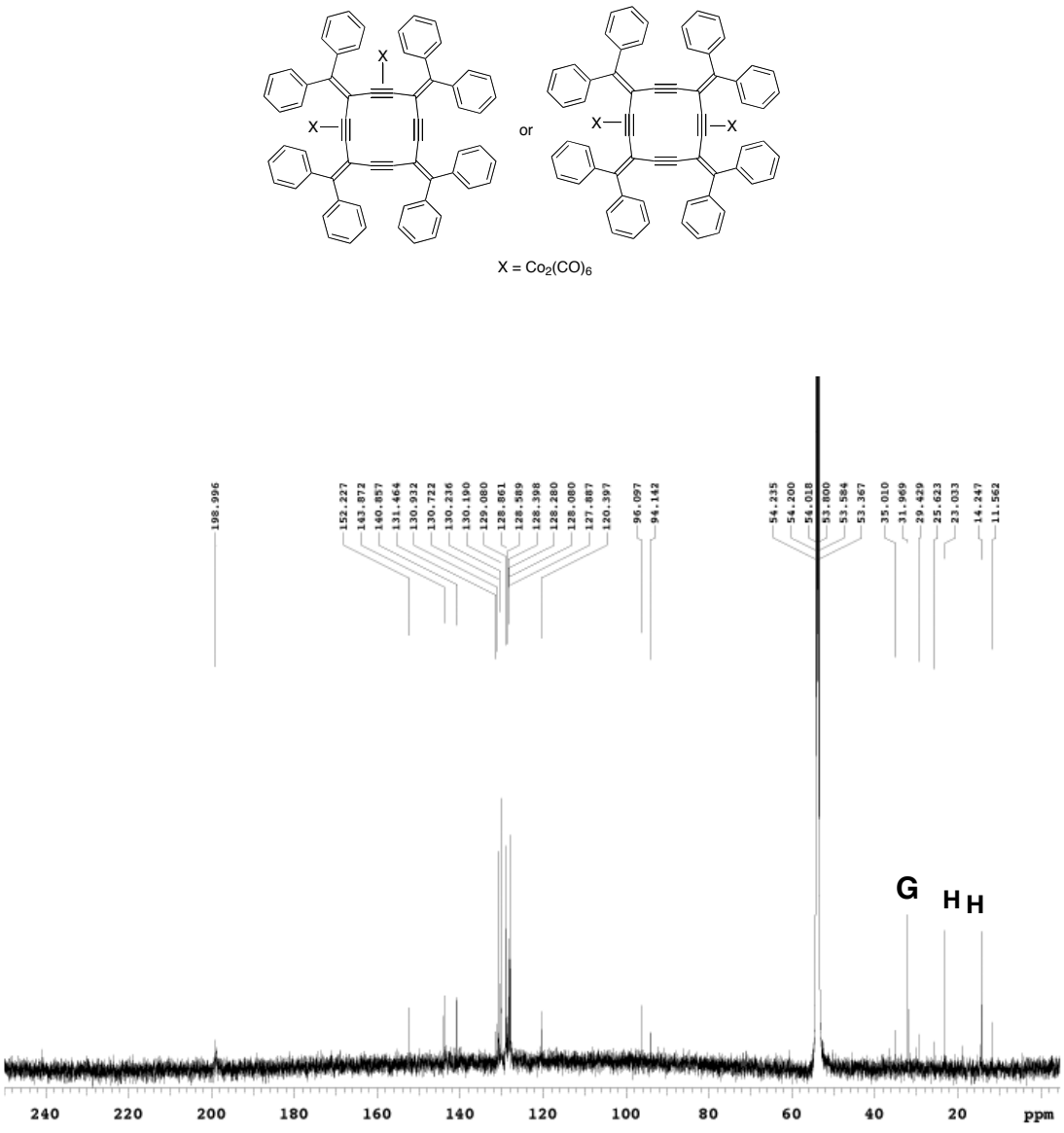

Figure 40 ^{13}C NMR spectrum for proposed structure **611** (CD_2Cl_2)

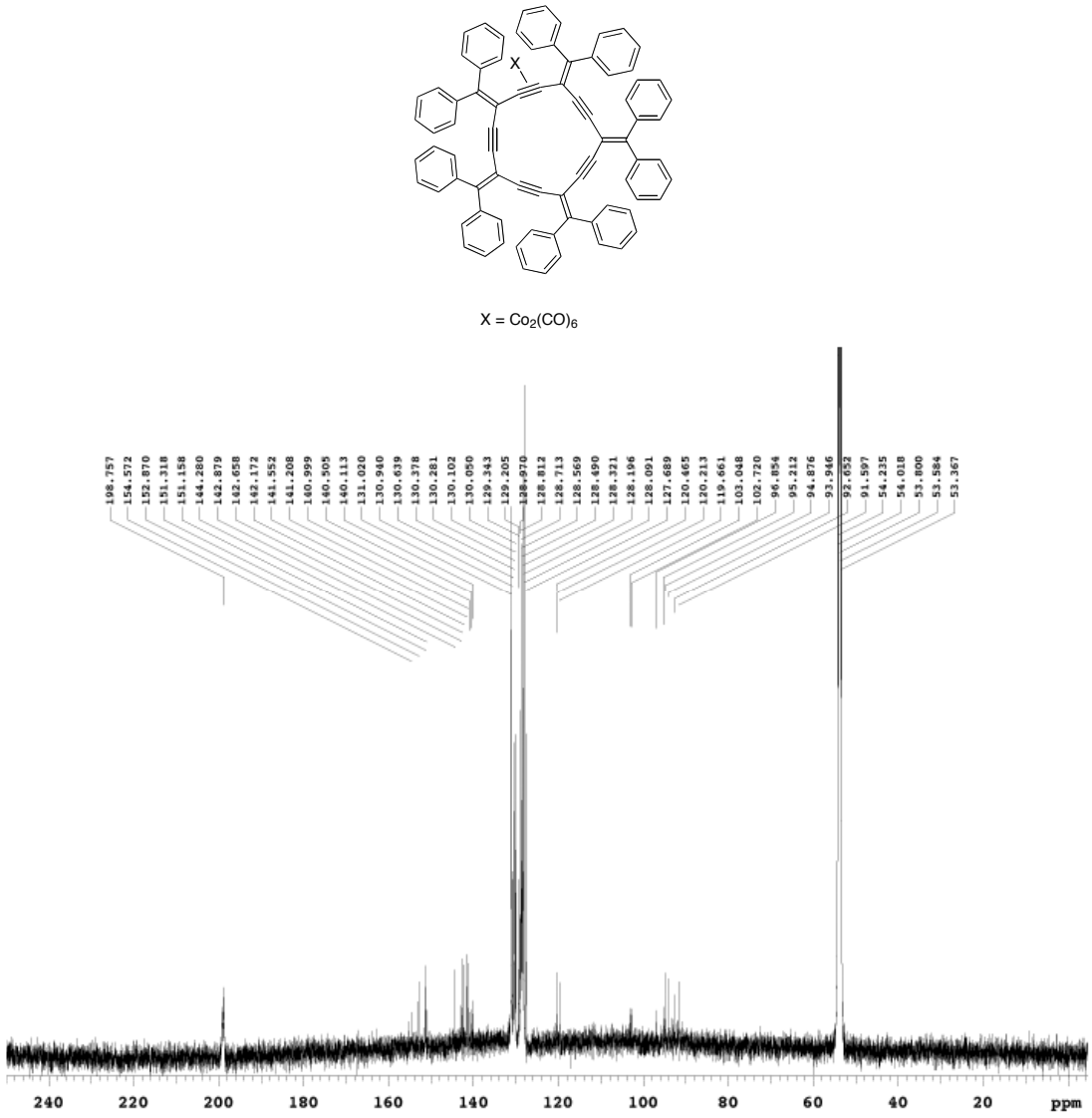

Figure A.41a ^{13}C NMR spectrum for proposed structure **612** (CD_2Cl_2)

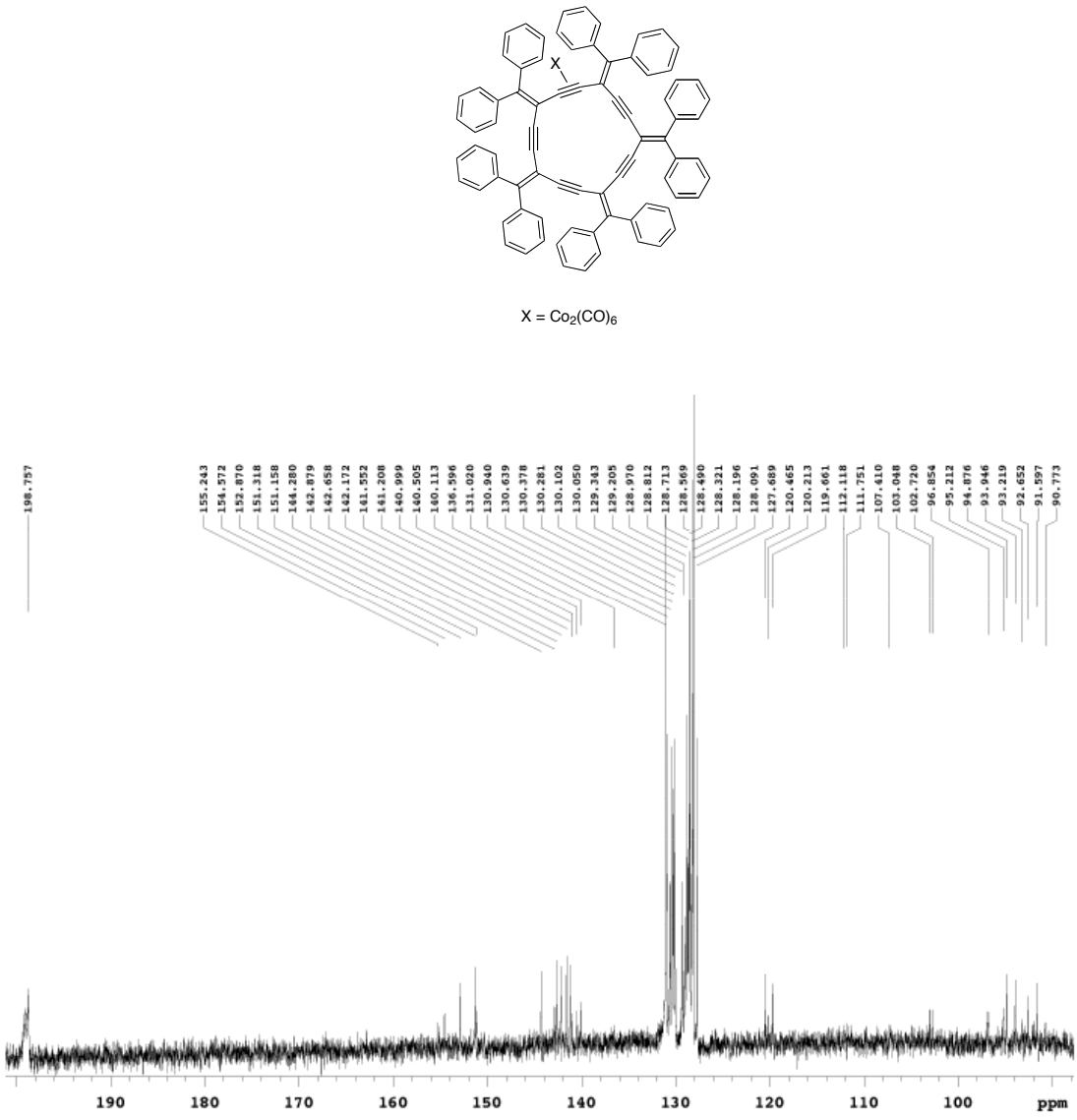

Figure A.41b Expanded ^{13}C NMR spectrum for proposed structure **612** (CD_2Cl_2)

Appendix

A1. **Monomers and their related derivatives (informative results)**

Through this thesis a series of different monomers used for the synthesis of the expanded radialenes that initiated from their corresponding dibromoolefins. Scheme **1** shows some of the most used desilylated monomers during this research and it is logical to discuss it here in order to have a deeper insight about their chemistry. Monomers **525** and **A1**–**A7** used for the synthesis of their corresponding trimers as discussed in Chapter **4**. Compounds **A1** and **A2** showed decomposition on TLC base line and they should be used as fast as possible for coupling reaction. Compounds **A3** also showed decomposition on the TLC base line and they also should be used also as fast as possible but compound **A6** showed significant decomposition and it was hard for usage in coupling reaction. Compound **A7** also showed significant decomposition.

Compound **A4** was used for the synthesis of the corresponding trimer with regard to the Scheme **2**. The yield of the trimer was very low and the low yield could be due to lack stability at high temperature and decomposition or lack of the solubility. The trimer **A8** was fully characterized but the experience and observation of the reaction provides an opportunity to think about a new strategy for the synthesis of trimers in general where there are some problems with desilylated monomers exist. The strategy is shown in the Scheme **3** and it is based on taking advantage of the selective protodesilylation of monomer **301** to give **302** and the following reaction of **302** with the targeted dibromoolefin that its corresponding monomer is not suitable for coupling reaction. The strategy is

applied to all vinyl trilates and their related monomers as shown in general Scheme **4**.

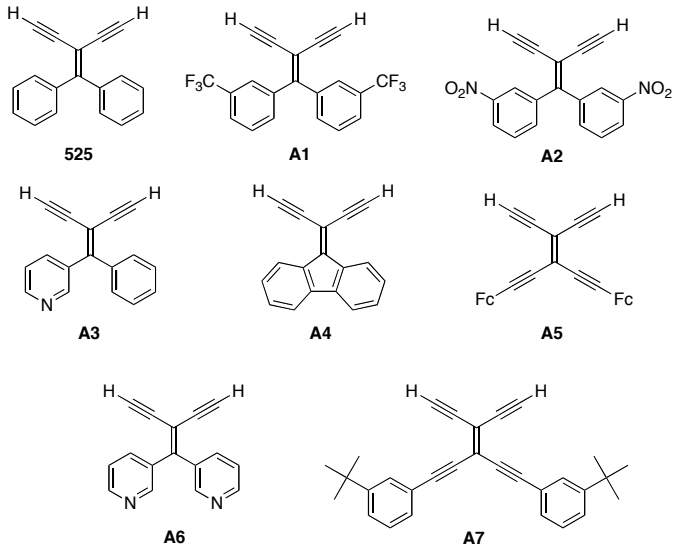

Scheme 1. A series of desilylated monomers

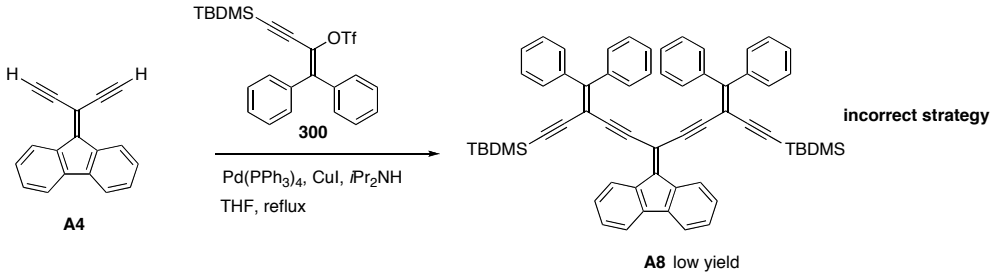

Scheme 2. Synthesis for trimer **A8**

Compound **302** is a useful starting material and it is possible to be subjected to chromatography or stored in fridge for a long time. This is a very useful compound that not only is applicable here but also it is very useful precursors for step-wise synthesis of unsymmetrical dibromoolefin.

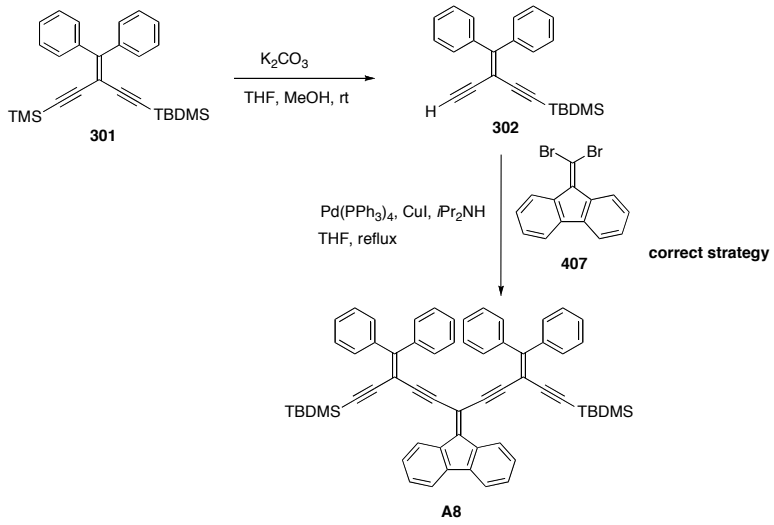

Scheme 3. Alternative synthesis for trimer **A8**

The second example related to this subject is with regard to the synthesis of the trimer from compound **A5.** The reaction began from compound **A9**[1], and only a small amount of the product trimer **A10** afforded (Scheme **5**). Two ways to synthesize ferrocenyl trimers avoiding the usage of **A5** are shown in Scheme **6**.

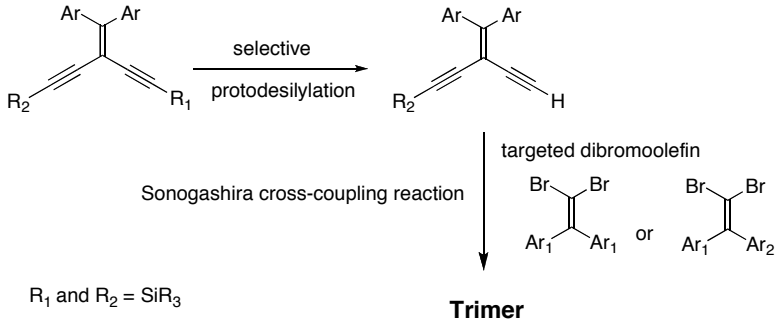

Scheme 4. Suggested method for synthesis of trimers

It should be mentioned that the synthesis of dibromoolefin **A11** has been reported by Ren and co-workers.[2]

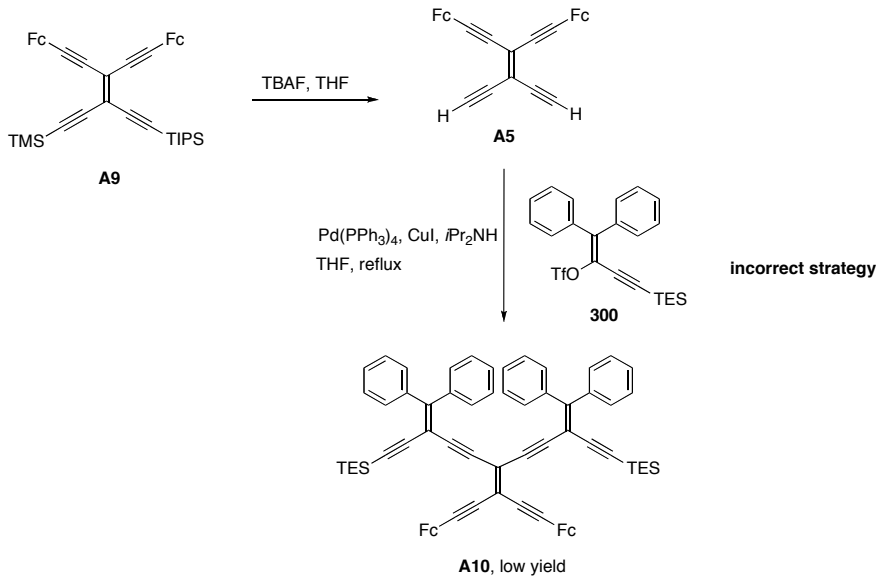

Scheme 5. Synthesis of ferrocenyl trimer **A10**

The third example with regard to the trimer synthesis is a trimer with methoxy groups at para position (Scheme **7**). Timer **A14** like trimer **A8** was synthesized in low yield from its corresponding monomer (not shown here) and it was not characterized further. Again, the correct strategy for the synthesis of trimer **A14** is according to the Scheme **7** using the corresponding dibromoolefin **416** instead. To summarize the application of monomer in the synthesis of trimer, if the desilylated monomers are not suitable for the corresponding trimer synthesis, the usage of Scheme **4** is recommended. Also, if the vinyl triflate of the corresponding aryl is available like ferrocenyl group, the synthesis direction is switched around as it is shown by Scheme **6**.

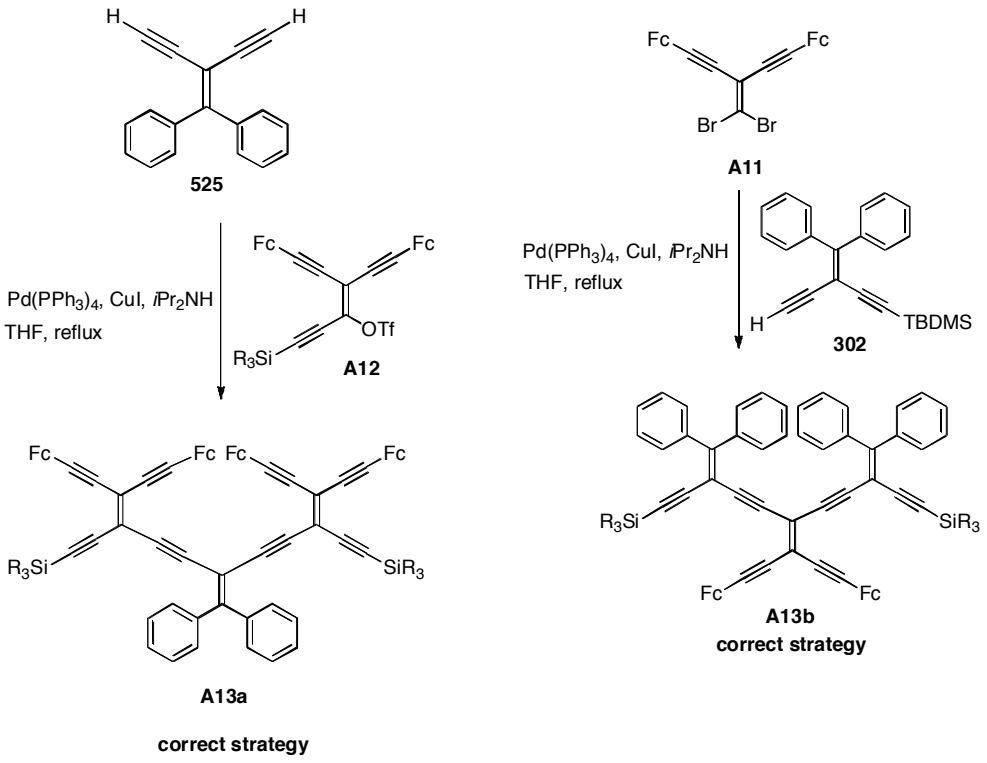

Scheme 6. Synthesis of ferrocenyl trimers

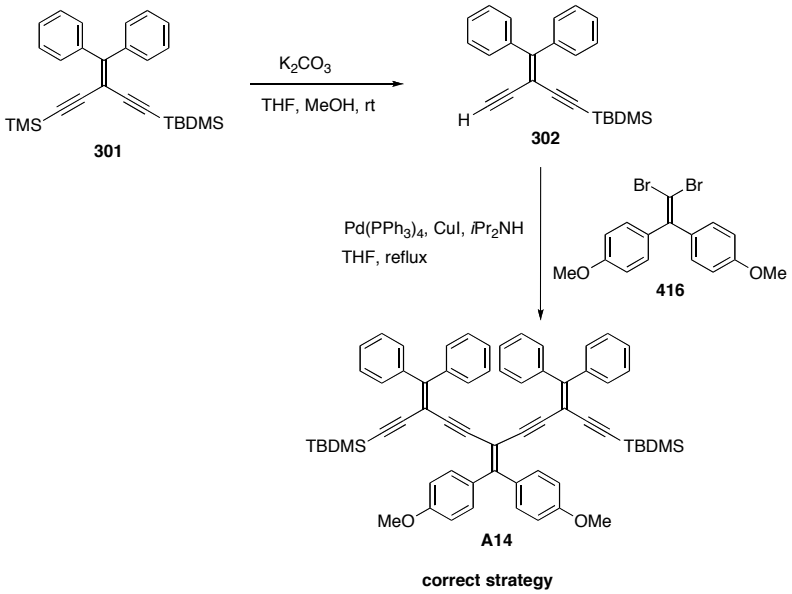

Scheme 7. Synthesis for trimer **A14**

A2. Synthesis of unsymmetrical dibromoolefins using the microwave technology

The application of the microwave in the synthesis of dibromoolefin further opens a door for the synthesis of symmetrical or even unsymmetrical ketone that are converted to their corresponding dibromoolefins through the dibromolefination reaction.[3] In Chapter **4**, one example of the synthesis of dibromoolefin using the microwave technology discussed. The application of microwave may be expanded to the synthesis of unsymmetrical ketones and consequently unsymmetrical dibromoolefins.

The synthesis is involved with reaction of two aryl halides in the same ratio or different ratio in the presence of $Co_2(CO)_8$ using the microwave reaction vessel (Scheme **8**).[4]

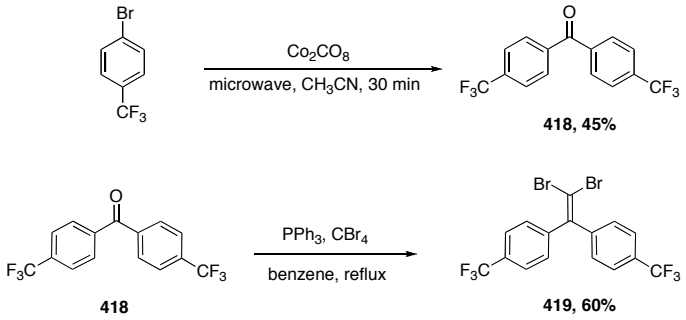

Scheme 8. Synthesis for ketone **418** and dibromoolefin **419**

An example of the unsymmetrical ketone is the reaction of boromoferrocene **A15** with 4-bromobenzotrifluoride (1:1 ratio) **A16** in CH_3CN at 130 °C for 45 min in the microwave in the presence of $Co_2(CO)_8$. The crude reaction product analysis showed three products as it was expected (Scheme **9**).

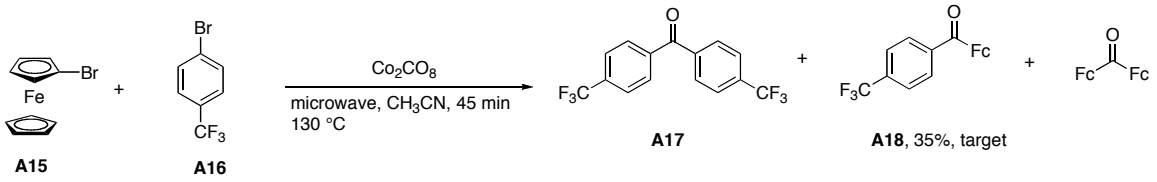

Scheme 9. Application of microwave technology in synthesis of **A18**

The ketone **A18** is confirmed only by EI mass spectrometry and it could be used for the synthesis of corresponding dibromooolefin.

A3. Miscellaneous side products from radialene syntheses

A series of side products also were separated from the synthesis of compounds **504, 507 and 508** according to the Schemes **10** to **12** respectively. All the side products **A19**–**A21** confirmed by HR MALDI-TOF MS.

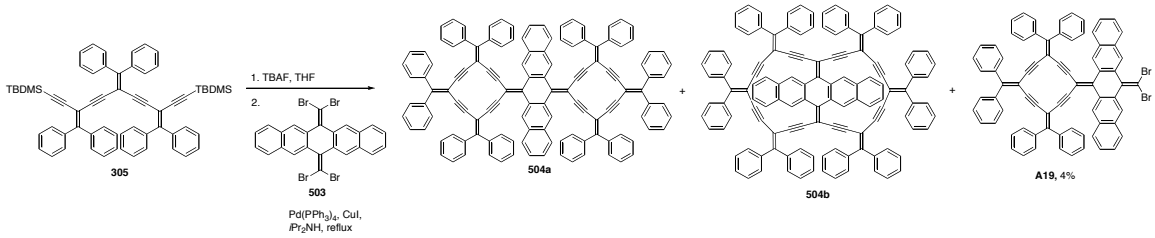

Scheme 10. Synthesis of radialenes **504a**, **504b**, and **A19**

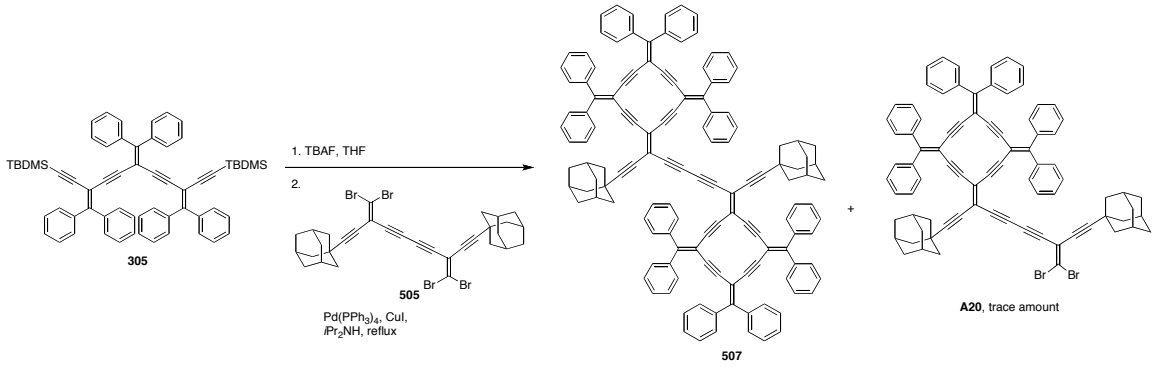

Scheme 11. Synthesis of radialenes **507** and **A20**

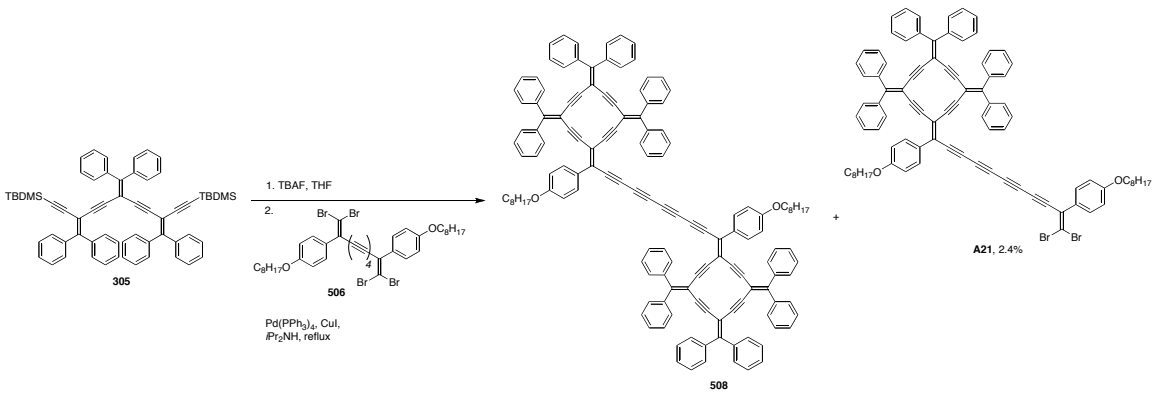

Scheme 6.12. Synthesis of radialenes **508** and **A21**

A series of side products also were separated from the synthesis of radialene **515** (Scheme **13**). The products separated on aluminum oxide plate (activity 2, hexanes/CH_2Cl_2, 1:1) and their constitutional formula confirmed by high resolution MALDI-TOF mass spectrometry. The UV-vis spectra of compounds were measured in THF and they are shown in Figure **1**.

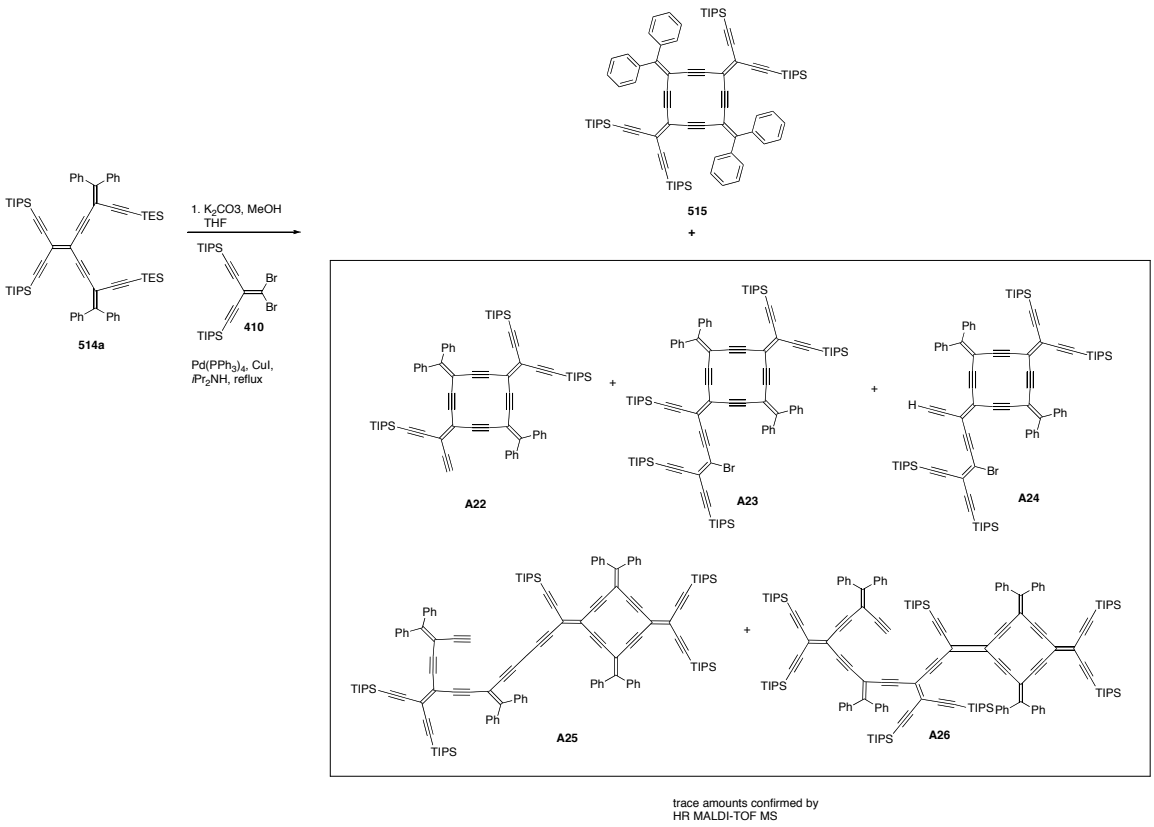

Scheme 13. Synthesis of radialenes **A22**–**A26**

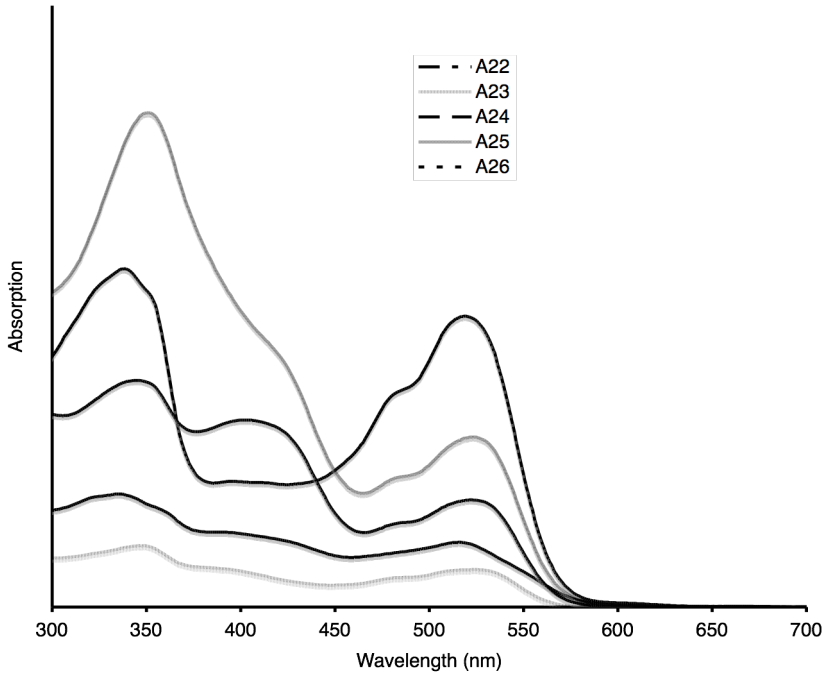

Figure 1. UV-vis spectra for **A22–A26** measured in THF

Basically, the above result is very useful for the concept of the derivatization of the expanded radialenes that are discussed in Chapter **5**. Interestingly all the compounds are very soluble in common organic solvents. Also, this confirms the design of frameworks that carry the trialkylsilylethynyl groups is a correct assumption in terms of solubility and the use for further Sonogashira cross coupling reactions.

A.4 The synthesis of expanded radialene derivatives (enyne-butadiyne)

Previous discussion of the derivatization of the expanded radialenes in Chapter **5** has been a base for further investigation with regard to the synthesis of novel and unprecedented skeletons that originate from two radialenes, **411** and **515**.

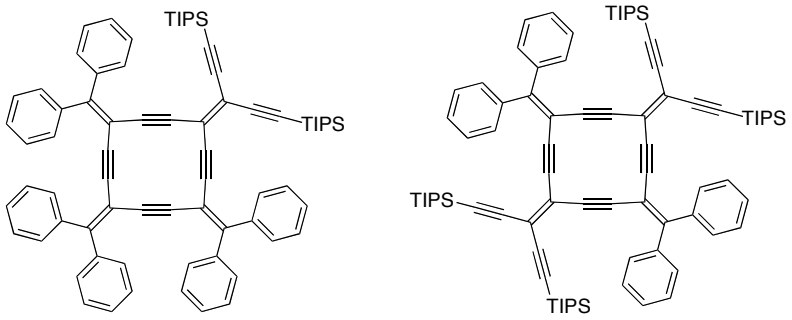

411 **515**

Scheme 14. Radialenes **411** and **515** with TIPS acetylene moieties for further derivatization of the radialene skeletons

Both compounds have appropriate design with regard to the presence of trialkylsilylethynyl groups that provides an opportunity for protodesilylation and formation of the corresponding terminal alkynes for coupling reactions. As discussed and shown in Chapter **5,** the protodesilylated radialene **411** is suitable for further cross-coupling reactions, such as the reaction with a vinyl triflate or an aryl halide (Scheme **15**).

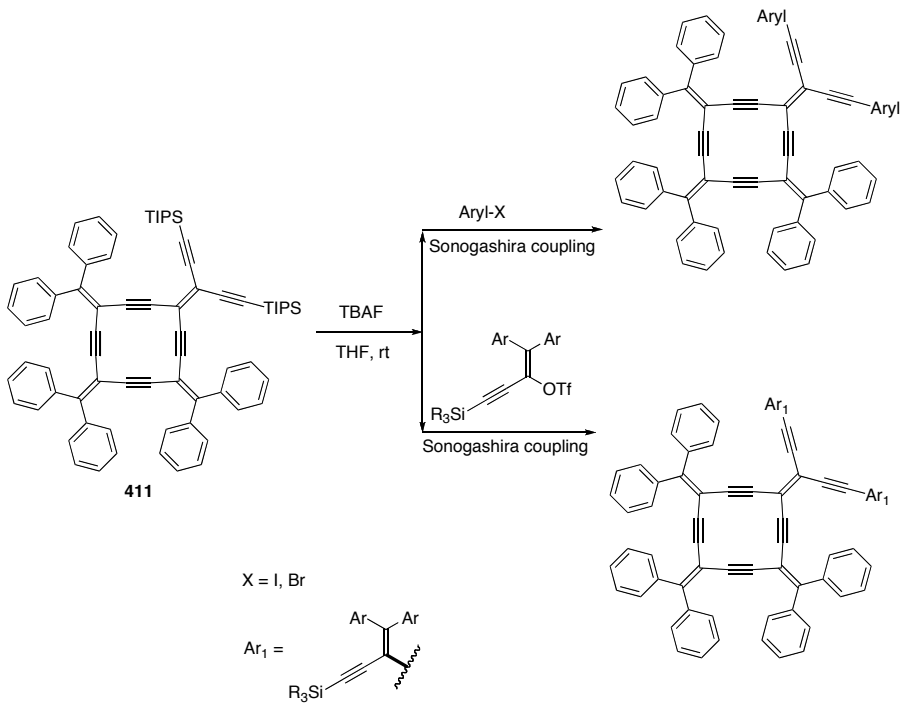

Scheme 15. General strategies for the incorporation of radialene **411** in the synthesis of radialene derivatives

One of the most interesting aspects of **411** is its use in synthesis of expanded radialene derivative **A27** in which the desilylated **411** is reacted in the presence of TMEDA, CuCl in CH_2Cl_2 at room temperature.[5] The oxidative coupling reaction could potentially lead to oligomeric cross-conjugated macrocycles. The experimental result has confirmed this hypothesis. While all the possible products should be unique in terms of skeleton and potential electronic makeup, only the smallest member of the series that carries a [3]expanded radialene skeleton in its central cavity has been the primary interest (compound **A28**) shown in Scheme **16**.

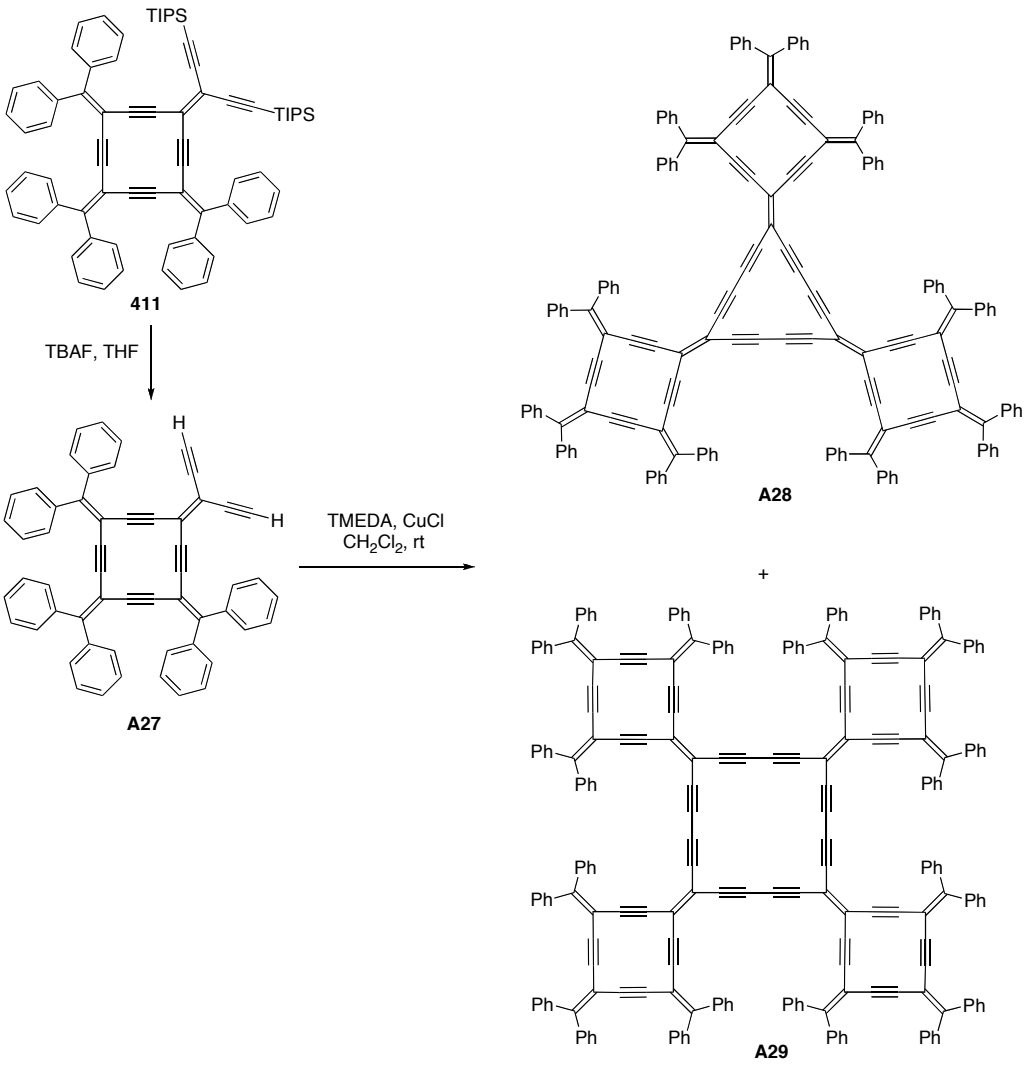

Scheme 16. Synthesis of enyne-butadiyne expanded radialenes **A28** and **A29**

Based on the MALDI-TOF mass spectrometric analysis, the reaction afforded **A28** and **A29** (Scheme **17**), as well as the un-cyclized products **A30** and **A31** (Scheme **17**). As a matter of fact, the major products were the side products **A30** and **A31**. The challenge for executing this reaction is to minimize the larger macrocycle such as**A29** and the unwanted side products.

The presence of compound **A31** is due to two factors, the reaction was stopped too early or the conditions (e.g., concentration) used were not the optimal.

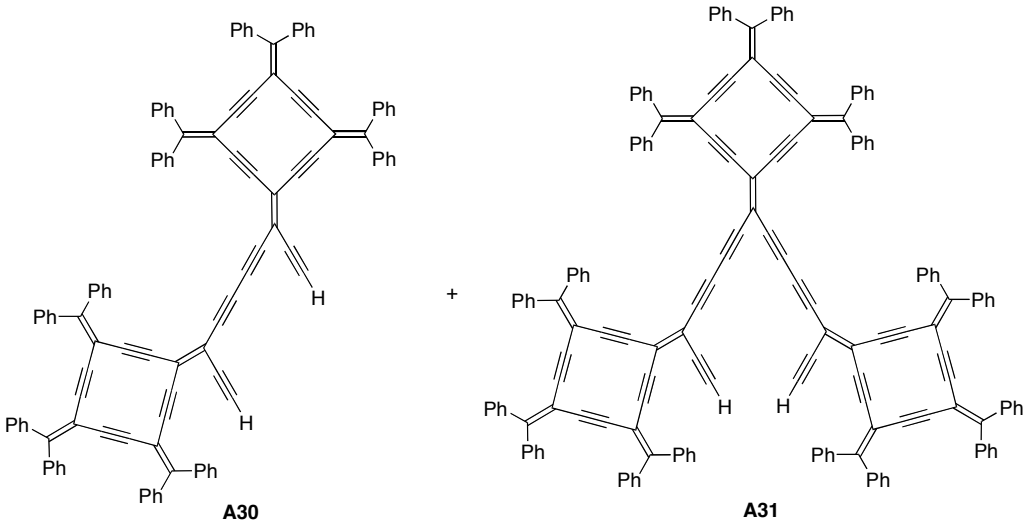

Scheme 17. Radialene **A30** and **A31**

In terms isolation and identification, **A30** (red solid) first collected from the silica gel column (hexanes/CH_2Cl_2, 5:1 to 2:1), followed by **A31** as a red solid, and then a mixture of radialenes **A28** and **A29** (dark green solid). Figures **2**, **3** and **4** show MALDI-TOF mass spectra of compounds **A28**–**A31**.

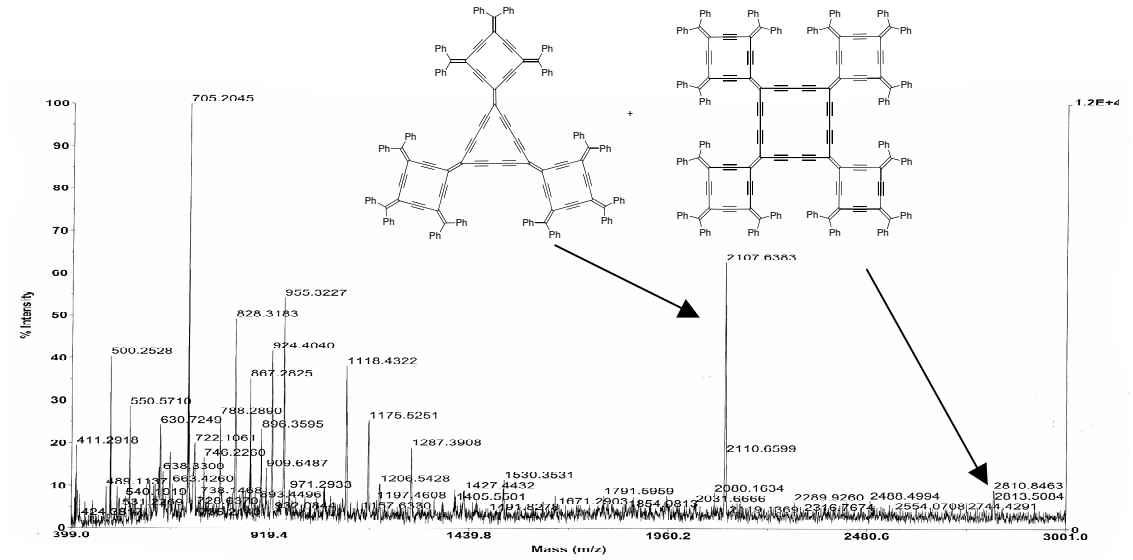

Figure 2. LR MALDI-TOF mass spectrum of a crude mixture of compounds **A28** and **A29**.

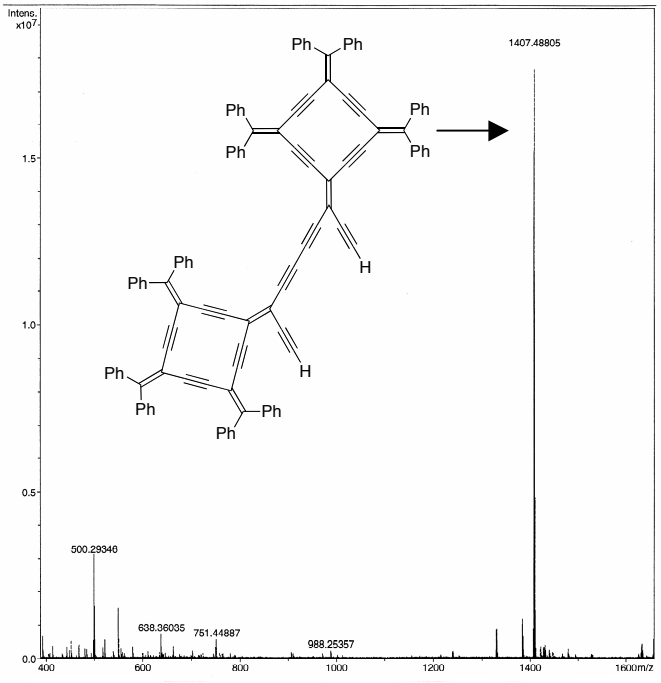

Figure 3. HR MALDI-TOF mass spectrum of compound **A30**

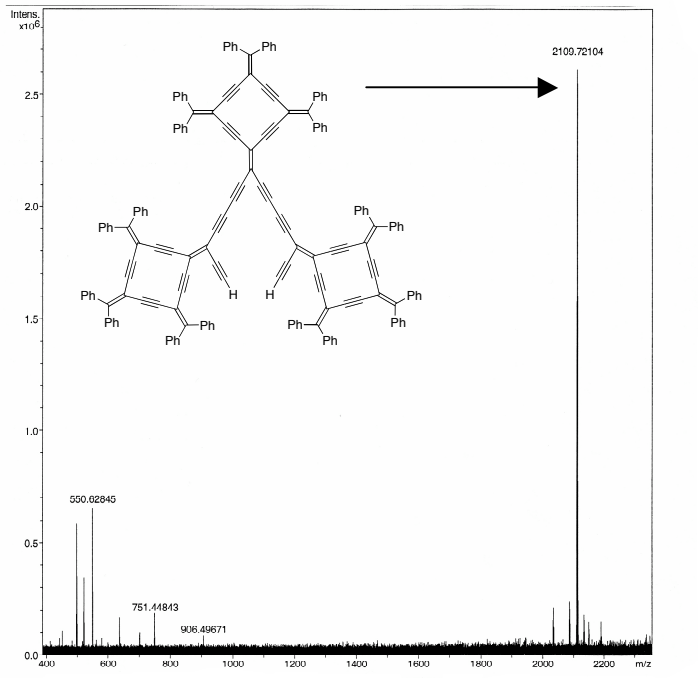

Figure 4. HR MALDI-TOF mass spectrum of compound **A31**

The synthesis of macrocycle **A28** could provide a new framework in the chemistry of the expanded radialenes and it would serve as new pattern for future exploratory studies in this field. A final note suggests the enyne-butadiyne protocol could be applied generally with functional groups and it may be executed according to the below proposed reaction in Scheme **18**. The synthesis could be also expanded to [3]expanded radialene derivatives of enyne-butadiyne.

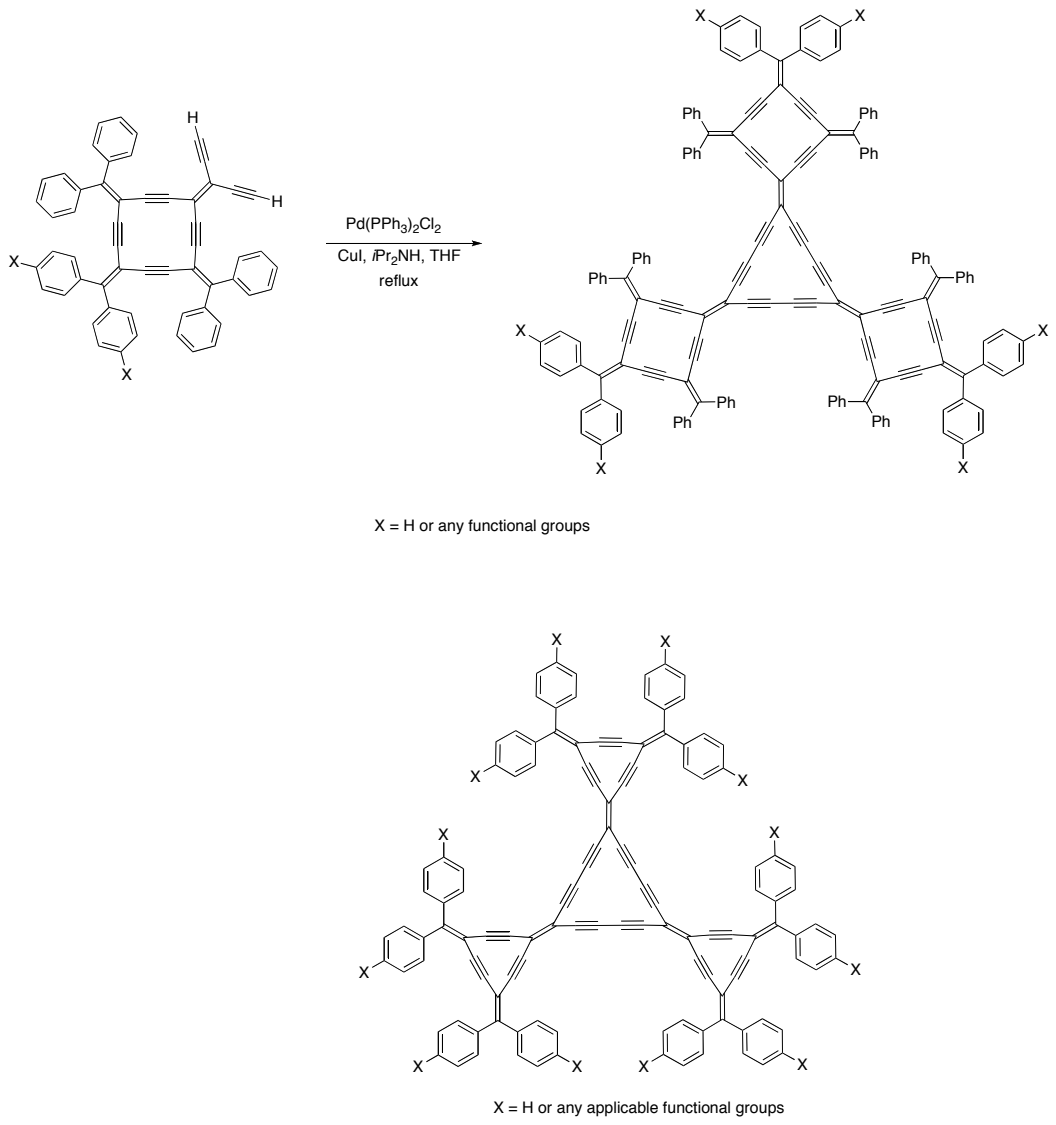

Scheme 18. Future plan for enyne-butadiyne [3]–, and [4]radialenes

A5. **Synthesis of cage expanded radialene (a future plan)**

The synthesis of **515** opens opportunities for the synthesis of carbon-rich skeletons including tube and cage molecules. It is honest to say that the synthesis of such molecules would be more challenging than any of other discussed through this thesis. This is due to many factors that are involved during their synthesis. The author believes these challenges could be minimized with a

smart synthetic plan, patience, and skill. A synthetic plan will be discussed briefly here only a proposal. The first step of the synthesis is protodesilylation of **511** using TBAF, in order to provide compound **A32** which in turn, would be reacted with excess of triflate **300** (6-fold excess at least) in the presence of $Pd(PPh_3)_4$ to give compound **A33** (Scheme **19**). It should be noted that **A32** contains four terminal alkynes that susceptible to oxidative coupling.

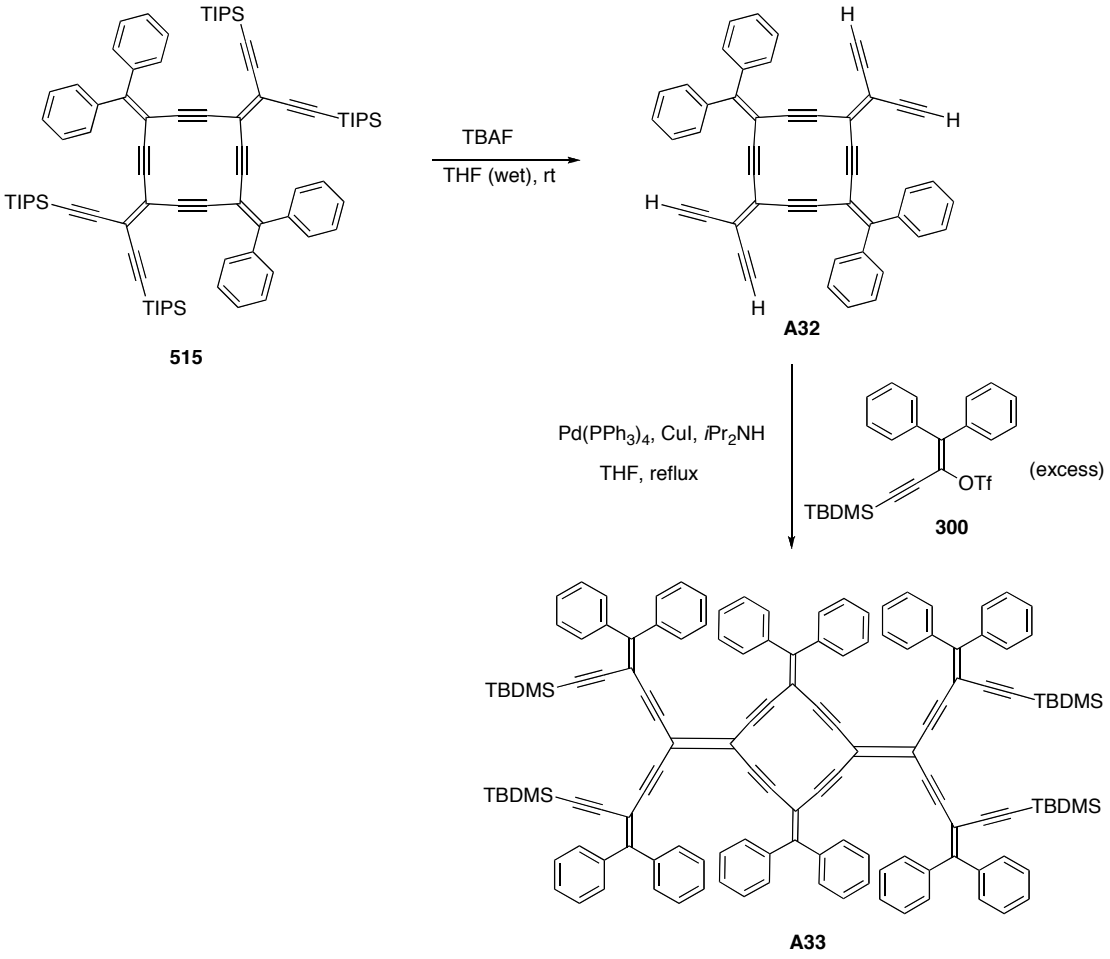

Scheme 19. Synthesis of radialene **A33**

Based on previous observations in the chemistry of macrocyclic radialene **A33** should be stable and suitable for further coupling reactions. The TBDMS groups address the solubility issue that usually is encountered in this chemistry. Protodesilylation of the compound **607** and reaction of the corresponding terminal alkyne under Hay (or any appropriate conditions) condition could be one of the strategies to synthesize the desired cage molecule (Scheme **6.7**).[5]

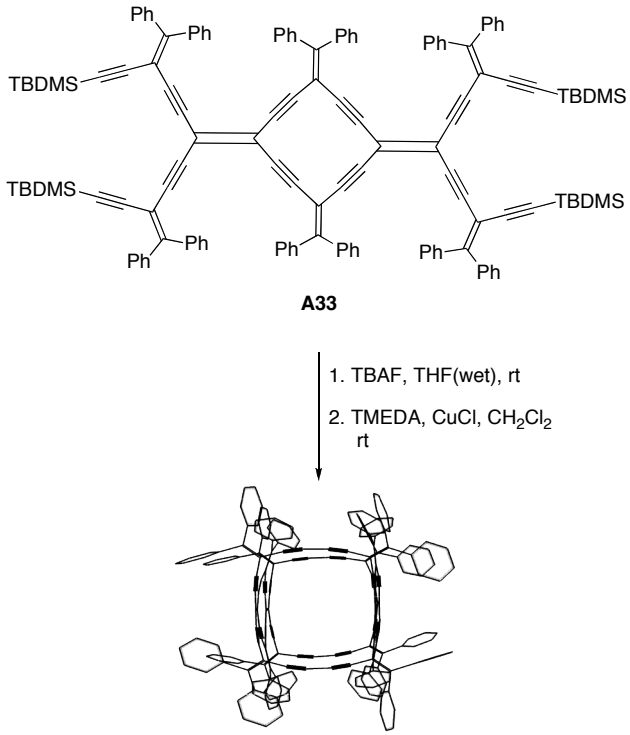

Scheme 20. Proposed synthesis for cage molecule (Spartan minimized geometry, molecular mechanics, MMFF94 force field)

A6. **Synthesis of 2-pyridyl dibromoolefin and its related reactions**

The synthesis of a dibromoolefin incorporating the 2-pyridyl group was considered as a building block for the synthesis of expanded radialenes.

The synthesis of the pyridyl dibromoolefin **A35**, began with preparation of the corresponding ketone according to Scheme **21**.[6] The synthesis of the ketone **A34** according to Scheme **21** is more versatile compared to the original synthesis reported for **A34** because it shorter and easier in terms of separation and purification.[7] Ketone **A34** has been used to synthesize compound **A35** in 75% as an off-white solid (Scheme **21**, **A**). An alternative method for the synthesis of **A34** that tried and it is outlined in Scheme **21** (**B**).

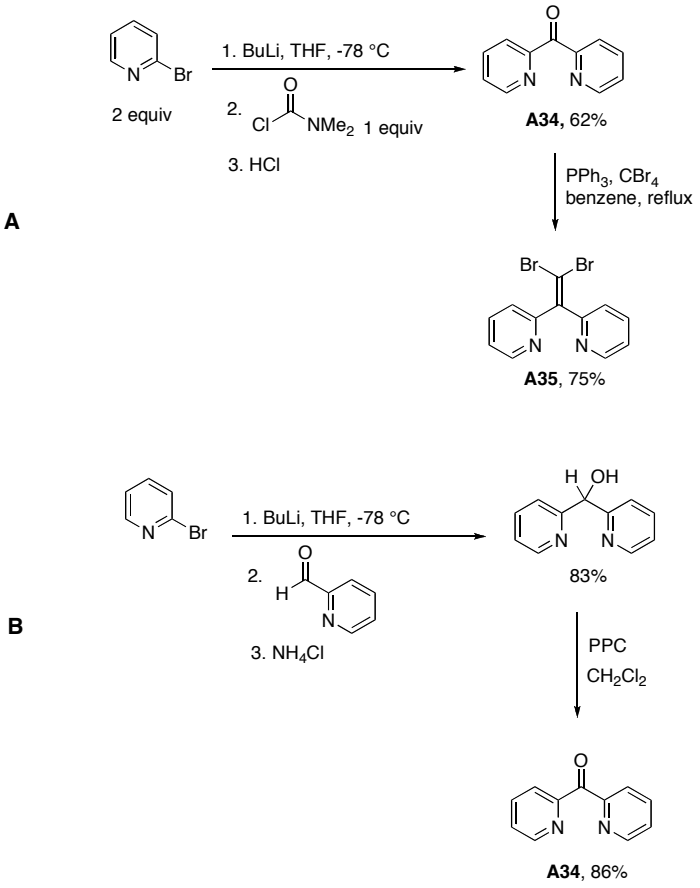

Scheme 21. Synthesis of ketone **A34** (**A** and **B**) and dibromoolefin **A35**

Dibromoolefin **A35** reacted with excess of trimethylsilylacetylene in the presence of $Pd(PPh_3)_2Cl_2$ in THF under reflux. Analysis of the reaction (TLC) did not show the expected product. The crude reaction product was very complex in contrast to expectations. Such reactions usually give three main compounds, (excluding homo-coupled product of the trimethylsilylacetylene) the first the un-reacted dibromoolefin, second the mono-substituted product, and third the target product as outlined by Scheme **22**.

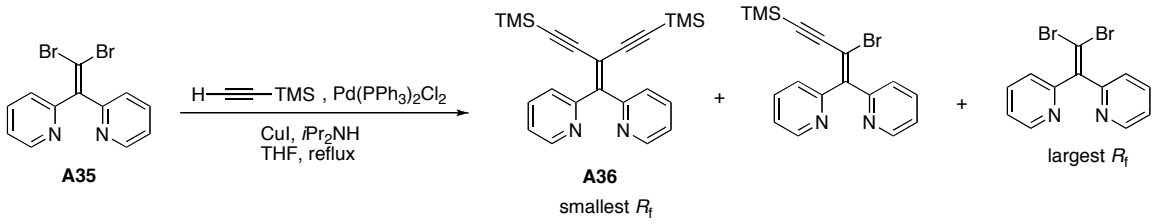

Scheme 22. Expected products from coupling reaction of compound **A35** with trimethylsilylacetylene

Compound **A36** was not observed. Only the first compound from column chromatography was isolated in sufficient yield for partial characterization (unstable) and the other products were all quite minor. Preliminary analysis by high resolution electrospray mass spectrometry showed, surprisingly product **A37** as the main product. The product was also observed from the reaction at room temperature (Scheme **23**).

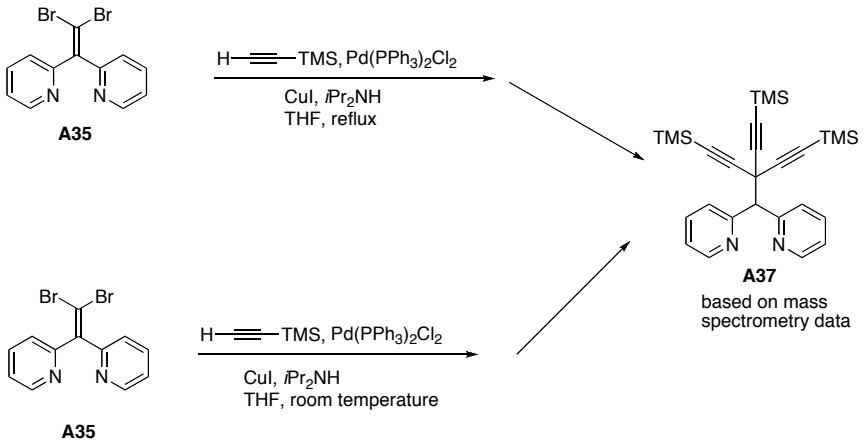

Scheme 23. Possible side product of coupling reaction of **A35**

Given that the reaction of trimethylsilylacetylene with **A35** missing, it was logical to look at a larger trialkylsilylethynyl group like triisopropylsilylacetylene. Reaction of **A35** with triisopropylsilylacetylene is shown in Scheme **24**. The reaction gave the desired product **A38** as colorless solid, but in 26% yield only.

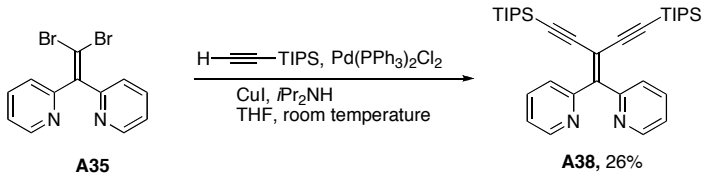

Scheme 24. Synthesis of monomer **A38**

Monomer **A38** was desilylated with TBAF in THF, however, the reaction showed a large amount of decomposition during the desilylation (from TLC baseline observation). Never the less, It was reacted with triflate **300** (Scheme **25**)**.** Some **A39** formed based on mass spectrometric analysis of the crude reaction product but it did not survive after leaving the crude reaction product in the fridge.

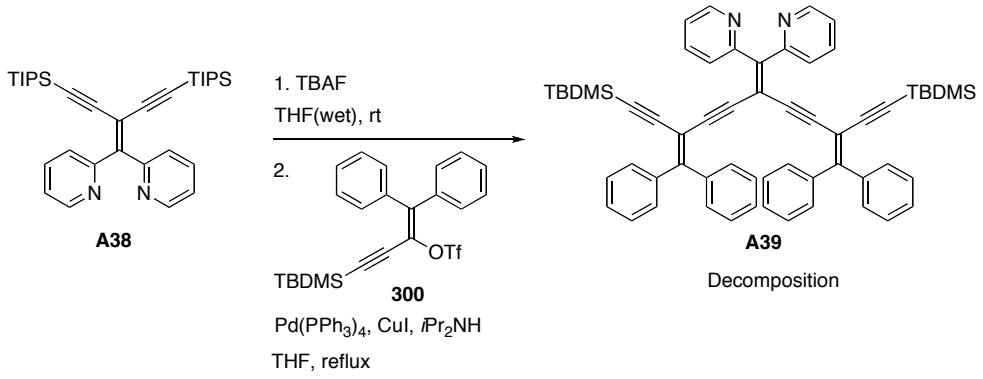

Scheme 25. Synthesis of trimer **A39**

The lack of stability of desilylated **A38** and also trimer **A39** that was observed during the reaction makes it very hard to use trimer **A39** for the radialene cyclization recation.

A7. **Synthesis of expanded radialenes with alky substitutents (informative results)**

So far thesis mainly covered the synthesis of the expanded radialenes that contain aryl or substituted aryls substituents. Expanded radialenes that carry alkyl groups are another alternative that could potentially produce different physical properties. The only synthesis of the alkyl-expanded radialene was discussed in Chapter **1** and reported by the Tykwinski group.[8] However, the compound was not as stable as the expanded radialenes discussed in this thesis. Nevertheless, it was logical again to look at the other skeletons that carry alkyl groups pendent to the expanded radialene skeleton.

Compound **A40**[9] was desilylated and reacted with triflate **300** under the standard Sonogashira protocol to give compound **A41** (unstable, light-orange solid). Compound **A41** was protodesilylated with TBAF in THF (decomposition

was observed) and reacted with dibromoolefin **308** under the standard Sonogashira protocol. The crude reaction product did not show any evidence of the desired product (bis[4]expanded radialene) only a black residue was observed (Scheme **26**). The reason behind the decomposition is probably the same concept that was discussed with regard to the alkyl radialene in Chapter **1**.[10]

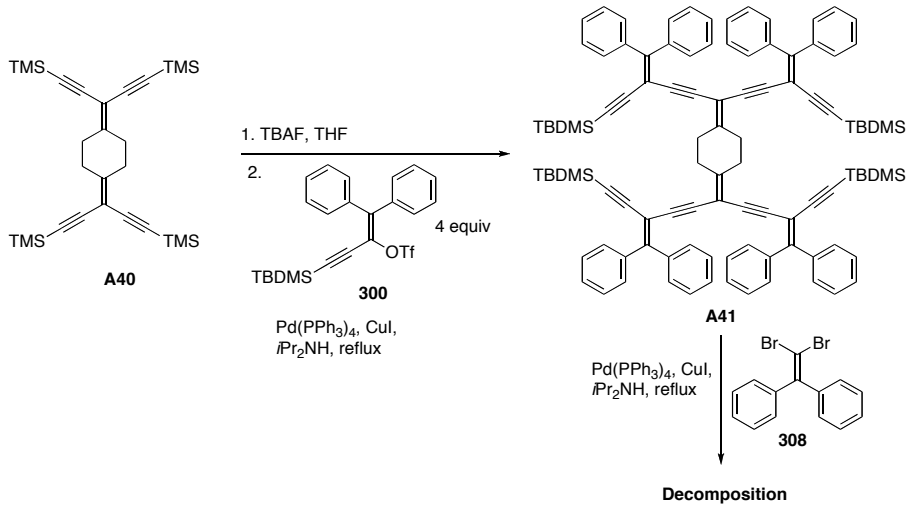

Scheme 26. Attempted synthesis of alkyl expanded radialene

A8. **Failed dibromoolefin synthesis (informative results)**

There were attempts to synthesize four dibromoolefins that were to carry different functional groups, as it is outline by Scheme **27.** In Scheme **27** the first two reaction products decomposed after column chromatography and did not survive long enough for full characterization while the last two reactions did not proceed to give the desired products. Perfluorinated benzophenone was reacted with PPh_3 and CBr_4 in dry benzene under reflux. The crude reaction product showed the usual pattern with regard to TLC and contained a series of products.

The major product was separated in trace amount as a colorless solid that was not the desired dibromoolefin. Instead, according to mass spectrometry analysis and Infrared spectroscopy, the major product was a dibromoolefin in which one of its fluoride atoms was replaced by OH group (Scheme **28**). The OH group may be originated from moisture in the CBr_4. The position of hydroxyl group in Scheme **28** is arbitrary.

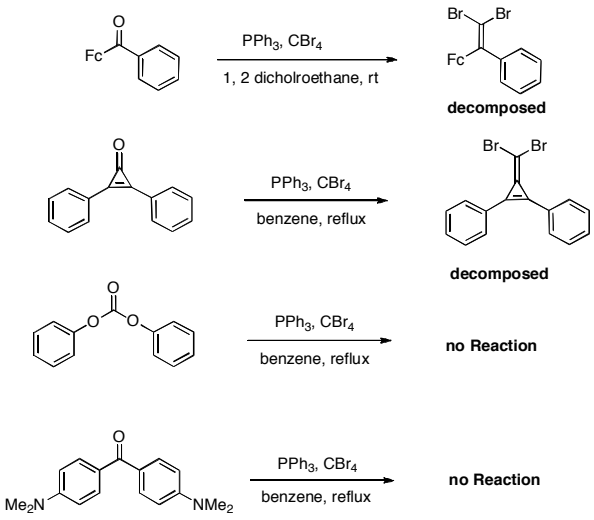

Scheme 27. Attempted synthesis of dibromoolefins

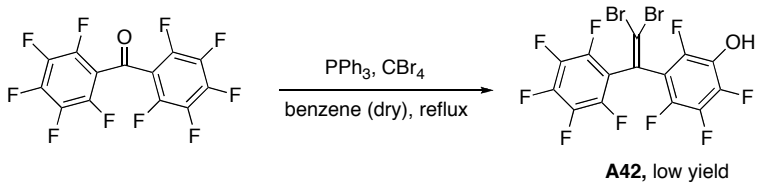

Scheme 28. Possible product from dibromoolefination reaction

Finally in a related attempt, ferroceyl ketone[11] reacted in the presence of PPh_3 and CBr_4 but the reaction did not produce the corresponding dibromoolefin **A43** (Scheme **29**).

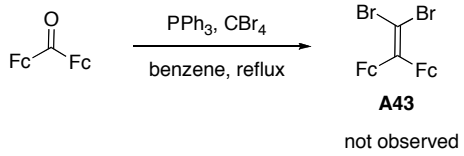

Scheme 29. Dibromoolefination of ferrocenyl ketone

A9. **Synthesis of anthracenylidene [3]expanded radialene derivatives**

Following the synthesis of a [4]expanded radialene based on an anthracenylidene framework it was logical to explore the synthesis of its [3]expanded radialene derivative because it had become clear that [3]radialenes are more interesting in terms of optical and electronic properties. This attempted synthesis revealed very unexpected results that again confirms the very unique behavior of [3]expanded radialenes (Scheme **30**).

Dimer **303** desilylated by TBAF in THF and reacted according to the Sonogashira protocol with compound **501** under reflux (Scheme **30**). The crude reaction product showed a complex pattern based on TLC analysis and after column chromatographic separation, using silica gel (hexanes/CH_2Cl_2, 5:1 to 2:1) a series of fractions were collected. HR MALDI-TOF mass spectrometry showed the presence of three major products. Target product **A44** was isolated as a red solid that had lowest R_f. It should be mentioned also the compound **A44** could be a mixture of two isomers but here only one isomer is presented for simplification

in Scheme **A44**. The first side product, **A45** (highest R_f, yellow solid) is the result of bromination of compound **A44**, and the second side product **A46** (yellow solid) seemed to be from cycloaddition reaction of compound **501** with the radialene **A44**. The overall yield for this reaction was about 10%. Unfortunately due to the side reactions, there was not enough material available for full characterization of each of the proposed products, which have been tentatively assigned as compounds **A44**–**A46**. It should be mentioned also that he reaction afforded also compound **A47** that has highest R_f among the products and its constitutional formula confirmed by HR MALDI-TOF mass spectrometry. ^{13}C NMR spectroscopy of **A47** shows the alkyne peaks at 95.1, 92.4 and 91.4 ppm. Other spectroscopic evidence comes from Infrared spectroscopy that also shows different absorptions for **A45** and **A46** compared to **A44**. Compound **A45** shows a peak at 2189 cm^{-1} and compound **A46** shows peaks at 2187 and 1946 cm^{-1}. More interesting data comes from UV-vis spectroscopic study for the three products in THF as shown in Figure **5**. The UV-vis spectrum of compound **A44** shows two absorptions, the first at 383 nm and the second at 532 nm.

The above reaction shows potentially new features in the chemistry of the [3]expanded radialenes and it is required to be repeated in order to fully understand and characterized the products of the bromination and cycloaddition reaction. it is worth noting that this is the third observation documenting the tendency of the [3]expanded radialenes to undergo the cycloaddition reaction.

The above observations demonstrate the special reactivity of the [3]radialenes and their related derivatives.

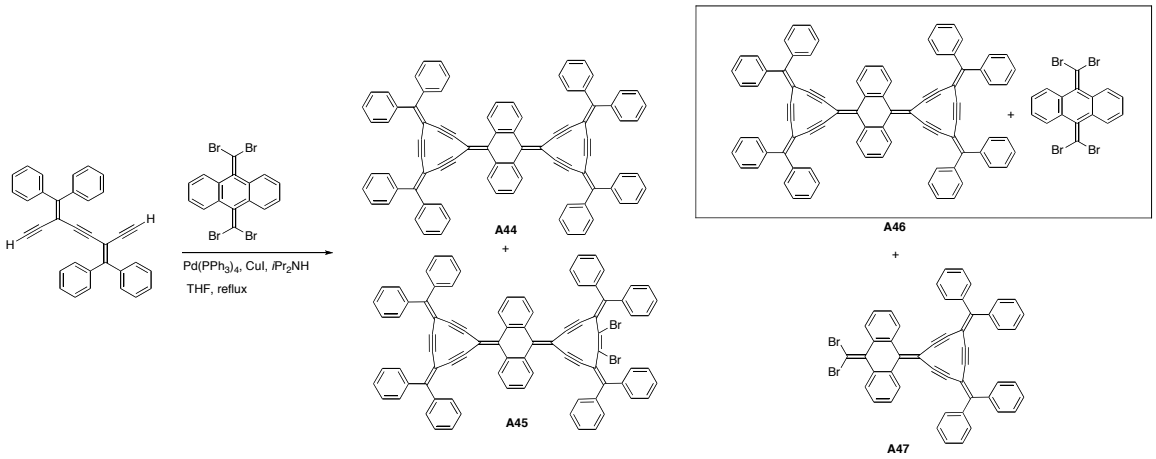

Scheme 30. Synthesis of radialene **A44** and its side products (the bromide position is arbitrary in compound **A45**)

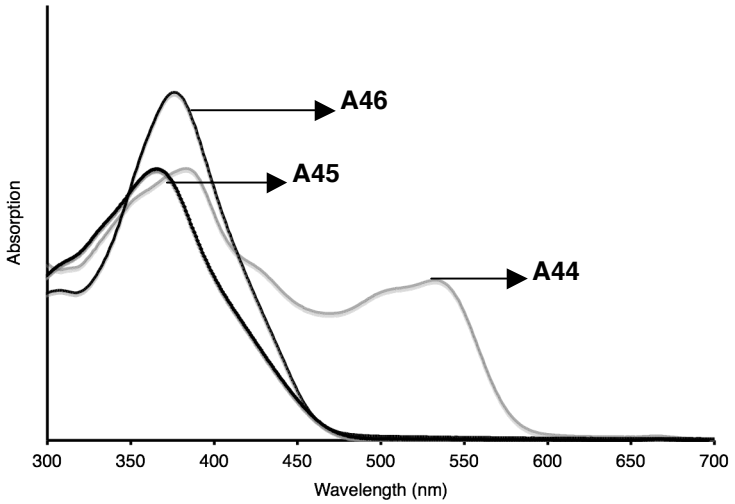

Figure 5. UV-vis spectra of radialene **A44–A46** measured in THF

A10. **Synthesis of bis[4]expanded radialenes (incomplete project)**

The incorporation of phenyl ring into bis[4]expanded radialene is shown according to Scheme **31**. Tetraiodobenzne[11] **A48** is not stable at high temperature; nevertheless, the reaction afforded the desired product **A49** (yellow solid) in low yield as well as compound **A50**. Both products show low solubility and make their characterization were very challenging. Radialene **A49** constitutional formula has been confirmed by HR MALDI-TOF mass. The ^{13}C NMR spectrum of compound **A49** shows the presence of more than one product according to a series of peaks at 98.8, 95.9, 95.1, 94.3, 93.1, 92.5, 91.8, 91.1, 90.4 ppm and other peaks with very low intensity (possibly an isomer). Also, ^{13}C NMR spectroscopy of the compound **A50** shows the alkyne carbons at 96.1, 93.9, 92.5 and 88.0 ppm.

The synthesis of the radialene **A49** should be repeated in which using tetrabromobenzene instead of the tetraiodobenzene in order to stop the decomposition during the reaction.

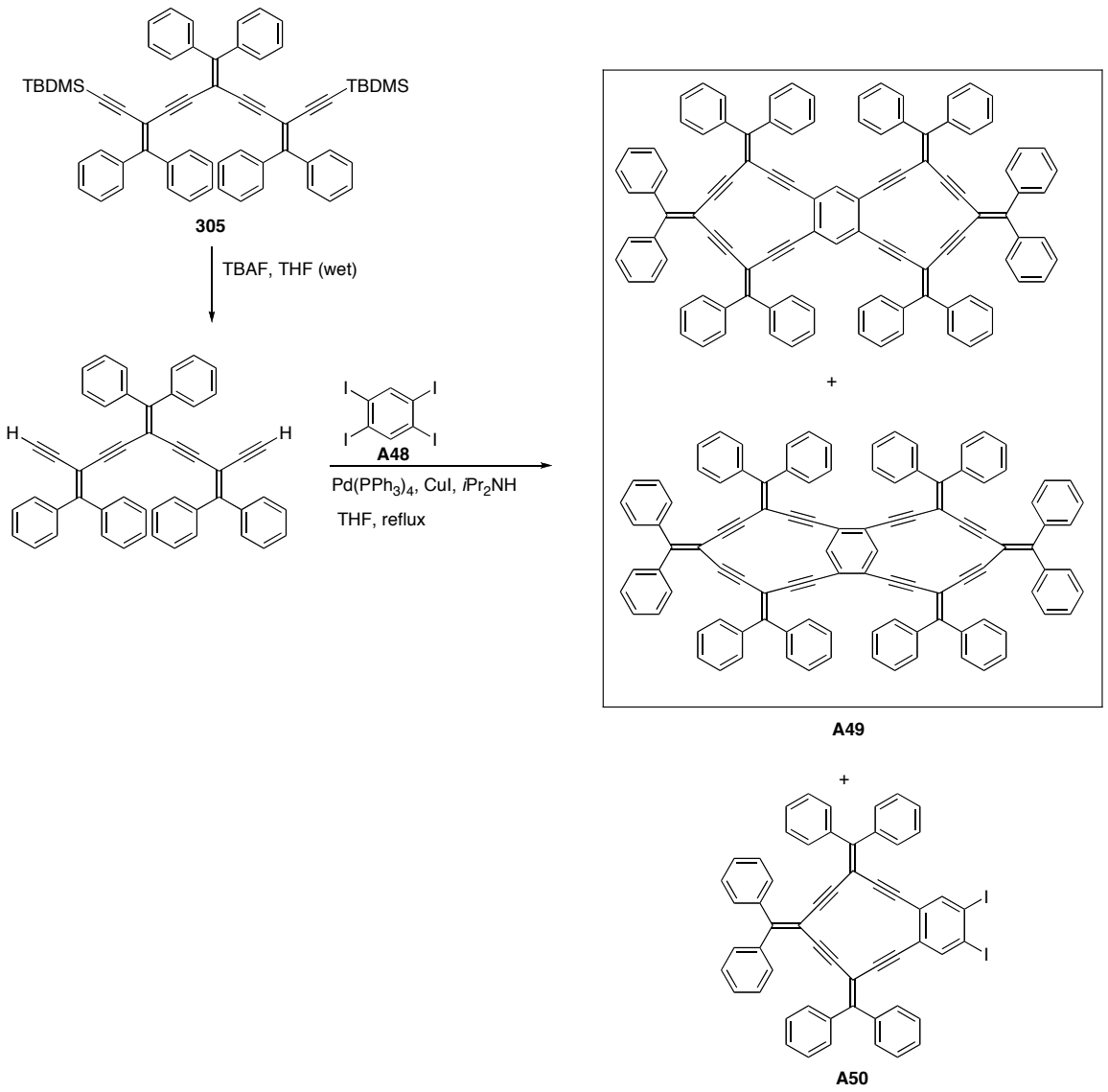

Scheme 31. Synthesis of radialene **A49** and **A50**

A11. **Synthesis of bis[3]expanded radialene (a stepwise approach)**

In Chapter **3**, the synthesis and characterization of radiaannulene **316a** was discussed. In this reaction, however, only a trace amount of bisexpanded radialene **316b** was obtained (Scheme **32**). Therefore, a few synthetic strategies has been explored that could potentially lead to the **316b**.

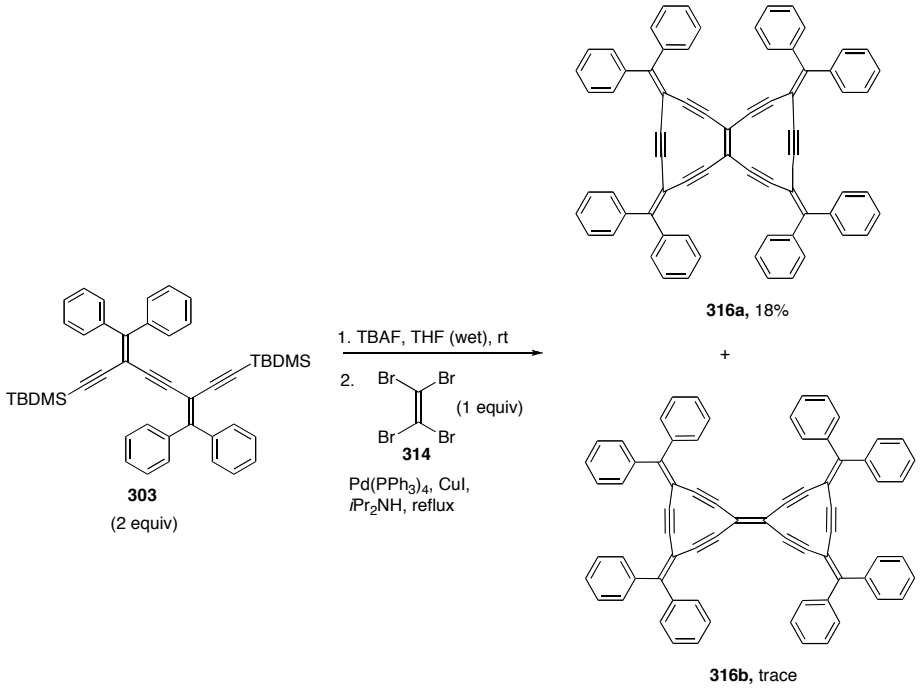

Scheme 32. One-pot synthesis for **316a** and **316b**

The first strategy is shown in Scheme **33**, and begins with the coupling reaction of vinyl triflate **300** with porpargyl alcohol gives compound **A51** as a brown solid in 92% (confirmed by mass spectrometry and ^{13}C NMR spectroscopy). Compound **A51** was reacted with MnO_2 in dry CH_2Cl_2 and gave compound **A52**, which was not stable and decomposed as the synthesis progressed. Due to the lack of stability of **A52,** the strategy was abandoned.

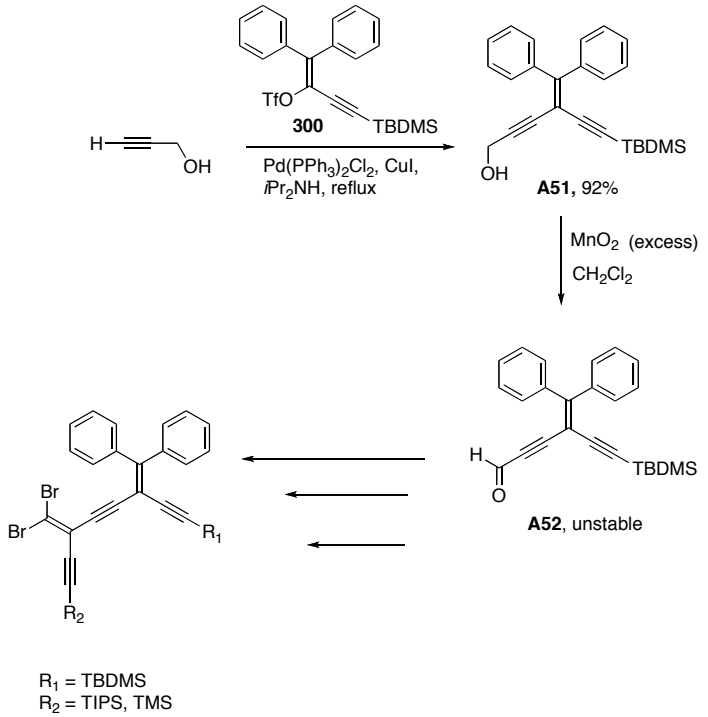

Scheme 33. Attempted synthesis for unsymmetrical dibromoolefin (route 1)

The second strategy is shown in Scheme **34**. First, the coupling reaction of carbamyl chloride with compound **512** was attempted, but the reaction did not give compound **A53** so the strategy was not suitable.

So far, both strategies have been based on the formation of a ketone that carries the diphenylalkylidene building block. The third unsuccessful strategy that was tested is shown in Scheme **35**. The synthesis is based on the coupling reaction of the vinyl triflate **300** with ethyl propiolate, but it did not produce the targeted molecule. However, the reaction is unique and gives ketone **A54** in quantitative yield**.**

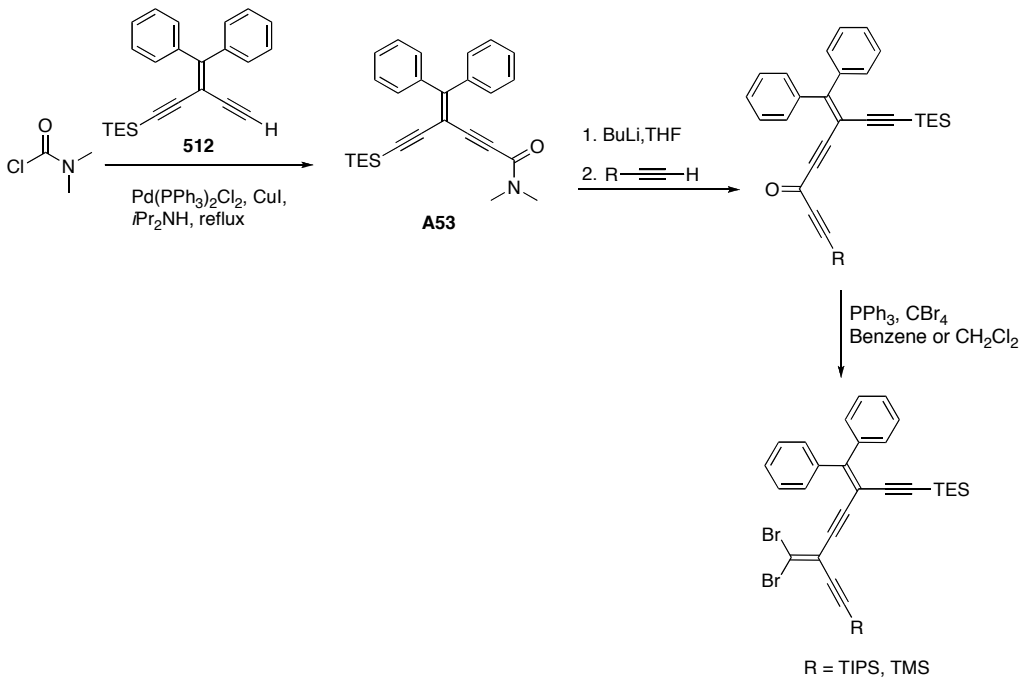

Scheme 34. Attempted synthesis for unsymmetrical dibromoolefin (route 2)

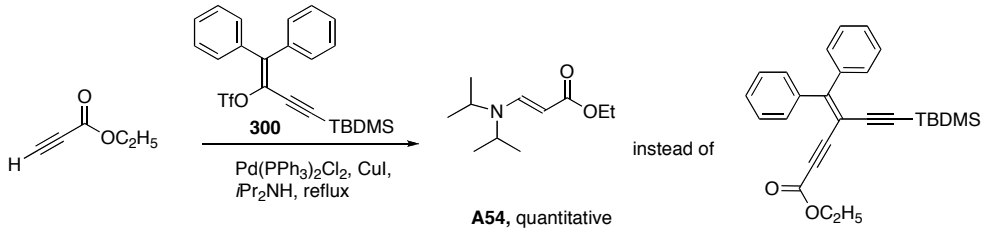

Scheme 35. Attempted synthesis for unsymmetrical dibromoolefin (route 3)

The most promising strategy to date is shown Scheme **36**. This strategy is shorter when compared to the strategies discussed above (three steps compared to five steps). As a matter of fact, the first step is crucial because it establishes a method that is applicable to the other oligomers. Lithiation of compound **302** and reaction with carbamyl chloride gave ketone **A55** as an off-white solid in 65% yield. The following two steps in Scheme **36** are established procedure and reported in the literature for similar systems (while two reactions

attempted and the results was promising based on ^{13}C NMR, but because of time shortage related characterization was not completed for report).[3,6] The unsymmetrical dibromoolefin potentially is a very useful compound that opens the door to the synthesis of not only bisexpanded radialene **316b** but also other unprecedented derivatives of expanded radialene. Scheme **37** shows some of the most important applications of the unsymmetrical dibromoolefin.

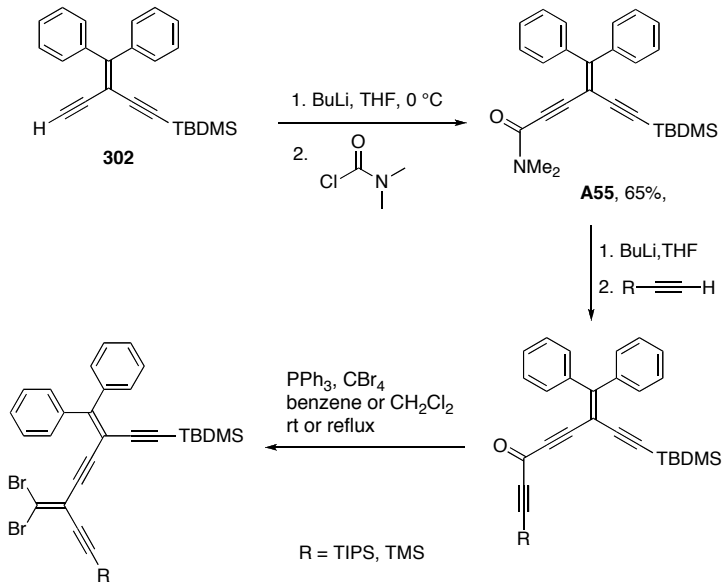

Scheme 36. Synthesis of unsymmetrical dibromoolefin **A55**

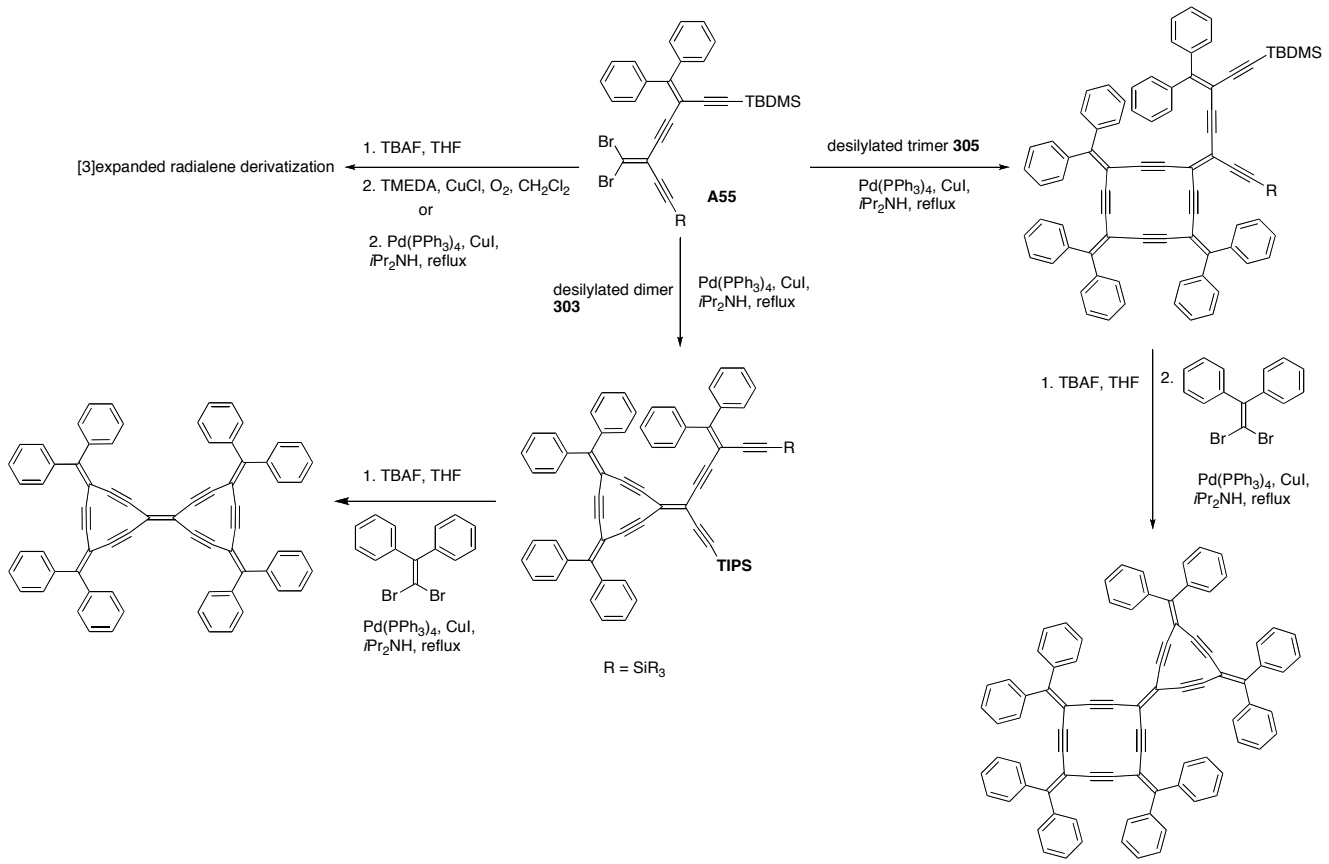

Scheme 37. Proposed synthetic applications of the unsymmetrical dibromoolefin **A55** (future plan)

A.12 Discussion of homo-coupled and side-reaction products

The synthesis of bis[5]expanded radialenes or radiaannulenes has been discussed in Chapter **3**. The synthesis also gave compound **A56** (yellow solid, 10%) as the result of oxidative coupling reaction of desilylated tetramer **304** (Scheme **38**).

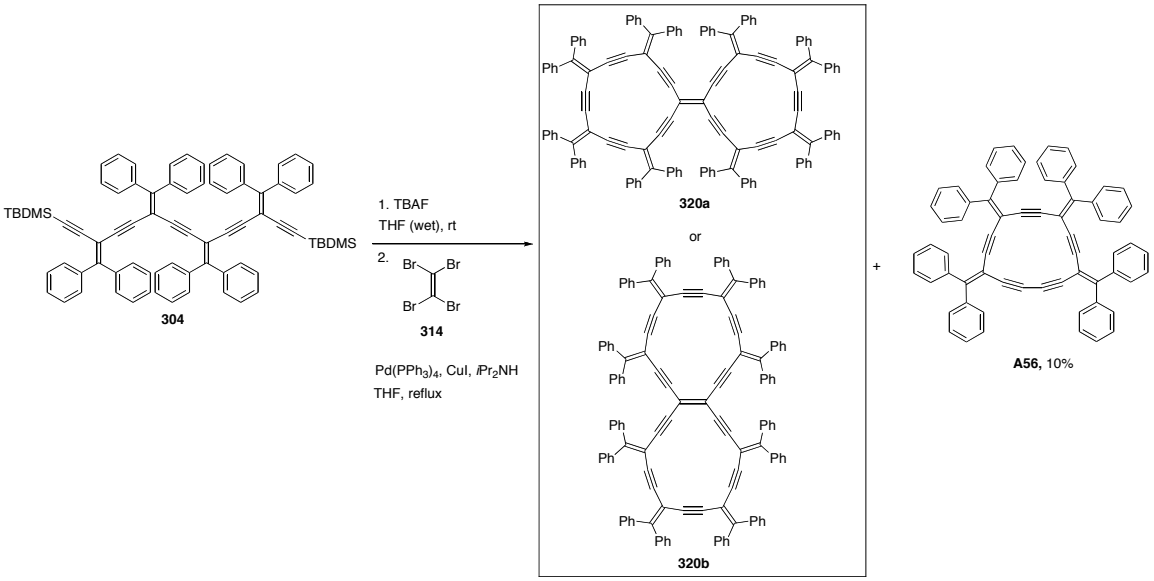

Scheme 38. Synthesis of radialenes **320a/b** and **A56**

Radialene **A56** is confirmed by HR MALDI-TOF mass spectrometry and ^{13}C NMR spectroscopy. The UV-vis spectrum of compound **A56** shows one main absorption at (λ_{max} is defined here as the lowest energy absorbance observed in the spectrum) λ_{max} = 397 nm in comparison to compound **318** that shows a main absorption at λ_{max} = 370 nm (Figure **6**).

Cyclic voltammetry of compounds **318** and **A56** was done in CH_2Cl_2. Compound **318** shows reductions at –1.72, –1.94, –2.04 and –2.35 V, and compound **A56** shows reductions at –1.77, –1.98, and –2.26 V. Radialene **318**

shows an oxidation event at 0.89 V in contrast to radialene **A56** which shows oxidations at 0.85 and at 0.98 V.

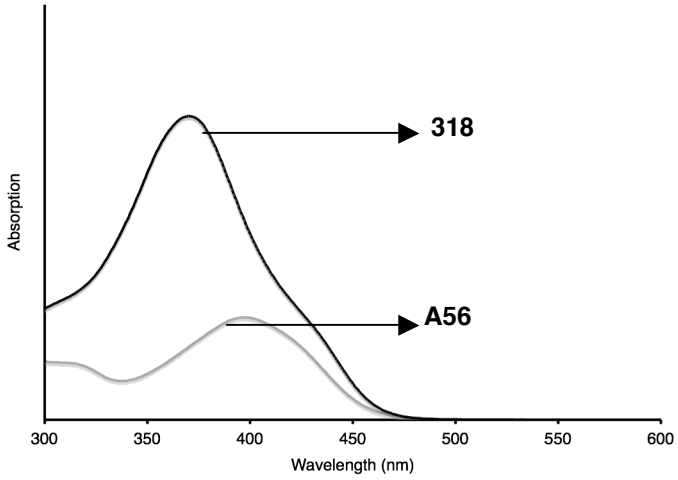

Figure 6. UV-vis spectra of compounds **318** and **A56** measured in THF

In addition to compounds **318** and **A56** a smaller member of this series compound **A57** that was obtained as a purple solid (< 1%) from the reaction in Scheme **38.** A compound with the constitutional formula according to compound **A57** was identified by HR MALDI-TOF mass spectrometry after subjecting the crude reaction product to the column chromatography. The amount of the radialene **A57** was however insufficient for characterization. The UV-vis spectrum of compound **A57** in THF (BHT) is shown in Figure **7**.

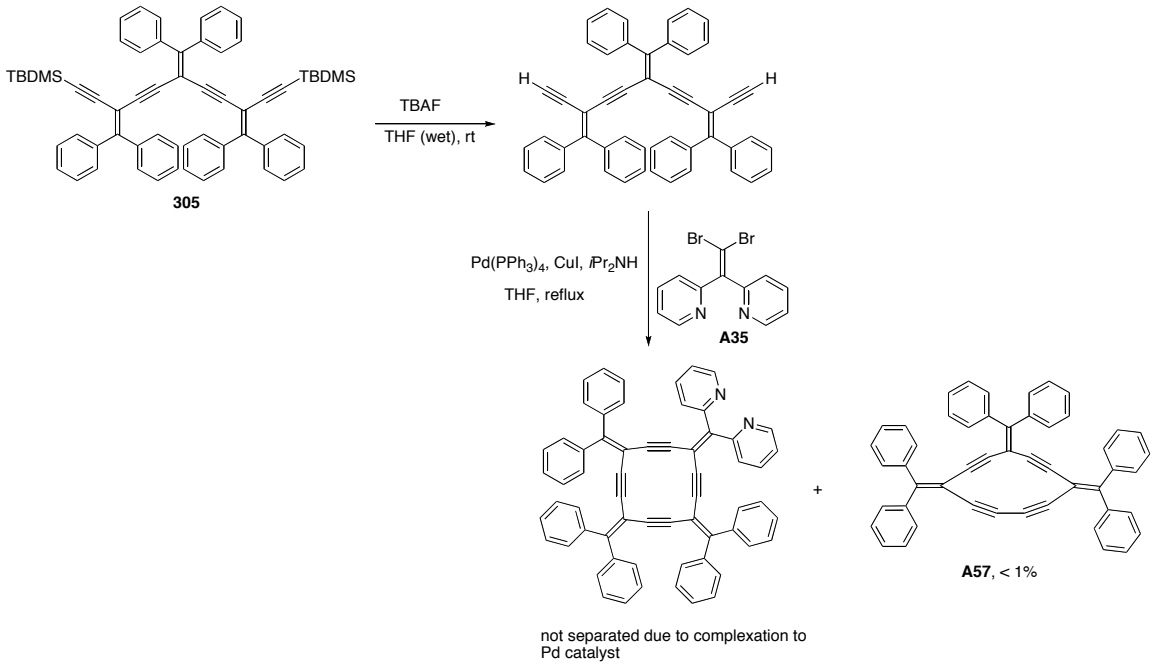

Scheme **39**. Synthesis of compound **A57**

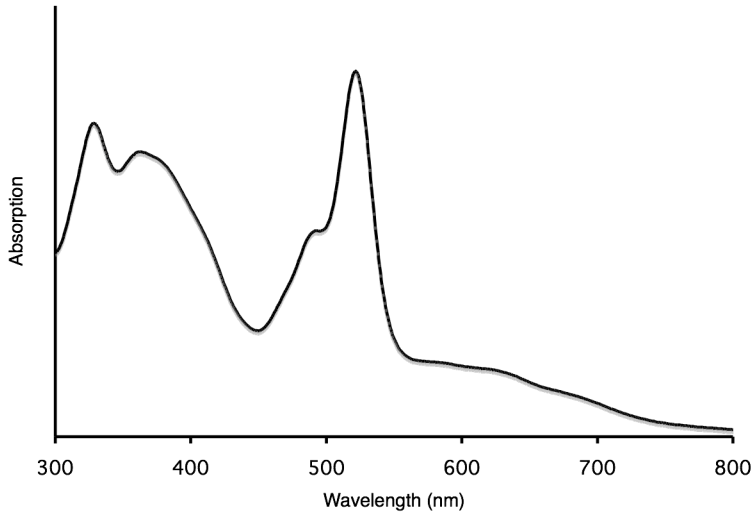

Figure 7. UV-vis spectrum of compound **A57** measured in THF (BHT)

After, the UV-vis spectroscopic analysis, however the THF solution showed that compound **A57** was not the only species present in the solution (Scheme **40**, possible reaction during UV-vis analysis?). The mixture from the UV-vis study was subjected to chromatography on aluminum oxide plate (activity 2, hexanes/CH_2Cl_2, 1.5:1), and the first compound was identified as **A57**. The second compound **A58** (smaller R_f) showed one additional degree of unsaturation based on HR MALDI-TOF mass spectrometry. For compound **A57** ($C_{50}H_{30}$) the calculated value is 630.23240 while the MS shows a molecular ion at (M^+) at m/z 630.23445. For compound **A58** ($C_{50}H_{28}$) MS shows a molecular ion is at m/z 628.21874 that matches with the calculated molecular value of 628.21855.

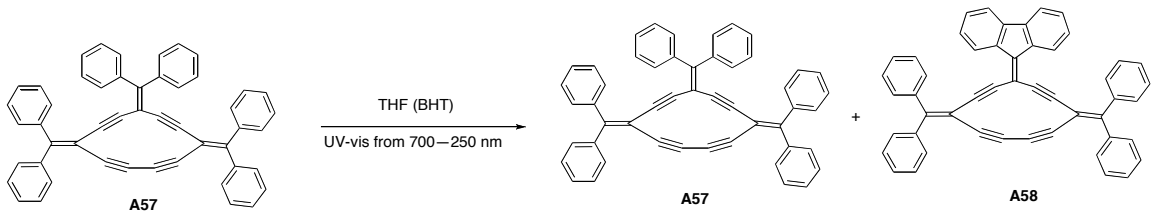

Scheme 40. Possible reaction during UV-vis study in THF (BHT)

Therefore, the spectrum shown in Figure **7** does not show electronic absorption either compound **A57** or **A58**. UV-vis spectroscopy for compounds **A57** and **A58** in CH_2Cl_2 revealed their absorptions according to the Figure **8**. Figure **8** shows the two compounds are very different in their electronic makeup.

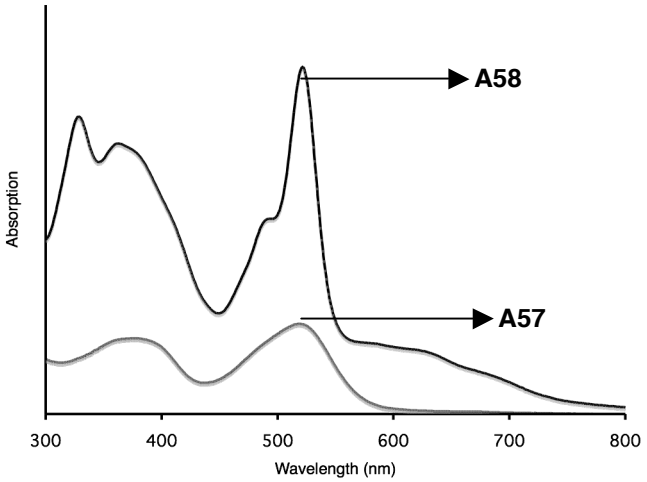

Figure 8. UV-vis spectra of compound **A57** and **A58** measured in CH_2Cl_2

There should be a way to re-examine and confirm the above results. The reexamination may include the synthesis of compound **A57** through desilylation of the trimer **305** and its reaction under oxidative coupling protocols (Scheme **41**). The resulted compound **A57** could be irritated by UV-vis radiation In THF (BHT) to provide hopefully a large quantity of compound **A58** for complete characterization and structural assignment.

Figure **9** shows UV-vis spectra for compounds **A57**, **A56** and **318**. The spectra show that as the macrocycles become more strained, the absorptions shift to lower energy. Also, the highly strained compound **A57** has an absorption at much higher wavelength compared to the less strained macrocycles **318** and **A56**. Again, the more strained the macrocycles, the more interesting their physical properties.

†Due to the shortage of compound **A57** and consequently low absorption in the UV-vis spectroscopy (under 0.1), It should be noted that the data for compound **A57** from Figure **8** multiplied by 3 in order to increase its intensity (the absorption intensity) and readers have a better visual comparison in Figure **9**.

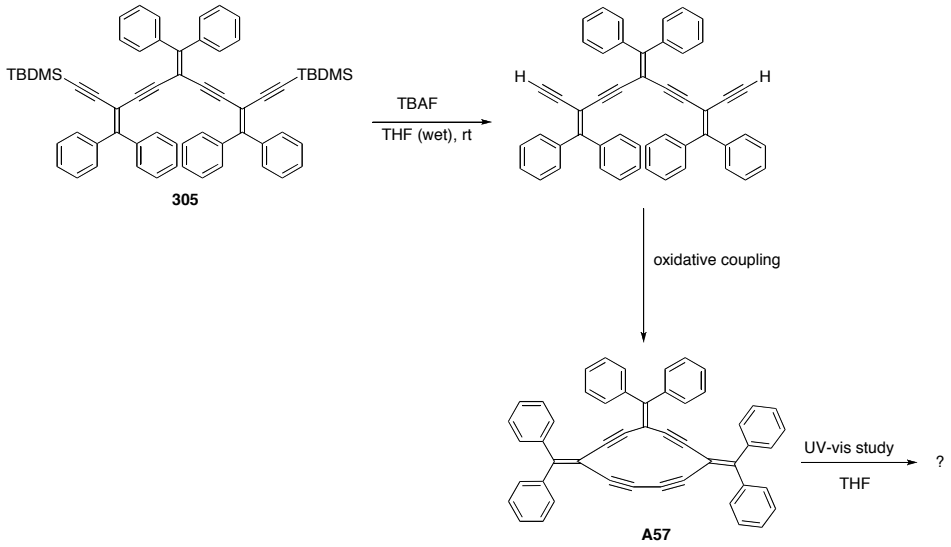

Scheme 41. Proposed strategy for synthesis of compound **A57**

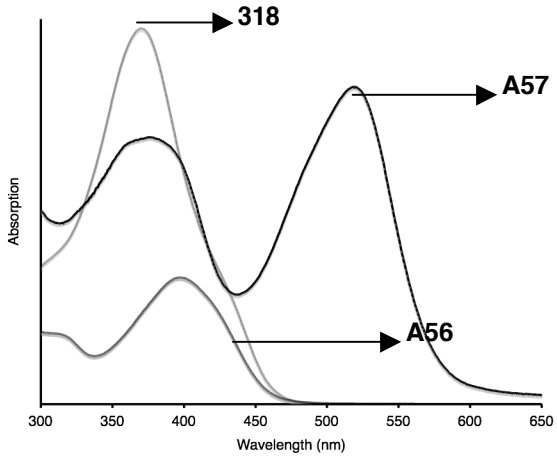

Figure 9. UV-vis spectra for radialenes **318**, **A56** (THF) and **A57** (CH_2Cl_2) (refer to above statement, page 421)†

A13. Side products from [3]expanded radialene reactions

The synthesis of [3]expanded radialenes was discussed in Chapters **3** and **4**. In the synthesis of compound **420** and **423**, both reactions shared a side product as a result of the oxidative coupling of the desilylated dimer **303** (Schemes **42** and **43**). Compound **A59** shows very low solubility in the most common organic solvents, and the proposed structure was supported by ^{13}C NMR spectroscopy and HR MATDI-TOF mass spectrometry. The UV-vis spectrum of **A59 (**in THF) shows an absorption at 329 nm. Cyclic voltammetry of compound **A59** in CH_2Cl_2 shows reductions at –1.67, –1.86, and –2.11 V, as well as an oxidation event at 0.96 V.

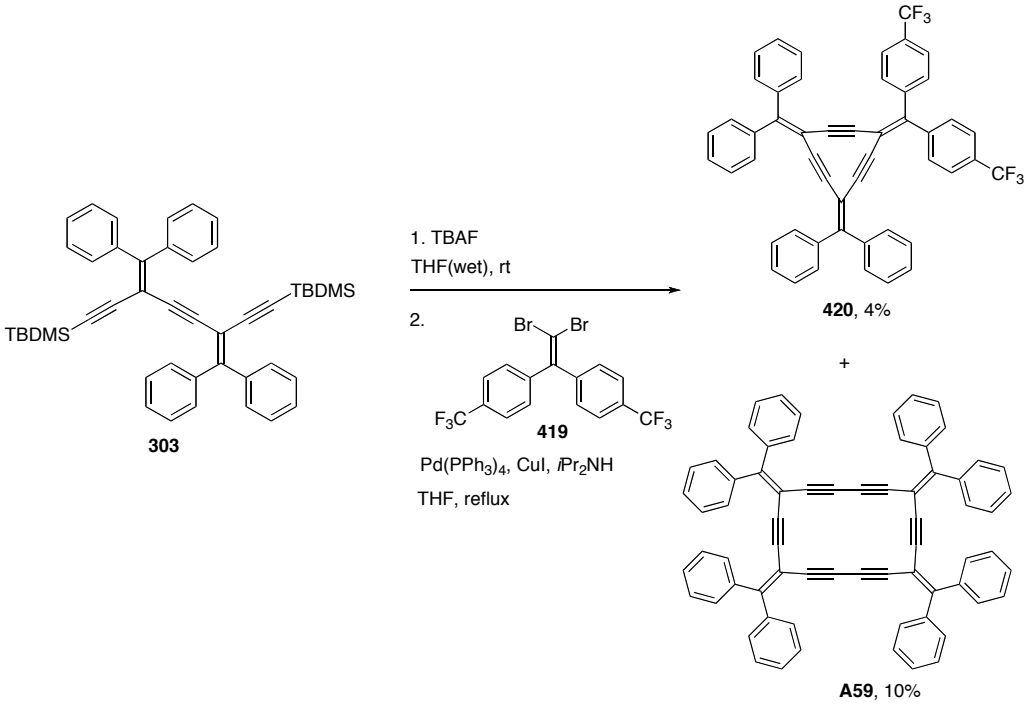

Scheme 42. Synthesis of compounds **420** and **A59**

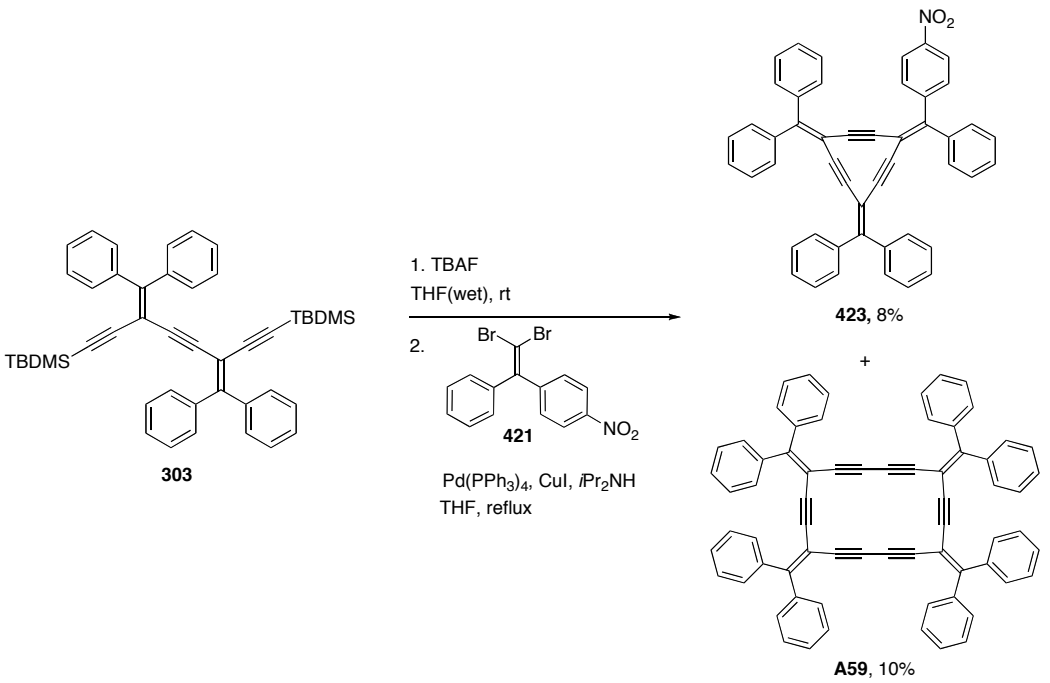

Scheme 43. Synthesis of compound **423** and **A59**

A.14 Tetraphenylcyclopentadienylidene expanded radialenes (incomplete projects)

There was also an attempt to synthesize [3]expanded radialene **A60** according to Scheme **44**. The product of the reaction was isolated in low yield and there was not enough time to repeat the reaction in order to provide sufficient material for full characterization of the compound **A60** (note: it is believed that compound **432** used in the reaction contained some PPh_3 that may cause the reaction did not work properly). Initial confirmation for constitutional formula for **A60** comes from HR MALDI-TOF mass spectrometry that shows a molecular ion (M^+) of m/z 808.31253, while the calculated for $C_{64}H_{40}$ is m/z 808.31245. Furthermore, Scheme **45** shows two radialenes **A61** and **A62** that remained for

future synthesis. Both compounds should be synthesized according to the general Scheme **4** in appendix.

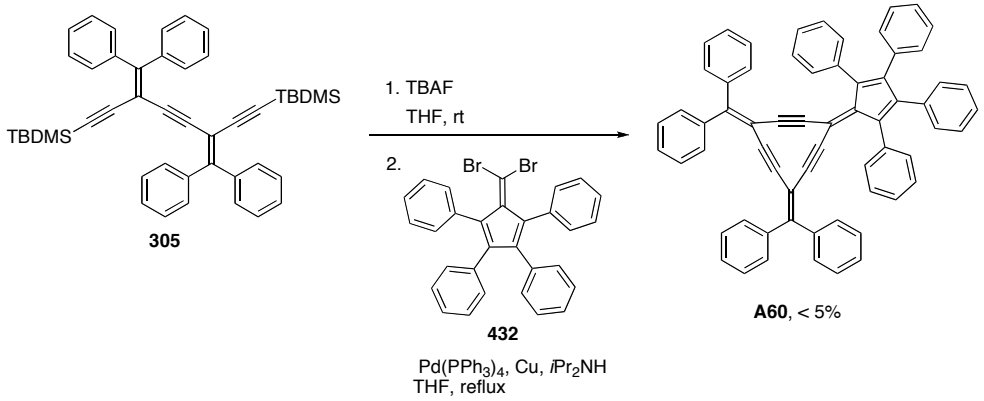

Scheme 44. Synthesis of [3]expanded radialenes **A60**

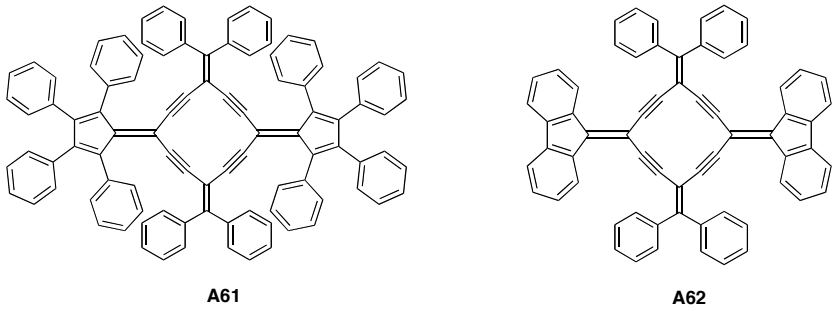

Scheme 45. Two radialenes for future synthesis

A.15 The last note for the expanded radialene chemistry

The two most useful starting materials used in this chemistry and widely applicable are compound **314** and **410** (Scheme **46**). However, a piece of this puzzle is still missing. For the synthesis of radiaannulenes, there is a clear need to have dibromoolefin **A63** (Scheme **46**). Compound **A63** allows for

stepwise synthesis of the radiaannulenes. The author at this stage does propose any strategies for the synthesis of compound **A63** and it remains for future students.

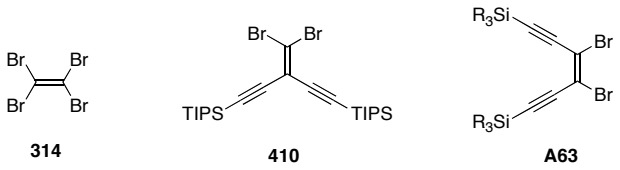

Scheme 46. Useful building blocks for the chemistry of radialenes and radiaannulenes

A16. **Conclusion**

This chapter has covered some valuables projects that are incomplete and are extensions to the chemistry that developed in this thesis and would provide new compounds with interesting skeletons.

A.17 References

(1) Rankin, T.; Tykwinski, R. R. *Org. Lett*. **2003**, *5*, 213–216.

(2) Xu, G.-L.; Xi, B.; Updegraff, J. B.; Protasiewicz, J. D.; Ren, T. *Orgaometallics* **2006**, *25*, 5213–5215.

(3) (a) Ramirez, F.; Desai, N. B.; McKelvie, N. *J. Am. Chem. Soc*. **1962**, *84*, 1745–1747; (b) Corey, E. J.; Fuchs P. L. *Tetraherdon Lett.* **1972**, *13*, 3769–3772; (c) Neidlein, R.; Winter, M. *Synthesis* **1998**, 1362–1366.

(4) Enquist, P.–A.; Nilsson, P.; Larhed, M. *Org. Lett*. **2003***, 5*, 4875–4878.

(5) Gibtner, T.; Hampel, F.; Gisselbrecht, J.-P.; Hirsch, A. *Chem. Eur. J*. **2002**, *8*, 408–432.

(6) O'Connor, D.C.; Cowan, D.O. *J. Organomet. Chem.* **1991**, *408*, 113–117.

(7) Minn, F. L.; Trichilo, C. L.; Hurt, C. R.; Filipescu N. *J. Am. Chem. Soc.* **1970**, *92*, 3600–3601.

(8) Eisler, S.; Tykwinski, R. R. *Angew. Chem. Int. Ed.* **1999**, *38*, 1940–1943.

(9) Clement Osei Akoto, University of Alberta, 2001–2004.

(10) Tykwinski, R. R.; Zhao, Y. *Synlett* **2002**, 1939–1953.

(11) Gan, Z.; Roy, R. *Can. J. Chem*. **2002**, *80*, 908–916.

Compound **A8**

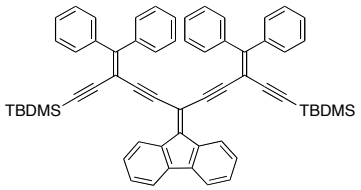

A mixture of **527** (150 mg, 0.39 mmol) and K_2CO_3 (10.7 mg, 0.0770 mmol) in wet THF (1 mL) and MeOH (1 mL) was stirred for 1 h. Et_2O and H_2O were added, the organic phase separated, washed with saturated NH_4Cl (2 x 20 mL), dried ($MgSO_4$) and reduced to 2 mL. The Et_2O solution was added to a degassed mixture of triflate **300** (350 mg, 0.750 mmol), CuI (22 mg, 0.11 mmol), $Pd(PPh_3)_4$ (24 mg, 0.020 mmol), iPr$_2$NH (3 mL) and dry THF (5 mL). The resulting mixture was refluxed for 20 h. Solvent removal and purification by column chromatography (silica gel, hexanes/CH_2Cl_2, 8:1 to 5:1) afforded **A8** (17 mg, 5%) as an orange solid. Mp 70 °C. R_f = 0.4 (hexanes/CH_2Cl_2, 1:1). IR (CH_2Cl_2, cast) 3058, 3030, 2953, 2927, 2984, 2856, 2144, 1600, 1579 cm^{-1}; ^{1}H NMR ($CDCl_3$, 500 MHz) δ 8.37 (d, J = 8 Hz, 2H), 7.55 (d, J = 8 Hz, 2H), 7.51–7.49 (m, 4H), 7.41–7.39 (m, 4H), 7.35–7.33 (m, 6H), 7.28–7.23 (m, 8H), 7.11–7.08 (t, J = 7 Hz, 2H), 0.87-0.86 (m, 18H), 0.09–0.07 (m, 12H); ^{13}C NMR (125 MHz, $CDCl_3$) δ 157.9, 145.1, 140.3, 134.0, 139.7, 137.2, 130.5, 130.4, 129.3, 129.0, 128.6, 127.9, 127.8, 127.5, 125.3, 119.2, 103.2, 101.9, 101.9, 101.1, 97.4, 96.9, 90.2, 26.1, 16.8, –4.7. MALDI-TOF HRMS (DCTB) calcd. for $C_{62}H_{58}Si_2$ 858.40716 (M^+), found 858.40627.

Compound **A28**, **A29**, **A30** and **A31** (incomplete project)

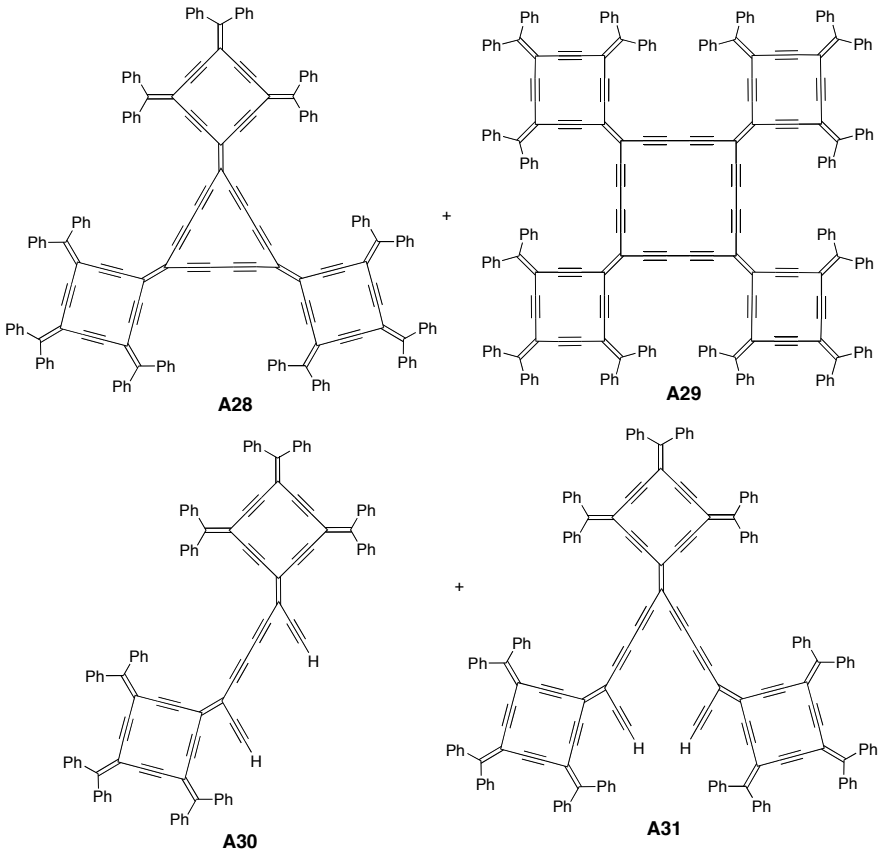

A mixture of radialene **411** (50.0 mg, 0.0490 mmol) and TBAF (0.2 mL, 0.2 mmol, 1M in THF) in wet THF (2 mL) was stirred for 1 h. CH_2Cl_2 and H_2O were added, the organic phase separated, washed with saturated NH_4Cl (2 x 20 mL), dried ($MgSO_4$) and reduced to 2 mL. The CH_2Cl_2 solution was added to a mixture of TMEDA (160 mg, 1.37 mmol, 0.205 mL), CuCl (26 mg, 0.26 mmol), and dry CH_2Cl_2 (25 mL). The resulting mixture was stirred for 12 h under air. Solvent removal and purification by column chromatography (silica gel, hexanes/CH_2Cl_2, 5:1 to 1:1) first afforded **A30** as a red solid and second **A31** as a red solid and

third a mixture of **A28** and **A29** (green) based on MALDI-TOF mass spectrometry analysis.

Compound **A28**: MALDI-TOF LRMS (DCTB) calcd. for $C_{168}H_{90}$ 2106.7042 (M^+), found 2107.6383.

Compound **A29**: MALDI-TOF LRMS (DCTB) calcd. for $C_{234}H_{120}$ 2808.9390 (M^+), found 2810.8463.

Compound **A30**: MALDI-TOF HRMS (DCTB) calcd. for $C_{112}H_{62}$ 1406.48460 (M^+), found 1406.48473.

Compound **A31**: MALDI-TOF HRMS (DCTB) calcd. for $C_{168}H_{92}$ 2108.71935 (M^+), found 2108.71728.

Compound **A34**[1]

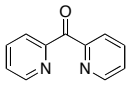

To dry THF (7 mL) was added 2-bromopyridine (1 g, 6 mmol) and the resulting solution was stirred for 5 min and then cooled to −78 °C. *n*BuLi (2.5 mL, 6.3 mmol, 2.5 M in hexanes) was added drop-wise to the solution and the mixture stirred for 15 min at −78 °C. Dimethyl carbamylchloride (340.0 mg, 0.3380 mmol, 0.2910 mL) was added to the mixture in one portion. The resulting mixture was stirred at −78 °C for 30 min followed by raising the temperature to room temperature and treating the mixture with HCl solution (5 mL, 10%). After work-up, the crude reaction product was subjected to column chromatography (silica gel, hexanes/ethyl acetate, 5:1) and afforded ketone **A34** (361 mg, 62%) as a creamy solid. IR (CH_2Cl_2, cast) 3054, 3006, 1685, 1612, 1582, 1569 cm^{-1}; ^1H NMR ($CDCl_3$, 400 MHz) δ 8.78–8.04 (m, 2H), 8.04–8.02 (m, 2H), 7.85–7.82 (m, 2H), 7.81–7.41 (m, 2H); ^{13}C NMR (125 MHz, $CDCl_3$) δ 192.9, 154.2, 149.1, 136.6, 126.3, 125.1. EI HRMS calcd. for $C_{11}H_8ON_2$ 184.0637 (M^+), found 184.0631.

Compound **A35**

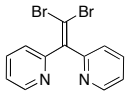

To a mixture of PPh_3 (6 g, 20 mmol) in dry benzene (40 mL), was added CBr_4 (4.3 g, 13 mmol) and the resulting mixture was stirred at room temperature for 30 min. Ketone **A34** (0.82 g, 4.4 mmol) was added in one portion and the resulting mixture was refluxed for 4 days. The crude reaction product was filtered and washed with benzene (2 x 40 mL). Solvent removal and purification by column chromatography (silica gel, hexanes/ethyl acetate, 10:1 to 5:1) afforded dibromoolefin **A35** (1.2 g, 75%) as a white solid. Mp 115 °C. R_f = 0.4 (aluminum oxide, CH_2Cl_2). IR (CH_2Cl_2, cast) 3063, 3007, 2976, 1582, 1566 cm^{-1}; ^1H NMR ($CDCl_3$, 500 MHz) δ 8.58–8.57 (m, 2H), 7.71–7.68 (m, 2H), 7.56–7.55 (m, 2H), 7.20–7.18 (m, 2H); ^{13}C NMR (125 MHz, $CDCl_3$) δ 157.9, 149.5, 146.5, 136.5, 124.7, 122.8, 95.6. EI HRMS calcd. for $C_{12}H_8N_2{}^{79}Br_2$ 337.9054 (M^+), found 337.9048.

Compound **A38**

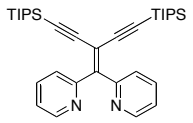

To a degassed mixture of **A35** (40.7 mg, 0.119 mmol), CuI (2.3 mg, 0.012 mmol), $Pd(PPh_3)_2Cl_2$ (4.2 mg, 0.0059 mmol), *i*Pr_2NH (3 mL) and dry THF (5 mL) was added triisopropylsilylacetylene (53 mg, 0.29 mmol, 0.076 mL) and the resulting mixture stirred for 20 h at room temperature. Solvent removal and purification by column chromatography (aluminum oxide, activity 1, hexanes/ethyl acetate, 9:1) afforded **A38** (17 mg, 26%) as an off white solid. Mp 30 °C. R_f = 0.3 (hexanes/ethyl acetate, 5:1). IR (CH_2Cl_2, cast) 3049, 2942, 2891, 2865, 2144, 2125, 1584, 1567 cm^{-1}; ^1H NMR ($CDCl_3$, 500 MHz) δ 8.56–8.55 (m, 2H), 7.92–7.90 (m, 2H), 7.66–7.62 (dt, *J* = 7.5, 2 Hz, 2H), 7.15–7.13 (m, 2H), 1.00–0.98 (s, 42H); ^{13}C NMR (125 MHz, $CDCl_3$) δ 157.5, 153.2, 149.3, 135.6, 125.9, 122.5, 107.3, 104.1, 97.3, 18.5, 11.2. EI HRMS calcd. for $C_{34}H_{50}N_2Si_2$ 542.3513 (M^+), found 542.3508.

Compound **A44**, **A45**, **A46**, and **A47** (incomplete project)

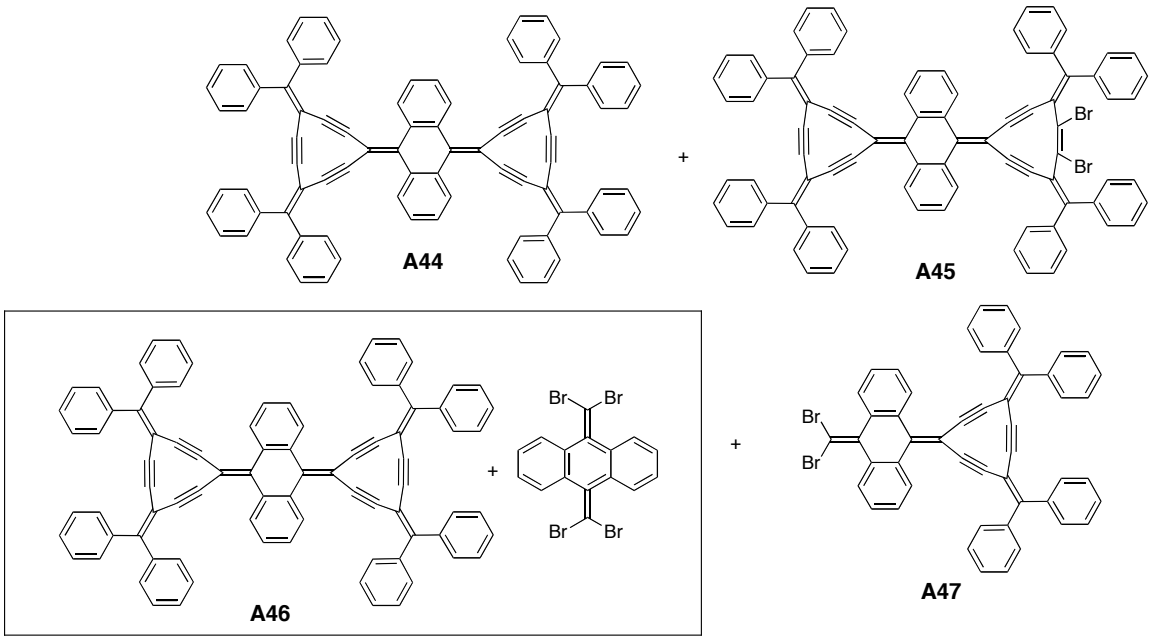

A mixture of dimer **303** (60 mg, 0.09 mmol) and TBAF (0.1 mL, 0.1 mmol, 1M in THF) in wet THF (2 mL) was stirred for 1 h. Et_2O and H_2O were added, the organic phase separated, washed with saturated NH_4Cl (2 x 20 mL), dried ($MgSO_4$) and reduced to 2 mL. The Et_2O solution was added to a degassed mixture of compound **501** (23 mg, 0.039 mmol), CuI (5 mg, 0.03 mmol), $Pd(PPh_3)_4$ (3.5 mg, 0.0030 mmol), *i*Pr_2NH (3 mL) and dry THF (5 mL). The resulting mixture was refluxed for 18 h. Solvent removal and purification by column chromatography (aluminum oxide, neutral, hexanes/CH_2Cl_2, 1.5:1) afforded first afforded first **A47** then **A44** (red solid) and then **A45** as yellow solid followed by **A46** as a yellow solid.

Compound **A44**: MALDI-TOF HRMS (DCTB) calcd. for $C_{84}H_{48}$ 1056.37505 (M^+), found 1056.37486; IR (CH_2Cl_2, cast) 2954, 2923, 2853, 1730, 1675, 1598 cm^{-1}.

Compound **A45**: MALDI-TOF HRMS (DCTB) calcd. for $C_{84}H_{48}{}^{79}Br_2$ 1214.21138 (M^+), found 1214.21267; IR (CH_2Cl_2, cast) 3059, 3029, 2953, 2924, 2853, 2187, 1949, 1730 cm^{-1}.

Compound **A46:** MALDI-TOF HRMS (DCTB) calcd. for $C_{100}H_{56}{}^{79}Br_4$ 1572.11100 (M^+), found 1572.11100; IR (CH_2Cl_2, cast) 3055, 3020, 2954, 2924, 2854, 2189, 1951, 1856, 1726 cm^{-1}.

Compound **A47**: MALDI-TOF HRMS (DCTB) calcd. for $C_{50}H_{28}{}^{79}Br_2$ 786.05523 (M^+), found 786.05539; IR (CH_2Cl_2, cast) 2954, 2921, 2850, 1729 cm^{-1}.

Compound **A49** and **A50** (incomplete project)

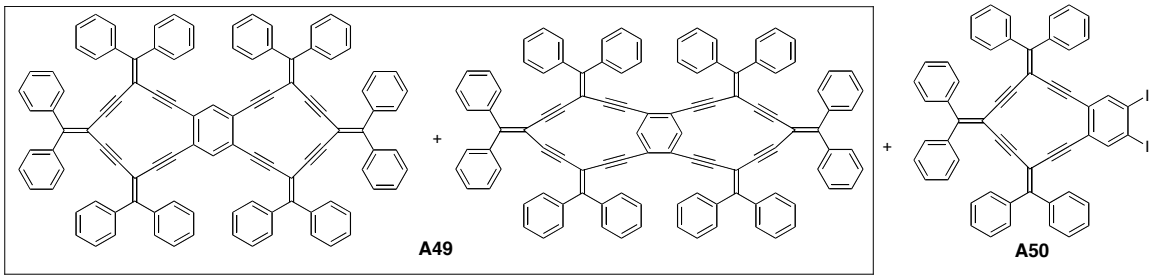

A mixture of trimer **305** (72 mg, 0.084 mmol) and TBAF (0.198 mL, 0.198 mmol, 1M in THF) in wet THF (2 mL) was stirred for 1 h. Et_2O and H_2O were added, the organic phase separated, washed with saturated NH_4Cl (2 x 20 mL), dried ($MgSO_4$) and reduced to 2 mL. The Et_2O solution was added to a degassed mixture of tetraiodobenzene **A48** (23 mg, 0.039 mmol), CuI (3.5 mg, 0.018 mmol), $Pd(PPh_3)_4$ (3.5 mg, 0.0030 mmol), *i*Pr_2NH (3 mL) and dry THF (5 mL). The resulting mixture was refluxed for 18 h. Solvent removal and purification by column chromatography (silica gel, hexanes/CH_2Cl_2, 5:1 to 2:1) afforded first afforded **A50** then **A49** both as yellow solids

Compound **A49**: MALDI-TOF LRMS (DCTB) calcd. for $C_{106}H_{62}$ 1334 (M^+), found 1334.5. ^{13}C NMR (125 MHz, CD_2Cl_2) δ 157.6, 156.4, 147.9, 142.2, 142.1, 140.7, 140.4, 140.1, 139.9, 132.7, 131.3, 130.9, 130.7, 130.4, 130.32, 130.30, 129.5, 129.3, 128.6, 128.4, 128.3, 128.29, 128.21, 126.1, 108.8, 107.3, 107.1, 101.9, 101.7, 101.6, 99.9, 98.7, 95.9, 95.1, 94.3, 93.1, 92.5, 91.7, 91.1, 90.4, 88.9, 88.3.

Compound **A50**: MALDI-TOF HRMS (DCTB) calcd. for $C_{56}H_{32}I_2$ 958.05879 (M^+), found 958.05793.

Compound **A54**[2]

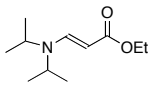

To a degassed mixture of triflate **300** (0.5 g, 1 mmol), CuI (20.5 mg, 0.188 mmol), $Pd(PPh_3)_2Cl_2$ (38 mg, 0.054 mmol), *i*Pr_2NH (3 mL) and dry THF (10 mL) was added ethyl propiolate (0.29 gr, 2.9 mmol, 0.29 mL) and the resulting mixture refluxed for 6h. Et_2O and H_2O were added to the crude reaction product, the organic phase separated, washed with saturated NH_4Cl (2 x 20 mL) and dried ($MgSO_4$). Solvent removal and purification by column chromatography (silica gel, hexanes/ethyl acetate 5:1) afforded ester **A54** (0.65 g, 96%) as a brown oil that becomes crystalline at low temperature (about 4 °C). R_f = 0.65 (hexanes/ethyl acetate, 1:1). IR (CH_2Cl_2, cast) 2976, 2934, 2873, 1688, 1602 cm^1; ^1H NMR (400 MHz, $CDCl_3$) δ 7.48 (dd, *J* = 6.6, 1.2 Hz, 1H), 4.58 (dd, *J* = 6.6, 0.8 Hz, 1H), 4.05 (dq, *J* = 7, 1.2 Hz, 2H), 3.57 (bs, 2H), 1.17 (dt, *J* = 7, 1.2 Hz, 3H), 1.12 (dd, *J* = 3.2, 1.2 Hz, 12H); ^{13}C NMR (125 MHz, CD_2Cl_2) δ 170.1, 147.0, 83.2, 58.5, 47.8, 20.4 (br), 14.6. ES HRMS calcd. for $C_{11}H_{21}NO_2Na$ 222.14645 (M^+), found 222.14652. X-ray.

Compound **A55**

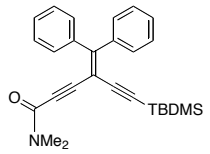

A mixture of **301** (150 mg, 0.362 mmol), K_2CO_3 (10 mg, 0.072 mmol) in wet THF (1 mL) and MeOH (1 mL) was stirred for 2h. Et_2O and H_2O were added, the organic phase separated, washed with saturated NH_4Cl (2 x 20 mL), dried ($MgSO_4$) and dissolved in dry THF (5 mL). To the THF solution at 0 °C was added drop-wise *n*BuLi (0.15 mL, 0.37 mmol, 2.5 mL in hexanes) and the resulting mixture stirred at 0 °C for 20 min. To the resulting mixture was added dimethylcarbamyl chloride (234 mg, 2.18 mmol, 0.170 mL) at 0 °C in one portion. The mixture stirred for 30 min at 0 °C and further 30 min as the temperature was raised to room temperature. The mixture was quenched with H_2O (5 mL). Et_2O was added (50 mL), the organic phase separated, washed with H_2O (2 x 20 mL) and dried ($MgSO_4$). Solvent removal and purification by column chromatography (silica gel, hexanes/CH_2Cl_2, 6:1 to 2:1) afforded amide **A55** (90 mg, 60%) as an off-white solid. Mp 96 °C. R_f = 0.47 (hexanes/ethyl acetate, 1:1). IR (CH_2Cl_2, cast) 3055, 2953, 2928, 2885, 2857, 2199, 2144, 1639 cm^{-1}; ^1H NMR ($CDCl_3$, 400 MHz) δ 7.37–7.35 (m, 2H), 7.23–7.20 (m, 8H), 2.80 (s, 3H), 2.73 (s, 3H), 0.77 (s, 9H), 0.02 (s, 6H); ^{13}C NMR (125 MHz, $CDCl_3$) δ 160.3, 154.2, 139.9, 139.3, 130.2, 130.0, 129.03, 128.95, 128.0, 127.7, 102.3, 100.5, 97.6, 88.5, 83.4, 37.6,

34.0, 26.1, 16.7, –4.9. EI HRMS calc. for $C_{27}H_{31}NOSi$ 413.21750 (M^+), found 413.2174.

Compound **A57** and **A58** (incomplete project)

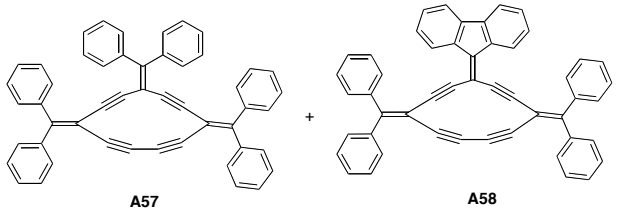

A mixture of trimer **305** (65 mg, 0.075 mmol) and TBAF (0.1 mL, 0.1 mmol, 1M in THF) in wet THF (5 mL) was stirred for 2 h. Et_2O and H_2O were added, the organic phase separated, washed with saturated NH_4Cl (2 x 20 mL), and dried ($MgSO_4$), and reduced to 2 mL. The Et_2O solution was added to a degassed mixture of dibromoolefin **A35** (25.3 mg, 0.0750 mmol), CuI (4.7 mg, 0.025 mmol), $Pd(PPh_3)_4$ (4.33 mg, 0.00375 mmol), *i*Pr_2NH (3 mL) and dry THF (10 mL). The resulting mixture was refluxed for 18 h. Solvent removal and purification by column chromatography (silica gel, hexanes/CH_2Cl_2, 4:1 to 2:1) afforded **A57** (< 1%, due to oxidative coupling reaction, only isolated product) as a purple solid. MALDI-TOF HRMS (DCTB) calcd. for $C_{50}H_{30}$ 630.23240 (M^+), found 630.23445.

Compound **A57** after non-quantitative UV-vis study in THF (refer to **A12**, page 416 for detailed discussion) was subjected to chromatography on aluminum oxide plate (activity 2) using hexanes/CH_2Cl_2 (1.5:1) as solvent system that gave two products, first gave compound **A57** (purple solid) and second gave a purple solid (**A58**).

Compound **A57**: TOF HRMS (DCTB) calcd. for $C_{50}H_{30}$ 630.23240 (M^+), found 630.23445; UV-vis (CH_2Cl_2) λ_{max} 375, 519 nm.

Compound **A58**: MALDI-TOF HRMS, calculated for $C_{50}H_{28}$ is 628.21855 (M^+), found 628.21874; UV-vis (CH_2Cl_2) λ_{max} 521 nm and a shoulder around 490 nm.

Compound **A60** (incomplete project)

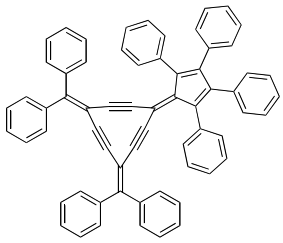

A mixture of dimer **303** (100.0 mg, 0.1517 mmol) and TBAF (0.1 mL, 0.1 mmol, 1M in THF) in wet THF (2 mL) was stirred for 1 h. Et_2O and H_2O were added, the organic phase separated, washed with saturated NH_4Cl (2 x 20 mL), and dried ($MgSO_4$) and reduced to 2 mL. The Et_2O solution was added to a degassed mixture of compound **432** (82 mg, 0. 15 mmol), CuI (9 mg, 0.05 mmol), $Pd(PPh_3)_4$ (3.5 mg, 0.0031 mmol), *i*Pr_2NH (3 mL) and dry THF (5 mL). The resulting mixture was refluxed for 18 h. Solvent removal and purification by column chromatography (silica gel hexanes/CH_2Cl_2, 5:1 to 2:1) afforded **A60** as a brown (3 mg, 2.5%) solid. MALDI-TOF HRMS (DCTB) calcd. for $C_{64}H_{40}$ 808.31245 (M^+), found 808.31523.

References

(1) Hlasta, D. J.; Court, J. J. *Tetrahedron Lett*. 1**989**, *30*, 1773–1776.
(2) Talley, J. J. *Tetrahedron Lett*. **1981**, *22*, 823–826.

Table A.1. Redox potentials of radialenes and related derivatives[†]

comp.	Ep, ox_1	E1/2, ox_1	Ep, ox_2	Ep, red_1	E1/2, red_1	Ep, red_2	E1/2, red_2	Ep, red_3	Ep, red_4
303	1.14			–2.09		–2.22		–2.38	
304	1.08			–2.15		–2.28		–2.45	
305	0.99			–2.22		–2.38			
309					–2.03		–2.23		
310		0.82	1.11		–1.9	–2.12		–2.33	
311		0.81	1.01		–1.9	–2.16			
312		0.83			–1.91	–1.98			
315a	0.78		0.86		–1.29		–1.59		
316a		0.68			–1.36		–1.71		
318	0.89				–1.72	–1.94		–2.04	–2.35
404	0.93		1.14		–1.08		–2.01	–2.42	
405	0.79			–1.79		–2.02			
406	1.08			–2.15		–2.28		–2.45	
408		0.83	1.01		–1.51		1.81	–2.37	
409		0.83	1.11		–1.55	–1.88		–2.03	
411		0.92			–1.58	–1.88			
412		0.94	1.19		–1.59	–1.98		–2.2	
414	0.92		1.16		–1.42	–1.8		–1.89	
433	0.65		0.83		–1.26		–1.54	–1.69	
434		0.81	1.21		–1.58	–2.05			
502	0.66		0.8		–1.48				
504	0.69		0.85		–1.54	–2.09			
507	0.85		1.05		–1.29		–1.43	–2.03	–2.14
508	0.77		0.93		–1.4	–1.88		–1.99	–2.19
515	0.95				–1.61		–1.85	–2.11	
519	0.81		1.03		–1.87	–2.19			
526	0.75				–1.97		–2.15	–2.41	
527	0.95				–1.82		–2.14	–2.39	
528	0.88				–1.50		–1.65	–2.30	
A56	0.85		0.98		–1.77		–1.98	–2.26	
A59	0.96			–1.67		–1.80		–2.11	

[†] Cyclic voltammetry measured in CH_2Cl_2 + 0.1 M nBu_4NPF6 at a scan rate 100 mV s1. All potentials are reported versus the ferrocenium/ferrocene (Fc^+/Fc) couple.

Table A.2. Optical and electrochemical gaps of radialenes and related derivatives[†]

comp.	spectral onset (nm)	optical H-L (ev)	Electrochemical H-L (V)
303	511	2.42	3.23
304	509	2.43	3.23
305	516	2.41	3.21
309	600	2.06	–
310	480	2.58	2.72
311	480	2.58	2.70
312	480	2.58	2.70
315a	664	1.86	2.07
316a	623	1.99	2.04
318	648	2.42	2.61
404	520	2.38	2.73
405	548	2.26	2.58
406	590	2.13	2.77
408	520	2.38	2.34
409	530	2.34	2.43
411	510	2.43	2.51
412	510	2.43	2.53
414	523	2.37	2.34
433	610	2.01	1.90
434	720	1.72	2.39
502	580	2.13	2.14
504	545	2.27	2.23
507	584	2.11	2.14
508	640	1.93	2.17
515	510	2.43	2.56
519	510	2.43	2.68
526	470	2.63	2.72
527	516	2.45	2.77
528	520	2.38	2.38
A56	500	2.48	2.62
A59	502	2.47	2.63

[†]Note: The electrochemical HOMO–LUMO gap is calculated from the first reduction potential minus the first oxidation potential (E_{1red}–E_{1ox}), and the optical

HOMO–LUMO gap is obtained from the onset of the UV-vis band ($E_{HOMO-LUMO}$=1240/onset (nm)).

There are a few ways to find out which wavelength should be used for the calculation of optical band gap (such as using the value at epsilon (ε) = 1000 or using a tangential line from the spectrum to the x-axis. The method used here is the tangential line that naturally is involved with some errors.

LR MALDI-TOF Mass Spectrum of DCTB Matrix

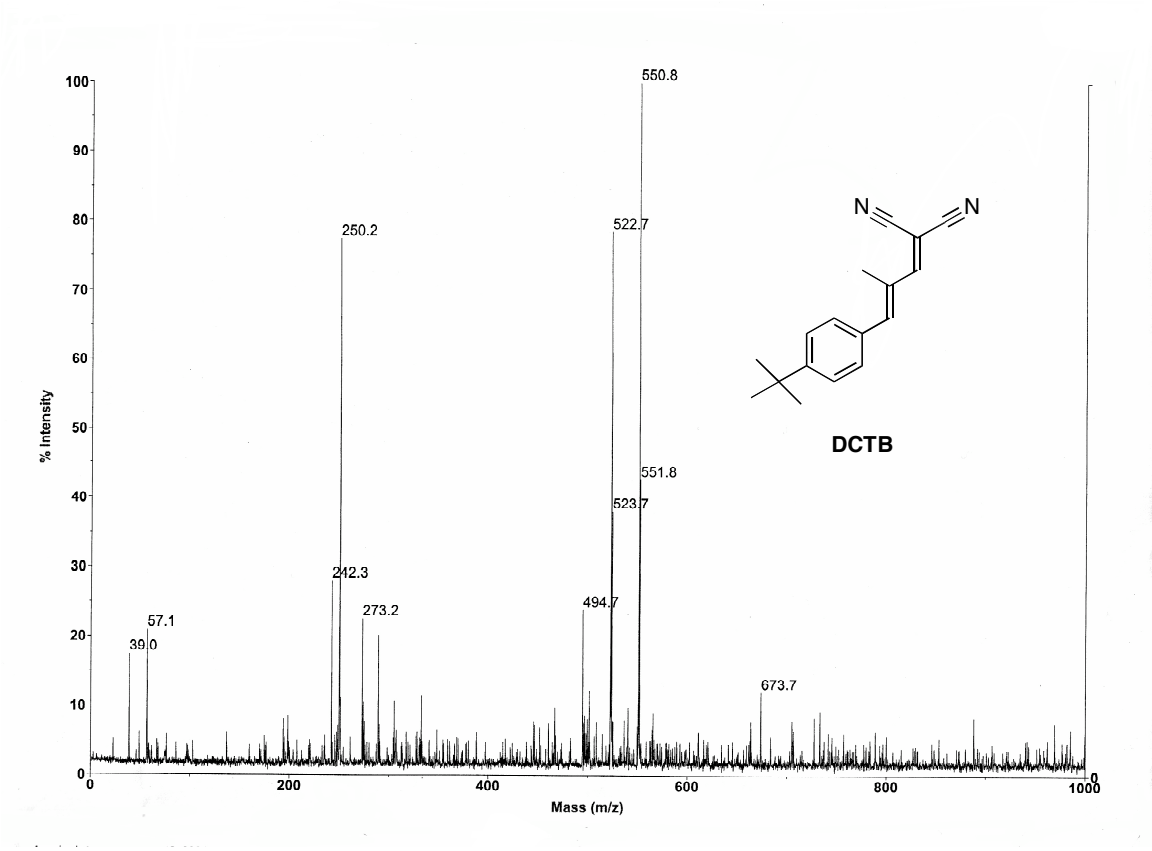

Figure 11. DCTB mass spectrum finger print ($C_{17}H_{18}N_2$ exact mass = 250.33822)

Crystal structures (compounds that are not discussed throughout this thesis)

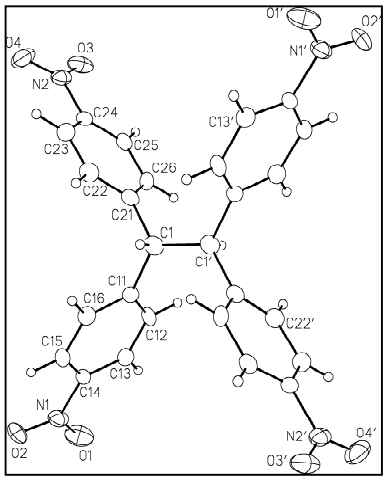

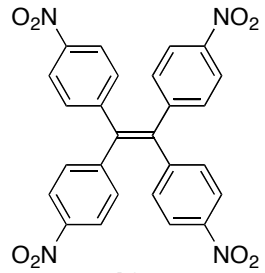

A64

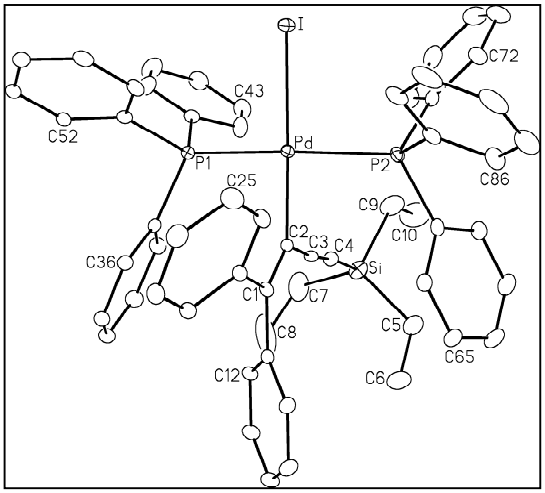

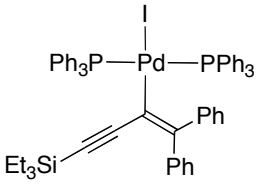

A65

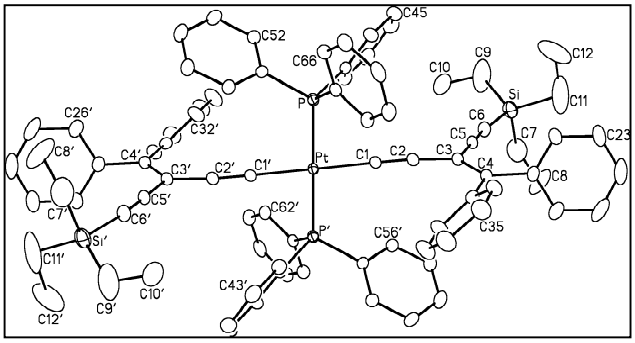

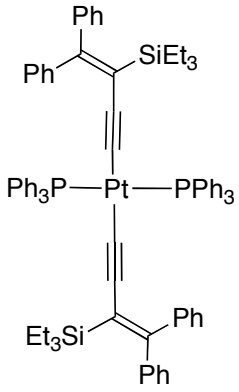

A66

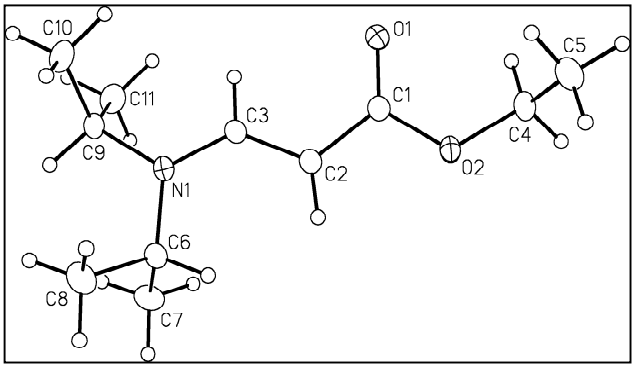

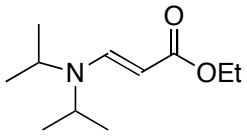

A67

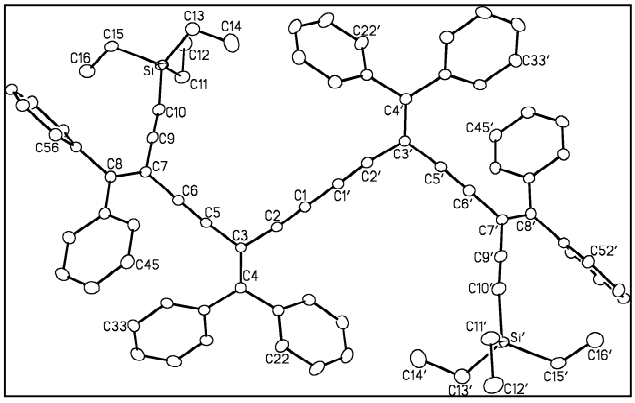

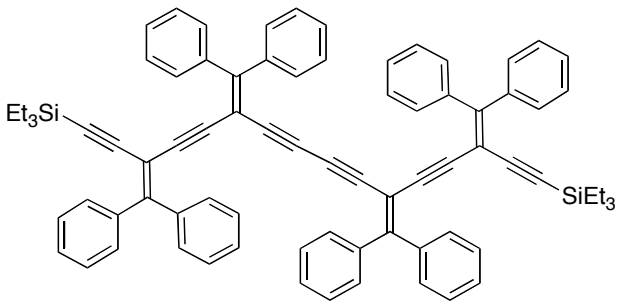

A68

Suitable single crystals of compounds **A64**–**A67** for X-ray crystallographic analysis grown from slow evaporation of a solution of CH_2Cl_2 at 4–5 °C. For compound **A68** THF was used as solvent.